

UNIVERSITY OF EAST ANGLIA

**A combined approach of electronic
structure calculations and spectroscopy
for elucidating reaction mechanisms in
organic and bioinorganic systems**

A Thesis submitted to the University of East Anglia

For the degree of Doctor of Philosophy

Submitted October 2012

Jamie N. T. Peck

School of Chemistry

University of East Anglia

Norwich

This copy of the thesis has been supplied on the condition that anyone who consults it is understood to recognise that its copyright rests with the author and that no quotation from the thesis, nor any information derived therefrom, may be published without the author's prior, written consent ©.

Abstract

This thesis describes the use of density functional theory (DFT) to assist the interpretation of advanced spectroscopic techniques such as stopped flow Fourier transform infrared spectroscopy (FTIR), muon spin resonance (μ SR), and nuclear inelastic scattering (NIS). These complementary techniques are used to investigate the structure and mechanism of a variety of important chemical systems, some of which are relevant to biological energy transduction and energy harvesting.

The mechanisms by which [FeFe] and [NiFe] hydrogenase enzymes catalyse the reversible reduction of protons to dihydrogen are of intrinsic interest in the context of a developing hydrogen technology for energy transduction. Gas phase DFT calculations are used to simulate and assign structure to experimental solution phase FTIR spectra for a family of [FeFe]-hydrogenase model complexes. Further, the Mulliken charge distribution across the Fe centres are compared for different dithiolate bridge groups and PMe_3 ligand positions. In the pursuit of understanding the protonation mechanism of [FeFe]-hydrogenases, transition state theory is used and the energetics of reaction pathways leading to terminal and bridging hydrides calculated and compared.

NIS demonstrates great potential for characterising the [FeFe]-hydrogenase mimics. In order to further develop and validate the technique, a combination of NIS, DFT calculations, FTIR and Raman spectroscopies are applied to a small Fe(III) model system in order to provide complete a characterisation of the low frequency metal–ligand vibrational modes.

Experimental μ SR spectroscopy is combined with DFT and applied to study the kinetics and mechanism of a simple microemulsion system in the measurement of the rate of molecular transfer through an oil-water interfacial layer. μ SR spectroscopy is then applied to a [FeFe]-hydrogenase mimic in order to identify products of muonium addition. In each application of the technique, the magnitude of the hyperfine interactions of all possible radical species are simulated using DFT calculations and compared with the experimental data, thus facilitating structural assignment.

Acknowledgments

First and foremost I would like to extend my sincerest gratitude to my primary supervisor, Dr. Vasily Oganessian and secondary supervisors, Dr. Upali Jayasooriya ("Jas") and Prof. Chris Pickett. I greatly appreciate their patience, kindness and academic experience, particularly during the final stages of writing. The conception and delivery of this thesis would not have been possible without their guidance. Special thanks go to Jas, who has been involved in my supervision since my undergraduate days. His passion and spirit of adventure towards research have been an inspiration to me.

I am thankful to Dr. Joseph Wright for his valuable advice regarding my research as well as in the art of LaTeX. I would also like to express my gratitude to all members of the Energy Materials Laboratory, for providing me with such interesting systems to work with and for their insightful discussion. I would like to thank Prof. Michael Hall for hosting me at Texas A&M University and providing me with guidance during the first year of my postgraduate study. The help of the beamline scientists at the Paul Scherrer Institut and Rutherford Appleton Laboratory has been invaluable, and I would like to particularly acknowledge Dr. Stephen Cottrell.

I gratefully acknowledge the EPSRC and CCLRC for providing me with the funding to make my research possible.

My time at UEA has been enriched by the many friends both inside and outside of University. I am grateful for the time spent with Paul and Trevor during tea breaks, and with Brad and Sam during beer breaks. This was often a welcome break from my research. I am especially thankful to my best friend Ellie, whose love and faithful support during the preparation of this thesis proved an invaluable source of motivation. Good one.

Finally, I would like to thank my family. I have a profound admiration for my mother who has provided me with unlimited love, support and encouragement throughout my life, thanks Mum. I am also grateful for the support of Alex and Frances, who have also been a huge source of inspiration to me during my life.

Wonderful, the process which fashions and transforms us! What is it going to turn you into next, in what direction will it use you to go?

Chuang-tzu, 6

Table of Contents

Abstract	i
Acknowledgments	ii
List of Figures	vii
List of Tables	xvii
Publications arising from this work	xx
1 Electronic structure theory	1
1.1 Introduction	1
1.2 The Schrödinger equation	1
1.3 Born-Oppenheimer approximation	2
1.4 Hartree-Fock theory	3
1.5 Basis sets	5
1.5.1 Slater and Gaussian type orbitals	5
1.5.2 Basis set classification	7
1.6 Correlation energy	8
1.7 Density functional theory	10
1.8 The potential energy surface (PES)	10
1.8.1 Stationary points	12
1.9 Solvation methods	16
1.10 Computational details	17
2 Experimental techniques	18
2.1 Principles of muon spectroscopy	18
2.1.1 Muon production and decay	19
2.1.2 Muons implanted in matter	21
2.1.3 Energy levels resulting from the interaction of spin $\frac{1}{2}$ particles	23
2.1.4 Sign of the hyperfine coupling constant	25
2.1.5 μ SR geometries	26
2.2 Principles of infrared spectroscopy	31
2.3 Principles of electron paramagnetic resonance (EPR) spectroscopy	35

2.4	Principles of nuclear inelastic scattering spectroscopy	39
3	Protonation regiochemistry in $[\text{Fe}_2(\mu\text{-Xdt})(\text{CO})_4(\text{PMe}_3)_2]$	41
3.1	Introduction	41
3.2	Computational details	48
3.3	Isomers of $[\text{Fe}_2(\mu\text{-Xdt})(\text{CO})_4(\text{PMe}_3)_2]$ model subsites	49
3.3.1	$[\text{Fe}_2(\mu\text{-pdt})(\text{CO})_4(\text{PMe}_3)_2]$	49
3.3.2	$[\text{Fe}_2(\mu\text{-edt})(\text{CO})_4(\text{PMe}_3)_2]$	58
3.3.3	$[\text{Fe}_2(\mu\text{-odt})(\text{CO})_4(\text{PMe}_3)_2]$	59
3.3.4	$[\text{Fe}_2(\mu\text{-mpdt})(\text{CO})_4(\text{PMe}_3)_2]$	61
3.3.5	$[\text{Fe}_2(\mu\text{-dmpdt})(\text{CO})_4(\text{PMe}_3)_2]$	63
3.3.6	$[\text{Fe}_2(\mu\text{-mpdt-S})(\text{CO})_4(\text{PMe}_3)_2]$	64
3.4	Effects of the dithiolate bridgehead	65
3.4.1	Trends in the $\nu(\text{CO})$ frequencies	65
3.4.2	Rotational energy barriers with changing dithiolate bridge	66
3.4.3	Trends in geometries	68
3.5	Relative stabilities of $[(\text{H})\text{Fe}_2(\mu\text{-Xdt})(\text{CO})_4(\text{PMe}_3)_2]^+$ subsites	69
3.5.1	The $[(\text{H})\text{Fe}_2(\mu\text{-pdt})(\text{CO})_4(\text{PMe}_3)_2]^+$ subsite	70
3.5.2	$[(\text{H})\text{Fe}_2(\mu\text{-Xdt})(\text{CO})_4(\text{PMe}_3)_2]^+$ subsites	81
3.6	Summary and conclusions	81
4	Protonation mechanism of $[\text{Fe}_2(\mu\text{-Xdt})(\text{CO})_4(\text{PMe}_3)_2]$ model subsites	83
4.1	Computational details	85
4.2	Protonation of the Fe–Fe bond to form bridging hydrides	85
4.2.1	Protonation to form terminal hydrides	95
4.3	Isomerisation pathways from terminal to bridging hydrides	111
4.3.1	Rearrangement from terminal hydrides 3A3 ^(*) , 3A4 ^(*) and 6AInt ^(*)	111
4.3.2	Rearrangement from terminal hydrides 3C1 ^(*) , 3A2 ^(*) , 6CInt ^(*) and 3D2 ^(*)	115
4.3.3	Rearrangement from terminal hydrides 3D1 ^(*) , 3A1 ^(*) , 3C2 ^(*) and 6DInt ^(*)	118
4.4	Summary and conclusions	121
5	Mixed valence $[(\mu\text{-H})\text{Fe}_2(\mu\text{-Xdt})(\text{CO})_4(\text{PMe}_3)_2]$ Subsites	123
5.1	Computational details	124
5.2	Relative energies of the isomers of $[(\mu\text{-H})\text{Fe}_2(\mu\text{-Xdt})(\text{CO})_4(\text{PMe}_3)_2]$ subsites	124
5.3	Simulated infrared of $[(\mu\text{-H})\text{Fe}_2(\mu\text{-Xdt})(\text{CO})_4(\text{PMe}_3)_2]$ subsites	125
5.4	EPR of mixed valence subsites	130
5.4.1	Summary and conclusions	132

5.5	Investigating [Fe(I)Fe(II)]-hydrogenase model systems using muon spectroscopy and DFT calculations	132
5.5.1	Experimental	134
5.5.2	Results and discussion	135
5.5.3	Summary and conclusions	144
6	Characterising the normal modes of tris(acetylacetonate)iron(III) using NIS and DFT	146
6.1	Introduction	146
6.2	Experimental	147
6.2.1	Nuclear inelastic scattering spectroscopy	147
6.2.2	Infrared spectroscopy	148
6.2.3	Raman spectroscopy	148
6.2.4	Computational parameters	148
6.3	Results and discussion	149
6.4	Summary and conclusions	154
7	Measuring the rate of interfacial transfer using muon spectroscopy	158
7.1	Introduction	158
7.2	Experimental	161
7.2.1	Sample preparation	161
7.2.2	Data fitting	162
7.2.3	Computational parameters	162
7.3	Results and discussion	162
7.3.1	Transverse field experiments	162
7.3.2	ALC- μ -SR experiments	165
7.3.3	Monte-Carlo simulation of ALC spectra	168
7.3.4	Assignment of ALC resonances using DFT calculations	170
7.4	Summary and conclusions	179
8	Final remarks and future work	180

List of Figures

1.1	Specification of molecule ABC in Cartesian space.	11
1.2	The potential energy surface of H ₂ O, characterised by variations in r_1 and θ_1 . Calculated at HF/3-21G level of theory.	12
1.3	Schematics of the allyl alcohol radical corresponding to: (a), the minimum energy conformation; (b), a first-order saddle point from the torsional rotation of the H7–C1–C2–C3; and (c), a second-order saddle point. Atom labels are indicated in red. (d) shows two slices of the potential energy surface of an allyl alcohol radical, characterised by the variation in H7–C1–C2–C3 and C1–C2–C3–O4 torsional angles.	15
1.4	Simplified schematic of the PCM model.	17
2.1	Decay of the positive pion in its resting frame, demonstrating muon spin polarisation. Where the blue arrows represent the momentum vectors, \mathbf{P} , and red arrows represent particle spin, \mathbf{I}	20
2.2	Decay of the positive muon into a positron, neutrino, and anti-neutrino. Where the blue arrows represent the momentum vectors, \mathbf{P} , and red arrows represent particle spin, \mathbf{I}	20
2.3	Muonium addition to ethene.	21
2.4	Angular distribution of the positron emission resulting from muon decay. The red curve represents the emission probability for maximum energy, $A = 1$. Averaging over the positrons energy spectrum gives the green curve, $A = \frac{1}{3}$	23
2.5	Energies of an electron, proton and muon as a function of magnetic field, \mathbf{B} . 24	
2.6	The Briet-Rabi diagram describing the energy levels of a muon-electron system as a function of magnetic field.	26

2.7	Left: Schematic of the TF Muon spectrometer geometry. The muon beam arrives from the left with its spin (red arrow) anti-parallel to its momentum (blue arrow). The externally applied magnetic field, \mathbf{H} , is transverse to the muon spin direction. The sample is represented by a yellow cube and the grey boxes around the sample indicate the positions of the detectors; forward (F), backward (B), left (L), and right (R), which are defined by the direction of the incoming muon spin. Right: An example μ SR histogram and corresponding asymmetry of the forward detector in a transverse-field experiment. Scheme adapted from [29].	27
2.8	Schematic of the LF Muon spectrometer geometry. Scheme adapted from [29].	29
2.9	Breit-Rabi diagram at high magnetic field showing the energy levels of a three spin system; muon, μ^+ , electron, e^- , and proton, p^+ . The three types of avoided level crossings are shown, $\Delta M=0$, 1, and 2 which correspond to muon-proton spin flip-flop, muon spin flip, and muon-proton spin flip-flop, respectively.	30
2.10	(a) Energy parabola for a vibrating spring and (b) energy parabola with quantised energy levels.	34
2.11	Morse potential energy curve for the anharmonic oscillator.	34
2.12	Example of the first derivative EPR spectrum.	38
3.1	Schematic representation of the H-cluster ($X = \text{CH}_2$, NH , or O and $L =$ vacant, H_2O , OH^- , H^- , or H_2).	43
3.2	Proposed mechanism for the catalytic turnover of H_2/H^+ by the $[\text{FeFe}]$ -hydrogenase. Adapted from [47, 62, 65].	44
3.3	Wright-Pickett proposed mechanism for protonation of the $[\text{Fe}_2(\mu\text{-pdt})(\text{CO})_4(\text{PMe}_3)_2]$ model subsite [68].	46
3.4	Family of $[\text{Fe}_2(\mu\text{-Xdt})(\text{CO})_4(\text{PMe}_3)_2]$ model systems investigated in this work.	47
3.5	Possible hydrides produced from the protonation of $[\text{Fe}_2(\mu\text{-Xdt})(\text{CO})_4(\text{PMe}_3)_2]$ (Xdt 1).	47
3.6	Isomers of the $[\text{Fe}_2(\mu\text{-pdt})(\text{CO})_4(\text{PMe}_3)_2]$ model system. Atom and functional group labels are reported in red. Associated relative free energies and Mulliken charges are reported in Table 3.1 and bond distances and angles are reported in Table A17 and Table A18.	50
3.7	Highest occupied molecular orbitals (HOMOs) for isomers (a) pdt 1A , (b) pdt 1A' , (c) pdt 1B , (d) pdt 1C , and (e) pdt 1D of the $[\text{Fe}_2(\mu\text{-pdt})(\text{CO})_4(\text{PMe}_3)_2]$ model complex. Isosurface = 0.04.	52
3.8	Schematic of an octahedron undergoing (a) Bailar twist and (b) Ray-Dutt twist.	55

3.9	Solvent corrected free energy barriers associated with rearrangement of the isomers of $[\text{Fe}_2(\mu\text{-pdt})(\text{CO})_4(\text{PMe}_3)_2]$. Rotating groups in transition states are highlighted in red.	56
3.10	Comparison of experimental IR spectra [67] of $[\text{Fe}_2(\mu\text{-pdt})(\text{CO})_4(\text{PMe}_3)_2]$ with the simulated spectra of the most stable isomer, 1A	58
3.11	Structural isomers of the $[\text{Fe}_2(\mu\text{-SCH}_2\text{CH}_2\text{S})(\text{CO})_4(\text{PMe}_3)_2]$ model system. Relative solvent corrected free energies are reported in Table A1 Selected bond distances and bond angles are reported in Table A2 and Table A3, respectively.	59
3.12	Comparison of experimental IR spectra [69] of $[\text{Fe}_2(\mu\text{-edt})(\text{CO})_4(\text{PMe}_3)_2]$ with the simulated spectra of the most stable isomer, 1A	59
3.13	Structural isomers of the $[\text{Fe}_2(\mu\text{-SCH}_2\text{OCH}_2\text{S})(\text{CO})_4(\text{PMe}_3)_2]$ model system. Relative solvent corrected free energies are reported in Table A31 Selected bond distances and bond angles are reported in Table A32 and Table A33, respectively.	60
3.14	Comparison of experimental IR spectra [105] of $[\text{Fe}_2(\mu\text{-odt})(\text{CO})_4(\text{PMe}_3)_2]$ with the simulated spectra of the most stable isomer, 1A'	61
3.15	Structural isomers of the $[\text{Fe}_2(\mu\text{-SCH}_2\text{CH}(\text{CH}_3)\text{CH}_2\text{S})(\text{CO})_4(\text{PMe}_3)_2]$. Relative solvent corrected free energies are reported in Table A46 Selected bond distances and bond angles are reported in Table A47 and Table A48, respectively.	62
3.16	Comparison of $[\text{Fe}_2(\mu\text{-mpdt})(\text{CO})_4(\text{PMe}_3)_2]$ experimental IR spectra [128] with the simulated spectra of the most stable isomer, 1A'	63
3.17	Structural isomers of the $[\text{Fe}_2(\mu\text{-SCH}_2\text{C}(\text{CH}_3)_2\text{CH}_2\text{S})(\text{CO})_4(\text{PMe}_3)_2]$ model system. Relative solvent corrected free energies are reported in Table A60. Selected bond distances and bond angles are reported in Table A61 and Table A62, respectively.	64
3.18	Comparison of the experimental IR spectra [120] of $[\text{Fe}_2(\mu\text{-dmpdt})(\text{CO})_4(\text{PMe}_3)_2]$ with the simulated spectra of the most stable isomer, 1A'	64
3.19	Structural isomers of the $[\text{Fe}_2(\mu\text{-SCH}_2\text{CH}(\text{CH}_3)(\text{CH}_2\text{S})\text{CH}_2\text{S})(\text{CO})_4(\text{PMe}_3)]$ tripodal model system, including 1A' and 1B' ; the isomers with a wagged S-CH ₃ group. Relative solvent corrected free energies and Mulliken charges are reported in Table A69. Selected bond distances and bond angles are reported in Table A70 and Table A71, respectively.	65
3.20	Comparison of the experimental IR spectra [129] of $[\text{Fe}_2(\mu\text{-mpdt-S})(\text{CO})_4(\text{PMe}_3)_2]$ with the simulated spectra of the most stable isomer, 1A	65
3.21	HOMOs of (a) isomer pdt 1C and (b) pdt TS_{1A-1C} of the $[\text{Fe}_2(\mu\text{-pdt})(\text{CO})_4(\text{PMe}_3)_2]$ (pdt 1) model complex.	69
3.22	Comparison of the experimental IR spectra [68] of $[(\text{H})\text{Fe}_2(\mu\text{-pdt})(\text{CO})_4(\text{PMe}_3)_2]^+$ with the simulated spectra of isomer 1D	72

3.23	Isomers of $[(\mu\text{-H})\text{Fe}_2(\mu\text{-pdt})(\text{CO})_4(\text{PMe}_3)_2]^+$. Relative free energies and bond distances are reported in Table 3.7.	72
3.24	Energy profile for the interconversion of the isomers of 2 through the rotation of the $\text{Fe}(\text{CO})_2(\text{PMe}_3)$ moiety. Free energies are reported in kcal/mol relative to 2D . Groups coloured red indicate the positional change characterising the transition state.	74
3.25	Isomers of the terminally protonated $[(\text{H})\text{Fe}_2(\mu\text{-pdt})(\text{CO})_4(\text{PMe}_3)_2]^+$. Relative free energies and bond distances are reported in Table 3.7. Selected bond distances and bond angles are reported in Table A23 and Table A24, respectively.	78
3.26	Relative solvent corrected free energies of the sulphur protonated isomers of $(\mu\text{-SCH-2CH}_2\text{CH}_2\text{SH})\text{Fe}_2(\text{CO})_4(\text{PMe}_3)_2^+$ calculated using the Becke, three-parameter (exchange), Lee-Yang-Parr (correlation) (B3LYP) functional. Energies are reported relative to 2D of the same functional, and are reported in kcal/mol.	79
3.27	Relative solvent corrected free energies of the formyl isomers of $(\mu\text{-pdt})\text{-Fe}_2(\text{COH})(\text{CO})_3(\text{PMe}_3)_2^+$ calculated using the B3LYP functional. Energies are reported relative to 2D of the same functional, and are reported in kcal/mol.	80
4.1	Possible ether mediated protonation pathways: terminal path and bridging path.	85
4.2	(a) Energy profile for the formation of 2A and 2A' through the diethyl ether mediated protonation of 1A and 1A' to the Fe–Fe bond. Energies are given in kcal/mol relative to 1A ; and optimised geometries of the (b) ether mediated intermediate (6Aba) and the (c) transition state (TS _{6Aba–6HAba}). For clarity, hydrogen atoms of the PMe_3 groups and the ether have been omitted, bond distances are reported in Å.	88
4.3	(a) Energy profile for the formation of 2B through the diethyl ether mediated protonation of 1B to the Fe–Fe bond. Energies are given in kcal/mol relative to 1B ; and optimised geometries of the (b) ether mediated intermediate (6Bba) and the (c) transition state (TS _{6Bba–6HBba}). For clarity, hydrogen atoms of the PMe_3 groups and the ether have been omitted, bond distances are reported in Å.	90
4.4	(a) Energy profile for the formation of 2C through the diethyl ether mediated protonation of 1C to the Fe–Fe bond. Energies are given in kcal/mol relative to 1C ; and optimised geometries of the (b) ether mediated intermediate (6Cba) and the (c) transition state (TS _{6Cba–6HCba}). For clarity, hydrogen atoms of the PMe_3 groups and the ether have been omitted, bond distances are reported in Å.	92

- 4.5 (a) Energy profile for the formation of **2D** through the diethyl ether mediated protonation of **1D** to the Fe–Fe bond. Energies are given in kcal/mol relative to **1D**; and optimised geometries of the (b) ether mediated intermediate (**6Dba**) and the (c) transition state (**TS_{6Dba-6Dba}**). For clarity, hydrogen atoms of the PMe_3 groups and the ether have been omitted, bond distances are reported in Å. 94
- 4.6 (a) Energy profile for the formation of **3A1** and **3A1'** through the diethyl ether mediated protonation of **1A** and **1A'**. Energies are given in kcal/mol relative to **1A**; and optimised geometries of the (b) ether mediated intermediate (**8Aba**) and the (c) transition state (**TS_{8Aba-8HAba}**). For clarity, hydrogen atoms of the PMe_3 groups and the ether have been omitted, bond distances are reported in Å. 99
- 4.7 (a) Energy profile for the formation of **3A2** and **3A2'** through the diethyl ether mediated protonation of **1A** and **1A'**. Energies are given in kcal/mol relative to **1A**; and optimised geometries of the (b) ether mediated intermediate (**10Aba**) and the (c) transition state (**TS_{10Aba-10HAba}**). For clarity, hydrogen atoms of the PMe_3 groups and the ether have been omitted, bond distances are reported in Å. 100
- 4.8 (a) Energy profile for the formation of **3A3** and **3A3'** through the diethyl ether mediated protonation of **1A** and **1A'**. Energies are given in kcal/mol relative to **1A**; and optimised geometries of the (b) ether mediated intermediate (**6Aap**) and the (c) transition state (**TS_{pdT_TS_{6Aap-6HAap}}**). For clarity, hydrogen atoms of the PMe_3 groups and the ether have been omitted, bond distances are reported in Å. 101
- 4.9 (a) Energy profile for the formation of **3A4** and **3A4'** through the diethyl ether mediated protonation of **1A** and **1A'**. Energies are given in kcal/mol relative to **1A**; and optimised geometries of the (b) ether mediated intermediate (**9Aba**) and the (c) transition state (**TS_{9Aba-9HAba}**). For clarity, hydrogen atoms of the PMe_3 groups and the ether have been omitted, bond distances are reported in Å. 102
- 4.10 (a) Energy profile for the formation of **3B** and **3B'** through the diethyl ether mediated protonation of **1B**. Energies are given in kcal/mol relative to **1A**; and optimised geometries of the (b) ether mediated intermediate (**7Bba**) and the (c) transition state (**TS_{7Bba-7HBba}**). For clarity, hydrogen atoms of the PMe_3 groups and the ether have been omitted, bond distances are reported in Å. 104

- 4.11 (a) Energy profile for the formation of **3C1** and **3C1'** through the diethyl ether mediated protonation of **1C**. Energies are given in kcal/mol relative to **1A**; and optimised geometries of the (b) ether mediated intermediate (**6Cap**) and the (c) transition state (**TS_{pdt_rS₆Cap-6HCap}**). For clarity, hydrogen atoms of the PMe_3 groups and the ether have been omitted, bond distances are reported in Å. 106
- 4.12 (a) Energy profile for the formation of **3C2** and **3C2'** through the diethyl ether mediated protonation of **1C**. Energies are given in kcal/mol relative to **1A**; and optimised geometries of the (b) ether mediated intermediate (**7Cba**) and the (c) transition state (**TS_{pdt_rS₇Cba-7HCba}**). For clarity, hydrogen atoms of the PMe_3 groups and the ether have been omitted, bond distances are reported in Å. 107
- 4.13 LUMOs associated with the **TS_{7Cba7HCba}** for (a) the pdt dithiolate bridge (b) the edt dithiolate bridge and (c) the odt bridge. Isosurface = 0.04. . . . 108
- 4.14 (a) Energy profile for the formation of **3D2** and **3D2'** through the diethyl ether mediated protonation of **1D**. Energies are given in kcal/mol relative to **1A**; and optimised geometries of the (b) ether mediated intermediate (**8DBa**) and the (c) transition state (**TS_{pdt_rS₈DBa-8HDBa}**). For clarity, hydrogen atoms of the PMe_3 groups and the ether have been omitted, bond distances are reported in Å. 110
- 4.15 Isomerisation pathways for the rearrangement of terminal hydrides **3A3** and **3A3'** to the bridging hydride **2B**: black line pathway: **3A3** → **3A4** → **2B**; red line pathway: the pdt bridge flipped path **3A3'** → **3A4'** → **2B**) is coloured red. Energies are reported relative to **1A**. 112
- 4.16 Alternative isomerisation pathways for the rearrangement of terminal hydrides **3A3** and **3A3'** to bridging hydrides **2A** and **2A'**: black line pathway: **3A3** → **6AInt** → **2A**; red line pathway: the pdt bridge flipped path **3A3'** → **6AInt'** → **2A'**. Energies are reported relative to **1A**. 113
- 4.17 Isomerisation pathways for the rearrangement of terminal hydrides **3A3** and **3A3'** to bridging hydrides **2A** and **2A'**: black line pathway: **3A3** → **3B** → **2A**; red line pathway: the pdt bridge flipped path **3A3'** → **3B'** → **2A'**. Energies are reported relative to **1A**. 114
- 4.18 Isomerisation pathways for the rearrangement of terminal hydrides **3C1** and **3C1'** to the bridging hydride **2D**: black line pathway: **3C1** → **3A2** → **2D**; red line pathway: the pdt bridge flipped path **3C1'** → **3A2'** → **2D**. Energies are reported relative to **1A**. 116
- 4.19 Isomerisation pathways for the rearrangement of terminal hydrides **3C1** and **3C1'** to bridging hydrides **2A** and **2A'**: black line pathway: **3C1** → **3D2** → **2A**; red line pathway: the pdt bridge flipped path **3C1'** → **3D2'** → **2A'**. Energies are reported relative to **1A**. 117

4.20	Isomerisation pathways for the rearrangement of terminal hydrides 3C1 and 3C1' to the bridging hydride 2D : black line pathway: 3C1 → 6CInt → 2D ; red line pathway: the pdt bridge flipped path 3C1' → 6C'Int → 2D . Energies are reported relative to 1A	117
4.21	Isomerisation pathways for the rearrangement of terminal hydrides 3D1 and 3D1' to the bridging hydride 2C : black line pathway: 3D1 → 3A1 → 2C ; red line pathway: the pdt bridge flipped path 3D1' → 3A1' → 2C . Energies are reported relative to 1A	119
4.22	Isomerisation pathways for the rearrangement of terminal hydrides 3D1 and 3D1' to the bridging hydrides 2A and 2A' : black line pathway: 3D1 → 3C2 → 2A ; red line pathway: the pdt bridge flipped path 3D1' → 3C2' → 2A' . Energies are reported relative to 1A	120
4.23	Isomerisation pathways for the rearrangement of terminal hydrides 3D1 and 3D1' to the bridging hydrides 2C : black line pathway: 3D1 → 6DInt → 2C ; red line pathway: the pdt bridge flipped path 3D1' → 6D'Int → 2C . Energies are reported relative to 1A	120
4.24	Comparison of the three most energetically favoured reaction pathways for the protonation of $[\text{Fe}_2(\mu\text{-Xdt})(\text{CO})_4(\text{PMe}_3)_2]$ with edt, pdt and odt dithiolate bridges. Solvent correct free energy barriers are reported in kcal/mol.	122
5.1	SOMO for the 2D isomer of the (a) edt (b) pdt and (c) odt dithiolate bridged complexes. Isosurface=0.4.	125
5.2	Top: Experimental difference IR spectrum of the reduction of the pdt dithiolate bridged system. Bottom: Calculated difference spectrum of the reduction of isomer pdt 2D	127
5.3	Top: Experimental difference IR spectrum of the reduction of the edt dithiolate bridged system. Bottom: Calculated difference spectrum of the reduction of isomer edt 2D	127
5.4	Isosurface of the spin density distribution of the singly reduced form of the basal/basal transoid isomer of $(\mu\text{-H})(\mu\text{-pdt})\text{Fe}_2(\text{CO})_4(\text{PMe}_3)_2$ (a) top view and (b) side view	130
5.5	Continuous-wave X-band EPR spectra in THF: (top) reduced pdt 2D at 165 K; (bottom) reduced deuterio-pdt 2D at 164 K. The line-width variation across the spectra, which is due to the sign of the coupling constants, is most pronounced in the spectrum of reduced protio-pdt 2D	131
5.6	Isosurface of the spin density distribution of the singly reduced form of the basal/basal transoid isomer of $(\mu\text{-H})(\mu\text{-pdt})\text{Fe}_2(\text{CO})_4(\text{PMe}_3)_2$ (a) top view and (b) side view	132

5.7	Artificial hydrogenase subsite analogues $[\text{Fe}_2(\mu\text{-pdt})(\text{CO})_4(\text{PMe}_3)_2]$ and $[\text{Fe}_2(\mu\text{-pdt})(\text{CO})_4(\text{CN})_2]^{2-}$ chosen for Longitudinal Field- μSR investigation.	134
5.8	$\mu\text{-SR}$ spectra of (a) $[\text{Fe}_2(\mu\text{-pdt})(\text{CO})_4(\text{CN})_2]^{2-}$ recorded at 5 K and (b) $[\text{Fe}_2(\mu\text{-pdt})(\text{CO})_4(\text{PMe}_3)_2]$ recorded at 5 K. Raw spectra are reported at the top and background subtracted spectra at the bottom. The background of the aluminium plate was recorded at 5 K.	137
5.9	Structural isomers of possible $[\text{MuFe}_2(\mu\text{-pdt})(\text{CO})_4(\text{CN})_2]^{2-}$ muoniated radicals.	141
5.10	Structural isomers of possible $[\text{MuFe}_2(\mu\text{-pdt})(\text{CO})_4(\text{PMe}_3)_2]$ muoniated radicals.	142
5.11	Spin densities of the (a) bisCN 5 and (b) bisCN 6 isomers. Isosurface = 0.004	142
5.12	Spin densities of the (a) bisPMe₃ 4 and (b) bisPMe₃ 5 isomers. Isosurface = 0.004	143
5.13	Structural isomers of $[\text{MuFe}_2(\mu\text{-pdt})(\text{CO})_4(\text{CN})_2]^{2-}$ muoniated radicals with predicted resonances in agreement with the experimental spectrum. .	145
5.14	Structural isomers of $[\text{MuFe}_2(\mu\text{-pdt})(\text{CO})_4(\text{PMe}_3)_2]$ muoniated radicals with predicted resonances in agreement with the experimental spectrum. .	145
6.1	Structure of tris(acetylacetonate)iron(III), Fe(III)(acac)_3	147
6.2	Comparison of (a) the experimental infrared spectrum of Fe(III)(acac)_3 with (b) the simulated infrared spectrum of an isolated molecule of $^{57}\text{Fe(III)(acac)}_3$ and $^{56}\text{Fe(III)(acac)}_3$ shown by solid and dashed lines, respectively.	151
6.3	Comparison of (a) the experimental Raman spectrum of solid state Fe(III)(acac)_3 with (b) the simulated Raman spectra of an isolated molecule of $^{57}\text{Fe(III)(acac)}_3$ and $^{56}\text{Fe(III)(acac)}_3$ shown by solid and dashed lines, respectively.	151
6.4	Comparison between (a) relative PDOS intensities obtained from nuclear inelastic scattering (NIS) of $^{57}\text{Fe(III)(acac)}_3$ with (b) those predicted from an <i>ab initio</i> DFT calculation for an isolated molecule.	152
6.5	Simulated A_2 normal modes of $^{57}\text{Fe(III)(acac)}_3$ for NIS active vibrations, hydrogen atoms omitted for clarity.	155
6.6	Simulated E normal modes of $^{57}\text{Fe(III)(acac)}_3$ for NIS active vibrations, hydrogen atoms omitted for clarity.	156

7.1	(a) Schematic illustrating a probe molecule, X residing in either the oil or water phases, travelling through the interface with a rate constant, k. Right: line broadening resulting from a two site chemical exchange where the rate of exchange is (b) much less than the peak HWHH, $\Delta\nu$ (c) approximately equal to $\Delta\nu$, or (d) much greater than $\Delta\nu$	159
7.2	Schematic of the system of choice.	160
7.3	Formation of the two muoniated allyl alcohol radicals.	162
7.4	TF- μ SR spectrum from 0.5 M allyl alcohol in water at 288.5 K in a transverse magnetic field of 3000 Gauss. The spectral feature at 40.67 MHz (truncated to better view the other signals) is from muons in the diamagnetic environment. The pair of signals at 113.60 MHz and 200.81 MHz result from one of the two radicals.	163
7.5	Temperature dependence of the position of (a) peak 1 and (b) peak 2 in water (blue), heptane (green), and micro-emulsion (red).	164
7.6	Temperature dependence of the peak width (HWHH) of (a) peak 1 and (b) peak 2 in water (blue), heptane (green), and micro-emulsion (red).	164
7.7	Temperature dependence of the peak width (HWHH) of (a) peak 1 and (b) peak 2 in water (blue), heptane (green), and micro-emulsion (red).	165
7.8	The allyl alcohol radicals with assignment of peaks based on the DFT investigation reported in 7.3.4.	166
7.9	ALC spectra showing peaks in water, micro-emulsion and heptane at 290 K. Labels are linked to Figure 7.8	166
7.10	Variance in ALC resonances in water and oil phases, $\nu_W - \nu_O$ in (a) peak 1, (b) peak 2 and (c) peak 4.	167
7.11	ALC spectra of AA in the micro-emulsion indicating the variation in line broadening with temperature.	167
7.12	Temperature dependence of the ALC resonance HWHH of (a) peak 1, (b) peak 2 and (c) peak 4.	168
7.13	Monte-Carlo simulation of ALC resonance of AA in the micro-emulsion based on a rate of exchange of (a) 0 seconds, (b) 10^{-7} seconds and (c) 10^{-9} seconds. All simulations assume a A_μ value of 376 MHz for both water and oil phases, and A_p values of 127 MHz and 122 MHz for water and oil phases, respectively. All simulations use 100 steps and 1,000,000 muons.	168
7.14	Experimentally fitted spectra for (a) peak 1 and (b) peak 2 for AA in water, heptane and microemulsion.	169
7.15	Monte-Carlo simulation of ALC resonance.	170
7.16	Atom labels used to describe muonium and the allyl alcohol molecule.	170
7.17	Spin density for (a) centrally muoniated AA, and (b) terminally muoniated AA. Isosurface=0.04.	171

7.18	The lowest energy simulated modes of vibration for terminally and centrally muoniated radicals of AA.	172
7.19	Schematic illustrating the overlap as a function of the angle between the p_z orbital and the muon bond.	173
7.20	(a) Atom labels for the centrally muonated radical. (b) Total energy of the centrally muoniated radical as a function of dihedral angles $\mathbf{H}_7\text{-C}_1\text{-C}_2\text{-C}_3$ and $\mathbf{C}_1\text{-C}_2\text{-C}_3\text{-O}_4$. Cross section of the potential energy surface (PES) taken from the equilibrium structure of the centrally muoniated radical showing energy as a function of the dihedral angle made by (c) $\mathbf{H}_7\text{-C}_1\text{-C}_2\text{-C}_3$ and (d) $\mathbf{C}_1\text{-C}_2\text{-C}_3\text{-O}_4$. The labelled dotted lines correspond to the ground state, E_0 and excited states, E_n	173
7.21	(a) Atom labels for the terminally muonated radical. (b) Total energy of the terminally muoniated radical as a function of dihedral angles $\mathbf{H}_7\text{-C}_1\text{-C}_2\text{-C}_3$ and $\mathbf{C}_1\text{-C}_2\text{-C}_3\text{-O}_4$. Cross section of the PES taken from the equilibrium structure of the terminally muoniated radical showing energy as a function of the dihedral angle made by (c) $\mathbf{H}_7\text{-C}_1\text{-C}_2\text{-C}_3$ and (d) $\mathbf{C}_1\text{-C}_2\text{-C}_3\text{-O}_4$. The labelled dotted lines correspond to the ground state, E_0 and excited states, E_n	174
7.22	$A_{\mu e}$ as a function of dihedral angles $\mathbf{H}_7\text{-C}_1\text{-C}_2\text{-C}_3$ and $\mathbf{C}_1\text{-C}_2\text{-C}_3\text{-O}_4$ for the (a) centrally and (b) terminally muoniated radicals.	174
7.23	Simulated $A_{p(6)}$ as a function of dihedral angles $\mathbf{H}_7\text{-C}_1\text{-C}_2\text{-C}_3$ and (b) $\mathbf{C}_1\text{-C}_2\text{-C}_3\text{-O}_4$ for the (a) centrally and (b) terminally muoniated radicals.	177
7.24	Simulated $A_{p(7)}$ as a function of dihedral angles $\mathbf{H}_7\text{-C}_1\text{-C}_2\text{-C}_3$ and (b) $\mathbf{C}_1\text{-C}_2\text{-C}_3\text{-O}_4$ for the (a) centrally and (b) terminally muoniated radicals.	177
7.25	Simulated $A_{p(8)}$ as a function of dihedral angles $\mathbf{H}_7\text{-C}_1\text{-C}_2\text{-C}_3$ and (b) $\mathbf{C}_1\text{-C}_2\text{-C}_3\text{-O}_4$ for the (a) centrally and (b) terminally muoniated radicals.	177
7.26	Simulated $A_{p(9)}$ as a function of dihedral angles $\mathbf{H}_7\text{-C}_1\text{-C}_2\text{-C}_3$ and (b) $\mathbf{C}_1\text{-C}_2\text{-C}_3\text{-O}_4$ for the (a) centrally and (b) terminally muoniated radicals.	178
7.27	Simulated $A_{p(10)}$ as a function of dihedral angles $\mathbf{H}_7\text{-C}_1\text{-C}_2\text{-C}_3$ and (b) $\mathbf{C}_1\text{-C}_2\text{-C}_3\text{-O}_4$ for the (a) centrally and (b) terminally muoniated radicals.	178

List of Tables

2.1	Comparison of the properties of the muon, electron, and proton.	19
2.2	Comparison of the chemical properties of muonium, hydrogen, deuterium, and tritium.	21
2.3	Energy levels and wavefunctions of a muon-electron spin system in zero field.	25
2.4	Energy levels and wavefunctions of a muon-electron spin system in a non-zero field.	25
3.1	Calculated gas phase and solvent corrected free energies and Fe Mulliken charges for isomers of $[\text{Fe}_2(\mu\text{-pdt})(\text{CO})_4(\text{PMe}_3)_2]$ and the transition states that connect them; either through rotation of the $\text{Fe}(\text{CO})_2(\text{PMe}_3)$ moiety or by the propane-1,3-dithiolate (pdt) bridge flip. Energies are reported relative to the 1A isomer. Calculations using the B3LYP functional were carried out by Liu [118].	51
3.2	Selected geometric parameters for the unprotonated $[\text{Fe}_2(\mu\text{-pdt})(\text{CO})_4(\text{PMe}_3)_2]$ isomer 1D from x-ray crystallography compared to calculated values [69].	51
3.3	Energy comparison of the HOMOs of $[\text{Fe}_2(\mu\text{-pdt})(\text{CO})_4(\text{PMe}_3)_2]$ isomers.	54
3.4	DFT simulated $\nu(\text{CO})$ bands of $[\text{Fe}_2(\mu\text{-pdt})(\text{CO})_4(\text{PMe}_3)_2]$ isomers compared to those experimentally determined in CH_3CN [67].	57
3.5	DFT simulated $\nu(\text{CO})$ bands of $[\text{Fe}_2(\mu\text{-xdt})(\text{CO})_4(\text{PMe}_3)_2]$ isomers compared to those experimentally determined in CH_3CN [67, 69, 105, 120, 128, 129].	67
3.6	DFT simulated $\nu(\text{CO})$ bands of $[(\mu\text{-H})\text{Fe}_2(\mu\text{-pdt})(\text{CO})_4(\text{PMe}_3)_2]^+$ isomers compared to those experimentally determined in CH_3CN [68].	71
3.7	Selected bond lengths and calculated gas phase and solvent corrected free energies of the bridging hydride isomers $[(\mu\text{-H})\text{Fe}_2(\mu\text{-pdt})(\text{CO})_4(\text{PMe}_3)_2]^+$. Also included the free energy barriers associated with the rotation of the $\text{Fe}(\text{CO})_2(\text{PMe}_3)$ moiety and the pdt bridge flip. Energies are relative to 2D . A comparison with the B3LYP functional is also included [119].	73

3.8	Comparison of selected geometric parameters from x-ray crystallography study [69] with calculated values the 2D isomer of $[(\mu\text{-H})\text{Fe}_2(\mu\text{-pdt})(\text{CO})_4(\text{PMe}_3)_2]^+$	73
3.9	Selected bond lengths and calculated gas phase and solvent corrected free energies of the terminally protonated isomers of $[(\text{H})\text{Fe}_2(\mu\text{-pdt})(\text{CO})_4(\text{PMe}_3)_2]^+$. Energies are relative to 2D	76
3.10	DFT simulated $\nu(\text{CO})$ bands of the terminally protonated isomers of $[(\text{H})\text{Fe}_2(\mu\text{-pdt})(\text{CO})_4(\text{PMe}_3)_2]^+$ compared to those experimentally determined in CH_3CN [68].	77
3.11	Selected bond lengths and calculated gas phase and solvent corrected free energies of the isomers of $[(\text{H})\text{Fe}_2(\mu\text{-pdt})(\text{CO})_4(\text{PMe}_3)_2]^+$. Energies are relative to 2D	77
4.1	Comparison of the relative stabilities between $[\text{Et}_2\text{OH}]^+$ and $[\text{CH}_3\text{CNH}]^+$ calculated at the B3LYP/6-31++G** level of theory $\Delta G_{\text{sol}v}(\text{H}^+) = 260.2$ kcal/mol = -0.41465 Hartree.	85
4.2	Free energy comparison between the pdt, edt and odt dithiolate bridge in the isomerisation pathways from kinetic products 3C2' leading to the thermodynamic product 2D . Energies are reported in kcal/mol.	89
4.3	Comparison of the calculated gas phase and solvent corrected free energies and iron Mulliken charges of the TS _{6Bba→6HBba} for pdt, edt and odt dithiolate bridges.	89
4.4	Comparison of selected bond distances of the TS _{6Bba→6HBba} for pdt, edt and odt dithiolate bridges.	91
4.5	Comparison of selected bond angles of the TS _{6Bba→6HBba} for pdt, edt and odt dithiolate bridges.	91
4.6	Comparison of the calculated gas phase and solvent corrected free energies and Fe Mulliken charges of the TS _{8Cba→8HCba} for pdt, edt and odt dithiolate bridges.	105
4.7	Free energy comparison between the pdt, edt and odt dithiolate bridge in the isomerisation pathways from kinetic products 3C2' leading to the thermodynamic product 2D . Energies are reported in kcal/mol.	112
4.8	Free energy comparison between the pdt, edt and odt dithiolate bridge in the isomerisation pathways from one of the kinetic products leading to the thermodynamic product 2D . Energies are reported in kcal/mol.	114
4.9	Free energy comparison between the pdt, edt and odt dithiolate bridge in the isomerisation pathways leading from kinetic products 3D2 and 3A2' to the thermodynamic product, 2D . Energies are reported in kcal/mol.	116
4.10	Free energy comparison between the pdt, edt and odt dithiolate bridge in the isomerisation pathways from kinetic products 3C2' leading to the thermodynamic product 2D . Energies are reported in kcal/mol.	119

5.1	DFT simulated $\nu(\text{CO})$ bands of singly reduced bridging hydride isomers of $[(\mu\text{-H})\text{Fe}_2(\mu\text{-pdt})(\text{CO})_4(\text{PMe}_3)_2]$ compared to those experimentally determined in CH_3CN [67, 137].	128
5.2	DFT simulated $\nu(\text{CO})$ bands of singly reduced bridging hydride isomers of $[(\mu\text{-H})\text{Fe}_2(\mu\text{-edt})(\text{CO})_4(\text{PMe}_3)_2]$ compared to those experimentally determined in CH_3CN [67].	128
5.3	DFT simulated $\nu(\text{CO})$ bands of doubly reduced bridging hydride isomers of $[(\mu\text{-H})\text{Fe}_2(\mu\text{-pdt})(\text{CO})_4(\text{PMe}_3)_2]^-$ compared to those experimentally determined in CH_3CN [137].	128
5.4	DFT simulated $\nu(\text{CO})$ bands of singly reduced terminal hydride isomers of $[(\text{H})\text{Fe}_2(\mu\text{-pdt})(\text{CO})_4(\text{PMe}_3)_2]$ compared to those experimentally determined in CH_3CN [67].	129
5.5	DFT simulated $\nu(\text{CO})$ bands of singly reduced terminal hydride isomers of $[(\text{H})\text{Fe}_2(\mu\text{-edt})(\text{CO})_4(\text{PMe}_3)_2]$ compared to those experimentally determined in CH_3CN [137].	130
5.6	Relative stabilities of the isomers of the $[\text{Fe}_2(\mu\text{-pdt})(\text{CO})_4(\text{CN})_2]^{2-}$ model complex.	136
5.7	Calculated muon-electron hyperfine coupling constants, $A_{e\mu}$, and associated resonance fields of the $[\text{MuFe}_2(\mu\text{-pdt})(\text{CO})_4(\text{CN})_2]^{2-}$ model complex.	140
5.8	Calculated muon-electron hyperfine coupling constants, $A_{e\mu}$, and associated resonance fields of the $[\text{MuFe}_2(\mu\text{-pdt})(\text{CO})_4(\text{PMe}_3)_2]$ model complex.	143
6.1	Assignment of experimental infrared, Raman, and NIS vibrational modes based on comparison with DFT calculations. ^a Peak masked by neighbouring E mode at 434 cm^{-1}	157
7.1	Experimental TF- μSR and ALC- μSR data at 290 K used for the Monte-Carlo simulation of the exchange process.	169
7.2	Results from geometry optimisations showing the binding energies for the formation of the two radical species, C-Mu bond distances and $A_{\mu e}$	170
7.3	Averaged hyperfine couplings and resonance positions for centrally and terminally muoniated radicals. Atom labels correspond to those presented in Figure 7.16.	179

Publications arising from this work

- (1) P. J. Turrell, J. A. Wright, J. N. T. Peck, V. S. Oganessian and C. J. Pickett, 'The Third Hydrogenase: A Ferracyclic Carbamoyl with Close Structural Analogy to the Active Site of Hmd', *Angew. Chem. Int. Ed.*, 2010, **49**, 7508–7511, DOI: 10.1002/anie.201004189.
- (2) C. Liu, J. N. T. Peck, J. A. Wright, C. J. Pickett and M. B. Hall, 'Density Functional Calculations on Protonation of the [FeFe]-Hydrogenase Model Complex $\text{Fe}_2(\mu\text{-pdt})(\text{CO})_4(\text{PMe}_3)_2$ and Subsequent Isomerization Pathways', *Eur. J. Inorg. Chem.*, 2011, 1080–1093, DOI: 10.1002/ejic.201001085.
- (3) A. Jablonskyte et al., 'Paramagnetic Bridging Hydrides of Relevance to Catalytic Hydrogen Evolution at Metallosulfur Centers', *J. Am. Chem. Soc.*, 2011, **133**, 18606–18609, DOI: 10.1021/ja2087536.
- (4) U. A. Jayasooriya et al., 'Nuclear inelastic scattering spectroscopy of tris(acetylacetonate)iron(III); a vibrational probe via the iron atom', *Chem. Phys. Lett.*, DOI: 10.1016/j.cpllett.2011.10.063.
- (5) J. N. T. Peck, U. A. Jayasooriya, D. Steytler, V. S. Oganessian, R. Scheurmann and N. J. Clayden, 'Fast Molecular Transfer Through an Oil-Surfactant-Water Interface Measured by Muon Spectroscopy', *In Preparation*.
- (6) J. N. T. Peck, U. A. Jayasooriya, V. S. Oganessian, S. Cottrell, J. A. Wright and C. J. Pickett, 'Determining the Sites of Radical Addition in Artificial [FeFe]-Hydrogenases using Muon Spectroscopy', *In preparation*.

Chapter 1

Electronic structure theory

1.1 Introduction

Computational chemistry is a sub-branch of theoretical chemistry concerned with predicting the properties of atomic and molecular systems. It involves the application of the fundamental laws of quantum mechanics to predict structure, electronic charge distribution, dipoles and the higher multipole moments, vibrational frequencies and other spectroscopic quantities, interaction energies as well as elucidating unobserved phenomena such as chemical reaction pathways. It is widely used to complement and help explain experimentally observed phenomena and can assist in the development of new materials with specific chemical properties. The application of computational chemistry has become more widespread over recent years, this is partly due to the available software packages becoming more user friendly and a substantial increase in available computer power.

1.2 The Schrödinger equation

The energy and all other observable properties of an atom or molecule can be determined by knowledge of the coordinates of its component atoms. These properties can be obtained by the time-independent, non-relativistic Schrödinger equation:

$$\hat{H}|\Psi\rangle = E|\Psi\rangle \tag{1.1}$$

where \hat{H} represents the Hamiltonian operator, Ψ is a time-independent multi electron wavefunction, and E denotes the observable energy.

1.3 Born-Oppenheimer approximation

The general form of the Hamiltonian for a molecule consisting of M nuclei and N electrons is given by the sum of the contributions of kinetic and potential energy terms:

$$\hat{H} = \hat{T}_e + \hat{T}_n + \hat{V}_{ne} + \hat{V}_{ee} + \hat{V}_{nn} \quad (1.2)$$

where the first two terms, \hat{T}_e and \hat{T}_n refer to the kinetic energy operators of electrons (i and j) and nuclei (A and B), respectively. \hat{V}_{ne} is the nuclear-electron Coulomb interaction between electrons and nuclei. The last two terms, \hat{V}_{ee} and \hat{V}_{nn} are the Coulomb interactions between electrons and the nuclear-nuclear potential interactions, respectively. When expressed in atomic units, the Hamiltonian operator for a molecular system composed of N electrons and M nuclei is represented by:

$$\hat{H} = -\frac{1}{2} \sum_{i=1}^N \nabla_i^2 - \sum_{A=1}^M \frac{1}{2M_A} \nabla_A^2 - \sum_{i=1}^N \sum_{A=1}^M \frac{Z_A}{r_{iA}} + \sum_{i=1}^N \sum_{j>i}^N \frac{1}{r_{ij}} + \sum_{A=1}^M \sum_{B>A}^M \frac{Z_A Z_B}{R_{AB}} \quad (1.3)$$

where the operator ∇ is equivalent to the partial differentiation with respect to x , y and z :

$$\nabla_i^2 = \frac{\delta^2}{\delta x_i^2} + \frac{\delta^2}{\delta y_i^2} + \frac{\delta^2}{\delta z_i^2} \quad (1.4)$$

M_A is the ratio of the mass of nucleus A to the mass of an electron, Z_A is atomic number of nuclei A , $r_{iA} = |r_{iA} - R_A|$ and $r_{ij} = |r_i - r_j|$. The size of the Hamiltonian operator can be reduced in size by implementing the Born-Oppenheimer approximation to give the Hamiltonian in an electronic form:

$$\hat{H}_e = -\frac{1}{2} \sum_{i=1}^N \nabla_i^2 - \sum_{i=1}^N \sum_{A=1}^M \frac{Z_A}{r_{iA}} + \sum_{i=1}^N \sum_{j>i}^N \frac{1}{r_{ij}} \quad (1.5)$$

The Born-Oppenheimer approximation may be imposed based on the fact that protons are much heavier than electrons ($m_p \approx 1836 m_e$), meaning that they move much more

slowly. Therefore, the nuclei may be considered frozen in a single arrangement so the kinetic energy of the nucleus becomes zero and the repulsion can be treated as constant. The electrons respond instantaneously to changes in nuclear positions. The solution to the time-independent Schrödinger equation with the electronic Hamiltonian produces the electronic energy, E_e , and the electronic wave function, Ψ_e :

$$\hat{H}_e \Psi_e(X_1, X_2, \dots, X_N | R_1, R_2, \dots, R_M) = E_e \Psi_e(X_1, X_2, \dots, X_N | R_1, R_2, \dots, R_M) \quad (1.6)$$

where X_i and R_i represent the three spatial and spin degrees of freedom of the i^{th} electron and nucleus, respectively. Although the Schrödinger equation presented in (1.6) can be solved for the ground state and electronically excited states of small molecular systems, it is demanding from a computational perspective.

1.4 Hartree-Fock theory

An approximate electronic wave function for an atomic or molecular system can be constructed by its component atomic and molecular orbitals. Spin orbitals, $\chi_i(\mathbf{x}_i)$ are composed of a spacial orbital, $\phi(\bar{r})$ and a spin function, σ . There are two spin functions α (*spin up*) and β (*spin down*).

$$\chi(\vec{x}) = \phi(\vec{r})\sigma \quad (1.7)$$

The spin orbitals are assumed to form an orthonormal basis:

$$\langle \Psi_i(\vec{r}) | \Psi_j(\vec{r}) \rangle = \delta_{ij} \quad (1.8)$$

where δ_{ij} is the Kronecker delta function which equals 1 for $i = j$ and 0 otherwise. The spin functions are orthonormal, i.e., $\langle \alpha | \beta \rangle = \langle \beta | \alpha \rangle = 0$ and $\langle \alpha | \alpha \rangle = \langle \beta | \beta \rangle = 1$. The Pauli exclusion principle forbids any two electrons from occupying the same spin orbital. Additionally, the wave functions for a multi-electron system must satisfy the antisymmetry principle; an N -electron wave function must be totally antisymmetric with respect

to the interchange of electrons. The Slater determinant respects the antisymmetric nature of the electronic wave function and is composed of an antisymmetrised product of N one-electron wave functions:

$$\Psi_{SD}(\vec{x}_1, \vec{x}_2, \dots, \vec{x}_N) = \frac{1}{\sqrt{N!}} \begin{vmatrix} \chi_1(\vec{x}_1) & \chi_2(\vec{x}_1) & \cdots & \chi_N(\vec{x}_1) \\ \chi_1(\vec{x}_2) & \chi_2(\vec{x}_2) & \cdots & \chi_N(\vec{x}_2) \\ \vdots & \vdots & \ddots & \vdots \\ \chi_1(\vec{x}_N) & \chi_2(\vec{x}_N) & \cdots & \chi_N(\vec{x}_N) \end{vmatrix} \quad (1.9)$$

The coefficient $\frac{1}{\sqrt{N!}}$ is a normalisation factor. The shorthand of the above equation takes only diagonal elements of the matrix:

$$\Psi_{SD} = \frac{1}{\sqrt{N!}} \det \{ \chi_1(\vec{x}_1) \chi_2(\vec{x}_2) \dots, \chi_N(\vec{x}_N) \} \quad (1.10)$$

The basic idea behind the Hartree-Fock (HF) theory is that the motion of each electron of a molecular system resides in an orbital, and experiences an average potential produced by other electrons [1, 2]. In order to find the best Slater determinant, i.e. the Slater determinant that produces the lowest energy, the Variational principle is implemented [3, 4]. The variational principle provides the starting point for finding an approximate solution to the Schrödinger equation. It simply states that the energy calculated using an approximate trial wave function is always greater than the true energy of the system, E_0 :

$$\frac{\langle \Psi_{trial} | \hat{H} | \Psi_{trial} \rangle}{\langle \Psi_{trial} | \Psi_{trial} \rangle} = E_{trial} \geq E_0 = \frac{\langle \Psi_0 | \hat{H} | \Psi_0 \rangle}{\langle \Psi_0 | \Psi_0 \rangle} \quad (1.11)$$

When comparing different trial wave functions, the one that generates the lowest energy is a better approximation for the true wave function.

$$\hat{f}_i \chi_i = \varepsilon_i \chi_i \quad (1.12)$$

The Fock operator, \hat{f} for each electron is expressed as:

$$\hat{f}_i = -\frac{1}{2} \nabla_i^2 - \sum_{A=1}^M \frac{Z_A}{r_{ij}} + V_{HF}(\vec{x}_i) \quad (1.13)$$

where the first two terms are the kinetic and potential energy arising from the attraction of the electron and nucleus. The third term, V_{HF} is the HF potential and has two components:

$$V_{HF}(\vec{x}_1) = \sum_j^N (\hat{J}(\vec{x}_1) - \hat{K}_j(\vec{x}_1)) \quad (1.14)$$

The first of which is the Coulomb operator, \hat{J} , defined by:

$$\hat{J}_j(\vec{x}_1) = \int |\chi_j(\vec{x}_2)|^2 \frac{1}{r_{12}} d\vec{x}_2 \quad (1.15)$$

In the above equation ((1.15)) $|\chi_j(\vec{x}_2)|^2 d\vec{x}_2$ represents the probability of finding the electron in $d\vec{x}_2$. Thus, the Coulomb operator represents the average potential that an electron at position \vec{x}_1 experiences as a result of an electron in spin orbital χ_j . The second term in (1.14) is the exchange operator, \hat{K} :

$$\hat{K}_j(\vec{x}_1)\chi_i(\vec{x}_1) = \int \chi_j^* \frac{1}{r_{12}} \chi_i(\vec{x}_2) d\vec{x}_2 \chi_j(\vec{x}_1) \quad (1.16)$$

We now have all that is needed to solve the HF equations. The Fockian operator treats the single electron orbitals of the multi-electron wave function (1.12) in the same way that the Hamiltonian operator treats the Slater determinant. Initially, a set of guessed one electron orbitals are diagonalised to produce an improved set of one electron orbitals and associated energies. These are pumped back in to solve the HF equations again. This process is repeated until the changes in energy between iterations are less than the given threshold and are said to be converged.

1.5 Basis sets

1.5.1 Slater and Gaussian type orbitals

A basis set is a set of functions used to describe the orbitals within a system, they provide the foundation of a theoretical calculation. There are two main types of basis functions, Slater type orbitals (STOs) [5] and Gaussian type orbitals (GTOs) [6]. STO take the gen-

eral form:

$$\Psi_{STO}(r) = r^L e^{-\zeta r} \quad (1.17)$$

where L denotes the angular momentum quantum number of the orbital and ζ represents the spacial extent of the orbital. Although STOs represent orbitals accurately in close proximity to the nucleus and far away, they are problematic and time consuming to integrate. As a result of this, they are more commonly used on atomic and diatomic systems that require a high level of accuracy [7]. GTOs are more commonly used for larger molecular systems. The shape of the STO can be approximated with either a single GTO (referred to as *uncontracted*) or as a linear combination of Gaussian functions (referred to as *contracted functions*), where the component Gaussian functions are termed *primitives*. Cartesian Gaussian functions can be expressed as:

$$\begin{aligned} \Psi_{GTO}(r) &= x^l y^n z^m e^{-\alpha r^2} \\ \Psi_{STO}(r) &= \sum_i C_i \Psi_{GTO}^i(r) \end{aligned} \quad (1.18)$$

where x , y and z are Cartesian coordinates. The l , n and m are the angular momentum, principle and magnetic quantum numbers, respectively. α provides a definition of the spacial extent of the orbital. The sum of l , n and m determines the nature of the orbital. For example, when $l + n + m = 0$, Ψ -*GTO* represents an *s*-orbital; when having a value of 1, Ψ -*GTO* represents a *p*-orbital; and so on.

GTOs are inferior to STOs because of their r^2 dependence in the exponential. Unlike STOs, Gaussian functions prove problematic in representing the orbital close to the nucleus because they have no cusp in this region. Additionally, GTOs do not fall away in the correct manner far from the nucleus compared to STOs. However, GTOs are much simpler to integrate and have the additional benefit of being added together more easily.

1.5.2 Basis set classification

Basis sets differ in the number of component functions used. The *minimal basis set* employs a single Slater function or its Gaussian counterpart for each occupied atomic orbital in the ground state. For example, hydrogen would be described by a single *s*-function and carbon would be described by two *s*-functions and a set of 3 *p*-functions. The most popular *minimum basis set* is the STO-*n*G, where *n* is the number of Gaussian functions. The STO-3G is a *single zeta* (SZ) basis set, it implements three primitives per function. The valence orbitals play a greater role in chemical bonding than core orbitals, as such a more sophisticated basis set is required in order to better model valence orbitals. Basis sets can be improved by increasing the number of basis functions per atom. Split valence basis sets do just this, and can be expressed as *a-bcdG*, where *a* represents the number of primitives used for inner shells and *bcd* are the number of primitives used in the valence shell. Doubling, tripling or quadrupling all the basis functions gives *double zeta* (DZ), *triple zeta* (TZ) and *quadruple zeta* (QZ), respectively. A popular example is 6-31G, a DZ basis set. Here, the core orbitals are described by six primitive GTO and the valence orbitals are represented by two functions, with the first composed of three primitive GTOs, while the second consists of a single GTO.

Split valence basis sets can be further improved through the addition of polarisation and diffuse functions. Polarisation functions have higher values of angular momentum than those present on a particular orbital on an atom in the ground state. For example, the *p*-orbital introduces polarisation to the *s*-orbital, and the *d*-orbital adds polarisations to the *p*-orbital. This polarisation allows the shape orbital to be modified so as to better cover a bonding region between two atoms. The molecular orbitals (MOs) of anions and excited states have a tendency to be more spatially diffuse than ground state MOs. To account for this, basis sets are augmented with diffuse functions which essentially increase the size of the orbital.

To accurately describe an orbital would require an infinite number of basis functions. Sadly, the number of functions present within a basis set is limited. There will therefore

be a level of error in the description of the orbital, this is referred to as the Basis Set Limit.

As the number of electrons in a system increases, so does the computational expense. Transition metals and elements from the lower end of the Periodic Table have a large number of core electrons, requiring a large number of basis functions to describe them. Chemically, these electrons are deemed as unimportant, since it is the valence electrons that are involved in bonding. However, if core electrons are excluded, the valence electrons would be inadequately described due to a poor description of electron–electron repulsion. In order to remedy this, the valence electrons can be treated explicitly and the core electrons may be replaced by an analytical function known as an effective core potential (ECP) [8, 9]. From a computational perspective this is a much more efficient approach, and is common practice in modelling systems involving heavier elements.

1.6 Correlation energy

The quality of the predicted properties is observed to increase by increasing the number and type of basis functions. At a certain point however, the HF energy reaches a minimum value, termed the HF limit. However, at this point, the addition of extra basis functions does not improve the wave function. As a result, the calculated energy of a given system is always greater than the true energy and the difference is referred to as the correlation energy [10]:

$$E_{corr} = E_{exact} - E_{HFlimit} \quad (1.19)$$

This difference in energy arises because the HF method treats electron-electron interactions using a mean-field of the other electrons, and therefore provides an inaccurate description of how electrons influence other electrons. The wave function derived from the Slater determinant only includes exchange correlation. In a real atomic or molecular system, the motions of electrons are not independent, and avoid each other. Even with an infinite basis set, the HF method cannot account for this. Therefore, the predicted energy

of a system can be significantly improved through the addition of electron correlation. There are several commonly used electron correlation techniques referred to as post-HF methods.

Similarly to the HF method, configuration interaction (CI) is based on the variational principle in that the trial wave function is composed of a linear combination of Slater determinants. The expansion coefficients used in the linear combination are chosen by ensuring that the energy is at a minimum [11]. The HF wave function is taken as a starting point and additional determinants are included through the excitation of electrons from occupied orbitals into unoccupied orbitals:

$$\Psi_{CI} = c_0\Psi_{HF} + \sum_S c_S\Psi_S + \sum_D c_D\Psi_D + \sum_T c_T\Psi_T + \dots \quad (1.20)$$

The number of excitations used to construct each determinant serves as a classification to the CI calculation. A single-excitation (CIS) calculation involves only the promotion of one electron for each determinant. Where two electrons are promoted for each determinant, the calculation is referred to as a single-and-double excitation (CISD) calculation. If all possible excitations are considered, the calculation is termed a full CI.

Perturbation theory is another method for obtaining the correlation energy, with Moeller-Plesset perturbation theory being the most commonly used technique. At the heart of perturbation methods is the idea that the true wave function is very similar to the wave function already solved by the Hartree-Fock method [12]. The basic principle is to add a small perturbation to a zero-order Hamiltonian. The technique is non-variational and in some cases the calculation predicts that the total energy is below that of the true total energy.

Notably, methods for accounting for electron correlation can increase the computational expense of the calculation significantly, making them viable for use on only small molecules. Electron correlation can be accounted for in a far more elegant manner through the use of Density Functional Theory (DFT).

1.7 Density functional theory

The field of DFT is based on two theorems proved by Hohenberg and Kohn and a set of equations derived by Kohn and Sham in 1960s [13, 14]. The theorems state that molecular systems can be described by their electron density, $\rho(\mathbf{r})$ and, consequently, all properties of the ground state are functionals of $\rho(\mathbf{r})$. This has profound implications, as it reduces the problem of calculating the electronic wavefunction in $3N$ dimensional space (as in the HF, CI and perturbation theory calculations) to calculating the electron density in 3 dimensional space with a single set of coordinates. For this reason, DFT is able to accurately predict the total energy of molecular system with a similar computational expense to a HF calculation.

The Kohn-Sham Hamiltonian can be expressed as:

$$\hat{H}_{KS} = -\frac{1}{2}\nabla^2 + v_H + v_{XC} + v_{ext} \quad (1.21)$$

where $-\frac{1}{2}\nabla^2$ and v_H are the kinetic energy and the electron-electron repulsion energy, respectively. The third term, v_{XC} is the exchange correlation energy and v_{ext} is the external potential.

1.8 The potential energy surface (PES)

Central to the concept of the PES is the invocation of the Born-Oppenheimer approximation. In the most simple terms, the PES is the relationship between the energy of a molecular system and its geometry. The PES has $3N - 6$ coordinate dimensions, where N is the number of atoms and is defined by the potential energy as a function of all atomic arrangements. It is from this perspective that geometry optimisation and transition state optimisation are best explained.

The concept of the PES is best illustrated by example, so consider the triatomic molecule ABC. If ABC is built in vector space atom by atom, and atom A is taken as the

point of origin. The position of atom B is defined by its distance from A with a bond length (r_1). Atom C can be specified either by its distance from B, (r_2) and A, (r_3), or by its distance from B and the angle between A–B–C, θ_1 (see Figure 1.1). Each structure of ABC represents a point on the PES, and can be defined by:

$$\mathbf{X} \equiv (x_A, y_A, z_A, x_B, y_B, z_B, x_C, y_C, z_C) \quad (1.22)$$

Distortion of either r_1 or θ_1 from their equilibrium positions will result an increase in potential energy. A plot of potential energy as a function of r_1 gives a one-dimensional PES, where the potential energy is at its minimum when r_1 is at its equilibrium distance, r_e (see Figure 2.10). Of course, in reality, molecules are not found residing at the bottom of the PES, and are instead found to occupy one or another vibrational energy level (this is described in more detail in 2.2). However, for the sake of this model these vibrational energy levels are ignored and the molecule is said to be resting on the PES [7]. While the harmonic oscillator model approximately describes the shape of the PES in close vicinity to r_e , a significant deviation from r_e is better described by the anharmonic oscillator model (see Figure 2.11). If now, r_2 is considered to vary in addition to r_1 , the result is a two-dimensional PES. Plotting the potential energy as a function of r_1 and r_2 produces a 3D graph (see Figure 1.2). In addition to r_1 and r_2 , angle θ_1 can bend from its equilibrium state. In order to plot all these variables as a function of energy would require a four-dimensional graph. Such a plot is not possible and the PES of molecule ABC is therefore referred to as a hypersurface.

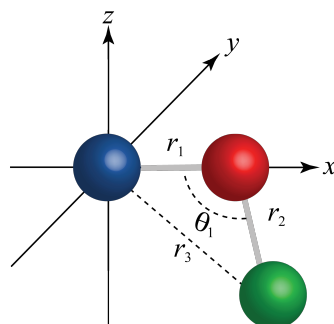


Figure 1.1: Specification of molecule ABC in Cartesian space.

1.8.1 Stationary points

Stationary points on the PES are of particular interest as they correspond to either global minima, local minima and saddle points (transition states or higher order saddle points). Finding the location of the global energy minimum is referred to as a geometry optimisation. Geometry optimisations require a starting structure, this needs to resemble the desired stationary point or the calculation could optimise to some other stationary point. If a crystal structure of the system of interest is available then it is common to use this. The calculation systematically changes the positions of all the component atoms until a stationary point is found. The PES around the stationary point is characterised as a minimum or as a saddle point by determining the second derivatives of energy as a function of atomic positions. Considering the H₂O molecule as an example. H₂O is in the C_{2v} point group, so its O–H bond lengths can be considered as equivalent. The PES of H₂O is therefore characterised by the O–H bond distance and H–O–H bond angle, this is shown in Figure 1.2.

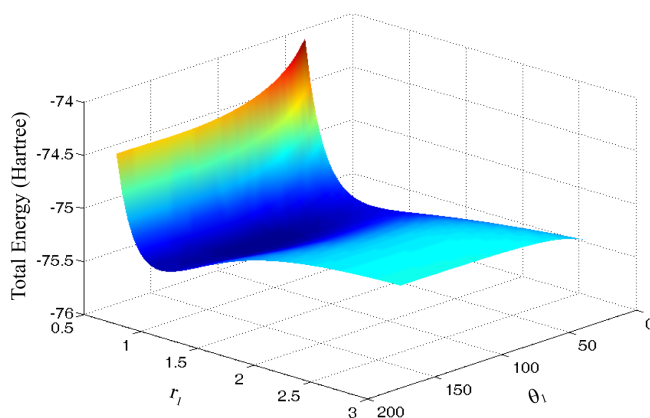


Figure 1.2: The potential energy surface of H₂O, characterised by variations in r_1 and θ_1 . Calculated at HF/3-21G level of theory.

In this particular example there is only one stationary point, which corresponds to the global minimum where $\frac{\partial E}{\partial r_1} = \frac{\partial E}{\partial \theta_1} = 0$. The starting structure can be described as being at a point $P(E_i, r_i)$ and the optimised structure as $P(E_0, r_0)$. Geometry optimisations are typically performed in Cartesian space where each atom of an N atom system has an x , y and z coordinate. This gives geometric parameters of $r_1, r_2, r_3, \dots, r_N$. In order to

find the equilibrium geometry, the first and second derivatives of E as a function of r_N are required [15]. This involves constructing a coordinate matrix corresponding to the starting structure:

$$\mathbf{r}_i = \begin{pmatrix} r_{i1} \\ r_{i2} \\ \vdots \\ r_{iN} \end{pmatrix} \quad (1.23)$$

The gradient matrix for the starting structure is expressed as:

$$\mathbf{g}_i = \begin{pmatrix} (\partial E / \partial r_1)_i \\ (\partial E / \partial r_2)_i \\ \vdots \\ (\partial E / \partial r_N)_i \end{pmatrix} \quad (1.24)$$

The second derivative matrix is a Hessian:

$$\mathbf{H} = \begin{pmatrix} \partial^2 E / \partial r_1 r_1 & \partial^2 E / \partial r_1 r_2 & \cdots & \partial^2 E / \partial r_1 r_N \\ \partial^2 E / \partial r_2 r_1 & \partial^2 E / \partial r_2 r_2 & \cdots & \partial^2 E / \partial r_2 r_N \\ \vdots & \vdots & & \vdots \\ \partial^2 E / \partial r_N r_1 & \partial^2 E / \partial r_N r_2 & \cdots & \partial^2 E / \partial r_N r_N \end{pmatrix} \quad (1.25)$$

The Hessian is of notable importance for the characterisation of all stationary points, and in the calculation of vibrational modes. The geometry optimised structure is expressed as:

$$\mathbf{r}_0 = \begin{pmatrix} r_{01} \\ r_{02} \\ \vdots \\ r_{0N} \end{pmatrix} \quad (1.26)$$

and can therefore be obtained through:

$$\mathbf{q}_0 = \mathbf{q}_i - \mathbf{H}^{-1} \cdot \mathbf{g}_i \quad (1.27)$$

This procedure is not strictly accurate, as the equilibrium structure is not found in one step. Instead, it is an iterative process where the matrix generated from equation (1.27) is fed back into equation (1.27) as a new starting structure. The process is continued until the change in energy is below a predetermined threshold.

The stationary point is confirmed as a minimum by calculating the vibrational frequencies. Vibrational frequencies are discussed in more detail in Chapter 2.2. As Figure 1.2 illustrates, the geometry optimisation of H₂O starting from any molecular configuration will result in the global minimum being found. Therefore, in order to illustrate the phenomena of local minima and saddle points, a larger molecular system is required.

The topic of investigation in Chapter 7 is a small organic molecule, the allyl alcohol radical, characterised by a potential energy hypersurface. Plotting the potential energy of the allyl alcohol radical as a function of H7–C1–C2–C3 and C1–C2–C3–O4 torsional angles produces the two-sliced PES displayed in Figure 1.3 (d). The plot shows nine stationary points as indicated by blue regions. Since H6, H7 and H11 are equivalent, the three energy minima labelled 1, 2 and 3 are equivalent. Therefore, if a starting geometry resembling that shown in Figure 1.3 (a) was used, the global minimum structure would be found. However, starting with a structure where the OH group is out of plane with respect to the molecular frame would result in a stationary point known as a local minimum. In order to differentiate between the global minimum and local minima, the energies would need to be compared.

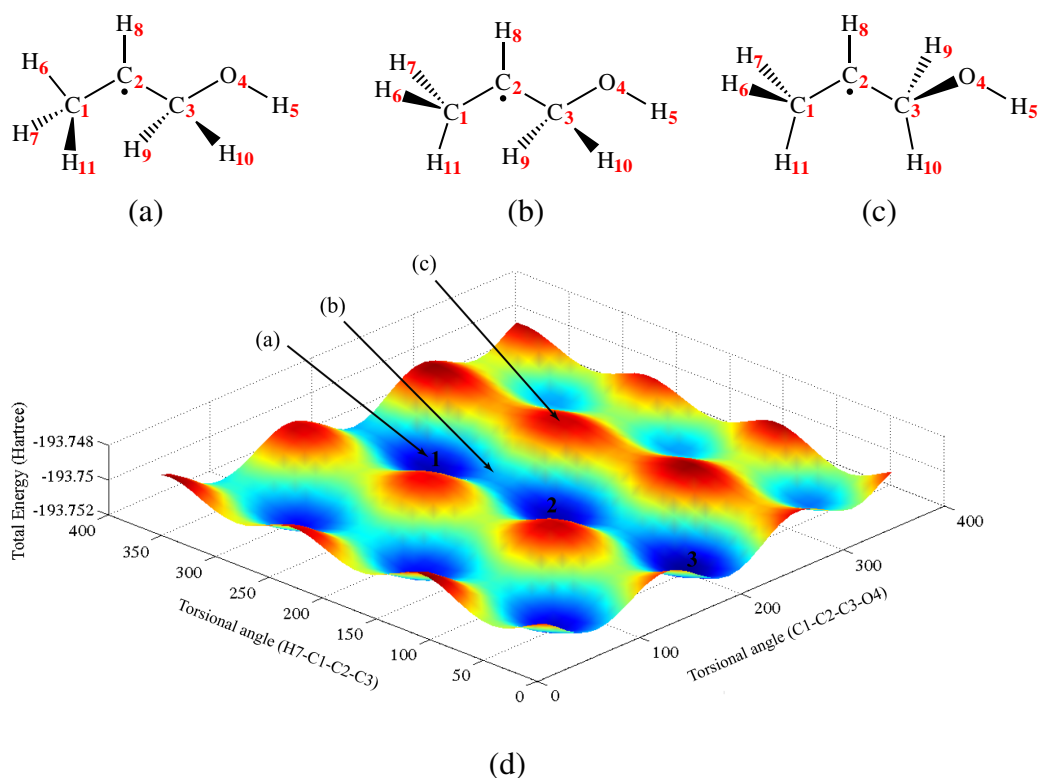


Figure 1.3: Schematics of the allyl alcohol radical corresponding to: (a), the minimum energy conformation; (b), a first-order saddle point from the torsional rotation of the H7–C1–C2–C3; and (c), a second-order saddle point. Atom labels are indicated in red. (d) shows two slices of the potential energy surface of an allyl alcohol radical, characterised by the variation in H7–C1–C2–C3 and C1–C2–C3–O4 torsional angles.

As well as locating energy minima, calculations also facilitate the characterisation of transition states on the PES. A transition state structure is a saddle point on the PES defined as having a zero derivative of energy for all but one reaction coordinate, where the energy is at its maximum. The allyl alcohol PES displayed in Figure 1.3 provides an example of a transition state. The two energy minima (1 and 2) with structures (a) are connected to each other by the transition state corresponding to structure (b). This could be confirmed through calculating the vibrational frequencies. If the structure is indeed a transition state it has a single negative Hessian eigenvalue. Structure (c) corresponds to a second-order saddle point, i.e., the second derivative of the energy with respect to two reaction coordinates. As well as characterising isomerisations, saddle points can also describe chemical reactions between two molecular fragments, which are looked at in more detail in Chapter 4. Access to useful information such as activation energy parameters is provided through the evaluation of a saddle points thermochemical properties.

For example, like the isomerising allyl alcohol radical, transition state structures can be guessed with relative ease and optimised directly. However, the PES describing some molecular systems or chemical reactions can be a little more complicated. This may be because the PES is relatively flat, with multiple energy minima around the product and reactant structures. In this case the structure corresponding to a saddle point is rather less obvious. In such cases it may be necessary to use other methods of finding the transition state, such as following the intrinsic reaction coordinate (IRC). When mass-weighted coordinates are used to describe the PES, the IRC is the shortest path joining the products and reactants. Notably, even if the transition state structure is known, it may be prudent to follow the IRC as the pathway leads to a better understanding of the nature of the saddle point. In many cases where the transition state structure is guessed, the structure that is found corresponds with some other process other than the one desired, and this is not obvious from merely visualising the imaginary frequency. Following the IRC in either direction leads to the product or reactant, in this way it is absolutely clear what the saddle point is connecting.

1.9 Solvation methods

Gas phase calculations are inappropriate for describing properties of molecular systems in solution such as the [FeFe]-hydrogenase model complexes reported in Chapters 3, 4 and 5. The local environment of a molecule can have a significant effect on properties, especially if the molecule is polarised. It has therefore become standard practice to include the effects of solvent when modelling chemical processes. The methods for dealing with the effects of solvent can be split in two; those which explicitly model individual solvent molecules and those that treat the solvent as a polarisable continuum [16, 17].

Calculations presented in this thesis where solvent is considered implement the continuum model, also referred to as Self-consistent Reaction Field (SCRF). In SCRF models the solvent is treated as a uniform polarisable with a dielectric constant, ϵ . The solute mo-

lecule is placed within a cavity of the medium. The dielectric medium has a constant value of ϵ , which is solvent dependant. In the calculations presented in the following chapters the solvent is always acetonitrile, where $\epsilon = 35.688$. The solvation free energy is described by:

$$\Delta G_{solvation} = \Delta G_{cavity} + \Delta G_{dispersion} + \Delta G_{electronic} \quad (1.28)$$

where ΔG_{cavity} is a destabilisation energy caused by creating the hole within the reaction field. $\Delta G_{dispersion}$ is a stabilisation energy roughly equivalent to the van der Waals interactions felt between the solute and solvent. $\Delta G_{electronic}$ is a stabilisation energy brought about by the charge distribution of the solute molecule. These induce charges in the dielectric medium, which impacts the electron density of the solute molecule. Several SCRF approaches have been developed that differ depending on the definition of the cavity size and shape. In the work presented in the following chapters, the Polarised Continuum Model (PCM) is exclusively applied to systems where solvent is considered. The PCM considers the cavity to be composed of a series of interlocking atomic spheres (Figure 1.4).

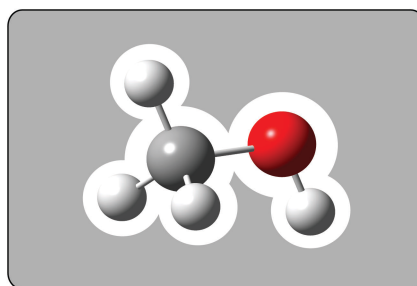


Figure 1.4: *Simplified schematic of the PCM model.*

1.10 Computational details

The calculations presented within this thesis were performed using the Gaussian 03 software package [18, 19]. The theoretical method and basis set used depend on the type and complexity of the system being investigated. A complete description of the computational details is given on a chapter by chapter basis.

Chapter 2

Experimental techniques

The experimental techniques applied to the chemical problems presented in this thesis are described hereafter: muon spectroscopy (μ SR), infrared spectroscopy (IR), Electron Paramagnetic Resonance spectroscopy (EPR) and Nuclear Inelastic Scattering (NIS). The high level of complementarity of these techniques when combined with DFT calculations is demonstrated in the proceeding chapters.

2.1 Principles of muon spectroscopy

μ SR is a less well known technique than the traditional spin-spectroscopic techniques such as Nuclear Magnetic Resonance (NMR), EPR and Mössbauer spectroscopy. The principles and their application have been reviewed on several occasions [20–24]. μ SR is a method of investigating the structure and dynamics of chemical systems in a way no other technique can. Once implanted into the sample the spin polarisation of the muon evolves according to the magnetic field (internal or applied) conveying information about the site it occupies through its decay positrons.

The muon is a fundamental particle belonging to the second generation of the lepton family. Table 2.1 compares some of its important physical properties with those of the electron and proton. Thus, it can be seen that the muon is analogous to either a heavy electron or a light proton. Because it has a spin of $\frac{1}{2}$, the muon can interact with and probe the local magnetic environment of its host species. In negative muon spectroscopy, the neg-

ative muon, μ^- can add to atomic nuclei by dislodging a lighter electron and occupying the 1s state where it is more sensitive to magnetic phenomena at the nucleus. The positive muon however, μ^+ , preferentially adds to areas of delocalised electron density in order to avoid the repulsive interaction with the nucleus and is a much more versatile probe than μ^- .

Table 2.1: Comparison of the properties of the muon, electron, and proton. Compiled from data within [26].

<i>property</i>	Muon (μ)	Electron (e)	Proton (p)
charge (q)	± 1	-1	+1
spin (s)	$\frac{1}{2}$	$\frac{1}{2}$	$\frac{1}{2}$
mass (m)	1.8835 x 10 ⁻²⁸ kg 207 m_e 0.1126 m_p 105.7 MeV	9.02094 x 10 ⁻³¹ kg m_e $m_p/1836.2$ 0.511 MeV	1.6726 x 10 ⁻²⁷ kg 1836 m_e m_p 938.27 MeV
magnetic moment (μ)	4.4904 x 10 ⁻²⁶ J T ⁻¹ 3.1833 μ_p	-928.48 x 10 ⁻²⁶ J T ⁻¹ -658.21 μ_p	1.4106 x 10 ⁻²⁶ J T ⁻¹ μ_p
gyromagnetic ratio, $\gamma/2\pi$	13.553 kHz G ⁻¹	2802.421 kHz G ⁻¹	4.258 kHz G ⁻¹
lifetime (τ)	2.197 x 10 ⁻⁶ s	>4 x 10 ²³ years	>2 x 10 ²⁶ years [25]

2.1.1 Muon production and decay

Muons are produced in a two-step process where a graphite or beryllium target is bombarded with high energy protons using a synchrotron. This high energy interaction between the incoming protons and the target protons or neutrons produces particles known as pions.



Pions can exist in two charge states, π^+ and π^- , and decay into positive and negative muons, respectively. Notably, negative pions and negative muons are not of any use in the context of the work presented in this thesis and so are not discussed any further. Pions

are transient particles which have an average lifetime of $\tau_\pi = 26.04$ ns, after which they decay into a muon, μ^+ , and muon neutrino, ν_μ .



At the time of decay on the target surface, the pion is in its resting frame. By considering that the pion is a spinless particle [21], the decay muon and neutrino must be emitted in opposite directions to conserve momentum and emitted with opposing spin vectors in order to conserve angular momentum. In addition to this, the neutrino possesses a negative helicity (neutrinos have spin vectors opposite to their momentum vectors). Therefore, by selecting only pions that stop in the target, the decay muons, known as surface muons always have their spin vector anti-parallel to their momentum. The result is $\sim 100\%$ spin polarised muons.

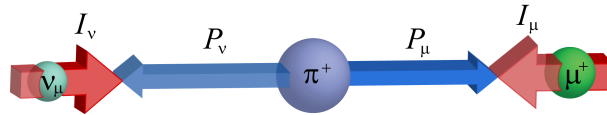


Figure 2.1: Decay of the positive pion in its resting frame, demonstrating muon spin polarisation. Where the blue arrows represent the momentum vectors, \mathbf{P} , and red arrows represent particle spin, \mathbf{I} . Adapted from [22].

The muon has a half-life, τ_μ , of $2.197 \mu\text{s}$ before decaying into a positron, e^+ , a neutrino, ν_e , and an anti-neutrino, $\bar{\nu}_\mu$.

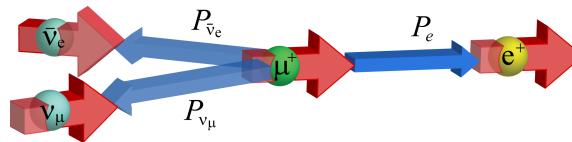


Figure 2.2: Decay of the positive muon into a positron, neutrino, and anti-neutrino. Where the blue arrows represent the momentum vectors, \mathbf{P} , and red arrows represent particle spin, \mathbf{I} . Adapted from [22]

2.1.2 Muons implanted in matter

Following their production, the $\sim 100\%$ spin polarised muons are directed towards the sample using steering magnets and collimators. These incident muons have a high energy (>4 MeV) and may be implanted into solid, liquid, or gaseous samples in a multi-step process, the radiolysis track. At each stage of the radiolysis track the muon loses energy, initially by ionising the atoms of the host material and scattering electrons. At lower energies, the muon can acquire an electron to form muonium (Mu), the muon usually undergoes several cycles of electron capture and electron loss. Muonium thermalisation is reached through collisions with atoms where it can dissociate to form a thermalised muon. The nature of the sample dictates the final chemical environment of the muon. In some cases the muons end up in the diamagnetic environment, μ^+ , these can either occupy an interstitial site in a solid sample and precess in its local magnetic field or they can react with the sample to produce a positively charged muonated species. Some muons retain the electron captured in the radiolysis track and exist as muonium. If the sample contains a centre of unsaturation the muonium can add to this to form a muoniated radical species, as shown in Figure 2.3. Once bound, the muon acts as a spin label. The similarity of the ionisation potential, Bohr radius, and reduced masses of muonium compared with protium, deuterium, and tritium justifies the claim for muonium being thought of as the lightest isotope of hydrogen (see Table 2.2).

Table 2.2: Comparison of the chemical properties of muonium, hydrogen, deuterium, and tritium.

<i>property</i>	Muonium (μ^+e^-)	Protium (p^+e^-)	Deuterium (d^+e^-)	Tritium (t^+e^-)
mass ($/m_H$)	0.1131	1.0000	1.998	2.993
reduced mass ($/m_e$)	0.9952	0.9995	0.9997	0.9998
ionisation potential ($/eV$)	13.539	13.598	13.601	13.602
bohr radius ($/pm$)	53.17	52.94	52.93	52.93
hyperfine coupling constant ($/GHz$)	4.463	1.420	0.218	1.516

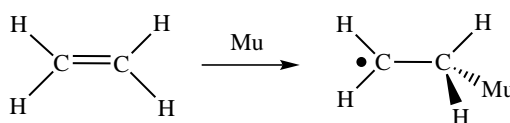


Figure 2.3: Muonium addition to ethene.

Although the muon was first discovered in cosmic rays by Carl Anderson and Seth

Neddermeyer in 1936 [27], the possibility of using muons as a magnetic probe only became viable after Garwin *et al.* observed the parity violation in the muon decay [28]. In this weak nuclear decay process, the positron is the only one of the three particles to be detected. The energy of the decay positron ranges from a value of 0 (when the neutrinos are emitted in opposite directions and the positron remains stationary) to a maximum, E_{max} , of 52.3 MeV (when the neutrinos are emitted in the same direction, but anti-parallel to the positrons momentum vector). The energy variation therefore depends on the momentum distribution of the three particles. It is this that leads to the tendency of the positron to be emitted preferentially in the direction of the muon spin at the instant of muon decay.

Upon implantation the muon polarisation is initially conserved, with its spin pointing in the direction from which it came. As soon as the muon experiences a foreign magnetic field, it begins to precess about it with a frequency, ω_μ which is proportional to the field:

$$\omega_\mu = \gamma_\mu B \tag{2.4}$$

where γ_μ is the gyromagnetic ratio of the muon ($\gamma_\mu = 2\pi \times 135.5 \text{ MHz T}^{-1}$). This foreign field may originate from an applied magnetic field or from a local magnetic field originating from the host material. With this born in mind, and knowing the time of implantation, it is possible to follow the muon spin evolution inside the host material. These types of experiments are known as time differential techniques. According to the theory of weak interaction, the probability of the positron being emitted at an angle θ is given by:

$$W(\theta) = 1 + a(\epsilon)\cos\theta \tag{2.5}$$

where θ is the angle between the spin of the muon and the direction of positron emission and a is an asymmetry factor. Figure 2.4 shows the angular distribution, $W(\theta)$, of positron emission. The highest energy positrons have an asymmetry factor close to 1, and are emitted anti-parallel to the neutrinos with spin aligned to that of the decaying muon. This situation is shown by the red curve in Figure 2.4. Lower energy positrons have a corresponding lower asymmetry factor, and in some rare cases they are negative in sign. In the reality of an experiment, a whole spectrum of positron energies are emitted

and when averaged, the asymmetry factor takes a value of $\sim \frac{1}{3}$. It is therefore possible to measure the spin evolution of a muon ensemble by measuring statistically significant number of decay positrons.

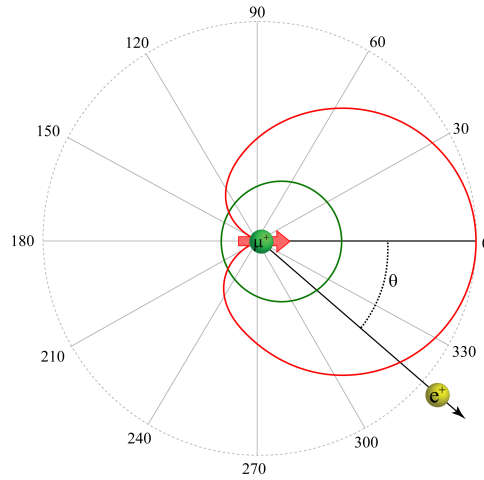


Figure 2.4: Angular distribution of the positron emission resulting from muon decay. The red curve represents the emission probability for maximum energy, $A = 1$. Averaging over the positrons energy spectrum gives the green curve, $A = \frac{1}{3}$. Adapted from [29].

2.1.3 Energy levels resulting from the interaction of spin $\frac{1}{2}$ particles

The experimental results presented in the following chapters can be interpreted through the energy levels arising from the hyperfine coupling between spin $\frac{1}{2}$ particles; the muon, the unpaired electron and protons. These particles possess a z -component of spin, m_I , of $\pm \frac{1}{2}$. The magnitude of the z -component of the magnetic moment, μ_z , is represented by:

$$\mu_z = \frac{\pm \frac{1}{2} \gamma h}{2\pi} \quad (2.6)$$

where h is Planck's constant. In an applied magnetic field, B , each particle can have two orientations ($m_I = \pm \frac{1}{2}$). Their energy is given by the scalar product of vectors μ and B . So for a magnetic field applied along the z -axis, the energy is represented by:

$$\begin{aligned} E &= \mu_z \cdot B_z \\ &= \frac{\pm \frac{1}{2} \gamma B_z h}{2\pi} \\ &\equiv \pm \frac{1}{2} \gamma B_z \hbar \end{aligned} \quad (2.7)$$

The degeneracy of the energy levels is lifted by the application of a magnetic field (Figure 2.5). The particle spin tends to precess around the magnetic field with a frequency, ν , known as the Larmor frequency. With an applied field of 1 Tesla the Larmor frequency will induce a transition between the energy levels.

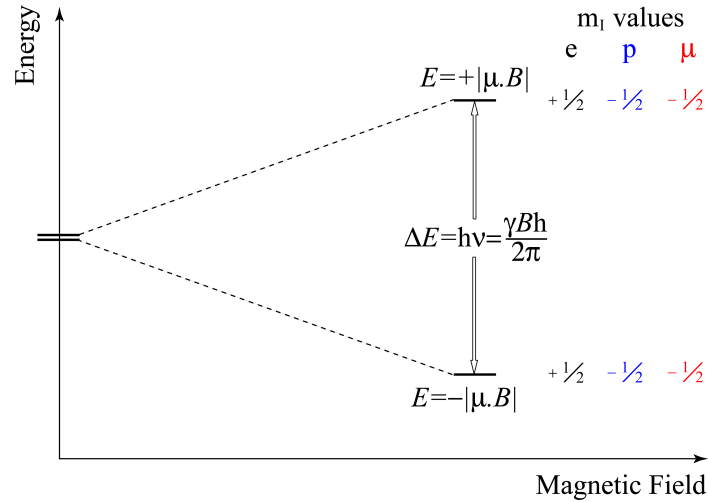


Figure 2.5: Energies of an electron, proton and muon as a function of magnetic field, \mathbf{B} . Adapted from [20].

If applying a magnetic field along the z -axis, the difference in energy between the two spin states is given by the Zeeman energy:

$$\begin{aligned} \Delta E &= -B_z \nu \left\{ \left\langle -\frac{1}{2} |\bar{I}_z| - \frac{1}{2} \right\rangle - \left\langle +\frac{1}{2} |\bar{I}_z| + \frac{1}{2} \right\rangle \right\} \\ &= \gamma \hbar B_z \end{aligned} \quad (2.8)$$

where ν is the Larmor frequency of the muon and \bar{I}_z is the z -component for spin angular momentum.

In the ground state, muonium may be described by a 1s hydrogenic like wavefunction. The unpaired electron spin, \mathbf{S} , couples with that of the muon, \mathbf{I} through the hyperfine, Fermi, or contact interaction, $\mathbf{A} \cdot \mathbf{I} \cdot \mathbf{S}$. This can be initially considered as isotropic in isolated muonium and provides a measure of electron density at the muon core. The Breit-Rabi diagram is commonly used to interpret μ SR investigations, the one displayed in Figure 2.6 plots the energy levels of muonium as a function of magnetic field. At zero field, muonium has two energy levels. The higher energy state is triply degenerate $\frac{1}{4}A$ state with a total

spin of 1 and z -components of +1, 0 and -1. The lower energy singly degenerate $-\frac{3}{4}A$ state has a total spin and z -component value of 0 [20].

Table 2.3: Energy levels and wavefunctions of a muon-electron spin system in zero field [20].

	Energy	M
E1	$+\frac{1}{4}A$	+1
E1	$+\frac{1}{4}A$	0
E1	$+\frac{1}{4}A$	-1
E2	$-\frac{3}{4}A$	0

The two energy levels are separated by an energy splitting equal to the hyperfine coupling, and when the electron is in the $1s$ atomic orbital this corresponds to a hyperfine coupling constant of $A=4.4633$ GHz. An externally applied magnetic field with z -component, B_z lifts the degeneracy of the $E1$ energy levels giving four energy levels (see Figure 2.6), as shown in Table 2.4.

Table 2.4: Energy levels and wavefunctions of a muon-electron spin system in a non-zero field [20].

	Energy	M_I
E1	$+\frac{1}{4}A - \frac{1}{2}B_z(\nu_\mu - \nu_e)$	+1
E2	$-\frac{1}{4}A + \frac{1}{2}((B_z(\nu_\mu + \nu_e))^2 + A^2)^{\frac{1}{2}}$	0
E3	$+\frac{1}{4}A + \frac{1}{2}B_z(\nu_\mu - \nu_e)$	-1
E4	$-\frac{1}{4}A - \frac{1}{2}((B_z(\nu_\mu + \nu_e))^2 + A^2)^{\frac{1}{2}}$	0

2.1.4 Sign of the hyperfine coupling constant

The sign of the hyperfine coupling constant can be derived from spin polarisation. The muon-electron hyperfine coupling constant is generally of a positive sign. Upon addition to an unsaturated bond, the muon spin is always parallel to the spin of the unpaired electron. For proton-electron hyperfine coupling constants, the sign can be negative. Taking the spin of the unpaired electron as a starting point, and considering Hund's rule which states that the spin of an adjacent electron is parallel, and the spin of an electron within an orbital is anti-parallel. Therefore, if the spin of the proton is parallel or anti-parallel to the unpaired electron, the sign of the hyperfine coupling is positive and negative, respectively.

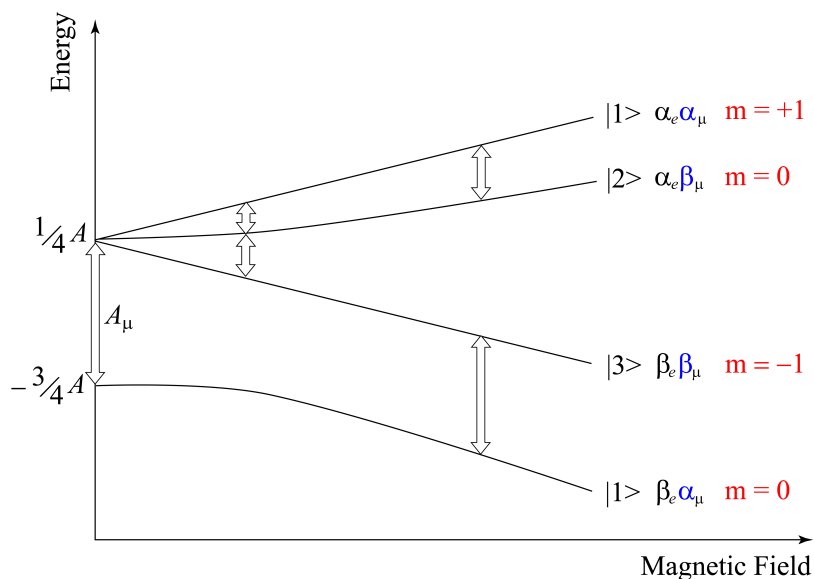


Figure 2.6: The Breit-Rabi diagram describing the energy levels of a muon-electron system as a function of magnetic field.

2.1.5 μ SR geometries

There are two techniques used for the characterisation of implanted muons, Transverse-Field Muon Spectroscopy (TF- μ SR) and Longitudinal-Field Muon Spectroscopy (LF- μ SR), of which the former and a variant of the latter, Avoided-Level Crossing Muon Spectroscopy (ALC- μ SR) will be discussed below. TF- μ SR is most readily used to measure the muon-electron hyperfine coupling and ALC- μ SR is used to measure nuclear hyperfine interactions. The two geometries differ in the relative orientation of the incident muon beam and the externally applied magnetic field.

Transverse field μ SR

TF- μ SR is a time differential technique that uses an external magnetic field applied perpendicular to the implanted muon spin polarisation. Figure 2.7 shows a schematic representation of a TF- μ SR spectrometer. Each muon that passes through the muon detector starts a fast electronic clock in preparation for the detection of a decay positron. The muon is subsequently implanted into the sample and it's spin precesses about the applied magnetic field, providing information about the magnetic environment of it's host through the hyperfine coupling. At the instant of decay, the positron is emitted preferentially in the direction of the muon spin. Positron detectors that are positioned around the plane

perpendicular to the applied field stop the electronic clock once the decay positron is detected.

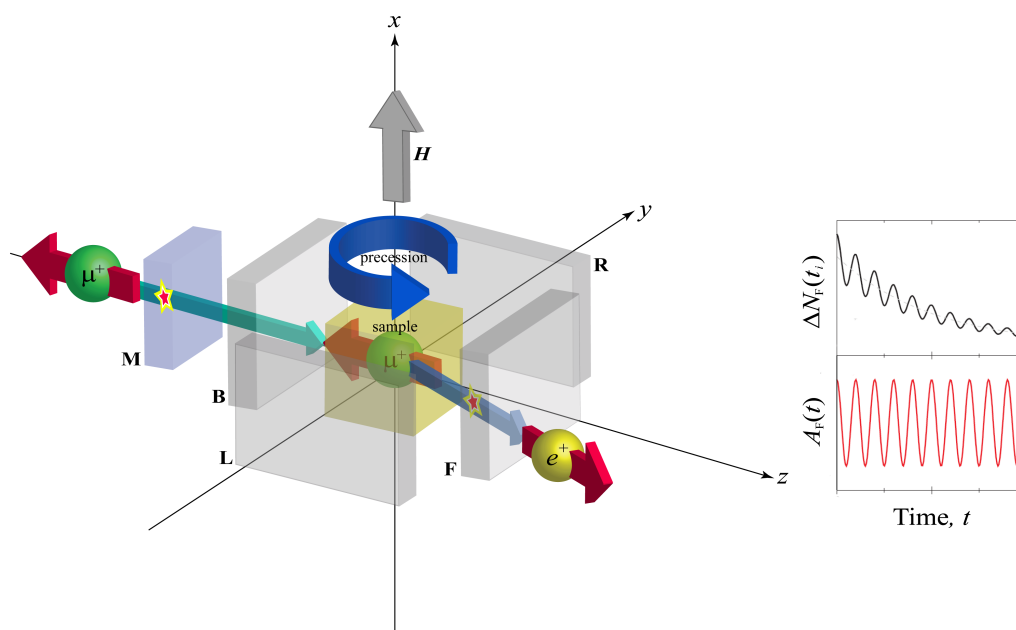


Figure 2.7: *Left: Schematic of the TF Muon spectrometer geometry. The muon beam arrives from the left with its spin (red arrow) anti-parallel to its momentum (blue arrow). The externally applied magnetic field, \mathbf{H} , is transverse to the muon spin direction. The sample is represented by a yellow cube and the grey boxes around the sample indicate the positions of the detectors; forward (\mathbf{F}), backward (\mathbf{B}), left (\mathbf{L}), and right (\mathbf{R}), which are defined by the direction of the incoming muon spin. Right: An example μ SR histogram and corresponding asymmetry of the forward detector in a transverse-field experiment. Scheme adapted from [29].*

Each positron detector records a μ SR histogram similar to the schematic displayed in Figure 2.7 right, and can be expressed by:

$$\Delta N_D(t_i) = e^{-\frac{t_i}{\tau_\mu}} \frac{\Delta t}{\tau_\mu} N_D (1 + A_D(t_i)) + B_D \quad (2.9)$$

where N_D is the total number of decay positrons detected by detector D, Δt is the width of the time bin, τ_μ is the muon lifetime, A_D is the detectors asymmetry factor and B_D is the background of the detector.

The magnetic moments of all the spins couple together resulting in numerous spin states. In zero/low magnetic fields, the muon polarisation is distributed between a multitude of spin states. Consequently, identification of the muoniated radical is inherently difficult. In higher magnetic fields the Zeeman energy dominates the hyperfine interac-

tions meaning the muon-electron hfcc is resolvable. Following Fourier transformation, the frequency spectrum is characterised by a strong diamagnetic peak resulting from μ^+ precessing at its Larmor frequency and eventually decaying in a diamagnetic environment. Additionally, a pair of resonances is symmetrically placed about the diamagnetic signal, the difference of which gives the muon-electron hyperfine coupling constant, $A_{\mu e}$ for the paramagnetic species.

$$\nu_R = \nu_d \pm \frac{1}{2}A_{\mu} \quad (2.10)$$

$A_{\mu e}$ provides a measure of the interaction between the muon and the unpaired electron.

Avoided level crossing μ SR

ALC- μ SR is a time-integral technique that investigates the energy levels of a spin system by investigating the time evolution of the muon spin polarisation. A schematic for an ALC- μ SR experiment is shown in Figure 2.8. In this type of experiment the $\sim 100\%$ spin polarised muon beam impinges the sample with spin parallel to the applied magnetic field. Here again, at the moment of implantation the muon spin is initially conserved, and as soon as it experiences the local magnetic field of the host material it begins to precess. The evolution of the muon spin is monitored as a function of time by two position detectors placed in the forward and backward directions relative to the muon momentum vector. This gives two histograms representing the muon spin polarisation along the axis defined by the forward and backward detectors.

$$\begin{aligned} N_B(t) &= N_0 \exp\left(-\frac{t}{\tau_{\mu}}\right) [1 + A_0 P(t)] \\ N_F(t) &= N_0 \exp\left(-\frac{t}{\tau_{\mu}}\right) [1 - A_0 P(t)] \end{aligned} \quad (2.11)$$

The forward-backward (FB) asymmetry function is given by the difference-and-sum ratio between the forward and backward histograms:

$$A_{FB} = \frac{N_B(t) - N_F(t)}{N_B(t) + N_F(t)} \quad (2.12)$$

Extending the Breit-Rabi diagram to higher magnetic fields (see Figure 2.9), sees the

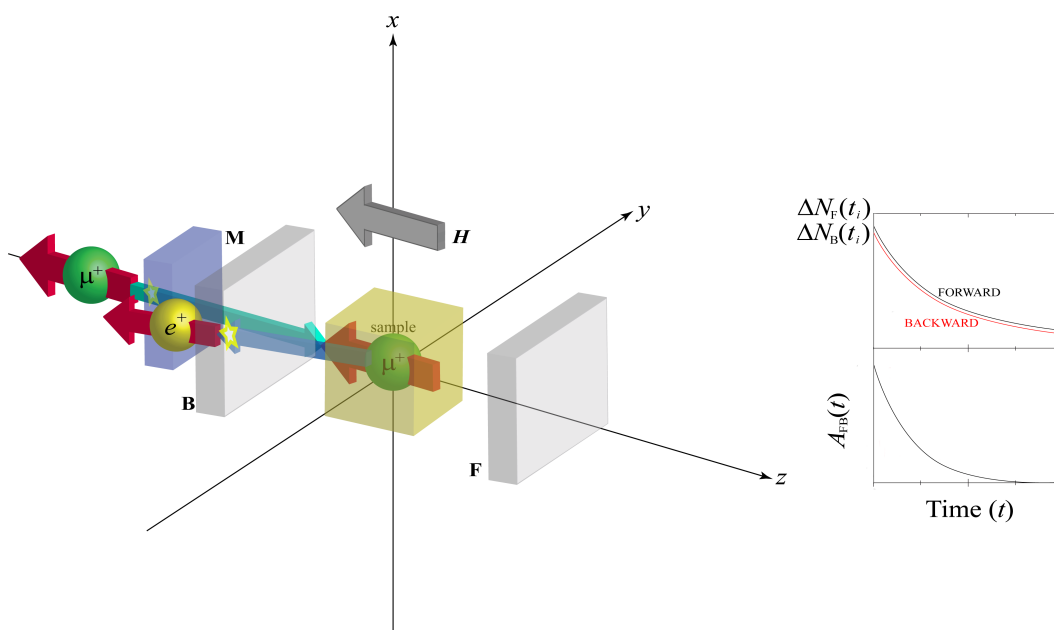


Figure 2.8: Schematic of the LF Muon spectrometer geometry. Scheme adapted from [29].

eigenstates of the muoniated radical becoming pure Zeeman states. In such a regime the asymmetry becomes independent of the applied magnetic field and there is no evolution of the muon spin with time. As the magnetic field increases, two energy levels become near degenerate and are mixed through the isotropic and anisotropic components of the hyperfine coupling. The spins oscillate between the two states resulting in a depolarisation of the muon spin, causing a resonance as the magnetic field is swept. The magnitude of the associated hyperfine interactions dictates the magnetic field at which the avoided-level crossing occurs. The field is given by [30]:

$$B_{res} = \left| \frac{A_{\mu e}(\theta, \psi) + (|\Delta M| - 1) [A_{ep}(\theta, \psi)]}{2 [\gamma_{\mu} + (|\Delta M| - 1) \gamma_p]} \right| \quad (2.13)$$

where $A_{\mu e}(\theta, \psi)$ and $A_{pe}(\theta, \psi)$ are the hyperfine coupling constants of the muon and proton, respectively and γ_{μ} and γ_p are the gyromagnetic ratios of the muon and proton, respectively.

The selection rule, $|\Delta M|=0, 1,$ and 2 dictates three types of resonance, where M denotes the sum of the quantum numbers for the z-components of the muon, electron, and nuclear spins. Δ_0 resonances allow a complete characterisation of radicals with known muon hyperfine coupling. They can occur in muoniated radicals formed in solids, liquids,

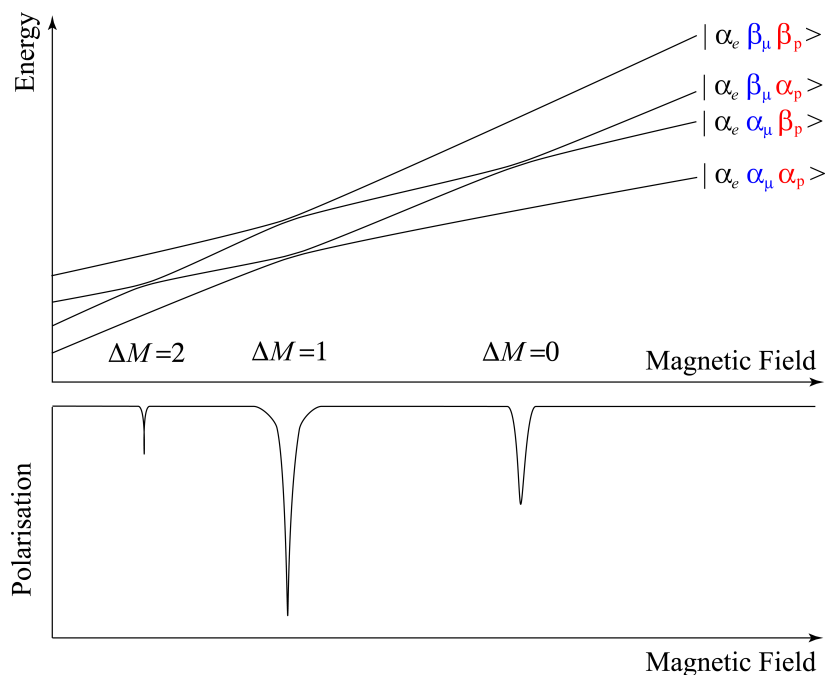


Figure 2.9: Breit-Rabi diagram at high magnetic field showing the energy levels of a three spin system; muon, μ^+ , electron, e^- , and proton, p^+ . The three types of avoided level crossings are shown, $\Delta M=0$, 1, and 2 which correspond to muon-proton spin flip-flop, muon spin flip, and muon-proton spin flip-flop, respectively.

and gases and arise from transitions between energy levels that have the same electron spin, but opposing muon and nuclear spins that are able to mix through the hyperfine interaction. They are thus termed muon-nuclear spin flip-flop transitions and occur at magnetic fields:

$$B_{res}(\Delta_0) = \frac{A_{e\mu} - A_{ep}}{2(\gamma_\mu - \gamma_p)} - \frac{A_{e\mu} + A_{ep}}{2\gamma_e} \quad (2.14)$$

Δ_1 resonances are due to the mixing of energy levels that have the same electron and nuclear spins, and opposite muon spin and so are termed muon spin flip transitions. The mixing of these energy levels is only possible in the presence of anisotropy, so are characteristic of anisotropic motion in a frozen state. The magnetic field at which a Δ_1 transition occurs may be calculated from:

$$B_{res}(\Delta_1) = \frac{A_{e\mu}}{2(\gamma_\mu)} - \frac{A_{e\mu}}{2\gamma_e} \quad (2.15)$$

The Δ_2 resonance is a muon-nuclear spin flip-flop transition. The crossing is only possible in the presence of anisotropy. It is a characteristically very weak and narrow signal and

as such is not typically observed.

The geometry and electronic structure of a radical species dictates the orientation of the principle axes of the hyperfine tensors, A_{μ} and A_p relative to each other. Additionally, at any given time the radical has a certain orientation with respect to the externally applied magnetic field, obviously with crystal samples this will remain constant. Single crystals with only one orientation are characterised by Lorentzian shape resonances at a field given by (2.13). In polycrystalline samples, a plethora of crystal orientations exist relative to the magnetic field. The observed resonances are characteristically asymmetric, made up of superpositioned single crystal Lorentzians, and the shapes of these powder patterns are determined by the symmetry of the hyperfine tensors.

2.2 Principles of infrared spectroscopy

The experimental IR spectra presented in Chapters 3 and 5 were recorded by either Dr. Joseph Wright or Ausra Jablonskyte of the Energy Materials Laboratory, UEA.

IR is a technique that uses electromagnetic radiation (EMR) to excite the vibrations of molecules in the sample. EMR consists of oscillating electric and magnetic fields propagating in a certain direction, at the same frequency, but perpendicular to each other. The velocity of propagation of all EMR is constant (in a vacuum) in every region of the spectrum, and has a value of $c=2.997\ 925 \times 10^8\text{m s}^{-1}$. It may be considered as either a propagating wave or as a stream of particles, photons or quanta. Taking the former point of view, the velocity of a wave is given by:

$$c = \lambda\nu \tag{2.16}$$

where λ is the wavelength (defined by the distance between two adjacent peaks) and ν is the frequency (the number of cycles per second). If viewed as a stream of photons, their

energy is given by:

$$E = h\nu \quad (2.17)$$

where $h=6.626 \times 10^{-34}$ J s is the Planck constant. The IR region of the EMR is divided into three sections, near-infrared (NIR), mid-infrared (MIR) and far-infrared (FIR). NIR has a wavenumber range of 14,000 to 4,000 cm^{-1} and can be used to excite harmonic and overtone vibrations. MIR has a range of 4,000 to 600 cm^{-1} which is able to excite the fundamental vibrations in molecules. It is routinely used for the characterisation of molecules in chemistry. FIR has a wavenumber range of 400 to 10 cm^{-1} and is able to excite lattice vibrations and also has applications in rotational spectroscopy.

The total energy of a molecule is defined by components of electronic, vibrational, rotational and translational energy:

$$E = E_{\text{electronic}} + E_{\text{vibrational}} + E_{\text{rotational}} + E_{\text{translational}} \quad (2.18)$$

where $E_{\text{electronic}}$ represents energy transitions of electrons into higher energy orbitals (typically the most energetic component, with UV wavelengths required); $E_{\text{vibrational}}$ corresponds to the energy that is absorbed by the molecule as its component atoms vibrate, $E_{\text{rotational}}$ is the observed oscillating motion of the molecule brought about through absorption of FIR to microwave radiation and $E_{\text{translational}}$ corresponds to the translational displacement of the molecules in space as a function of their thermal motions (this energy is typically small compared to the energy required for a vibrational transition).

The energy of a molecular system is quantised and the molecule can reside in discrete vibrational energy levels E_0, E_1, E_2 , etc. When the molecule interacts with IR radiation it is excited into a higher energy level if the energy matches the difference between the two levels. Therefore the frequency of an absorption for a transition between energy levels E_0

→ E_1 is given by:

$$\nu = \frac{E_1 - E_0}{h} \quad (2.19)$$

In the simplest case of a diatomic molecule, there are no bending modes, just a stretching mode causing the atoms to converge and separate. This may be modelled as a simple harmonic oscillator composed of 2 masses connected to each other by a spring. The energy curve for a simple harmonic oscillator is a simple parabola (see Figure 2.10). Hooke's law provides the relationship between the frequency of vibration to the two masses and force constant, k of the spring;

$$\nu = \frac{1}{2\pi c} \sqrt{\frac{k}{m}} \quad (2.20)$$

where m is the reduced mass which is defined by:

$$m = \frac{m_A \cdot m_B}{m_A + m_B} \quad (2.21)$$

where m_A and m_B are the masses of the atoms involved. The force constant in (2.20) is dependant on the strength of the chemical bond in A–B, resulting from electronic effects such as bond order. It therefore follows that larger force constants (stronger bond) and smaller reduced masses result in higher vibrational frequencies. However, vibrational motion is quantised, and as such must follow the rules of quantum mechanics. Therefore, transitions are only permitted when they follow;

$$E = \left(n + \frac{1}{2} \right) h\nu \quad (2.22)$$

where n is the quantum number and has allowed values of $n = 0, 1, 2, 3, \dots$. The energy of the lowest energy level is therefore given by $E_0 = \frac{1}{2}h\nu$ and the next energy level is $E_1 = \frac{3}{2}h\nu$. The selection rule stipulates that only transitions to the next highest energy level are allowed. This rule does not always hold true, and sometimes transitions of $2h\nu$ and $3h\nu$ are observed, appearing as overtones and combinations in the IR spectrum, because real systems are not strictly harmonic.

The harmonic oscillator is actually an insufficient model for diatomic molecules. A chemical bond can reach a critical point where the two atoms dissociate. The anharmonic model accounts for this, as the interatomic distances reach the point of dissociation the energy levels become more closely spaced (see Figure 2.11).

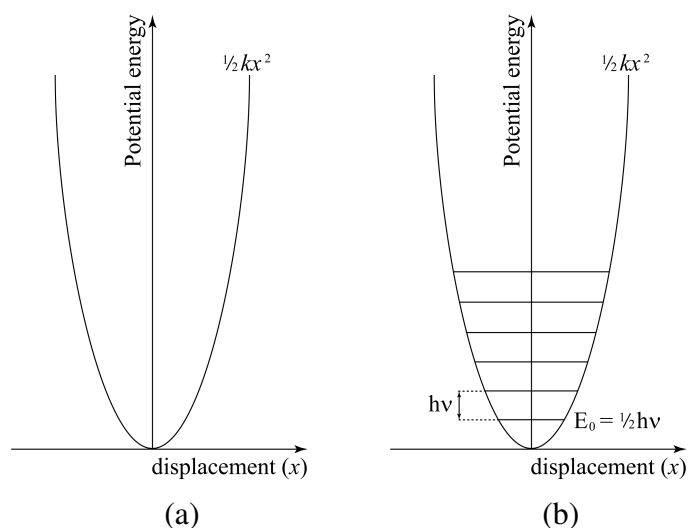


Figure 2.10: (a) Energy parabola for a vibrating spring and (b) energy parabola with quantised energy levels.

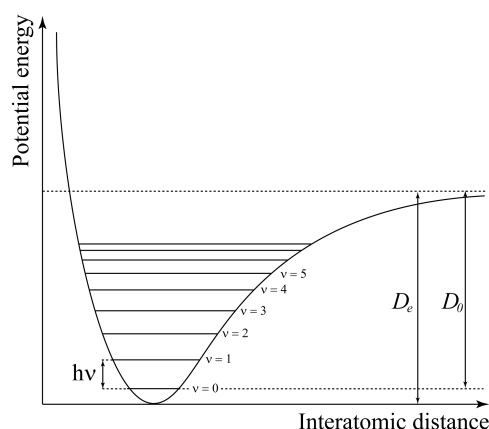


Figure 2.11: Morse potential energy curve for the anharmonic oscillator.

However, energy is not always absorbed when it matches the difference between two energy levels. As was mentioned previously, electromagnetic radiation has an associated oscillating electric field. If a vibration causes a change in molecular dipole moment, it can also be viewed as an oscillating electric field. In this manner oscillating electric fields

can interact. Therefore, in order for radiation to be absorbed, the vibration must cause a change in molecular dipole moment - the IR selection rule. The triatomic CO₂ provides one of the best examples of this with its symmetric stretch being IR inactive. Polyatomic molecules containing N atoms have $3N$ degrees of freedom (cartesian coordinates x, y, z), of which 3 of these are translational and if nonlinear 3 are rotational (2 if linear). Therefore, nonlinear polyatomic molecules have $3N-6$ fundamental modes of vibration while linear ones have $3N-5$. The vibrational frequency of each functional group within a molecule is unique.

The types of vibration fall under two main categories, stretching and bending. There are two varieties of stretch in polyatomic molecules, the symmetric and asymmetric stretch. There are four types of bending modes; rocking, scissoring, wagging and twisting.

The Beer-Lambert law is an empirical relationship between the absorbance, A , and the concentration, c , of the absorbing species:

$$\begin{aligned} A &= -\log_{10}\left(\frac{I}{I_0}\right) \\ &= \epsilon cL \end{aligned} \tag{2.23}$$

where I is the intensity of transmitted radiation, I_0 is the intensity of incident radiation and ϵ is the molar extinction coefficient.

2.3 Principles of electron paramagnetic resonance (EPR) spectroscopy

The EPR measurements presented in Chapter 5 were carried out at the John Innes Centre by Dr. Shirley Fairhurst.

EPR is a spectroscopic technique for investigating systems containing unpaired electrons. Similar to μ SR, the technique detects transitions between the energy levels of electron spins in the presence of an applied magnetic field. EPR has been most readily

applied to the investigation of organic and inorganic free radicals, transition metal complexes (containing Fe, Cu, Co, Ni, Mn) as well as reaction intermediates. Theoretical and experimental aspects of EPR have been comprehensively reviewed in a number of texts [31, 32].

The behaviour of the free electron is the basis behind the phenomenon of EPR. As well as having an associated magnetic moment, the negative charge of the unpaired electron is also spinning about its own axis giving rise to the electron spin angular moment, P_S , which can be expressed through;

$$P_S = \frac{h}{2\pi} \sqrt{S(S+1)} \quad (2.24)$$

where S is the spin quantum number and takes a value of $\frac{1}{2}$. The relationship between the electron magnetic moment and its spin angular moment can be represented by;

$$\begin{aligned} \mu_S &= -P_S \frac{e}{m} \\ &= M_S \frac{eh}{2\pi m} \end{aligned} \quad (2.25)$$

where M_S is the magnetic quantum number and takes a value of $\pm\frac{1}{2}$. The relationship between the magnetic and angular moments is called the gyromagnetic ratio, γ . Its components; orbital motion and spin motion are represented by $\gamma = -\frac{2}{2m}$ and $\gamma = -\frac{2}{m}$, respectively. The proportionality coefficient was introduced for cases where the contributions from spin and orbital motion differ, and is represented by;

$$\gamma = -g \frac{e}{2m} \quad (2.26)$$

where g represents the proportionality coefficient, also known as the g -factor. In zero-field, the electron's magnetic moment orientates randomly with respect to one another and their energy is degenerate. Under the influence of an externally applied magnetic field, the electron's magnetic moment become aligned with the field and the energy degeneracy is lifted to give two levels, $E_S = pm\frac{1}{2}$ (see Figure 2.5). The interaction energy between

the externally applied magnetic field H_o , and the electron is represented by;

$$\begin{aligned} E &= \mu_S H_o \\ &= \frac{1}{2} g_e \beta_e H_o \end{aligned} \quad (2.27)$$

where g_e is equal to 2.0023 and is a 2^{nd} rank tensor of g (g is a spectroscopic splitting factor) and β_e is the Bohr magneton. It therefore follows that the difference in energy between two levels, ΔE corresponds to:

$$\begin{aligned} \Delta E &= g_e \beta_e H_o \\ &= \hbar \omega \end{aligned} \quad (2.28)$$

where the Hamiltonian is given by:

$$\bar{H} = g_e \beta_e H_o \cdot S \quad (2.29)$$

When incident EMR is equivalent to the separation of the two energy levels, the system absorbs it. This is the origin of an EPR signal. The number of electrons in either energy level is determined by the Boltzmann distribution. The ratio of the number of electrons in the upper level, $N_{+\frac{1}{2}}$ and those in the lower level, $N_{-\frac{1}{2}}$ is represented by;

$$\begin{aligned} \frac{N_{+\frac{1}{2}}}{N_{-\frac{1}{2}}} &= e^{-\frac{\Delta E}{kT}} \\ &= e^{-\frac{g\beta_e H_o}{kT}} \end{aligned} \quad (2.30)$$

where k is the Boltzmann constant and T is the temperature. There are two mechanisms for radiation to induce an EPR signal; induced emission and resonant absorption. Induced emission occurs when electrons in the upper energy level interact with EMR and drop to the lower energy level, emitting a photon in the process. The process of resonant absorption occurs when electrons in the lower energy level absorb energy from the incident EMR and transfer it to the upper energy level. It follows from (2.30) that the population of the lower energy level exceeds the upper level. Thus, the process of resonant absorption will dominate.

The EPR spectrum is typically presented as the first derivative of the absorption spectrum (see Figure 2.12).

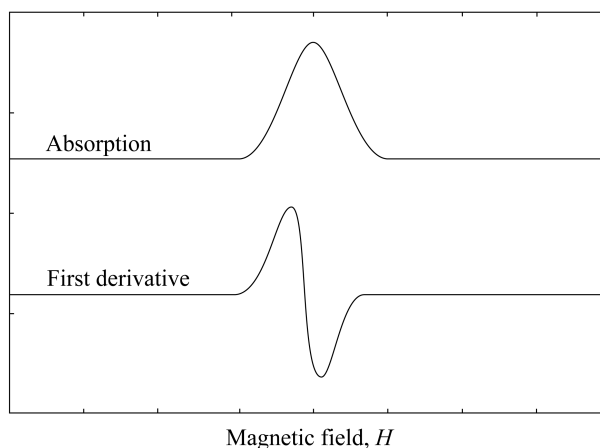


Figure 2.12: Example of the first derivative EPR spectrum.

The presence of neighbouring nuclei can result in the EPR signal being split into several lines, this occurs through the phenomenon of the hyperfine interaction. Nuclei possess an intrinsic spin, characterised by the nuclear angular momentum spin quantum number I . This gives rise to an observable magnetic moment:

$$\mu_N = g_N \beta_N I \quad (2.31)$$

where g_N is the nuclear g -factor and β_N is the nuclear Bohr magneton. In a paramagnetic species, the interaction of the unpaired electron density with a nucleus possessing nonzero I results in a small perturbation of the electron energy levels. This causes each energy level to split into sublevels. The perturbation adds an additional term to the spin Hamiltonian:

$$\hat{H} = \beta_e H_0 g_e S + A_i I_i S \quad (2.32)$$

There are two kinds of hyperfine coupling: coupling of the electron's magnetic moment to the magnetic moment of the nucleus of the atom to which the electron belongs; and superfine splitting where the electron couples to a nucleus of a neighbouring atom. In such cases the spectral line is split with intensities following Pascal's triangle.

2.4 Principles of nuclear inelastic scattering spectroscopy

The NIS spectrum reported in Chapter 6 was recorded by Dr. Vasily Oganessian and Dr. Upali Jayasooriya at ESRF in Grenoble. NIS spectra reported in Chapter 6 were simulated using a MATLAB program developed by Dr. Vasily Oganessian.

NIS can be used to measure the vibrational density of states (VSOS) in materials possessing a Mössbauer active atomic nucleus, i.e. ^{57}Fe . The technique of Mössbauer spectroscopy probes the rigidity of a materials atomic lattice by measuring the Lamb-Mössbauer factor (fLM), i.e. the recoilless fraction of resonant absorption of γ -rays by nuclei. The presence of lattice dynamics can be identified through measurement of the supplemental recoil fraction, $1-fLM$. NIS offers the ability to probe deeper than this single parameter, and in doing so providing valuable information on the energy spectrum of this recoil. Mössbauer spectroscopy provides an insight into the energy differences between the source and absorber, such as chemical shifts. Even the mechanical movement of the whole sample or the source is enough to provide a sufficient Doppler shift in the energy of the radiation to provide an energy match for absorption to occur. NIS harnesses this process in order to measure the rapid motion of a Mössbauer active atom in a normal mode of vibration. It is able to do this by tuning the energy of the source to match the much larger Doppler energy shifts needed by the motion of an absorbing atom. For example, the ^{57}Fe atom in a normal mode of vibration. Tunable energy with high resolution in the γ -ray region is typically provided by synchrotron radiation. There have been numerous reviews describing the theory and principles of the technique [33–40].

In the approximation of Einstein-like modes where there is no momentum dependence of vibrational frequency and polarisation vector and, under the condition of random distribution of molecules in powder, the so-called partial density of states (PDOS) is calculated according to equation (2.33)[33–40]:

$$D_{Fe}(\nu) = \frac{1}{3} \sum_{\alpha} e_{Fe,\alpha}^2 \cdot f(\nu - \nu_{\alpha}) \quad (2.33)$$

where $f(\nu-\nu_\alpha)$ is the line shape function, characterised by a convolution of Gaussian and Lorentzian functions. The composition factor, $e_{Fe,\alpha}^2$, for the resonant Mössbauer active atom in the normal mode α is given by:

$$e_{Fe,\alpha}^2 = \frac{(\Delta r_{Fe,\alpha})^2 m_{Fe}}{\sum_{k=1}^N (\Delta r_{k,\alpha})^2 m_k} \quad (2.34)$$

where $(\Delta r_{k,\alpha})^2$ is the mean square displacement of atom k in mode α . Summation in the denominator of this expression is taken over all atoms; m_k is the mass of the k^{th} atom.

Chapter 3

Protonation regiochemistry in



3.1 Introduction

As the demand for energy increases over the coming decades, providing a clean and renewable alternative to fossil fuels as an energy vector is crucial, not only for the protection of the world economy but more importantly for its ecology as well. In the long-term it is clear why H_2 is such a promising alternative. It has a high enthalpy of reaction with O_2 , gram for gram releasing more energy than any other fuel when burnt or oxidised in a fuel cell, producing only energy and pure water [41, 42].

Before hydrogen can become a viable alternative to fossil fuels, several key technological hurdles need to be overcome. One of the most important hurdles is finding a clean method of producing it. Despite hydrogen being the most abundant element in the universe [43], elemental hydrogen is scarcely available for use as an energy vector. Before it can be utilised, it has to be separated from the chemical compounds to which it is bound. The current methods for hydrogen production are based on fossil fuels and include hydrocarbon reforming, ammonia cracking, and the less common techniques of pyrolysis and aqueous phase reforming [44]. All these techniques are viewed as relatively energy inefficient and lead to the emission of significant quantities of undesired greenhouse gases [43]. They may however prove vital in providing a transitional method for producing hy-

drogen until more environmentally friendly means are developed, such as solar, wind, nuclear and wind power. The cleanest and most efficient method of converting the energy stored in H₂ into electrical energy is using fuel cells [45]. These are based on the reversible interconversion of protons and electrons, a process that requires catalysis to proceed reversibly at diffusion controlled rates and temperatures. Currently platinum is the preferred electrocatalyst used in hydrogen fuel cells. Unfortunately the supply of platinum is limited and its use is therefore unsustainable in the long term [45].

Di-iron and nickel-iron hydrogenase enzymes exist in nature and have evolved to either cleave dihydrogen for use as energy or to create it as a product of their energy metabolism. As such, considerable research has been devoted to the design and synthesis of species to mimic the active sites of these hydrogenases [46–48]. There are three main classes of hydrogenase, distinguished according to the composition of the transition metal containing active site: [FeFe] hydrogenase; [NiFe]-hydrogenase; and [Fe]-hydrogenases or Hmd [46–53]. Notably, [Fe]-hydrogenase does not cleave H₂, it is not a redox enzyme.

[FeFe]-hydrogenases play a pivotal role in the energy metabolism of microbial organisms in their ability to catalyse the reversible reduction of protons and electrons to molecular hydrogen (3.1).



The structure of [FeFe]-hydrogenase was revealed by X-ray crystallographic studies of two different organisms, the H₂ producing hydrogenase *Clostridium pasteurianum* (CpI), and the H₂ uptake hydrogenase *Desulphovibrio desulfuricans* (DdH) [54–57]. They both show similarities in structure and feature a 6-Fe active site cluster, the H-cluster. The H-cluster of both enzymes was found to be buried deep within the protein and connected to the surface by a hydrophobic channel. It was suggested that this channel is responsible for the delivery and release of H₂ [58]. The H-cluster is composed of a [2Fe2S] subsite (the site of H₂ oxidation and H⁺ reduction) linked to a [4Fe4S] cubane cluster by a protein bound cysteine ligand. The irons in the di-iron centre are labelled Fe_d (distal; furthest

from the $[4Fe4S]$ cluster) or Fe_p (proximal; closest to the $[4Fe4S]$ cluster). The Fe centres are bridged by a dithiolate ligand, with a pair of CO and CN^- ligands on each iron completing their coordination spheres. One of the structural differences observed between CpI and DdH hydrogenases is the L ligand present in CpI and absent in DdH [54, 55]. This was assigned to either H_2O , OH^- , H^- , or H_2 (see Figure 3.1). Depending on the oxidation state of the di-iron cluster, a third CO is either found bridging the two irons (H_{ox} -CO) or in a terminal position on the distal iron [57]. The identity of the central atom in the dithiolate bridge of DdH was unresolvable in the X-ray diffraction data. It was initially assigned as CH_2 , [55]. However, O, or NH are thought to be more likely from a mechanistic perspective, as they can participate in electron transfers [56, 59]. Studies combining hyperfine sublevel correlation spectroscopy (HYSCORE) with DFT calculations on DdH in the H_{ox} state [60] and synthetic model systems [61] by Lubitz and co-workers provide compelling evidence that the identity of the X group is NH.

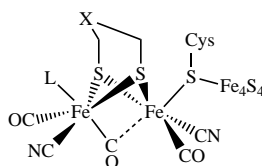


Figure 3.1: Schematic representation of the H-cluster ($X = CH_2$, NH , or O and $L =$ vacant, H_2O , OH^- , H^- , or H_2).

Numerous studies of the $[FeFe]$ hydrogenase using the techniques of fourier transform infrared spectroscopy (FTIR), DFT and quantum mechanical and molecular mechanical (QM/MM) over recent years have led to several proposals for catalytic mechanisms for the turnover of H_2/H^+ [46, 47, 62]. The current model of the $[FeFe]$ hydrogenase uses the central nitrogen of the dithiolate bridge to relay protons to the Fe centre (see Figure 3.2). Essential to the proposed mechanism is the formation of a terminal hydride species. Various DFT based investigations of the enzyme have eluded to the formation of such a species during catalysis [63, 64]. However, to date there has been no direct spectroscopic evidence that such a species exists during the turnover of the $[FeFe]$ hydrogenase.

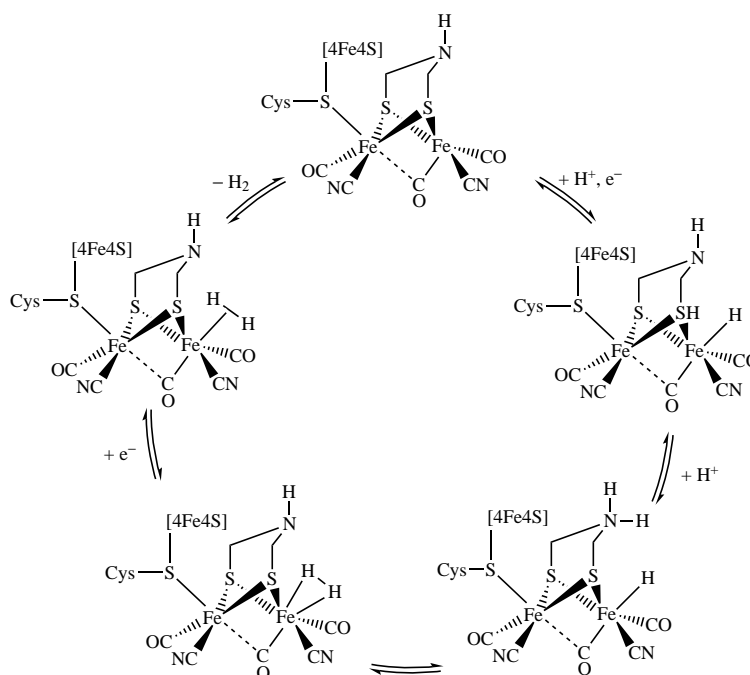


Figure 3.2: Proposed mechanism for the catalytic turnover of H_2/H^+ by the $[FeFe]$ -hydrogenase. Adapted from [47, 62, 65].

To understand the nature of hydrogen evolution at diiron sites and to explore the possibility of a synthetic catalyst, organometallic diiron complexes possessing key structural features of the active site of $[FeFe]$ -hydrogenases have been intensively and widely explored [46, 65–87]. The natural and synthetic systems have also received much attention from theoretical chemists. DFT studies have played a key role in understanding $[FeFe]$ -hydrogenase chemistry, key reviews are [47, 62, 63, 88–91]. For the initial step in the hydrogen evolution at a multi-iron site, the proton can either bind to two iron centres to form a bridging-hydride or to a single iron centre to form a terminal-hydride [65–68, 92–98]. It is also possible that the protonation can occur at sulphur or CO [85, 99, 100]. Many experimental observations have shown that the bridging hydride species is thermodynamically favoured [67–69, 92–98, 101–103]. However, several studies suggest that at low temperature the terminal-protonation can be observed by NMR spectroscopy especially for the complexes possessing strong donor and chelating ligands, and that upon warming the terminal hydrides isomerise to the bridging-hydrides [74–78, 95–98, 101–103]. Therefore, it is important to gain a better understanding of the protonation process.

Wright and Pickett recently reported a kinetic study on the protonation of a subsite analogue of $[FeFe]$ -hydrogenase: $Fe_2(\mu-pdt)(CO)_4(PMe_3)_2$ [67]. They proposed a two

step mechanism: (1) protonation of the Fe–Fe bond of the apical-basal isomer; (2) rearrangement to the trans-basal bridging hydride isomer (see Figure 3.3) [67]. Later, using time-resolved NMR, stopped-flow UV and IR, Pickett and co-workers explored a series of similar diiron subsite models [68, 104]. For the complexes with two PMe_3 ligands, their observations were consistent with direct protonation at the bridging site, followed by isomerisation to the thermodynamic product. For complexes containing cyanide ligands instead of PMe_3 ligands however, the proton was thought to bind to the cyanide, before migrating to the bridging site. Protonation to a single iron centre to form the terminal hydride was not observed [68]. Additionally, Wright and Pickett investigated the influence that the identity of the dithiolate bridge had on the activation energy parameters for protonation. They found that the protonation kinetics were significantly influenced by the identity of the bridgehead linker with the pdt bridged system reacting an order of magnitude slower than the ethane-1,3-dithiolate (edt) and 2-oxapropane-1,3-dithiolate (odt) bridged systems, which suggested that bridge length was not a determinant of reactivity [104, 105]. The subsequent rearrangement to the thermodynamic product was observed to follow a similar pattern.

Because the formation of a terminal hydride, which appears to be responsible for the H_2 evolution in the enzyme [47, 54–56], could also be applicable to the synthetic systems [69, 78, 95, 98], many researchers have explored the possibilities of the formation of terminal-hydrides. Recent theoretical studies have shown that the activation barriers for formation of terminal-hydrides were lower than or close to those of the bridging-hydrides [91, 106, 107].

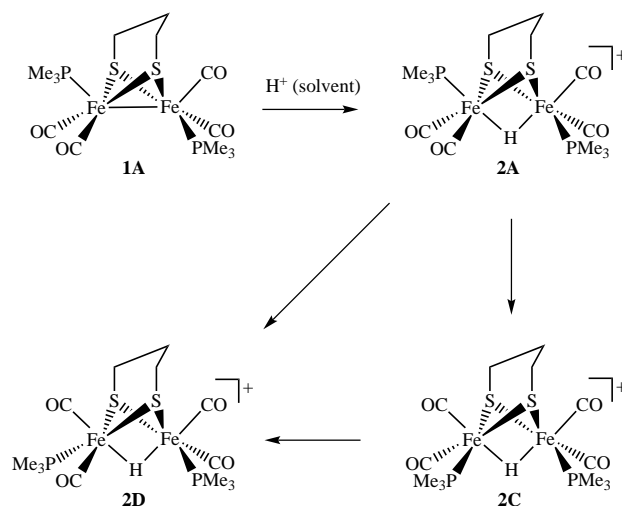


Figure 3.3: Wright-Pickett proposed mechanism for protonation of the $[Fe_2(\mu-pdt)(CO)_4(PMe_3)_2]$ model subsite [68].

In an attempt to provide insight into the experimental observations described above, this work analyses the protonation regiochemistry for a family of $[Fe_2(\mu-(Xdt)(CO)_4(PMe_3)_2)]$ model systems (see Figure 3.4) (where: Xdt = edt, pdt, odt, 2-methyl-1,3-propanedithiolate (mpdt), 2,2-dimethyl-1,3-propanedithiolate (dmpdt) and 2-methyl-1,3-propanedithiolate-S (mpdt-S)). All systems investigated in this work have been synthesised by the Pickett group. A portion of the computational work was carried out in collaboration with the Hall research group at Texas A&M University. They investigated the $[Fe_2(\mu-pdt)(CO)_4(PMe_3)_2]$ system using the B3LYP exchange functional, while my calculations on all systems use exclusively the Tao, Perdew, Staroverov, and Scuseria (TPSS) exchange functional (see 3.2 for full details).

Computational models of the Xdt model systems have been labelled into four isomeric types apical/basal (**A**), apical/apical (**B**), basal/basal *cisoid* (**C**), and apical/basal *transoid* (**D**) according to the relative positions of the trimethylphosphine (PMe_3) ligands. For the pdt, odt and dmpdt bridged systems, an additional isomer of **A** exists where the direction of the dithiolate bridgehead atom is reversed, this is labelled **A'** (see Figure 3.6, Figure 3.13 and Figure 3.17). For the mpdt bridged model compounds, the methyl (CH_3) group attached to the bridgehead can be either orientated parallel or perpendicular to the Fe–Fe bond vector so it is possible that an additional isomer for each type can exist, giving ten in total (see Figure 3.15). For the mpdt-S model complex, the CH_3 group of the

apically coordinated sulphur can be positioned either side of the Fe–Fe vector giving rise to the additional isomer **1A'** (see Figure 3.19).

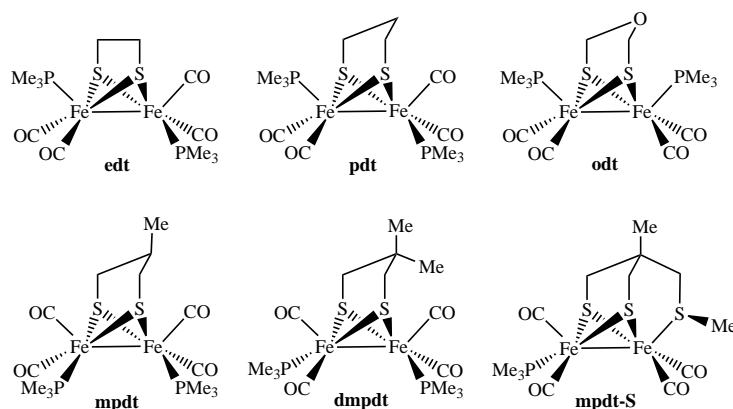


Figure 3.4: Family of $[Fe_2(\mu-Xdt)(CO)_4(PMe_3)_2]$ model systems investigated in this work.

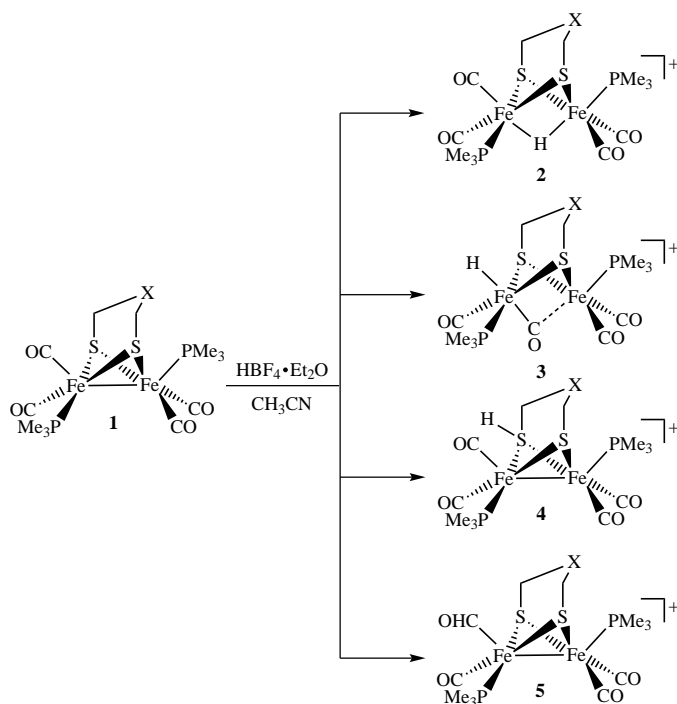


Figure 3.5: Possible hydrides produced from the protonation of *Xdt* **1**.

The pdt dithiolate bridged system will be considered as a starting point for the following investigation. The relative stabilities of the unprotonated isomers of the pdt bridged system and the rotational transition states that link them are considered first. In an attempt to assign structure to the experimental infrared spectrum, a comparison with computed infrared spectra is performed. In order to help understand the protonation regiochemistry of these complexes, the Mulliken charges are investigated. The effects that the steric bulk

of the dithiolate bridge have on these parameters is then evaluated through the systematic investigation of the pdt, odt, mpdt, dmpdt and mpdt-S dithiolate bridged systems. The same properties are investigated in the protonated Xdt model subsites, along with the effects of a single electron reduction.

As shown in Figure 3.5, the reaction of Xdt **1** with an acid may produce any of the four hydride species **2**, **3**, **4**, or **5**. The relative energies of these protonated species are compared in section 3.5 and the experimental IR is compared with simulated IR in order to assign structure. A similar investigation of the protonated species with the different dithiolate bridges is then carried out. A comparative investigation of protonation mechanism of the pdt system is then reported in Chapter 4, including the effects that the edt and odt dithiolate bridges have on the energy pathways. Finally, the energetics of isomerisation processes of the edt, pdt, and odt bridged systems are reported in Chapter 4.3.

Unless it is otherwise stated, all computed energies reported in the text, figures, and tables are the solvent corrected free energies reported in kcal/mol using the TPSS functional.

3.2 Computational details

All calculations have been performed using the Gaussian software package [18, 19]. DFT calculations have been performed at two levels of theory; using the Beck3LYP (B3LYP) hybrid GGA functional [108–110] and the hybrid meta-GGA functionals of Tao-Perdew-Staroverov-Scuseria (TPSS) [111]. All calculations were carried out using the same basis sets; to characterise iron, phosphorus, and sulphur, the effective core potentials of Hay and Wadt have been employed along with the double-zeta valence basis set (LanL2DZ) [112–114]. In the case of iron, the two outermost *p* functions have been replaced by re-optimised *4p* functions [115], with the addition of the *f* polarisation function [116]. For sulphur and phosphorus, the basis sets were augmented with the *d* polarisation functions proposed by Höllwarth *et al* [117]. All other atoms are described by the 6-31++G** basis set. Geomet-

ric isomers were optimised in the gas phase using the crystal structure [69] as a starting point. Frequency calculations were carried out at the same level of theory to provide thermochemistry data and to confirm stationary points as having no negative frequencies, and transition states as having a single negative frequency. All geometries were optimised in the gas phase. Solvation was accounted for in single point energy calculations, using the integral equation formalism polarisable continuum model (**IEFPCM**) in CH₃CN in combination with the united atom topological model for radii setting (**RADII=UAHF**).

3.3 Isomers of [Fe₂(μ-Xdt)(CO)₄(PMe₃)₂] model subsites

3.3.1 [Fe₂(μ-pdt)(CO)₄(PMe₃)₂]

The possible isomers of the pdt subsite are shown in Figure 3.6. X-ray crystallographic studies revealed that pdt **1** adopts a basal/basal-*transoid* geometry in the solid state [69]. In agreement with this, gas phase DFT calculations predict isomer **1D** as the most stable with the order of stability predicted as **1D** > **1A'** > **1A** > **1C** > **1B** (see Table 3.1). Comparison of selected geometric parameters shows good agreement with the X-ray crystal structure [69] at all levels of theory, with the B3LYP functional used by Lui [118] giving the best agreement (see Table 3.2). Isomer pdt **1B** is predicted to have the shortest Fe–Fe bond length (2.4892 Å) and the longest Fe–Fe bond length is observed in isomer pdt **1C** with a distance of 2.5977 Å. The identity of the L_{apical} ligand is important in understanding these observations, since it is this ligand that is *transoid* to the Fe–Fe bond. Analysis of the highest occupied molecular orbitals (HOMOs) of both complexes reveals mainly Fe–Fe bonding and Fe–L_{apical} anti-bonding contributions (see Figure 3.7). This means that electron density from this orbital is most easily accessible for back donation into the π* MO of the CO. Since the CO ligand is a stronger π acceptor than the PMe₃ ligand, more Fe *d*-electron density is donated back into the π* MO of the CO than in the case of the PMe₃ ligand. This should result in a weaker Fe–Fe bond when CO ligands are apically coordinated. In agreement with this, isomers with a single apical PMe₃ group (pdt **1A**⁽⁹⁾) have the next shortest bond length. As might be expected, this difference in bond

length corresponds to a 4.6° increase in $\angle Fe-S-Fe$ in pdt **1C** relative to pdt **1B**. Long Fe–Fe bond lengths are also associated with longer Fe–S bond lengths. Comparing the two extremes, isomers pdt **1C** and pdt **1B** show that the Fe–S bond lengths are on average 0.03 \AA shorter in isomer pdt **1C**. Comparing the Fe–P bond distances between the isomers reveals that they are consistently shorter when apically coordinated, by an average of 0.02 \AA .

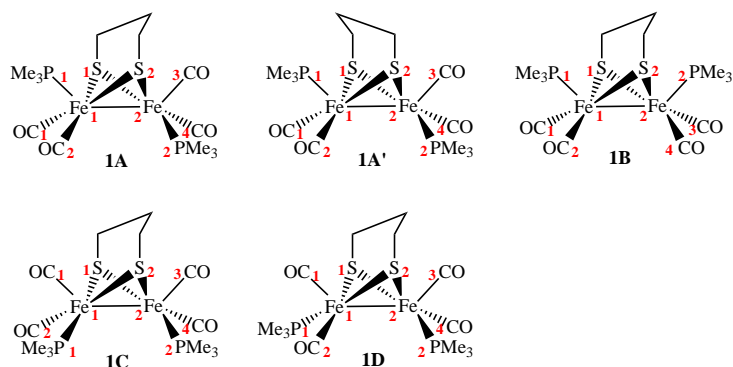


Figure 3.6: Isomers of the $[Fe_2(\mu\text{-pdt})(CO)_4(PMe_3)_2]$ model system. Atom and functional group labels are reported in red. Associated relative free energies and Mulliken charges are reported in Table 3.1 and bond distances and angles are reported in Table A17 and Table A18.

Table 3.1: Calculated gas phase and solvent corrected free energies and Fe Mulliken charges for isomers of $[Fe_2(\mu-pdt)(CO)_4(PMe_3)_2]$ and the transition states that connect them; either through rotation of the $Fe(CO)_2(PMe_3)$ moiety or by the *pdt* bridge flip. Energies are reported relative to the **1A** isomer. Calculations using the B3LYP functional were carried out by Liu [118].

Isomer	B3LYP		TPSS			
	Free Energies (kcal/mol)				Mulliken charges	
	ΔG_g	ΔG_{solv}	ΔG_g	ΔG_{solv}	Fe ₁	Fe ₂
pdt 1A	0.0	0.0	0.0	0.0	-0.698	-0.310
pdt 1A'	1.1	1.1	0.8	0.9	-0.701	-0.177
pdt 1B	0.8	0.8	2.9	2.9	-0.467	-0.531
pdt 1C	3.9	3.9	2.7	3.0	-0.365	-0.516
pdt 1D	-1.2	0.9	-1.8	0.4	-0.511	-0.514
TS_{pdt 1A→1B}	8.7	9.0	10.2	9.1	-0.489	-0.717
TS_{pdt 1A→1C}	9.2	9.8	9.5	9.3	-0.932	-0.530
TS_{pdt 1A→1D}	8.6	9.1	7.2	8.3	-0.810	-0.503
TS_{pdt 1C→1D}	22.8	23.6	22.6	23.6	-0.044	-1.081
TS_{pdt 1C→1D-flipped}	^a	^a	20.9	19.7	-0.012	-0.965
TS_{pdt 1A'→1C}	5.9	6.0	7.2	7.4	-0.725	-0.554
TS_{pdt 1A'→1D}	4.1	4.4	3.6	4.6	-0.743	-0.467
TS_{pdt 1A'→1B}	10.8	11.2	9.5	8.5	-0.461	-0.743
TS_{pdt 1A→1A'}	8.8	9.4	9.1	10.1	-0.626	-0.172
TS_{pdt 1B→1B}	10.7	10.8	10.5	10.4	-0.407	-0.407
TS_{pdt 1C→1C}	11.0	12.1	12.9	13.9	-0.365	-0.293
TS_{pdt 1D→1D}	8.1	9.5	8.1	10.2	-0.499	-0.500

^a not calculated using B3LYP functional

Table 3.2: Selected geometric parameters for the unprotonated $[Fe_2(\mu-pdt)(CO)_4(PMe_3)_2]$ isomer **1D** from x-ray crystallography compared to calculated values [69].

	bond length/Å				bond angle/°	
	Fe-Fe	Fe-S _{av}	Fe-CO _{av}	Fe-P _{av}	S-Fe-S	Fe-S-Fe
Exp.	2.5573	2.2519	1.7580	2.2374	84.326	69.194
B3LYP	2.5617	2.3086	1.7608	2.2925	85.015	67.396
TPSS	2.4892	2.3208	1.7563	2.2398	85.086	68.858

Pickett and co-workers showed the apical/basal (**pdt 1A**) isomer to be most prevalent in solution (acetonitrile (CH₃CN) solvent) [67]. After accounting for the effects of solvation, the calculations are in agreement with this observation, predicting **pdt 1A** to be most stable, albeit by only 0.4 kcal/mol. The order of stability for the remaining isomers is predicted to remain the same as in the gas phase. Use of the B3LYP functional lowers the relative energy of **pdt 1B**, so that instead of being the fourth most stable it is the second most stable (see Table 3.1) [118]. Isomer **pdt 1C** is found to be the least thermodynamically

ically stable by both functionals (see Table 3.1). The flipping of the pdt bridge has little effect on the energy of pdt **1A** relative to pdt **1A'**, with a difference of only 0.93 kcal/mol.

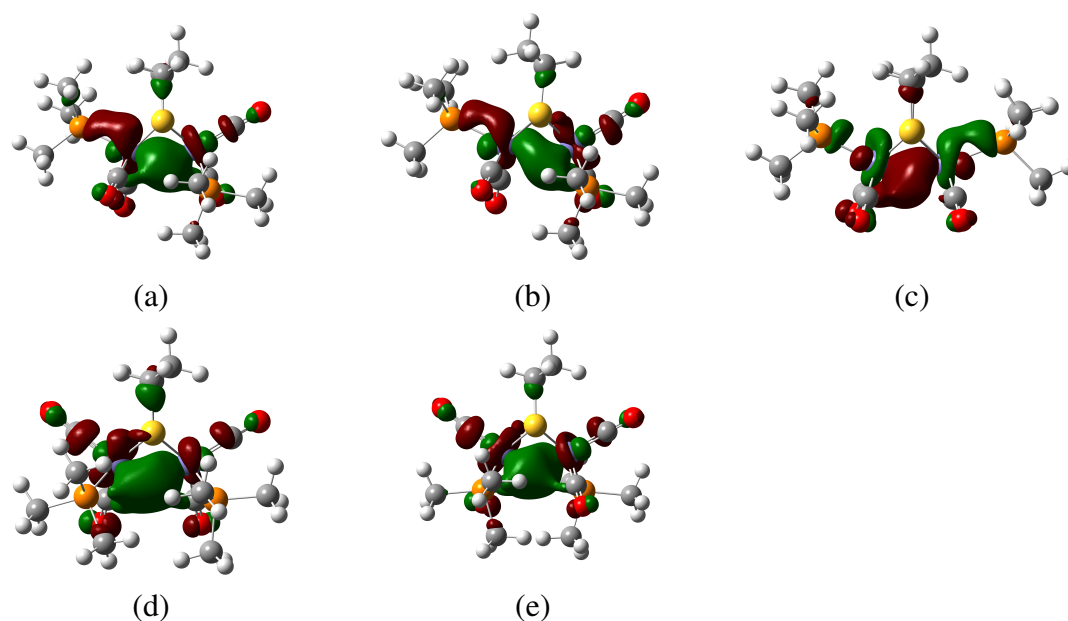


Figure 3.7: Highest occupied molecular orbitals (HOMOs) for isomers (a) pdt **1A**, (b) pdt **1A'**, (c) pdt **1B**, (d) pdt **1C**, and (e) pdt **1D** of the $[Fe_2-(\mu-pdt)-(CO)_4-(PMe_3)_2]$ model complex. Isosurface = 0.04.

In order to characterise any structural distortions brought about by the substitution of CO by sterically bulky ligands, Φ and Ψ angles have previously been employed [119]. The Φ angle is defined by the torsional angle between the two apical ligands and the Fe–Fe bond vector [119], while Ψ is given by the angle between a given basal ligand and the Fe–Fe bond vector. In the relatively undistorted $[Fe_2(\mu-pdt)(CO)_6]$ model compound the Ψ angle is reported to be ca. 100° , while a semi-bridging CO yields a Ψ angle of ca. 140° [120]. Comparing isomers **1A** and **1A'** of pdt **1**, the Ψ angle for the basal carbonyl (CO) (of Fe_1) orientated *transoid* to the basal PMe_3 group is 1.6° less for isomer **1A'**. Further, observing the basal CO (of Fe_2), the Ψ angle decreases by 1.8° when the bridgehead atom of the dithiolate linker is above it. These small changes in the dihedral angle stem from a slight rotation of the $Fe(CO)_2(PMe_3)$ moiety caused by the steric bulk of the methylene (CH_2) bridgehead. In isomer **1B**, both PMe_3 groups are apically coordinated. The PMe_3 group next to the pdt bridge is more sterically hindered and so should be partially rotated to avoid the steric clash. However, the CH_3 hydrogens of the the PMe_3 and the CH_2

hydrogens fit snugly together seemingly preventing any rotation (in order to rotate the hydrogens must first move out of the way, perhaps during a bridge flip). Predictably, the more sterically hindered \angle Fe–Fe–P in **1B** is 3.1° more than the less sterically hindered angle. In isomer **1C**, the Fe₂(CO)₂(PMe₃) moiety is slightly rotated (to avoid clash of the apical CO with CH₂ bridgehead hydrogens) resulting in an almost semi-bridging CO from the basal CO on Fe₂, \angle 91.0°. This effect may be exaggerated by the basal/basal-*cisoid* PMe₃ groups. For isomer **1D** there is no obvious distortion, but the Ψ angle for basal CO is ca. 2° less for the more hindered Fe₂.

Matthews and Heinekey found that the Fe₂(μ-S₂C₃H₆)(CO)₆ model subsite possesses a very low basicity, the subsite only protonates in the presence of a superacid [121]. The subsite can be protonated by weaker acids if CO ligands are replaced with less basic ligand sets such as PMe₃. Several groups have demonstrated how the electron density of the Fe centres in diiron hydrogenase can be modified by substitution of carbonyl ligands with σ/π -electron donors such as cyanides, phosphines, amines or thioethers [120, 122–126]. The geometry optimised structures of pdt **1** show electronic inequivalence between the two Fe centres. For example, comparison of the Mulliken charges of Fe₁ and Fe₂ in **1A** and **1A'** shows slight enrichment of the electron density of the Fe centre where the PMe₃ group is apically coordinated. In each case, the Fe–PMe₃*apical* bond distance is 0.02 Å shorter than the basal PMe₃ group. Analysis of the HOMOs of pdt **1** (see Figure 3.7), reveals mainly Fe–Fe bonding and Fe–L_{apical} anti-bonding contributions. The high electron withdrawing nature of the CO ligand relative to the PMe₃ ligand means that when it is coordinated in the apical position (*transoid* to the Fe–Fe bond) more electron density is withdrawn from the Fe–Fe bond centre than with a PMe₃ ligand. This results in charge asymmetry when there is apical PMe₃ on one Fe centre and apical CO on the other Fe centre (see Table 3.1 and Figure 3.6). This is an important observation; to make the subsite sufficiently basic to protonate, the PMe₃ group has to be in the apical position. This was also observed experimentally by Pickett and co-workers in their proposed mechanism; **1A** isomer is protonated to the bridging position to give the kinetic product (isomer **2A**), before rearranging to isomer **2D** (see Figure 3.3) [67]. Comparing the energies of the

HOMOs of each isomer should give an indication of the basicity of the subsite as a whole. A higher energy HOMO will make the *d*-electrons more accessible for back donation to the CO ligands. Table 3.3 shows the energies of the HOMOs for each of the isomers of pdt **1**. Isomer **1B** has the lowest energy and so in theory should be most desirable for proton addition.

Table 3.3: Energy comparison of the HOMOs of [Fe₂(μ-pdt)(CO)₄(PMe₃)₂] isomers.

Isomer	HOMO energy (kcal/mol)
1A	-107.86
1A'	-108.41
1B	-109.36
1C	-107.07
1D	-108.88

As noted by Darensbourg *et al.*[122] the direction of the pdt bridge impacts the charge distribution, with Fe₂ being more positive by 0.13 when the pdt is flipped from being above Fe₂ in **1A** to above Fe₁ in **1A'**. In isomers **1B**, **1C**, and **1D**, the PMe₃ groups are in equivalent sites to each other (apical/apical, basal/basal and basal/basal, respectively) and in each case the Fe centre beneath the pdt linker is calculated to be more electronegative (see Figure 3.6 and Table 3.1). In **1D** the Φ angle is at its smallest for all the isomers, at 6.8°, and the charge of the Fe centres is symmetrically distributed. Having both PMe₃ groups apically coordinated as in **1B**, distorts the Φ angle to 14.5°. The PMe₃ that faces the pdt linker in **1B** is more sterically hindered seemingly making the rotated Fe₂ centre more electron rich by 0.06. For the **1C** isomer, the PMe₃ groups are basal/basal-*cisoid* to each other. In order to accommodate the bulk of the ligands in the same area, one of the Fe(CO)₂(PMe₃) units is rotated slightly relative to the other, giving a Φ angle of 27.1°. This slight rotation is coupled with the electron enrichment of the Fe₂ centre, more electronegative by 0.15 (see Table 3.1). In addition to the structure reported for isomer **1C**, there exists another local minimum for this ligand arrangement which is 1.1 kcal/mol less stable. The structure is characterised by the distortion of both Fe centres, with the PMe₃ groups being twisted away from each other, this time resulting in Fe₁ being 0.13 more electronegative than Fe₂.

Octahedral complexes are able to rotate via trigonal twisting type mechanisms. These are known as Bailar twist and the Ray-Dutt twist. Both mechanisms involve two consecutive rotations of ca. 60° .

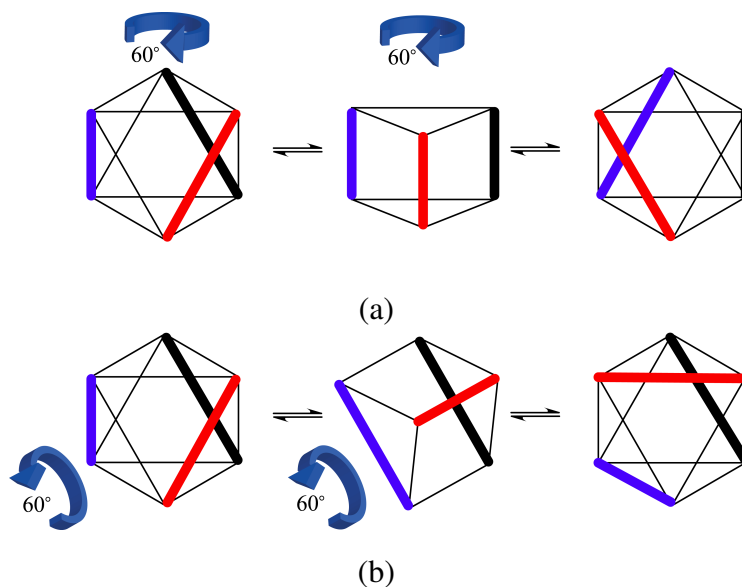


Figure 3.8: Schematic of an octahedron undergoing (a) Bailar twist and (b) Ray-Dutt twist.

Rotation of the $Fe(CO)_2(PMe_3)$ moiety by $\sim 60^\circ$ in a Bailar type twist results in transition states (TSs) that bring either a CO or PMe_3 group into the semi-bridging position (see Figure 3.9). During the rotation of pdt **1** the Fe–Fe bond lengthens by an average 0.042 \AA relative to the unrotated structures. While both iron centres retain their square pyramidal geometry, the rotated Fe square pyramid is inverted relative to the unrotated square pyramid. As previously noted, the semi-bridging CO group has a modified $\angle Fe-C-O$ compared to the typical terminal CO [122]. The typical $\angle Fe-C-O$ for a terminal CO ligand is predicted to be ca. 180° , while the $\angle Fe-C-O$ for a semi-bridging CO is calculated at an average of 169° . The average $Fe-C_{semi-bridging}$ bond distance is ca. 2.69 \AA , which would suggest some electronic interaction. Transition states with a semi-bridging CO are stabilised by the π -acceptor interaction and have relatively low energy barriers; 3.2 kcal/mol to 8.5 kcal/mol (see Table 3.1). Conversely, a higher energy barrier is observed for the transition state that links **1C** and **1D** brings the PMe_3 group into the semi-bridging position. The bulky PMe_3 group prevents any Fe–P interaction and as a consequence, this TS has a higher rotational energy barrier, 20.6 kcal/mol. The energy barrier associated with the flip of bridgehead in the pdt linker is predicted to be 9.7 kcal/mol. The

energy barrier for the bridge flip of the other isomers is almost isoenergetic with this (see Table 3.1). In undergoing the flip, the Fe–Fe bond is predicted to lengthen by an average of 0.02 Å while the Fe–S bonds shorten by an average of 0.01 Å.

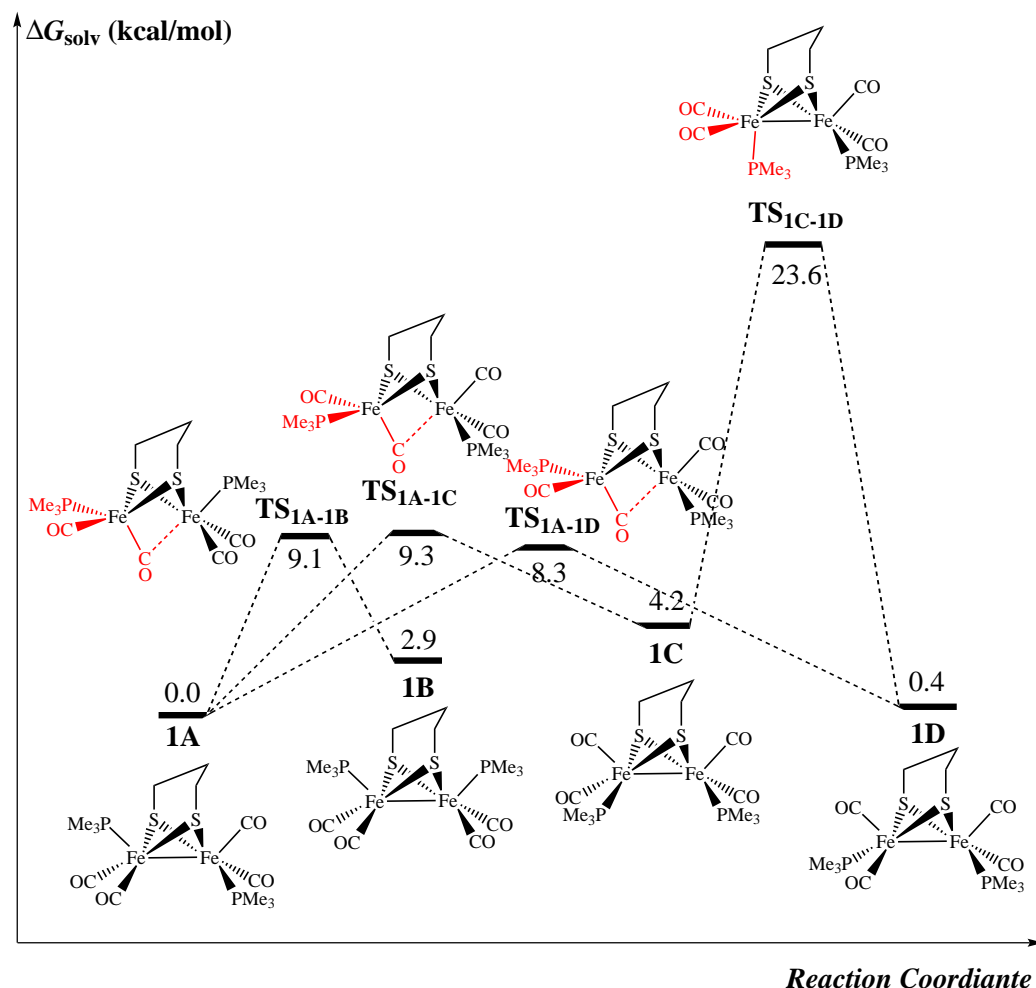


Figure 3.9: Solvent corrected free energy barriers associated with rearrangement of the isomers of $[Fe_2(\mu-pdt)(CO)_4(PMe_3)_2]$. Rotating groups in transition states are highlighted in red.

In contrast to findings of Georgakaki *et al.* [122], both iron centres in all the rotated TSs are predicted to be more electronegative than the unrotated iron centres. The exception to this is for pdt **TS_{1C-1D}**, where the PMe_3 group is in the semi-bridging position. For example, Fe_1 and Fe_2 in pdt **TS_{1A-1C}** have Mulliken charges 0.234 and 0.220 more negative, respectively than those found in **1A**. Comparing pdt **TS_{1A-1C}** with pdt **TS_{1A'-1C}**, the charges of the un-rotated Fe_2 are unaffected by the presence of the pdt linker, while the presence of the pdt linker makes the rotated Fe_1 0.207 more electronegative. This same pattern can be seen in pdt **TS_{1A-1D}** (see Table 3.1). For pdt **TS_{1C-1D}**, Fe_2 is at its most electronegative with a predicted Mulliken charge of -1.081 compared to the values

of -0.273 and -0.514 in isomers pdt **1C** and pdt **1D** respectively, and Fe_1 becomes more electropositive (-0.04 compared to -0.402 and -0.511 for isomers pdt **1C** and pdt **1D** respectively).

The experimental IR spectrum of pdt **1** (recorded in CH_3CN) gave three bands in the carbonyl region, at 1898 cm^{-1} (broad), 1943 cm^{-1} , and 1980 cm^{-1} [67]. Table 3.4 compares the experimental spectrum to the simulated spectrum for all isomers. In each case the simulated spectrum exhibits four $\nu(CO)$ spectral bands, characterised by the four combinations of each CO moving in and out of phase with one another. It is difficult to assign structure to the experimentally observed spectra since all isomers are predicted to produce spectral features with very similar peak position. Due to the similarity in energy of the isomers and the low energy rotational barriers, it is feasible for all of the isomers to coexist in solution at room temperature. The simulated spectra of pdt **1A** (most stable solvent corrected isomer) overlaps well with the experimental one, with only a small shift in the wavenumber of the lower frequency band (see Figure 3.10). This could presumably be caused by the absence of the solvent in the simulated spectra.

Table 3.4: DFT simulated $\nu(CO)$ bands of $[Fe_2(\mu-pdt)(CO)_4(PMe_3)_2]$ isomers compared to those experimentally determined in CH_3CN [67].

Isomer	$\nu(CO)$ (cm^{-1})			
Exp.	1898		1943	1980
1A	1919	1928	1954	1987
1A'	1919	1927	1955	1987
1B	1930	1953	1960	2004
1C	1914	1929	1951	1983
1D	1909	1916	1951	1968

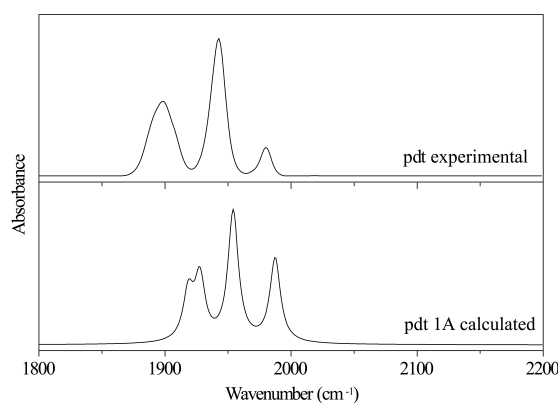


Figure 3.10: Comparison of experimental IR spectra [67] of $[Fe_2(\mu-pdt)(CO)_4(PMe_3)_2]$ with the simulated spectra of the most stable isomer, **1A**.

3.3.2 $[Fe_2(\mu-(edt)(CO)_4(PMe_3)_2]$

With only four isomers, edt is the most simple dithiolate bridge investigated in this work, and has the bridge with the least steric bulk (see Figure 3.11). The X-ray crystal structure of $[Fe_2(\mu-edt)(CO)_4(PMe_3)_2]$ (**edt 1**) indicates the PMe_3 groups are in an apical/basal configuration, with the same arrangement dominant in solution [69]. The simulated geometric parameters for isomer **edt 1A** are in excellent agreement with those observed experimentally, with small deviations of ca. 0.2 Å for bond distances and ca. 2° for the selected bond angles. Gas phase DFT calculations predict **edt 1A** to be the most stable isomer, albeit only 1 kcal/mol more stable than isomer **edt 1D**. Isomers **edt 1B** and **edt 1C** are 1.3 kcal/mol and 4.5 kcal/mol less stable respectively, than **edt 1A**. Considering the influence of the solvent, isomer **edt 1B** is stabilised and becomes the most stable (see Table A1).

A comparison of the experimental peak positions with those simulated for the four isomers of **edt 1** is given in Table 3.5. The experimental spectrum shows IR maxima at 1895, 1908, 1945 and 1981 cm^{-1} . Isomers **edt 1A** and **edt 1C** give best agreement with the experimental spectra and considering their energy separation and the low energy barrier to inter-convert them, it is reasonable that they could coexist in solution. They are both predicted to give peaks at ca. 1920, 1930, 1955 and 1987 cm^{-1} . This is a slight overestimate of the peak positions of the lower frequency bands but the intensity is in good agreement (see Figure 3.12). The simulated spectra of isomer **edt 1B** gives peaks at 1932, 1954, 1961 and 2004 cm^{-1} with peaks 2 and 3 appearing unresolvable. This

is not consistent with the experimentally observed spectra. Isomer edt **1D** actually gives the best agreement in terms of peak position with bands at 1914, 1921, 1950 and 1971 cm^{-1} . However, due to symmetry the peak at 1971 cm^{-1} is predicted to have a negligible intensity.

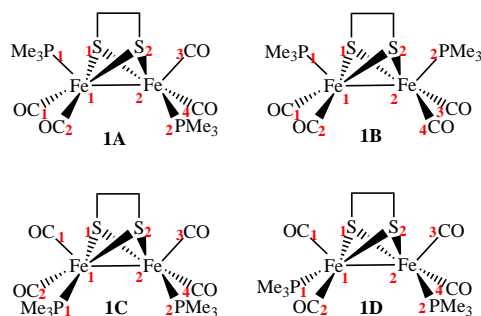


Figure 3.11: Structural isomers of the $[Fe_2(\mu-SCH_2CH_2S)(CO)_4(PMe_3)_2]$ model system. Relative solvent corrected free energies are reported in Table A1 Selected bond distances and bond angles are reported in Table A2 and Table A3, respectively.

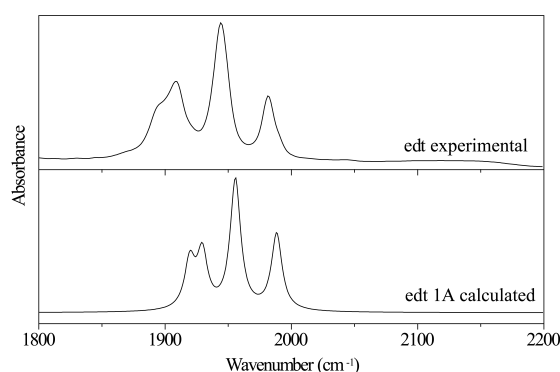


Figure 3.12: Comparison of experimental IR spectra [69] of $[Fe_2(\mu-(edt)(CO)_4(PMe_3)_2]$ with the simulated spectra of the most stable isomer, **1A**.

3.3.3 $[Fe_2(\mu-odt)(CO)_4(PMe_3)_2]$

The odt bridged species is similar in structure to the pdt bridged system, with the central CH_2 group replaced by an oxygen atom. The X-ray crystal structure of $[Fe_2(\mu-odt)(CO)_4(PMe_3)_2]$ (odt **1**) gives an apical/basal arrangement of the PMe_3 groups [105]. Gas phase DFT calculations agree with this finding, also predicting the apical/basal arrangement to be most stable by 2.1 kcal/mol. Interestingly, it is the odt **1A'** isomer where the bridge faces the more sterically hindered Fe_1 with the apical PMe_3 that is most stable. Gas phase DFT calculations on the isomers of odt predict the order of stability as **1A'** > **1B** > **1D** >

1A > **1C**. The geometry optimised structure of odt **1A'** (Table A32 and Table A33) shows good agreement with the reported crystal structure [105], with deviations of ca. 1% for bond distances and ca. 1° for bond angles. However, the $PMe_3-Fe_1-Fe_2-CO$ torsional angle underestimated by ca. 8°. Solvation makes isomer odt **1B** less stable than odt **1A'**, but the order of the remaining isomers is the same. The relative energy barriers associated with the dithiolate bridge flip are on average 0.9 kcal/mol lower for the isomers with the odt bridge compared to the pdt bridged systems, presumably because of the reduced sterics involved. The difference is greatest for the **1C** bridge flip, being 1.8 kcal/mol lower for the odt bridged system.

Table 3.5 displays a comparison of the experimental IR with those simulated for the five isomers with an odt dithiolate bridge. The experimental spectrum showed carbonyl stretches at 1915 cm^{-1} , 1922 cm^{-1} , 1953 cm^{-1} and 1974 cm^{-1} [105]. Although isomer odt **1B** is predicted to be the most stable in the solution phase, the simulated spectrum associated with this isomer is not matched well in peak position or intensities. Peak ν_2 is unobservable due to symmetry while ν_2 and ν_3 appear unresolvable. This is instead of peaks ν_1 and ν_2 which appear unresolvable in the experimental spectrum. Although isomer **1D** gives the best agreement with the experimental spectrum out of the isomers in terms of peak positions, ν_4 is predicted to be of negligible intensity due to symmetry. Out of the remaining isomers **1A'** gives best agreement (see Figure 3.14).

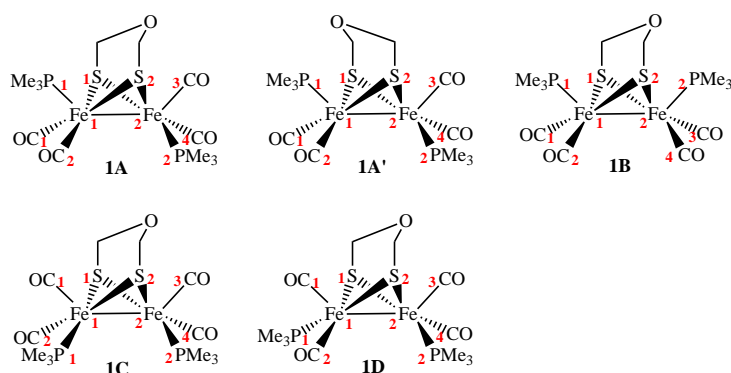


Figure 3.13: Structural isomers of the $[Fe_2(\mu-SCH_2OCH_2S)(CO)_4(PMe_3)_2]$ model system. Relative solvent corrected free energies are reported in Table A31 Selected bond distances and bond angles are reported in Table A32 and Table A33, respectively.

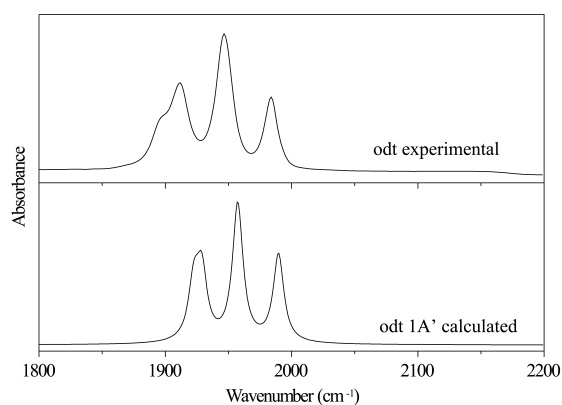


Figure 3.14: Comparison of experimental IR spectra [105] of $[Fe_2(\mu-odt)(CO)_4(PMe_3)_2]$ with the simulated spectra of the most stable isomer, **1A'**.

3.3.4 $[Fe_2(\mu-mpdt)(CO)_4(PMe_3)_2]$

There are a large number (ten) of structural isomers for the mpdt bridged system, owing to the fact that the CH_3 group of the dithiolate bridge can be either orientated perpendicular to the Fe–Fe bond vector or parallel to it. There is therefore an extra isomer of each of the types (see Figure 3.15). The crystal structure of the mpdt bridged system shows the PMe_3 groups in a basal/basal-*transoid* configuration with the Me group of the dithiolate bridge orientated perpendicular to the Fe–Fe bond vector (isomer mpdt **1D1**) [127]. The predicted geometric parameters for isomer mpdt **1D1** are in good agreement, deviating by a maximum of ca. 0.04 Å and ca. 2° (see Table A47). In the gas phase the basal/basal-*transoid* arrangement of PMe_3 groups is favoured for both orientations of the CH_3 group with isomer mpdt **1D1** predicted the most stable. Within all the isomer types, the isomer with the CH_3 group pointing up, in the least sterically demanding position is the most stable. Predictably, the sterically most hindered isomer mpdt **1B2** is the least stable in the gas phase, some 13 kcal/mol less stable than mpdt **1D1**. In isomers where the Me group of the dithiolate linker is parallel to the Fe–Fe bond vector, a rotated state with semibridging CO is the ground state. This can be seen most strongly in isomer mpdt **1D2**. Solvation stabilises the majority of the isomers, with the exception of isomer mpdt **1D** (which is still the most stable) and isomer mpdt **1A'**. Solvation also makes the energy range smaller. Relative to the edt, pdt and odt bridged systems the energy range is greatest here. Table 3.5 displays a comparison of the experimental peak positions with the predicted peak positions for each of the ten isomers of the mpdt bridged system. The

most stable isomer, mpdt **1D1** gives best agreement with the peak positions and intensities observed experimentally (see Figure 3.16).

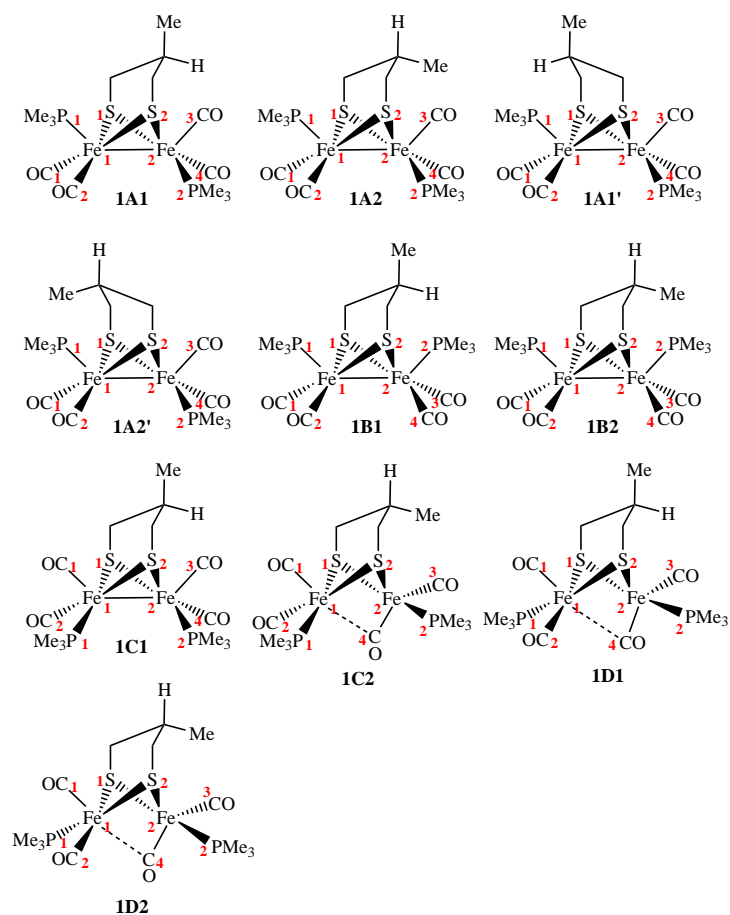


Figure 3.15: Structural isomers of the $[Fe_2(\mu-SCH_2CH(CH_3)CH_2S)(CO)_4(PMe_3)_2]$. Relative solvent corrected free energies are reported in Table A46 Selected bond distances and bond angles are reported in Table A47 and Table A48, respectively.

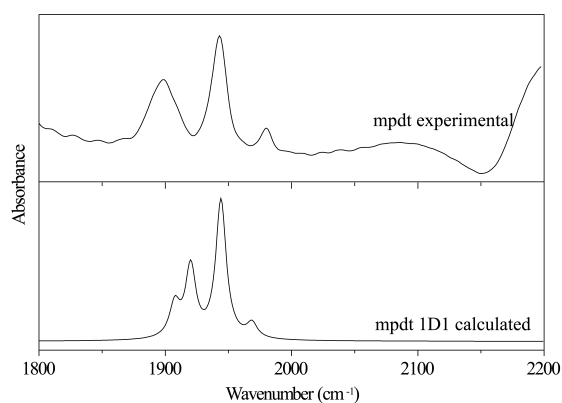


Figure 3.16: Comparison of $[Fe_2(\mu\text{-mpdt})(CO)_4(PMe_3)_2]$ experimental IR spectra [128] with the simulated spectra of the most stable isomer, **1A'**.

3.3.5 $[Fe_2(\mu\text{-dmpdt})(CO)_4(PMe_3)_2]$

The X-ray crystal structure of the dmpdt bridged system was first reported by Darensbourg and co-workers. They found basal/basal-*transoid* arrangement of the PMe_3 ligands (isomer dmpdt **1D**) [119]. The simulated geometric parameters of isomer dmpdt **1D** are in good agreement with those experimentally observed, deviating by a maximum of 0.05 Å for bond distances and 2° for bond angles (see Table A61). In the gas phase the order of stability is the same as for the pdt bridged isomers, with **1D** being most stable by around 3 kcal/mol. However, the energy range of the isomers is roughly double that of the range of the pdt isomers. Unlike the pdt bridged isomers, solvation has no effect on the order of stability. The bulky dithiolate bridge is seen to distort the geometry, this is most apparent in the **1A**^(s) isomers. When the bridgehead faces the apical PMe_3 group (**1A'**) the $\angle Fe_1-Fe_2-P$ increases by 4.25°. The Φ angle is also seen to change considerably between these isomers, from 37.6° in **1A** to 63.0° in **1A'**. The steric hindrance is so profound in isomers **1C** and **1D** that the $Fe(PMe_3)(CO)_2$ moiety is rotated so that a CO is semi-bridging. The experimental IR spectrum of the dmpdt is displayed in Figure 3.18. The simulated spectrum of isomer **1D** gives excellent agreement with both peak positions and peak intensities (see Figure 3.18).

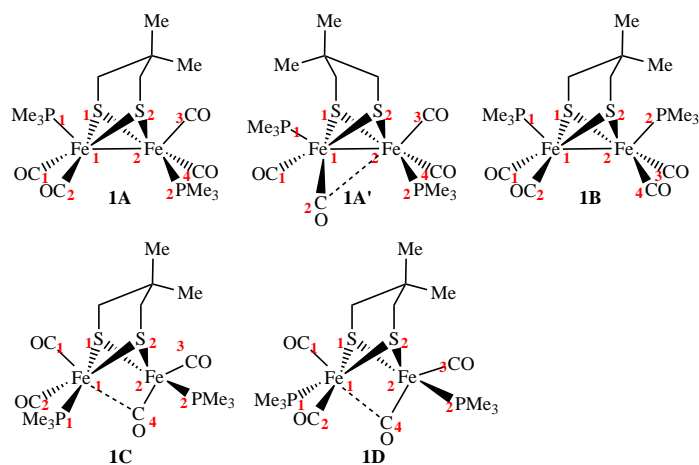


Figure 3.17: Structural isomers of the $[Fe_2(\mu-SCH_2C(CH_3)_2CH_2S)(CO)_4(PMe_3)_2]$ model system. Relative solvent corrected free energies are reported in Table A60. Selected bond distances and bond angles are reported in Table A61 and Table A62, respectively.

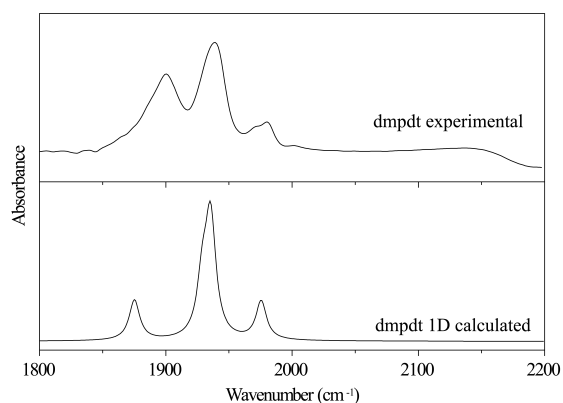


Figure 3.18: Comparison of the experimental IR spectra [120] of $[Fe_2(\mu-dmpdt)(CO)_4(PMe_3)_2]$ with the simulated spectra of the most stable isomer, **1A'**.

3.3.6 $[Fe_2(\mu-mpdt-S)(CO)_4(PMe_3)_2]$

The geometry of one end of the mpdt-S bridged complex is fixed by the chelating dithiolate bridge. Scanning the potential energy surface of the complex revealed three isomers, one with the PMe_3 ligands in an apical position (mpdt-S **1A**) and two with the PMe_3 ligand in a basal position (mpdt-S **1B**). Within these types the CH_3 group coordinated to the chelating apical sulphur can face either side of the complex (see Figure 3.19). The X-ray crystal structure gives the PMe_3 ligand in the basal position *transoid* to the S–Me group [128]. The simulated geometric parameters for the corresponding isomer, mpdt-S **1A1**, are in excellent agreement with these, deviating by a maximum of ca. 0.4 Å for bond distances and ca. 2° for bond angles (see Table A70 and Table A71). The experimental IR for the mpdt-S complex gives peak maxima at 1898, 1910, 1946 and 1985 cm^{-1} . Isomers

mpdt-S **1A**⁽⁹⁾ are predicted to give best agreement (see Table 3.5 and Figure 3.20) with only a small discrepancy in wavenumber.

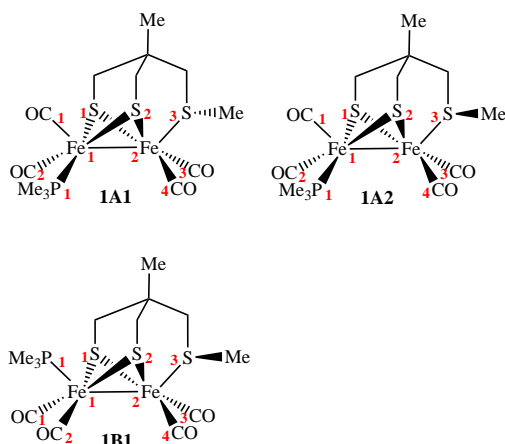


Figure 3.19: Structural isomers of the $[Fe_2(\mu-SCH_2CH(CH_3)(CH_2S)CH_2S)(CO)_4(PMe_3)_2]$ tripod model system, including **1A'** and **1B'**; the isomers with a wagged $S-CH_3$ group. Relative solvent corrected free energies and Mulliken charges are reported in Table A69. Selected bond distances and bond angles are reported in Table A70 and Table A71, respectively.

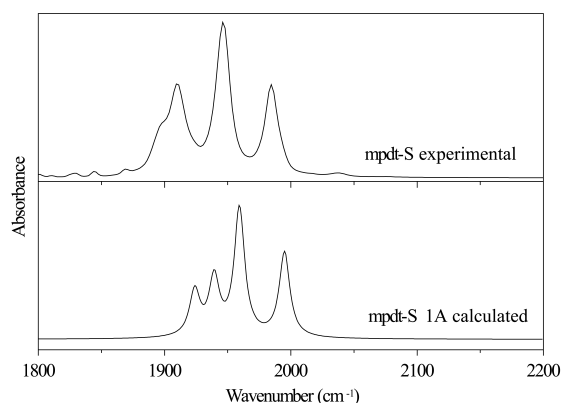


Figure 3.20: Comparison of the experimental IR spectra [129] of $[Fe_2(\mu-mpdt-S)(CO)_4(PMe_3)_2]$ with the simulated spectra of the most stable isomer, **1A**.

3.4 Effects of the dithiolate bridgehead

3.4.1 Trends in the $\nu(CO)$ frequencies

The stronger the Fe–C bond, the weaker the corresponding CO bond. The backbonding from the d -orbital of the Fe centre to the π^* anti-bonding orbital serves to weaken the CO bond resulting in a lower stretching frequency. One would expect that decreasing the steric bulk of the dithiolate bridge would decrease the electron density associated with the d -orbitals of the iron centres. This would serve to decrease the level of π backbonding

from the Fe *d*-orbitals to the π^* of the CO ligand, thus giving a stronger CO bond requiring a greater energy frequency to bring it into resonance. This effect is only expected to be slight, and comparing the frequencies of the edt with the pdt there is very little difference. Comparing the **1D** isomer of the pdt and edt systems, ν_1 , ν_2 and ν_4 are shifted by approx. 5 cm^{-1} higher in frequency, while ν_3 remains roughly the same. A similar trend can be observed for the other isomers. Interestingly, replacement of the central CH₂ group with an O atom also shifts the CO frequencies higher in wavenumber (see Table 3.5). Progressively loading the dithiolate bridge with bulkier groups in the mpdt and dmpdt systems does not effect the peak positions, suggesting that the dithiolate bridge does not have a significant electronic effect on the iron centres (see Table 3.4 and Table 3.5). This has important implications in understanding the protonation kinetics, i.e. it is not an electronic effect that causes the difference in reaction rate observed between the different bridges.

3.4.2 Rotational energy barriers with changing dithiolate bridge

In a series of calculations on $Fe_2(\mu-Xdt)(CO)_6$ model subsites Georgakaki and co-workers found that the direction of the S-to-S linker impacted the activation energy barrier to rotation of the $Fe(CO)_3$ moiety [122]. It was found that rotating the more hindered end of the molecule lowered the energy barrier comparative to the rotation of the less hindered end. Additionally, they found that increasing the steric bulk of the S-to-S linker accentuated this effect, a difference of 1.68 kcal/mol in pdt and 2.17 kcal/mol in o-xyldt [122]. The systems in this work are complicated by the presence of the two PMe_3 ligands, which for reasons of sterics would be presumably more difficult to rotate. However, in agreement with their findings, rotations of the $Fe(CO)_2(PMe_3)$ moiety in pdt **1** show that rotation the more hindered end occurs with a slightly lower energy barrier (see Table 3.1). For example, converting pdt **1A** to pdt **1D** proceeds through transition state pdt **TS_{1A→1D}** with an energy barrier of 8.3 kcal/mol. The same rotation, this time from pdt **1A'** sees the energy barrier for rotation being reduced by 3.7 kcal/mol (see Table 3.1). In the conversion of pdt **1C** to pdt **1D**, either end of the complex can rotate, the calculations predict that rotating the less hindered end proceeds over an energy barrier 3.9 kcal/mol higher

Table 3.5: DFT simulated $\nu(CO)$ bands of $[Fe_2(\mu-xdt)(CO)_4(PMe_3)_2]$ isomers compared to those experimentally determined in CH_3CN [67, 69, 105, 120, 128, 129].

Isomer	$\nu(CO)$ (cm^{-1})			
Exp. edt	1895	1908	1945	1981
edt 1A	1920	1929	1956	1988
edt 1B	1932	1954	1961	2004
edt 1C	1916	1934	1954	1986
edt 1D	1914	1921	1950	1971 ⁿ
Exp. odt	1898	1913	1947	1984
odt 1A	1922	1936	1964	1992
odt 1A'	1923	1929	1957	1990
odt 1B	1933	1954	1963	2005
odt 1C	1915	1936	1959	1989
odt 1D	1915	1922	1953	1974
Exp. mdt	1897		1943	1980
mpdt 1A1	1919	1927	1954	1987
mpdt 1A1'	1919	1927	1954	1986
mpdt 1A2	1914	1927	1952	1987
mpdt 1A2'	1913	1928	1949	1984
mpdt 1B1	1930	1952	1960	2003
mpdt 1B2	1928	1950	1958	2002
mpdt 1C1	1915	1930	1952	1984
mpdt 1C2	1900	1931	1939	1983
mpdt 1D	1908	1920	1944	1969
Exp. dmdt	1900		1939	1978
dmpdt 1A	1914	1927	1952	1987
dmpdt 1A'	1910	1927	1946	1983
dmpdt 1B	1928	1949	1958	2001
dmpdt 1C	1899	1931	1940	1984
dmpdt 1D	1875	1929	1935	1976
Exp. mdt-S 1A	1898	1910	1946	1985
mpdt-S 1A	1923	1939	1959	1995
mpdt-S 1A'	1924	1936	1959	1999
mpdt-S 1B	1936	1955	1966	2008

ⁿ indicates a peak of negligible intensity

than for the rotation of the more hindered end (activation energy barriers of 20.6 and 16.7 kcal/mol respectively). When comparing the rotational energy barriers of pdt **1** with edt **1**, reducing the steric bulk of the dithiolate bridge consistently increases the energy barriers to rotation. For example, $TS_{1A \rightarrow 1B}$, $TS_{1A \rightarrow 1C}$, $TS_{1A' \rightarrow 1D}$ and $TS_{1C \rightarrow 1D}$ are 0.8, 0.2, 1.9 and 0.9 kcal/mol higher, respectively, with the edt bridge. Replacing the central CH_2 group in the dithiolate linker with an oxygen atom serves to reduce all energy barriers to rotation (see Table 3.1 and Table A31). Additionally, the energy barriers associated with the bridge flip are predicted on average 1.2 kcal/mol lower with an odt bridge. Rotation of the mpdt and dmpdt is problematic to simulate as the CH_3 group that protrudes out toward Fe_2 has already forced a semi-bridging CO from Fe_2 in the ground state, making it

difficult to have a semi-bridging CO originating from Fe₁. For the mpdt bridged systems, the only rotational transition states that could be modelled were when the CH₃ group was perpendicular to the Fe–Fe bond vector. However, comparing the transition states for rotation that could be modelled for the mpdt with edt and pdt bridgeheads, the same pattern was observed; increasing the steric bulk of the dithiolate linker is accompanied by a lower energy barrier for rotation (see Table A1, Table 3.1 and Table A46). This is an important observation to bear in mind for investigating protonation mechanism (the subject of Chapter, 4), as in order for terminal protonation to proceed a partial rotation must first occur. If increasing the steric bulk of the dithiolate linker lowers the energy barriers to rotation, this also lowers the energy barrier for protonation. The only transition states corresponding to bridge flips that could be found for the mpdt bridged system were mpdt **TS**_{1A1→1A2'} and mpdt **TS**_{1A2→1A1'}. These barriers were ca. 2 kcal/mol higher in energy than with the pdt bridge. Unfortunately, no rotational or bridge flip transition states could be found for the dmpdt system. For the mpdt-S bridged system, the rotational energy barrier from **1A1**→**1B1** is found to have a height of 9.7 kcal/mol, similar to that found for the pdt bridged system. Although this should be expected as the sterics imposed on this end of the molecule are similar in both systems. An activation energy barrier of 14.7 kcal/mol is predicted when wagging the CH₃ group of the apical sulphur of Fe₂ to inter-convert isomers **1A1** with **1A2**, the same wag has an energy barrier 0.7 kcal/mol higher in the case of **1B1**.

3.4.3 Trends in geometries

Experimentally, the Fe–Fe bond in solid state pdt **1** is found to be significantly less than in the edt, 2.5551(6) Å [69] and 2.5159(2) Å [92], respectively [68]. It was suggested that the Fe–Fe bond in the edt model system is much stronger than that of the pdt model system, and that this may effect it's reactivity toward proton addition [68]. DFT calculations predict that the average Fe–Fe bond distances get progressively shorter as the bulk of the dithiolate bridge increases (see Table A2, Table 3.2, Table A47, Table A61 and Table A70). Interestingly, the odt bridge has the longest average bond distance in the

family of systems investigated. In all the systems investigated, the same order of Fe–Fe bond distances between the isomers exists, $C > D > A > B$ (see Table A2, Table A17, Table A32, Table A47, Table A61 and Table A70). This suggests that having an apical PMe_3 has an effect of reducing the Fe–Fe bond distance. In complexes with a bridge flipped isomer, the A' isomer (where the central CH_2 group faces the apical PMe_3 group) is calculated to have a longer Fe–Fe bond distance. In the *pdt 1* system this difference is only 0.0003 Å. The difference becomes more marked as the steric bulk of the dithiolate bridge increases, with a 0.01 Å difference in the $[Fe_2(\mu-dmpdt)(CO)_4(PMe_3)_2]$ (*dmpdt 1*) system.

In all cases, in order to rotate the $Fe(CO)_2(PMe_3)$ moiety the Fe–Fe bond distance significantly increases. Examining the HOMO of the ground and rotated states, upon rotation the electron density associated with the Fe–Fe bond is disrupted (see Figure 3.21) which would increase the bond distance.

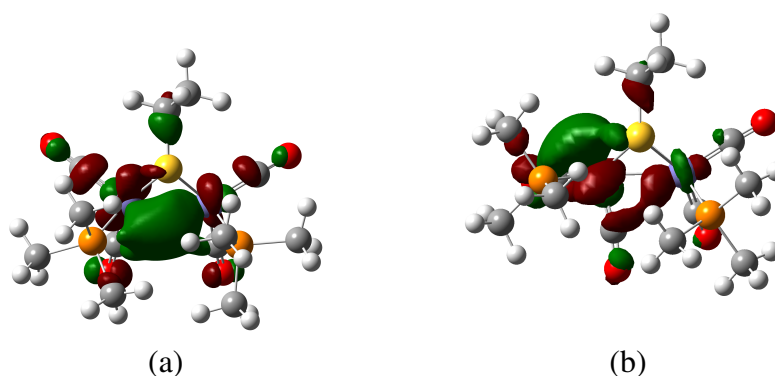


Figure 3.21: HOMOs of (a) isomer *pdt 1C* and (b) *pdt TS_{1A-1C}* of the *pdt 1* model complex.

3.5 Relative stabilities of $[(H)Fe_2(\mu-Xdt)(CO)_4(PMe_3)_2]^+$ subsites

In the following sections, the bridging hydrides (**2**), terminal hydrides (**3**), thiol isomers (**4**) and formyl isomers (**5**) are reported for the *pdt* dithiolate bridged system. Based on the relative stabilities of these, bridging and terminal hydrides of the *edt*, *odt*, *mpdt*, *dmpdt*

and mpdt-S bridged systems are then investigated.

3.5.1 The $[(H)Fe_2(\mu-pdt)(CO)_4(PMe_3)_2]^+$ subsite

Bridging-hydride isomers

Like pdt **1**, there are five phosphine positional isomers of $[(\mu-H)Fe_2(\mu-pdt)(CO)_4(PMe_3)_2]^+$, pdt **2** in which both irons have octahedral geometry (see Figure 3.23). The X-ray crystal structure of the pdt bridged system gave the PMe_3 ligands in an a basal/basal-*transoid* arrangement [69]. With respect to the calculations, the presence of the bridging hydride seems to increase their energy separation relative to those of **1** (see Table 3.1 and Table 3.7). In agreement with the crystal structure, all functionals [118] find the **2D** isomer to be the most stable. In the case of the TPSS functional by 5.3 kcal/mol, suggesting that at higher temperatures the other isomers would isomerise to this. The TS energy barrier for rotating $Fe(CO)_2(PMe_3)$ in pdt **2** is significantly higher in energy than predicted in pdt **1**, ranging from 24 – 31 kcal/mol (see Table 3.7). During these rotations, the CO group is hampered from moving into the semi-bridging position by the presence of the bridging hydride. As such, the intermediate is not stabilised by the π -accepter interaction, the Fe–Fe bond is elongated and the Fe–H bond lengths become more asymmetric relative to both irons. The flipped isomer **2A'** is almost isoenergetic with pdt **2A** and the energy barrier associated with the flip is 12.3 kcal/mol, 2.6 kcal/mol lower in comparison to pdt **TS**_{1A–1A'}.

Wright *et al.* recorded stopped-flow IR over a three minute duration in CH_3CN , and suggested that pdt **1A** was rapidly protonated to form an intermediate species before slowly isomerising to the thermodynamic product. The kinetic product was reported to give two peaks at 2001 cm^{-1} and 2055 cm^{-1} while the peaks of the thermodynamic product were shifted slightly downfield, at 1990 cm^{-1} and 2031 cm^{-1} [67].

Like their unprotonated counterparts, all of the bridging hydride isomers exhibit four $\nu(CO)$ spectral features. The simulated spectrum of pdt **2D** is in excellent agreement with the experimental spectrum, producing two unresolvable bands at 1996 cm^{-1} and two un-

resolvable bands at 2035 cm^{-1} (see Figure 3.22). Isomers pdt **2A**, pdt **2A'**, pdt **2C** and pdt **2C** give a near identical simulated spectrum, with four bands at 1996, 2000, 2033 and 2050 cm^{-1} (Table 3.6). Considering the relative energies of pdt **2** and the corresponding energy barriers to rotation it seems possible for any of the isomers, or a mixture of them could produce the observed experimental spectrum for the kinetic product, before rearranging to the thermodynamic product. Time-resolved $^{31}\text{P}\{^1\text{H}\}$ NMR spectra of the reaction of pdt **1** with $\text{BF}_4\cdot\text{Et}_2\text{OH}$ in CH_3CN at 10°C indicated the initial formation of a mixture of three products. These were all thought to be bridging hydride species, assigned to pdt **2A**, pdt **2C**, and pdt **2D**. As the reaction progress was tracked, the signal associated with pdt **2D** was found to intensify while the other two signals weakened [67]. Neither the experimental IR or NMR spectra indicated any evidence for a terminal hydride species, although during the postulated isomerisation to pdt **2A** a semi-bridging hydride species was suggested [67].

Table 3.6: *DFT simulated $\nu(\text{CO})$ bands of $[(\mu\text{-H})Fe_2(\mu\text{-pdt})(\text{CO})_4(\text{PMe}_3)_2]^+$ isomers compared to those experimentally determined in CH_3CN [68].*

Isomer		$\nu(\text{CO})/\text{cm}$			
Exp._K	2001				2055
Exp._T	1989				2031
2A	1996	2000	2033		2049
2A'	1996	2001	2033		2049
2B	2004 ⁿ	2014	2039		2058
2C	1996	2002	2035		2049
2D	1996	1997	2032		2042 ⁿ

ⁿ indicates a band of negligible intensity

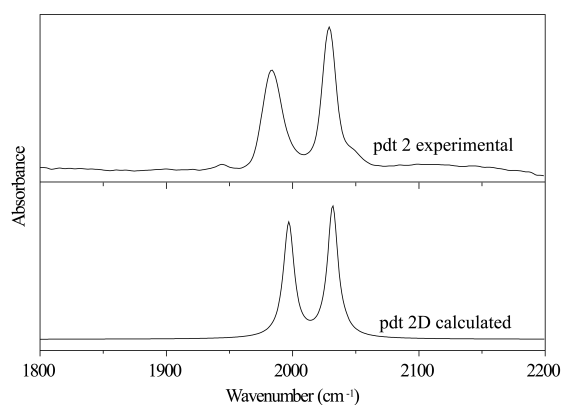


Figure 3.22: Comparison of the experimental IR spectra [68] of $[(H)Fe_2(\mu-(pdt)(CO)_4(PMe_3)_2)]^+$ with the simulated spectra of isomer **1D**.

The deviation of the calculated bond lengths of pdt **2D** with the X-ray crystallographic data [69] is found to be less than 0.034 Å, with the TPSS functional giving the best agreement (Table 3.8). The calculated Fe–Fe bond length is similar in all isomers of pdt **2** and elongated by an average of 0.05 Å relative to isomers of pdt **1**. The calculated Fe–H bond length is predicted to be approximately equal between the two iron centres and averages at 1.67 Å. Fe–S, Fe–C and Fe–P bond lengths are all observed to increase by an average of 0.02, 0.02 and 0.03 Å, respectively, relative to the unprotonated isomers.

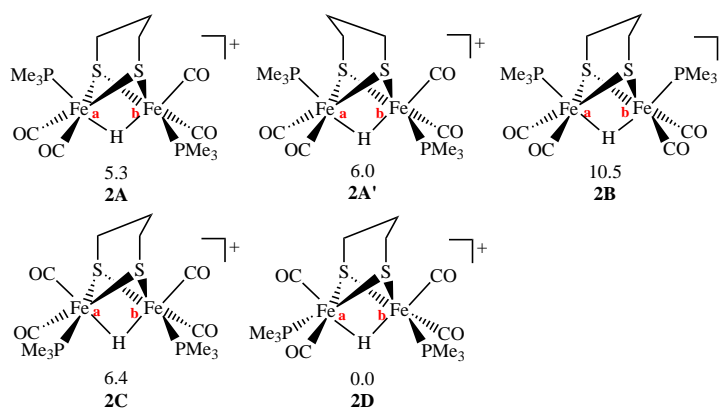


Figure 3.23: Isomers of $[(\mu-H)Fe_2(\mu-pdt)(CO)_4(PMe_3)_2]^+$. Relative free energies and bond distances are reported in Table 3.7.

Table 3.7: Selected bond lengths and calculated gas phase and solvent corrected free energies of the bridging hydride isomers $[(\mu-H)Fe_2(\mu-pdt)(CO)_4(PMe_3)_2]^+$. Also included the free energy barriers associated with the rotation of the $Fe(CO)_2(PMe_3)$ moiety and the pdt bridge flip. Energies are relative to **2D**. A comparison with the B3LYP functional is also included [119].

Isomer	B3LYP				TPSS		
	Free Energies (kcal/mol)				bond length / Å		
	ΔG_g	ΔG_{solv}	ΔG_g	ΔG_{solv}	Fe-Fe	Fe _a -H	Fe _b -H
2A	4.1	5.2	4.9	5.3	2.586	1.655	1.661
2A'	4.3	7.1	5.0	6.0	2.588	1.672	1.654
2B	10.9	10.3	11.2	10.5	2.580	1.644	1.656
2C	3.4	3.8	4.9	6.4	2.609	1.681	1.699
2D	0.0	0.0	0.0	0.0	2.599	1.696	1.678
TS _{2A→2B}	24.6	24.0	29.2	28.7	2.640	1.637	1.693
TS _{2A→2C}	24.1	24.4	27.1	27.2	2.647	1.702	1.649
TS _{2A→2D}	20.8	21.7	25.1	26.2	2.637	1.697	1.648
TS _{2C→2D}	23.8	24.1	28.2	28.9	2.679	1.719	1.682
TS _{2A'→2C}	21.6	21.9	25.2	25.2	2.651	1.647	1.722
TS _{2A'→2D}	20.2	21.0	23.0	24.1	2.643	1.644	1.717
TS _{2A'→2B}	28.7	29.0	31.3	31.9	2.637	1.679	1.642
TS _{2A→2A'}	3.9	4.2	12.0	12.3	2.600	1.663	1.675
TS _{2B→2B}	12.4	11.7	18.4	17.2	2.594	1.657	1.657
TS _{2C→2C}	6.2	7.4	7.8	9.8	2.626	1.699	1.699
TS _{2D→2D}	6.8	6.9	9.8	9.8	2.614	1.687	1.687

Table 3.8: Comparison of selected geometric parameters from x-ray crystallography study [69] with calculated values the **2D** isomer of $[(\mu-H)Fe_2(\mu-pdt)(CO)_4(PMe_3)_2]^+$.

	bond length/Å					bond angle/°	
	Fe-Fe	Fe-S _{av}	Fe-CO _{av}	Fe-P _{av}	Fe-H _{av}	S-Fe-S	Fe-S-Fe
Exp.	2.5786	2.2705	1.7850	2.2516	1.7089	85.046	69.199
B3LYP	2.6300	2.3281	1.7881	2.3198	1.6804	85.152	68.784
TPSS	2.6046	2.3042	1.7782	2.2296	1.6867	85.086	68.858

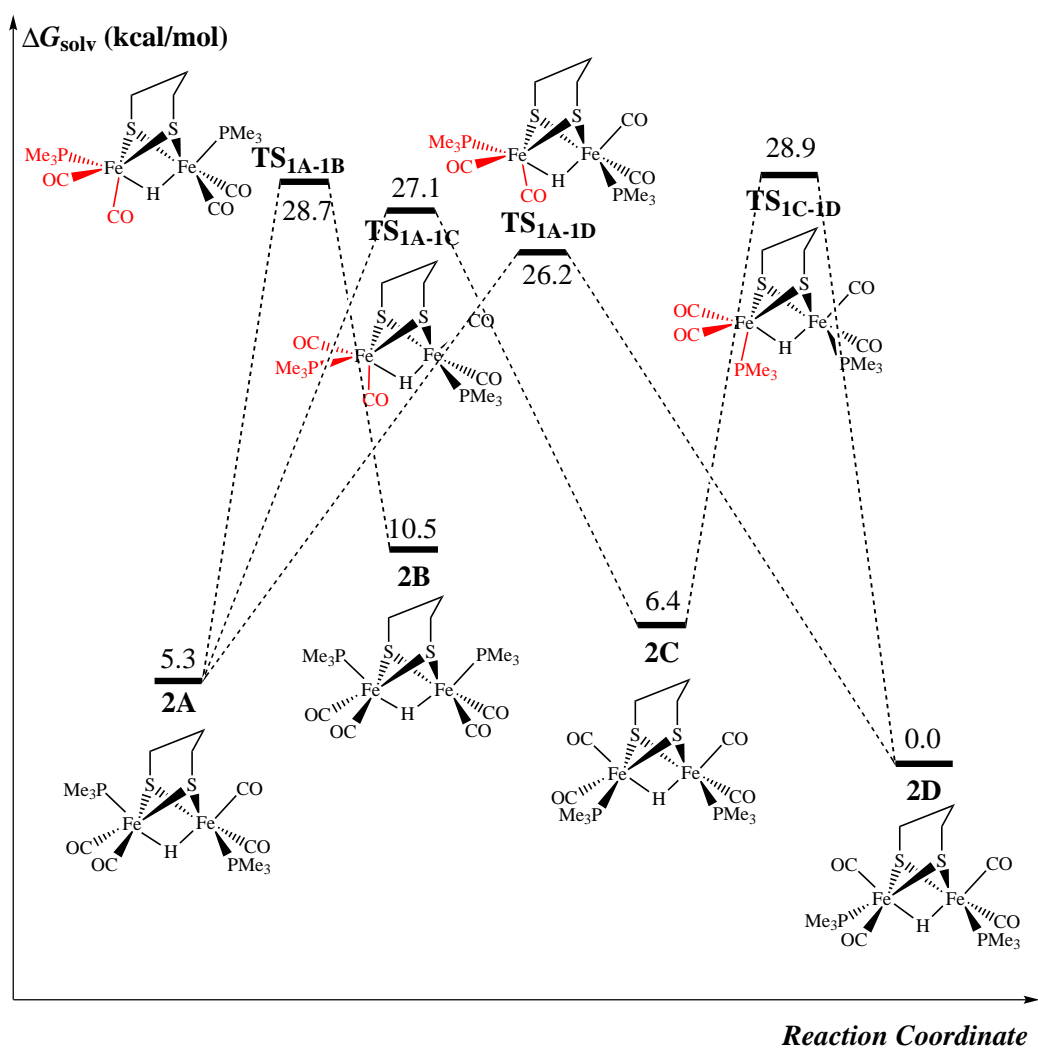


Figure 3.24: Energy profile for the interconversion of the isomers of **2** through the rotation of the $Fe(CO)_2(PMe_3)$ moiety. Free energies are reported in kcal/mol relative to **2D**. Groups coloured red indicate the positional change characterising the transition state.

Terminal hydride isomers

Crystallographic studies on the enzyme by Fontecilla-Camps and co-workers first led to the suggestion of terminal protonation [56]. Since then several groups have reported the proton binding to a single Fe centre in a terminal position in model complexes [74, 95, 98, 129–131]. DFT calculations were carried out on eighteen isomers of $[HFe_2(\mu-pdt)(CO)_4(PMe_3)_2]^+$ in which the hydride is terminally bound. In order to facilitate the hydride group in the apical site, a partial rotation of the $Fe(CO)_2(PMe_3)$ unit must first occur, moving a basal CO group into the semi-bridging position. In order to accommodate the hydride in the basal position no rotation is necessary, instead a terminal CO group must swing across into the semi-bridging position. The rotated iron takes on a face-bridged octahedral geometry, while the other iron retains its octahedral geometry (square pyramidal if the bridging hydride is counted as being coordinated). Comparison of the free energies of pdt **3** shows the basal/basal *transoid* isomers to be on average, the most stable of the group. However, it is the position of the hydride has the most significant effect on the relative stability of the isomers. Having the hydride positioned in the apical position results in the lowest energy. The energy is further reduced if the pdt linker is pointing toward the less sterically bulky group. For example, flipping the pdt linker from pointing toward the CO group in pdt **3D1** to facing the hydride in pdt **3D1'** lowers the energy by 1.7 kcal/mol. In comparison with the bridging hydrides pdt **2**, the Fe–Fe bonds in the terminal hydrides are shorter on average, but still longer than in the unprotonated species, pdt **1**. The semi-bridging CO is always found to be closer to the protonated iron by an average of 0.03 Å, while the Fe–H bond length is shorter on average by 0.19 Å compared to isomers of pdt **2**. Sampling of the potential energy surface led to the discovery of an additional six high energy isomers (see Figure A2). In these structures, the hydride bound iron adopts a trigonal prismatic geometry, while the other iron retains its square pyramidal geometry. The PMe_3 group adjacent to the hydride takes on a semi-bridging position, and the presence of this steric bulk increases the Fe–Fe bond length on average by 0.04 Å.

The simulated IR of the terminal hydrides pdt **3** all produce 5 bands in the carbonyl region (see Table 3.10). In each case the 2 lowest energy bands both correspond to a mix-

Table 3.9: Selected bond lengths and calculated gas phase and solvent corrected free energies of the terminally protonated isomers of $[(H)Fe_2(\mu-pdt)(CO)_4(PMe_3)_2]^+$. Energies are relative to **2D**.

Isomer	B3LYP				TPSS			
	Free Energies (kcal/mol)				bond length/Å			
	ΔG_g	ΔG_{solv}	ΔG_g	ΔG_{solv}	Fe-Fe	Fe-H	Fe _a - μ CO	Fe _b - μ CO
3A1	25.2	25.1	21.6	21.0	2.543	1.506	2.314	1.792
3A1'	25.8	25.6	20.1	20.3	2.525	1.502	2.205	1.817
3A2	24.9	24.7	21.1	20.3	2.552	1.502	2.342	1.791
3A2'	24.2	24.6	19.4	19.5	2.538	1.498	2.245	1.811
3A3	21.9	21.3	17.1	16.8	2.562	1.513	1.802	2.445
3A3'	21.5	22.0	17.6	18.4	2.575	1.516	1.801	2.532
3A4	24.8	24.1	21.2	20.9	2.553	1.501	1.781	2.450
3A4'	24.1	24.6	20.4	21.0	2.570	1.504	1.778	2.580
3B	31.0	30.4	26.2	25.4	2.538	1.497	1.799	2.311
3B'	29.2	29.0	25.7	25.0	2.552	1.501	1.786	2.410
3C1	20.7	20.2	17.3	16.6	2.583	1.514	1.801	2.530
3C1'	19.2	19.4	15.6	15.1	2.566	1.513	1.808	2.423
3C2	22.7	23.0	21.2	21.6	2.613	1.505	1.778	2.609
3C2'	22.1	23.0	20.7	21.3	2.583	1.503	1.786	2.445
3D1	17.6	18.1	13.6	14.4	2.571	1.515	1.798	2.487
3D1'	16.6	17.2	12.0	12.7	2.556	1.513	1.805	2.394
3D2	18.7	19.1	16.1	17.1	2.556	1.506	1.774	2.496
3D2'	18.4	19.3	15.9	17.2	2.537	1.504	1.786	2.364

ture of bridging CO and terminal hydride vibrations. Since the kinetic product observed in the stopped-flow IR study of Pickett and co-workers [67] did not give a peak of such low intensity it seems more likely that it corresponds to a bridging hydride.

Table 3.10: DFT simulated $\nu(CO)$ bands of the terminally protonated isomers of $[(H)Fe_2(\mu-pdt)(CO)_4(PMe_3)_2]^+$ compared to those experimentally determined in CH_3CN [68].

Isomer		$\nu(CO)/cm^{-1}$				
Exp._K	2001				2055	
Exp._T	1989				2031	
3A1	1922	1969	2000	2026	2051	
3A1'	1902	1990	2003	2022	2050	
3A2	1931	1988	2000	2015	2048	
3A2'	1915	1999	2002	2011	2047	
3A3	1939	1989	2004	2035	2053	
3A3'	1942	1985	2004	2034	2052	
3A4	1946	1999	2006	2019	2048	
3A4'	1961	1995	1999	2018	2045	
3B	1947	2005 ⁿ	2009	2022	2053	
3B'	1961	1993 ⁿ	2008	2025	2053	
3C1	1936	1996	2001	2037	2052	
3C1'	1924	1988	1999	2037	2051	
3C2	1952	1991	1994	2019	2043	
3C2'	1934	1996	2000	2018	2044	
3D1	1925 ⁿ	1986	1999	2031	2045	
3D1'	1915 ⁿ	1979	2001	2031	2045	
3D2	1928	1985	1996	2022	2039 ⁿ	
3D2'	1910	1994	1998	2018	2040 ⁿ	

ⁿ indicates a band of negligible intensity

Table 3.11: Selected bond lengths and calculated gas phase and solvent corrected free energies of the isomers of $[(H)Fe_2(\mu-pdt)(CO)_4(PMe_3)_2]^+$. Energies are relative to **2D**.

Isomer	Free Energies (kcal/mol)		bond length/Å	
	ΔG_g	ΔG_{solv}	Fe–Fe	Fe–H
3A5	28.3	28.3	2.602	1.505
3A5'	37.6	36.6	2.686	1.505
3D3	27.5	27.1	2.663	1.503
3D3'	31.0	30.7	2.652	1.502
3D4	30.0	29.9	2.681	1.506
3D4'	29.1	29.8	2.676	1.507

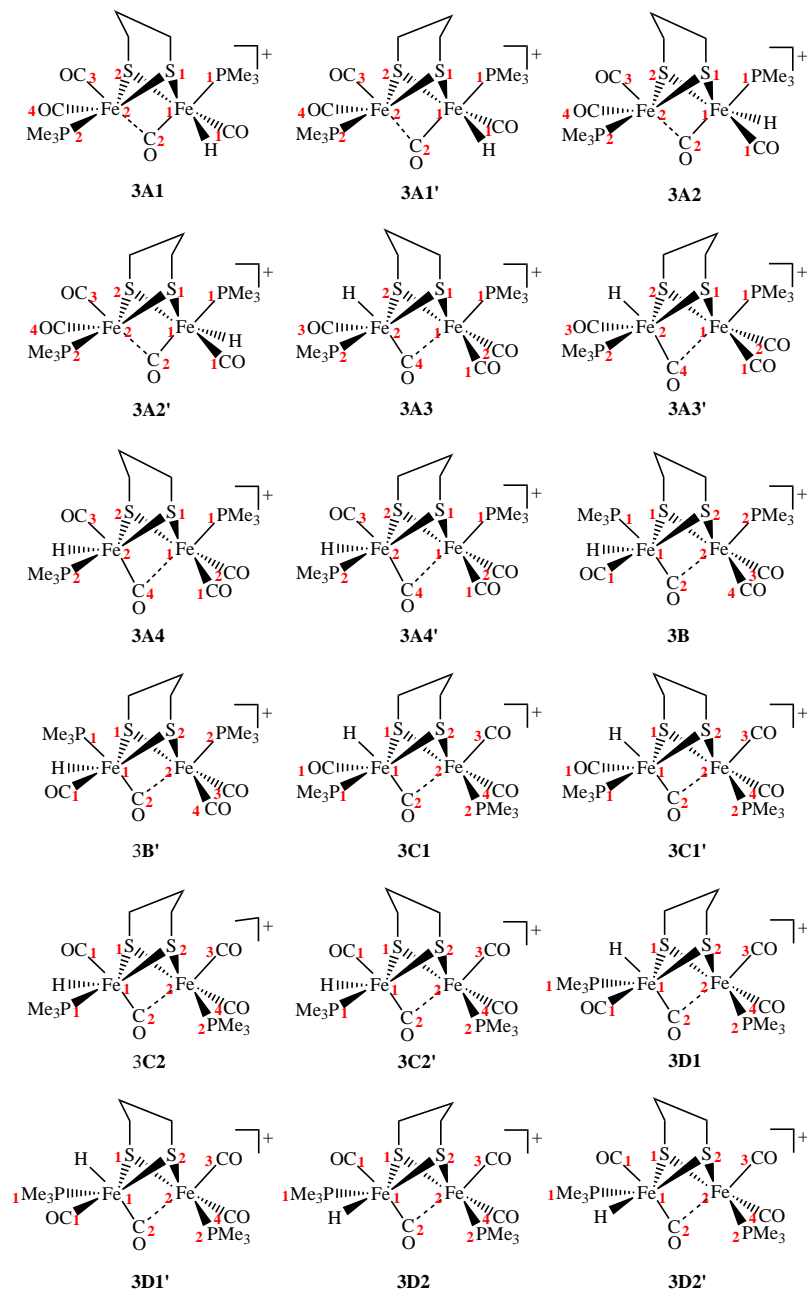


Figure 3.25: Isomers of the terminally protonated $[(H)Fe_2(\mu-pdt)(CO)_4(PMe_3)_2]^+$. Relative free energies and bond distances are reported in Table 3.7. Selected bond distances and bond angles are reported in Table A23 and Table A24, respectively.

Protonated sulphur and protonated carbonyl isomers

Lui considered protonation to either of the sulphur atoms in the dithiolate bridge, and found eight high energy isomers (see Figure 3.26) [118]. All of the isomers were found to have similar energies, around 29 kcal/mol higher in energy than **2D**. Interestingly, the two basal/basal *cisoid* isomers, **4C1** and **4C2** were found to be around 4 kcal/mol less stable than the others [118]. Due to the high energies of these isomers relative to the **2D** isomer, protonation to the sulphur was not modelled using the TPSS functional.

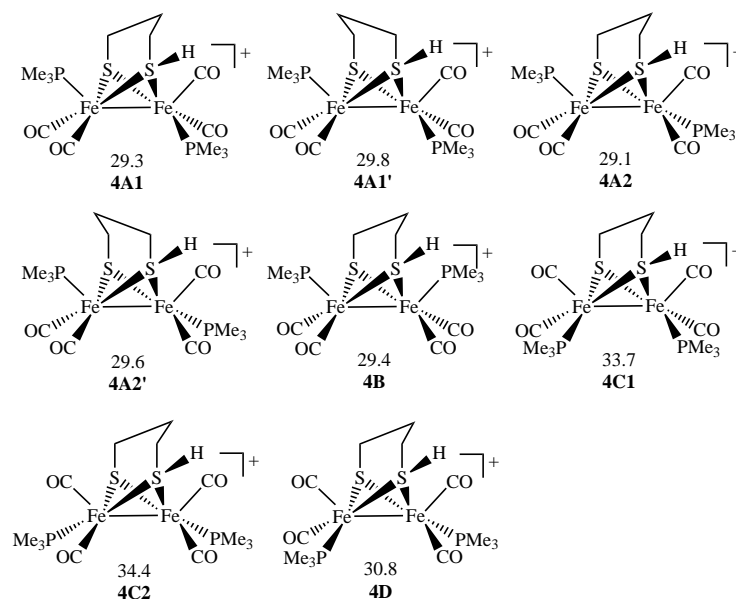


Figure 3.26: Relative solvent corrected free energies of the sulphur protonated isomers of $(\mu\text{-SCH}_2\text{CH}_2\text{SH})Fe_2(CO)_4(PMe_3)_2^+$ calculated using the B3LYP functional by Lui [118]. Energies are reported relative to **2D** of the same functional, and are reported in kcal/mol.

Best and Pickett have previously reported the possibility for the CO ligand to be protonated to produce a formyl species [85]. Lui calculated the energies of the formyl isomers and found them to be of the highest energy of all the protonated species (Figure 3.27) [118]. It was found that when the terminal CO group at the basal position is protonated, as in **5A3**, **5B1** and **5B2** (see Figure 3.27), the distance between this CO group and the iron is lengthened and the energy is even higher. A second class of isomers have the Fe–Fe bond broken and formation of a four-member ring, composed of two Fe atoms and C=O. The distance between two iron atoms averages 3.145 Å, and the Fe–O distance averages 2.051 Å. Although the second class of isomers presents species with free energies slightly lower than the S-protonated species, these formyl species may be difficult to generate because

Fe–Fe bond breaking will likely lead to a significant barrier. Formyl species of the first class may be kinetically accessible, but they are among the least stable protonated species (note that reduction of the system will stabilise these formyl species [132]).

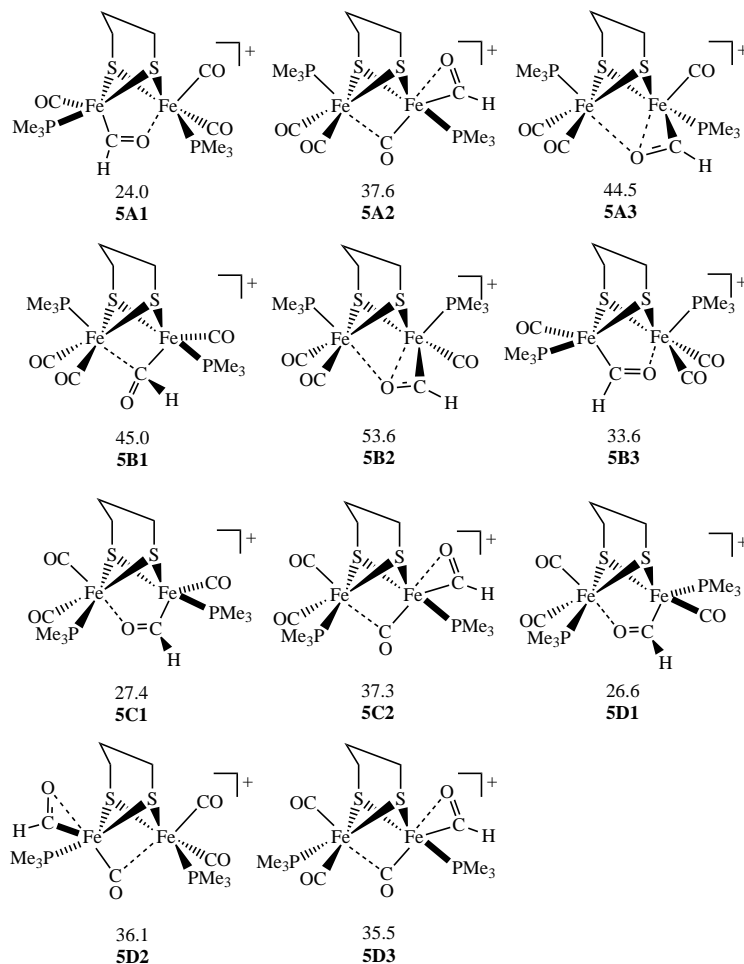


Figure 3.27: Relative solvent corrected free energies of the formyl isomers of $[(\mu\text{-pdt})Fe_2(COH)(CO)_3(PMe_3)_2]^+$ calculated using the B3LYP functional by Lui [118]. Energies are reported relative to **2D** of the same functional, and are reported in kcal/mol.

It is likely that neither the S–H or CHO species would be generated because of their high energy and, as there are numerous alternative reaction pathways significantly lower in energy. Therefore, these are not investigated for the other bridge types, nor is the mechanism in which they would be produced.

3.5.2 $[(H)Fe_2(\mu-Xdt)(CO)_4(PMe_3)_2]^+$ subsites

With respect to the relative energies and geometric parameters, the protonated isomers with the different dithiolate bridge head groups parallel the behaviour of the parent unprotonated isomers. Tables of IR and comparisons between experimental and calculated geometric parameters are reported in the appendix.

3.6 Summary and conclusions

With the aid of the density functional theory (DFT) calculations, the isomers for the family of $[FeFe]$ hydrogenase model complexes, $[Fe_2(\mu-(Xdt)(CO)_4(PMe_3)_2)]$ ($X = \text{edt, pdt, odt, mpdt, dmpdt}$ and mpdt-S), along with their protonated analogues have been studied in detail. It has been demonstrated that the IR spectra can be accurately predicted in terms of both peak position and intensity, and that the crystal structure can be accurately modelled with the computational parameters implemented. Analysis of the Mulliken charges of the unprotonated subsites indicated that the Fe is more electron rich when it has an apically coordinated PMe_3 group as opposed to CO. This is thought to be a consequence of the stronger electron withdrawing nature of CO relative to PMe_3 when in a position *transoid* to the Fe–Fe bond. The Fe centres are also predicted to become more electron rich as the Φ angle increases and is most pronounced during the rotation of the $Fe(PMe_3)(CO)_2$ moiety. Notably, increasing the steric bulk of the dithiolate bridge is coupled with an increase in the Ψ angle, which serves to enrich the rotated Fe centre. It is possible for a ratchet type mechanism to exist where, as the dithiolate bridge flips, the steric clash causes a partial rotation of the $Fe(PMe_3)(CO)_2$ moiety, thus enriching the Fe centre and making it a more attractive site for protonation.

The calculations show that the isomers of the sulphur-hydrides and formyl species are much less stable than the bridging or terminal hydrides. Furthermore, for bridging and terminal hydrides, the basal/basal *transoid* forms are found to be thermodynamically more stable than other corresponding isomers. This prediction is consistent with the experimental observation for the bridging-hydride species. In the investigation of the dithiolate

bridges, it was found that there was little to no change in the νCO peak positions, indicating that the level of steric bulk located on the bridgehead does not effect the electron density at the Fe centres. This is a crucial observation as it implies that the differences in the kinetics of protonation observed experimentally for the edt, pdt and odt bridges does not result from the electronic effects of the bridgehead. It was observed that progressively loading the bridgehead with steric bulk lowered the energy barriers to rotation. These effects are important as the first step of terminal protonation is a rotation to provide a vacant site. Presumably, lowering the energy barrier of this initial step will lower the the barrier to protonation.

Chapter 4

Protonation mechanism of [Fe₂(μ-Xdt)(CO)₄(PMe₃)₂] model subsites

Protonation mechanisms that involve the formation of either bridging or terminal hydride species are discussed below. Transition states are characterised by having a single negative frequency. Intermediate species are connected to the transition states by following the IRC in both the forward and backward direction. Identifying a global minimum associated with a particular subsite isomer and the [Et₂OH]⁺ acid proved problematic. The PES around these global minimum structures were characteristically flat and featured many local minima. Notably in some cases, following the IRC led to some other intermediate structure whose energy was an intermediate to the transition state and the global minimum for the two fragments.

De Gioia, Schollhammer and their respective co-workers have previously investigated the protonation kinetics of terminal vs. bridging hydrides and found terminal hydrides to be kinetic products [91, 106]. Wright *et al.* reported the activation parameters associated with the protonation of [FeFe] hydrogenase subsites with edt, pdt and odt dithiolate bridgeheads. In each complex they found rapid protonation was followed by rearrangement to the thermodynamic product, but no evidence for terminal protonation. Notably, the activation parameters for the initial protonation and isomerisations were found to be

an order of magnitude faster for the pdt bridge compared to edt and odt bridges [104, 105]). These pathways will be analysed in the following sections along with the effect that the identity of the dithiolate linker has on the energy barriers of these pathways. The experimental work on the [(μ-pdt)Fe₂(CO)₄(PMe₃)₂] model subsite by Pickett and co-workers used [Et₂OH]⁺...[BF₄]⁻ as the acid and [CH₃CN] as the solvent [67, 105]. Due to the equilibrium thought to exist between the two solvated species, both acid and solvent were investigated by Liu as potential protonating species [118]. The free energy of [Et₂OH]⁺ was found to be lower than [CH₃CNH]⁺ (see Table 4.1). This difference in free energy suggests that [Et₂OH]⁺ is the preferred acid, despite the fact that CH₃CN is present in higher concentration. [Et₂OH]⁺ is therefore modelled exclusively as the acid in subsequent reactions. During its approach, the proton of the [Et₂OH]⁺ appears to coordinate to the oxygen of a carbonyl of the subsite, forming an intermediate species. The Φ angle of this intermediate species is modified, which appears to electronically enrich the rotated Fe centre. Proton transfer can proceed via one of two pathways to form the bridging hydride product (see Figure 4.1). The bridging path: involves proton transfer along the Fe-Fe bond to form a bridging hydride species. The alternative terminal path: involves the transfer of the proton to a terminal position, followed by isomerisation to the bridging hydride product. In order to make energy comparison possible throughout, the number of species at each stage of the reaction pathway was maintained. To this end, the diiron complex plus the ion pair ([Et₂OH]⁺...[BF₄]⁻) were modelled as the reactants, and the protonated diiron complex plus ion (Et₂O...[BF₄]⁻) were taken as the product. Energies of all isomers and transition states are reported relative to isomer **1A** in each system. The transition states were followed along the IRC leading to, in the backward direction, an intermediate species where the [Et₂OH]⁺ is coordinated to the oxygen of a basal CO ligand and, in the forward direction, to an intermediate species where the Et₂O is weakly coordinated to the iron bound hydride.

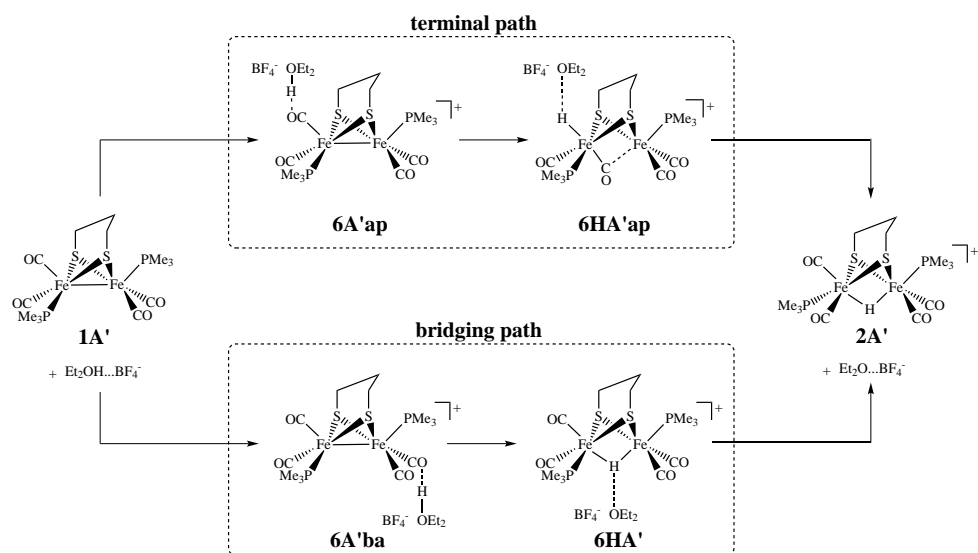


Figure 4.1: Possible ether mediated protonation pathways: terminal path and bridging path.

Table 4.1: Comparison of the relative stabilities between $[Et_2OH]^+$ and $[CH_3CNH]^+$ calculated at the B3LYP/6-31++G** level of theory $\Delta G_{solv}(H^+) = 260.2 \text{ kcal/mol} = -0.41465 \text{ Hartree}$.

	ΔG_{solv}
$H^+ + Et_2O \rightarrow [HOEt_2]^+$	17.8
$H^+ + CH_3CN \rightarrow [CH_3CNH]^+$	22.0

4.1 Computational details

All calculations have used the same computational parameters to those given in Chapter 3.2. In order to analyse reaction mechanism, the free energies in solution were used.

4.2 Protonation of the Fe–Fe bond to form bridging hydrides

Figure 4.2, Figure 4.3, Figure 4.4, and Figure 4.5 show the energetics of the reaction pathways leading to the formation of bridging hydrides pdt **2A**, pdt **2A'**, pdt **2B**, pdt **2C**, and pdt **2D**, respectively, through protonation of the Fe–Fe bond.

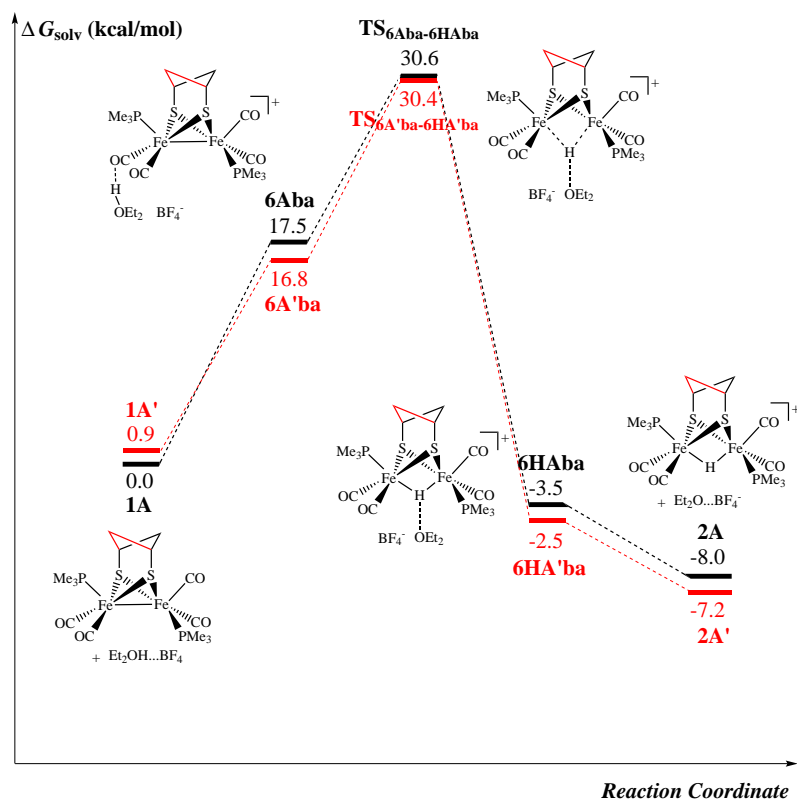
The energetics for protonating pdt **1A** along the Fe–Fe bond, forming pdt **2A** are outlined in Figure 4.2. The reaction proceeds through the intermediate pdt **6Aba** to pdt

TS_{6Aba-6HAb_a}, transferring the proton with a free energy barrier of 13.1 kcal/mol, with an absolute barrier to protonation of 30.6 kcal/mol. In forming the transition state pdt **TS**_{6Aba-6HAb_a} from pdt **6Aba**, the O–H bond is elongated by 0.27 Å and the proton moves from being weakly coordinated to the CO to a position asymmetrically beneath the Fe–Fe bond, 2.04 Å from Fe₁ and 2.50 Å from Fe₂ (transfer is presumably asymmetric due to the bulky PMe₃ ligand which the acid avoids). The initial product pdt **6HAb_a** is predicted to be an intermediate possessing a weak "H-bond" between the hydride and Et₂O. The product pdt **2A** is produced through the formation of the ether-ion pair Et₂O⋯[BF₄][−] (a more likely process is loss of the ether to the solvent, but this would mean explicitly modelling solvent molecules at every stage of the reaction). Throughout the reaction pathway, both PMe₃ groups maintain their apical/basal arrangement. Protonation along the Fe–Fe bond leads to the expansion of the bridging structure. In order to facilitate the steric bulk of the acid on approach the Fe–Fe bond lengthens slightly and the ligands on both irons tip away from the approaching acid. For example, comparing the structures pdt **6Aba** and pdt **TS**_{6Aba-6HAb_a}, the CO_{ba}–Fe₁–Fe₂–PMe₃ dihedral increases by 31.7°, and the Fe₁–Fe₂–CO_{ap} and Fe₂–Fe₁–PMe₃ bond angles decrease by 5.5° and 5.4° respectively. The flip of the pdt bridge (to face Fe₁ and the PMe₃ ligand) has a small effect on the energetics of the pathway, increasing the absolute barrier to protonation by 1.1 kcal/mol, although this is due to the difference in energy of pdt **1A** and pdt **1A'**. Comparison of the geometries of these transition states reveals that in the lower energy pathway (that of forming pdt **2A**), the Fe₁–H bond distance is 0.08 Å shorter, indicating a stronger bond to the Et₂O in this TS. pdt **6A'ba**, pdt **TS**_{6A'ba-6HA'ba}, and pdt **6HA'ba** show markedly similar geometric parameters to their bridge flipped analogues (see Figure 4.2). Interestingly, in both pdt **TS**_{6Aba-6HAb_a} and pdt **TS**_{6A'ba-6HA'ba}, [Et₂OH]⁺ is attacking Fe₁. Notably, this was found to be the more electronegative centre in the isolated subsites. Transition states for the alternative routes to produce pdt **2A** and pdt **2A'** which have the proton adding to the more electropositive iron centre, Fe₂, could not be found. In comparing the energetics of the two pathways with respect to the dithiolate bridgehead type (edt, pdt, odt and mpdt-S bridges investigated), the absolute energy barriers of protonation to form **2A** are lower for edt and odt, while in the formation of **2A'** they are higher (see Table B1). In the formation

of **2A'**, more structural distortion of the parent complex is present due to the direction of the bridge.

With both PMe₃ groups apically coordinated, the acid moiety is able to approach pdt **2B** relatively unhindered (see Figure 4.3). This is reflected by a relatively low absolute energy to protonation of 22.7 kcal/mol (7.8 kcal/mol lower in energy than in the formation of pdt **2A**). The acid approaches the Fe–Fe bond more symmetrically than in the formation of pdt **2A**. The same pathway is found to be 1.9 kcal/mol and 2.4 kcal/mol higher for the edt and odt bridges respectively (see Table B1). This difference is unlikely to be caused by an electronic influence of the bridgehead as the simulated IR of the carbonyl region in the isolated **2** systems showed negligible differences in peak position with varying bridge type. The difference must therefore arise from steric differences. Comparison of the geometric parameters of these transition states shows that in the edt and odt bridged systems, the O_{acid}–H bond is slightly stronger than in the pdt bridged system. While the absolute energy for protonation is computed to be higher by ca. 6 kcal/mol, the differences in barrier height between the different bridgeheads is in complete accord with the kinetics observed experimentally by Pickett and co-workers [67, 105].

The rotational energy barriers for interconverting bridging hydrides were discussed in Chapter 3.3.1. Recall that in order for pdt **2B** to convert to the thermodynamic product, pdt **2D**, both iron centres must undergo a Bailar twist, sequentially forming pdt **2A** and pdt **2D**. The energy barrier for the initial Bailar twist that forms pdt **2A** is predicted to have a height of 18.2 kcal/mol, this is 7.7 kcal/mol lower than the barrier associated with direct protonation to the Fe–Fe bond that produces pdt **2A'**. Notably, during this rotation, the pdt linker is facing the rotating iron centre. The alternative transition state, pdt **TS_{2B→2A'}** with the pdt linker facing away from the rotating iron has a barrier 7.7 kcal/mol higher in energy (see Table 4.2). The second Bailar twist is also predicted to be energetically more favourable when the pdt linker faces the rotating iron, giving energy barrier heights of 26.2 and 18.1 kcal/mol from pdt **2A** → **2D** and **2A'** → **2D**, respectively. In order to rotate from pdt **2A'**, a bridge flip must first occur, doing so with a low 7 kcal/mol energy bar-



(a)

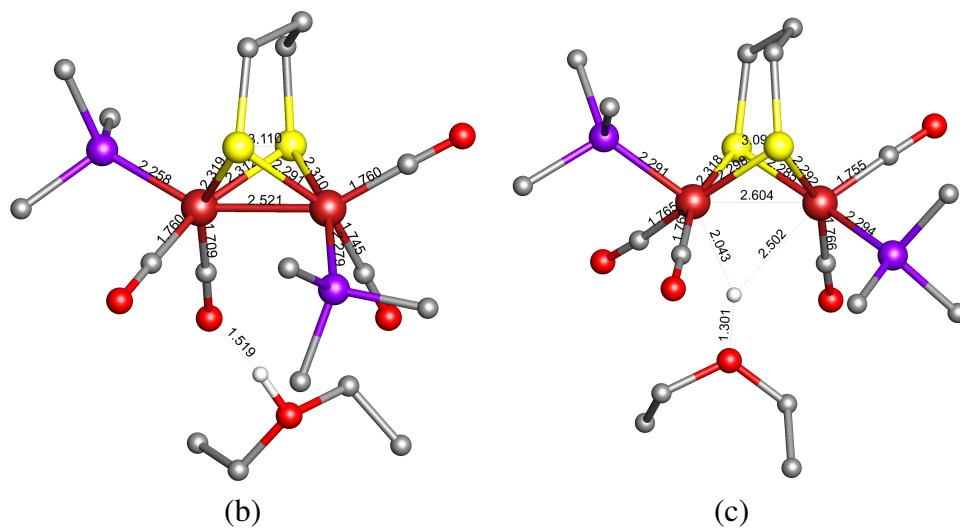


Figure 4.2: (a) Energy profile for the formation of **2A** and **2A'** through the diethyl ether mediated protonation of **1A** and **1A'** to the Fe–Fe bond. Energies are given in kcal/mol relative to **1A**; and optimised geometries of the (b) ether mediated intermediate (**6Aba**) and the (c) transition state (**TS_{6Aba-6HAba}**). For clarity, hydrogen atoms of the PMe_3 groups and the ether have been omitted, bond distances are reported in Å.

rier. These rotational barriers for rearrangement are lower than for the energy barrier for direct protonation to form pdt **2B**. This is inconsistent with the experimental kinetics data observed for the pdt bridged system, characterised by a rapid protonation, followed by a slower isomerisation process [67]. However, in comparing the reaction pathway of the pdt bridge with edt and odt bridges, good agreement with the experimental observations is seen [105]. The initial rotation of pdt **2B** → **2A** is computed to be 3.6 and 5 kcal/mol higher for edt and odt bridges, respectively. Additionally, the rotation of pdt **2A'** → **2D** is computed to be 3.1 and 4.5 kcal/mol higher for edt and odt bridges, respectively.

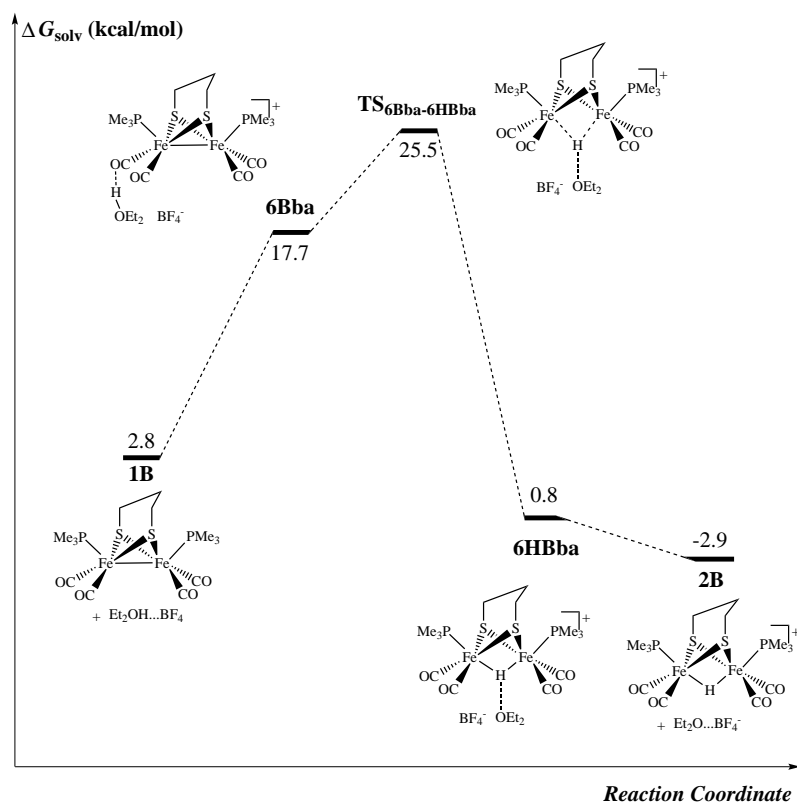
Table 4.2: Free energy comparison between the pdt, edt and odt dithiolate bridge in the isomerisation pathways from kinetic products **3C2**^(s) leading to the thermodynamic product **2D**. Energies are reported in kcal/mol.

Reaction coordinate	pdt	edt	odt
TS _{2B→2A}	18.2	21.8	23.2
TS _{2B→2A'}	25.9	21.8	21.5
TS _{2A→2A'}	7.0	-	10.0
TS _{2A→2D}	26.2	21.2	20.7
TS _{2A'→2D}	18.1	21.2	22.6

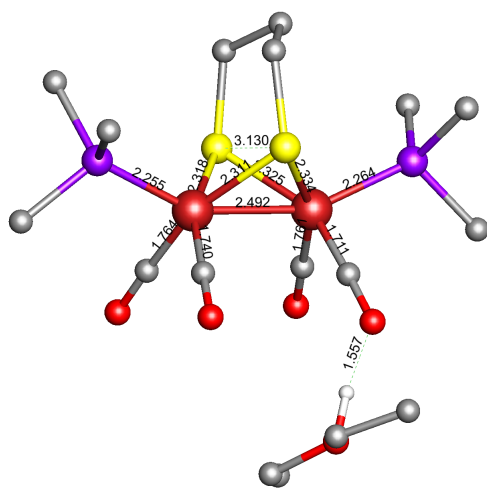
Table 4.3: Comparison of the calculated gas phase and solvent corrected free energies and iron Mulliken charges of the TS_{6Bba→6HBba} for pdt, edt and odt dithiolate bridges.

Isomer	ΔG_{solv} (kcal/mol)	Mulliken charges	
		Fe ₁	Fe ₂
pdt TS _{6Bba→6HBba}	22.7	-0.866	-0.841
edt TS _{6Bba→6HBba}	24.6	-0.904	-0.850
odt TS _{6Bba→6HBba}	25.1	-0.869	-0.750

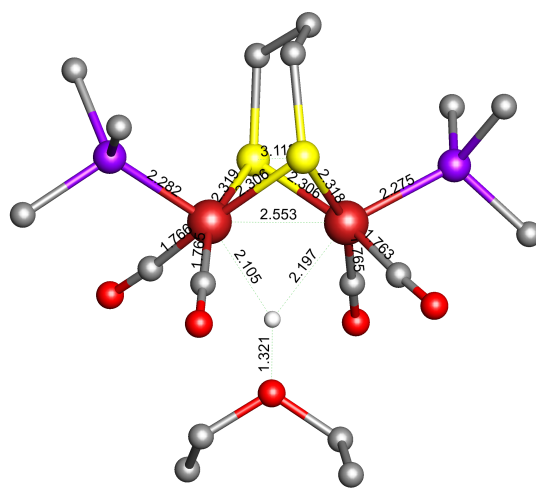
[Et₂OH]⁺ attacks pdt **1C** via intermediate pdt **6Cba**, and the subsequent proton transfer occurs in pdt TS_{6Cba→6HCba} with an absolute free energy barrier of 32.3 kcal/mol. This is 11.9 kcal/mol higher than the absolute barrier found in the formation of pdt **2B**. In this pathway, the acid approaches from beneath the Fe–Fe bond from the carbonyl side (avoiding the steric bulk of the PMe₃ ligands) and the proton is asymmetrically transferred to the Fe–Fe bond, more strongly associated with Fe₁. The corresponding pathways for the edt and odt were found to be 0.9 kcal/mol and 1.5 kcal/mol lower, respectively. Comparing the transition state structures for the different bridges shows that the pdt bridged system



(a)



(b)



(c)

Figure 4.3: (a) Energy profile for the formation of **2B** through the diethyl ether mediated protonation of **1B** to the Fe-Fe bond. Energies are given in kcal/mol relative to **1B**; and optimised geometries of the (b) ether mediated intermediate (**6Bba**) and the (c) transition state (**TS_{6Bba-6HBba}**). For clarity, hydrogen atoms of the PMe_3 groups and the ether have been omitted, bond distances are reported in Å.

Table 4.4: Comparison of selected bond distances of the $TS_{6Bba \rightarrow 6HBba}$ for pdt, edt and odt dithiolate bridges.

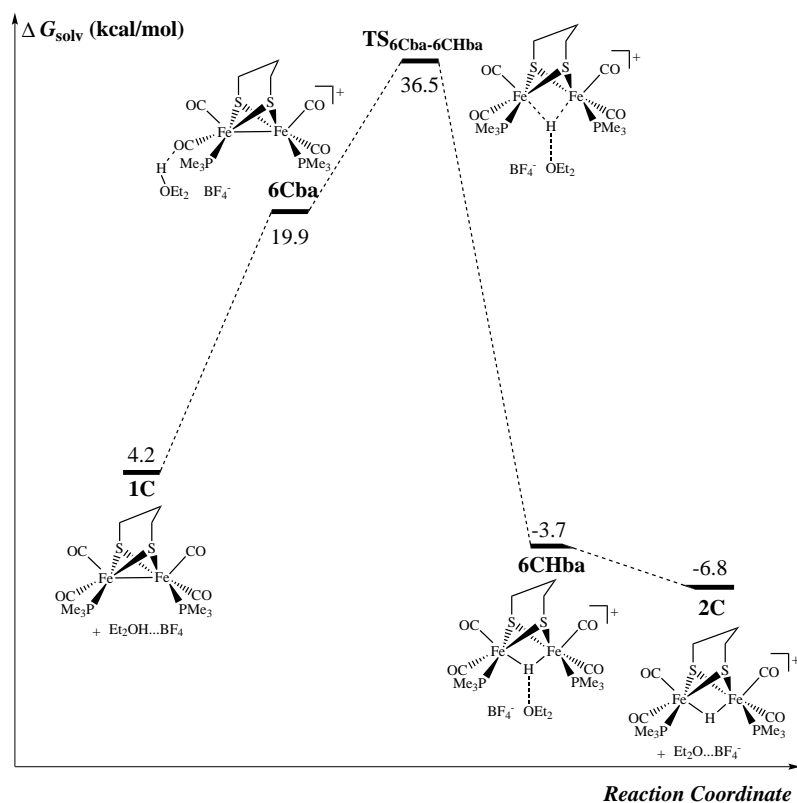
bond length/Å	pdt $TS_{6Bba \rightarrow 6HBba}$	edt $TS_{6Bba \rightarrow 6HBba}$	odt $TS_{6Bba \rightarrow 6HBba}$
Fe ₁ -Fe ₂	2.6772	2.6640	2.6856
Fe ₁ -S ₁	2.2800	2.2712	2.2787
Fe ₁ -S ₂	2.3159	2.2718	2.2801
Fe ₂ -S ₁	2.2933	2.2770	2.2865
Fe ₂ -S ₂	2.2663	2.2745	2.2870
Fe ₁ -H	2.1358	2.4061	2.4551
Fe ₂ -H	2.5257	2.2970	2.2877
Fe ₁ -CO ₁	1.7638	1.7559	1.7545
Fe ₁ -CO ₂	1.7612	1.7631	1.7655
Fe ₂ -CO ₁	1.7544	1.7590	1.7717
Fe ₂ -CO ₂	1.7576	1.7629	1.7594
Fe ₁ -P ₁	2.3166	2.2963	2.3021
Fe ₂ -P ₂	2.3176	2.2983	2.2975

Table 4.5: Comparison of selected bond angles of the $TS_{6Bba \rightarrow 6HBba}$ for pdt, edt and odt dithiolate bridges.

bond angle/°	pdt $TS_{6Bba \rightarrow 6HBba}$	edt $TS_{6Bba \rightarrow 6HBba}$	odt $TS_{6Bba \rightarrow 6HBba}$
∠ S ₁ -Fe ₁ -S ₂	84.9208	80.9957	85.5787
∠ S ₁ -Fe ₂ -S ₂	85.7595	80.8162	85.2385
∠ Fe ₁ -S ₁ -Fe ₂	71.6609	71.7069	72.0681
∠ Fe ₁ -S ₂ -Fe ₂	71.4922	71.7415	72.0343
∠ Fe ₁ -Fe ₂ -C ₃	141.7411	137.7865	137.3680
∠ Fe ₁ -Fe ₂ -C ₄	117.1888	111.2271	112.4413
∠ Fe ₁ -Fe ₂ -PMe ₃	112.7391	117.6320	118.7305
∠ Fe ₂ -Fe ₁ -C ₁	132.6249	138.4605	136.7393
∠ Fe ₂ -Fe ₁ -C ₂	104.4013	112.5093	113.9190
∠ Fe ₂ -Fe ₁ -PMe ₃	131.6760	116.7428	117.3991
∠ L-Fe ₁ -Fe ₂ -L	27.1143	10.7793	10.7836

has the strongest O_{acid} -H bond. Transition states with edt and odt dithiolate bridges have O_{acid} -H bonds ca. 0.03 Å longer.

Formation of the most stable protonated species, pdt **2D** (see Figure 4.5) proceeds from intermediate pdt **6Dba**, to pdt $TS_{6Dba \rightarrow 6HDba}$, transferring the proton with a free energy barrier of 18.2 kcal/mol and an absolute energy barrier of 35.2 kcal/mol, the highest bridging pathway energy barrier. The structure of the intermediate pdt **6Dba** is interesting as the $[Et_2OH]^+$ coordinated CO group is partially semi-bridging (see Figure 4.5(b)) with a C-Fe_{semi-coord} bond distance that is 0.28 Å, 0.26 Å, 0.22 Å, and 0.23 Å shorter than those calculated in pdt **6Aba**, pdt **6A'ba**, pdt **6Bba** and pdt **6Cba**, respectively. The trans-



(a)

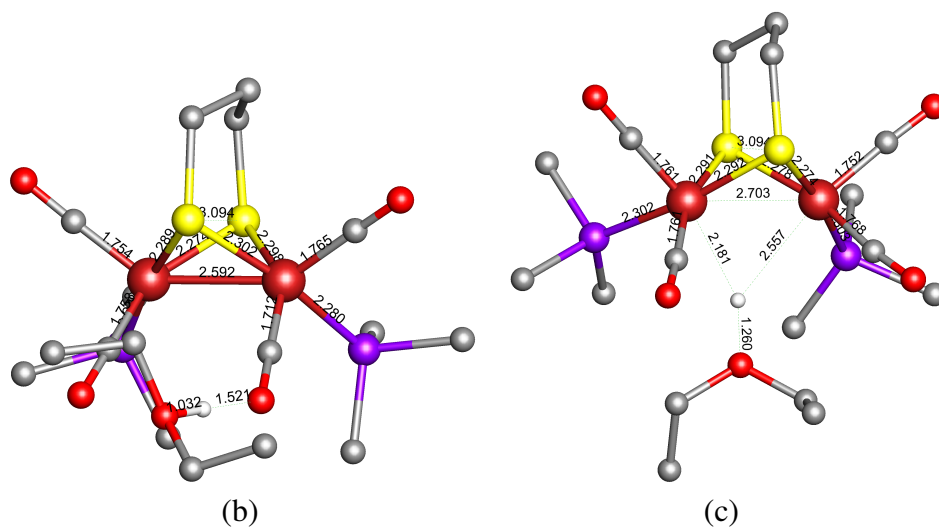


Figure 4.4: (a) Energy profile for the formation of **2C** through the diethyl ether mediated protonation of **1C** to the Fe-Fe bond. Energies are given in kcal/mol relative to **1C**; and optimised geometries of the (b) ether mediated intermediate (**6Cba**) and the (c) transition state (**TS_{6Cba-6CHba}**). For clarity, hydrogen atoms of the PMe_3 groups and the ether have been omitted, bond distances are reported in Å.

ition state has the shortest Et₂O–H bond length at 1.23 Å. The absolute energy barriers to protonation are predicted to be 1.0 and 0.7 kcal/mol lower in energy, respectively, than with edt and odt bridges. Here, the Et₂O–H bonds in the transition state are 0.14 Å and 0.12 Å longer for edt and odt bridged systems, respectively.

As discussed in Chapter 3.3.1, isomers of **1** are similar in energy, with a range of 4 kcal/mol. Additionally, the rotational free energy barriers are low enough (below 9 kcal/mol) to be feasible at room temperature. It is therefore possible for all isomers of **1** to co-exist in solution, so all are equally possible as starting points for protonation. Use of the B3LYP functional [118] has little effect on the energetics of the reaction pathways, showing the same order of barrier heights (see Table B1). The lowest energy barriers for proton transfer are found to occur at the more electronegative iron centre, and in most cases, this is the only route for bridging protonation that could be calculated. The relative free energy barriers for formation of **2** from the H-bonded precursor **6**, are lowest in the formation of **2B**, and significantly higher for **2A**, **2A'**, **2C** and **2D**. Interestingly it was **1B** that was found to have the shortest Fe–Fe bond distance, and it was previously suggested that this corresponded to a stronger Fe–Fe bond which would be harder to protonate [105]. For all bridge head types, the bridging path favours the initial formation of **2B**, characterised by a longer Et₂O–H bond length, which seems to have an impact on the relative stability of the transition state. Isomer **2B** could then rearrange to the more stable **2A**, **2A'** and **2D** isomers. Although this mechanism appears consistent with experimental observations, the calculations predict lower energy pathways for mechanisms investigated in the following section.

4.2.1 Protonation to form terminal hydrides

Figure 4.1 shows the alternative protonation reaction pathway, which also involves the initial formation of an intermediate species where [Et₂OH]⁺ is partially coordinated to a carbonyl group. Initial attack of apical or basal carbonyls produces corresponding apical and basal hydrides. In all reaction pathways described in the following section, the formation of the Fe–H bond occurs synchronously with the movement of the carbonyl group from a terminal to semi-bridging position; i.e. there is no distinct formation of an accessible site prior to proton transfer. Implicit in the current interpretation of the active site of the [FeFe]-hydrogenase is the availability of a vacant coordination site for proton binding. In the cases described herein, the rotated state is a transition state and not a stable intermediate. Of course, if the system were such that the geometry was stable in the rotated state, as was observed for some isomers of the mpdt and dmpdt bridged systems (see Chapter 3.3.4 and Chapter 3.3.5), and also as expected in the enzyme, the barrier would be comparatively low.

Mechanisms with 1A⁽⁹⁾ as the initial reactant

There are eight distinguishable coordination sites in isomers pdt **1A** and pdt **1A'** that would produce terminal hydrides. Figure 4.6 shows the protonation energy profiles that generate the terminal hydride pdt **3A1** and its bridged flipped analogue pdt **3A1'**. Both pathways involve [Et₂OH]⁺ initially attacking the basal CO of Fe₁ which lies *cis* to the basal PMe₃ group of Fe₂. This initial attack gives the terminal hydride intermediates pdt **8Aba** and pdt **8A'ba**. The overall barrier to protonation is fractionally lower in energy than for the alternative bridging route of pdt **1A**, albeit by only 0.4 kcal/mol (for comparison see Figure 4.2 and Figure 4.6). However, these intermediates are higher in energy by ~3 kcal/mol when compared to the intermediates involved in the bridging path, where [Et₂OH]⁺ attacks the basal CO *trans* to the PMe₃ group. In these pathways, H⁺ is transferred to Fe₁, previously identified as the more electronegative centre, which should be preferable. Although the energy barrier is similar to that of the bridging hydride analogues (pdt TS_{6Aba–6HAba}), the Et₂O–H bond is predicted to be stronger here, shorter by

ca. 0.15 Å. The extra stability is presumably caused by Et₂O–H not being so sterically hampered in the TS (not much space in the bridging case as the acid has to deal with the four basal ligands on its approach). The overall energy barrier for protonation is 2.6 kcal/mol lower when the pdt linker faces the PMe₃ group in pdt **1A'**. The lower energy TS has Et₂O–H bond and Fe–H bonds 0.006 Å and 0.003 Å shorter and longer, respectively. Having the proton more associated with the subsite than the acid seems to stabilise the resulting TS. Unfortunately, the TSs associated with these pathways could not be found for the odt bridged system. However, for the edt bridged system, the absolute energy barrier to protonation was found to be 0.8 kcal/mol lower in energy. The Et₂O–H bond in the edt bridged system is fractionally longer (by 0.0004 Å) and the Fe–H bond is shorter by 0.018 Å.

Alternatively, [Et₂OH]⁺ can attack the same carbonyl as taken in the corresponding bridging path to produce intermediates that are fractionally lower in energy (see Figure 4.7). The energy barriers for proton transfer to Fe₁ are also lower by 0.3 kcal/mol and 4.4 kcal/mol, respectively, than for the corresponding bridging path. These pathways are again characterised by proton transfer to what was previously identified as the more electronegative iron centre. Importantly, the overall energy barrier is 3.8 kcal/mol lower when the pdt linker faces Fe₁, the iron centre undergoing protonation. The TS in this lower energy pathway has a weaker Et₂O–H bond (0.006 Å longer), and a stronger Fe–H interaction (0.06 Å shorter) compared to the higher energy bridged flipped pathway.

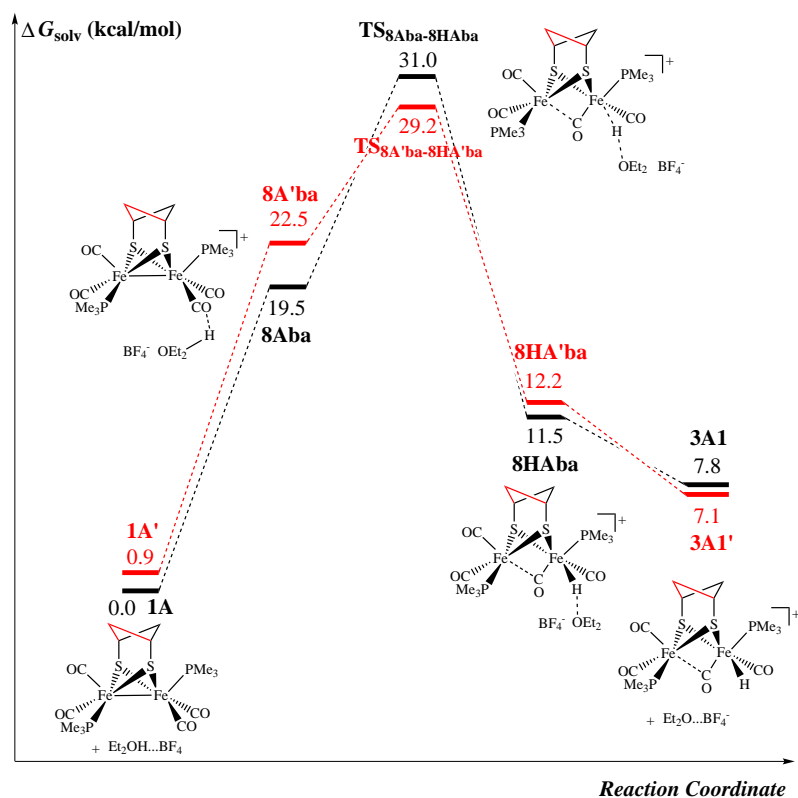
A third possible coordination pathway sees [Et₂OH]⁺ attacking the apical CO of Fe₂ to form pdt **3A3** and pdt **3A3'**. Interestingly, the Φ angle in intermediates pdt **6Aap** and pdt **6A'ap** are significantly increased from ~20° in pdt **1A** to ~64°, increasing the charge density on what was found to be the more electronically deficient Fe₂, and now giving almost symmetrical charge density across the iron centres. This also results in a partial semi-bridging CO with Fe–C_{semi} bond distances of 2.83 Å and 2.98 Å for pdt **6Aap** and pdt **6A'ap**, respectively. The Fe–C_{semi} bond distance is shorter when the pdt bridge is facing the apical CO which has the acid coordinated to it. The relative energies of interme-

diates pdt **6Aap** and pdt **6A'ap** are similar, but the free energy barriers to proton transfer are lower by 2.37 kcal/mol when the pdt linker is facing Fe₁. Comparing the structures of **TS**_{6Aap-6HAap} and **TS**_{6A'ap-6HA'ap} shows that the lower energy barrier for protonation is associated with the less sterically hindered approach of the acid (when the bridge is facing away). Although the Et₂O–H bond distances are similar in both these structures (1.1512 Å), the Fe–H interaction is 0.003 Å shorter in **TS**_{6A'ap-6HA'ap} and the ∠Fe–Fe–H is 9° higher (131.34 vs 140.39°). Additionally, C_{semi}–Fe₁ interaction is stronger in the structure associated with the lower energy pathway, with a bond distance 0.27 Å shorter (2.6028 Å compared to 2.3290 Å). The protonation energies for edt and odt bridged systems were predicted to be roughly the same at ca. 26 kcal/mol.

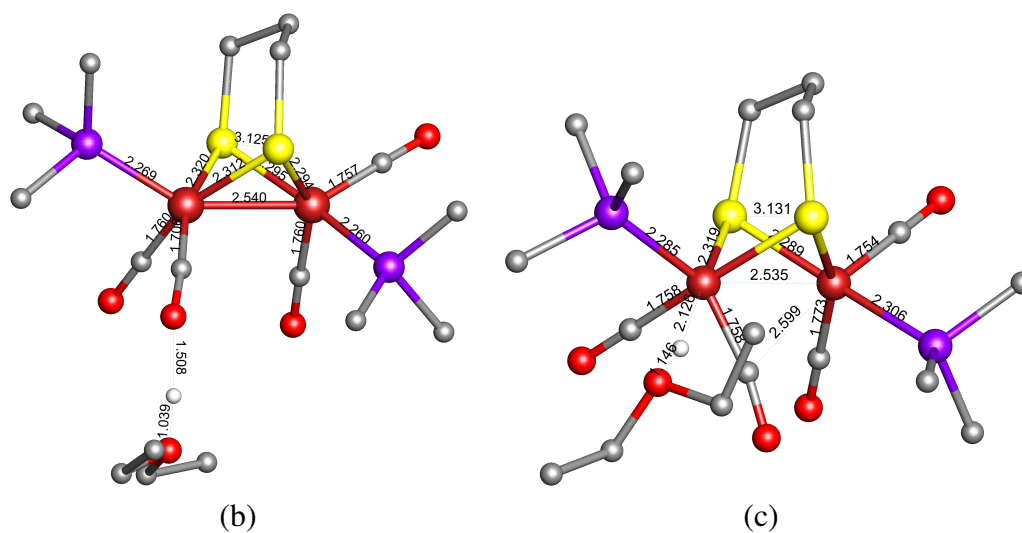
A final coordination pattern is considered for pdt **1A** and pdt **1A'** which involves [Et₂OH]⁺ approaching Fe₂ in a similar fashion to that modelled in **7Aba**, to the basal CO on Fe₂, where the PMe₃ group is basally coordinated (see Figure 4.9). Here, the position of the PMe₃ group relative to the attacking [Et₂OH]⁺ seems to have a significant effect on the energy barriers. The overall barrier from the neutral complex pdt **1A** is the lowest observed yet at only 19.9 kcal/mol (18.8 kcal/mol in the bridge flipped analogue), 10.7 kcal/mol lower when compared to the barrier to form the bridging hydride species seen in Figure 4.2. Further, the relative free energy barrier between **9A'ba** and **TS**_{9A'ba-9HA'ba} is only 3.8 kcal/mol, 9.8 kcal/mol lower than the difference between **6A'ba** and **TS**_{6A'ba-6HA'ba}. Intermediates **9** once again have a high Φ angle giving a semi-bridging CO character (this is the CO that [Et₂OH]⁺ is weakly coordinated to), more so in intermediate pdt **9Aba** where the pdt linker faces Fe₂. For this intermediate, the semi-bridging character is stronger with an Fe–C_{semi} bond distance 0.2 Å shorter than in pdt **9A'ba**. Although this pathway is predicted to have a slightly lower energy barrier with an odt dithiolate bridge, the edt bridged system is calculated to have an absolute energy barrier 3.4 kcal/mol higher in energy, which is consistent with experimental observations. Comparison of Et₂O–H and Fe–H bond distances shows agreement with previous observations. Section 4.3 will evaluate the isomerisation process in forming the thermodynamic product from **3A4**^(') in order to determine whether this is the favoured pathway (over that

of **2B**).

The energy barrier for protonation is highest when [Et₂OH]⁺ approaches from the most sterically hindered angle to form pdt **3A1** and lowest in the formation of pdt **3A4**⁽⁹⁾ where [Et₂OH]⁺ approaches from the least sterically hindered angle. In all of the reaction pathways leading to isomers of pdt **3A**, the energy barriers are lowered when the pdt bridge faces the Fe₁, this is also associated with a longer Et₂O–H bond and shorter Fe–H bond. Use of the B3LYP functional does not significantly effect the results of the pdt bridged system (see Table B2).



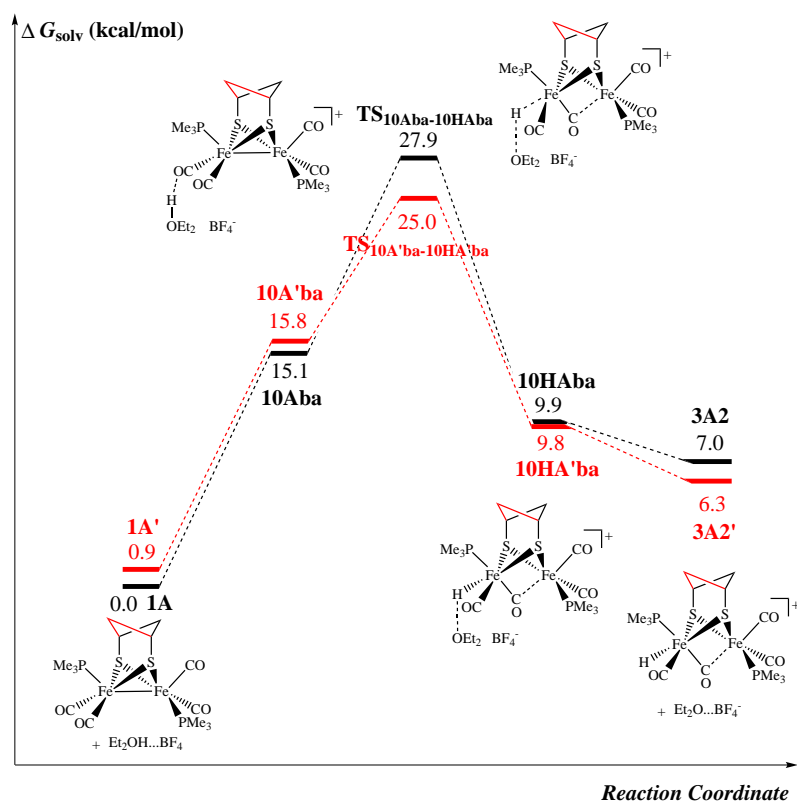
(a)



(b)

(c)

Figure 4.6: (a) Energy profile for the formation of **3A1** and **3A1'** through the diethyl ether mediated protonation of **1A** and **1A'**. Energies are given in kcal/mol relative to **1A**; and optimised geometries of the (b) ether mediated intermediate (**8Aba**) and the (c) transition state (**TS_{8Aba-8HAba}**). For clarity, hydrogen atoms of the PMe_3 groups and the ether have been omitted, bond distances are reported in Å.



(a)

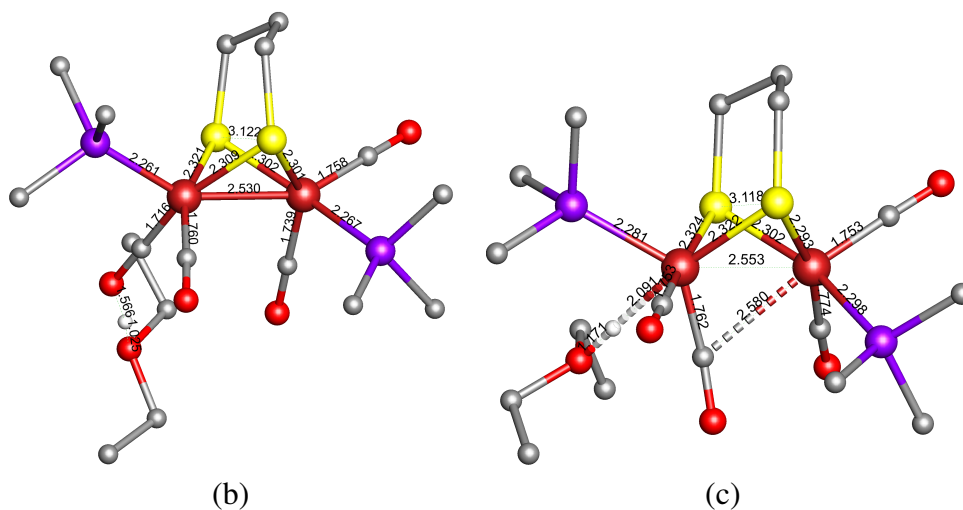
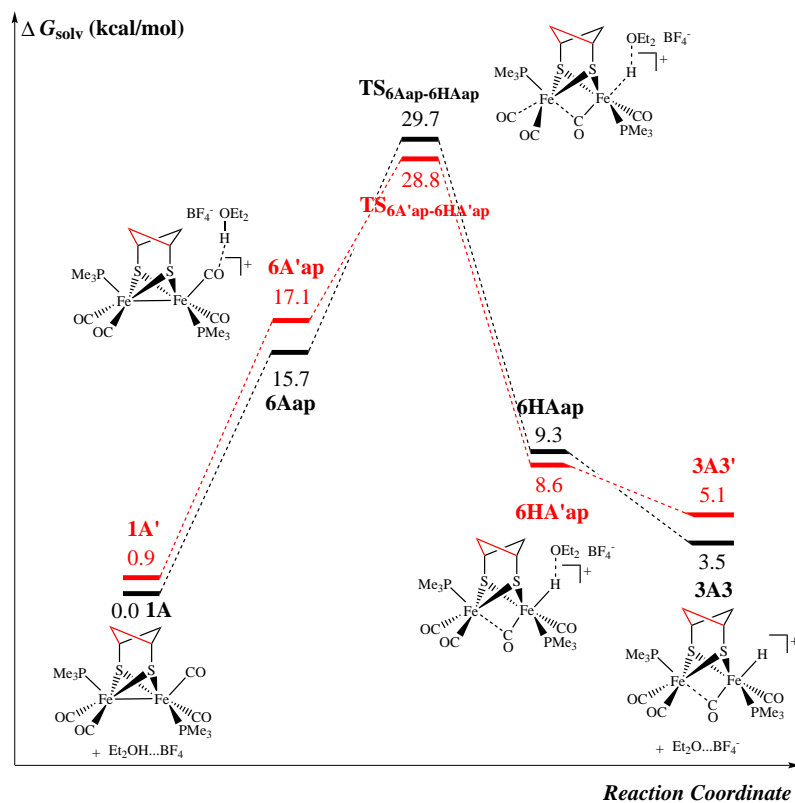


Figure 4.7: (a) Energy profile for the formation of **3A2** and **3A2'** through the diethyl ether mediated protonation of **1A** and **1A'**. Energies are given in kcal/mol relative to **1A**; and optimised geometries of the (b) ether mediated intermediate (**10Aba**) and the (c) transition state (**TS_{10Aba-10HAba}**). For clarity, hydrogen atoms of the PMe_3 groups and the ether have been omitted, bond distances are reported in Å.



(a)

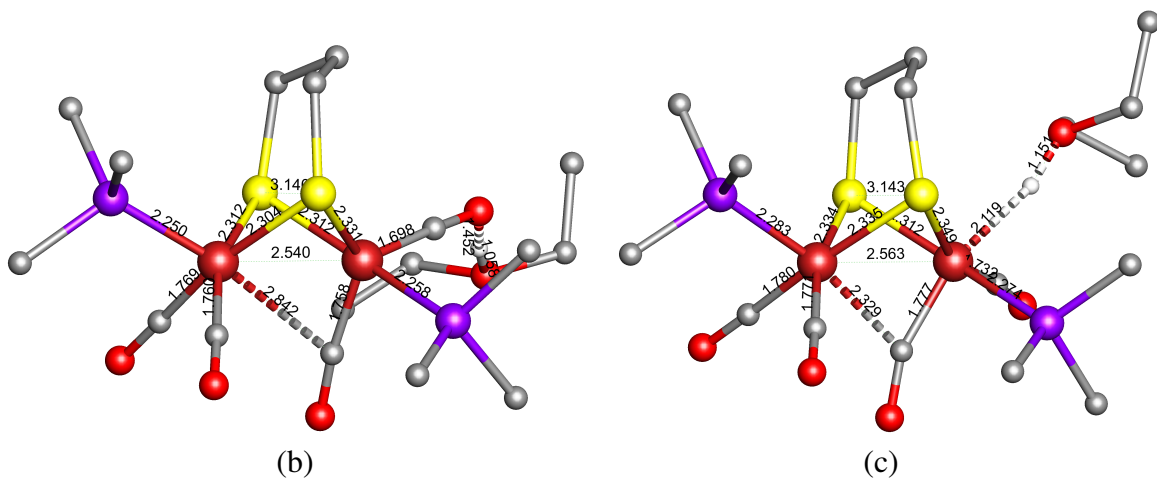


Figure 4.8: (a) Energy profile for the formation of $3A3$ and $3A3'$ through the diethyl ether mediated protonation of $1A$ and $1A'$. Energies are given in kcal/mol relative to $1A$; and optimised geometries of the (b) ether mediated intermediate ($6Aap$) and the (c) transition state ($TS_{pdt7S_6Aap-6HAap}$). For clarity, hydrogen atoms of the PMe_3 groups and the ether have been omitted, bond distances are reported in Å.

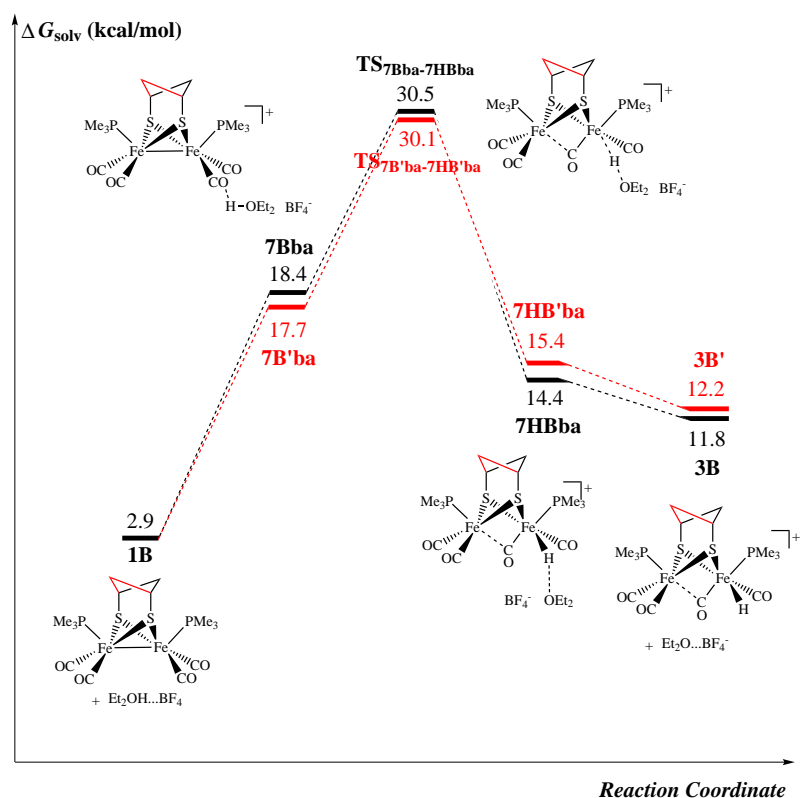
Mechanisms with **1B** as the initial reactant

There are two pathways that lead to terminal protonation on isomer **1B**. They are both basal attacks and differ only by the direction of the pdt linker. The absolute energy barrier to protonation is roughly the same for producing pdt **3B** and pdt **3B'**, with pdt **TS**_{7B'ba-7HB'ba} lower in energy by 0.5 kcal/mol with a height of 27.2 kcal/mol. In producing **3B** with edt and odt bridges, the barrier heights are predicted to be 2.1 kcal/mol and 0.1 kcal/mol higher, respectively. Here again, any reduction in barrier height predicted corresponds to a fractionally weaker Et₂O–H interaction and a stronger Fe–H interaction. Liu did not consider this pathway using the B3LYP functional so no comparison can be made here.

Mechanisms with **1C** as the initial reactant

As the unprotonated species **1A** is rapidly interconverting to isomers **1C** and **1D**, the ether-coordinated intermediates with two PMe₃ ligands either *transoid* or *cisoid* also need to be considered. Figure 4.11 plots the energy profiles of the pathways to the *cisoid* terminal-hydride. Coordination of [Et₂OH]⁺ to the apical CO group of Fe₁ in pdt **1C** forms the intermediate pdt **6Cap**. The structure of pdt **6Cap** has a semi-bridging CO in preparation for the proton to be apically coordinated. Proton transfer takes place via a transition state with the energy barrier of 8.5 kcal/mol above pdt **6Cap** to generate the apical-hydride pdt **3C1** with an overall barrier of 25 kcal/mol. In comparison with the apical path via pdt **6Aap** (Figure 4.8) the absolute free energy barrier to protonation is lower by 4.8 kcal/mol, but still not as low as for the protonation path going via **9Aba**, see Figure 4.9. The energy pathway is predicted to be 0.2 kcal/mol higher for the more sterically hindered approach, when the pdt linker faces Fe₁ and the incoming proton.

An unexpectedly low energy barrier is found for the formation of the terminal-hydride isomers pdt **3C2**⁽⁹⁾. As is shown in Figure 4.12, attack of [Et₂OH]⁺ on the basal CO of Fe₁ in pdt **1C** gives the transition state **TS**_{7Cba-7HCba}, some 7.2 kcal/mol lower in absolute free energy than the **TS**_{6Cap-6HCap} transition state (see Figure 4.11). Addi-



(a)

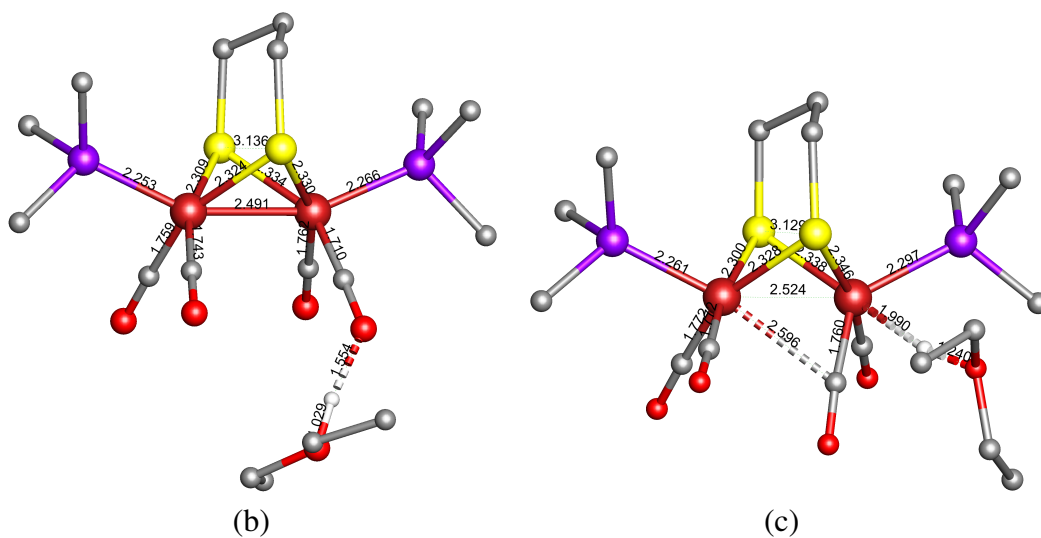
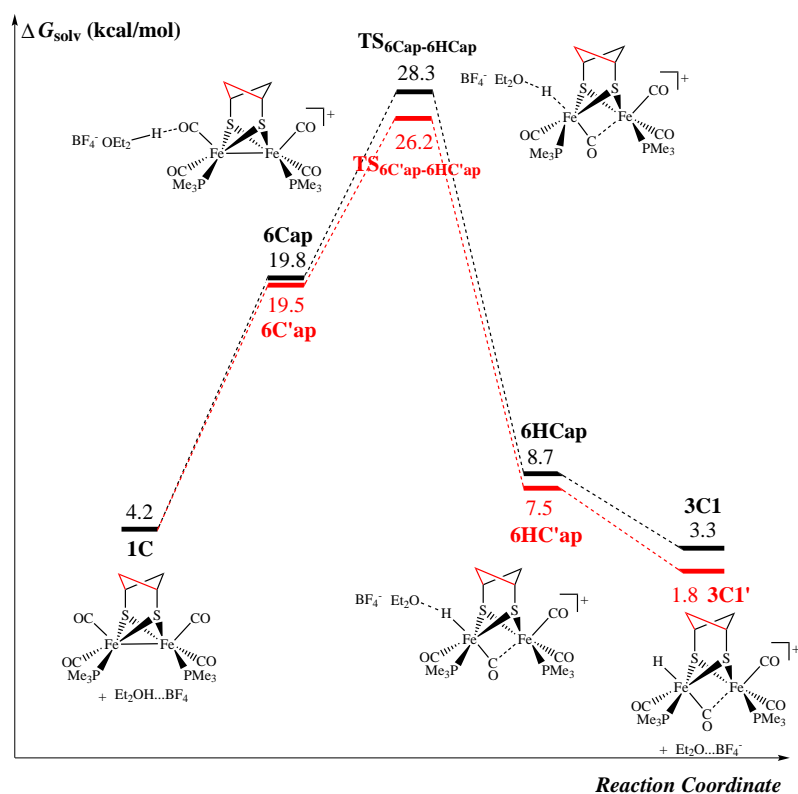


Figure 4.10: (a) Energy profile for the formation of **3B** and **3B'** through the diethyl ether mediated protonation of **1B**. Energies are given in kcal/mol relative to **1A**; and optimised geometries of the (b) ether mediated intermediate (**7Bba**) and the (c) transition state (**TS_{7Bba-7HBba}**). For clarity, hydrogen atoms of the PMe_3 groups and the ether have been omitted, bond distances are reported in Å.

tionally, **TS**_{7Cba-7HCba} is lower in both absolute and relative free energy compared to **TS**_{8Aba-8HAb} by 9.1 and 9.2 kcal/mol, respectively with a barrier of 18.9 kcal/mol. Comparing the pathways that generate basal terminal hydrides (Figure 4.9 and Figure 4.12), one can note similar energy barriers for the two pathways in which the Et₂O–H can transfer the proton to the subsite relatively unhindered. Here again, the energy barrier to protonation is predicted to be 1 kcal/mol lower (at 17.9 kcal/mol) when the pdt linker faces Fe₁ and the incoming proton, this agrees well with the experimental results which gave a 14.6 kcal/mol activation energy barrier [104]. Also in agreement with the experimental observations [104], comparison of the energy profiles that generate pdt **3C2'** with the different dithiolate bridges predicts a slower protonation reaction with the edt and odt bridges, with activation energy barriers 0.7 kcal/mol and 5.5 kcal/mol higher in energy, respectively. In agreement with previous geometric observations, lower energy transition states correspond to weaker Et₂O–H interactions and stronger Fe–H interactions. Observing the LUMOs associated with transition states for proton transfer (see Figure 4.13), all bridge types look markedly similar. The orbital coefficients of the MO associated with the dithiolate bridge sulphurs are *p*-type and roughly symmetrical and the irons have *d*_{z²} coefficients.

Table 4.6: Comparison of the calculated gas phase and solvent corrected free energies and Fe Mulliken charges of the **TS**_{8Cba→8HCba} for pdt, edt and odt dithiolate bridges.

Isomer	ΔG_{solv} (kcal/mol)	Mulliken charges	
		Fe ₁	Fe ₂
pdt TS _{8Cba→8HCba}	17.9	-0.480	-0.779
edt TS _{8Cba→8HCba}	18.6	-0.591	-0.782
odt TS _{8Cba→8HCba}	23.4	-0.732	-0.639



(a)

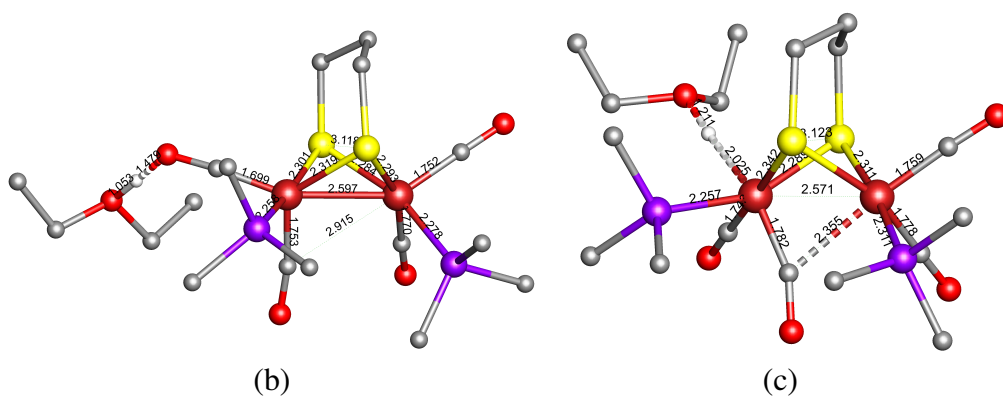
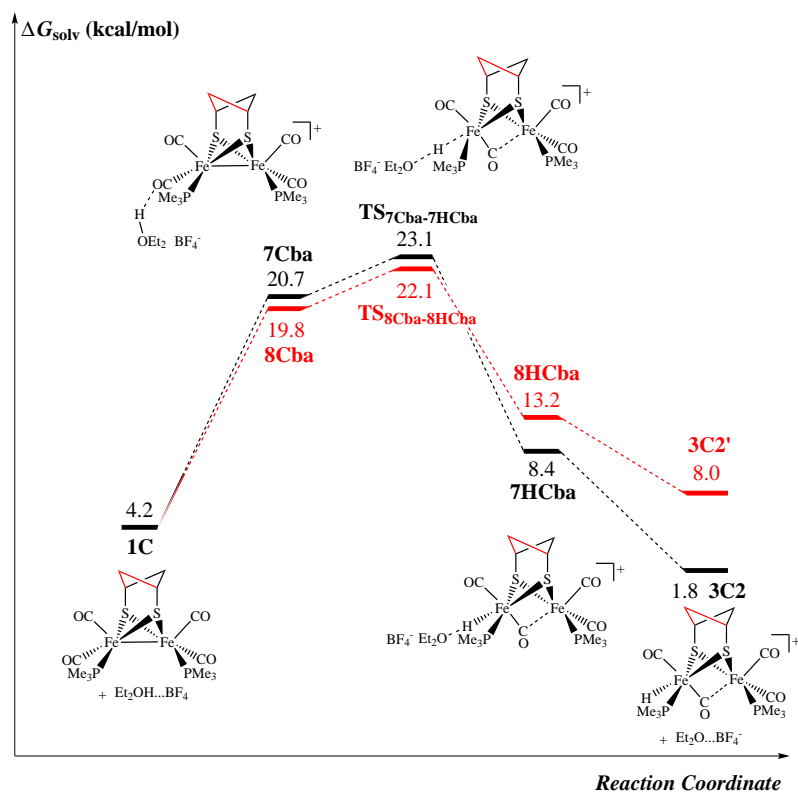
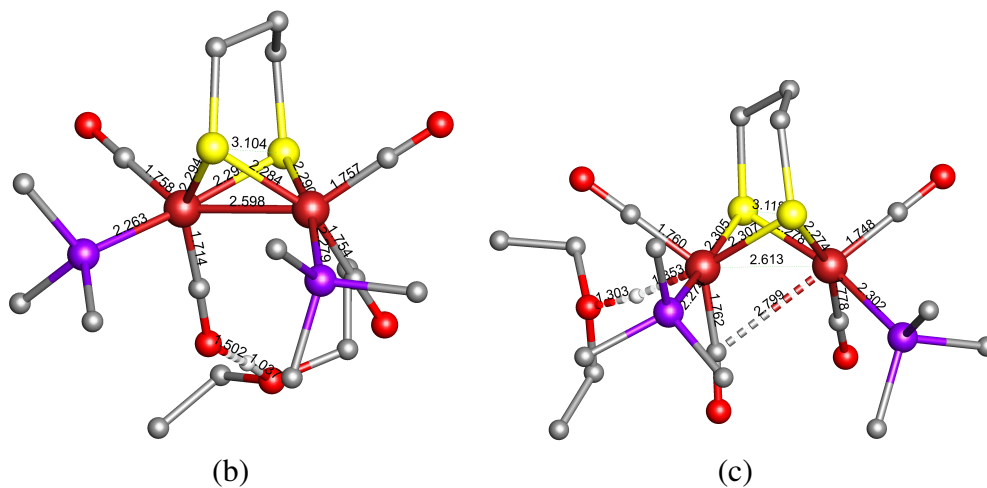


Figure 4.11: (a) Energy profile for the formation of **3CI** and **3CI'** through the diethyl ether mediated protonation of **1C**. Energies are given in kcal/mol relative to **1A**; and optimised geometries of the (b) ether mediated intermediate (**6Cap**) and the (c) transition state (**TS_{pdt7S6Cap-6HCap}**). For clarity, hydrogen atoms of the PMe_3 groups and the ether have been omitted, bond distances are reported in Å.



(a)



(b)

(c)

Figure 4.12: (a) Energy profile for the formation of **3C2** and **3C2'** through the diethyl ether mediated protonation of **1C**. Energies are given in kcal/mol relative to **1A**; and optimised geometries of the (b) ether mediated intermediate (**7Cba**) and the (c) transition state (**TS_{pdt_S7Cba-7HCba}**). For clarity, hydrogen atoms of the PMe_3 groups and the ether have been omitted, bond distances are reported in Å.

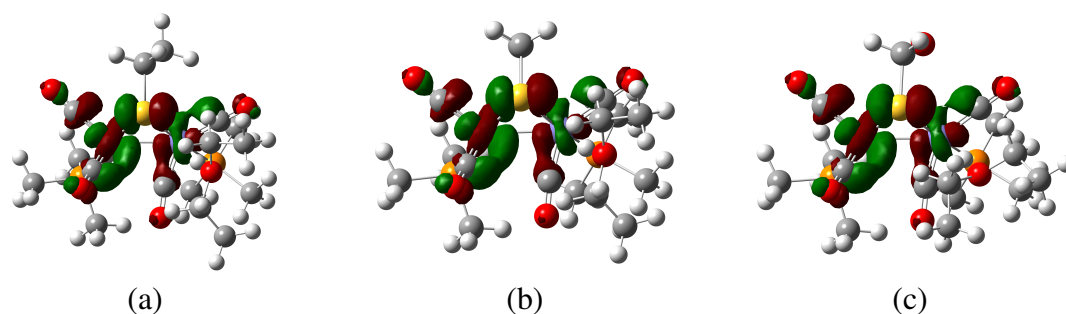


Figure 4.13: LUMOs associated with the $TS_{7Cba7HCba}$ for (a) the pdt dithiolate bridge (b) the edt dithiolate bridge and (c) the odt bridge. Isosurface = 0.04.

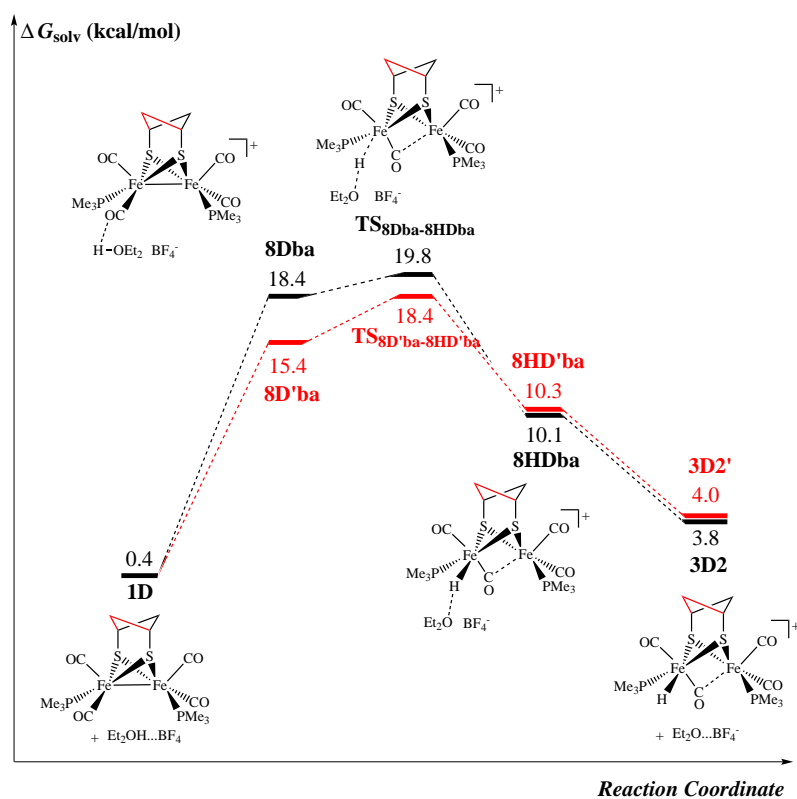
Mechanisms with **1D** as the initial reactant

Unfortunately, the transition states for proton transfer to form apical hydrides pdt **3D1** and pdt **3D1'** could not be found using the TPSS functional. Figure 4.14 shows that the *transoid* arrangement of the PMe_3 ligands produces pathways of similar energetics to those found for the *cisoid* arrangement. Here, however, slightly higher barriers are found for the initial attack of $[Et_2OH]^+$ on both apical and basal CO ligands, this is in agreement with the B3LYP calculations (see Table B4 and Table B5) [118]. Similarly, the relative order of the barriers are comparable between the pathways. Attack on the basal CO of Fe_1 gives pdt $TS_{8Dba-8HDba}$, which is 19.4 kcal/mol above pdt **1D**, a barrier that is 0.5 kcal/mol above the energy in the corresponding *cisoid* path, (see Figure 4.12) and 0.6 kcal/mol below the energy in the corresponding apical-basal path (see Figure 4.9). In the case where the PMe_3 ligands are *transoid*, the H-bonded intermediate is very weakly bound leading to a very small relative barrier between pdt **8Dba** and pdt $TS_{8Dba-8HDba}$ of 1.4 kcal/mol. Flipping the pdt linker so that it faces the incoming proton reduces the energy barrier by 0.6 kcal/mol, which makes it only 0.9 kcal/mol higher than the kinetically favoured path to produce pdt **3C2'** in Figure 4.12. The H-bonded intermediate is more strongly bound to the CO giving a higher barrier for proton transfer compared to its bridge flipped analogue, 3 kcal/mol higher. The lower energy pathway to produce pdt **3D2'** is predicted to be the same in energy and 0.7 and 0.4 kcal/mol higher in energy with edt and odt bridges, respectively (see Table B5).

As discussed above, the ether-mediated terminal-path mechanisms with attack of $[Et_2-$

OH]⁺ on basal CO groups to form terminal-hydrides **3A4**^('), **3C2**^(') and **3D2**^('), are more favourable than forming the more stable apical and bridging isomers, **2**. Furthermore, these pathways are also more favourable when the dithiolate bridgehead faces the attacking proton, except in the special case of the pathway to form **3A4** where the barrier was lowered when the dithiolate bridgehead faces the apical PMe₃ (as was the trend in the **3A** pathways). In all cases, lower energy transition states coincide with weaker Et₂O–H interactions and stronger Fe–H interactions. These effects are expected to be more prominent as the steric bulk of the dithiolate bridge increases, as in the mpdt and dmpdt systems.

In the following section the rearrangements from the terminal-hydride isomers to the bridging-hydride isomers will be examined.



(a)

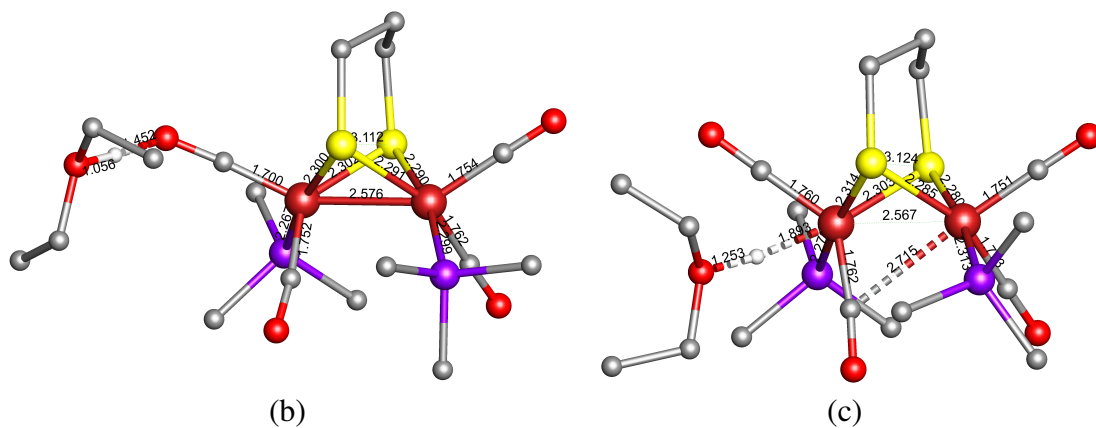


Figure 4.14: (a) Energy profile for the formation of **3D2** and **3D2'** through the diethyl ether mediated protonation of **1D**. Energies are given in kcal/mol relative to **1A**; and optimized geometries of the (b) ether mediated intermediate (**8Dba**) and the (c) transition state (**TS_{pdtT}S_{8Dba-8HDba}**). For clarity, hydrogen atoms of the PMe_3 groups and the ether have been omitted, bond distances are reported in Å.

4.3 Isomerisation pathways from terminal to bridging hydrides

The isomerisation pathways reported below map the rearrangement of terminal hydrides into bridging hydride species. Terminal hydride isomers **3A3**⁽⁹⁾, **3C1**⁽⁹⁾ and **3C2**⁽⁹⁾ are taken as starting points in the rearrangements where the proton and its adjacent ligands can rotate either clockwise or anti-clockwise in Bailar or Ray-Dutt twists to form bridging hydrides. In the process of these rotations all terminal hydride isomers are included. The interconversion of bridging hydrides has already been discussed in Chapter 3.4.2.

4.3.1 Rearrangement from terminal hydrides **3A3**⁽⁹⁾, **3A4**⁽⁹⁾ and **6AInt**⁽⁹⁾

As shown in Figure 4.17, Figure 4.15 and Figure 4.16, the isomerisation from apical terminal-hydride to bridging-hydrides takes place through a multi-step process. Taking pdt **3A3** as a starting point, there are three pathways to generate the bridging-hydrides pdt **2A** (see Figure 4.17 and Figure 4.16) and pdt **2B** (see Figure 4.15).

Following the pathway described in Figure 4.15; the three ligands of Fe₂: proton, basal PMe₃, and basal CO in pdt **3A3** can rotate anti-clockwise in a Bailar twist to form pdt **3A4**, doing so with a free-energy barrier of 15.4 kcal/mol. Unusually, the bridge flipped version where the pdt linker faces the rotating iron is predicted to be 2.3 kcal/mol higher in energy. The rearrangement of pdt **3A4**⁽⁹⁾ into the thermodynamic product is of particular importance as this was found to be one of the kinetic products. In a Ray-Dutt twist pdt **3A4** converts to pdt **2B** via the anti-clockwise rotation of the four ligands of Fe₂, through transition state pdt **TS**_{3A4-2B} with a free energy barrier of 12.0 kcal/mol. Again, the energy barrier to rotation was predicted 1.1 kcal/mol higher for the bridge flipped analogue where the pdt linker faces away from the rotating iron centre. Consistent with experimental kinetics observations, the pathways are less energetically favourable with edt and odt bridges (see Table 4.9). The remaining rearrangement steps from **2B** to **2D** were discussed in 4.2 along with the effects on rotational energy barriers that the dithi-

olate bridge has (see Table 4.2).

Table 4.7: Free energy comparison between the *pdt*, *edt* and *odt* dithiolate bridge in the isomerisation pathways from kinetic products $3C2^{(*)}$ leading to the thermodynamic product $2D$. Energies are reported in kcal/mol.

Reaction coordinate	<i>pdt</i>	<i>edt</i>	<i>odt</i>
$TS_{3A4 \rightarrow 2B}$	12.0	11.8	13.2
$TS_{3A4' \rightarrow 2B}$	13.1	16.5	21.4

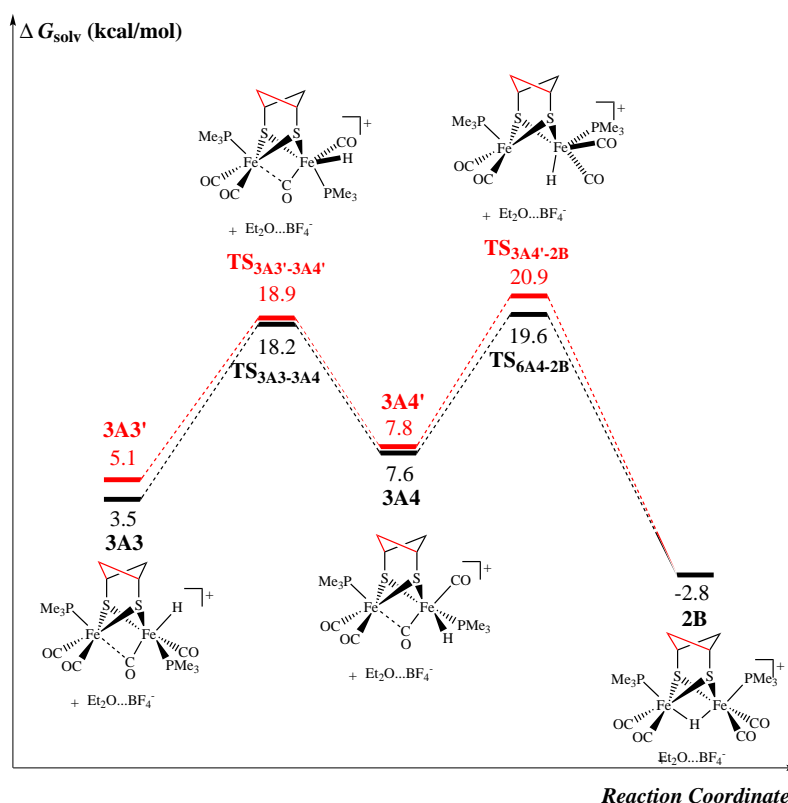


Figure 4.15: Isomerisation pathways for the rearrangement of terminal hydrides $3A3$ and $3A3'$ to the bridging hydride $2B$: black line pathway: $3A3 \rightarrow 3A4 \rightarrow 2B$; red line pathway: the *pdt* bridge flipped path $3A3' \rightarrow 3A4' \rightarrow 2B$ is coloured red. Energies are reported relative to $1A$.

In Figure 4.16; the four ligands of Fe_2 in *pdt* $3A3$: proton, basal PMe_3 , basal CO and the μ -CO rotate anti-clockwise to give intermediate $6AInt$, which presents a configuration with the PMe_3 ligand lying nearly in the plane defined by the apical PMe_3 and CO ligands and two irons. Although $6AInt$ is 13.9 kcal/mol less stable than $3A4$, this rotation is 1.5 kcal/mol lower in energy. Isomer $6AInt$ may undergo a further rotation to $2A$ with an energy barrier of 8.5 kcal/mol. This pathway is composed of two continuous Ray-Dutt twists in an anti-clockwise direction. In the bridge flipped analogue, where the *pdt* linker

faces away from the rotating iron the energy barriers to rotation are 1.3 kcal/mol lower and 3.2 kcal/mol higher.

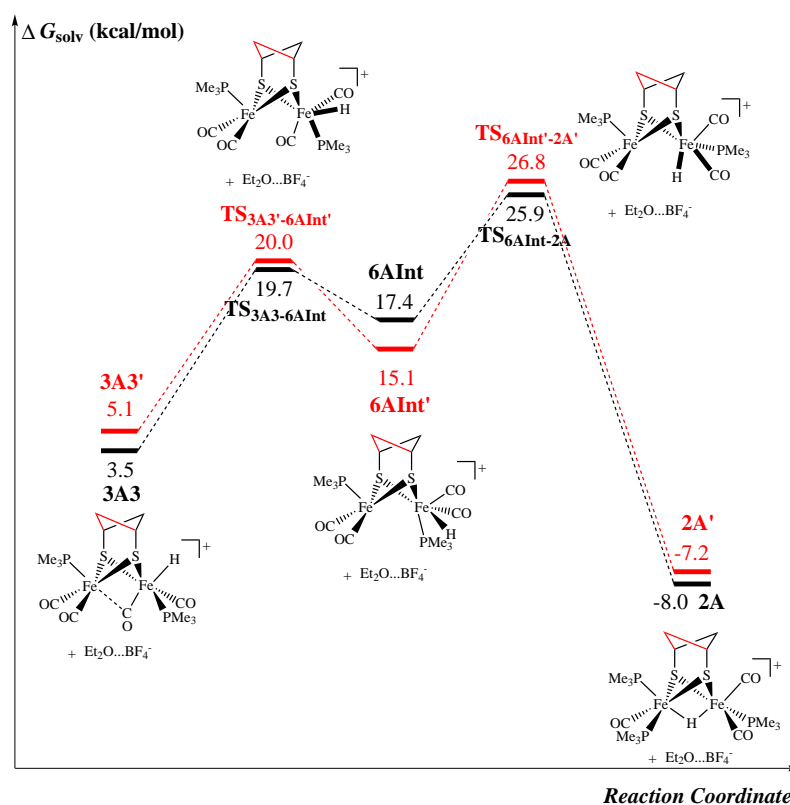


Figure 4.16: Alternative isomerisation pathways for the rearrangement of terminal hydrides **3A3** and **3A3'** to bridging hydrides **2A** and **2A'**: black line pathway: **3A3** → **6AInt** → **2A**; red line pathway: the *pdt* bridge flipped path **3A3'** → **6AInt'** → **2A'**. Energies are reported relative to **1A**.

Plotted in Figure 4.17; the three ligands coordinated to Fe_2 in **3A3**: proton, basal PMe_3 and basal CO rotate clockwise to generate **3B** through transition state TS_{3A3-3B} with a barrier of 15.5 kcal/mol. The next isomerisation from **3B** to **2A** involves rotation of the four ligands in a Ray-Dutt twist with a barrier of 6.9 kcal/mol. This pathway is similar to the first one (**3A3** → TS_{3A33A4} → **3A4** → TS_{3A4-2B} → **2B**), in which a Bailar twist is followed by a Ray-Dutt twist.

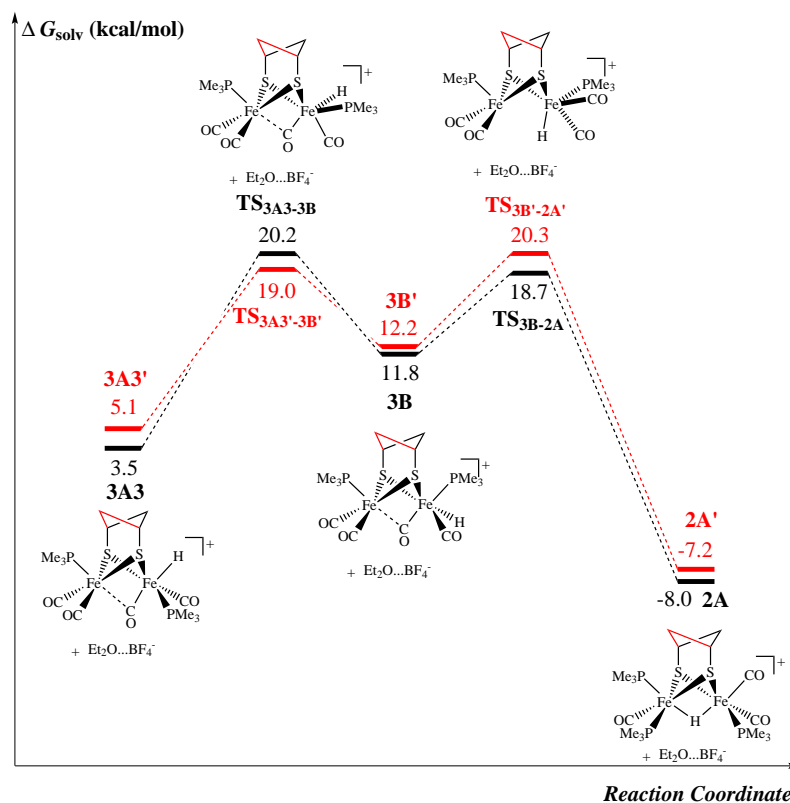


Figure 4.17: Isomerisation pathways for the rearrangement of terminal hydrides $3A3$ and $3A3'$ to bridging hydrides $2A$ and $2A'$: black line pathway: $3A3 \rightarrow 3B \rightarrow 2A$; red line pathway: the *pdt* bridge flipped path $3A3' \rightarrow 3B' \rightarrow 2A'$. Energies are reported relative to $1A$.

Table 4.8: Free energy comparison between the *pdt*, *edt* and *odt* dithiolate bridge in the isomerisation pathways from one of the kinetic products leading to the thermodynamic product $2D$. Energies are reported in kcal/mol.

Reaction coordinate	<i>pdt</i>	<i>edt</i>	<i>odt</i>
$TS_{3A4 \rightarrow 2B}$	12.0	11.8	13.2
$TS_{3A4' \rightarrow 2B}$	13.1	16.5	21.4
$TS_{2B \rightarrow 2A}$	18.2	21.8	23.2
$TS_{2A \rightarrow 2A'}$	7.0	-	10.0
$TS_{2A \rightarrow 2D}$	26.2	21.2	20.7
$TS_{2A' \rightarrow 2D}$	18.1	21.2	22.6

4.3.2 Rearrangement from terminal hydrides **3C1**^(s), **3A2**^(s), **6CInt**^(s) and **3D2**^(s)

Following three similar pathways for the rearrangement presented in Figure 4.19, Figure 4.20 and Figure 4.18, **pdt 3C1**^(s) can rearrange to form **pdt 2A**^(s) and **pdt 2D**. In Figure 4.19 the pathway via **3D2**^(s) shows a transition state **TS_{3C1-3D2}** with high energy barrier (24.8 kcal/mol). The magnitude of this energy barrier is predicted to be unaffected by the direction pdt linker. As observed in Chapter 4.2.1, isomers **pdt 3D2**^(s) are predicted to be among the kinetic products so their rearrangement to the thermodynamic product are of particular interest. The Ray-Dutt twist of the ligands coordinated to Fe₁ in **pdt 3D2** occurs through a low energy barrier of 14.3 kcal/mol, this is further lowered by 1 kcal/mol when the pdt linker is facing the rotating moiety. Rearrangement of **pdt 2A** to **pdt 2D** occurs via a TS with a barrier of 26.2 kcal/mol. However, if this rotation is proceeded by a bridge flip to **pdt 2A'** (with an energy of 7 kcal/mol), the barrier to **pdt 2D** is reduced to 18.1 kcal/mol. In the pathway from **3D2** leading to **2D** the rate limiting step in all bridge types is again the rotation of **2A'** into **2D**, which would be consistent with the experimentally observed kinetics data (see Table 4.9).

Plotted in Figure 4.20 is the path via **pdt 6CInt**^(s), predicted to be energetically more favourable by 4 kcal/mol compared to that of generating **3D2**. This converts directly into the thermodynamic product with an energy barrier of 5.5 kcal/mol. These energy barriers are predicted to be largely unaffected by the direction of the pdt dithiolate linker.

Anti-clockwise rotation of the ligands coordinated to Fe₁ in **pdt 3A2** is the most favoured pathway from **pdt 3C1** with a barrier of 15.4 kcal/mol (see Figure 4.18). This infers a strong influence of the relative position of the two PMe₃ ligands, resulting in high energy barriers, thus hindering the rearrangement from **pdt 3C1** to the bridging isomers. **3A2**^(s) converts directly into the thermodynamic product with a low energy barrier of 10.9 kcal/mol. The barrier to rotation is predicted to be unaffected by the direction of the pdt linker. Isomer **pdt 3A2'** was identified as one of the higher energy kinetic

products, and can convert to the thermodynamic product in a single rotation (barrier of 10.8 kcal/mol) making it an attractive pathway. Comparing the energies of this particular rotation between the different bridgehead types gives a slightly higher energy barrier with the edt bridge (by 0.3 kcal/mol) and slightly lower for odt bridge (0.3 kcal/mol lower) (see Table 4.9).

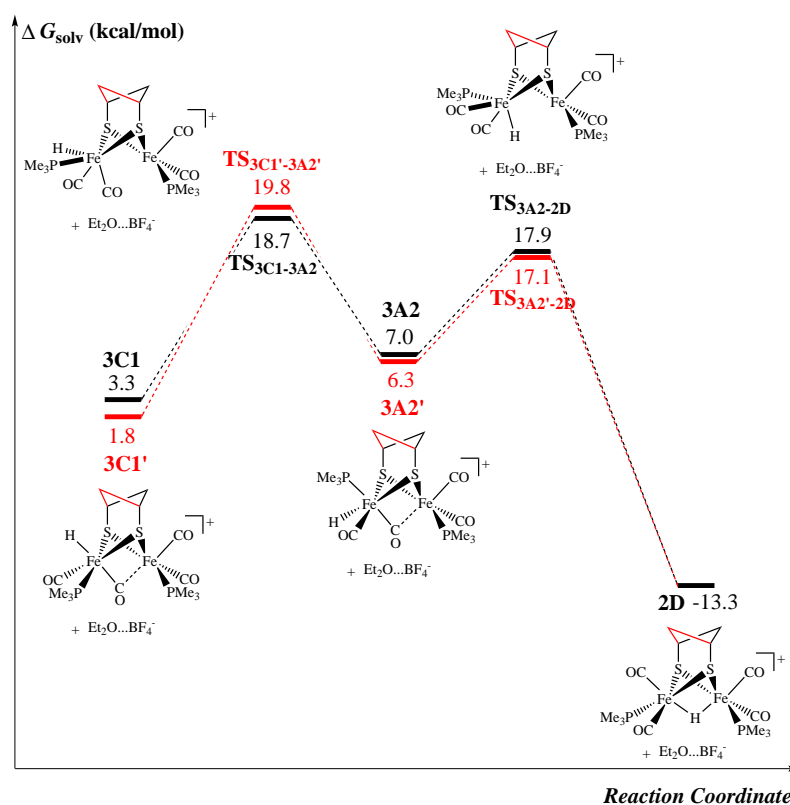


Figure 4.18: Isomerisation pathways for the rearrangement of terminal hydrides **3C1** and **3C1'** to the bridging hydride **2D**: black line pathway: **3C1** → **3A2** → **2D**; red line pathway: the *pdt* bridge flipped path **3C1'** → **3A2'** → **2D**. Energies are reported relative to **1A**.

Table 4.9: Free energy comparison between the *pdt*, *edt* and *odt* dithiolate bridge in the isomerisation pathways leading from kinetic products **3D2** and **3A2'** to the thermodynamic product, **2D**. Energies are reported in kcal/mol.

Reaction coordinate	<i>pdt</i>	<i>edt</i>	<i>odt</i>
TS _{3D2→2A}	14.3	12.8	14.7
TS _{3D2'→2A'}	13.1	12.8	14.3
TS _{2A→2A'}	7.0	-	10.0
TS _{2A→2D}	26.2	21.2	20.7
TS _{2A'→2D}	18.1	21.2	22.6
TS _{3A2'→2D}	10.8	11.1	10.5

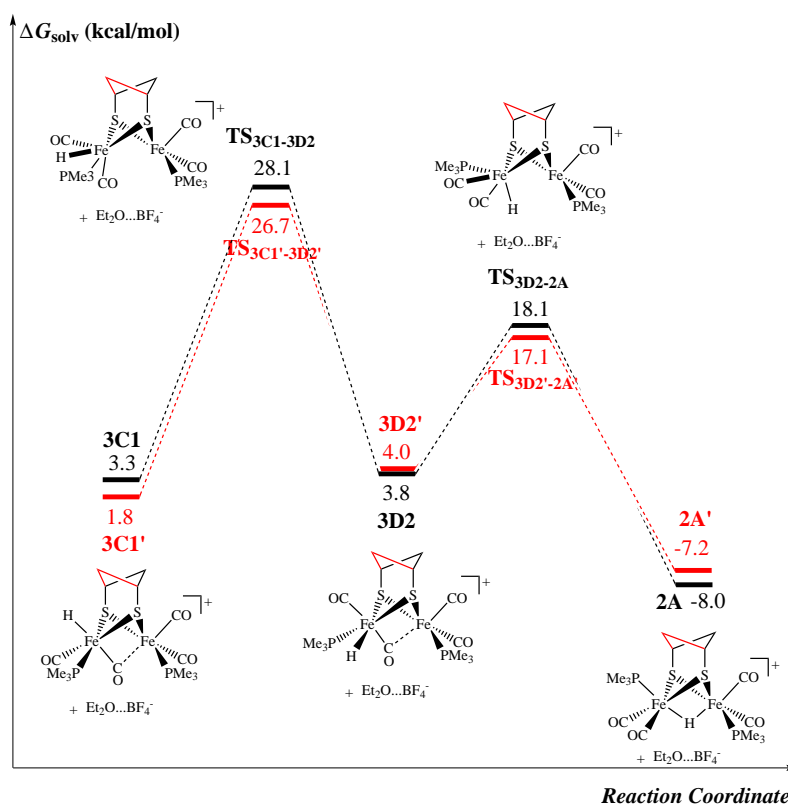


Figure 4.19: Isomerisation pathways for the rearrangement of terminal hydrides $3C1$ and $3C1'$ to bridging hydrides $2A$ and $2A'$: black line pathway: $3C1 \rightarrow 3D2 \rightarrow 2A$; red line pathway: the *pdt* bridge flipped path $3C1' \rightarrow 3D2' \rightarrow 2A'$. Energies are reported relative to $1A$.

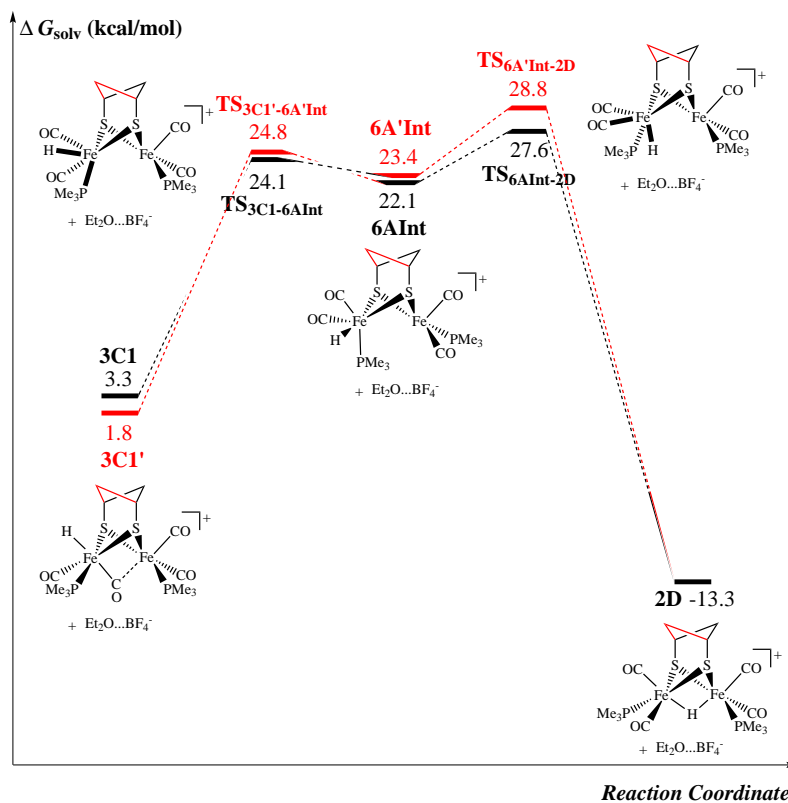


Figure 4.20: Isomerisation pathways for the rearrangement of terminal hydrides $3C1$ and $3C1'$ to the bridging hydride $2D$: black line pathway: $3C1 \rightarrow 6CInt \rightarrow 2D$; red line pathway: the *pdt* bridge flipped path $3C1' \rightarrow 6C'Int \rightarrow 2D$. Energies are reported relative to $1A$.

4.3.3 Rearrangement from terminal hydrides **3D1**^(*), **3A1**^(*), **3C2**^(*) and **6DInt**^(*)

As shown in Figure 4.21, Figure 4.22 and Figure 4.23 the overall energy barriers for rearrangement of pdt **3D1** anti-clockwise to pdt **2A**, or clockwise and anti-clockwise to pdt **2C** are 25.8 (see Figure 4.22), 34.2 (see Figure 4.21) and 17.5 (see Figure 4.23) kcal/mol for the three possible pathways, respectively. It turns out that the barriers to these limiting steps are lowered by 0.6 kcal/mol and 0.9 kcal/mol and 1.2 kcal/mol, respectively when the pdt bridge is flipped to face the rotating Fe₁. The rearrangement from terminal hydride pdt **3A1** appears simple, where a single Ray-Dutt twist generates the bridging-hydride pdt **2C**. The four ligands of Fe₁: basal proton, basal CO, apical PMe₃ and μ-CO rotate clockwise to form pdt **2C** and anti-clockwise to form pdt **2D**, respectively. Interestingly, these two rotational transition states pdt **TS**_{3A12D} and pdt **TS**_{3A12C} are predicted to be almost identical in energy. This indicates the probability of forming pdt **2C** and pdt **2D** from pdt **3A1** are roughly equal. This rearrangement would be fast as the energy barrier is only 11.1 kcal/mol, an advantageous pathway in comparison with those presented in Figure 4.17, Figure 4.15 and Figure 4.16.

Isomers pdt **3C2**^(*) are again special cases, as they were found to be among the kinetic products of the initial protonation. In order to reach the thermodynamic product, Fe₁ must undergo an anti-clockwise Ray-Dutt twist to pdt **2A**, followed by a Bailer twist to pdt **2D**, which has already been covered. The former rotation is predicted to occur with an energy barrier of 12.0 kcal/mol. Here again, the bridge flipped analogue where the pdt linker faces the rotating Fe₁ is predicted to reach the thermodynamic product with a barrier 0.9 kcal/mol lower in energy. Table 4.10 shows that having an edt and odt dithiolate bridge decrease and increase the rotational barriers, respectively.

It is clear that the arrangement of the two PMe₃ ligands has an effect on the rotational energy barriers. In the case of apical terminal hydrides, the barriers to rotate the hydride from apical to basal coordination sites are predicted to be significantly higher when the PMe₃ ligands are *cisoid* to each other. However, the direction of the pdt linker has a

Table 4.10: Free energy comparison between the *pdt*, *edt* and *odt* dithiolate bridge in the isomerisation pathways from kinetic products $3C2^{(s)}$ leading to the thermodynamic product **2D**. Energies are reported in kcal/mol.

Reaction coordinate	<i>pdt</i>	<i>edt</i>	<i>odt</i>
TS _{3C2→2A}	12.0	8.5	12.9
TS _{3C2'→2A'}	11.1	8.5	15.8
TS _{2A→2A'}	7.0	–	10.0
TS _{2A→2D}	26.2	21.2	20.7
TS _{2A'→2D}	18.1	21.2	22.6

greater impact on the energy barriers, lowering the barrier when the linker is facing the iron centre undergoing rotation.

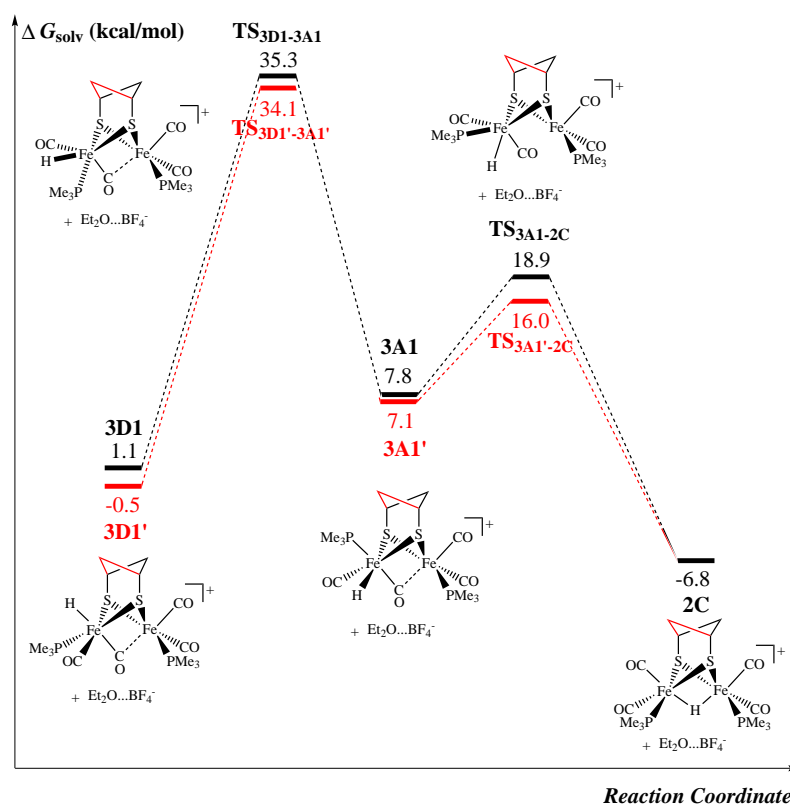


Figure 4.21: Isomerisation pathways for the rearrangement of terminal hydrides **3D1** and **3D1'** to the bridging hydride **2C**: black line pathway: **3D1** → **3A1** → **2C**; red line pathway: the *pdt* bridge flipped path **3D1'** → **3A1'** → **2C**. Energies are reported relative to **1A**.

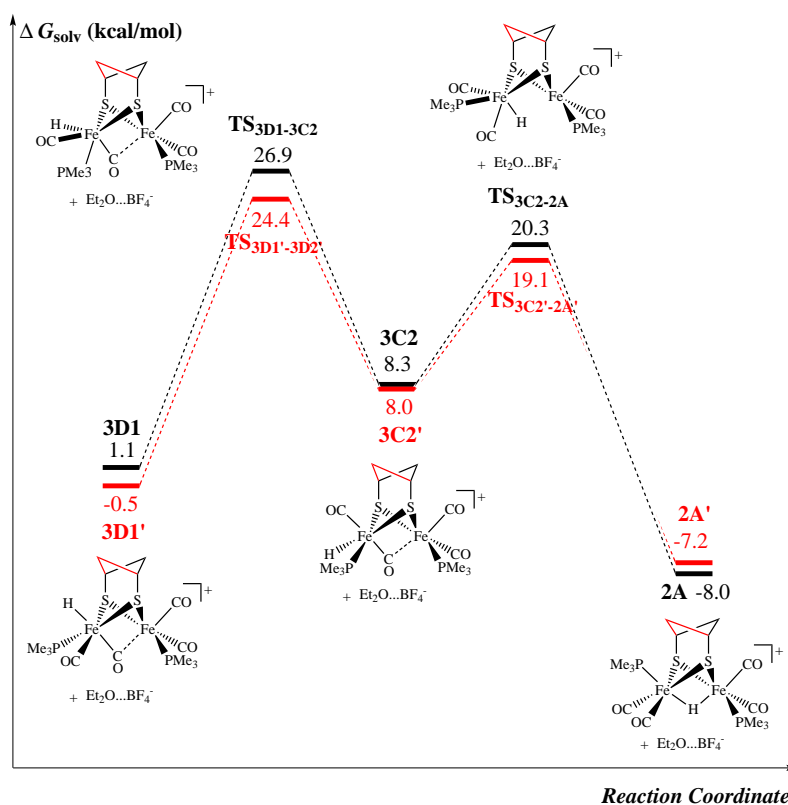


Figure 4.22: Isomerisation pathways for the rearrangement of terminal hydrides $3D1$ and $3D1'$ to the bridging hydrides $2A$ and $2A'$: black line pathway: $3D1 \rightarrow 3C2 \rightarrow 2A$; red line pathway: the ptd bridge flipped path $3D1' \rightarrow 3C2' \rightarrow 2A'$. Energies are reported relative to $1A$.

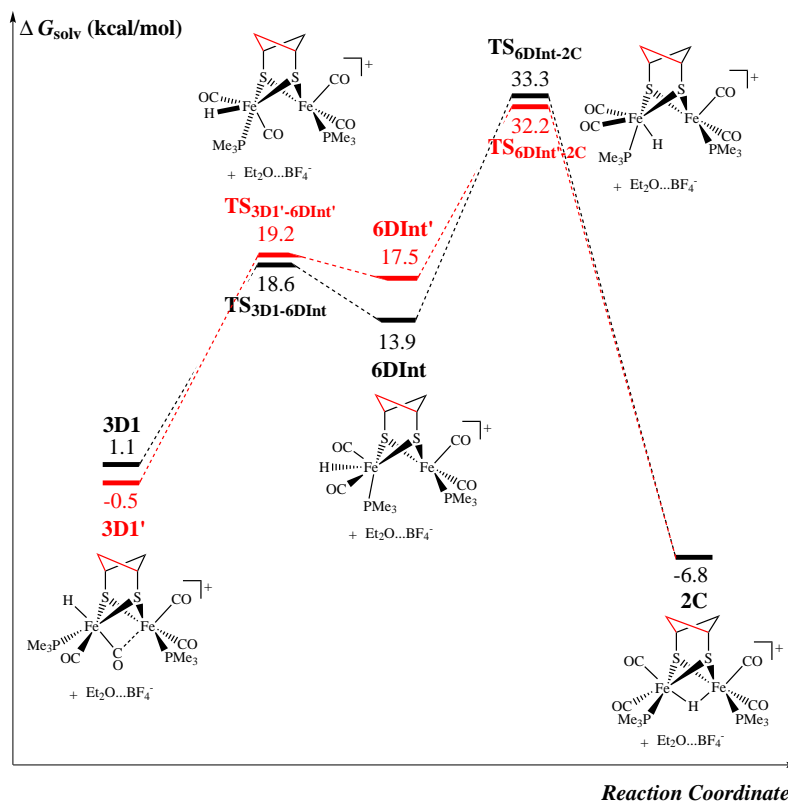


Figure 4.23: Isomerisation pathways for the rearrangement of terminal hydrides $3D1$ and $3D1'$ to the bridging hydride $2C$: black line pathway: $3D1 \rightarrow 6DInt \rightarrow 2C$; red line pathway: the ptd bridge flipped path $3D1' \rightarrow 6DInt' \rightarrow 2C$. Energies are reported relative to $1A$.

4.4 Summary and conclusions

DFT calculations have been used to explore the protonation mechanism for [FeFe] hydrogenase model complexes, [Fe₂(μ-(Xdt)(CO)₄(PMe₃)₂] (X = edt, pdt and odt). The calculations reveal that the diethyl ether (or solvent) may play a role in the protonation mechanism. With [Et₂OH]⁺ as the proton carrier, the proton transfer pathways appear to involve an intermediate with [Et₂OH]⁺ bound to a CO ligand followed by rearrangement to a terminal or bridging hydride. The calculations identified three preferable pathways to the thermodynamic product, all are very close in energy and involve the same rearrangement as the rate limiting step. These pathways involve the formation of basal terminal hydrides pdt **3A4**^(s), pdt **3C2**^(s) and pdt **3D2**^(s) followed by rearrangement to bridging hydrides, which then inter-convert between each other at a slower rate. These pathways are plotted in Figure 4.24. The pathway to pdt **3C2**^(s) has the lowest energy barrier. It not only involves the lowest energy barriers, but takes the fewest steps in order to reach the thermodynamic product. Protonation of **1C** occurs preferentially as the barrier for the protonation of **1A** is ~14 kcal/mol higher in free energy. The lowest energy path for protonation of **1C** produces **3C2**^(s), which rearranges rapidly to **2A**^(s) through a Ray-Dutt twist, this would be the species initially observed in the experiments. The species **2A**^(s) then rearranges through a Bailar twist **2A**^(s) → **2D**. Experimental and computational (for the proposed pathway) estimates for the protonation energy barrier for the pdt bridged system are 14.6 and 16.8 kcal/mol, respectively. Experimental activation parameters showed the barrier to increase to 16.5 and 17.4 kcal/mol with edt and odt dithiolate bridges, respectively [104, 105]. In accordance with this, the calculated barriers were also predicted to increase to 18.6 and 23.4 kcal/mol for edt and odt bridges, respectively. Activation parameters for the isomerisation process showed a barrier of 20.1 kcal/mol with a pdt bridge. This was seen to increase slightly to 20.8 and 21.1 kcal/mol for the edt and odt bridged systems, respectively [104, 105]. The calculations are again in agreement with the experimental observations, with energy barriers for the rearrangement of **2A**^(s) to **2D** predicted at 18.1, 21.2 and 22.6 kcal/mol for pdt, edt and odt dithiolate bridges, respectively.

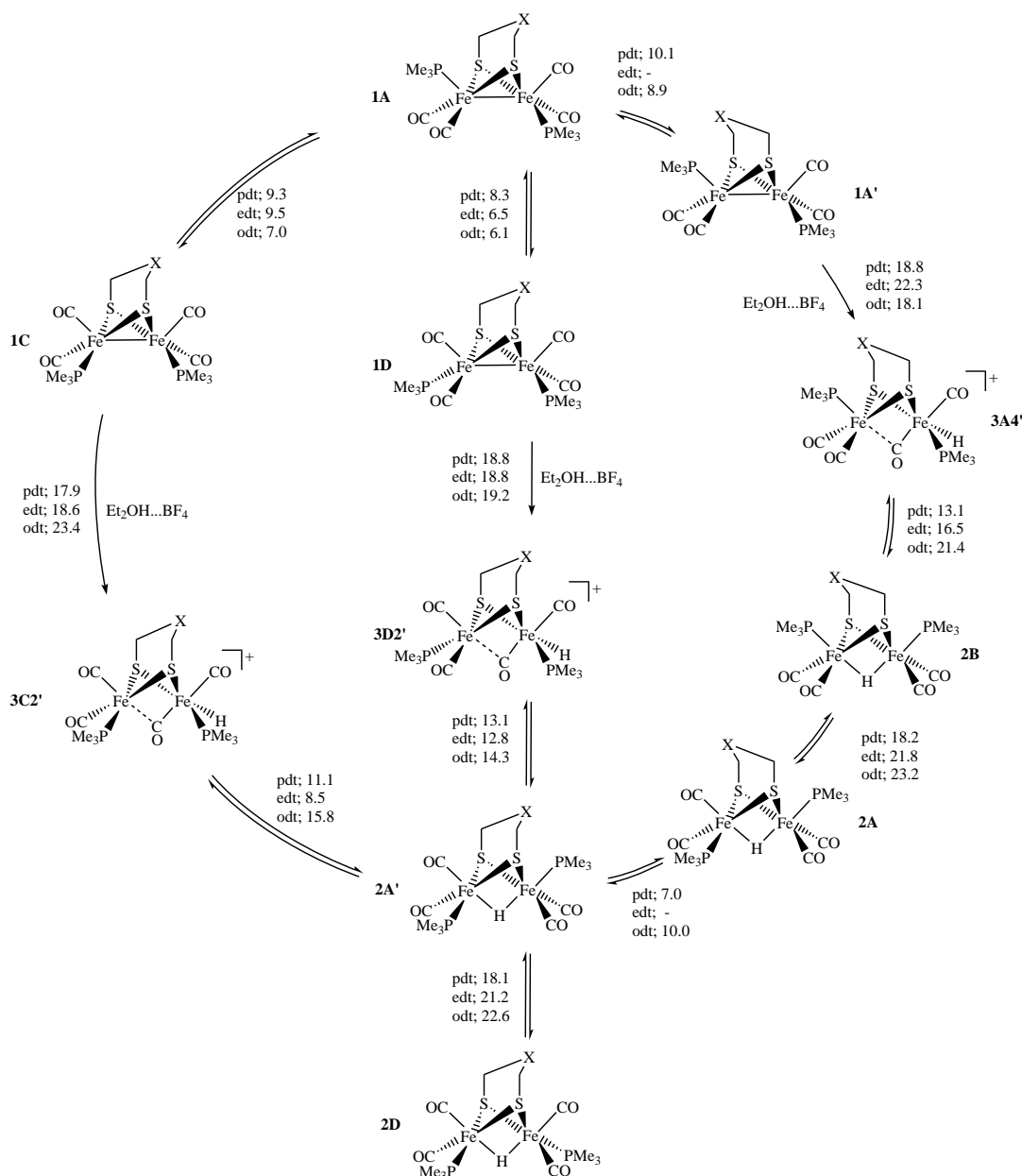


Figure 4.24: Comparison of the three most energetically favoured reaction pathways for the protonation of $[Fe_2(\mu-Xdt)(CO)_4(PMe_3)_2]$ with *edt*, *pdt* and *odt* dithiolate bridges. Solvent correct free energy barriers are reported in kcal/mol.

Chapter 5

Mixed valence



Subsites

Mixed-valence Fe(I)–Fe(II) hydrides have been postulated as intermediates in the turnover of the enzyme and also in electrocatalysis of proton reduction mediated by synthetic Fe(I)–Fe(I) subsite analogues [47, 70, 133, 134]. Quantum mechanics/molecular mechanics (QM/MM) studies suggest that only protonated Fe(I)–Fe(II) systems are competent for dihydrogen evolution [70]. De Gioia has noted from DFT calculations that dihydrogen formation may occur via mixed-valence Fe(I)–Fe(II) μ -hydride species [62]. The evidence that such mixed-valence hydrides exist rested solely with cyclic voltammetric experiments showing the generation of more or less unstable species by reduction of Fe(II)–Fe(II) hydride precursors [135].

The singly reduced isomers of pdt **2** and pdt **3** shall be termed pdt **2**^{*} and pdt **3**^{*} from here on. DFT simulations of pdt **2**^{*} and pdt **3**^{*}, along with their edt and odt bridged analogues are considered in the first sections of this chapter. A combined spectroelectrochemistry, EPR and DFT study was carried out on singly reduced species containing pdt or edt dithiolate linkers. In the latter part of the chapter, a combined μ SR and DFT study is carried out on $(\mu\text{-pdt})[\text{Fe}(\text{CO})_2(\text{PMe}_3)_2]_2$ and $(\mu\text{-pdt})[\text{Fe}(\text{CO})_2(\text{CN})_2]_2^{2-}$ model systems in order to help understand the mechanism of the radical hydrogen analogue ad-

dition. Notably, the addition of Mu to the subsites is analogous to adding the proton and the electron simultaneously.

5.1 Computational details

Geometry optimisations and frequency calculations on the reduced systems were carried out using the same computational parameters to those outlined in Chapter 3.2. EPR parameters were determined using the spin unrestricted Beck3LYP (B3LYP) hybrid GGA functional [108–110]. Iron, sulphur and phosphorus were characterised by the double-zeta split valence basis set with polarisation functions and diffuse functions, 6-31+G(d,p). Hydrogen, carbon, oxygen and nitrogen were characterised by the EPR-III basis set [136].

5.2 Relative energies of the isomers of $[(\mu\text{-H})\text{Fe}_2(\mu\text{-Xdt})(\text{CO})_4(\text{PMe}_3)_2]$ subsites

Observing bridging hydrides, $\mathbf{2}^*$, isomer $\mathbf{2D}$ is predicted to be the most stable before and after reduction, for all three bridge types investigated. In the case of the edt bridged system, the order of stability is predicted to remain the same after reduction (see Table A4 and Table A11 in appendix). However, for the pdt and odt systems the order of stability of the isomers is altered following reduction. Upon reduction, all isomers of $\mathbf{2}^*$ are stabilised relative to $\mathbf{2D}^*$, reducing the energy range of the isomers by ~ 1.5 kcal/mol, ~ 3.5 kcal/mol and 1.6 kcal/mol for pdt, edt and odt bridged systems, respectively (see Table A19, Table A34, Table A25 and Table A40 in appendix). The singly occupied molecular orbitals (SOMOs) for isomer $\mathbf{2D}^*$ for each bridge type are displayed in Figure 5.1. All are characterised by anti-bonding orbitals around Fe–Fe, anti-bonding orbitals between Fe and apically bound COs and bonding orbitals between Fe and basally bound COs. Therefore, reducing these complexes should be coupled with an increase in Fe–Fe bond distances, which is in fact the case, by an average of 0.150 Å, 0.148 Å and 0.141 Å for edt, pdt, and odt bridges, respectively. Additionally, reduction causes the Fe–CO_{ap} bond distances to increase and the Fe–CO_{ba} bond distances to shorten.

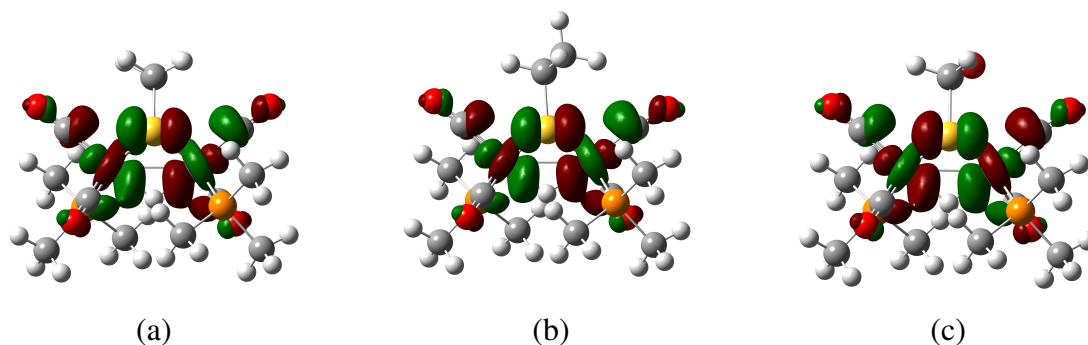


Figure 5.1: SOMO for the **2D** isomer of the (a) edt (b) pdt and (c) odt dithiolate bridged complexes. Isosurface=0.4.

Interestingly, the energy barriers associated with the rotation of the $\text{Fe}(\text{CO})_2(\text{PMe}_3)$ moiety are predicted to be significantly lower after reduction, by an average of 6.3, 8.7 and 8.9 kcal/mol for edt **2***, pdt **2***, and odt **2***, respectively. Additionally, the energy associated with the bridge flip is predicted to be lower after reduction (see Table A19 and Table A25). Terminal hydrides **3*** are stabilised relative to isomer **2D*** by an average of 5.7, 6.6 and 7.1 kcal/mol for edt, pdt, and odt bridged systems, respectively, relative to their unreduced counterparts. Since the rotational energy barriers that connect terminal hydrides to bridging hydrides are predicted to be lower after reduction, terminal hydrides are more energetically accessible following reduction.

5.3 Simulated infrared of $[(\mu\text{-H})\text{Fe}_2(\mu\text{-Xdt})(\text{CO})_4(\text{PMe}_3)_2]$ subsites

The singly reduced odt bridged system has not been investigated spectroscopically, so its part in the discussion ends here. Experimentally, pdt **2D** exhibits two peaks in the carbonyl region, at 1989 and 2031 cm^{-1} [67, 137]. Upon reduction, these are rapidly replaced by two new bands at 1900 cm^{-1} and 1948 cm^{-1} (see Figure 5.2) [137]. Wright *et al.* determined the kinetic product to have a half-life of 1.6 seconds, as measured by the loss of the absorption at 1948 cm^{-1} [137]. The thermodynamic product gave four spectral features at 1841, 1863, 1899 and 1943 cm^{-1} . It is possible that the complex/complexes

responsible for this spectrum could be a mixture of singly and doubly reduced isomers. Experimentally, the edt analogue was found to exhibit a similar pattern of reactivity to the pdt system, with starting material signals at 1994 cm^{-1} and 2035 cm^{-1} being replaced by peak maxima at 1902 cm^{-1} and 1951 cm^{-1} (see Figure 5.3) [137]. Here, the intermediate was found to be shorter lived, with a half-life of $\sim 0.4\text{ s}$. The thermodynamic product gave bands at 1870 cm^{-1} , 1902 cm^{-1} and 1937 cm^{-1} . In the primary reduction of pdt **2** and edt **2**, the retention of the peak pattern of the starting material suggests that the kinetic product has the same geometry as the parent compound, **2D**. The peak positions for the simulated spectra of pdt **2*** and edt **2*** isomers are given in Table 5.1 and Table 5.2. In the case of the pdt bridged system, the simulated spectra agree with the initial formation of isomer pdt **2D***, which gives an unresolvable feature at 1920 cm^{-1} and bands at 1958 and 1972 cm^{-1} (see Figure 5.2). There is a shift in the position of ν_1 and ν_2 by ca. 20 cm^{-1} in the simulated resonance positions relative to the experimentally observed peak positions. Here again, the feature at 1972 cm^{-1} is predicted to be of negligible intensity due to the symmetry of the vibration. In the case of the edt bridged complex, none of the simulated spectral features give agreement with the experimentally observed band at 1902 cm^{-1} . Isomer edt **2D*** gives rough agreement, but peaks ν_1 and ν_2 are again shifted again by $\sim 20\text{ cm}^{-1}$. With the exception of **2D***, all isomers are predicted to produce bands at $\sim 1980 - 2000\text{ cm}^{-1}$, a band at this frequency was not observed experimentally. The experimentally observed thermodynamic products of both bridge types give a poor match with the simulated peak positions of all bridging isomers, none are predicted to produce a peak near the 1841 cm^{-1} resonance. Notably, the presence of such low wavenumber spectral features is consistent with bridging CO (see Table 5.4 and Table 5.5) or, a terminal ν CO in a doubly reduced species (see Table 5.3). Comparing the peak positions of pdt **2*** ($1841, 1863, 1899$ and 1943 cm^{-1}) with those simulated for the doubly reduced isomer pdt **2A**** ($1858, 1871, 1907$ and 1937 cm^{-1}), good agreement can be observed.

Some isomers of pdt **3*** edt **3*** maintain a relatively short Fe–Fe bond distance relative to their unreduced counter-parts, while in other isomers the bond distance is significantly elongated. In the isomers of edt **3A***, the Fe–Fe bond distance is predicted to be at its

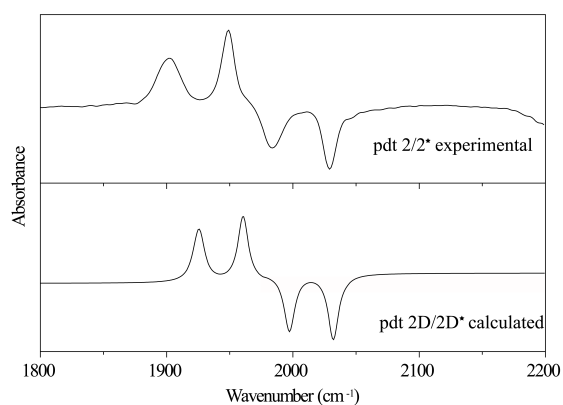


Figure 5.2: Top: Experimental difference IR spectrum of the reduction of the pdt dithiolate bridged system [67, 137]. Bottom: Calculated difference spectrum of the reduction of isomer pdt 2D.

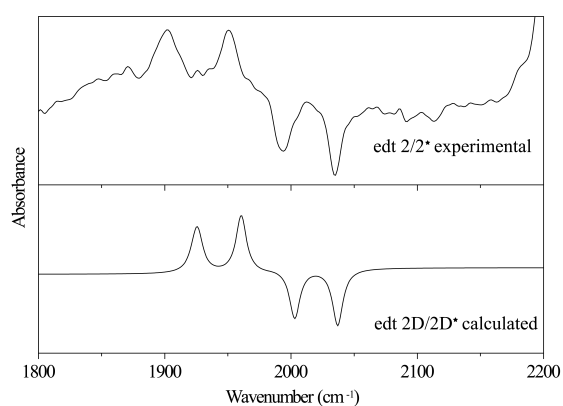


Figure 5.3: Top: Experimental difference IR spectrum of the reduction of the edt dithiolate bridged system [137]. Bottom: Calculated difference spectrum of the reduction of isomer edt 2D.

shortest when the hydride is basally coordinated to Fe_1 , adjacent to the apical PMe_3 and *cisoid* to the basal PMe_3 ligand of Fe_2 , as is found in isomer **3A1***. In this configuration, the semi-bridging CO is the closest to Fe_2 out of all isomers. In the pdt bridged complex, the Fe–Fe bond distance is further shortened, by 0.03 \AA when the dithiolate bridge faces the more sterically hindered apical PMe_3 ligand. Comparing pdt **3A1*** and pdt **3A1'***, the Fe–Fe– PMe_3 angle increases by 4° in the more hindered isomer which may force the irons to converge ever so slightly. The semi-bridging CO is consequently 0.1 \AA closer in pdt **3A1'**. Predictably, the additional back-donation from the iron into the π^* orbitals of CO, weakens the CO bond, causing a significant shift downfield in the bridging carbonyl frequency (here at its lowest for the bridging hydride isomers at 1802 cm^{-1} compared to the next lowest, in pdt **3A1** at 1827 cm^{-1}). Comparing the spin density of these two isomers, there is no observable difference (see Figure 5.4). In edt **3A2** the hydride is located *transoid* to the basal PMe_3 ligand of Fe_2 , which seems to slightly elongate the

Table 5.1: DFT simulated $\nu(CO)$ bands of singly reduced bridging hydride isomers of $[(\mu-H)Fe_2(\mu-pdt)(CO)_4(PMe_3)_2]$ compared to those experimentally determined in CH_3CN [67, 137].

Isomer	$\nu(CO)$ (cm ⁻¹)			
Exp. pdt 2[*]_K	1900			1948
Exp. pdt 2[*]_T	1841	1863	1899	1943
pdt 2A[*]	1925	1935	1971	1991
pdt 2A'[*]	1929	1933	1972	1990
pdt 2B[*]	1944 ⁿ	1953	1985	2006
pdt 2C[*]	1919	1925	1962	1982
pdt 2D[*]	1918	1923	1958	1972 ⁿ

ⁿ negligible peak intensity due to symmetry

Table 5.2: DFT simulated $\nu(CO)$ bands of singly reduced bridging hydride isomers of $[(\mu-H)Fe_2(\mu-edt)(CO)_4(PMe_3)_2]$ compared to those experimentally determined in CH_3CN [67].

Isomer	$\nu(CO)$ (cm ⁻¹)			
Exp. edt 2[*]_K	1902			1951
Exp. edt 2[*]_T	1870	1902		1937
edt 2A[*]	1931	1934	1972	1991
edt 2B[*]	1944 ⁿ	1954	1984	2006
edt 2C[*]	1924	1931	1963	1983
edt 2D[*]	1924	1926	1961	1974 ⁿ

ⁿ negligible peak intensity due to symmetry

Fe–Fe bond distance relative to **3A1** (by 0.009 Å), the C_{semi}–Fe₂ bond distance lengthens (by 0.03 Å). In the case of the pdt bridged system, when the pdt linker faces the apical PMe₃ in pdt **3A2'^{*}** the Fe–Fe bond distance is again shorter (shorter by 0.03 Å compared to pdt **3A2**), and is in fact shorter than in pdt **3A1^{*}**, indicating that the orientation of the dithiolate bridge dominates this effect, seemingly acting as a channel for the charge. Like the unreduced systems, isomers **3C1^{*}** are predicted to have the longest bond distances in

Table 5.3: DFT simulated $\nu(CO)$ bands of doubly reduced bridging hydride isomers of $[(\mu-H)Fe_2(\mu-pdt)(CO)_4(PMe_3)_2]^-$ compared to those experimentally determined in CH_3CN [137].

Isomer	$\nu(CO)$ (cm ⁻¹)			
Exp. pdt 2[*]_K	1900			1948
Exp. pdt 2[*]_T	1841	1863	1899	1943
pdt 2A^{**}	1858	1871	1907	1937
pdt 2A'^{**}	1819	1879	1885	1935
pdt 2B^{**}	1878 ⁿ	1889	1926	1945
pdt 2C^{**}	1856	1860	1898	1918
pdt 2D^{**}	1822	1831	1871	1889 ⁿ

ⁿ negligible peak intensity due to symmetry

both bridged systems.

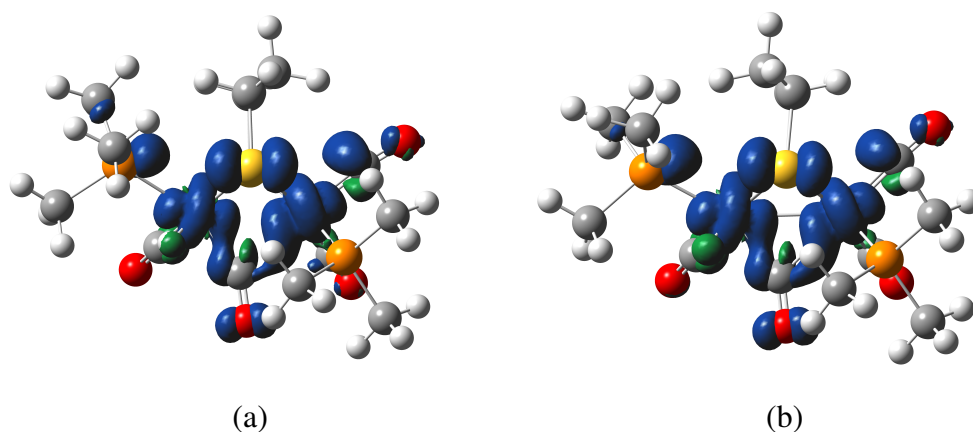
Table 5.4: DFT simulated $\nu(CO)$ bands of singly reduced terminal hydride isomers of $[(H)Fe_2(\mu-pdt)(CO)_4(PMe_3)_2]$ compared to those experimentally determined in CH_3CN [67].

Isomer	$\nu(CO)$ (cm ⁻¹)				
Exp. pdt 2 ^{*_K}	1900			1948	
Exp. pdt 2 ^{*_T}	1841	1863	1899	1943	
pdt 3A1 [*]	1827	1913	1927	1968	1992
pdt 3A1' [*]	1802	1922	1935	1964	1994
pdt 3A2 [*]	1836	1928	1934	1962	1990
pdt 3A2' [*]	1810	1936	1943	1959	1994
pdt 3A3 [*]	1896	1933	1952	1976	1998
pdt 3A3' [*]	1881	1934	1947	1976	1999
pdt 3A4 [*]	1906	1931	1949	1984	2002
pdt 3A4' [*]	1919	1930	1955	1975	1996
pdt 3B [*]	1872	1949 ⁿ	1953	1969	2003
pdt 3B' [*]	1917	1940 ⁿ	1944	1973	2001
pdt 3C1 [*]	1894	1908	1949	1962	1995
pdt 3C1' [*]	1897	1909	1952	1962	1994
pdt 3C2 [*]	1905	1919	1948	1958	1986
pdt 3C2' [*]	1902	1915	1947	1965	1988
pdt 3D1 [*]	1875 ⁿ	1910	1936	1960	1987
pdt 3D1' [*]	1877 ⁿ	1913	1938	1960	1985
pdt 3D2 [*]	1901	1912	1944	1953	1981 ⁿ
pdt 3D2' [*]	1825	1924	1935	1969	1980 ⁿ

ⁿ indicates a band of negligible intensity

Table 5.5: DFT simulated $\nu(\text{CO})$ bands of singly reduced terminal hydride isomers of $[(\text{H})\text{Fe}_2(\mu\text{-edt})(\text{CO})_4(\text{PMe}_3)_2]$ compared to those experimentally determined in CH_3CN [137].

Isomer	$\nu(\text{CO})$ (cm^{-1})				
Exp. edt 2^*_K	1902			1951	
Exp. edt 2^*_T	1870	1902		1937	
edt 3A1*	1815	1912	1939	1968	1995
edt 3A2*	1828	1936	1938	1960	1993
edt 3A3*	1917	1931	1957	1978	1998
edt 3A4*	1863	1935	1941	1977	2000
edt 3B*	1962	2006	2014	2022	2051
edt 3C1*	1878	1914	1943	1963	1996
edt 3C2*	1910	1923	1953	1963	1990
edt 3D1*	1859 ⁿ	1915	1928	1962	1987
edt 3D2*	1893	1918	1947	1957	1982 ⁿ

ⁿ indicates a band of negligible intensity**Figure 5.4:** Isosurface of the spin density distribution of the singly reduced form of the basal/basal transoid isomer of $(\mu\text{-H})(\mu\text{-pdt})\text{Fe}_2(\text{CO})_4(\text{PMe}_3)_2$ (a) top view and (b) side view

5.4 EPR of mixed valence subsites

In a collaboration with the EML, EPR studies were carried out on the pdt 2^* system. These confirmed the presence of a paramagnetic di-iron complex. Isomer pdt 2 was reduced using the acenaphthylene monoanion radical ($E_1 = -2.12$ V vs Fc^+/Fc) in THF at 195 K and examined using EPR spectroscopy. Figure 5.5(top) shows the well defined isotropic solution $S = \frac{1}{2}$ spectrum obtained at 165 K. Analysis revealed that this EPR spectrum is characterised by a g factor of 2.0066 and strong hyperfine interactions with three nuclei: two equivalent phosphorus atoms ($A_{iso} = -41.7$ MHz) and the bridging hydride ($A_{iso} = -75.8$ MHz). This assignment was confirmed by the reduction for the bridge-deuterated analogue of 2D . The spectrum of this species (see Figure 5.5, bottom) shows

the anticipated 1:1:1 splitting for coupling to the bridging deuteride, with the coupling constant reduced by the magnetogyric ratio γ_D/γ_H ($\gamma_D/\gamma_H=0.153523$, where γ_D and γ_H are the magnetogyric ratios of ^2H and ^1H respectively) ($A_{iso} = -11.6\text{MHz}$); the phosphorus coupling is unchanged. This pattern of coupling is in accord with a symmetrical disposition of the radical character. Isomer **2D**^{*} was predicted a g factor of 2.0061, which is in good agreement with the experimentally observed value. The spin density of pdt **2D**^{*} is primarily localised on the iron atoms (see Figure 5.6), with the iron centres bearing a total of 70% of the unpaired electron density (spin density is asymmetrically distributed because of the pdt bridge). Approximately 3% of the calculated spin density is located on the bridging hydride, while the two phosphorus atoms bear a total of 0.5%. In combination with the standard isotropic atomic hyperfine coupling values (1420 MHz for ^1H and 10178 MHz for ^{31}P) [31], the experimental coupling constants can be used to find empirical spin density dispositions: 5% for the bridging hydride and a total of 0.8% for the two phosphorus atoms.

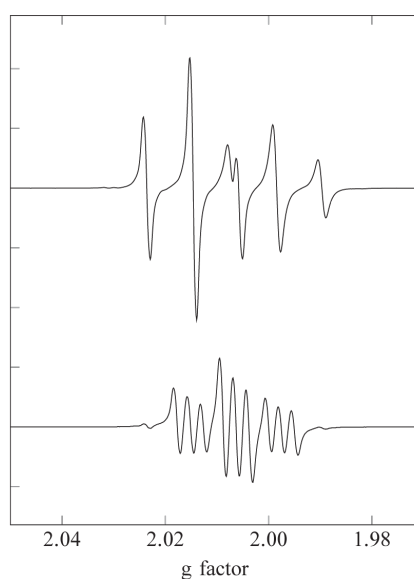


Figure 5.5: Continuous-wave X-band EPR spectra in THF: (top) reduced pdt **2D** at 165 K; (bottom) reduced deuterio-pdt **2D** at 164 K. The line-width variation across the spectra, which is due to the sign of the coupling constants, is most pronounced in the spectrum of reduced protio-pdt **2D** [137].

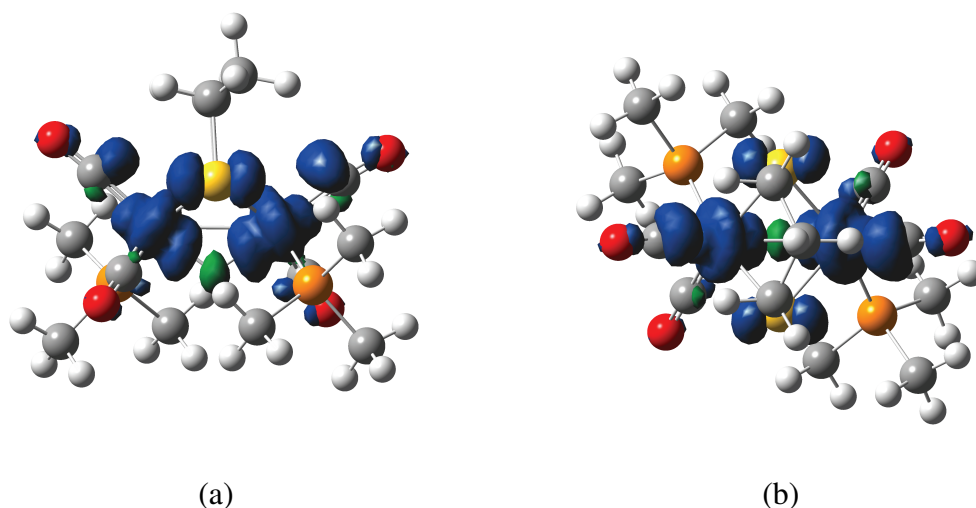


Figure 5.6: *Isosurface of the spin density distribution of the singly reduced form of the basal/basal transoid isomer of $(\mu\text{-H})(\mu\text{-pdt})\text{Fe}_2(\text{CO})_4(\text{PMe}_3)_2$ (a) top view and (b) side view*

5.4.1 Summary and conclusions

Paramagnetic metallohydrides seem likely candidates as intermediate species in the enzymic catalytic turnover of hydrogen. Studies using FTIR spectroscopy, DFT calculations, and EPR spectroscopy have enabled the characterisation of the first mixed-valence di-iron μ -hydride species. The FTIR and DFT calculations provide strong evidence that isomer p/edt **2D** forms **2D*** upon reduction. There is no evidence for the formation of a terminal hydride species on the basis of these results.

5.5 Investigating [Fe(I)Fe(II)]-hydrogenase model systems using muon spectroscopy and DFT calculations

The introduction to muon spectroscopy (see Chapter 2.1) discussed the similarity between μ and H. In this section, the regiochemistry of muonium addition to the di-iron centres is investigated. This concerted addition of muon and electron is analogous to the two-step process of protonation and reduction of the di-iron system discussed in the previous sections. This section describes a preliminary study in which μ SR spectroscopy is applied in combination with DFT calculations to investigate the binding sites of two artificial hy-

drogenase subsites, $[\text{Fe}_2(\mu\text{-pdt})(\text{CO})_4(\text{CN})_2]^{2-}$ and $[\text{Fe}_2(\mu\text{-pdt})(\text{CO})_4(\text{PMe}_3)_2]$ (see Figure 5.7). The study by Wright *et al.* using stopped flow IR investigated the protonation reaction of pdt **1** from ~ 0.1 seconds onwards. This indicated a two step mechanism: (1) protonation of the apical-basal isomer, **1A** to the Fe–Fe bond forming **2A**; (2) rearrangement from **2A** to the *trans*-basal isomer **2D** (see Figure 3.2) [104]. Notably, there was no evidence of the formation of a terminal hydride species within these time scales. Notably, the mechanistic study of the protonation of **1** discussed in Chapter 4 suggested a terminal hydride as the kinetic product. However, before this is formed the calculations predicted the formation of an intermediate species where the the $[\text{Et}_2\text{OH}]^+$ acid is weakly bound to the oxygen of a CO group of the subsite. This would presumably be too fast a process to be observed using the stopped flow techniques.

μSR spectroscopy offers a unique time window, allowing observation of the reaction between Mu and the subsite during the first few nano-seconds. The magnitude and sign of the muon-electron hyperfine coupling constant (hfcc) varies according to the muonium binding site. With the aid of DFT calculations it is possible to calculate the muon-electron hfccs associated with each radical structure. These can then be used to estimate the field at which Δ_0 and Δ_1 avoided level crossing corresponding to that structure occurs. Comparison of the predicted resonance positions with the experimental spectrum offers an insight into structure. Previous calculations on small organic systems have shown that in order to achieve accurate predictions of the isotropic hfcc, a high level of electron correlation and a flexible basis set are required. While this may be computationally achievable for small radicals species, large atoms such as iron, sulphur, and phosphorus make the calculation computationally expensive.

For the purposes of this section, the $[\text{Fe}_2(\mu\text{-pdt})(\text{CO})_4(\text{PMe}_3)_2]$ and $[\text{Fe}_2(\mu\text{-pdt})(\text{CO})_4(\text{CN})_2]$ subsites will be labelled *bisPMe₃* and *bisCN* from here on.

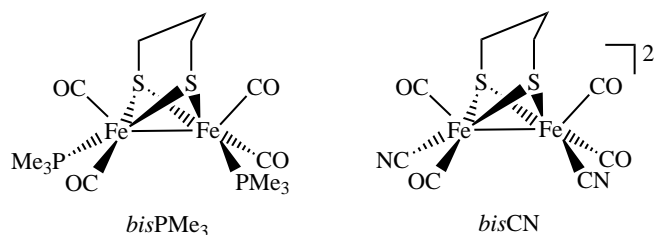


Figure 5.7: Artificial hydrogenase subsite analogues $[\text{Fe}_2(\mu\text{-pdt})(\text{CO})_4(\text{PMe}_3)_2]$ and $[\text{Fe}_2(\mu\text{-pdt})(\text{CO})_4(\text{CN})_2]^{2-}$ chosen for Longitudinal Field- μSR investigation.

5.5.1 Experimental

Sample environment

Solid samples of the $[\text{Fe}_2(\mu\text{-pdt})(\text{CO})_4(\text{PMe}_3)_2]$ and $[\text{N}(\text{Et})_4]_2[\text{Fe}_2(\mu\text{-pdt})(\text{CO})_4(\text{CN})_2]$ were prepared in the Energy Materials Laboratory. TF- μSR experiments were made using the EMU beamline at the ISIS pulsed muon facility at the Rutherford Appleton Laboratory (RAL, Chilton, UK). The sample environment was provided by a closed cycle refrigerator (CCR) cryostat. Samples were packed into ISIS titanium sample cells (25mm diameter) and covered with a mylar window, then mounted onto the cryostat. An initial 100 Gauss TF was taken in order to verify a missing fraction was present, this was observed to be $\sim 10\%$ for both complexes. μSR spectra were recorded between 2-5000 Gauss taking 10 MeV per scan. Scans were recorded at 5 K. A scan of the empty cell was taken prior to measurements to enable background subtraction. Data was fitted using two functions (a gaussian function corresponding to muons stopping in the titanium sample holder and a kubo-Toyabe function corresponding to muons stopping in the sample) with the WiMDA software package [138].

Computational details

Density functional calculations on the two systems were performed using the Gaussian software package [18, 19]. Muonation sites at the Fe–Fe bond, basal and apical terminal positions, at the sulphur of the dithiolate bridge, at each carbonyl and in the case of the *bisCN* complex, on the CN ligand, were considered. To this end, each hydrogenase radical was geometry optimised using the spin unrestricted Beck3LYP (B3LYP) hybrid GGA functional [108–110]. Iron, sulphur and phosphorus were characterised by the double-

zeta split valence basis set with polarisation functions and diffuse functions, 6-31+G(d,p). Hydrogen, carbon, oxygen and nitrogen were characterised by the EPR-III basis set [136]. Structures were confirmed as minima through frequency calculations. All calculations were performed by modelling the hydrogen analogue systems; where in each case the muon is modelled by a hydrogen atom. To account for the muons light mass relative to the hydrogen, the bond length was scaled by a factor of 1.02 [139]. Additionally, to account for the difference in the gyromagnetic ratio of the muon and the proton and thus obtain a more realistic muon hfcc, the proton hfcc was multiplied by a factor of 3.183.

5.5.2 Results and discussion

As discussed in Chapter 3.3.1, there are five structural isomers for both the *bis*PMe₃ and *bis*CN complexes, depending on the relative positions of the X ligands (X=CN or PMe₃). The x-ray crystal structures of the *bis*PMe₃ complex was isolated in a basal/basal *transoid* arrangement of the PMe₃ ligands, while the *bis*CN gave an apical/basal arrangement of the CN ligands [69, 140]. The DFT calculations reported in Chapter 3.3.1 showed that the apical/apical arrangement of the PMe₃ ligands was the most energetically favoured in the gas phase, with the cryptographically identified structure, **1D**, 1.0 kcal/mol less stable. The relative stabilities of the five *bis*CN isomers also gave the apical/apical arrangement as the most stable, with the apical/basal isomer 1.1 kcal/mol less stable (see Table 5.6). The barriers to rotation of the *bis*CN were not investigated. However, these are not expected to differ significantly from those of the *bis*PMe₃ complex, which were found to be ~10 kcal/mol. While this may be feasible at room temperature, at low temperatures these barriers are less likely to be overcome. With this in mind, only the geometry optimised structures corresponding to the crystal structures of *bis*PMe₃ and *bis*CN were investigated for possible muon binding. Muonium addition was considered to occur at numerous sites; to the Fe–Fe bond, apical and basal positions on the Fe, at the sulphur, carbonyl (bound to either oxygen or carbon) and cyanide ligands. These have been given numbered labels to differentiate them (see Figure 5.9 and Figure 5.10). The difficulty with these calculations comes with modelling iron, sulphur and phosphorus atoms.

Table 5.6: Relative stabilities of the isomers of the $[\text{Fe}_2(\mu\text{-pdt})(\text{CO})_4(\text{CN})_2]^{2-}$ model complex.

Isomer	ΔG_g (kcal/mol)
<i>bis</i> CN A	0.0
<i>bis</i> CN A'	1.1
<i>bis</i> CN B	-1.1
<i>bis</i> CN C	5.2
<i>bis</i> CN D	3.1

Figure 5.8 shows the ALC- μ SR spectra recorded from the muoniation of *bis*PMe₃ and *bis*CN complexes. Both of the polycrystalline samples produced a broad asymmetric feature located at ~ 0.12 Tesla, suggesting that the mode of binding is similar in both complexes. The initial rise in asymmetry observed in Figure 5.8 is due to the gain of the muon polarisation, as can be seen in the Breit-Rabi diagram (see Figure 2.6) when the field is swept up. The observed dip in polarisation may correspond to a Δ_1 resonance; a mixing of the spin states that have the same electron and nuclear spins but different muon spin (see 2.1). Since there are no protons or nuclei with a non-zero spin in the vicinity, Δ_0 resonances are unlikely to be observed. The broad asymmetric shape of the observed spectral feature appears like a powder pattern and could also be the result of several muon binding sites, each with a different Δ_1 resonance. The asymmetric nature of the spectral feature is due to it being a powder spectrum, this phenomenon was discussed in the Chapter 2.1.

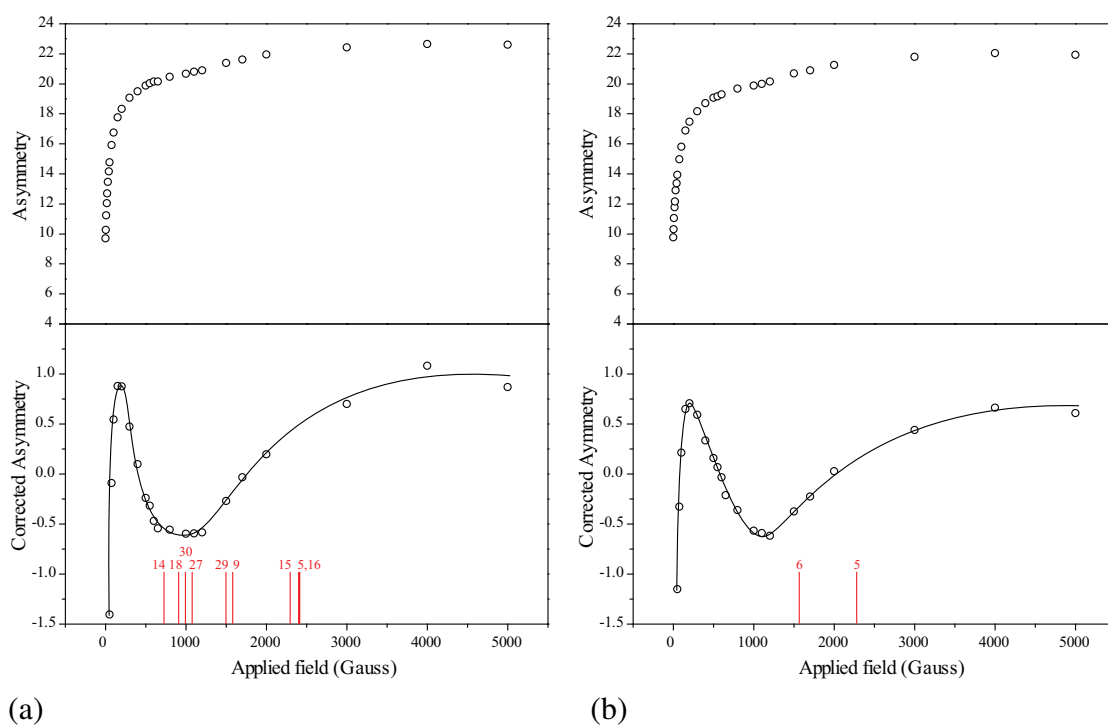


Figure 5.8: μ -SR spectra of (a) $[\text{Fe}_2(\mu\text{-pdt})(\text{CO})_4(\text{CN})_2]^{2-}$ recorded at 5 K and (b) $[\text{Fe}_2(\mu\text{-pdt})(\text{CO})_4(\text{PMe}_3)_2]$ recorded at 5 K. Raw spectra are reported at the top and background subtracted spectra at the bottom. The background of the aluminium plate was recorded at 5 K.

According to equation (2.15), the level crossing resonances observed for the *bis*CN and *bis*PMe₃ radicals correspond to hfc's of ~ 33 MHz. The calculated hfc and resonance fields associated with each of the investigated muonium adducts are displayed in Table 5.7 and Table 5.8. The solid state structure of the *bis*CN complex features an apical and basal CN ligand. As the pdt bridge can flip, there are a larger number of isomers available for the muon to bind to. It will be shown that the direction of the pdt bridge has a significant influence on the muon-electron hfc. There are a large number of muoniated radicals that could be responsible for resonances observed in the experimental spectrum. Structures **5** and **7**, where the muon is bound to the basal position *cisoid* to the basal CN or *cisoid* to the apical CN, give hfc's of 65 MHz and 24 MHz, respectively. Equation (2.15) predicts these hyperfines correspond to resonances centred at 0.24 Tesla and 0.09 Tesla, respectively, giving rough overlap with the experimental spectrum. Notably, these radicals are not predicted to be the most stable. The calculations indicate that the spin density in **5** is localised mainly on the Fe and S atoms. It is distributed asymmetrically between the Fe centres with 47% of the unpaired electron density on Fe₁ and 20% on Fe₂ (see Fig-ure 5.11(a)). An asymmetric distribution of unpaired electron density is also predicted

between S atoms, with approximately 4% on the S *cisoid* to the muonium and 3% on the S *transoid* to muonium. Interestingly, flipping of the pdt bridge seems to have a significant influence on the structure. When the dithiolate bridge faces the muonium bound iron (Fe_2) in **5**, the $\text{Fe}_1\text{-Fe}_2$ and $\text{Fe}_1\text{-C}_{\text{semi}}$ bond distances are 0.245 Å and 0.559 Å shorter than in **6** where it faces the unbound iron (Fe_2). This difference in structure modifies the predicted muon-electron hpc with a 60.4 MHz difference predicted between the two structures. The spin density of **6** has approximately 73% of the unpaired electron density on Fe_1 with only 3% on Fe_2 . This would account for the difference in hfcs observed between these radicals (see Figure 5.11). This indicates the possibility of an electron circuitry existing in the complexes that is better connected when the pdt bridge faces toward Fe_2 rather than Fe_1 . Radicals *bisCN-9*, *bisCN-14*, *bisCN-15*, and *bisCN-16* also give rise to hfcs that are in rough agreement with the resonance position in the experimental spectrum. These are radical structures where the muon is bound to the carbon atoms of the apical (in *bisCN-9*) and basally coordinated CO groups (in *bisCN-14*, *bisCN-15*, and *bisCN-16*). Radicals *bisCN-29* and *bisCN-30* see the muon bound to the carbon of apical CN ligands, and give hfcs of 40 MHz and 28 MHz, respectively. Radicals *bisCN-18* and *bisCN-27*, where the muon is either bound to the oxygen of a basal CO group or the nitrogen of an apical CN ligand, respectively, also give rough agreement with the experimental resonance with predicted hfcs of 26 MHz and 29 MHz, respectively. Like all radicals that feature the muon bound to oxygen of a CO ligand, radical *bisCN-18* shows that the formation of a 6-membered ring made up of the Fe, CO, CN, and Mu is predicted. These are all important findings because in modelling the ether mediated protonation mechanism (see Chapter 4), the proton was first predicted to form a weak hydrogen-bond with the carbonyl oxygen before migrating past the carbon and being transferred onto the iron. The most important observation here is that muonation to the Fe-Fe bond results in the most stable structure, but produces a large hyperfine coupling of 216 MHz corresponding to a resonance at 0.79 Tesla. This field region was not investigated since it is beyond the operating capacity of the EMU instrument. Further measurements on an instrument capable of scanning at higher fields are required to rule out the possibility of muonium binding to the Fe-Fe bond.

For the *bisPMe₃* complex, structures where the muonium is bound terminally in the basal position (*bisPMe₃*-**5**) and bound to the apical CO (*bisPMe₃*-**6**) have muon-electron hfcs of 64 MHz and 44MHz, which would produce resonances at 0.23 and 0.16 Tesla respectively. The unpaired electron density of *bisPMe₃*-**5** is primarily localised on the iron, sulphur, and apical carbon atoms (see Figure 5.12(b)), having 41% on Fe₁, 30% on Fe₂, ca. 5% on each S, and ca. 4% on each apical carbon. Flipping the pdt bridge seems to influence the stability of the structure of the *bisPMe₃* radicals. When the pdt bridge faces the muon bound iron (Fe₂) in *bisPMe₃*-**4** the Fe₁-Fe₂ and Fe₂-C_{semi} are 0.023 Å and 0.116 Å shorter than when the pdt linker faces the unbound iron (Fe₁) in **5**. The spin density of *bisPMe₃*-**5** is also more asymmetrically distributed across the irons, with 49% on Fe₁, 25% on Fe₂, ca. 5% on each S, and ca. 4% on each apical carbon. The influence that the pdt bridge has on structure and the spin density is less pronounced in the *bisPMe₃* radicals, than in the *bisCN* complexes. This suggests that it is the nature of the substituted ligand, i.e. how electron withdrawing or electron donating the groups are *transoid* to the sulphurs of the dithiolate bridge. This is expected to influence the connectedness of the electron circuitry of the radical structure. No other radicals produce hfccs close to the resonance observed in the experimental spectrum. Importantly again, binding muonium to the Fe-Fe bond results in a high hyperfine coupling of 203 MHz corresponding to a resonance at 0.75 Tesla. ALC measurements on the HIFI instrument at ISIS would need to be recorded in order to either confirm or rule out this bridging site.

Table 5.7: Calculated muon-electron hyperfine coupling constants, $A_{e\mu}$, and associated resonance fields of the $[\text{MuFe}_2(\mu\text{-pdt})(\text{CO})_4(\text{CN})_2]^{2-}$ model complex.

Radical	ΔG_g (kcal/mol)	$A_{e\mu}$ (MHz)	B_{res} (Tesla)
Exp.		~33	~0.12
<i>bis</i> CN-1	0.0	213.95	0.79
<i>bis</i> CN-2	-6.8	224.53	0.82
<i>bis</i> CN-3	8.7	295.08	1.08
<i>bis</i> CN-4	3.3	312.81	1.15
<i>bis</i> CN-5	13.0	65.14	0.24
<i>bis</i> CN-6	4.3	4.70	0.02
<i>bis</i> CN-7	11.1	23.92	0.09
<i>bis</i> CN-8	2.1	81.13	0.30
<i>bis</i> CN-9	-0.2	42.96	0.16
<i>bis</i> CN-10	1.8	76.23	0.28
<i>bis</i> CN-11	7.1	465.33	1.71
<i>bis</i> CN-12	8.9	400.77	1.47
<i>bis</i> CN-13	15.2	92.47	0.34
<i>bis</i> CN-14	15.8	19.59	0.07
<i>bis</i> CN-15	12.1	62.40	0.23
<i>bis</i> CN-16	13.6	65.35	0.24
<i>bis</i> CN-17	9.6	339.85	1.25
<i>bis</i> CN-18	10.8	25.61	0.09
<i>bis</i> CN-19	36.7	260.80	0.96
<i>bis</i> CN-20	39.6	309.35	1.14
<i>bis</i> CN-21	39.4	277.62	1.02
<i>bis</i> CN-22	41.1	270.08	0.99
<i>bis</i> CN-23	43.1	245.75	0.90
<i>bis</i> CN-24	43.4	235.24	0.86
<i>bis</i> CN-25	46.2	121.66	0.45
<i>bis</i> CN-26	43.2	-5.88	0.02
<i>bis</i> CN-27	23.5	28.73	0.11
<i>bis</i> CN-28	10.9	5.88	0.02
<i>bis</i> CN-29	26.7	40.17	0.15
<i>bis</i> CN-30	14.2	28.42	0.10
<i>bis</i> CN-31	15.2	711.86	2.61
<i>bis</i> CN-32	17.9	756.34	2.78
<i>bis</i> CN-33	12.8	721.85	2.65
<i>bis</i> CN-34	14.3	736.82	2.71

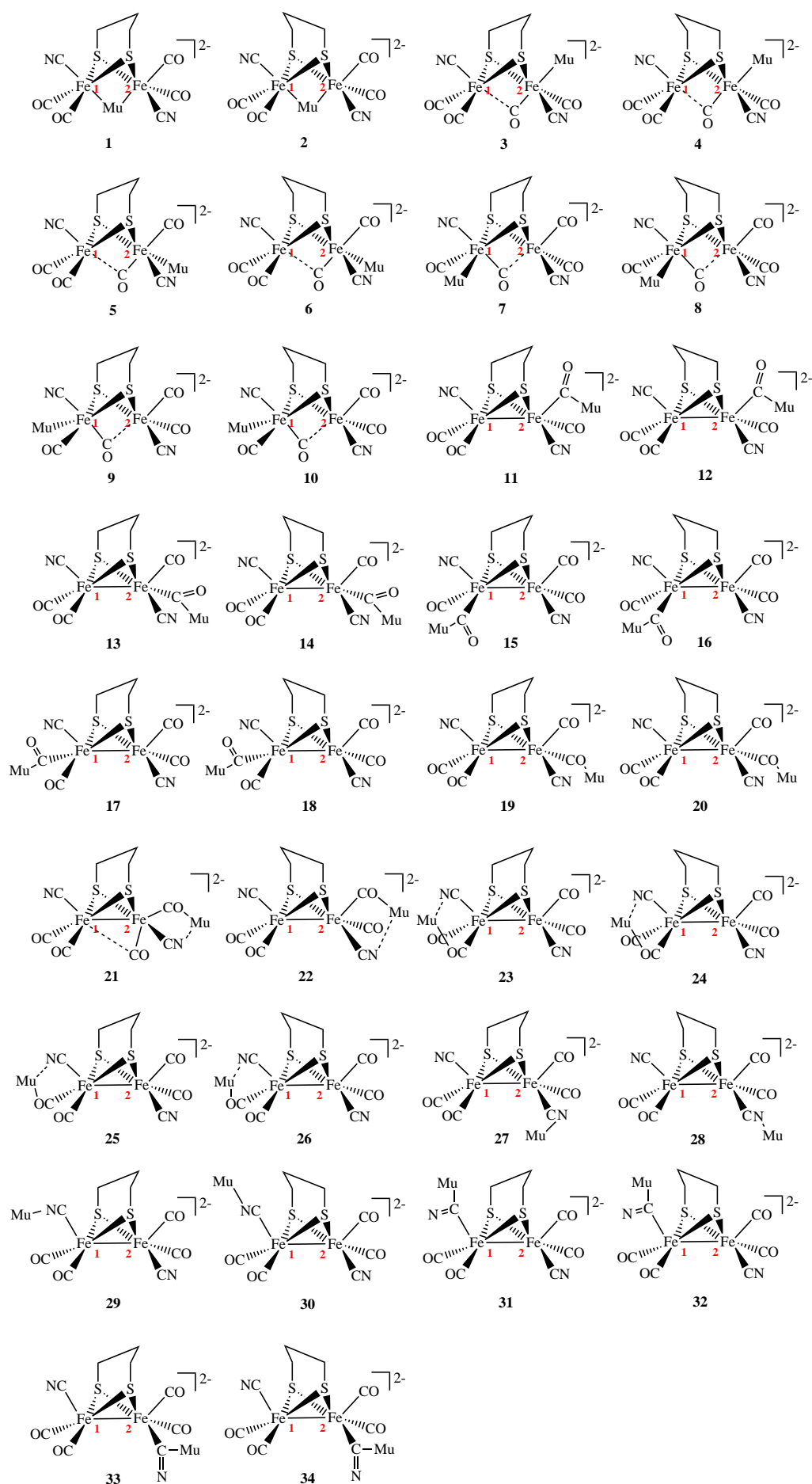


Figure 5.9: Structural isomers of possible $[MuFe_2(\mu-pdt)(CO)_4(CN)_2]^{2-}$ muoniated radicals.

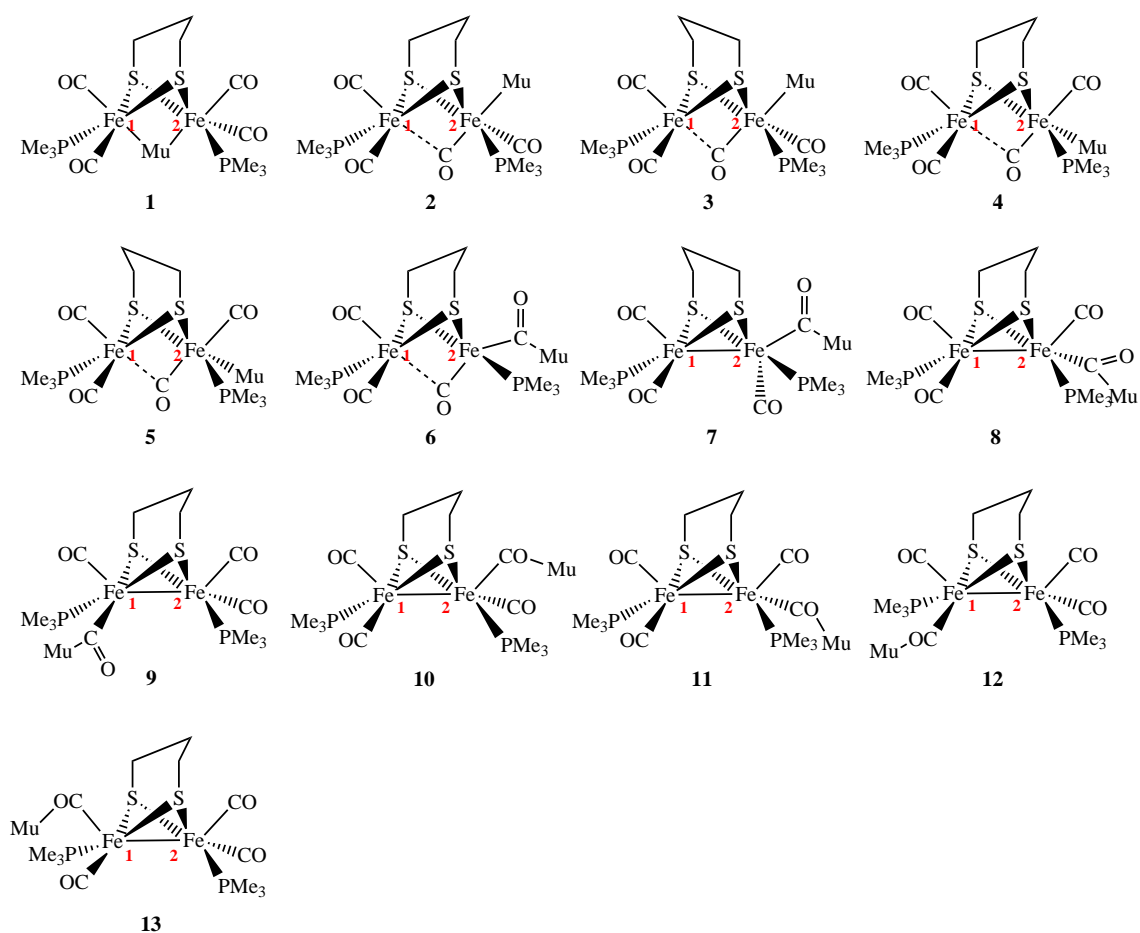


Figure 5.10: Structural isomers of possible $[MuFe_2(\mu-pdt)(CO)_4(PMe_3)_2]$ muoniated radicals.

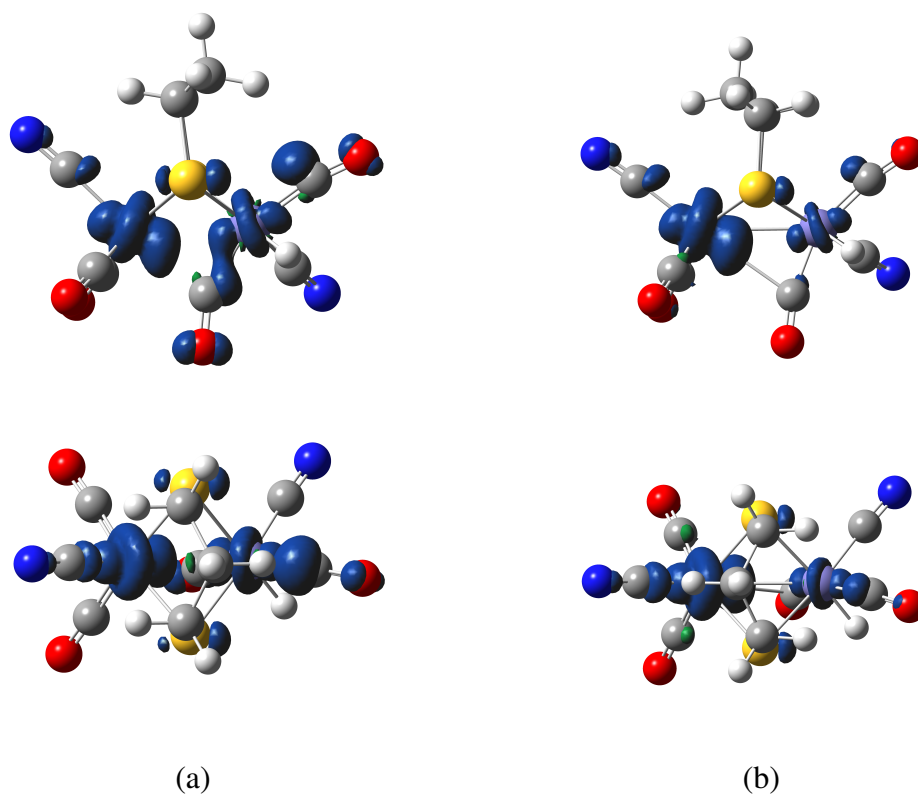


Figure 5.11: Spin densities of the (a) bisCN 5 and (b) bisCN 6 isomers. Isosurface = 0.004

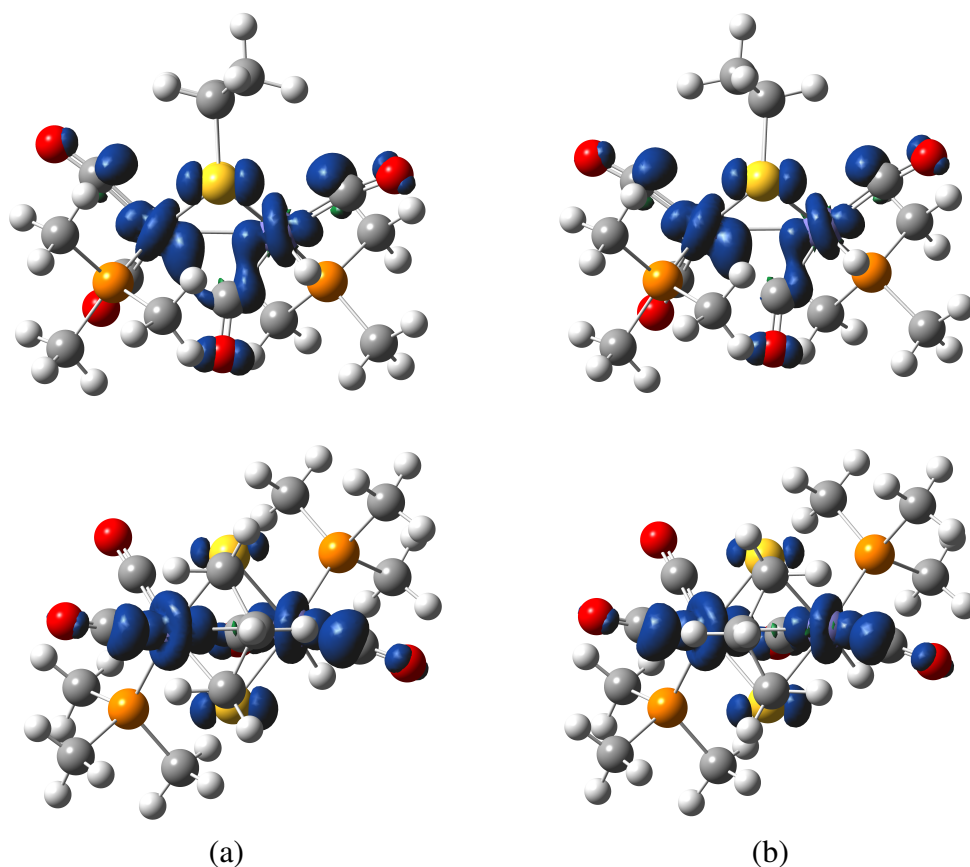


Figure 5.12: Spin densities of the (a) *bisPMe*₃ 4 and (b) *bisPMe*₃ 5 isomers. Isosurface = 0.004

Table 5.8: Calculated muon-electron hyperfine coupling constants, $A_{e\mu}$, and associated resonance fields of the $[\text{MuFe}_2(\mu\text{-pdt})(\text{CO})_4(\text{PMe}_3)_2]$ model complex.

Radical	ΔG_g (kcal/mol)	$A_{e\mu}$ (MHz)	B_{res} (Tesla)
Exp.		~33	~0.12
<i>bisPMe</i> ₃ -1	0.0	203.23	0.75
<i>bisPMe</i> ₃ -2	6.7	299.52	1.10
<i>bisPMe</i> ₃ -3	7.4	222.17	0.82
<i>bisPMe</i> ₃ -4	9.7	86.76	0.32
<i>bisPMe</i> ₃ -5	10.7	63.92	0.23
<i>bisPMe</i> ₃ -6	17.7	44.34	0.16
<i>bisPMe</i> ₃ -7	17.6	6.55	0.02
<i>bisPMe</i> ₃ -8	22.8	143.19	0.53
<i>bisPMe</i> ₃ -9	23.7	127.61	0.47
<i>bisPMe</i> ₃ -10	46.3	224.50	0.82
<i>bisPMe</i> ₃ -11	47.9	231.23	0.85
<i>bisPMe</i> ₃ -12	47.7	185.77	0.68
<i>bisPMe</i> ₃ -13	44.2	221.61	0.81

5.5.3 Summary and conclusions

This work presents the first muon implantation study in the [FeFe]-hydrogenase model subsite. The use of muons as substitutes for protons is demonstrated to offer a unique insight into the binding regiochemistry on the nanosecond timescale, a time window inaccessible by other techniques. Both complexes showed a broad asymmetric resonance at ~ 0.12 Tesla. The similarity in the experimentally observed resonances suggests similar modes of binding in both complexes. The resonance positions predicted for muonium adding to a basal site on the Fe centre or to the carbon atom of CO ligand are most consistent with the experimental spectra (see Figure 5.8, Figure 5.13 and Figure 5.14). These findings are consistent with the analogous ether mediated protonation mechanisms of Xdt bridged systems reported in Chapter 4, which indicated that the kinetic product, a terminal hydride is formed through an intermediate species with the proton bound to CO and the thermodynamic product, a bridging hydride can be reached by comparable activation barriers through rearrangement. The results from stopped flow IR, NMR, and EPR experiments, and from the DFT investigation provide strong evidence that protonation of the subsite results in a bridging hydride as the thermodynamic product [68, 104, 118, 137]. It is however possible that a terminal hydride is formed and rapidly rearranges to a bridging hydride, and that this process is too rapid to be observed using these techniques. The time window that μSR offers makes the technique complementary to other spectroscopic techniques. Preliminary results of this combined μSR and DFT study on the muonation of $[\text{Fe}_2(\mu\text{-pdt})(\text{CO})_4(\text{CN})_2]^{2-}$ and $[\text{Fe}_2(\mu\text{-pdt})(\text{CO})_4(\text{PMe}_3)_2]$ model complexes provide compelling evidence for the formation of CMuO species and terminally bound Mu. However, to rule out the possibility of binding to the Fe–Fe bond, an ALC investigation is required on an instrument able of reaching magnetic fields above 5000 Gauss. Calculations using basis sets offering a higher level of electron correlation could improve the calculated hfcc, and will be performed as a validation of the current technique at a later date. Notably, the effects that flipping the pdt bridge had on the structure and spin density of these complexes suggests that there is some level of electronic circuitry existing within the subsite. Observations taken from the analysis of the spin density suggest that the connectedness of this circuitry is affected not only by the direction of the pdt bridgehead, but

by the nature of the ligated group *transoid* to the S atoms of the dithiolate bridge, i.e. its electron withdrawing ability.

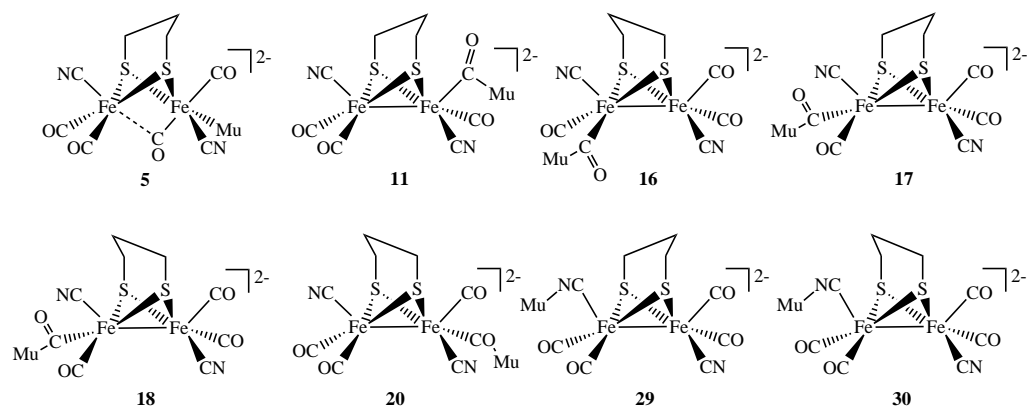


Figure 5.13: Structural isomers of $[MuFe_2(\mu-pdt)(CO)_4(CN)_2]^{2-}$ muoniated radicals with predicted resonances in agreement with the experimental spectrum.

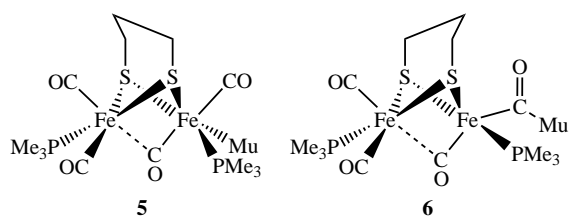


Figure 5.14: Structural isomers of $[MuFe_2(\mu-pdt)(CO)_4(PMe_3)_2]$ muoniated radicals with predicted resonances in agreement with the experimental spectrum.

Chapter 6

Characterising the normal modes of tris(acetylacetonate)iron(III) using NIS and DFT

6.1 Introduction

The work presented in this Chapter was performed in collaboration with Dr. Upali Jayasooriya, Dr. Elaine Barclay, Dr. Aleksandr Chumakov, Dr. David Evans, Professor Chris Pickett and Dr. Vasily Oganessian.

Element selective vibrational information is now accessible with such experimental techniques as NIS [141] spectroscopy. NIS (also sometimes referred to as nuclear resonance vibrational spectroscopy, NRVS, or nuclear resonant inelastic X-ray scattering, NRIXS) is showing great potential for its application to biological and materials systems [142–148]. It is therefore of importance to investigate the application of NIS to model systems. The direct and selective access to the metal-ligand vibrations gives NIS the potential to be a very powerful technique. This has therefore led to direct applications of complicated biological problems, with only a very few small molecule applications [33, 141, 149, 150] for technique validation. $[\text{Fe(III)(acac)}_3]$ (see Figure 6.1) is a relatively high symmetry molecule in both the molecular and the solid state. The latent symmetry approach is first used to predict the changes to be expected in the solid state when compared to the

isolated molecule. The predictions obtained using DFT vibrational modelling in order to provide a complete assignment of iron-active vibrational modes of $[\text{Fe(III)(acac)}_3]$ up to 700cm^{-1} , using NIS spectroscopy.

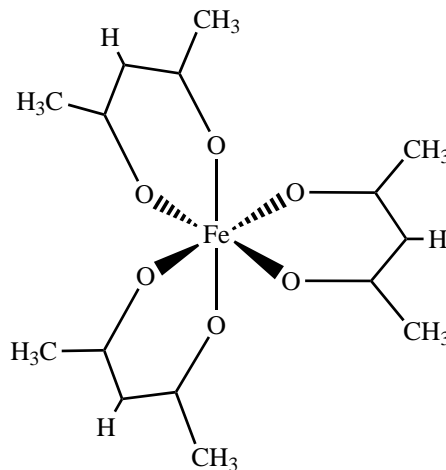


Figure 6.1: Structure of tris(acetylacetonate)iron(III), Fe(III)(acac)_3

6.2 Experimental

6.2.1 Nuclear inelastic scattering spectroscopy

A polycrystalline sample of $[\text{}^{57}\text{Fe(III)(acac)}_3]$, ca. 250 mg, was mounted into a copper block and covered with a Kapton film and Beryllium foil. NIS data were collected at the Nuclear Resonance beamline at the European Synchrotron Radiation Facility in Grenoble, France [34]. Details of sample preparations are given elsewhere [151]. Measurements have been carried out according to the previously published procedure [38]. Sample temperatures for NIS measurements were ca. 25 K. Samples were maintained at this temperature using a liquid helium cryostat. Spectra were recorded between -40 and 210 MeV with the energy resolution of the NIS experiment being ca. 0.59 MeV. For every measured point 15 scans were accumulated. The measurement time was 30 seconds per point in the NIS spectrum. The added scans were corrected for decaying intensity of the incident beam. The plot of the original NIS spectrum and the plot showing the relative errors in the PDOS spectrum for each value are displayed in Figure D3 and Figure D2, respectively (see appendix).

6.2.2 Infrared spectroscopy

[⁵⁶Fe(III)(acac)₃] was prepared as a nujol mull and applied to a polyethylene sample window. The absorption spectrum of the Far-infrared was recorded using a Perkin Elmer Spectrum 400 with the optics system and sample area continuously purged with dried air in order to minimise the presence of water vapour. The spectral resolution was set at 1cm⁻¹.

6.2.3 Raman spectroscopy

Raman spectra were recorded using a solid state sample of [⁵⁶Fe(III)(acac)₃] on a Bruker IFS66 FT-IR spectrometer, incorporating a FRA106 Raman module and a liquid nitrogen cooled germanium detector. The excitation source was a diode laser, lasing at 1064 nm, and the spectral resolution was set at 4cm⁻¹.

6.2.4 Computational parameters

The spectral simulation implemented an ab initio DFT calculation of an isolated molecule of [⁵⁷Fe(III)(acac)₃] with Fe in a high spin state (S=5/2). The X-ray crystal structure [152] was used as a starting point for the geometry optimisation and assumed an idealised D₃ molecular symmetry (see Figure 6.1). DFT calculations were performed using the Gaussian 03 [18] software package with Beckes three-parameter exchange functional (B3) [108] with the Lee, Yang, and Parr (LYP) correlation functional [109]. Carbon, Oxygen and Hydrogen used the 6-311++G** [153] basis set and Iron used the 6-31G** basis set [154]. An analytic Hessian calculation was performed on the optimised structure to verify its D₃ symmetry. The normal modes were used to simulate the NIS spectra according to equation (2.33) using an in-house built computer program. Simulated spectral lines were assigned a Lorentzian line shape with ahwhh of 1 cm⁻¹ for infrared and Raman spectra and 6 cm⁻¹ for PDOS.

6.3 Results and discussion

[Fe(III)(acac)₃] has D₃ symmetry and 48 low frequency fundamental modes of vibration (below 700 cm⁻¹) [144]; 16 doubly degenerate E modes, 8 A₂ and 8 A₁ modes. In this symmetry point group, A₁ and E modes are Raman active while E and A₂ modes are infrared active. In principle any of the E and A₂ modes can be NIS active. However, for an isolated molecule 9 E and 6 A₂ modes involve displacement of the Mössbauer active iron, thus showing non-zero intensities in the NIS spectrum. Vibrational modes which are NIS active and their associated composition factors are shown in Table 6.1.

[Fe(III)(acac)₃] crystallizes in the orthorhombic crystal class with the space group Pbca [155–157]. There are 8 symmetry related molecules per primitive unit cell with each occupying a site of no formal symmetry. The biggest difference between the vibrational density of states of an isolated molecule and that of it in the solid state is the additional modes due to lattice phonons, apart from any broadening of internal modes when significant intermolecular vibrational interactions are present. In the present case with 8 molecules per primitive unit cell, 21 translational and 24 rotational lattice phonon branches are to be expected in addition to the three acoustic branches. A careful examination of the crystal structure [152] of this material shows some important latent or near symmetries that may explain the differences to be observed between the solid state spectra and the calculated NIS intensities for an isolated molecule. The rationale behind the latent symmetry approach is that a relatively small distortion of a symmetric structure introduces small modifications to the vibrational spectra corresponding to the magnitude of the actual distortion [151, 158–160]. Figure D1 shows a unit cell of [Fe(III)(acac)₃] projected along the crystallographic *b*-axis. All molecular pseudo 3-fold axes are parallel to each other and to the crystallographic *b*-axis. Further, the eight molecules fall into two sets of four on each plane, and the molecules on each plane are on an approximately 4-fold grid, thus providing an approximate 4-fold near symmetry environment for each molecule. Therefore, one would expect the vibrations parallel to the molecular three fold axis to be independent of those along the other axes, thus implying no mixing between

the internal molecular A_2 and E modes in going from an isolated molecule to the solid state. Further the translational lattice modes with translations parallel to the molecular 3-fold axis, i.e. the crystallographic b -axis, are distinct from those parallel to the other two axes. This segregation of the phonons, between the unique b -axis and the rest, also segregates any possible mixing between the lattice modes and the internal modes. A_2 molecular modes being able to mix with only those lattice modes along the b -axis, whilst E molecular modes mix with those lattice modes along the other two axes. In short, one can consider the solid state spectrum as consisting of a sum of independent 1-D and 2-D components. Along the b -axis, the 1-D component, a single molecule is a reasonable approximation for the unit cell length, while such a simplification is not possible along the other two directions, the 2-D component.

Figure 6.2 displays a comparison of the experimental infrared spectrum of $[^{56}\text{Fe(III)}(\text{acac})_3]$ with the DFT simulated infrared spectrum of both $[^{56}\text{Fe(III)}(\text{acac})_3]$ and $[^{57}\text{Fe(III)}(\text{acac})_3]$ in the low frequency region (below 700 cm^{-1}). The computed spectra show very good agreement with the experiment, in terms of both peak position and intensity. The spectral region below ca 200 cm^{-1} is noisy due to the presence of trace amounts of water vapour in the purging gas which prevented the observation of the very weak features predicted for this region by the DFT calculation.

Experimental FT-Raman spectrum of a solid state sample of $[^{56}\text{Fe(III)}(\text{acac})_3]$ is shown in Figure 6.3(a). The region below ca. 130 cm^{-1} was inaccessible due to the Rayleigh line filter. The spectrum compares very well with that simulated with DFT calculations for an isolated molecule of $[^{56}\text{Fe(III)}(\text{acac})_3]$. The most intense Raman feature is at 448 cm^{-1} , assigned to an A_1 mode involving the symmetric stretch of the oxygen ligands relative to the iron. The next strongest set of Raman modes appear at ca. 209 and 168 cm^{-1} in the solid state spectrum. In the simulated spectrum these appear as three resolvable peaks at 163 , 184 , and 196 cm^{-1} , all of these modes involve O-Fe-O rocking motions. The peaks in the solid state spectrum are much broader, an effect which is likely to be caused by mixing of the internal E modes with lattice modes, as predicted by the latent symmetry

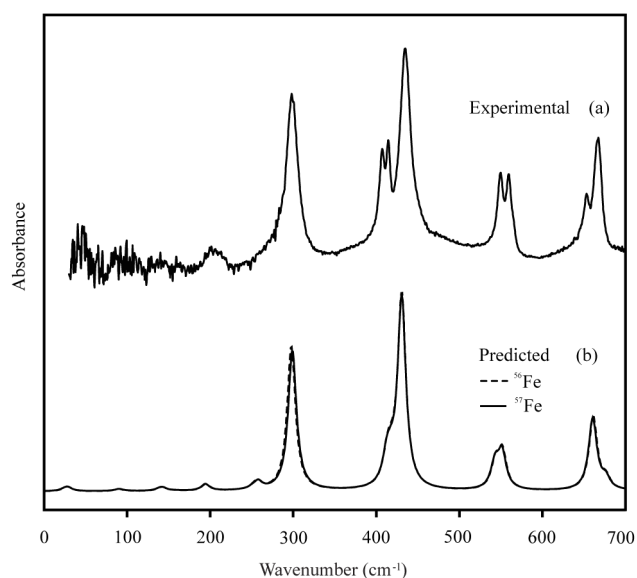


Figure 6.2: Comparison of (a) the experimental infrared spectrum of $Fe(III)(acac)_3$ with (b) the simulated infrared spectrum of an isolated molecule of $^{57}Fe(III)(acac)_3$ and $^{56}Fe(III)(acac)_3$ shown by solid and dashed lines, respectively.

approach.

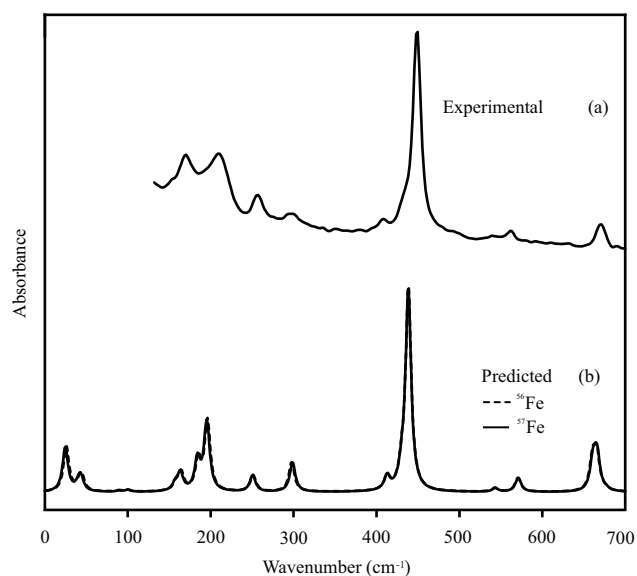


Figure 6.3: Comparison of (a) the experimental Raman spectrum of solid state $Fe(III)(acac)_3$ with (b) the simulated Raman spectra of an isolated molecule of $^{57}Fe(III)(acac)_3$ and $^{56}Fe(III)(acac)_3$ shown by solid and dashed lines, respectively.

The selection rules associated with NIS intensities are defined by equations (2.33) and (2.34) and are principally different from the selection rules of both infrared and Raman spectroscopies, thus making all three spectroscopic techniques complementary for the assignment and analysis of vibrational modes. Due to the invariance of the centre of the molecule where the iron atom is situated, in the totally symmetric modes, all A_1

modes are NIS inactive. In addition, several E and A₂ modes appear not to manifest NIS activity because of either totally constrained or fully symmetric stretching of the oxygen-containing ligands towards the centre of the molecule, thus suppressing the displacement of the Fe atom during the vibration. It is important to emphasise the role of NIS in the assignment and analysis of modes in the far infrared region since the amplitude Δ_{rFe} (and therefore the NIS intensity) of the iron motions is expected to increase with decreasing vibrational frequency ν according to $(\Delta_{rFe})^2 \propto k_B T / \nu^2$, using a simple harmonic model approximation (k_B and T are the Boltzmann constant and temperature, respectively).

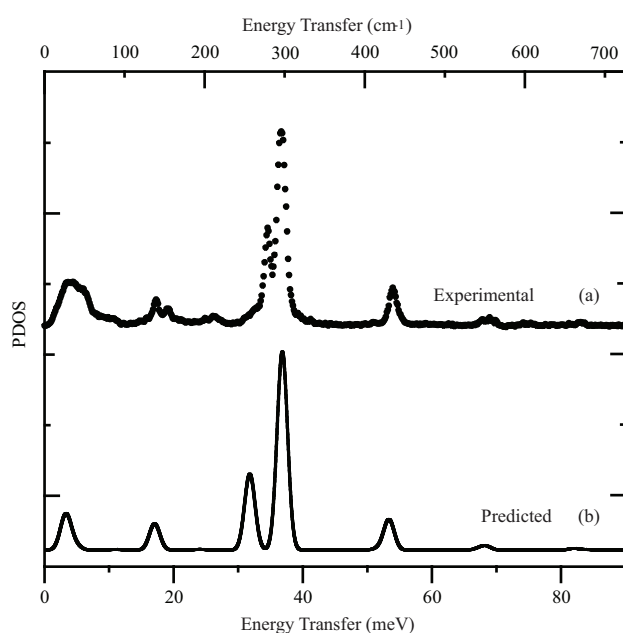


Figure 6.4: Comparison between (a) relative PDOS intensities obtained from nuclear inelastic scattering (NIS) of ⁵⁷Fe(III)(acac)₃ with (b) those predicted from an ab initio DFT calculation for an isolated molecule.

The partial density of states, PDOS, obtained from NIS data of polycrystalline [⁵⁷Fe(III)(acac)₃] run at a sample temperature of 5 K is shown in Figure 6.4(a). A large number of peaks associated with vibrational modes involving varying contributions from the displacement of the iron atom are observed in the low frequency region. The iron atom weighted PDOS given by the amplitude of motion of the ⁵⁷Fe atom in the direction of the incoming photon is predicted according to equation (2.33) and is shown in Figure 6.4(b). The calculated normal modes are shown in Figure 6.5 and Figure 6.6 for all the NIS active vibrations. For clarity, only the metal and primary ligand atoms are displayed. Doubly degenerate E modes involve Fe displacements in the xy plane while in A₂ modes the iron

displacement is along the z -axis. The assignment of normal modes is summarized in Table 6.1. Both experimental and theoretical values for IR spectra of $[\text{}^{56}\text{Fe(III)(acac)}_3]$, reported previously by Diaz-Acosta et. al [155] are confined to wavenumbers greater than ca 210 cm^{-1} . The present NIS data are in reasonable agreement with their assignments. The most intense PDOS spectral feature appears at 297 cm^{-1} in the experimental spectrum (298 cm^{-1} calculated). This band is assigned to the doubly degenerate E mode characterised by a combination of O-Fe-O bending and O-Fe stretching motions, which is in good agreement with previous assignments [155, 156] (Figure 6.6). Interestingly, non-negligible spectral features appearing at higher wavenumbers are all predicted to be of E symmetry. The intensity of the PDOS features progressively decreases with the increasing wavenumber as the character of the vibration becomes associated less with Fe displacements and more with the internal motions of the acetylacetonate groups. The medium intensity E band appearing at 434 cm^{-1} (430 cm^{-1} calculated) is primarily associated with Fe-O stretching (in agreement with previous assignment [155]) and also includes minor contributions from CH-C-CH₃ bending. During this vibrational mode the Fe atom moves along the x and y -axes towards the converging oxygen atoms of the acetylacetonate groups (Figure 6.6). The low intensity E mode at 547 cm^{-1} (542 cm^{-1} calculated) was previously assigned to O=C-CH₃ bending [155]. This mode also includes contributions from CH-C-CH₃ bending and O-Fe stretching. The E band at 655 cm^{-1} (660 cm^{-1} calculated) previously characterised by a mixture of Fe-O and C-CH₃ stretching [155], also includes O=C-CH₃ bending. Most of the non-trivial spectral features below the 297 cm^{-1} peak are of the A₂ irreducible representation. Although the experimentally observed NIS wavenumbers and intensities are both in good agreement with those predicted by the DFT calculation, the position of the A₂ mode at 279 cm^{-1} in the experimental PDOS spectrum appears down-shifted at 257 cm^{-1} in the simulated spectrum, explanation required here. Previously assigned to C=O-Fe and CH₃-C=C bending [155], this mode also includes major contributions from Fe-O stretching. The low intensity bands observed experimentally at 212 cm^{-1} appears as an E symmetry band at 194 cm^{-1} with a significantly lower intensity. Additionally, the doublet of bands at 139 and 154 cm^{-1} in experimental PDOS appear as a single A₂ band at 137 cm^{-1} in the predicted spectrum. This medium intensity

band is characterised by a mixture of components: O-Fe-O and C-C-CH₃ wagging, O-Fe-O rocking, O-Fe-O bending, and O-C-CH₃ twisting. The O-Fe-O bending component involves the motion of the Fe atom along the *z*-axis. In principle the higher wavenumber feature of the doublet could arise from the the E band at 142 cm⁻¹, which may become NIS active as a result of the distortion of molecular symmetry in the solid state. The medium intensity A₂ feature at 28 cm⁻¹ is characterised by torsions within the ligand rings. During the vibration the shape of the inner coordination sphere is maintained as it is translated along the *z*-axis.

An inspection of the *ab initio* DFT predictions shows that there are indeed several predicted vibrations of molecular E symmetry at 100, 142, 157, 184, and 194 cm⁻¹, but of negligibly small iron displacements for an isolated molecule. Mixing of vibrational wavefunctions between the lattice modes and internal modes, but still segregated mainly to *b*-axis and *a/c*-axes, *i.e.* A₂ modes being independent of E modes, as predicted by the latent symmetry approach given at the beginning of this section, explains the noticeable intensities of the experimental NIS bands at ~85, 154, and 212 cm⁻¹. It is only the E modes that should show the effects of the distortions from the latent to real symmetry of the crystal structure and hence the enhanced intensities due to coupling, whilst the A₂ modes being well explained by an isolated molecule model. The intensity enhancement appears to be greatest closer to the low frequency lattice modes and is explained by the fact that the mixing between the lattice modes and the internal modes decreases inversely with the energy separation between them. The significant intensity observed in the NIS spectrum for the E-modes at 85, and 154 cm⁻¹ and partially at 212 cm⁻¹, for which the molecular model predicts almost zero intensity is a clear manifestation of this expectation.

6.4 Summary and conclusions

The element selective vibrational spectroscopic technique of NIS (which in this case probes the vibrations via ⁵⁷Fe, the heaviest atom in the molecule), in combination with infrared and Raman spectroscopies and *ab initio* DFT calculations, is shown to provide

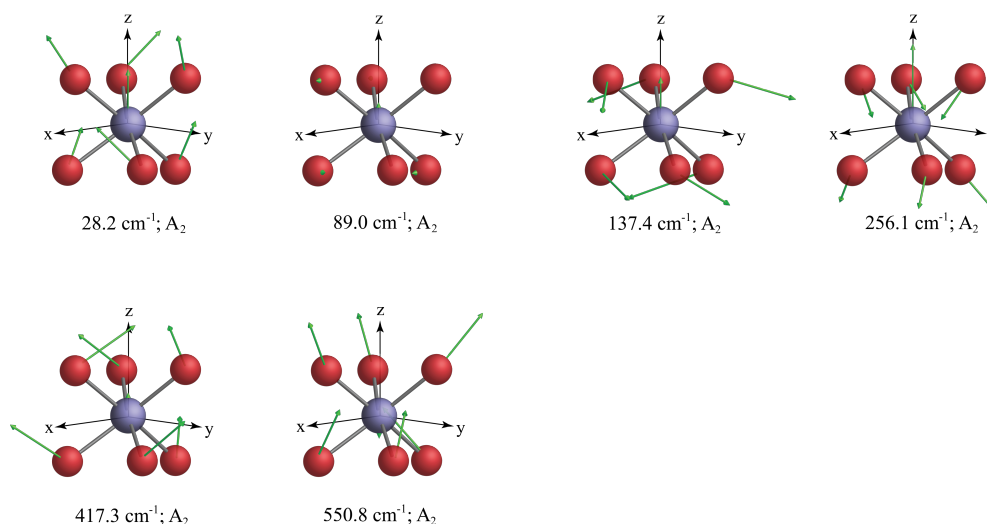


Figure 6.5: Simulated A_2 normal modes of $^{57}\text{Fe(III)}(\text{acac})_3$ for NIS active vibrations, hydrogen atoms omitted for clarity.

a complete and reliable assignment of the metal-active vibrations in the lower frequency region of this model compound. The predicted PDOS, infrared and Raman frequencies are all in good agreement with experimental spectra. NIS is a particularly valuable complementary technique for an accurate assignment of vibrations in the far infrared region. Analysis of NIS data for this compound provides good evidence for solid state induced mixing between lower frequency internal modes and external modes. The arguments developed herein explaining the spectral intensity differences between the experimental spectra for solid state and an isolated molecule are essentially symmetry based. It is concluded that the solid state E modes are enhanced by coupling with the lattice modes. This study also shows that a clear understanding of the solid state effects are accessible using the latent symmetry procedure, without always referring to a detailed solid state calculation. The results presented herein provide a validation for the NIS technique and demonstrate the potential to fully characterise the metal-ligand vibrational modes in more complicated bioinorganic systems such as the hydrogenase model complexes investigated in Chapter 3.

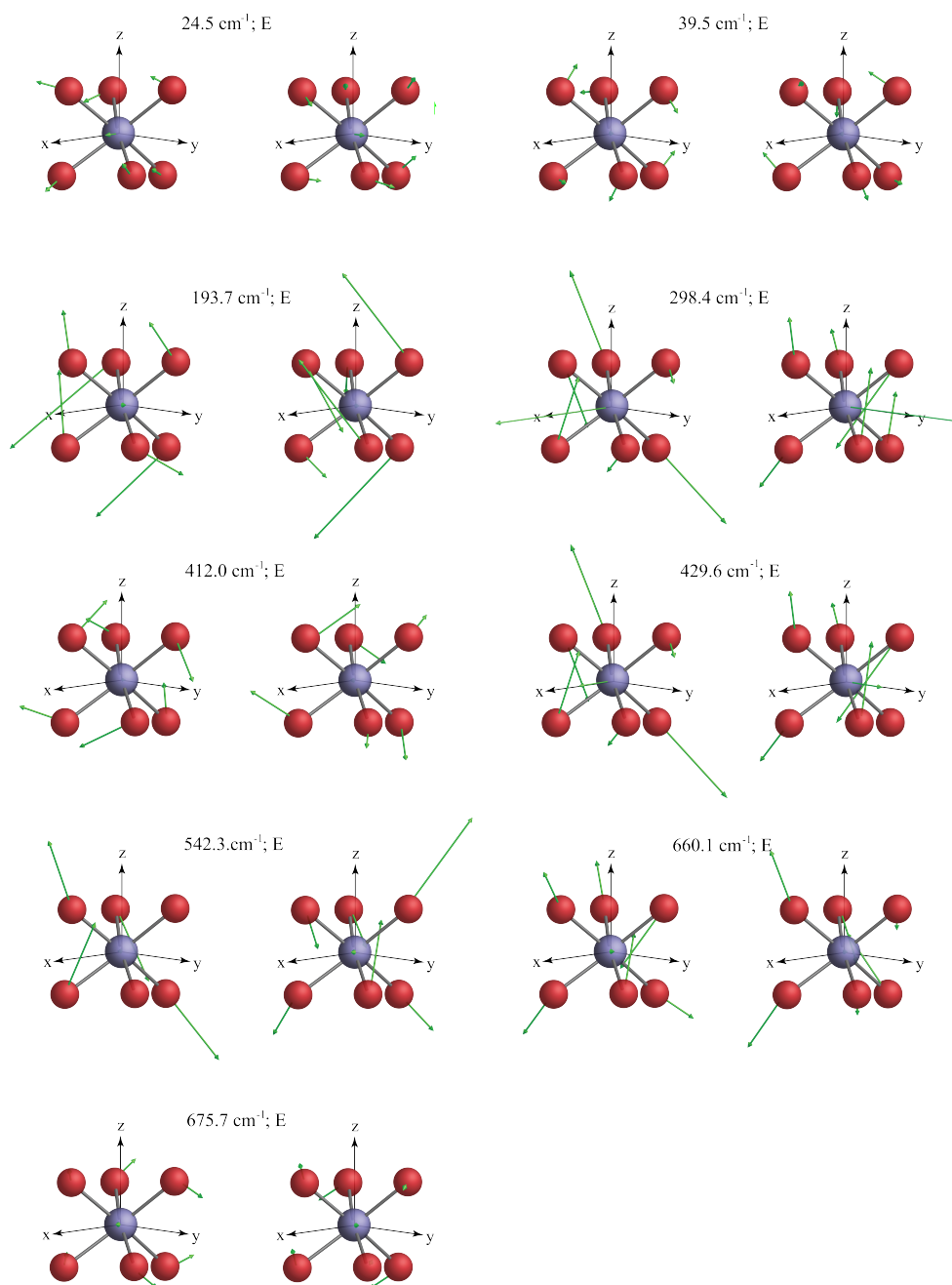


Figure 6.6: Simulated *E* normal modes of ⁵⁷Fe(III)(acac)₃ for NIS active vibrations, hydrogen atoms omitted for clarity.

Table 6.1: Assignment of experimental infrared, Raman, and NIS vibrational modes based on comparison with DFT calculations. ^aPeak masked by neighbouring E mode at 434 cm⁻¹

Symmetry	type	DFT	IR	Raman	⁵⁷ Fe NIS	<i>e</i> _{Fe,a} ²
		Frequency/cm ⁻¹				
		exp.	exp.	exp.	exp.	
E	O=C-CH ₃ wag	24.5			25	0.0492
A ₂	Fe-O=C wag	28.2			32	0.1424
E	C-CH-C-CH ₃ rock	39.5			47	0.0134
A ₁	C-CH-C-CH ₃ rock	43.1				
A ₂	C-CH-C-CH ₃ twist	89.0			85	0.0050
E	C-CH-C-CH ₃ twist	99.7				
A ₂	(O-Fe-O; C-CH-C) wag; O-Fe-O rock; O-Fe-O bend; O=C-CH ₃ twist	137.4			139	0.1696
E	(O-Fe-O; C-CH-C) wag; O-Fe-O rock; O-Fe-O bend; O-C-CH ₃ twist	142.0			154	0.0000
A ₂	C-CH-C-CH ₃ twist	156.5				
E	C-CH-C-CH ₃ twist	156.9				
A ₁	O-Fe-O rock; O-Fe-O bend	163.2		168		
E	O-Fe-O rock	183.8				
E	O-Fe-O bend; (O-Fe-O;C-CH-C) wag; O=C-CH ₃ twist	193.7	205	207	201	0.0028
E	O-Fe-O rock	195.6		209		
	unassigned				212	
E	(O-Fe-O;C-CH-C; O=C-CH ₃) bend	250.1		256		
A ₂	(CH ₃ -C=C; C=O-Fe) bend; Fe-O stretch	257.2			279	0.4886
E	Fe-O stretch; O-Fe-O wag; O-Fe-O bend	298.4	298	298	297	0.6340
E	(C=C-CH ₃ ; O=C=C; O-Fe-O) bend	412.0	406	408	410	0.0012
A ₂	(O-Fe-O; O-C-CH; C=C-CH ₃) bend	417.3	414	a		0.0098
E	Fe-O stretch; C-CH-C bend	430.0	434		434	0.0990
A ₁	Fe-O stretch; C-CH-C bend	437.8		448		
E	Fe-O stretch; (O=C-CH ₃ ; CH-C-CH ₃) bend	542.3	550	541	547	0.0236
A ₂	Fe-O stretch; (O=C-CH ₃ ; CH-C-CH ₃) bend	550.8	560		554	
A ₁	C-CH-CH ₃ twist	570.8		563		
E	(Fe-O; C-CH ₃) stretch; O=C-CH ₃ bend	660.1	653		655	0.0057
A ₁	Fe-O stretch; O=C-CH ₃ bend	665.1		670		
E	pi torsional	675.7	667		670	0.0020

Chapter 7

Measuring the rate of interfacial transfer using muon spectroscopy

7.1 Introduction

The work presented in this chapter was performed in collaboration with Dr. Upali Jayasooriya, Dr. David Steytler and Dr. Nigel Clayden.

The rate of molecular transfer through an interfacial layer is a rapid process that is close to being diffusion controlled. This process is of great importance in the context of drug delivery across the membranes of living cells. At present, there are no generally applicable methods for the determination of such rates. Existing methods include rotating diffusion cells[161–165], stopped-flow spectroscopic techniques, and the line broadening methods of NMR (where the signal originating from each environment is not easily distinguished) and EPR (this requires a stable radical species)[166–168]. With the correct choice of probe molecule and system, μ SR offers a unique opportunity to probe directly the interfacial transfer dynamics and energetics through a line broadening approach.

Figure 7.1 (a) shows a hypothetical model in which a probe molecule, X may travel in either direction through an interfacial layer. The line broadening technique may be applied to probe the frequency of exchange only if the probe molecules give distinct spectroscopic signals originating from each chemical environment (oil and water). Figure 7.1

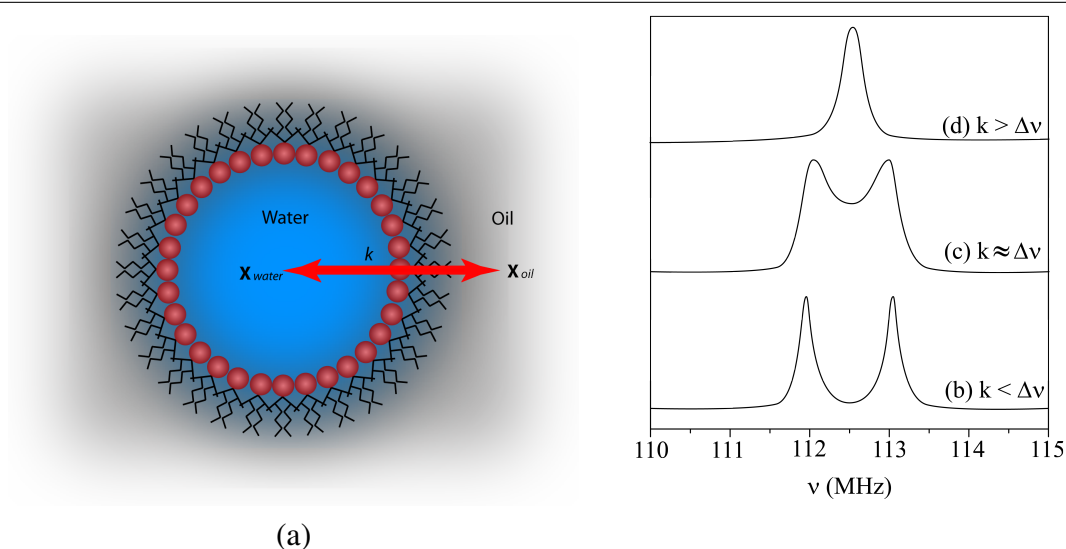


Figure 7.1: (a) Schematic illustrating a probe molecule, X residing in either the oil or water phases, travelling through the interface with a rate constant, k . Right: line broadening resulting from a two site chemical exchange where the rate of exchange is (b) much less than the peak HWHH, $\Delta\nu$ (c) approximately equal to $\Delta\nu$, or (d) much greater than $\Delta\nu$.

(b) shows the hypothetical situation of the probe molecules exchanging slowly (relative to time scale of the spectroscopic technique) or not at all between chemical environments. The result is two individual signals, corresponding to the probe molecules being present in each of the solvent phases. Rapid molecular exchange (relative to the time scale of the spectroscopic technique) would result in a sharp signal at an intermediate position to each of the solvent peaks (see Figure 7.1 (d)). A variety of chemical exchange lineshapes can be observed in between these two extreme examples.

In order for this type of line broadening experiment to succeed, several criteria were required from the micro-emulsion system, probe molecule and the spectroscopic technique. To provide the large interfacial area, a well characterised water-in-oil (w/o) microemulsion stabilised by bis(2-ethyl hexyl) sodium sulphosuccinate (Aerosol OT) was employed. Such a system is composed of thermodynamically stable nano-sized pools of water (the droplet size can be controlled by altering the water-to-surfactant molar ratio) separated from the bulk heptane phase by a surfactant monolayer of Aerosol OT (see Figure 7.2). The temperature stability window for the experiments was reasonably wide (15 - 50°C) for droplets with a core radius, R_{core} less than ~ 5 nm. The probe molecule of choice was allyl alcohol, AA ($\text{CH}_2=\text{CH}_2-\text{CH}_2-\text{OH}$). The unsaturated centre fulfils the

requirements for muon-capture and the size and polarity ensure the balanced partitioning between the water droplets ($P_W \sim 0.58$) and surrounding oil phase ($P_O \sim 0.42$) that is essential in the measurements. Moreover, AA can be added to the micro-emulsion system at the levels required for effective muon capture for TF and ALC experiments (1 mol dm^{-3}) without affecting the droplet structure, making it the ideal candidate. In the following sections, TF and ALC spectra of muoniated AA in water, heptane, and in the Aerosol OT microemulsion, at variable temperatures are reported.

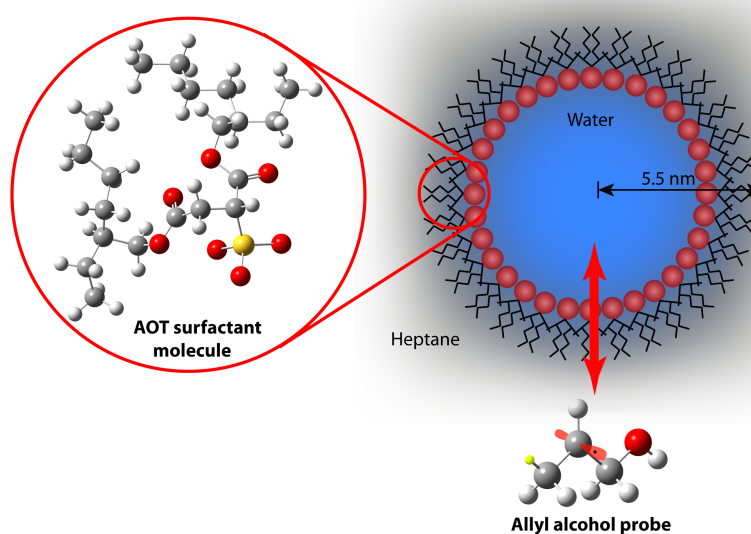


Figure 7.2: Schematic of the system of choice.



When the population of allyl alcohol in the micro-emulsion is distributed equally between the oil and water phases, the rate constant associated with exchange should be equal in both the forward (k_f) and backward (k_b) direction, giving a single rate constant for exchange, k . The half width at half height (HWHH) of the observed peak (in Hz) in the micro-emulsion system is given by;

$$\Delta\nu_M = P_O\Delta\nu_O + P_W\Delta\nu_W + P_O^2P_W^2(\nu_O - \nu_W)^2(\tau_O + \tau_W) \quad (7.2)$$

where ν_O and ν_W are the peak positions in the oil and water phases, respectively (with units of rad s^{-1}). $\Delta\nu_O$, $\Delta\nu_W$ and $\Delta\nu_M$ represent the HWHH of the peaks observed in oil,

water and micro-emulsion, respectively (with units of rad s^{-1}). P_O and P_W are the population of the probe molecule in the micro-emulsion found in the oil and water phases, respectively. τ_O and τ_W represent the lifetimes in the oil and water phases in the micro-emulsion system, and are proportional to k_f and k_b .

The exchange rates from linebroadening are derived from the following analytical expression:

$$k_f = \frac{1}{P_O} \left[\frac{2P_O^2 P_W^2 (\nu_O - \nu_W)^2}{\Delta\nu_M - (P_O \Delta\nu_O + P_W \Delta\nu_W)} \right] \quad (7.3)$$

$$k_b = k_f \left(\frac{P_O}{P_W} \right) \quad (7.4)$$

7.2 Experimental

Transverse Field (TF) and Avoided Level crossing (ALC) μSR experiments were carried out on the GPD and ALC instruments, respectively, at the Paul Scherrer Institut (PSI), Villigen, Switzerland over a period of 2 years starting in 2009. Latter experiments were conducted on the HIFI instrument at the Rutherford Appleton Laboratory, Didcot, UK.

7.2.1 Sample preparation

Solutions of 0.5 M allyl alcohol (Sigma Aldrich ≥ 99) in water (deionised) and allyl alcohol in heptane (Sigma Aldrich, Chromasolv [®]). Micro-emulsion samples were prepared by mixing the AOT stock (75 %), AA (7 %) and water (18 %). All samples were transferred into glass bulbs (diameter = 3.5 cm), subjected to 10 cycles of freeze-pump-thaw to remove any dissolved oxygen. For Transverse field measurements on the GPD instrument the bulbs could be directly loaded into the cryostat. For ALC measurements samples were transferred from the glass bulbs into the metal liquid cells at PSI under a helium atmosphere.

7.2.2 Data fitting

Transverse field data were fourier transformed using the ftx fitting program from PSI, and fitted in the time domain using minfit. Avoided level crossing data was background subtracted and fitted using the ROOT software package developed at CERN.

7.2.3 Computational parameters

DFT calculations were performed on an isolated molecule of allyl alcohol using the Gaussian software 03 package [18]. All calculations used the Becke3LYP (B3LYP) hybrid GGA functional [108–110] in conjunction with the EPR-III basis set[136]. Structures were confirmed as minima through frequency calculations. Calculations were performed by modelling hydrogen analogue systems; where in each case the muon was modelled by a H atom. To account for the light mass of the muon relative to the hydrogen, the bond length was scaled by a factor of 1.02. Moreover, to account for the difference in gyromagnetic ratio between the muon and the hydrogen, the hfcs were scaled by a factor of 3.183.

7.3 Results and discussion

7.3.1 Transverse field experiments

When allyl alcohol is irradiated with positive muons it is possible for two radicals to be formed, with the muonium terminally or centrally bonded.

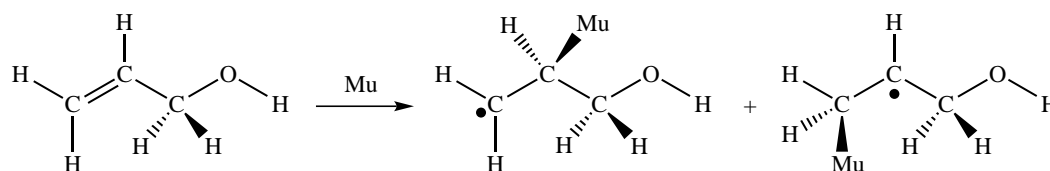


Figure 7.3: Formation of the two muoniated allyl alcohol radicals.

The sign and magnitude of the muon-electron hyperfine coupling (hpc) is specific to that radical. Figure 7.4 shows the TF- μ SR spectrum of 0.5 M AA in water at 288.5 K with 3000 Gauss field fitted in the frequency domain. The spectrum is characterised by

a diamagnetic signal positioned at 40.67 MHz and a pair of signals placed symmetrically about the diamagnetic signal which could correspond to either radical. The prominent radical of AA in water at 300 K gives rise to peaks at 112.5 MHz and 199.6 MHz, a hyperfine coupling of 312.1 MHz.

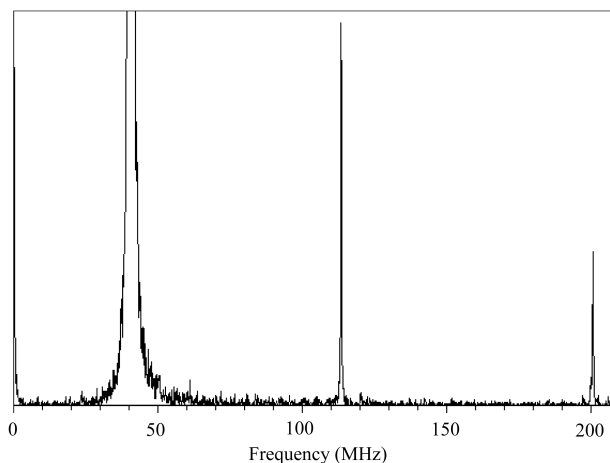


Figure 7.4: *TF- μ SR spectrum from 0.5 M allyl alcohol in water at 288.5 K in a transverse magnetic field of 3000 Gauss. The spectral feature at 40.67 MHz (truncated to better view the other signals) is from muons in the diamagnetic environment. The pair of signals at 113.60 MHz and 200.81 MHz result from one of the two radicals.*

The resonances were found to be solvent dependant, with a shift of ~ 2.3 MHz between the water and heptane phases. The signal in the micro-emulsion is found in an intermediate position between the water and heptane phases. This suggests a fast exchange of the radical between the two media, with a lower exchange rate limit of $\sim 2.3 \times 10^6 \text{ s}^{-1}$. The peak positions in all media also showed strong temperature dependence, with a 10° change in temperature corresponding to a ~ 1 MHz shift in peak position.

The TF data was fitted in the time domain using the MINFIT software package (see Figure 7.6). There is no observed temperature dependence of the peak widths within the error estimates for water and heptane, the micro-emulsion does show a slight broadening with increasing temperature, although the two measurements above $\sim 330\text{K}$ are beyond the phase separation observed in the micro-emulsion (the phase separation temperature of this micro-emulsion is $\sim 328\text{K}$). In the fast exchange limit, the position of the resonance in the micro-emulsion is expected to be in between that in water and heptane, with the ex-

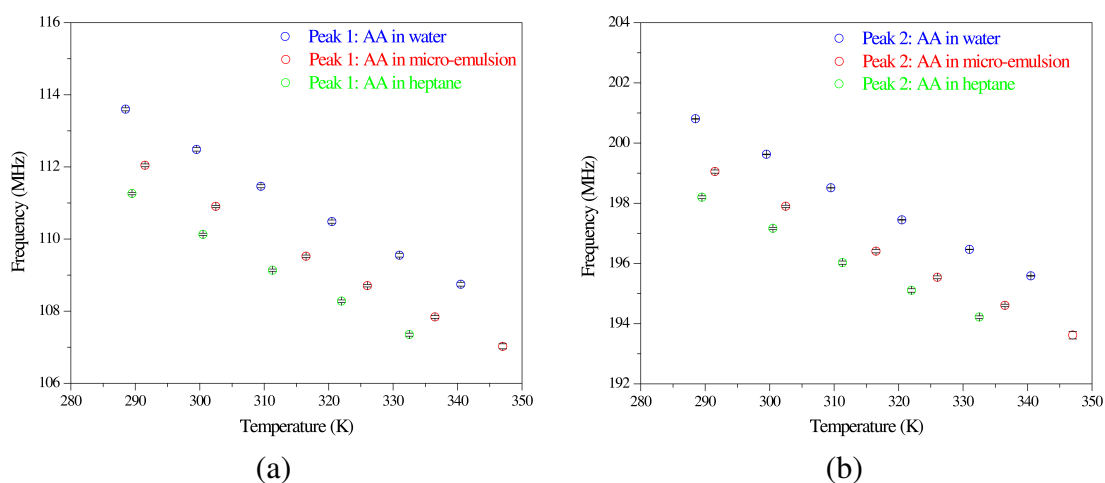


Figure 7.5: Temperature dependence of the position of (a) peak 1 and (b) peak 2 in water (blue), heptane (green), and micro-emulsion (red).

act position dependent on the weighted average partitioning between these two solvents. However, the observed values are in fact marginally above that in heptane. An accurate measurement of this difference should provide a measure of the intended rate.

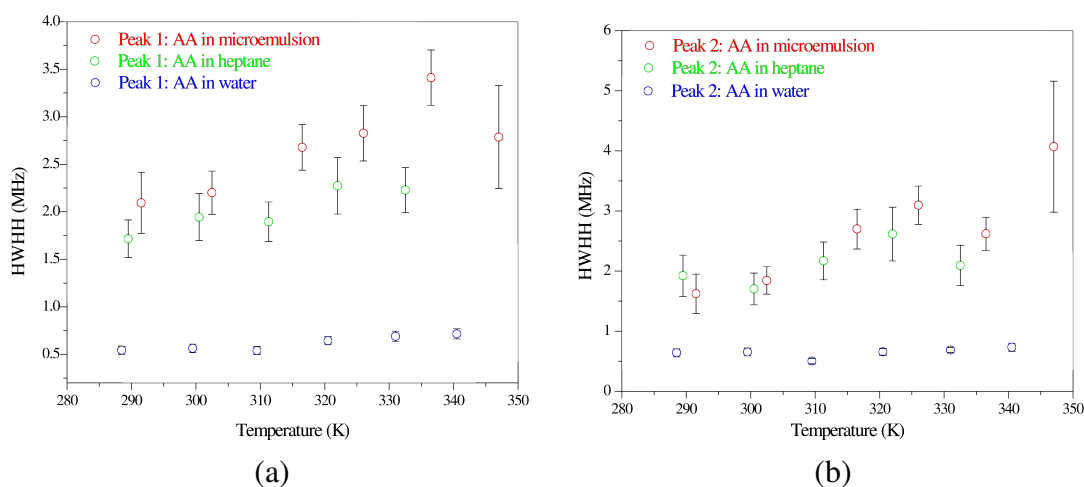


Figure 7.6: Temperature dependence of the peak width (HWHH) of (a) peak 1 and (b) peak 2 in water (blue), heptane (green), and micro-emulsion (red).

When paramagnetic ions are present in solution, the presence of these different spin orientations results in the muoniated radicals sensing a larger variation of the applied field and hence a broadening of the resonance would result. Ni^{2+} (0.1%) was added to a solution of AA in water and the TF- μ SR spectrum taken at two temperatures, 300 K and 321 K. The presence of Ni^{2+} did not seem to alter the peak positions relative to the undoped

water solutions. As expected however, a significant broadening of both resonances was observed (see Figure 7.7). When added to the micro-emulsion, Ni^{2+} is isolated within the nano-droplets of water and does not enter the heptane phase. The spectra of this system shows significant sharpening of both peaks. The intermediate relaxation of the micro-emulsion signals relative to the heptane and Ni^{2+} in water provides clear evidence of the AA–Mu radical shuttling between phases.

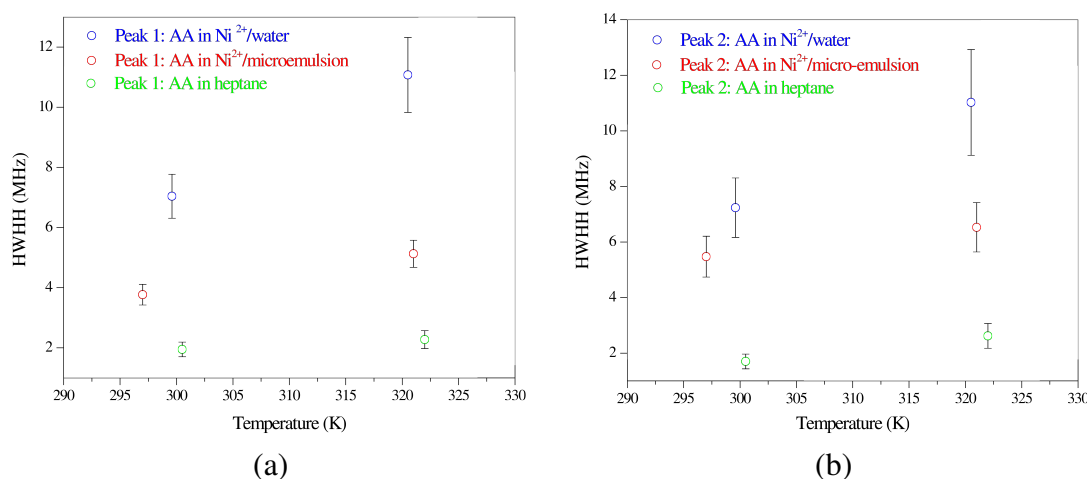


Figure 7.7: Temperature dependence of the peak width (HWHH) of (a) peak 1 and (b) peak 2 in water (blue), heptane (green), and micro-emulsion (red).

7.3.2 ALC- μ -SR experiments

ALC- μ SR demonstrates the presence of the exchange more clearly than TF - μ SR as well as highlighting the number of resonances which can be observed undergoing exchange. Like in the TF experiments, AA muoniated radicals were characterised in the water and heptane phases separately, then in the micro-emulsion, all at temperatures ranging from 275-330 K. DFT calculations revealed that the terminal muoniated radical was 3.8 kcal/mol more stable than the centrally muoniated radical. This radical has more resonance canonicals associated with it which could presumably account for some of the stabilisation energy. Each radical has three proton environments giving the possibility of six ALC resonances. However, only five were observed, however, three in a lower field range and two in an upper field range (see Figure 7.9). Assignment of these was based on the analysis of the muoniated allyl alcohol radicals presented in section 7.3.4. Peaks

corresponding to ALC resonances of the terminally muoniated radical (peaks 1, 2 and 4) give the best statistics and so are most suitable for line broadening measurements.

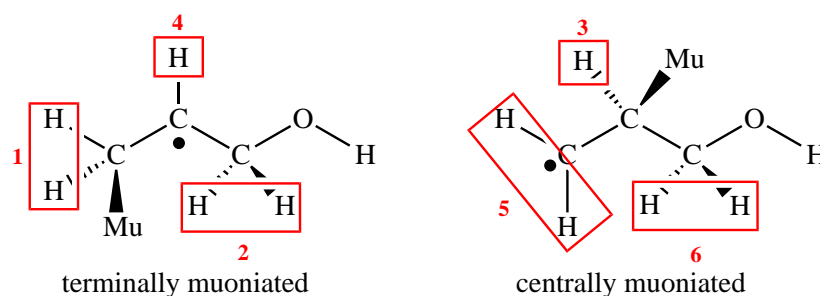


Figure 7.8: The allyl alcohol radicals with assignment of peaks based on the DFT investigation reported in 7.3.4.

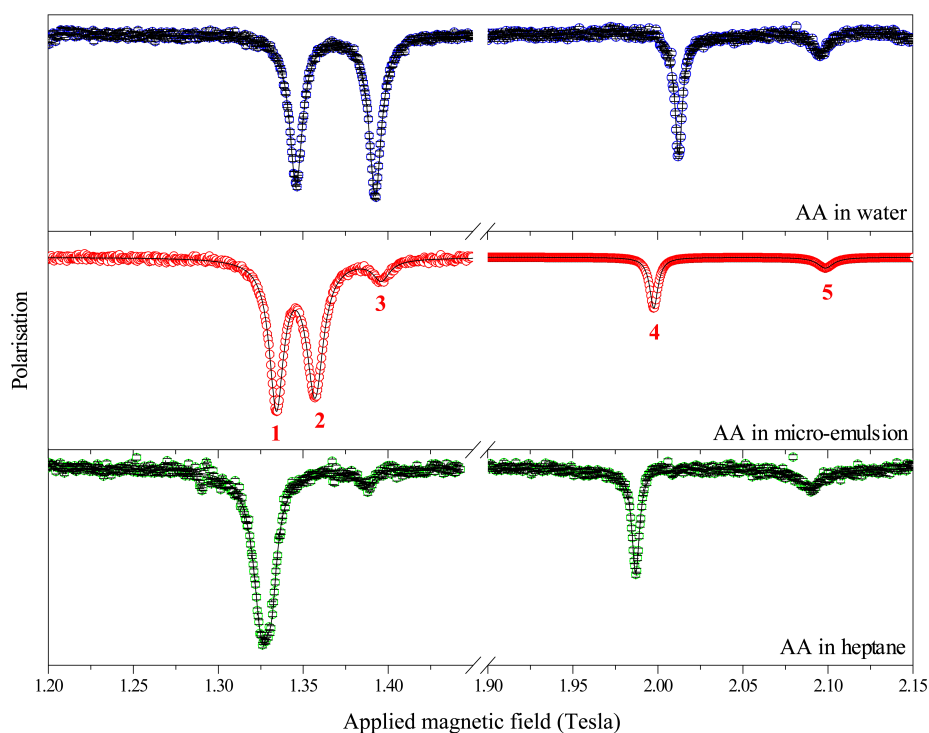


Figure 7.9: ALC spectra showing peaks in water, micro-emulsion and heptane at 290 K. Labels are linked to Figure 7.8

As with the TF spectra, each peak displays the same solvent dependence, heptane at lowest fields, water at highest fields, and the peaks from the micro-emulsion at intermediate positions to these. The solvent dependence of the field values of these resonances are dependant on the position of the resonating proton in the structure of the muoniated radical, thus providing different frequency windows for rate measurements depending on the resonance used (see Figure 7.10). It is clear that the greatest frequency separation

between oil and water phases, $\nu_W - \nu_O$ exists in peak 2 (see Figure 7.10). At temperatures below ~ 310 K in the heptane phase peak 2 is unresolvable from peak 1, the peaks only become distinguishable above ~ 310 K.

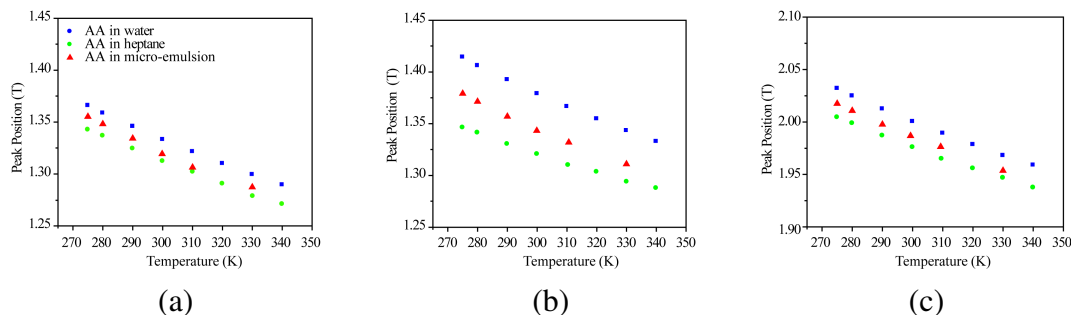


Figure 7.10: Variance in ALC resonances in water and oil phases, $\nu_W - \nu_O$ in (a) peak 1, (b) peak 2 and (c) peak 4.

The HWHH is observed to have considerable temperature dependence. Peaks 4 and 5 show almost no broadening with decreasing temperature whereas peak 2 shows considerable broadening with decreasing temperature, indicative of a slowing rate of transfer.

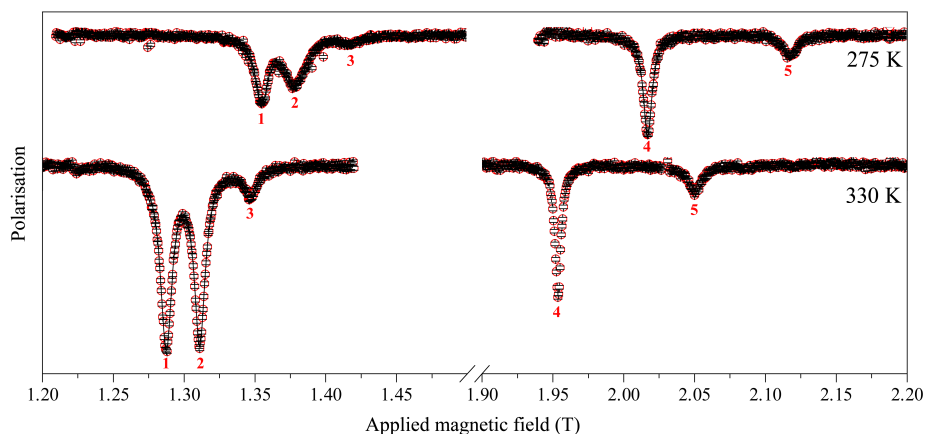


Figure 7.11: ALC spectra of AA in the micro-emulsion indicating the variation in line broadening with temperature.

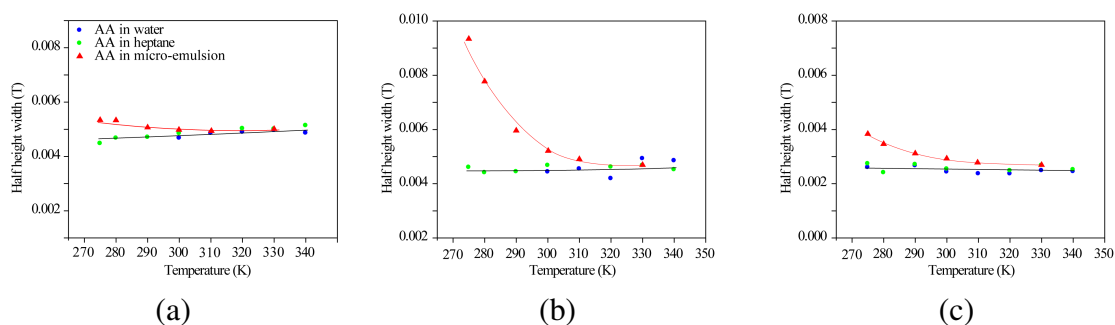


Figure 7.12: Temperature dependence of the ALC resonance HWHH of (a) peak 1, (b) peak 2 and (c) peak 4.

7.3.3 Monte-Carlo simulation of ALC spectra

A Monte-Carlo simulation of the exchange process was carried out on peaks 1 and 2. Dr Nigel Clayden modified the fortran code for the two site flip subroutine originally proposed by Tregenna-Piggott and co-workers [169]. The calculation takes into consideration the partitioning of the AA in water and in heptane ($P_W=0.58$, $P_O=0.42$). Figure 7.13 shows the simulated line shapes with no exchange occurring (peaks), an exchange rate of 1×10^{-7} s and an exchange rate of 1×10^{-9} s. This demonstrates that the rate that is being observed in the system investigated is $\sim 1 \times 10^{-9}$ s.

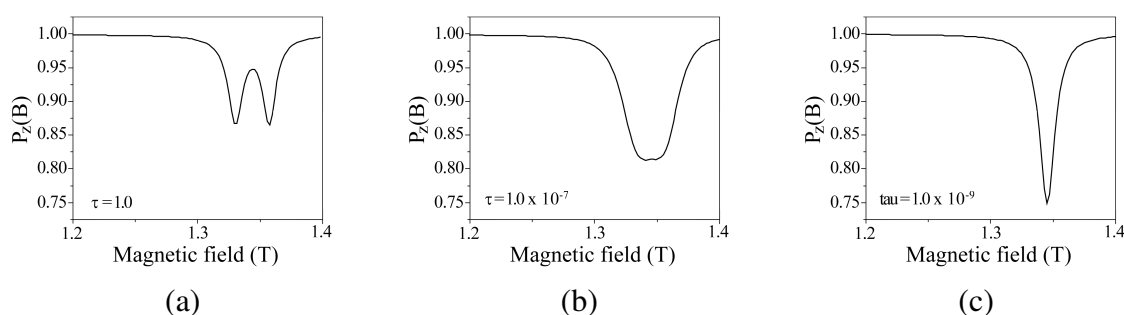


Figure 7.13: Monte-Carlo simulation of ALC resonance of AA in the micro-emulsion based on a rate of exchange of (a) 0 seconds, (b) 10^{-7} seconds and (c) 10^{-9} seconds. All simulations assume a A_μ value of 376 MHz for both water and oil phases, and A_p values of 127 MHz and 122 MHz for water and oil phases, respectively. All simulations use 100 steps and 1,000,000 muons.

Figure 7.14 shows the experimental peak positions of peaks 1 and 2 for AA in water, heptane and the microemulsion system fitted with Lorentzians. The positions of peaks 1 and 2 in each of the phases, along with the corresponding $A_{\mu e}$ values are presented in table Table 7.1. These values were used in the Monte-Carlo simulation. The simulation

is shown in Figure 7.15 accurately reproduces the experimentally observed line shape for peaks 1 and 2, giving a predicted exchange rate of $\tau=8.229 \times 10^{-9}$ s (121.65 MHz).

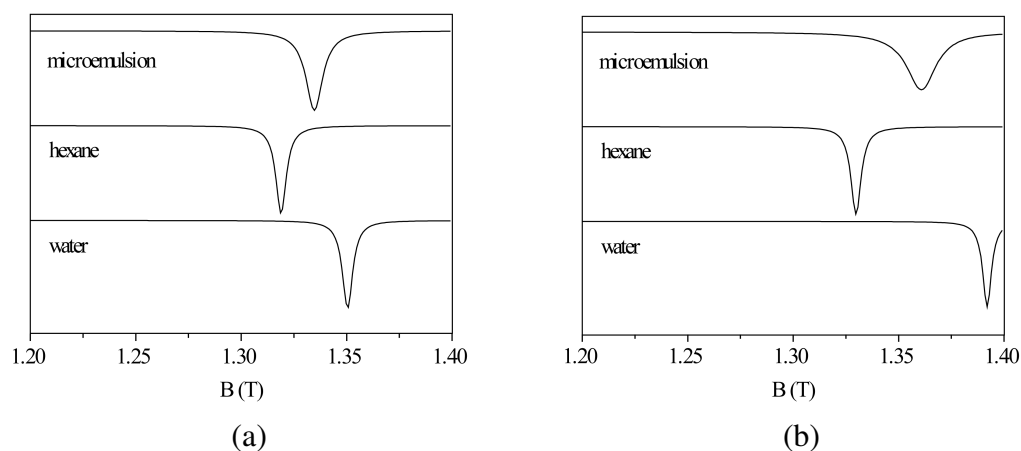


Figure 7.14: Experimentally fitted spectra for (a) peak 1 and (b) peak 2 for AA in water, heptane and microemulsion.

Table 7.1: Experimental TF- μ SR and ALC- μ SR data at 290 K used for the Monte-Carlo simulation of the exchange process.

	A_{μ} /MHz	A_p /MHz (1)	A_p /MHz (2)
AA_{water}	314.40	62.06	54.37
$AA_{heptane}$	309.46	63.00	60.98
$AA_{microemulsion}$	311.20	61.97	57.76
$AA_{water} - AA_{heptane}$	4.94	0.94	6.61

There are various diffusion controlled processes that could have been responsible for the observed chemical exchange phenomena. In order to verify that the observed phenomena was indeed associated with interfacial transfer and not one of these processes, Dr David Steytler determined their rates. The average time taken for AA to encounter an AOT droplet was found to be $\sim 5 \times 10^{-10}$ s $^{-1}$. The average collision frequency of AA with the microemulsion droplets was determined as $\sim 1.1 \times 10^{-8}$ s $^{-1}$ and the collision frequency of microemulsion droplets with AA $\sim 6.6 \times 10^{-10}$ s $^{-1}$. The diffusion time of AA across the diameter of the water droplets was determined to be $\sim 3.1 \times 10^{-9}$ s $^{-1}$.

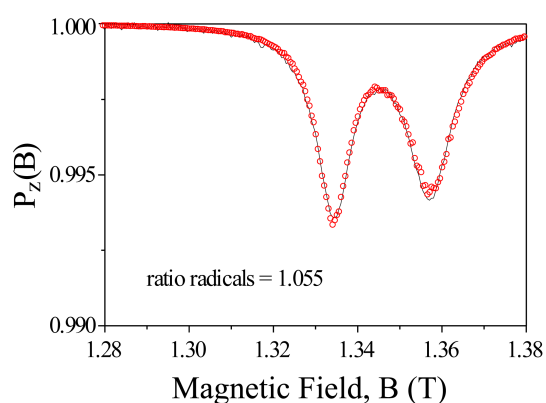


Figure 7.15: Monte-Carlo simulation of ALC resonance.

7.3.4 Assignment of ALC resonances using DFT calculations

Two sites in the AA molecule were investigated for muon binding, where the muon adds to the centre of unsaturation, at either C₁ or C₂ (see Figure 7.16 for atom labels). Both radicals were geometry optimised and the C–Mu bond distance scaled by a factor of 1.02 to account for the light mass of the muon relative to that of the proton [139]. The binding energies were calculated through comparing the total energy of each of the muoniated radicals with sum of the energies of the isolated AA molecule and muonium atom (see Table 7.2). This indicated that the most stable binding site is to C₁, generating the terminally muoniated radical.

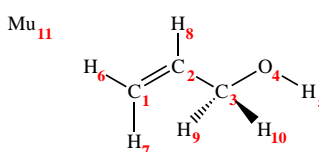


Figure 7.16: Atom labels used to describe muonium and the allyl alcohol molecule.

Table 7.2: Results from geometry optimisations showing the binding energies for the formation of the two radical species, C–Mu bond distances and $A_{\mu e}$.

site	Binding energy (kcal/mol)	bond length (Å)
terminal C ₁ –Mu	33.90	1.172
central C ₂ –Mu	30.15	1.182

DFT calculations of the optimised structure of the centrally and terminally muoniated radicals predict $A_{\mu e}$ values of 420 MHz and 356 MHz respectively. This is an overestimate

of 112 MHz (centrally muoniated) and 44 MHz (terminally muoniated) compared to the experimentally observed $A_{\mu e}$ values. Of course, a static representation of the equilibrium structure of these radicals is an insufficient model to accurately predict the $A_{\mu e}$ of each of the radicals. The bonds of the radical are in constant motion, vibrating and rotating around, which significantly influences the magnitude $A_{\mu e}$. Numerous studies on small organic molecules have demonstrated that the hyperfine interaction can be accurately determined through Boltzmann averaging of torsional angles [170–172]. Figure 7.17 shows the location of the unpaired electron density in the two radical species in their equilibrium geometries. For the centrally muoniated radical the electron density is primarily localised on the $2p_z$ orbital of the terminal carbon (C_1) while the terminally muoniated radical sees it localised in the $2p_z$ orbital of C_2 . Figure 7.18 shows the two lowest energy modes of vibration of both radicals as corresponding to torsional distortions about $H_7-C_1-C_2-C_3$ and $C_1-C_2-C_3-O_4$ (centrally muoniated: 101 cm^{-1} and 143 cm^{-1} ; terminally muoniated: 62 cm^{-1} and 109 cm^{-1}).

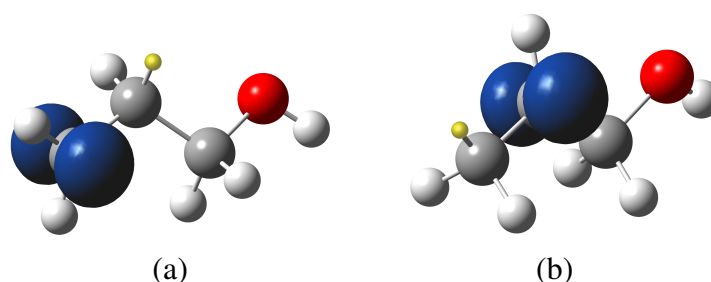


Figure 7.17: Spin density for (a) centrally muoniated AA, and (b) terminally muoniated AA. Isosurface=0.04.

Thus, the magnitude of the hyperfine coupling is strongly dependant on the torsional angle, θ between the direction of the $2p_z$ orbital and the C–Mu bond, with an angle of $\theta=0$ giving the greatest interaction (see Figure 7.19). Therefore, while maintaining a fixed C–Mu bond distance, two slices of the PES were calculated by rotating in 10° increments about torsional angles defined by $H_7-C_1-C_2-C_3$ and $C_1-C_2-C_3-O_4$. At each increment, the corresponding $A_{\mu e}$ and A_p values for each proton were calculated. Figure 7.20 (b) shows the calculated energy of the centrally muoniated radical as a function of dihedral angles defined by $H_7-C_1-C_2-C_3$ and $C_1-C_2-C_3-O_4$. The plot shows three energy min-

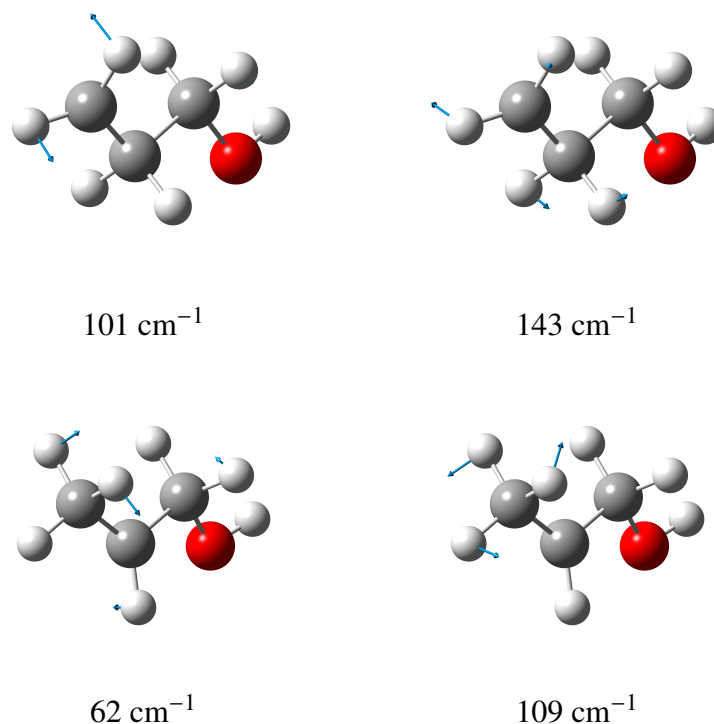


Figure 7.18: The lowest energy simulated modes of vibration for terminally and centrally muoniated radicals of AA.

ima down each cross-section. Following the energy as a function of $\text{H}_7\text{-C}_1\text{-C}_2\text{-C}_3$ gives the global minimum at ca. 0° , and two local minima at ca. 150° and 240° (see Figure 7.20 (c)). Rotation of the $\text{C}_1\text{-C}_2\text{-C}_3\text{-O}_4$ torsional angle gives the global minimum at ca. 180° and the two local minima at ca. 100° and 300° ((see Figure 7.20 (d)). Rotation of the $\text{H}_7\text{-C}_1\text{-C}_2\text{-C}_3$ torsional angle in the terminally muoniated radical again produces three energy minima at angles ca. 40° , ca. 160° and ca. 280° , with the former being the global minimum (see Figure 7.21 (c)). Rotation of the $\text{C}_1\text{-C}_2\text{-C}_3\text{-O}_4$ angle gives a surface with energy minima at ca. 70° , 320° and 200° , with the latter being the global minimum (see Figure 7.21 (d)). As a crude approximation, the rotations were treated as harmonic. The ground state energies, E_0 and excited state energies, $E_{1,2,3,\dots}$ were determined from the vibrational energies describing the corresponding torsions. For example, E_0 for the torsional angle described by $\text{H}_7\text{-C}_1\text{-C}_2\text{-C}_3$ in the centrally muoniated radical corresponds to an energy of $\frac{h \cdot 101}{2} \text{ cm}^{-1}$, where h is Plancks constant. These have been superimposed onto the PES plots (see Figure 7.20 (c) and (d) and Figure 7.21 (c) and (d)).

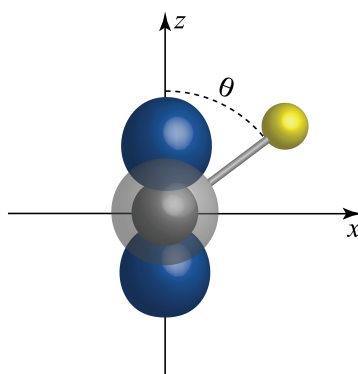


Figure 7.19: Schematic illustrating the overlap as a function of the angle between the p_z orbital and the muon bond. Adapted from [170].

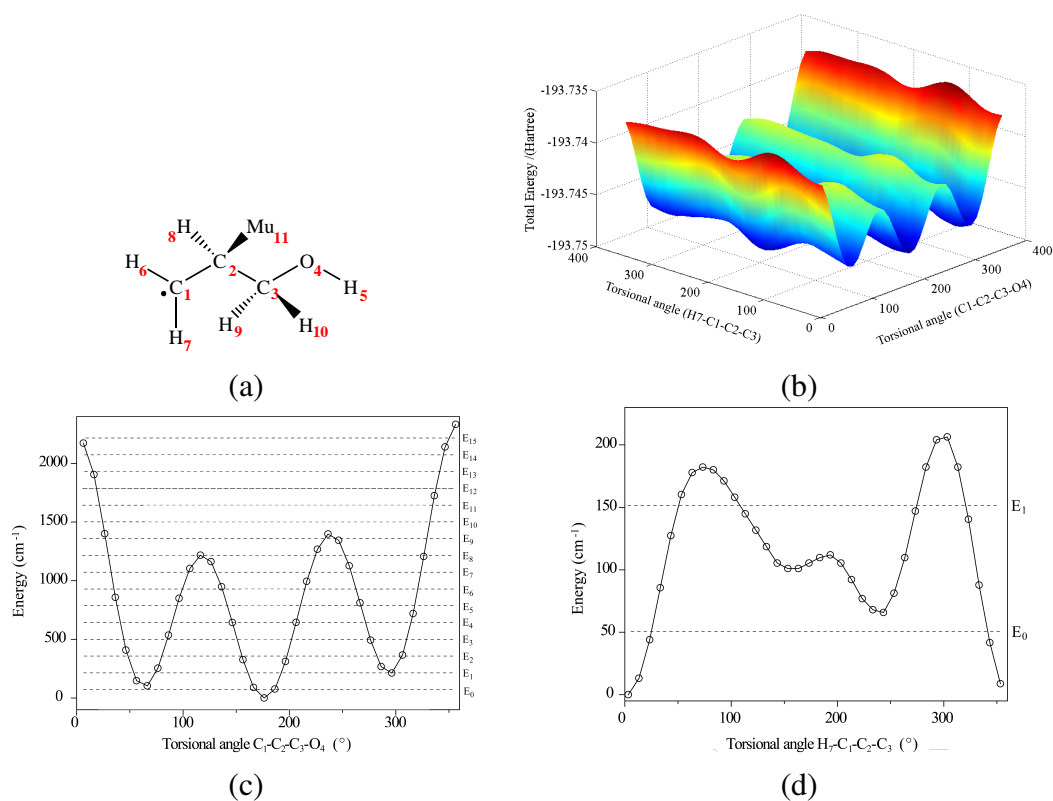


Figure 7.20: (a) Atom labels for the centrally muonated radical. (b) Total energy of the centrally muonated radical as a function of dihedral angles $H_7-C_1-C_2-C_3$ and $C_1-C_2-C_3-O_4$. Cross section of the PES taken from the equilibrium structure of the centrally muonated radical showing energy as a function of the dihedral angle made by (c) $H_7-C_1-C_2-C_3$ and (d) $C_1-C_2-C_3-O_4$. The labelled dotted lines correspond to the ground state, E_0 and excited states, E_n .

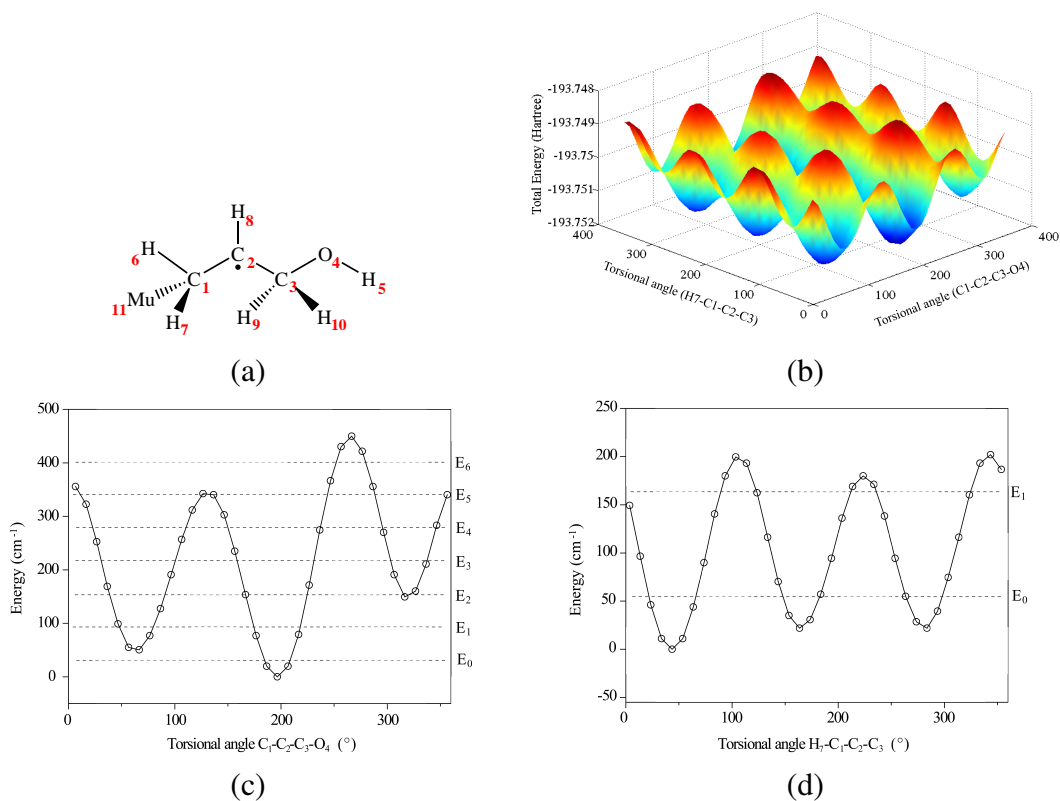


Figure 7.21: (a) Atom labels for the terminally muonated radical. (b) Total energy of the terminally muonated radical as a function of dihedral angles $H_7-C_1-C_2-C_3$ and $C_1-C_2-C_3-O_4$. Cross section of the PES taken from the equilibrium structure of the terminally muonated radical showing energy as a function of the dihedral angle made by (c) $H_7-C_1-C_2-C_3$ and (d) $C_1-C_2-C_3-O_4$. The labelled dotted lines correspond to the ground state, E_0 and excited states, E_n .

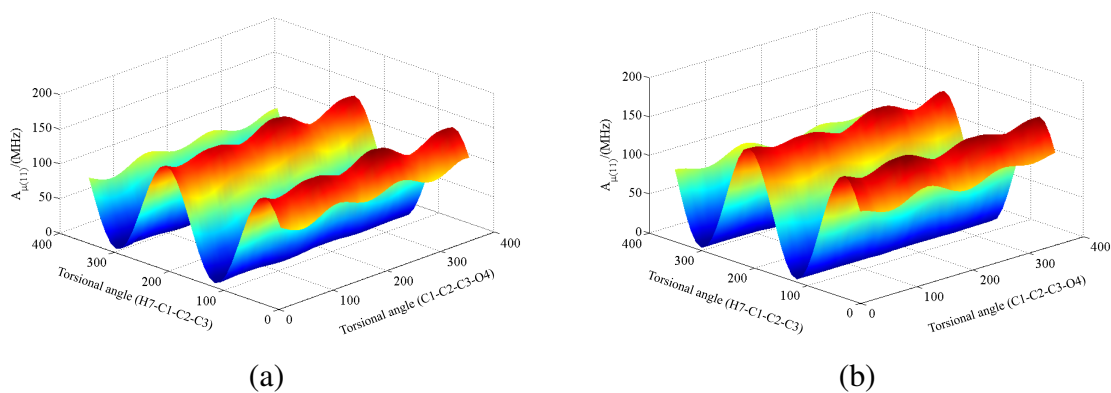


Figure 7.22: $A_{\mu e}$ as a function of dihedral angles $H_7-C_1-C_2-C_3$ and $C_1-C_2-C_3-O_4$ for the (a) centrally and (b) terminally muonated radicals.

For each muoniated radical and torsional angle, the fractional population, $\frac{n_i}{N}$ associated with each energy level was determined using:

$$\frac{n_i}{N} = \frac{e^{\left(\frac{-E_i}{kT}\right)}}{\sum e^{\left(\frac{-E_j}{kT}\right)}} \quad (7.5)$$

where k is the Boltzmann constant (1.38×10^{-23}) and T is the temperature (298 K). Finally, the average hyperfine coupling constant was obtained using:

$$A = \sum A(\theta_i) \cdot \frac{n_i}{N} \quad (7.6)$$

The average muon-electron hyperfine couplings were predicted to be 334 MHz and 319 MHz for centrally and terminally muoniated radicals, respectively. Notably, these were modelled in the gas phase at 298 K and as the experiments have demonstrated, temperature and the nature of solvent medium effects their magnitudes. While this is still not an ideal model, it clearly produces a more accurate estimation of $A_{\mu e}$ than a static model, and is in rough agreement with the experimentally observed value of ca. 312 MHz.

However, this still does not provide a means of distinguishing between the two muoniated radicals. The experimental ALC spectra seems to indicate the presence of both radical species, with a set of sharp Δ_0 resonances presumably corresponding to the dominant radical and the weaker resonances to the minor radical. A_p values were also calculated for the two radicals, and again their magnitudes are also strongly linked to the torsional angles. The same rotational averaging procedure was used to predict A_p values associated with the protons on each radical, these are reported in Table 7.3. Equation (2.14) (see Chapter 2.1) was used to predict the Δ_0 resonance positions associated with the protons from each radical, these are reported in Table 7.3. It must be stressed again that these resonances were simulated for the radicals in the gas phase at 298 K, and that the nature of the solvent and temperature have been demonstrated to significantly alter their positions, possibly to a different degree in each radical. In spite of this, the simulations indicate the terminally muoniated radical as the dominant species. Taking the terminally muoniated species first; protons 6 and 7 are in a similar chemical environment with respect to

the unpaired electron and are predicted to show Δ_0 resonances at 1.346 and 1.331 Tesla, respectively. These have been assigned to *peak 1* in the experimental spectra (see Figure 7.9). Protons 9 and 10 are also in a similar chemical environment with respect to the unpaired electron and are predicted to give resonances at 1.404 and 1.403 Tesla, respectively. These have been assigned to *peak 2* in the experimental spectrum (see Figure 7.9). Notably, below ~ 310 K, the experimental spectrum of AA in heptane shows these two resonances as unresolvable (see Figure 7.9). This is due to the large frequency window of *peak 2* which gives the resonance large variability with temperature relative to *peak 1*. Proton 8 is bound to the same carbon atom as the unpaired electron resides and after rotational averaging is predicted to give a Δ_0 resonance at 2.02 Tesla. This has been assigned to *peak 4* (see Figure 7.9). All resonance positions associated with the terminally muoniated radical give good agreement with the intense features observed experimentally. For the centrally muoniated radical, protons 6 and 7 are coordinated on the carbon on which the unpaired electron resides. These are predicted to produce resonances at 2.108 and 2.105 Tesla, respectively. This accounts for the weak intensity resonance (*peak 5*) appearing in this region of the experimental spectra. The weak intensity resonance appearing slightly upfield from *peak 1* and *peak 2* has been assigned to proton 8 in the centrally muoniated radical. Experimentally, this resonance is unobservable in the water phase as *peak 2* dominates the region. Protons 9 and 10 are both predicted to give resonances at 1.799, a region in the experimental spectrum which is featureless. Notably, these protons are separated from the unpaired electron density by two carbon bonds which could explain the absence of this resonance in the experimental spectra.

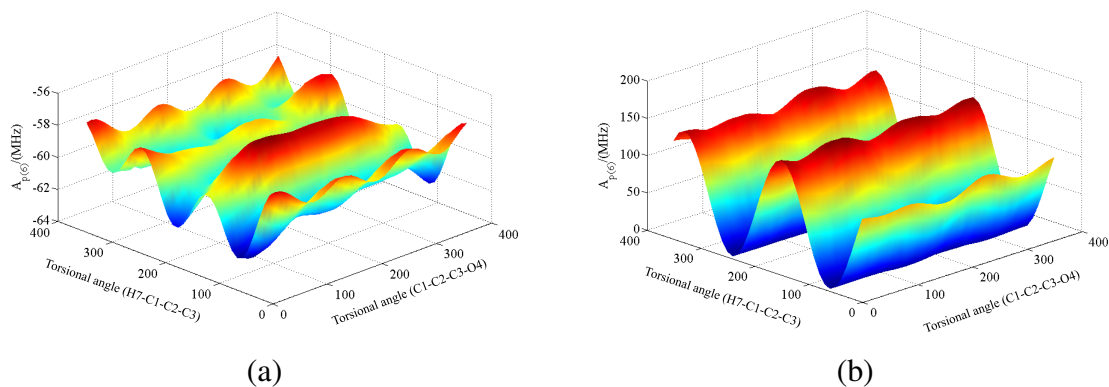


Figure 7.23: Simulated $A_{p(6)}$ as a function of dihedral angles $H_7-C_1-C_2-C_3$ and (b) $C_1-C_2-C_3-O_4$ for the (a) centrally and (b) terminally muoniated radicals.

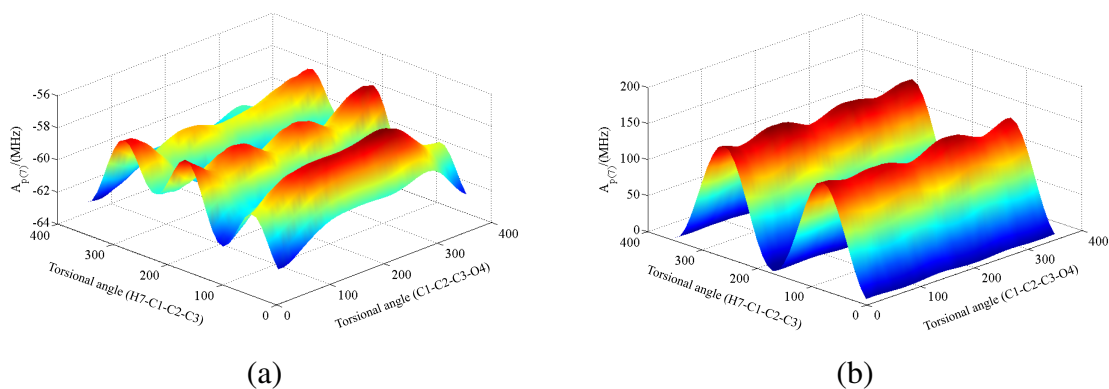


Figure 7.24: Simulated $A_{p(7)}$ as a function of dihedral angles $H_7-C_1-C_2-C_3$ and (b) $C_1-C_2-C_3-O_4$ for the (a) centrally and (b) terminally muoniated radicals.

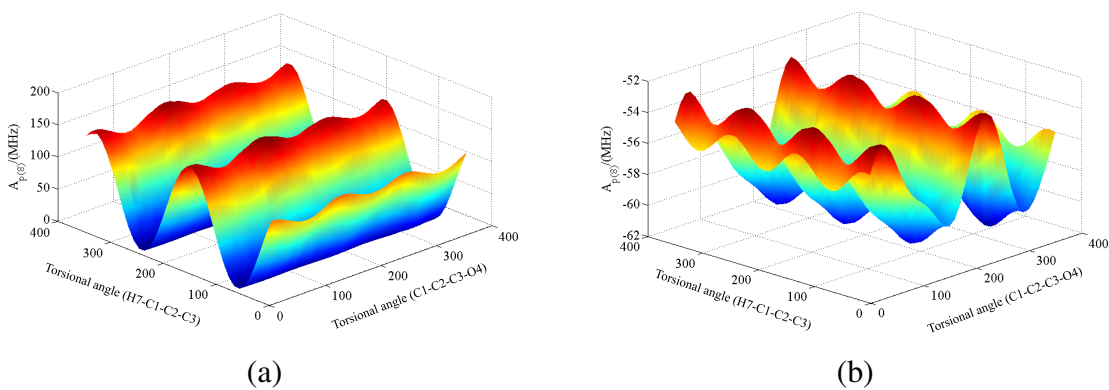


Figure 7.25: Simulated $A_{p(8)}$ as a function of dihedral angles $H_7-C_1-C_2-C_3$ and (b) $C_1-C_2-C_3-O_4$ for the (a) centrally and (b) terminally muoniated radicals.

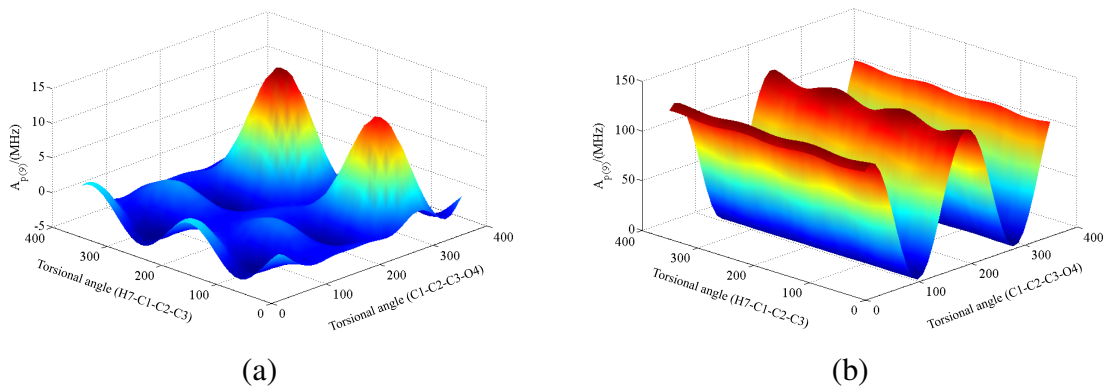


Figure 7.26: Simulated $A_{p(9)}$ as a function of dihedral angles $H_7-C_1-C_2-C_3$ and (b) $C_1-C_2-C_3-O_4$ for the (a) centrally and (b) terminally muoniated radicals.

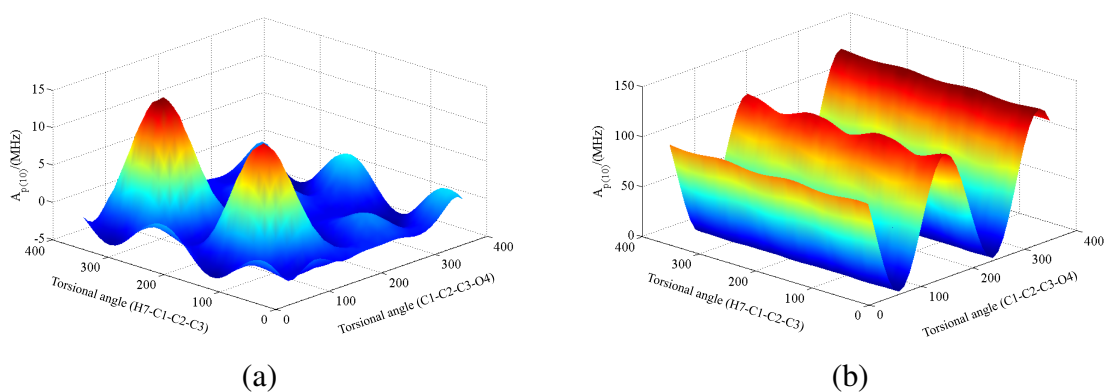


Figure 7.27: Simulated $A_{p(10)}$ as a function of dihedral angles $H_7-C_1-C_2-C_3$ and (b) $C_1-C_2-C_3-O_4$ for the (a) centrally and (b) terminally muoniated radicals.

Table 7.3: Averaged hyperfine couplings and resonance positions for centrally and terminally muoniated radicals. Atom labels correspond to those presented in Figure 7.16.

atom	centrally muoniated (298 K)			terminally muoniated (298 K)		
	A (MHz)	B _{res} (Tesla)	Exp. (μ -emuls.)	A (MHz)	B _{res} (Tesla)	Exp. (μ -emuls.)
μ (11)	334.542			319.026		
p (6)	-58.238	2.108	2.086	67.637	1.346	1.321
p (7)	-57.662	2.105	2.086	70.326	1.331	1.321
p (8)	82.648	1.348	1.381	-57.849	2.02	1.985
p (9)	-0.965	1.799	"	56.836	1.404	1.344
p (10)	-0.987	1.799	"	56.975	1.403	1.344

" indicates peak unobserved

7.4 Summary and conclusions

The rate of molecular transfer across an oil-water interface has been determined using a combination of TF- μ SR, ALC- μ SR and Monte-Carlo simulations. The system chosen for this investigation was an oil-in-water microemulsion consisting of AOT surfactant molecules separating the bulk heptane and water phases. The probe molecule, allyl alcohol was chosen as it demonstrated a balanced partitioning between both phases. Initial TF measurements were used as a proof of principle, with muon-electron hyperfine coupling constants demonstrating temperature and solvent dependence, crucial for line broadening type experiments. ALC measurements on the system resulted in spectra characterised by five resonances, three of which possessed good enough statistics for the line broadening experiment (peaks 1, 2 and 4). DFT calculations and rotational averaging enabled reliable assignment of the observed resonances. Considering the calculated binding energies and predicted resonance positions, the three intense resonances were assigned to the terminally muoniated radical while the two weaker intensity resonances were assigned to the centrally muoniated radical. Experimentally, all resonances demonstrated solvent and temperature dependence, but peaks 1 and 2 demonstrated the broadest frequency window of observation, and were therefore chosen for the Monte-Carlo simulation. The simulation predicted a rate of transfer of $\tau=8.229 \times 10^{-9}$ s (121.65 MHz). Notably, this is the first measurement of its kind.

Chapter 8

Final remarks and future work

The underlying theme of Chapters 3, 4 and 5 was the investigation of protonation regio-chemistry and mechanism of [FeFe]-hydrogenase model subsites. These systems were characterised by the Pickett group using stopped-flow spectroscopic techniques. They found that the size and nature of the dithiolate bridge significantly affected the rate of protonation. These observations provided the motivation for a large portion of this work. The findings presented herein add to the current understanding of how coordination sphere ligands affect the properties and dynamics of [FeFe]-hydrogenase mimics. Continued work in this area has the potential to aid the design of hydrogenase mimics able to catalyse H₂ at rates which make it viable for energy production.

Chapter 3 presents a rigorous DFT investigation of a family of [FeFe]-hydrogenase model complexes, Fe₂(μ-Xdt)(CO)₄(PMe₃)₂ (X= edt, pdt, odt, mpdt, dmpdt and mpdt-S). It was demonstrated that the IR and geometric parameters of these subsites could be reliably simulated, thus complementing previous structural assignment made from experimental observations. Based on observations made in this work, a ratchet type mechanism was proposed. This mechanism primes the subsite for protonation and is strongly affected by the identity of the Fe bound ligands. The relative position of PMe₃ ligands was found to affect the Mulliken charge distribution across the two Fe centres. An apically coordinated PMe₃ group was found to electronically enrich the Fe centre compared to having a CO in this position. Additionally increasing the steric bulk of the dithiolate bridge causes the apically bound ligand to become more sterically hindered. As a result, the Ψ angle

increases in order to minimise the energy of the structure. This rotational distortion appears to further enrich the Mulliken charge of the rotated Fe centre. For the dithiolate bridges investigated, the activation energy barriers associated with the interconversion of isomers was predicted to decrease with increasing bridge bulk. A full understanding of this mechanism could help design of a subsite with a ligand set that optimises the ratchet mechanism, thus minimising the energy barrier associated with initial protonation. With additional time, calculations on the more bulky dithiolate bridged systems would be carried out to confirm these observations. It may also be interesting to experiment with CO substituted ligands other than PMe₃, such as CN in the [Fe₂(μ-Xdt)(CO)₄(PMe₃)(CN)]⁻ and [Fe₂(μ-Xdt)(CO)₄(CN)₂]²⁻ systems. This could provide further insight into the effects that their position has on the Mulliken charge distribution.

Consistent with experimental observations, the DFT calculations showed that bridging hydrides are the most thermodynamically stable. Increasing the steric bulk of the dithiolate bridge was shown to have little affect on the IR νCO peak positions. This suggested that the differences in rates of protonation between the different dithiolate bridges were unlikely to be caused by the electronic effects of the bridgehead itself. Wright and Picket identified a two-step reaction pathway when protonating the Fe₂(μ-pdt)(CO)₄(PMe₃)₂ model complex [67]. They identified the product of protonation as a bridging hydride with the PMe₃ ligands basal/basal-*transoid* to each other, isomer **2D**. Chapter 4 presented the simulated reaction pathways of protonation reactions with an HBF₄·Et₂O acid. Notably, for all reaction pathways, the approaching acid first appears to weakly coordinate to a CO ligand, before transferring the proton to the Fe centre. The energy barriers associated with protonation to the basal position in isomers **1C** (basal/basal-*cisoid*), **1D** (basal/basal-*transoid*) and **1A** (apical/basal) were predicted to be lower in energy than for the analogous pathways for protonation directly to the Fe–Fe bond. Additionally, modelling the isomerisation pathways from these terminal products to the thermodynamic bridging product showed that the predicted barrier heights were still lower than for protonation directly to the bridging position. This work could be built upon by calculating the energetics of protonation pathways for bulkier dithiolate bridged systems, as well

calculating analogous pathways for subsites where PMe_3 ligands are substituted for CN ligands. Further insight into the Approaching the problem from a DFT/MD perspective may also offer additional insight into mechanism.

Chapter 5 presents a study in which the $[(\mu\text{-H})\text{Fe}_2(\mu\text{-pdt})(\text{CO})_4(\text{PMe}_3)_2]$ model complex was reduced to form a stable paramagnetic species. Characterisation using FTIR and EPR showed that the product had retained its basal/basal-transoid geometry following reduction, with a symmetrical disposition of the unpaired spin. Addition of muonium is analogous to the two-step process of protonation and reduction, and offers a means of studying the structure and dynamics of radical addition on the nano-second timescale. Preliminary experiments on $[\text{Fe}_2(\mu\text{-pdt})(\text{CO})_4(\text{PMe}_3)_2]$ and $[\text{Fe}_2(\mu\text{-pdt})(\text{CO})_4(\text{CN})_2]^{2-}$ model subsites confirmed that muonium addition produces a transient paramagnetic species. The repolarisation curves showed a rapid recovery at fields of ~ 0.06 T and a produced broad asymmetric ALC resonance features at ~ 0.12 T in both complexes. This data suggests a similar mode of binding in each compound and is consistent with a hyperfine coupling of ~ 33 MHz. The hfccs associated with all possible binding sites were calculated using DFT. Predicted resonance positions associated with the basal muonation to Fe and muonation to the CO group produce simulated hfccs most consistent with those observed experimentally. This is an interesting observation, in agreement with the mechanism predicted for the protonated analogue where a CO-acid intermediate is formed first. Unfortunately, the resonance associated with muonation to the Fe–Fe bond could not be investigated as the resonance is predicted to occur at ~ 0.8 T, a field region inaccessible to the instrument used. Future experiments will use ALC– μ SR to measure around the regions where other resonances were predicted by DFT, particularly the resonance associated with the Fe–Fe bridging muonium. Molecular dynamics of the subsite are expected to manifest as a change in the width of the resonance while a secondary chemical reaction would reduce the resonance intensity. In order to identify these dynamics, an investigation into how the ALC line shapes evolve as a function of temperature could be investigated. By measuring ALC spectra over a number of dilute concentrations the total addition rate could be measured. DFT calculations demonstrated that the size and nature of the dith-

iolate bridge, as well as the direction in which it pointed, influenced the magnitude of the predicted hyperfine couplings. Experiments measuring the resonance positions of the different dithiolate bridged systems would allow a means of investigating the first point while a temperature study would investigate the effect of the bridge flip on the resonance position. This is an important measurement in the context of the ratchet mechanism proposed.

In Chapter 6 a combination of NIS, FTIR, Raman, and DFT were used to provide a complete assignment of the metal-active vibrations in the lower frequency region of the $^{57}\text{Fe}(\text{acac})_3$ model complex. The predicted PDOS, infrared and Raman spectral features were all found to be in excellent agreement with experimental spectra. This investigation provides proof of principle and demonstrates the potential for its use in characterising of more complex systems. The next step in this work would be to label the $[\text{Fe}_2(\mu\text{-pdt})(\text{CO})_4(\text{PMe}_3)_2]$ model system with ^{57}Fe to provide a complete assignment of the low energy metal-active vibrations. Investigations using varying coordination spheres could help shed further light into the properties of the hydrogenase mimic.

An investigation into the rates of molecular transfer across an oil-water interface using a combination of TF- μ SR, ALC- μ SR and Monte-Carlo simulations was presented in Chapter 7. Monte-Carlo simulations on the selected ALC resonances predicted a rate of transfer of $\tau \sim 122$ MHz. Rotational averaged DFT calculations provided a means of calculating hyperfine coupling constants and enabled the unambiguous assignment of the experimentally observed ALC resonances associated with centrally and terminally muoniated radical species.

Bibliography

- (1) V. Fock, 'Näherungsmethode zur Lösung des quantenmechanischen Mehrkörperproblems', *Z. Phys.*, 1930, **61**, 126–148.
- (2) W. Pauli, 'Über den Zusammenhang des Abschlusses der Elektronengruppen im Atom mit der Komplexstruktur der Spektren', *Z. Phys.*, 1925, **31**, 765–783, DOI: 10.1007/BF02980631.
- (3) N. M. Hugenholtz, 'Variational Principle in Quantum Mechanics', *Phys. Rev.*, 1954, **96**, 1158–1159, DOI: 10.1103/PhysRev.96.1158.
- (4) W. Kock and M. C. Holthausen, *A Chemist's Guide to Density Functional Theory, Second Edition*, WILEY-VCH Verlag, 2001.
- (5) J. C. Slater, 'Atomic Shielding Constants', *Phys. Rev.*, 1930, **36**, 57–64, DOI: 10.1103/PhysRev.36.57.
- (6) S. F. Boys, 'Electronic Wave Functions. I. A General Method of Calculation for the Stationary States of Any Molecular System', *Proc. R. Soc.*, 1950, **200**, 542–554, DOI: 10.1098/rspa.1950.0036.
- (7) C. J. Cramer, *Essentials of Computational Chemistry: Theories and Models, Second Edition*, John Wiley & Sons, Inc., 2008.
- (8) G. Frenking et al., 'Pseudopotential Calculations of Transition Metal Compounds: Scope and Limitations', *Rev. Comp Chem.*, 1996, **8**, ed. K. B. Lipkowitz and D. B. Boyd, 63–143.
- (9) T. Cundari, M. T. Benson, M. L. Lutz and S. O. Sommerer, 'Effective Core Potential Approaches to the Chemistry of the Heavier Elements.', *Rev. Comp Chem.*, 1996, **8**, ed. K. B. Lipkowitz and D. B. Boyd, 145–202.
- (10) P.-O. Löwdin, 'Quantum Theory of Many-Particle Systems. III. Extension of the Hartree-Fock Scheme to Include Degenerate Systems and Correlation Effects', *Phys. Rev.*, 1955, **97**, 1509–1520, DOI: 10.1103/PhysRev.97.1509.
- (11) F. Jensen, *Introduction to Computational Chemistry, Second Edition*, John Wiley & Sons, Inc., 2007.
- (12) C. Miller and M. S. Plesset, 'Note on an Approximation Treatment for Many-Electron Systems', *Phys. Rev.*, 1934, **46**, 618–622, DOI: 10.1103/PhysRev.46.618.

- (13) P. Hohenberg and W. Kohn, 'Inhomogeneous Electron Gas', *Phys. Rev.*, 1964, **136**, B864–B871, DOI: 10.1103/PhysRev.136.B864.
- (14) W. Kohn and L. J. Sham, 'Self-Consistent Equations Including Exchange and Correlation Effects', *Phys. Rev.*, 1965, **140**, A1133–A1138, DOI: 10.1103/PhysRev.140.A1133.
- (15) E. Lewars, *Computational Chemistry: Introduction to the Theory and Applications of Molecular and Quantum Mechanics*, Kluwer Academic Publishers, 2003.
- (16) H. Agren and K. V. Mikkelsen, 'Theory of solvent effects on electronic spectra', *J. Mol. Struct-theochem.*, 1991, **234**, 425–467, DOI: 10.1016/0166-1280(91)89027-X.
- (17) C. J. Cramer and D. G. Truhlar, 'Implicit Solvation Models: Equilibria, Structure, Spectra, and Dynamics', *Chem. Rev.*, 1999, **99**, 2161–2200, DOI: 10.1021/cr960149m.
- (18) M. J. Frisch et al., *Gaussian 03, Revision E.02*, Gaussian, Inc., Wallingford, CT, 2004.
- (19) M. J. Frisch et al., *Gaussian 09 Revision C.01*, Gaussian Inc. Wallingford CT 2009.
- (20) U. A. Jayasooriya and R. Grinter, Muon Spectroscopy, in *digital Encyclopedia of Applied Physics*, Wiley-VCH Verlag GmbH & Co. KGaA, 2009, DOI: 10.1002/3527600434.eap700.
- (21) A. Yaouanc and P. Dalmas De Reotier, *Muon Spin Rotation, Relaxation, and Resonance: Applications to Condensed Matter*, ed. J. Birman, S. F. Edwards, R. Friend, M. Rees, D. Sherrington and G. Veneziano, Oxford Science Publications, 2011.
- (22) S. F. J. Cox, 'Implanted muon studies in condensed matter science', *J. Phys. C*, 1987, **20**, 3187–3319.
- (23) S. J. Blundell, 'Muon-Spin Rotation Studies of Electronic Properties of Molecular Conductors and Superconductors', *Chem. Rev.*, 2004, **104**, 5717–5736, DOI: 10.1021/cr030632e.
- (24) K. Nagamine, *Introductory Muon Science*, Cambridge University Press, 2003.
- (25) S. N. Ahmed et al., 'Constraints on Neutron Decay via Invisible Modes from the Sudbury Neutrino Observatory', *Phys. Rev. Lett.*, 2004, **92**, 102004, DOI: 10.1103/PhysRevLett.92.102004.
- (26) P. J. Mohr and B. N. Taylor, *The 2010 CODATA Recommended Values of the Fundamental Physical Constants*, <http://physics.nist.gov/constants>, 2010.

- (27) C. D. Anderson and S. H. Neddermeyer, 'Cloud Chamber Observations of Cosmic Rays at 4300 Meters Elevation and Near Sea-Level', *Phys. Rev.*, 1936, **50**, 263–271, DOI: 10.1103/PhysRev.50.263.
- (28) R. L. Garwin, L. M. Lederman and M. Weinrich, 'Observations of the Failure of Conservation of Parity and Charge Conjugation in Meson Decays: the Magnetic Moment of the Free Muon', *Phys. Rev.*, 1957, **105**, 1415–1417, DOI: 10.1103/PhysRev.105.1415.
- (29) J. Piroto Duarte, MA thesis, University of Coimbra, 2006.
- (30) E. Roduner, 'Polarized positive Muons probing free radicals: a variant of magnetic resonance', *Chem. Soc. Rev.*, 1993, **22**, 337–346, DOI: 10.1039/CS9932200337.
- (31) J. E. Wertz and J. R. Bolton, *Electron Spin Resonance: Elementary Theory and Practical Applications*, McGraw-Hill: New York, 1972.
- (32) C. P. J. Poole, *Electron Spin Resonance: A Comprehensive Treatise on Experimental Techniques*, John Wiley & Sons, Inc., 1983.
- (33) B. M. Leu et al., 'Quantitative Vibrational Dynamics of Iron in Nitrosyl Porphyrins', *J. Am. Chem. Soc.*, 2004, **126**, 4211–4227, DOI: 10.1021/ja038526h.
- (34) R. Ruffer and A. Chumakov, 'Nuclear Resonance Beamline at ESRF', *Hyperfine Interact.*, 1996, **97–98**, 589–604.
- (35) M. Seto, Y. Yoda, S. Kikuta, X. W. Zhang and M. Ando, 'Observation of Nuclear Resonant Scattering Accompanied by Phonon Excitation Using Synchrotron Radiation', *Phys. Rev. Lett.*, 1995, **74**, 3828–3831, DOI: 10.1103/PhysRevLett.74.3828.
- (36) W. Sturhahn et al., 'Phonon Density of States Measured by Inelastic Nuclear Resonant Scattering', *Phys. Rev. Lett.*, 1995, **74**, 3832–3835.
- (37) A. I. Chumakov et al., 'Energy Dependence of Nuclear Recoil Measured with Incoherent Nuclear Scattering of Synchrotron Radiation', *Europhys. Lett.*, 1995, **30**, 427–432.
- (38) A. I. Chumakov and W. Sturhahn, 'Experimental aspects of inelastic nuclear resonance scattering', *Hyp. Interact.*, 1999, **123**, 781–808.
- (39) M. C. Smith et al., 'Normal-Mode Analysis of FeCl_4^- and $\text{Fe}_2\text{S}_2\text{Cl}_4^{2-}$ via Vibrational Mossbauer, Resonance Raman, and FT-IR Spectroscopies', *Inorg. Chem.*, 2005, **44**, 5562–5570, DOI: 10.1021/ic0482584.
- (40) W. Sturhahn, 'Nuclear resonant spectroscopy', *J. Phys.: Condens. Matter*, 2004, **16**, S497–S530, DOI: 10.1088/0953-8984/16/5/009.
- (41) R. F. Service, 'The Hydrogen Backlash', *Science*, 2004, **305**, 958–961, DOI: 10.1126/science.305.5686.958.

- (42) K. A. Vincent, A. Parkin and F. A. Armstrong, 'Investigating and Exploiting the Electrocatalytic Properties of Hydrogenases', *Chem. Rev.*, 2007, **107**, 4366–4413, DOI: 10.1021/cr050191u.
- (43) W. Lubitz and W. Tumas, 'Hydrogen: An Overview', *Chem. Rev.*, 2007, **107**, 3900–3903, DOI: 10.1021/cr050200z.
- (44) J. D. Holladay, Y. Wang and E. Jones, 'Review of Developments in Portable Hydrogen Production Using Microreactor Technology', *Chem. Rev.*, 2004, **104**, 4767–4790, DOI: 10.1021/cr020721b.
- (45) M. Winter and R. J. Brodd, 'What Are Batteries, Fuel Cells, and Supercapacitors', *Chem. Rev.*, 2004, **104**, 4245–4270, DOI: 10.1021/cr020730k.
- (46) C. Tard and C. J. Pickett, 'Structural and Functional Analogues of the Active Sites of the [Fe]-, [NiFe]-, and [FeFe]-Hydrogenases', *Chem. Rev.*, 2009, **109**, 2245–2274, DOI: 10.1021/cr800542q.
- (47) P. E. M. Siegbahn, J. W. Tye and M. B. Hall, 'Computational Studies of [NiFe] and [FeFe] Hydrogenases', *Chem. Rev.*, 2007, **107**, 4414–4435, DOI: 10.1021/cr050185y.
- (48) J. W. Tye, M. B. Hall and M. Y. Darensbourg, 'Better than platinum; Fuel cells energized by enzymes', *Natl. Acad. Sci. USA*, 2005, **102**, 16911–16912, DOI: 10.1073/pnas.0508740102.
- (49) M. W. Adams, 'The structure and mechanism of iron-hydrogenases', *Biochimica et Biophysica Acta*, 1990, **1020**, 115–145, DOI: 10.1016/0005-2728(90)90044-5.
- (50) S. P. Albracht, 'Nickel hydrogenases: in search of the active site', *Biochimica et Biophysica Acta*, 1994, **1188**, 167–204, DOI: 10.1016/0005-2728(94)90036-1.
- (51) E. Garcin, X. Vernede and E. C. Hatchikian, 'The crystal structure of a reduced [NiFeSe] hydrogenase provides an image of the activated catalytic center', *Structure*, 1999, **7**, 557–566, DOI: 10.1016/S0969-2126(99)80072-0.
- (52) M. Korbas et al., 'The Iron-Sulfur Cluster-free Hydrogenase (Hmd) Is a Metalloenzyme with a Novel Iron Binding Motif', *J. Biol. Chem.*, 2006, **281**, 30804–30813, DOI: 10.1074/jbc.M605306200.
- (53) X. Yang and M. B. Hall, 'Monoiron Hydrogenase Catalysis: Hydrogen Activation with the Formation of a Dihydrogen, Fe–H⁻H⁺–O, Bond and Methenyl–H₄MPT⁺ Triggered Hydride Transfer', *J. Am. Chem. Soc.*, 2009, **131**, 10901–10908, DOI: 10.1021/ja902689n.

- (54) J. W. Peters, W. N. Lanzilotta, B. J. Lemon and L. C. Seefeldt, 'X-ray Crystal Structure of the Fe-Only Hydrogenase (CpI) from *Clostridium pasteurianum* to 1.8 Angstrom Resolution', *Science*, 1998, **282**, 1853–1858, DOI: 10.1126/science.282.5395.1853.
- (55) Y. Nicolet, C. Piras, P. Legrand, C. E. Hatchikian and J. C. Fontecilla-Camps, 'Desulfovibrio desulfuricans iron hydrogenase: the structure shows unusual coordination to an active site Fe binuclear center', *Structure*, 1999, **7**, 13–23.
- (56) Y. Nicolet, A. L. de Lacey, X. Vernde, V. M. Fernandez, E. C. Hatchikian and J. C. Fontecilla-Camps, 'Crystallographic and FTIR Spectroscopic Evidence of Changes in Fe Coordination Upon Reduction of the Active Site of the Fe-Only Hydrogenase from *Desulfovibrio desulfuricans*', *J. Am. Chem. Soc.*, 2001, **123**, 1596–1601, DOI: 10.1021/ja0020963.
- (57) B. J. Lemon and J. W. Peters, 'Binding of Exogenously Added Carbon Monoxide at the Active Site of the Iron-Only Hydrogenase (CpI) from *Clostridium pasteurianum*', *Biochem.*, 1999, **38**, 12969–12973, DOI: 10.1021/bi9913193.
- (58) Y. Nicolet, B. J. Lemon, J. C. Fontecilla-Camps and J. W. Peters, 'A novel FeS cluster in Fe-only hydrogenases', *Trends. Biochem. Sci.*, 2000, **25**, 138–143, DOI: 10.1016/S0968-0004(99)01536-4.
- (59) A. S. Pandey, T. V. Harris, L. J. Giles, J. W. Peters and R. K. Szilagyi, 'Dithiomethylether as a Ligand in the Hydrogenase H-Cluster', *J. Am. Chem. Soc.*, 2008, **130**, 4533–4540, DOI: 10.1021/ja711187e.
- (60) A. Silakov, B. Wenk, E. Reijerse and W. Lubitz, '¹⁴N HYSCORE investigation of the H-cluster of [FeFe] hydrogenase: evidence for a nitrogen in the dithiol bridge', *Phys. Chem. Chem. Phys.*, 2009, **11**, 6592–6599, DOI: 10.1039/B905841A.
- (61) O. F. Erdem et al., 'A Model of the [FeFe] Hydrogenase Active Site with a Biologically Relevant Azadithiolate Bridge: A Spectroscopic and Theoretical Investigation', *Angew. Chem. Int. Ed.*, 2011, **50**, 1439–1443, DOI: 10.1002/anie.201006244.
- (62) C. Greco, M. Bruschi, L. De Gioia and U. Ryde, 'A QM/MM Investigation of the Activation and Catalytic Mechanism of Fe-Only Hydrogenases', *Inorg. Chem.*, 2007, **46**, 5911–5921, DOI: 10.1021/ic062320a.
- (63) Z. Cao and M. B. Hall, 'Modeling the Active Sites in Metalloenzymes. 3. Density Functional Calculations on Models for [Fe]-Hydrogenase: Structures and Vibrational Frequencies of the Observed Redox Forms and the Reaction Mechanism at the Diiron Active Center', *J. Am. Chem. Soc.*, 2001, **123**, 3734–3742, DOI: 10.1021/ja000116v.

- (64) M. Bruschi, C. Greco, P. Fantucci and L. D. Gioia, 'Structural and Electronic Properties of the [FeFe] Hydrogenase H-Cluster in Different Redox and Protonation States. A DFT Investigation', *Inorg. Chem.*, 2008, **47**, 6056–6071, DOI: 10.1021/ic8006298.
- (65) S. J. Borg, S. K. Ibrahim, C. J. Pickett and S. P. Best, 'Electrocatalysis of hydrogen evolution by synthetic diiron units using weak acids as the proton source: Pathways of doubtful relevance to enzymic catalysis by the diiron subsite of [FeFe] hydrogenase', *C. R. Chim.*, 2008, **11**, 852–860, DOI: 10.1016/j.crci.2008.04.008.
- (66) A. I. Stewart et al., 'Structure and Vibrational Dynamics of Model Compounds of the [FeFe]-Hydrogenase Enzyme System via Ultrafast Two-Dimensional Infrared Spectroscopy', *J. Phys. Chem. B*, 2008, **112**, 10023–10032, DOI: 10.1021/jp803338d.
- (67) J. A. Wright and C. J. Pickett, 'Protonation of a subsite analogue of [FeFe]-hydrogenase: mechanism of a deceptively simple reaction revealed by time resolved IR spectroscopy', *Chem. Comm.*, 2009, 5719–5721, DOI: 10.1039/b912499c.
- (68) A. Jablonskyte, J. A. Wright and C. J. Pickett, 'Mechanistic aspects of the protonation of [FeFe]-hydrogenase subsite analogues', *Dalton Trans.*, 2010, **39**, 3026–3034, DOI: 10.1039/B923191A.
- (69) X. Zhao, I. P. Georgakaki, M. L. Miller, J. C. Yarbrough and M. Y. Darensbourg, 'H/D Exchange Reactions in Dinuclear Iron Thiolates as Activity Assay Models of Fe-H₂ase', *J. Am. Chem. Soc.*, 2001, **123**, 9710–9711, DOI: doi : 10.1021/ja0167046.
- (70) D. Chong, I. P. Georgakaki, R. Mejia-Rodriguez, J. Sanabria-Chinchilla, M. P. Soriaga and M. Y. Darensbourg, 'Electrocatalysis of hydrogen production by active site analogues of the iron hydrogenase enzyme: structure/function relationships', *Dalton Trans.*, 2003, 4158–4163, DOI: 10.1039/B304283A.
- (71) C. M. Thomas, O. Rdiger, T. Liu, C. E. Carson, M. B. Hall and M. Y. Darensbourg, 'Synthesis of Carboxylic Acid-Modified [FeFe]-Hydrogenase Model Complexes Amenable to Surface Immobilization', *Organometallics*, 2007, **26**, 3976–3984, DOI: 10.1021/om7003354.
- (72) C. M. Thomas, T. Liu, M. B. Hall and M. Y. Darensbourg, 'Series of Mixed Valent Fe(II)Fe(I) Complexes that Model the Hox State of [FeFe]Hydrogenase: Redox Properties, Density-Functional Theory Investigation, and Reactivities with Extrinsic CO', *Inorg. Chem.*, 2008, **47**, 7009–7024, DOI: 10.1021/ic800654a.

- (73) M. L. Singleton, N. Bhuvanesh, J. H. Reibenspies and M. Y. Darensbourg, 'Synthetic Support of De Novo Design: Sterically Bulky [FeFe]-Hydrogenase Models', *Angew. Chem. Int. Ed.*, 2008, **47**, 9492–9495, DOI: 10.1002/anie.200803939.
- (74) J.-F. Capon, S. El Hassnaoui, F. Gloaguen, P. Schollhammer and J. Talarmin, 'N-Heterocyclic Carbene Ligands as Cyanide Mimics in Diiron Models of the All-Iron Hydrogenase Active Site', *Organometallics*, 2005, **24**, 2020–2022, DOI: 10.1021/om049132h.
- (75) S. Ezzaher et al., 'Evidence for the Formation of Terminal Hydrides by Protonation of an Asymmetric Iron Hydrogenase Active Site Mimic', *Inorg. Chem.*, 2007, **46**, 3426–3428, DOI: 10.1021/ic0703124.
- (76) S. Ezzaher et al., 'Diiron chelate complexes relevant to the active site of the iron-only hydrogenase', *C. R. Chim.*, 2008, **11**, 906–914, DOI: 10.1016/j.crci.2008.04.002.
- (77) J.-F. Capon, F. Gloaguen, F. Y. Petillon, P. Schollhammer and J. Talarmin, 'Organometallic Diiron Complex Chemistry Related to the [2Fe]H Subsite of [FeFe]-H₂ase', *Eur. J. Inorg. Chem.*, 2008, **30**, 4671–4681, DOI: 10.1002/ejic.200800717.
- (78) J.-F. Capon, S. Ezzaher, F. Gloaguen, F. Y. Petillon, P. Schollhammer and J. Talarmin, 'Electrochemical Insights into the Mechanisms of Proton Reduction by [Fe₂(CO)₆μ-SCH₂N(R)CH₂S] Complexes Related to the [2Fe]H Subsite of [FeFe]Hydrogenase', *Chem. Eur. J.*, 2008, **14**, 1954–1964, DOI: 10.1002/chem.200701454.
- (79) F. Gloaguen, J. D. Lawrence and T. B. Rauchfuss, 'Biomimetic Hydrogen Evolution Catalyzed by an Iron Carbonyl Thiolate', *J. Am. Chem. Soc.*, 2001, **123**, 9476–9477, DOI: 10.1021/ja016516f.
- (80) A. K. Justice, T. Rauchfuss and S. R. Wilson, 'Unsaturated, Mixed-Valence Diiron Dithiolate Model for the H_{ox} State of the [FeFe]-Hydrogenase', *Angew. Chem.*, 2007, **119**, 6264–6266, DOI: 10.1002/ange.200702224.
- (81) M. T. Olsen, M. Bruschi, L. De Gioia, T. B. Rauchfuss and S. R. Wilson, 'Nitrosyl Derivatives of Diiron(I) Dithiolates Mimic the Structure and Lewis Acidity of the [FeFe]-Hydrogenase Active Site', *J. Am. Chem. Soc.*, 2008, **130**, 12021–12030, DOI: 10.1021/ja802268p.
- (82) A. K. Justice, M. J. Nilges, T. B. Rauchfuss, S. R. Wilson, L. De Gioia and G. Zampella, 'Diiron Dithiolato Carbonyls Related to the H_{ox}CO State of [FeFe]-Hydrogenase', *J. Am. Chem. Soc.*, 2008, **130**, 5293–5301, DOI: 10.1021/ja7113008.
- (83) Z. Heiden, G. Zampella, L. De Gioia and T. Rauchfuss, '[FeFe]-Hydrogenase Models and Hydrogen: Oxidative Addition of Dihydrogen and Silanes', *Angew. Chem.*, 2008, **120**, 9902–9905, DOI: 10.1002/ange.200804400.

- (84) M. H. Cheah, S. J. Borg, M. I. Bondin and S. P. Best, 'Electrocatalytic Proton Reduction by Phosphido-Bridged Diiron Carbonyl Compounds: Distant Relations to the H-Cluster', *Inorg. Chem.*, 2004, **43**, 5635–5644, DOI: 10.1021/ic049746e.
- (85) S. J. Borg, T. Behrsing, S. P. Best, M. Razavet, X. Liu and C. J. Pickett, 'Electron Transfer at a Dithiolate-Bridged Diiron Assembly: Electrocatalytic Hydrogen Evolution', *J. Am. Chem. Soc.*, 2004, **126**, 16988–16999, DOI: 10.1021/ja045281f.
- (86) M. H. Cheah, S. J. Borg and S. P. Best, 'Steps along the Path to Dihydrogen Activation at [FeFe] Hydrogenase Structural Models: Dependence of the Core Geometry on Electrocatalytic Proton Reduction', *Inorg. Chem.*, 2007, **46**, 1741–1750, DOI: 10.1021/ic0623361.
- (87) M. H. Cheah et al., 'Modeling [Fe-Fe] Hydrogenase: Evidence for Bridging Carbonyl and Distal Iron Coordination Vacancy in an Electrocatalytically Competent Proton Reduction by an Iron Thiolate Assembly That Operates through Fe(0)-Fe(II) Levels', *J. Am. Chem. Soc.*, 2007, **129**, 11085–11092, DOI: 10.1021/ja071331f.
- (88) Z.-P. Liu and P. Hu, 'A Density Functional Theory Study on the Active Center of Fe-Only Hydrogenase: Characterization and Electronic Structure of the Redox States', *J. Am. Chem. Soc.*, 2002, **124**, 5175–5182, DOI: 10.1021/ja0118690.
- (89) H.-J. Fan and M. B. Hall, 'A Capable Bridging Ligand for Fe-Only Hydrogenase: Density Functional Calculations of a Low-Energy Route for Heterolytic Cleavage and Formation of Dihydrogen', *J. Am. Chem. Soc.*, 2001, **123**, 3828–3829, DOI: 10.1021/ja004120i.
- (90) G. Zampella, C. Greco, P. Fantucci and L. De Gioia, 'Proton Reduction and Dihydrogen Oxidation on Models of the [2Fe]H Cluster of [Fe] Hydrogenases. A Density Functional Theory Investigation', *Inorg. Chem.*, 2006, **45**, 4109–4118, DOI: 10.1021/ic051986m.
- (91) G. Zampella, P. Fantucci and L. D. Gioia, 'Unveiling How Stereoelectronic Factors Affect Kinetics and Thermodynamics of Protonation Regiochemistry in [FeFe] Hydrogenase Synthetic Models: A DFT Investigation', *J. Am. Chem. Soc.*, 2009, **131**, 10909–10917, DOI: 10.1021/ja902727z.
- (92) X. Zhao, Y.-M. Hsiao, C.-H. Lai, J. H. Reibenspies and M. Y. Darensbourg, 'Oxidative Addition of Phosphine-Tethered Thiols to Iron Carbonyl: Binuclear Phosphinothiolate Complexes, $(\mu\text{-SCH}_2\text{CH}_2\text{PPh}_2)_2\text{Fe}_2(\text{CO})_4$, and Hydride Derivatives', *Inorg. Chem.*, 2002, **41**, 699–708, DOI: 10.1021/ic010741g.

- (93) X. Zhao, I. P. Georgakaki, M. L. Miller, R. Mejia-Rodriguez, C.-Y. Chiang and M. Y. Darensbourg, 'Catalysis of H₂/D₂ Scrambling and Other H/D Exchange Processes by [Fe]-Hydrogenase Model Complexes', *Inorg. Chem.*, 2002, **41**, 3917–3928, DOI: 10.1021/ic020237r.
- (94) P. I. Volkers and T. B. Rauchfuss, 'Extending the motif of the [FeFe]-hydrogenase active site models: Protonation of Fe₂(NR)₂(CO)_{6-x}L_x species', *J. Inorg. Biochem.*, 2007, **101**, 1748–1751, DOI: 10.1016/j.jinorgbio.2007.05.005.
- (95) J. I. van der Vlugt, T. B. Rauchfuss, C. M. Whaley and S. R. Wilson, 'Characterization of a Diferrous Terminal Hydride Mechanistically Relevant to the Fe-Only Hydrogenases', *J. Am. Chem. Soc.*, 2005, **127**, 16012–16013, DOI: 10.1021/ja055475a.
- (96) D. Morvan et al., 'N-Heterocyclic Carbene Ligands in Nonsymmetric Diiron Models of Hydrogenase Active Sites', *Organometallics*, 2007, **26**, 2042–2052, DOI: 10.1021/om061173l.
- (97) P.-Y. Orain et al., 'Use of 1,10-phenanthroline in diiron dithiolate derivatives related to the [Fe-Fe] hydrogenase active site', *Dalton Trans.*, 2007, 3754–3756, DOI: 10.1039/B709287C.
- (98) B. E. Barton and T. B. Rauchfuss, 'Terminal Hydride in [FeFe]-Hydrogenase Model Has Lower Potential for H₂ Production Than the Isomeric Bridging Hydride', *Inorg. Chem.*, 2008, **47**, 2261–2263, DOI: 10.1021/ic800030y.
- (99) J. W. Tye, M. Y. Darensbourg and M. B. Hall, 'The reaction of electrophiles with models of ironiron hydrogenase: A switch in regioselectivity', *J. Mol. Struct-theochem.*, 2006, **771**, 123–128, DOI: 10.1016/j.theochem.2006.03.022.
- (100) J. A. Franz et al., 'Activation of the S-H group in Fe(μ₂-SH)Fe clusters: S-H bond strengths and free radical reactivity of the Fe(μ₂-SH)Fe cluster', *J. Am. Chem. Soc.*, 2009, **131**, 15212–15224, DOI: 10.1021/ja904602p.
- (101) B. E. Barton, M. T. Olsen and T. B. Rauchfuss, 'Aza- and Oxadithiolates Are Proton Relays in Functional Models for the [FeFe]-Hydrogenases', *J. Am. Chem. Soc.*, 2008, **130**, 16834–16835, DOI: 10.1021/ja8057666.
- (102) D. Morvan et al., 'Modeling [FeFe] hydrogenase: Synthesis and protonation of a diiron dithiolate complex containing a phosphine-N-heterocyclic-carbene ligand', *J. Organomet. Chem.*, 2009, **694**, 2801–2807, DOI: 10.1016/j.jorganchem.2009.01.018.
- (103) B. E. Barton, G. Zampella, A. K. Justice, L. De Gioia, T. B. Rauchfuss and S. R. Wilson, 'Isomerization of the hydride complexes [HFe₂(SR)₂(PR₃)_x(CO)_{6-x}]⁺ (x = 2, 3, 4) relevant to the active site models for the [FeFe]-hydrogenases', *Dalton Trans.*, 2010, **39**, 3011–3019, DOI: 10.1039/B910147K.

- (104) J. A. Wright, L. Webster, A. Jablonskyte, P. M. Woi, S. K. Ibrahim and C. J. Pickett, 'Protonation of [FeFe]-hydrogenase sub-site analogues: revealing mechanism using FTIR stopped-flow techniques', *Faraday Discuss.*, 2011, **148**, 359–371, DOI: 10.1039/C004692B.
- (105) A. Jablonskyte, J. A. Wright and C. J. Pickett, '[FeFe]-Hydrogenase Models: Unexpected Variation in Protonation Rate between Dithiolate Bridge Analogues', *Eur. J. Inorg. Chem.*, 2011, (7), 1033–1037, DOI: 10.1002/ejic.201001072.
- (106) P.-Y. Orain et al., 'Investigation on the Protonation of a Trisubstituted [Fe₂(CO)₃-(PPh₃)(κ²-phen)(μ-pdt)] Complex: Rotated versus Unrotated Intermediate Pathways', *Inorg. Chem.*, 2010, **49**, 5003–5008, DOI: 10.1021/ic100108h.
- (107) P. Surawatanawong and M. B. Hall, 'Density functional study of the thermodynamics of hydrogen production by tetrairon hexathiolate, Fe₄[MeC(CH₂S)₃]₂(CO)₈, a hydrogenase model.', *Inorg. Chem.*, 2010, **49**, 5737–5747.
- (108) A. D. Becke, 'Density-functional thermochemistry. III. The role of exact exchange', *J. Chem. Phys.*, 1993, **98**, 5648–5652, DOI: 10.1063/1.464913.
- (109) C. Lee, W. Yang and R. G. Parr, 'Development of the Colle-Salvetti correlation-energy formula into a functional of the electron density', *Phys. Rev. B*, 1988, **37**, 785–789, DOI: 10.1103/PhysRevB.37.785.
- (110) B. Miehlich, A. Savin, H. Stoll and H. Preuss, 'Results obtained with the correlation energy density functionals of Becke and Lee, Yang and Parr', *Chem. Phys. Lett.*, 1989, **157**, 200–206, DOI: 10.1016/0009-2614(89)87234-3.
- (111) J. Tao, J. P. Perdew, V. N. Staroverov and G. E. Scuseria, 'Climbing the Density Functional Ladder: Nonempirical Meta-Generalized Gradient Approximation Designed for Molecules and Solids', *Phys. Rev. Lett.*, 2003, **91**, 146401, DOI: 10.1103/PhysRevLett.91.146401.
- (112) W. R. Wadt and P. J. Hay, 'Ab initio effective core potentials for molecular calculations. Potentials for main group elements Na to Bi', *J. Chem. Phys.*, 1985, **82**, 284–298, DOI: 10.1063/1.448800.
- (113) P. J. Hay and W. R. Wadt, 'Ab initio effective core potentials for molecular calculations. Potentials for the transition metal atoms Sc to Hg', *J. Chem. Phys.*, 1985, **82**, 270–283, DOI: doi:10.1063/1.448799.
- (114) P. J. Hay and W. R. Wadt, 'Ab initio effective core potentials for molecular calculations. Potentials for K to Au including the outermost core orbitals', *J. Chem. Phys.*, 1985, **82**, 299–310, DOI: doi:10.1063/1.448975.
- (115) M. Couty and M. B. Hall, 'Basis sets for transition metals: Optimized outer p functions', *J. Comput. Chem.*, 1996, **17**, 1359–1370, DOI: 10.1002/(SICI)1096-987X(199608)17:11<1359::AID-JCC9>3.0.CO;2-L.

- (116) A. Ehlers et al., 'A set of f-polarization functions for pseudo-potential basis sets of the transition metals Sc-Cu, Y-Ag and La-Au', *Chem. Phys. Lett.*, 1993, **208**, 111–114, DOI: 10.1016/0009-2614(93)80086-5.
- (117) A. Hollwarth et al., 'A set of d-polarization functions for pseudo-potential basis sets of the main group elements Al-Bi and f-type polarization functions for Zn, Cd, Hg', *Chem. Phys. Lett.*, 1993, **208**, 237–240, DOI: 10.1016/0009-2614(93)89068-S.
- (118) C. Liu, J. N. T. Peck, J. A. Wright, C. J. Pickett and M. B. Hall, 'Density Functional Calculations on Protonation of the [FeFe]-Hydrogenase Model Complex $\text{Fe}_2(\mu\text{-pdt})(\text{CO})_4(\text{PMe}_3)_2$ and Subsequent Isomerization Pathways', *Eur. J. Inorg. Chem.*, 2011, 1080–1093, DOI: 10.1002/ejic.201001085.
- (119) M. L. Singleton, R. M. Jenkins, C. L. Klemashevich and M. Y. Darensbourg, 'The effect of bridgehead steric bulk on the ground state and intramolecular exchange processes of $(\text{SCH}_2\text{CR}_2\text{CH}_2\text{S})[\text{Fe}(\text{CO})_3][\text{Fe}(\text{CO})_2\text{L}]$ complexes', *C. R. Chim.*, 2008, **11**, 861–874, DOI: 10.1016/j.crci.2008.01.018.
- (120) E. J. Lyon, I. P. Georgakaki, J. H. Reibenspies and M. Y. Darensbourg, 'Carbon Monoxide and Cyanide Ligands in a Classical Organometallic Complex Model for Fe-Only Hydrogenase', *Angew. Chem. Int. Ed.*, 1999, **38**, 3178–3180, DOI: 10.1002/(SICI)1521-3773(19991102)38:21<3178::AID-ANIE3178>3.CO;2-4.
- (121) S. L. Matthews and D. M. Heinekey, 'A Carbonyl-Rich Bridging Hydride Complex Relevant to the Fe-Fe Hydrogenase Active Site', *Inorg. Chem.*, 2010, **49**, 9746–9748, DOI: 10.1021/ic1017328.
- (122) I. P. Georgakaki, L. M. Thomson, E. J. Lyon, M. B. Hall and M. Y. Darensbourg, 'Fundamental properties of small molecule models of Fe-only hydrogenase: computations relative to the definition of an entatic state in the active site', *Coord. Chem. Rev.*, 2003, **238239**, 255–266, DOI: 10.1016/S0010-8545(02)00326-0.
- (123) C. Liu, L.-K. Tu, T.-H. Yen, G.-H. Lee and M.-H. Chiang, 'Influences on the rotated structure of diiron dithiolate complexes: electronic asymmetry vs. secondary coordination sphere interaction', *Dalton Trans.*, 2011, **40**, 2528–2541, DOI: 10.1039/C0DT01332C.
- (124) C. Liu, L.-K. Tu, T.-H. Yen and M.-H. Chiang, *Design of Biomimetic Models Related to the Active Sites of Fe-Only Hydrogenase, Biomimetic Based Applications*. Ed. P. M. Cavrak, 2011.

- (125) J. D. Lawrence, H. Li, T. B. Rauchfuss, M. Bnard and M.-M. Rohmer, 'Diiron Azadithiolates as Models for the Iron-Only Hydrogenase Active Site: Synthesis, Structure, and Stereoelectronics', *Angew. Chem. Int. Ed.*, 2001, **40**, 1768–1771, DOI: 10.1002/1521-3773(20010504)40:9<1768::AID-ANIE17680>3.0.CO;2-E.
- (126) X. Liu, S. K. Ibrahim, C. Tard and C. J. Pickett, 'Iron-only hydrogenase: Synthetic, structural and reactivity studies of model compounds', *Coord. Chem. Rev.*, 2005, **249**, 1641–1652, DOI: 10.1016/j.ccr.2005.04.009.
- (127) J. A. Wright, A. Jablonskyte and C. J. Pickett, *Unpublished*, 2013.
- (128) J. A. Wright, A. Jablonskyte and C. J. Pickett, *Unpublished*, 2013.
- (129) J. Capon, F. Gloaguen, F. Petillon, P. Schollhammer, J. Talarmin and S. Ezzaher, 'Evidence for the formation of terminal hydrides by protonation of an asymmetric iron hydrogenase active site mimic', *Inorg. Chem.*, 2007, **46**, 3426–3428, DOI: 10.1021/ic0703124.
- (130) B. E. Barton, G. Zampella, A. K. Justice, L. D. Gioia, T. B. Rauchfuss and S. R. Wilson, 'Isomerization of the hydride complexes $[\text{HFe}_2(\text{SR})_2(\text{PR}_3)_x(\text{CO})_{6-x}]^+$ ($x = 2, 3, 4$) relevant to the active site models for the $[\text{FeFe}]$ -hydrogenases', *Dalton Trans.*, 2010, **39**, 3011–3019, DOI: 10.1039/b910147k.
- (131) D. Chouffai et al., 'Electrochemical and Theoretical Studies of the Impact of the Chelating Ligand on the Reactivity of $[\text{Fe}_2(\text{CO})_4(2\text{-LL})(\mu\text{-pdt})]^+$ Complexes with Different Substrates (LL = IMe-CH₂-IMe, dppe; IMe = 1-Methylimidazol-2-ylidene)', *Organometallics*, 2012, **31**, 1082–1091, DOI: 10.1021/om201143p.
- (132) S. J. Borg, J. W. Tye, M. B. Hall and S. P. Best, 'Assignment of Molecular Structures to the Electrochemical Reduction Products of Diiron Compounds Related to $[\text{Fe-Fe}]$ Hydrogenase: A Combined Experimental and Density Functional Theory Study', *Inorg. Chem.*, 2007, **46**, 384–394, DOI: 10.1021/ic061211t.
- (133) A. L. De Lacey, C. Stadler, C. Cavazza, E. C. Hatchikian and V. M. Fernandez, 'FTIR Characterization of the Active Site of the Fe-hydrogenase from *Desulfovibrio desulfuricans*', *J. Am. Chem. Soc.*, 2000, **122**, 11232–11233, DOI: 10.1021/ja002441o.
- (134) M. Razavet, S. J. Borg, S. J. George, S. P. Best, S. A. Fairhurst and C. J. Pickett, 'Transient FTIR spectroelectrochemical and stopped-flow detection of a mixed valence Fe(I)-Fe(II) bridging carbonyl intermediate with structural elements and spectroscopic characteristics of the di-iron sub-site of all-iron hydrogenase', *Chem. Commun.*, 2002, 700–701, DOI: 10.1039/B111613B.
- (135) S. Tschierlei, S. Ott and R. Lomoth, 'Spectroscopically characterized intermediates of catalytic H₂ formation by $[\text{FeFe}]$ hydrogenase models', *Energy Environ. Sci.*, 2011, **4**, 2340–2352, DOI: 10.1039/C0EE00708K.

- (136) V. Barone, *Recent Advances in Density Functional Methods, Part I*, ed. D. P. Chong, World Scientific Publ. Co., 1996.
- (137) A. Jablonskyte et al., 'Paramagnetic Bridging Hydrides of Relevance to Catalytic Hydrogen Evolution at Metallosulfur Centers', *J. Am. Chem. Soc.*, 2011, **133**, 18606–18609, DOI: 10.1021/ja2087536.
- (138) F. Pratt, 'WIMDA: a muon data analysis program for the Windows PC', *Physica B*, 2000, **289290**, 710–714, DOI: 10.1016/S0921-4526(00)00328-8.
- (139) Y. K. Chen, D. G. Fleming and Y. A. Wang, 'Theoretical Calculations of Hyperfine Coupling Constants for Muoniated Butyl Radicals', *J. Phys. Chem. A*, 2011, **115**, 2765–2777, DOI: 10.1021/jp1096212.
- (140) M. Schmidt, S. M. Contakes and T. B. Rauchfuss, 'First Generation Analogues of the Binuclear Site in the Fe-Only Hydrogenases: $\text{Fe}_2(\mu\text{-SR})_2(\text{CO})_4(\text{CN})_2^{2-}$ ', *J. Am. Chem. Soc.*, 1999, **121**, 9736–9737, DOI: 10.1021/ja9924187.
- (141) U. Jayasooriya, S. Malone, A. Chumakov, R. Ruffer, A. Overweg and C. Nicklin, 'Atom-selective vibrational spectroscopy: Ferrocene probed via the iron atom', *ChemPhysChem*, 2001, **2**, 177–180.
- (142) W. Scheidt, S. Durbin and J. Sage, 'Nuclear resonance vibrational spectroscopy - NRVS', *J. Inorg. Biochem.*, 2005, **99**, 60–71, DOI: 10.1016/j.jinorgbio.2004.11.004.
- (143) Y. Guo et al., 'Characterization of the Fe Site in Iron-Sulfur Cluster-Free Hydrogenase (Hmd) and of a Model Compound via Nuclear Resonance Vibrational Spectroscopy (NRVS)', *Inorg. Chem.*, 2008, **47**, 3969–3977, DOI: 10.1021/ic701251j.
- (144) Z. J. Tonzetich et al., 'Identification of Protein-Bound Dinitrosyl Iron Complexes by Nuclear Resonance Vibrational Spectroscopy', *J. Am. Chem. Soc.*, 2010, **132**, 6914–6916, DOI: 10.1021/ja101002f.
- (145) W. R. Scheidt, A. Barabanschikov, J. W. Pavlik, N. J. Silvernail and J. T. Sage, 'Electronic Structure and Dynamics of Nitrosyl Porphyrins', *Inorg. Chem.*, 2010, **49**, 6240–6252, DOI: 10.1021/ic100261b.
- (146) V. Pelmeshnikov, Y. Guo, H. Wang, S. P. Cramer and D. A. Case, 'Fe-H/D stretching and bending modes in nuclear resonant vibrational, Raman and infrared spectroscopies: Comparisons of density functional theory and experiment', *Faraday Discuss.*, 2011, **148**, 409–420, DOI: 10.1039/c004367m.
- (147) B. M. Leu et al., 'Bulk Modulus of a Protein Active-Site Mimic', *J. Phys. Chem. B*, 2011, **115**, 4469–4473, DOI: 10.1021/jp112007z.
- (148) V. S. Oganessian, J. E. Barclay, S. M. Hardy, D. J. Evans, C. J. Pickett and U. A. Jayasooriya, 'Nuclear inelastic scattering spectroscopy of iron-sulfur cubane compounds', *Chem. Commun.*, 2004, 214–215.

- (149) Y. Xiao, M. Koutmos, D. A. Case, D. Coucouvanis, H. Wang and S. P. Cramer, 'Dynamics of an $[\text{Fe}_4\text{S}_4(\text{SPh})_4]^{2-}$ cluster explored via IR, Raman, and nuclear resonance vibrational spectroscopy (NRVS)-analysis using S-36 substitution, DFT calculations, and empirical force fields', *Dalton Trans.*, 2006, 2192–2201, DOI: 10.1039/b513331a.
- (150) J. Sage et al., 'Long-Range Reactive Dynamics in Myoglobin', *Phys. Rev. Lett.*, 2001, **86**, 4966–4969, DOI: 10.1103/PhysRevLett.86.4966.
- (151) U. A. Jayasooriya, 'Vibrational spectroscopic analysis of group 6 metal hexacarbonyls in the solid state', *J. Chem. Soc., Faraday Trans.*, 1994, **90**, 1265–1269, DOI: 10.1039/ft9949001265.
- (152) J. Iball and C. H. Morgan, 'A refinement of the crystal structure of ferric acetylacetonate', *Acta Cryst.*, 1967, **23**, 239–244, DOI: 10.1107/S0365110X67002531.
- (153) R. Krishnan, J. S. Binkley, R. Seeger and J. A. Pople, 'Self-consistent molecular orbital methods. XX. A basis set for correlated wave functions', *J. Chem. Phys.*, 1980, **72**, 650–654, DOI: 10.1063/1.438955.
- (154) V. A. Rassolov, J. A. Pople, M. A. Ratner and T. L. Windus, '6-31G* basis set for atoms K through Zn', *J. Chem. Phys.*, 1998, **109**, 1223–1229, DOI: 10.1063/1.476673.
- (155) I. Diaz-Acosta, J. Baker, W. Cordes and P. Pulay, 'Calculated and Experimental Geometries and Infrared Spectra of Metal Tris-Acetylacetonates: Vibrational Spectroscopy as a Probe of Molecular Structure for Ionic Complexes. Part I', *J. Phys. Chem. A.*, 2001, **105**, 238–244, DOI: 10.1021/jp0028599.
- (156) J. P. Dismukes, L. H. Jones and J. C. Bailar, 'The Measurement of Metal-Ligand Bond Vibrations in Acetylacetonate Complexes ¹', *J. Phys. Chem.*, 1961, **65**, 792–795, DOI: 10.1021/j100823a021.
- (157) N. N. Greenwood and T. C. Gibb, *Mossbauer Spectroscopy*, Chapman and Hall, Ltd., 1971.
- (158) U. A. Jayasooriya and S. F. A. Kettle, 'Lattice vibrations in relatively complicated crystal structures: Aragonite', *Phys. Rev. B*, 1984, **29**, 2227–2231, DOI: 10.1103/PhysRevB.29.2227.
- (159) M. A. Ismail, U. A. Jayasooriya and S. F. A. Kettle, 'Relative vibrational spectral intensities of the internal modes of phase II potassium nitrate', *J. Chem. Phys.*, 1983, **79**, 4459–4462, DOI: 10.1063/1.446331.
- (160) U. A. Jayasooriya, S. F. A. Kettle and S. Mahasuverachai, 'Manifestations of latent space group symmetry in the vibrational spectra of three alkali metal perchlorates', *J. Chem. Phys.*, 1987, **86**, 3127–3133, DOI: 10.1063/1.452023.

- (161) W. J. Albery, J. F. Burke, E. B. Leffler and J. Hadgraft, 'Interfacial transfer studied with a rotating diffusion cell', *J. Chem. Soc., Faraday Trans. 1*, 1976, **72**, 1618–1626, DOI: 10.1039/F19767201618.
- (162) R. H. Guy, 'Solute Transfer Across Liquid-liquid Interfaces', *Ann. N. Y. Acad. Sci.*, 1983, **404**, 194–197, DOI: 10.1111/j.1749-6632.1983.tb19457.x.
- (163) D. E. Leahy and A. R. Wait, 'Solute transport resistance at water-oil interfaces', *J. Pharm. Sci.*, 1986, **75**, 1157–1161, DOI: 10.1002/jps.2600751208.
- (164) J.-P. Simonin, P. Turq and C. Musikas, 'Rotating stabilised cell: a new tool for the investigation of interfacial extraction kinetics between liquid phases', *J. Chem. Soc., Faraday Trans.*, 1991, **87**, 2715–2721, DOI: 10.1039/FT9918702715.
- (165) B.-J. Molloy, K. Y. Tam, J. Matthew Wood and R. A. W. Dryfe, 'A hydrodynamic approach to the measurement of the permeability of small molecules across artificial membranes', *Analyst*, 2008, **133**, 655–659, DOI: 10.1039/B719634B.
- (166) M. Peric, M. Alves and B. L. Bales, 'Combining precision spin-probe partitioning with time-resolved fluorescence quenching to study micelles: Application to micelles of pure lysomyristoylphosphatidylcholine (LMPC) and LMPC mixed with sodium dodecyl sulfate', *Chem. Phys. Lipids*, 2006, **142**, 1–13, DOI: 10.1016/j.chemphyslip.2006.02.003.
- (167) H. Yoshioka, 'Exchange of the position of a spin probe in an aerosol OT reversed micelle', *J. Colloid. Interf. Sci.*, 1983, **95**, 81–86, DOI: 10.1016/0021-9797(83)90074-7.
- (168) H. Yoshioka, 'Temperature dependence of motion of a spin probe in aerosol of reversed micelles', *J. Colloid. Interf. Sci.*, 1981, **83**, 214–220, DOI: 10.1016/0021-9797(81)90026-6.
- (169) P. L. Tregenna-Piggott, E. Roduner and S. Santos, 'Calculation of the avoided level-crossing muon spin resonance response for various stochastic motions using Monte Carlo methods', *Chem. Phys.*, 1996, **203**, 317–337, DOI: 10.1016/0301-0104(95)00385-1.
- (170) M. I. J. Probert and A. J. Fisher, 'An *ab initio* study of muons in ethanal', *J. Phys-Condens. Mat.*, 1997, **9**, 3241–3257.
- (171) P. L. Hubbard, V. S. Oganessian, N. Sulaimanov, J. N. Butt and U. A. Jayasooriya, 'Avoided Level Crossing Muon Spectroscopy of Free Radicals Formed by Muonium Addition to the Constituents of DNA', *J. Phys. Chem. A*, 2004, **108**, 9302–9309, DOI: 10.1021/jp0475335.
- (172) R. Macrae and T. Briere, 'The muonium adduct to biacetyl – *ab initio* calculations and vibrational averaging', *Hyperfine Interact.*, 1997, **106**, 169–174, DOI: 10.1023/A:1012693925163.

Appendices

Appendix A

[Fe₂(μ-Xdt)(CO)₄(PMe₃)₂] systems

[Fe₂(μ-edt)(CO)₄(PMe₃)₂] systems

Table A1: Calculated gas phase and solvent corrected free energies and Fe Mulliken charges of [Fe₂(μ-edt)(CO)₄(PMe₃)₂] isomers and the transition states that connect them. Energies are reported relative to the 1A isomer.

Isomer	Free Energies / kcal/mol		Mulliken charges	
	ΔG_g	ΔG_{solv}	Fe ₁	Fe ₂
edt 1A	0.0	0.0	-0.618	-0.515
edt 1B	1.3	-0.4	-0.561	-0.561
edt 1C	4.5	4.0	-0.224	-0.415
edt 1D	1.0	1.3	-0.341	-0.341
TS _{edt 1A→1B}	11.6	9.9	-0.544	-0.855
TS _{edt 1A→1C}	10.6	9.5	-0.955	-0.587
TS _{edt 1A→1D}	6.3	6.5	-0.849	-0.619
TS _{edt 1C→1D}	22.8	22.7	-0.016	-1.144

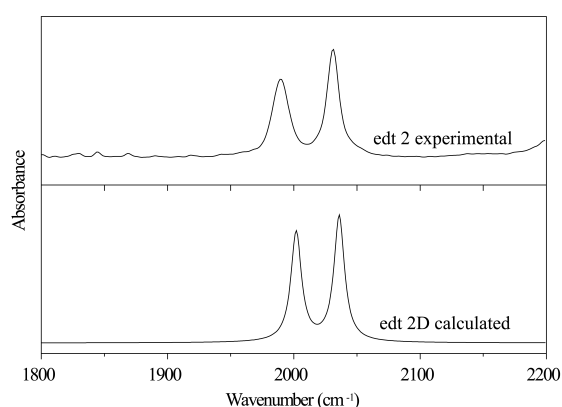


Figure A1: Comparison of the experimental IR spectra of [(H)Fe₂(μ-edt)(CO)₄(PMe₃)₂]⁺ with the simulated spectra of isomer 1D.

Table A2: Selected bond distances of the unprotonated [$\text{Fe}_2(\mu\text{-edt})(\text{CO})_4(\text{PMe}_3)_2$] from x-ray crystallography (in bold) [69], compared to calculated values of all isomers and transition states inter-converting them.

	bond length/Å										
	$\text{Fe}_1\text{-Fe}_2$	$\text{Fe}_1\text{-S}_1$	$\text{Fe}_1\text{-S}_2$	$\text{Fe}_2\text{-S}_1$	$\text{Fe}_2\text{-S}_2$	$\text{Fe}_1\text{-CO}_1$	$\text{Fe}_1\text{-CO}_2$	$\text{Fe}_2\text{-CO}_1$	$\text{Fe}_2\text{-CO}_2$	$\text{Fe}_1\text{-P}_1$	$\text{Fe}_2\text{-P}_2$
Exp.	2.515	2.254	2.256	2.248	2.250	1.763	1.753	1.770	1.761	2.208	2.221
edt IA	2.5194	2.2972	2.2907	2.2803	2.2823	1.7547	1.7473	1.7542	1.7603	2.2340	2.2535
edt IB	2.4830	2.3066	2.3023	2.3024	2.3066	1.7570	1.7538	1.7538	1.7570	2.2344	2.2344
edt IC	2.5958	2.2729	2.2699	2.2689	2.2712	1.7509	1.7631	1.7519	1.7637	2.2472	2.2344
edt ID	2.5765	2.2699	2.2766	2.2766	2.2699	1.7511	1.7546	1.7511	1.7546	2.2545	2.2545
$\text{TS}_{\text{edt IA}\rightarrow\text{IB}}$	2.5342	2.3032	2.3088	2.3141	2.3340	1.7604	1.7618	1.7435	1.7418	2.2357	2.2094
$\text{TS}_{\text{edt IA}\rightarrow\text{IC}}$	2.5756	2.2941	2.3197	2.2768	2.3052	1.7421	1.7403	1.7494	1.7686	2.2180	2.2604
$\text{TS}_{\text{edt IA}\rightarrow\text{ID}}$	2.5516	2.3207	2.2941	2.2942	2.2964	1.7408	1.7375	1.7505	1.7645	2.2107	2.2663
$\text{TS}_{\text{edt IC}\rightarrow\text{ID}}$	2.6980	2.3101	2.3190	2.2623	2.2613	1.7441	1.7429	1.7513	1.7613	2.2219	2.2708

Table A3: Selected bond angles of the unprotonated $[Fe_2(\mu\text{-edt})(CO)_4(PMe_3)_2]$ from x-ray crystallography (in bold)[69], compared to calculated values of all isomers and transition states interconverting them.

	bond angle/ °				
	$\angle S_1\text{-Fe}_1\text{-S}_2$	$\angle S_1\text{-Fe}_2\text{-S}_2$	$\angle Fe_1\text{-S}_1\text{-Fe}_2$	$\angle Fe_1\text{-S}_2\text{-Fe}_2$	$L_{ap}\text{-Fe}_1\text{-Fe}_2\text{-L}_{ap}$
Exp.	79.94	80.17	67.93	67.86	19.35
edt 1A	80.6773	81.2181	66.7879	66.8637	17.6335
edt 1B	80.9049	80.9047	65.1944	65.1946	13.3872
edt 1C	81.1275	81.1852	69.7151	69.7278	8.5888
edt 1D	81.3198	81.3193	69.0395	69.0392	36.6959
TS_{edt 1A→1B}	80.8256	80.0698	66.5761	66.1619	89.0904
TS_{edt 1A→1C}	80.5748	81.2497	68.5931	67.6835	82.0421
TS_{edt 1A→1D}	80.3243	80.8377	67.1289	67.5361	95.6957
TS_{edt 1C→1D}	79.6982	81.9456	72.3140	72.1665	75.5037

Table A4: Calculated gas phase and solvent corrected free energies, Fe–Fe bond lengths, and Fe Mulliken charges of the isomers of $[(\mu\text{-H})Fe_2(\mu\text{-edt})(CO)_4(PMe_3)_2]^+$. Energies are reported relative to the **2D** isomer.

Isomer	Free Energies / kcal/mol		Mulliken charges	
	ΔG_g	ΔG_{solv}	Fe ₁	Fe ₂
edt 2A	2.3	2.9	-1.206	-0.156
edt 2B	6.4	5.5	-0.592	-0.592
edt 2C	2.8	3.1	-0.521	-0.564
edt 2D	0.0	0.0	-0.303	-0.305
TS_{edt 2A→2B}	27.7	27.3	-1.053	-0.222
TS_{edt 2A→2C}	25.7	25.6	-0.348	-0.807
TS_{edt 2A→2D}	23.1	24.1	-0.390	-0.669
TS_{edt 2C→2D}	26.6	27.3	0.182	-1.040

Table A5: Selected bond distances of the bridged protonated $[(\mu\text{-H})\text{Fe}_2(\mu\text{-edt})(\text{CO})_4(\text{PMe}_3)_2]^+$ from x-ray crystallography (in bold) [69], compared to calculated values of all isomers and transition states inter-converting them.

Exp.	bond length/Å													
	Fe₁-Fe₂	Fe₁-S₁	Fe₁-S₂	Fe₂-S₁	Fe₂-S₂	Fe₁-H	Fe₂-H	Fe₁-CO₁	Fe₁-CO₂	Fe₂-CO₁	Fe₂-CO₂	Fe₁-P₁	Fe₂-P₂	
2.571	2.262	2.253	2.253	2.262	1.771	1.771	1.776	1.785	1.776	1.776	1.785	2.240	2.240	
2.5752	2.3043	2.3108	2.3050	2.3034	1.6607	1.6587	1.7764	1.7742	1.7652	1.7767	1.7767	2.2727	2.2865	
2.5663	2.3108	2.3210	2.3209	2.3109	1.6506	1.6506	1.7752	1.7790	1.7790	1.7752	1.7752	2.2761	2.2761	
2.6033	2.2903	2.2973	2.2883	2.2958	1.6870	1.6871	1.7630	1.7789	1.7633	1.7788	1.7788	2.2894	2.2893	
2.6001	2.2929	2.2920	2.2919	2.2927	1.6854	1.6857	1.7628	1.7740	1.7627	1.7741	1.7741	2.2905	2.2908	
2.6249	2.2970	2.3058	2.3792	2.3669	1.6366	1.6799	1.7760	1.7774	1.7550	1.7477	1.7477	2.2766	2.2558	
2.6375	2.3594	2.3663	2.2826	2.2989	1.7065	1.6459	1.7547	1.7457	1.7675	1.7781	1.7781	2.2501	2.2821	
2.6320	2.3549	2.3594	2.2890	2.2887	1.7008	1.6458	1.7528	1.7452	1.7671	1.7752	1.7752	2.2576	2.2858	
2.6648	2.3565	2.3659	2.2829	2.2893	1.7128	1.6714	1.7523	1.7488	1.7680	1.7749	1.7749	2.2467	2.2955	
TS _{edt 2A→2B}														
TS _{edt 2A→2C}														
TS _{edt 2A→2D}														
TS _{edt 2C→2D}														

Table A6: Selected bond angles of the bridged protonated $[(\mu\text{-H})\text{Fe}_2(\mu\text{-edt})(\text{CO})_4(\text{PMe}_3)_2]^+$ from x-ray crystallography (in bold)[69], compared to calculated values of all isomers and transition states inter-converting them.

	bond angle/°				
	$\angle \text{S}_1\text{-Fe}_1\text{-S}_2$	$\angle \text{S}_1\text{-Fe}_2\text{-S}_2$	$\angle \text{Fe}_1\text{-S}_1\text{-Fe}_2$	$\angle \text{Fe}_1\text{-S}_2\text{-Fe}_2$	$\angle \text{L-Fe}_1\text{-Fe}_2\text{-L}$
Exp.	80.46	80.46	69.42	69.42	14.01
edt 2A	80.3952	80.5369	67.9331	67.8498	10.3154
edt 2B	80.2368	80.2369	67.2945	67.2927	9.3929
edt 2C	80.9491	81.0227	69.3023	69.0530	2.3484
edt 2D	81.1545	81.1594	69.0962	69.0986	0.6711
TS_{edt 2A→2B}	80.8632	77.9488	68.2688	68.3383	74.4794
TS_{edt 2A→2C}	78.4265	81.4003	69.2227	68.8370	73.6277
TS_{edt 2A→2D}	78.4308	81.2488	69.0330	68.9591	75.5373
TS_{edt 2C→2D}	78.6528	81.7756	70.0934	69.8196	75.7533

Table A7: DFT simulated $\nu(\text{CO})$ bands of $[(\text{H})\text{Fe}_2(\mu\text{-edt})(\text{CO})_4(\text{PMe}_3)_2]^+$ isomers compared to those experimentally determined in CH_3CN [69].

Isomer	$\nu(\text{CO})$ (cm ⁻¹)			
Exp. edt	1989			2032
edt 2A	2000	2004	2036	2051
edt 2B	2006	2016	2040	2060
edt 2C	2002	2007	2038	2053
edt 2D	2001	2002	2035	2045 ⁿ

ⁿ peak of negligible intensity

Table A8: Calculated gas phase and solvent corrected free energies, Fe–Fe bond lengths, and Fe Mulliken charges of the isomers of terminal hydride isomers of $[(\mu\text{-H})\text{Fe}_2(\mu\text{-edt})(\text{CO})_4(\text{PMe}_3)_2]^+$. Energies are reported relative to the **2D** isomer.

Isomer	Free Energies / kcal/mol		Mulliken charges	
	ΔG_g	ΔG_{solv}	Fe ₁	Fe ₂
edt 3A1	19.2	18.4	-1.205	-0.524
edt 3A2	18.9	18.3	-1.143	-0.653
edt 3A3	16.6	16.2	-0.603	-1.375
edt 3A4	19.5	19.3	-0.565	-0.963
edt 3B	23.1	21.5	-1.156	-0.588
edt 3C1	16.5	15.8	-1.278	-0.573
edt 3C2	21.6	21.8	-0.238	-0.694
edt 3D1	12.8	13.5	-1.277	-0.550
edt 3D2	16.2	16.8	-0.567	-0.796

Table A9: Selected bond distances of the terminal hydride isomers of $[HFe_2(\mu-edt)(CO)_4(PMe_3)_2]^+$.

	bond length/Å												
	Fe ₁ -Fe ₂	Fe ₁ -S ₁	Fe ₁ -S ₂	Fe ₁ -S ₁	Fe ₂ -S ₁	Fe ₂ -S ₂	Fe-H	Fe ₁ -CO ₁	Fe ₁ -CO ₂	Fe ₂ -CO ₁	Fe ₂ -CO ₂	Fe-CO _{semi}	Fe ₁ -P ₁
edt 3A1	2.5279	2.3074	2.3112	2.3051	2.2931	1.5049	1.7717	1.7989	1.7579	1.7859	2.2775	2.2609	2.3198
edt 3A2	2.5401	2.3076	2.3107	2.2940	2.3021	1.5016	1.7679	1.7975	1.7549	1.7858	2.3117	2.2666	2.3041
edt 3A3	2.5551	2.2775	2.2968	2.3035	2.3134	1.5153	1.7816	1.7830	1.7706	1.8034	2.4697	2.2572	2.2681
edt 3A4	2.5521	2.2813	2.2921	2.3210	2.3176	1.5025	1.7830	1.7787	1.7774	1.7767	2.5190	2.2558	2.2773
edt 3B	2.5332	2.3218	2.3227	2.3109	2.3019	1.4991	1.7728	1.7911	1.7848	1.7805	2.3654	2.2696	2.2713
edt 3C1	2.5948	2.3017	2.3037	2.2720	2.2792	1.5029	1.7769	1.7787	1.7456	1.7882	2.4645	2.2781	2.3078
edt 3C2	2.5687	2.2837	2.3043	2.2727	2.2845	1.5134	1.7733	1.8015	1.7493	1.7881	2.5404	2.2683	2.3160
edt 3D1	2.5492	2.2976	2.2891	2.2867	2.2720	1.5131	1.7683	1.8011	1.7509	1.7848	2.4173	2.2733	2.3088
edt 3D2	2.5413	2.2998	2.3067	2.2903	2.2718	1.5050	1.7761	1.7759	1.7515	1.7825	2.4288	2.2770	2.3207

Table A10: Selected bond angles of the terminal hydride isomers of $[HFe_2(\mu-edt)(CO)_4(PMe_3)_2]^+$.

	bond angle/°							
	$\angle S_1-Fe_1-S_2$	$\angle S_1-Fe_2-S_2$	$\angle Fe_1-S_1-Fe_2$	$\angle Fe_1-S_2-Fe_2$	$\angle L-Fe_1-Fe_2-L$	$\angle Fe-Fe-C_{semi}$	$\angle Fe-C-O_{semi}$	
edt 3A1	81.0382	81.4736	66.4687	66.5998	31.6765	60.7820	156.3336	
edt 3A2	81.0834	81.5557	67.0071	66.8238	30.4374	61.6302	157.8927	
edt 3A3	81.4728	80.5661	67.8006	67.3160	5.3490	66.4551	164.1728	
edt 3A4	81.9874	80.5956	67.3506	67.2315	16.3589	68.4920	165.7093	
edt 3B	80.4092	81.0737	66.2955	66.4250	34.0441	63.6337	160.5081	
edt 3C1	81.1900	82.3643	69.1258	68.9672	19.8912	65.9654	162.6999	
edt 3C2	81.1782	81.8440	68.6315	68.0787	2.5079	68.0977	164.8391	
edt 3D1	81.1010	81.7071	67.5690	67.9588	0.5184	64.8753	162.1386	
edt 3D2	81.0047	81.9605	67.2361	67.4234	26.1305	65.7101	162.8768	

Table A11: Calculated gas phase and solvent corrected free energies, Fe–Fe bond lengths, and Fe Mulliken charges of the singly reduced isomers of $[(\mu\text{-H})\text{Fe}_2(\mu\text{-edt})(\text{CO})_4(\text{PMe}_3)_2]^+$. Energies are reported relative to the reduced **2D*** isomer.

Isomer	Free Energies / kcal/mol		Mulliken charges	
	ΔG_g	ΔG_{solv}	Fe ₁	Fe ₂
edt 2A*	1.4	2.0	-1.184	-0.141
edt 2B*	5.1	4.0	-0.825	-0.825
edt 2C*	3.4	3.5	-0.598	-0.595
edt 2D*	0.0	0.0	-0.558	-0.559
TS _{edt 2A*→2B*}	22.2	21.4	-0.073	-1.195
TS _{edt 2A*→2C*}	19.1	19.8	-0.533	-0.889
TS _{edt 2A*→2D*}	16.4	17.6	-0.510	-0.822
TS _{edt 2C*→2D*}	19.1	20.4	-1.148	-0.199

Table A12: Selected bond distances of the singly reduced bridging hydrides of $[(\mu-H)Fe_2(\mu-edt)(CO)_4(PMe_3)_2]^+$ and transition states convert them into each other.

	bond length/Å												
	Fe ₁ -Fe ₂	Fe ₁ -S ₁	Fe ₁ -S ₂	Fe ₂ -S ₁	Fe ₂ -S ₂	Fe ₁ -H	Fe ₂ -H	Fe ₁ -CO ₁	Fe ₁ -CO ₂	Fe ₂ -CO ₁	Fe ₂ -CO ₂	Fe ₁ -P ₁	Fe ₂ -P ₂
edt 2A*	2.7150	2.3341	2.3544	2.3451	2.3588	1.6944	1.6553	1.7606	1.7574	1.7917	1.7553	2.3476	2.2456
edt 2B*	2.6989	2.3501	2.3643	2.3643	2.3501	1.6579	1.6578	1.7585	1.7599	1.7599	1.7585	2.3341	2.3341
edt 2C*	2.7717	2.3140	2.3621	2.3160	2.3552	1.7172	1.7004	1.7954	1.7595	1.7970	1.7581	2.2454	2.2453
edt 2D*	2.7612	2.3501	2.3219	2.3219	2.3502	1.7052	1.7053	1.7955	1.7545	1.7955	1.7545	2.2477	2.2477
TS _{edt 2A*→2B*}	2.8293	2.3284	2.3519	2.4094	2.4093	1.5819	1.8350	1.7557	1.7572	1.7466	1.7804	2.3300	2.2399
TS _{edt 2A*→2C*}	3.2227	2.3709	2.3605	2.3349	2.3683	2.6654	1.5264	1.7550	1.7970	1.7885	1.7465	2.2504	2.2309
TS _{edt 2A*→2D*}	3.1821	2.3585	2.3761	2.3452	2.3565	2.5936	1.5250	1.7535	1.7983	1.7893	1.7476	2.2539	2.2289
TS _{edt 2C*→2D*}	3.3215	2.3695	2.3673	2.3457	2.3510	2.8077	1.5323	1.7564	1.7638	1.7865	1.7504	2.3065	2.2410

Table A13: Selected bond angles of the singly reduced bridging hydrides of $[(\mu\text{-H})\text{Fe}_2(\mu\text{-edt})(\text{CO})_4(\text{PMe}_3)_2]^+$ and transition states convert them into each other.

	bond angle/°				
	$\angle \text{S}_1\text{-Fe}_1\text{-S}_2$	$\angle \text{S}_1\text{-Fe}_2\text{-S}_2$	$\angle \text{Fe}_1\text{-S}_1\text{-Fe}_2$	$\angle \text{Fe}_1\text{-S}_2\text{-Fe}_2$	$\angle \text{L-Fe}_1\text{-Fe}_2\text{-L}$
edt 2A*	80.4287	80.1128	70.9351	70.3461	4.7240
edt 2B*	80.2642	80.2648	69.8463	69.8470	5.7153
edt 2C*	80.4573	80.5621	73.5449	71.9665	4.7956
edt 2D*	80.7459	80.7448	72.4549	72.4523	1.6955
TS_{edt 2A*→2B*}	80.5829	77.8237	73.3128	72.9048	81.7587
TS_{edt 2A*→2C*}	77.0087	77.5519	86.4415	85.9208	76.7926
TS_{edt 2A*→2D*}	77.2491	77.8912	85.1455	84.5027	76.7430
TS_{edt 2C*→2D*}	76.7670	77.5434	89.5643	89.4925	73.6451

Table A14: Calculated gas phase and solvent corrected free energies, Fe–Fe bond lengths, and Fe Mulliken charges of the singly reduced terminal hydride isomers of $[\text{HFe}_2(\mu\text{-edt})(\text{CO})_4(\text{PMe}_3)_2]^+$. Energies are reported relative to the singly reduced **2D** isomer.

Isomer	Free Energies / kcal/mol		Mulliken charges	
	ΔG_g	ΔG_{solv}	Fe ₁	Fe ₂
edt 3A1*	14.2	12.9	-0.539	-0.629
edt 3A2*	13.2	11.9	-1.404	-0.496
edt 3A3*	9.5	9.2	-1.455	-0.508
edt 3A4*	12.6	12.7	-1.082	-0.572
edt 3B*	16.8	14.7	-1.327	-0.592
edt 3C1*	10.5	10.4	-0.960	-0.544
edt 3C2*	14.0	14.3	-1.316	-0.605
edt 3D1*	7.9	8.5	-1.439	-0.444
edt 3D2*	11.5	12.2	-0.567	-0.796

Table A15: Selected bond distances of the singly reduced terminal hydride isomers of $[Fe_2(\mu-edt)(CO)_4(PMe_3)_2]^+$.

	bond length/Å													
	Fe₁-Fe₂	Fe₁-S₁	Fe₁-S₂	Fe₂-S₁	Fe₂-S₂	Fe-H	Fe₁-CO₁	Fe₁-CO₂	Fe₂-CO₁	Fe₂-CO₂	Fe-CO_{semi}	Fe₁-P₁	Fe₂-P₂	
edt 3A1*	2.6832	2.3235	2.3654	2.3435	2.3549	1.5133	1.7459	1.8273	1.7932	1.7652	2.2007	2.3054	2.2731	
edt 3A2*	2.6921	2.3584	2.3307	2.3318	2.3619	1.5087	1.7442	1.8246	1.7917	1.7607	2.2311	2.3029	2.2683	
edt 3A3*	2.8282	2.3142	2.3289	2.3444	2.3643	1.5336	1.7663	1.7634	1.7468	1.8077	2.6689	2.3336	2.2307	
edt 3A4*	2.7975	2.3780	2.3534	2.3312	2.3234	1.5027	1.7712	1.7877	1.7632	1.7648	2.6600	2.2300	2.3335	
edt 3B*	2.7209	2.3688	2.3586	2.3488	2.3418	1.5066	1.7487	1.8021	1.7646	1.7686	2.3767	2.2868	2.3448	
edt 3C1*	2.9561	2.3595	2.3276	2.3412	2.2924	1.5311	1.7484	1.8005	1.7926	1.7698	2.8398	2.2309	2.2519	
edt 3C2*	2.9469	2.3018	2.3442	2.3349	2.3636	1.5056	1.7940	1.7651	1.7702	1.7856	2.8419	2.2533	2.2310	
edt 3D1*	2.8702	2.3489	2.3373	2.3105	2.3159	1.5331	1.7481	1.8033	1.7972	1.7642	2.7091	2.2298	2.2665	
edt 3D2*	2.8306	2.3496	2.3516	2.3161	2.3268	1.5075	1.7760	1.7841	1.7953	1.7654	2.6598	2.2297	2.2628	

Table A16: Selected bond angles of the singly reduced terminal hydride isomers of $[Fe_2(\mu-edt)(CO)_4(PMe_3)_2]^+$.

	bond angle/°									
	$\angle S_1-Fe_1-S_2$	$\angle S_1-Fe_2-S_2$	$\angle Fe_1-S_1-Fe_2$	$\angle Fe_1-S_2-Fe_2$	$\angle L-Fe_1-Fe_2-L$	$\angle Fe-Fe-C_{semi}$	$\angle Fe-C-O_{semi}$			
edt 3A1*	81.2572	81.0642	70.1869	69.2833	23.9642	54.4915	149.8911			
edt 3A2*	81.2595	81.1638	70.0544	70.0125	25.6950	55.2580	151.1341			
edt 3A3*	80.7618	79.4086	74.7541	74.1095	5.9473	66.0951	166.0272			
edt 3A4*	79.6691	81.2561	72.8794	73.4725	13.4252	66.7631	165.2562			
edt 3B*	80.1942	80.9526	70.4459	70.7413	29.6271	59.3313	157.4350			
edt 3C1*	78.9283	80.0184	77.9324	79.5557	5.9951	68.4156	168.1904			
edt 3C2*	80.3488	79.2756	78.9185	77.5049	14.0251	68.8567	166.8862			
edt 3D1*	79.3579	80.5919	76.0445	76.1670	2.0495	66.3597	166.3276			
edt 3D2*	79.8243	81.0331	74.6951	74.4600	23.7808	65.9214	164.4611			

[Fe₂(μ-edt)(CO)₄(PMe₃)₂] Cartesian Coordinates**edt 1A**

Fe	0.98358000	-0.40171700	0.11033900
Fe	-1.31646000	0.61002000	0.29410000
S	0.55080100	1.60101300	1.14901500
S	-0.06165100	0.69055900	-1.61056400
P	3.19261100	-0.20440500	-0.15777400
P	-2.67854200	-0.98247500	-0.53481900
O	1.03801700	-1.79951100	2.68259900
O	-2.20954800	-0.12464000	2.98932800
O	0.74998600	-2.91374900	-1.36936900
O	-3.08383000	2.90816500	-0.12266100
C	1.01982800	-1.22368700	1.66017000
C	-1.83421300	0.15773400	1.91462000
C	0.83979700	-1.90232700	-0.77304200
C	-2.38882300	1.97400000	0.03570700
C	1.00868900	2.86763300	-0.15132200
C	0.54815600	2.45941700	-1.55283200
C	4.12801500	-1.82133600	-0.14379300
C	-4.49301800	-0.58227300	-0.34162700
C	3.86112400	0.57536100	-1.72348800
C	-2.58164100	-1.39172300	-2.35251300
C	4.10920900	0.74483000	1.16611100
C	-2.59823800	-2.67311300	0.25327500
H	-1.60907300	-3.10884300	0.08501800
H	3.78640500	-2.44943500	-0.97418700
H	-4.72571400	0.33208900	-0.89852900
H	3.92429300	-2.34764500	0.79567100
H	-4.71557000	-0.41053200	0.71777000
H	3.54644100	1.62345800	-1.77854900
H	-3.35573100	-2.12639100	-2.60928300
H	3.45117600	0.04436600	-2.58987800
H	-1.59560600	-1.80315700	-2.59106900
H	4.95792700	0.52812200	-1.75018600
H	-2.72952400	-0.47795300	-2.93791900
H	5.20810300	-1.64961000	-0.23758800
H	-5.11637300	-1.40523700	-0.71441200
H	5.19037100	0.74315200	0.97518400
H	-3.36575000	-3.33074500	-0.17554900
H	3.90865600	0.27994600	2.13783800
H	-2.76240900	-2.57823400	1.33225200
H	3.74544900	1.77735400	1.20248300
H	0.54746200	3.81044400	0.16665900
H	2.09815800	2.98611200	-0.10089900
H	-0.29581400	3.07054400	-1.89177200
H	1.35424500	2.54517900	-2.29153600

edt 1B

Fe	1.24011400	-0.41423300	0.04189000
Fe	-1.24011400	-0.41423600	-0.04188900
S	-0.05480100	0.82545800	1.49463200
S	0.05479900	0.82546000	-1.49463000
P	3.25029800	0.55960300	-0.00245700
P	-3.25029700	0.55960200	0.00245600
O	1.82122900	-2.30592600	2.20121700
O	-1.82122400	-2.30593100	-2.20121500
O	1.85485600	-2.41263700	-2.00581600
O	-1.85485500	-2.41264200	2.00581500
C	1.58491900	-1.54519100	1.34102000
C	-1.58491500	-1.54519500	-1.34101900
C	1.60570100	-1.60892700	-1.18893900
C	-1.60570000	-1.60893100	1.18893800
C	-0.13789100	2.54163600	0.75262400
C	0.13787500	2.54163700	-0.75262200
C	3.80990000	1.24341600	-1.65062000
C	-4.67453700	-0.57754200	-0.40678600
C	3.60237300	1.99737000	1.14461600
C	-3.80991200	1.24337800	1.65062900
C	4.67454200	-0.57755200	0.40674300
C	-3.60235900	1.99739700	-1.14458800
H	-2.95773300	2.84442000	-0.88444200
H	3.10475300	2.00746900	-1.99590200
H	-4.66623400	-1.42633700	0.28639800
H	3.81685700	0.43155400	-2.38663100
H	-4.55401500	-0.96206300	-1.42573300
H	4.65215700	2.31043800	1.06877900
H	-4.81509500	1.67901600	1.57724100
H	3.38240100	1.69715600	2.17512000
H	-3.10475300	2.00740300	1.99594700
H	2.95769500	2.84437600	0.88454100
H	-3.81690300	0.43149400	2.38661500
H	4.81509400	1.67902800	-1.57723700
H	-5.63460200	-0.05131300	-0.32643300
H	5.63460400	-0.05131300	0.32642600
H	-4.65216000	2.31041800	-1.06880200
H	4.66625200	-1.42631100	-0.28648500
H	-3.38231200	1.69723000	-2.17509000
H	4.55401200	-0.96212700	1.42566800
H	-1.14336600	2.91926700	0.97502900
H	0.58155300	3.16323900	1.30014200
H	-0.58157500	3.16323300	-1.30013900
H	1.14334700	2.91927800	-0.97502700

edt 1C

Fe	-1.258728	-0.464874	0.277869
Fe	1.336304	-0.458801	0.213351
S	0.060700	-2.234348	0.820271
S	-0.008352	-0.562185	-1.614114
P	-2.362897	1.390606	-0.345033
P	2.197584	1.546749	-0.351388
O	-3.624629	-2.132836	-0.151801
O	2.046145	0.057910	3.015075
O	-1.555061	0.364202	3.079571
O	3.671123	-2.030693	-0.586564
C	-2.687123	-1.438466	-0.000162
C	1.739103	-0.143260	1.901210
C	-1.410813	0.022121	1.965518
C	2.745735	-1.374855	-0.280056
C	0.028039	-3.260016	-0.745441
C	-0.010633	-2.395639	-2.010725
C	-4.068110	1.499849	0.412159
C	4.057067	1.537434	-0.546947
C	-1.734174	3.106319	0.059506
C	1.702038	2.331184	-1.975259
C	-2.753180	1.543071	-2.163819
C	2.020316	2.956697	0.865678
H	0.966984	3.139993	1.093679
H	-3.978989	1.516946	1.504280
H	4.337287	0.856153	-1.357755
H	-4.655859	0.621483	0.125069
H	4.515997	1.179012	0.381461
H	-2.478038	3.862319	-0.223904
H	2.210607	3.295726	-2.100204
H	-0.802924	3.302900	-0.479384
H	0.618251	2.477972	-2.019030
H	-1.542452	3.173793	1.136395
H	1.983895	1.657687	-2.791941
H	-4.582991	2.408744	0.075233
H	4.429876	2.545331	-0.770659
H	-3.354962	2.439829	-2.359644
H	2.477510	3.871727	0.467482
H	-3.308246	0.652510	-2.479236
H	2.526610	2.677771	1.796761
H	-1.821816	1.584974	-2.738966
H	-0.918837	-2.575653	-2.597097
H	0.862869	-2.571436	-2.648849
H	0.925272	-3.888831	-0.711667
H	-0.855121	-3.904493	-0.666157

edt 1D

Fe	-1.15352600	0.17728000	0.57358300
Fe	1.15340600	0.17710100	-0.57365200
S	-0.66489500	1.32321500	-1.32393700
S	0.66464000	1.32398600	1.32328500
P	-2.78606200	-0.88992300	-0.55727500
P	2.78606700	-0.88924200	0.55781600
O	-0.82055100	-2.14146600	2.33303100
O	-3.05513300	1.72585900	2.16949400
O	0.82064900	-2.14286800	-2.33148100
O	3.05609700	1.72253400	-2.17134500
C	-0.91331800	-1.20593700	1.62602900
C	-2.31774600	1.10501400	1.49567600
C	0.91333300	-1.20680600	-1.62516400
C	2.31778200	1.10392500	-1.49648200
C	-0.35153700	3.05749900	-0.68218400
C	0.35116700	3.05788400	0.68055100
C	-3.76392000	-2.13216100	0.43327000
C	-4.12546400	0.26922600	-1.14739000
C	-2.42417300	-1.84439200	-2.11754900
C	2.42430300	-1.84311200	2.11848300
C	4.12519000	0.27044600	1.14751200
C	3.76420900	-2.13170700	-0.43215900
H	4.14096800	-1.65310800	-1.34305800
H	-1.33602500	3.53648900	-0.62767300
H	0.24638100	3.56557300	-1.44740700
H	1.33562500	3.53690200	0.62576800
H	-0.24679500	3.56636500	1.44546900
H	-4.60839200	-2.51490400	-0.15368800
H	-3.11475000	-2.96577500	0.72193300
H	-4.14074200	-1.65324500	1.34397700
H	-4.55855800	0.79613600	-0.29016600
H	-3.67818000	1.00577500	-1.82429700
H	-4.91449200	-0.28235700	-1.67466500
H	-3.35855600	-2.24172900	-2.53482200
H	-1.95272100	-1.17979500	-2.84939500
H	-1.73734500	-2.66815800	-1.90242500
H	3.35875700	-2.24008800	2.53593900
H	1.95271200	-1.17829500	2.85004000
H	1.73763700	-2.66709900	1.90368900
H	4.55820100	0.79709400	0.29008400
H	3.67771400	1.00717600	1.82409900
H	4.91431600	-0.28074600	1.67505000
H	4.60873400	-2.51405300	0.15498200
H	3.11519800	-2.96556100	-0.72049200

TS_{edt 1A→1B}

Fe	1.13998900	-0.44109800	-0.05394900
Fe	-1.30981200	-0.06332400	0.47328900
S	0.41851800	0.84939700	1.71211200
S	-0.16271900	1.07274000	-1.21224500
P	3.23211000	0.32410500	-0.24266700
P	-3.18329500	0.21947500	-0.66318500
O	1.93436400	-2.59620600	1.76660700
O	-1.32930500	-2.93328500	-0.02692700
O	1.27394600	-2.11446400	-2.45899700
O	-2.79546300	-0.24785600	2.98077400
C	1.60988400	-1.73852300	1.03916800
C	-1.22284900	-1.76798700	0.12649600
C	1.21175500	-1.45629700	-1.49201800
C	-2.20579100	-0.17008900	1.96508100
C	0.63559900	2.58716400	1.04612900
C	0.13103400	2.73182000	-0.39112200
C	4.43364000	-0.91958100	-0.94800800
C	-4.65949500	-0.73118300	-0.03146300
C	3.59230800	1.81315300	-1.31698400
C	-3.87832400	1.95085400	-0.80245200
C	4.09190600	0.77570200	1.35341500
C	-3.13834000	-0.31968900	-2.44969100
H	-2.37227800	0.25227800	-2.98364500
H	4.13288200	-1.18338300	-1.96794700
H	-4.90924300	-0.39848400	0.98174500
H	4.41564100	-1.82758600	-0.33475000
H	-4.41070500	-1.79787000	0.00370500
H	3.12037500	2.70434700	-0.88943700
H	-4.81689100	1.95160800	-1.37297900
H	3.18042300	1.64569800	-2.31830000
H	-3.14772300	2.59069300	-1.31028800
H	4.67494000	1.98154900	-1.38890200
H	-4.06020800	2.34966800	0.20180300
H	5.45254400	-0.51167400	-0.96273400
H	-5.52513700	-0.58048800	-0.68891900
H	5.11477800	1.12489700	1.16105700
H	-4.11609900	-0.16219400	-2.92320000
H	4.12496600	-0.10823300	2.00010300
H	-2.87739700	-1.38280500	-2.49278300
H	3.52873900	1.55617700	1.87571300
H	0.09521200	3.24848700	1.73440200
H	1.70536500	2.82025800	1.12097800
H	-0.83456500	3.24857000	-0.42214200
H	0.83847100	3.28801000	-1.01934400

TS_{edt 1A→1C}

Fe	1.28312600	0.16258900	0.42644200
Fe	-1.29073900	0.24540600	0.47319300
S	0.05034900	1.90942000	1.25817800
S	-0.03774200	0.61168900	-1.42676900
P	2.80725500	-0.81574000	-0.85391200
P	-2.17327900	-1.65235800	-0.38068700
O	3.45994300	1.11076300	2.12641100
O	-2.12736000	-0.42297500	3.20804900
O	0.68134500	-2.29036900	1.88173500
O	-3.60817700	1.91957700	-0.13520300
C	2.59608000	0.73685300	1.41706400
C	-1.77138100	-0.17968200	2.12124600
C	0.80639000	-1.27424300	1.28475800
C	-2.68289100	1.23393600	0.09215400
C	0.09754200	3.13613700	-0.15867700
C	-0.14697300	2.48123200	-1.52161500
C	4.05562000	-1.85949900	0.05936100
C	-3.47022200	-1.35604700	-1.69026300
C	2.32039500	-1.96505100	-2.24582300
C	-1.06102300	-2.86440400	-1.25564400
C	3.89946200	0.38867300	-1.77546000
C	-3.06606600	-2.76771600	0.81690200
H	-2.35937100	-3.11441200	1.57888800
H	3.53432800	-2.67810900	0.56791500
H	-3.01876800	-0.78261600	-2.50796900
H	4.55997000	-1.24750300	0.81482800
H	-4.29514800	-0.77172100	-1.26828600
H	1.61764900	-1.45051400	-2.91006300
H	-1.65418000	-3.69769700	-1.65459300
H	1.84035600	-2.85990900	-1.83741900
H	-0.31466100	-3.24731800	-0.55313900
H	3.21132600	-2.26139300	-2.81443800
H	-0.55666400	-2.34980200	-2.07923200
H	4.80087700	-2.27215600	-0.63248200
H	-3.85834900	-2.30671000	-2.07830400
H	4.66852600	-0.13950800	-2.35501700
H	-3.49014600	-3.63141600	0.28958000
H	4.37849400	1.06456800	-1.05886600
H	-3.87103900	-2.21339200	1.31192200
H	3.27399200	0.98178100	-2.45215200
H	-0.66344700	3.89493800	0.06384700
H	1.08631800	3.60487000	-0.10538200
H	-1.14669000	2.71215800	-1.90558600
H	0.59624900	2.80159100	-2.26204100

TS_{edt 1A→1D}

Fe	1.08493500	-0.22032700	-0.41397900
Fe	-1.21732700	0.50089800	0.41660400
S	0.68071800	1.74523300	0.75175100
S	-0.52376400	0.70422900	-1.76311400
P	3.12691400	-0.23592800	0.43291500
P	-2.64825200	-1.13194400	-0.23341100
O	0.26575400	-2.51694200	1.17364400
O	-1.44998600	-0.13466100	3.27172000
O	1.96225400	-1.79902000	-2.70784600
O	-3.16723400	2.67891900	0.47404000
C	0.49380500	-1.50646200	0.59363100
C	-1.34105100	0.09112400	2.12838400
C	1.62486800	-1.15282400	-1.78118400
C	-2.39555900	1.79536000	0.43589100
C	0.53277200	3.05755700	-0.57555300
C	-0.12289200	2.53128100	-1.85640800
C	4.10157600	-1.80677600	0.18422600
C	-3.33242100	-2.23188800	1.10628800
C	4.30311100	1.06345400	-0.21414300
C	-4.19659300	-0.49348000	-1.05494100
C	3.26288600	-0.00681600	2.28040400
C	-2.04754400	-2.37590800	-1.48749000
H	-1.69101500	-1.85456800	-2.38260500
H	4.23618300	-1.99441800	-0.88637100
H	-3.85404500	-1.62284200	1.85306300
H	3.54445700	-2.64466000	0.61830400
H	-2.50403400	-2.75680200	1.59396300
H	3.89291100	2.05406000	0.01200000
H	-4.84127500	-1.32561100	-1.36541600
H	4.38799800	0.95841000	-1.30144300
H	-3.91345800	0.09826700	-1.93274900
H	5.29611500	0.96551200	0.24472200
H	-4.74443300	0.15172700	-0.35938600
H	5.08346700	-1.73229400	0.66862400
H	-4.03124800	-2.96285000	0.68008500
H	4.31412800	-0.03058700	2.59610900
H	-2.87124700	-3.04841100	-1.76082700
H	2.71326400	-0.81242700	2.78010300
H	-1.22393700	-2.95774200	-1.06347500
H	2.81440400	0.95157600	2.56321800
H	-0.04958700	3.87503800	-0.13392300
H	1.55159100	3.41650300	-0.76373500
H	-1.07402600	3.03824100	-2.05842800
H	0.53074000	2.65160600	-2.72793700

TS_{edt 1C→1D}

Fe	1.44897000	-0.48108500	0.19635300
Fe	-1.17425600	-0.39143200	-0.42807100
S	0.31287800	-1.89209200	-1.23714200
S	-0.33154700	-1.09906700	1.54744900
P	1.85613100	1.65318900	-0.26818400
P	-2.35063500	1.25483700	0.60261300
O	2.94931200	-0.39772100	2.70013700
O	-1.40664500	0.91453700	-3.04505500
O	3.76047700	-1.38885500	-1.33944900
O	-3.46523300	-2.17320000	-0.78658200
C	2.34707000	-0.42130300	1.68885800
C	-1.27751200	0.41705500	-1.98947100
C	2.83288100	-1.00385700	-0.72742900
C	-2.56410700	-1.44009800	-0.61694900
C	0.01901400	-3.37009300	-0.12095000
C	-0.30573200	-2.96157100	1.31975100
C	3.69993800	1.99247000	-0.22145900
C	-4.17288500	0.86864200	0.77136300
C	1.45103400	2.42647700	-1.92248500
C	-1.96149500	1.69736800	2.37776600
C	1.30344400	2.99338400	0.91699100
C	-2.46617900	2.92652900	-0.23290200
H	-1.47444800	3.37211100	-0.35865500
H	4.20562300	1.40358600	-0.99435500
H	-4.29564300	-0.04625800	1.36151400
H	4.10456200	1.70522800	0.75556500
H	-4.60905700	0.70269200	-0.21991200
H	1.93887000	3.40657900	-2.01014700
H	-2.60159100	2.52705600	2.70402400
H	0.37002500	2.54082800	-2.03750700
H	-0.91011400	1.97441300	2.49302800
H	1.81125700	1.76950100	-2.72191400
H	-2.15050100	0.81928500	3.00435100
H	3.89705500	3.05856600	-0.39492900
H	-4.69759000	1.69578700	1.26672500
H	1.72459800	3.96341700	0.62070300
H	-3.09684400	3.60579600	0.35473400
H	1.65315500	2.74112300	1.92482800
H	-2.90996000	2.79252300	-1.22601700
H	0.21329200	3.06394600	0.93173600
H	0.43697900	-3.34190000	2.02965800
H	-1.29885500	-3.31355400	1.62442900
H	-0.80518000	-3.93173300	-0.57696100
H	0.93189900	-3.97349500	-0.17847100

edt 2A

Fe	1.03939100	-0.46803000	0.18388900
Fe	-1.34662900	0.49498300	0.32881300
S	0.52588500	1.56182400	1.14522600
S	-0.06517800	0.52897600	-1.58462700
P	3.23623200	-0.08580100	-0.25829600
P	-2.88550300	-0.96766100	-0.52076800
O	1.71477900	-1.62620900	2.79779600
O	-2.43733000	0.10004600	3.02835500
O	1.02854700	-3.03008600	-1.25315700
O	-2.96091500	2.85800800	-0.29743800
C	1.47028300	-1.16420600	1.76054400
C	-2.01095900	0.26172700	1.96001100
C	1.05718400	-2.01599500	-0.68341000
C	-2.32872600	1.91360500	-0.04582500
C	0.92036100	2.79060100	-0.20326500
C	0.46344800	2.31831600	-1.58677200
C	4.25039400	-1.64564900	-0.26186300
C	-4.65098800	-0.44749500	-0.25746800
C	3.69484600	0.69049500	-1.88653900
C	-2.80950800	-1.30191300	-2.34729200
C	4.11740400	0.95842100	1.00422800
C	-2.83080300	-2.66572300	0.23517000
H	-1.86416800	-3.13445400	0.02402300
H	3.91361400	-2.31133700	-1.06378700
H	-4.84223300	0.49994300	-0.77271000
H	4.14312200	-2.16363600	0.69754400
H	-4.84574200	-0.31497500	0.81252100
H	3.36916300	1.73493700	-1.91752400
H	-3.62098100	-1.98542600	-2.62555200
H	3.22283300	0.14104400	-2.70785400
H	-1.84785700	-1.75587400	-2.60842400
H	4.78460500	0.65840900	-2.00691000
H	-2.91632000	-0.36294100	-2.90052100
H	5.30735200	-1.39984500	-0.42037000
H	-5.32777400	-1.21451100	-0.65266500
H	5.17565700	1.05526000	0.73302700
H	-3.63257100	-3.28581400	-0.18365300
H	4.03933000	0.48138600	1.98711700
H	-2.96206300	-2.59366700	1.32031000
H	3.66655300	1.95374400	1.06649800
H	0.43036200	3.72646200	0.09002800
H	2.00339200	2.95414100	-0.16794600
H	-0.40994600	2.87811000	-1.93803200
H	1.25147800	2.41975500	-2.34068700
H	-0.50012100	-0.89954300	0.63212200

edt 2B

Fe	1.28261000	-0.50855400	-0.03785200
Fe	-1.28260800	-0.50848300	0.03804300
S	0.05325800	0.71218700	1.49139100
S	-0.05318600	0.71198500	-1.49128500
P	3.24611800	0.64214100	-0.00164800
P	-3.24615300	0.64211800	0.00129400
O	2.27406000	-2.31228400	2.05670700
O	-2.27321700	-2.31283400	-2.05637200
O	2.13437700	-2.21440100	-2.27520800
O	-2.13524800	-2.21349900	2.27569900
C	1.89779600	-1.59042700	1.22807200
C	-1.89734300	-1.59072200	-1.22778400
C	1.81985600	-1.53299700	-1.38937400
C	-1.82033700	-1.53244800	1.38973100
C	0.14017400	2.42289200	0.75196400
C	-0.14006000	2.42277800	-0.75200300
C	4.71509800	-0.41118600	-0.44154400
C	-4.71526400	-0.41149800	0.44007700
C	3.44437600	2.09321200	-1.15131900
C	-3.44482600	2.09259100	1.15163700
C	3.73142300	1.30978100	1.66655300
C	-3.73093800	1.31050700	-1.66676200
H	-2.95998300	1.98136300	-2.05817100
H	4.63314900	-0.75782800	-1.47719800
H	-4.63362200	-0.75887400	1.47550800
H	4.76306800	-1.28209000	0.22117200
H	-4.76306800	-1.28192800	-0.22327300
H	4.48369600	2.44253500	-1.12175900
H	-4.48408900	2.44206000	1.12181700
H	2.78890000	2.91552700	-0.84768200
H	-2.78910100	2.91498400	0.84873700
H	3.19254500	1.79080800	-2.17332800
H	-3.19345700	1.78960700	2.17358800
H	5.63549800	0.17459100	-0.33075100
H	-5.63561900	0.17437600	0.32943800
H	4.68110400	1.85296100	1.59039800
H	-4.68104200	1.85297000	-1.59076800
H	3.84995700	0.47511500	2.36616300
H	-3.84849600	0.47621100	-2.36697700
H	2.96017300	1.97980800	2.05880900
H	-0.57079300	3.04585100	1.30626900
H	1.14559300	2.79736600	0.97482100
H	-1.14548800	2.79722100	-0.97484900
H	0.57089300	3.04567500	-1.30639400
H	-0.00002100	-1.54671300	0.00094400

edt 2C

Fe	-1.27966800	-0.41503000	0.29167500
Fe	1.32327300	-0.41952200	0.25001900
S	0.02918000	-2.21862800	0.82007500
S	-0.00725500	-0.51022900	-1.61866600
P	-2.40303700	1.49136200	-0.29583800
P	2.34207400	1.55804100	-0.29054800
O	-3.51699400	-2.05935400	-0.63386000
O	2.36833600	-0.22328400	2.99095600
O	-2.16188500	-0.11849900	3.08034300
O	3.51567900	-2.03678300	-0.81861300
C	-2.63824100	-1.39289800	-0.26169500
C	1.96372400	-0.29918100	1.90517500
C	-1.82898500	-0.24194300	1.97480100
C	2.65793100	-1.37957400	-0.38737400
C	0.00200900	-3.21292300	-0.76096200
C	-0.01604400	-2.33430100	-2.02057600
C	-4.15140600	1.53149900	0.33969200
C	4.18578400	1.44082400	-0.50973600
C	-1.73909700	3.11928900	0.31392800
C	1.81102500	2.38932300	-1.86912200
C	-2.62559100	1.75781000	-2.12303800
C	2.19082400	2.88700300	1.00439200
H	1.14089000	3.05086300	1.26379600
H	-4.15100900	1.51082800	1.43493500
H	4.42321500	0.78709000	-1.35575000
H	-4.70797900	0.66369600	-0.02993200
H	4.64325200	1.02787500	0.39611400
H	-2.41677500	3.93016800	0.02053100
H	2.35660500	3.33297500	-1.99038100
H	-0.75029400	3.30843000	-0.11411600
H	0.73514900	2.58986900	-1.85530000
H	-1.65827300	3.09722300	1.40637100
H	2.02867800	1.73056700	-2.71643000
H	-4.64903800	2.44749100	-0.00067400
H	4.60093800	2.43824200	-0.69830900
H	-3.20457200	2.67225500	-2.30010800
H	2.63134100	3.82291300	0.64051000
H	-3.16111200	0.90241100	-2.54957200
H	2.72501400	2.57087100	1.90730300
H	-1.65220400	1.83612800	-2.61794600
H	-0.91397900	-2.50635800	-2.62394200
H	0.86184100	-2.50960400	-2.65185100
H	0.88958900	-3.85437700	-0.72547900
H	-0.88532200	-3.85262500	-0.69814100
H	0.03126100	0.53585600	0.76402900

edt 2D

Fe	1.17511000	0.16926200	-0.55652000
Fe	-1.17541800	0.17130600	0.55494400
S	0.63685200	1.33035300	1.34580100
S	-0.63663000	1.32657500	-1.35098800
P	2.69992500	-1.06853400	0.62270500
P	-2.70047000	-1.06958600	-0.62018900
O	1.36647400	-1.57820500	-2.90912300
O	3.20595600	2.04581400	-1.51398900
O	-1.36684300	-1.56776400	2.91366600
O	-3.20223500	2.04947400	1.51795000
C	1.28293300	-0.88949100	-1.97595700
C	2.40899100	1.28830200	-1.13310100
C	-1.28341600	-0.88241700	1.97800100
C	-2.40819100	1.29238400	1.13022700
C	0.33603400	3.05354300	0.68573700
C	-0.33540900	3.05160200	-0.69582900
C	3.62927200	-2.34344400	-0.36091300
C	4.05816600	-0.06241100	1.39612500
C	2.02940800	-2.04445100	2.05453200
C	-2.03076700	-2.04875400	-2.05018400
C	-4.05964000	-0.06575800	-1.39500400
C	-3.62873500	-2.34261200	0.36691400
H	-4.14562300	-1.86095700	1.20411800
H	-0.00039900	-0.90252100	0.00107800
H	1.31590900	3.54285800	0.65993600
H	-0.28105200	3.55770700	1.43749300
H	-1.31517500	3.54120900	-0.67146400
H	0.28182500	3.55342600	-1.44903200
H	4.36708300	-2.83858100	0.28143700
H	2.93538800	-3.09317100	-0.75579400
H	4.14694100	-1.86330200	-1.19850900
H	4.63595100	0.44609500	0.61669100
H	3.62293700	0.68702600	2.06557800
H	4.72644500	-0.71698900	1.96878500
H	2.84393100	-2.61199400	2.52073600
H	1.59426700	-1.36854900	2.79785300
H	1.25900100	-2.73913900	1.70487400
H	-2.84565200	-2.61702900	-2.51485800
H	-1.59564800	-1.37458400	-2.79509200
H	-1.26046200	-2.74294100	-1.69930100
H	-4.63679100	0.44459700	-0.61629400
H	-3.62526800	0.68207100	-2.06681400
H	-4.72831700	-0.72200400	-1.96529400
H	-4.36705200	-2.83911600	-0.27378600
H	-2.93430600	-3.09144100	0.76255300

TS_{edt 2A→2B}

Fe	1.30401400	-0.47759900	-0.00079900
Fe	-1.31831800	-0.36334500	0.01298600
S	0.12995600	0.87289800	1.43937300
S	0.08936000	0.73297700	-1.54221300
P	3.32953000	0.56163600	0.00892900
P	-2.92286200	-0.09848600	-1.55031300
O	2.16243600	-2.20454600	2.21406700
O	-2.00800100	-3.19600300	0.03669100
O	2.07973300	-2.35718300	-2.12197200
O	-3.21910800	0.25865400	2.14222600
C	1.83922200	-1.51582100	1.33702300
C	-1.74245200	-2.05880800	0.00629000
C	1.79851800	-1.60936800	-1.27891500
C	-2.46664500	0.01439900	1.28531800
C	0.22654400	2.54995000	0.62992500
C	0.03670900	2.48219000	-0.88658400
C	4.73903800	-0.59593800	-0.35435600
C	-4.56956100	-0.80338600	-1.05648500
C	3.61057600	1.94082100	-1.20837800
C	-3.34780900	1.63902600	-2.05843900
C	3.82266700	1.29621400	1.64491900
C	-2.54685400	-0.95347400	-3.15504300
H	-1.61872400	-0.55503700	-3.57684600
H	4.64271000	-0.99842200	-1.36837100
H	-4.95500700	-0.28057000	-0.17490400
H	4.73159400	-1.42703700	0.35915600
H	-4.46873200	-1.86855400	-0.82403500
H	4.66765700	2.23322100	-1.19217500
H	-4.22796500	1.61735200	-2.71299000
H	3.00115000	2.80939300	-0.94058500
H	-2.50981500	2.07836100	-2.60918900
H	3.34009100	1.60737000	-2.21566300
H	-3.57166700	2.24830700	-1.17628300
H	5.69123300	-0.05868500	-0.26984400
H	-5.27785100	-0.68240400	-1.88474500
H	4.81318400	1.75999600	1.56279200
H	-3.37005400	-0.79128800	-3.86177700
H	3.85692400	0.50625900	2.40288600
H	-2.42905400	-2.02766900	-2.97744400
H	3.09525500	2.04928400	1.96369000
H	-0.54051700	3.16740100	1.11131800
H	1.20625500	2.96229200	0.89912400
H	-0.93895800	2.88151400	-1.18044800
H	0.80691000	3.04518600	-1.42565300
H	-0.02312700	-1.42845800	0.11372800

TS_{edt 2A→2C}

Fe	1.03795300	-0.36573500	0.11908800
Fe	-1.39728200	0.64079000	0.23235600
S	0.45817400	1.77296300	0.92944300
S	-0.17273300	0.52269200	-1.70962900
P	2.35206200	-1.31584300	-1.44078200
P	-2.94798200	-0.80401700	-0.61379200
O	3.41378000	0.26149200	1.69844800
O	-2.37650400	0.36042300	2.98834200
O	0.72767500	-2.98603000	1.35710100
O	-3.04068600	2.98369500	-0.40105200
C	2.46849100	0.01974200	1.05920800
C	-2.00065100	0.47652500	1.89690800
C	0.86733100	-1.94427200	0.84474500
C	-2.39281800	2.04907000	-0.15459100
C	0.87780500	2.86754100	-0.52263300
C	0.37957500	2.30494500	-1.85682300
C	3.67882500	-2.41332400	-0.74155300
C	-4.36024100	-1.23111100	0.51535700
C	1.49484000	-2.42368900	-2.66107000
C	-3.79539000	-0.19335600	-2.15156500
C	3.30538300	-0.12866900	-2.50734600
C	-2.28999000	-2.46537700	-1.12518600
H	-1.49176600	-2.32921700	-1.86233200
H	3.22733800	-3.22034900	-0.15526900
H	-4.88836100	-0.31786800	0.81059300
H	4.34871400	-1.83575500	-0.09613700
H	-3.98241700	-1.72830200	1.41517700
H	0.73191600	-1.85689100	-3.20405900
H	-4.49140600	-0.95607600	-2.52096600
H	1.02389100	-3.25690700	-2.12895400
H	-3.04609700	0.02115300	-2.92106300
H	2.23062600	-2.81899200	-3.37193700
H	-4.35257900	0.72359100	-1.93164800
H	4.25974700	-2.84890600	-1.56331300
H	-5.05820000	-1.90084800	-0.00096200
H	3.97185100	-0.69034400	-3.17394600
H	-3.09595900	-3.06183400	-1.56975100
H	3.90354700	0.53698600	-1.87627300
H	-1.88795400	-2.99166300	-0.25318500
H	2.61404600	0.46682300	-3.11218200
H	0.42563400	3.84202800	-0.30113300
H	1.96675300	2.98227900	-0.50655200
H	-0.49509400	2.85043300	-2.22677400
H	1.15773900	2.34117500	-2.62740200
H	-0.56239600	-0.73351900	0.58355900

TS_{edt 2A→2D}

Fe	1.01109300	-0.41155600	0.28043200
Fe	-1.41369700	0.60582800	0.39252200
S	0.46051300	1.74677800	1.04449600
S	-0.21231300	0.44004300	-1.54841900
P	2.91707600	-0.06406000	1.43936200
P	-2.92052900	-0.90211800	-0.43244500
O	0.72520700	-2.92944600	1.71968000
O	-2.40961800	0.40798600	3.14775200
O	2.51315600	-1.65192500	-1.89449800
O	-3.06705000	2.91678300	-0.32512100
C	0.86216600	-1.91298600	1.15755000
C	-2.02804500	0.48712600	2.05383500
C	1.92436700	-1.14879200	-1.02134100
C	-2.41536200	1.99515000	-0.04242000
C	0.74292200	2.86012600	-0.43141500
C	0.47714200	2.15922500	-1.76810800
C	4.10021000	-1.49521500	1.36596600
C	-3.79136100	-0.33955400	-1.97443500
C	3.96081400	1.37240000	0.89098400
C	-2.18860200	-2.53797700	-0.92425800
C	2.67153000	0.20822300	3.25907800
C	-4.30949600	-1.36650200	0.71002100
H	-3.90795100	-1.83327800	1.61584700
H	4.41697100	-1.66927700	0.33243100
H	-3.04988000	-0.11225300	-2.74785700
H	3.62184900	-2.40184800	1.75049900
H	-4.37843600	0.56119200	-1.76591800
H	3.44020300	2.31127600	1.10488500
H	-2.96411900	-3.16737500	-1.37747800
H	4.16003400	1.29934000	-0.18341000
H	-1.78210200	-3.04329500	-0.04209500
H	4.91219600	1.35892500	1.43710300
H	-1.38194600	-2.37925300	-1.64828000
H	4.98137000	-1.26862500	1.97802200
H	-4.46089000	-1.13071500	-2.33277600
H	3.64335700	0.37383600	3.74027100
H	-4.98218200	-2.07213900	0.20824500
H	2.19607700	-0.67528800	3.69836900
H	-4.87196400	-0.46993500	0.99272600
H	2.03003800	1.08034300	3.42055600
H	0.07194500	3.71294600	-0.28009800
H	1.77527200	3.22038400	-0.36508800
H	-0.26183300	2.70140500	-2.37005000
H	1.38910300	2.04395800	-2.36331200
H	-0.57760300	-0.75813300	0.77893400

TS_{edt 2C→2D}

Fe	1.37907200	-0.33765300	0.09796700
Fe	-1.24361700	-0.30023300	-0.37254200
S	0.20944900	-1.72812700	-1.40264700
S	-0.30722700	-1.22293500	1.50160800
P	2.20254200	1.74279000	-0.10515900
P	-2.41243300	1.23767600	0.86757300
O	2.96655800	-0.70455100	2.51686200
O	-1.79026900	1.11732800	-2.88617100
O	3.54196800	-1.22214500	-1.65180200
O	-3.51977000	-2.13620100	-0.56581800
C	2.32994200	-0.54110700	1.55153400
C	-1.58759300	0.55553100	-1.88902800
C	2.66952200	-0.84882400	-0.97159200
C	-2.62803700	-1.39427500	-0.48356900
C	0.05160600	-3.29618800	-0.40565900
C	-0.22147100	-3.03906800	1.08111700
C	4.05085000	1.84844100	0.05903100
C	-4.19274500	0.79494800	1.17475700
C	1.86559200	2.52368100	-1.75574300
C	-1.79444700	1.57519000	2.59061200
C	1.62043000	3.01163400	1.12216200
C	-2.55398700	2.93439800	0.11168600
H	-1.56080800	3.35789800	-0.07138600
H	4.53513500	1.23636600	-0.70842200
H	-4.24860700	-0.14737200	1.73039400
H	4.36032000	1.49243900	1.04743300
H	-4.72093600	0.67632100	0.22257600
H	2.34659300	3.50811800	-1.80770800
H	-2.39184100	2.37861800	3.03855200
H	0.78672500	2.63436800	-1.90213000
H	-0.74101500	1.86927500	2.57355900
H	2.26339000	1.88232700	-2.54928900
H	-1.89215400	0.66934400	3.19764200
H	4.36564900	2.89194700	-0.06240600
H	-4.67607100	1.58727100	1.75888100
H	2.12749800	3.96530600	0.93030000
H	-3.11082100	3.59757900	0.78451500
H	1.85368000	2.67743600	2.13887100
H	-3.08511400	2.86780000	-0.84399800
H	0.54023500	3.15464200	1.02785100
H	0.56300200	-3.45992200	1.71911700
H	-1.18463100	-3.45932200	1.39375300
H	-0.76231700	-3.86114000	-0.87549400
H	0.98678400	-3.84503100	-0.56069600
H	0.07100900	0.72081900	-0.22203300

edt 2A*

Fe	1.07207700	-0.49498100	0.23904200
Fe	-1.44592700	0.51744400	0.31719600
S	0.46668900	1.53945300	1.20981600
S	-0.04806100	0.49006300	-1.58257700
P	3.30990000	-0.02946300	-0.29642200
P	-2.88877400	-0.97264500	-0.54329400
O	1.79051600	-1.62155700	2.84948400
O	-2.59630900	0.13661700	2.98219600
O	1.06736500	-3.08770200	-1.12923700
O	-3.06401500	2.90546900	-0.36220600
C	1.50427200	-1.17106600	1.80617600
C	-2.13332200	0.28438500	1.91543900
C	1.08602900	-2.05121400	-0.57728700
C	-2.38985800	1.97629500	-0.11966700
C	0.90516000	2.74524200	-0.14335700
C	0.45847200	2.28284600	-1.53939400
C	4.37389700	-1.56893700	-0.29888600
C	-4.68979600	-0.52351400	-0.34830600
C	3.80916700	0.72568600	-1.93843600
C	-2.78069900	-1.35492400	-2.36532000
C	4.26978900	1.03221300	0.91153800
C	-2.83738200	-2.67804100	0.21060800
H	-1.84543300	-3.11289600	0.04897700
H	4.01942600	-2.25866700	-1.07341800
H	-4.88981700	0.41724600	-0.87309400
H	4.28880600	-2.06824500	0.67328000
H	-4.91602600	-0.38345900	0.71485700
H	3.47483100	1.76822100	-1.98672700
H	-3.56691100	-2.06686800	-2.64847400
H	3.33273200	0.16952100	-2.75385900
H	-1.79871000	-1.78337900	-2.59267100
H	4.89944900	0.69569800	-2.06465800
H	-2.89295600	-0.42925100	-2.93979200
H	5.42678300	-1.32202400	-0.48811200
H	-5.33463500	-1.31264200	-0.75576000
H	5.32234600	1.12196600	0.61226600
H	-3.59946800	-3.32717400	-0.23982600
H	4.21307000	0.57456600	1.90586200
H	-3.01377800	-2.60306000	1.28941600
H	3.82481200	2.03157600	0.97434300
H	0.43625200	3.70051000	0.12500300
H	1.99311200	2.87710400	-0.10007700
H	-0.41795100	2.84677000	-1.87795600
H	1.25620000	2.41715100	-2.28058500
H	-0.54181600	-0.83380100	0.62817400

edt 2B*

Fe	-1.34911600	-0.57274300	0.03092100
Fe	1.34909900	-0.57271300	-0.03088200
S	-0.04726100	0.62192800	-1.51853300
S	0.04724500	0.62172600	1.51870000
P	-3.27831100	0.74087200	0.00945800
P	3.27834300	0.74083900	-0.00954800
O	-2.39050100	-2.33621300	-2.06433800
O	2.39058000	-2.33626800	2.06425500
O	-2.25306300	-2.28579200	2.23019900
O	2.25287700	-2.28570700	-2.23027500
C	-1.97694200	-1.63146400	-1.22502500
C	1.97697900	-1.63148800	1.22498900
C	-1.90364100	-1.59899300	1.34866200
C	1.90354700	-1.59891200	-1.34870100
C	-0.14779000	2.31863200	-0.75301500
C	0.14780200	2.31853100	0.75342500
C	-4.80659400	-0.24663500	0.44418600
C	4.80652400	-0.24661600	-0.44474900
C	-3.50209700	2.21356100	1.14881800
C	3.50197200	2.21376000	-1.14863800
C	-3.80403300	1.44839100	-1.64240800
C	3.80436600	1.44802700	1.64236500
H	3.03262400	2.11932700	2.03499400
H	-4.72473500	-0.61365100	1.47351800
H	4.72450300	-0.61336300	-1.47416500
H	-4.88252800	-1.11113200	-0.22529100
H	4.88252500	-1.11128800	0.22449400
H	-4.53814900	2.57584200	1.12035200
H	4.53805200	2.57597100	-1.12029700
H	-2.83400700	3.02815800	0.84705800
H	2.83399400	3.02833000	-0.84655800
H	-3.24835700	1.91623000	2.17281100
H	3.24801300	1.91667400	-2.17264800
H	-5.71238300	0.36611900	0.34881600
H	5.71234900	0.36608200	-0.34935200
H	-4.75144600	1.99617900	-1.55504000
H	4.75170900	1.99592300	1.55492600
H	-3.92630700	0.62411200	-2.35446000
H	3.92686600	0.62359900	2.35420500
H	-3.03227800	2.11985600	-2.03472500
H	0.54972900	2.96637700	-1.29923000
H	-1.16180100	2.68458000	-0.95219700
H	1.16181600	2.68443600	0.95266700
H	-0.54971700	2.96621000	1.29972000
H	0.00003000	-1.53575800	-0.00011900

edt 2C*

Fe	-1.35792400	-0.41755000	0.30215400
Fe	1.41291200	-0.43223000	0.23582900
S	0.02970900	-2.19449100	0.82314600
S	-0.01238700	-0.44592200	-1.63908200
P	-2.43607000	1.46053600	-0.29120800
P	2.36643900	1.54042600	-0.25504300
O	-3.63819700	-2.12334100	-0.53084800
O	2.48725900	-0.28325700	2.95846400
O	-2.18071300	-0.09064800	3.09758100
O	3.60565000	-2.08134200	-0.89901100
C	-2.72243600	-1.44207500	-0.25642000
C	2.04764200	-0.33457500	1.87243600
C	-1.84773000	-0.21614600	1.98009600
C	2.72658700	-1.42877800	-0.47854200
C	-0.01348700	-3.15905300	-0.77362400
C	-0.04085300	-2.26830200	-2.03186300
C	-4.16565100	1.58419800	0.40346400
C	4.22931200	1.49907600	-0.38386300
C	-1.75705100	3.13612900	0.18697800
C	1.91598600	2.38054700	-1.86226400
C	-2.75547400	1.68673900	-2.11633000
C	2.13827300	2.91046500	0.99467300
H	1.07123500	3.09444400	1.15174900
H	-4.12056900	1.59315000	1.49813800
H	4.52432900	0.82757400	-1.19764300
H	-4.74838000	0.71231100	0.08662100
H	4.64816100	1.11271400	0.55223900
H	-2.45430100	3.93325800	-0.10210700
H	2.44360600	3.33853800	-1.95682400
H	-0.79766000	3.30235500	-0.31321800
H	0.83479900	2.54865800	-1.90630500
H	-1.59975600	3.16696600	1.27107600
H	2.18724200	1.72394700	-2.69590800
H	-4.66051300	2.49916000	0.05319700
H	4.63106000	2.50252600	-0.57471500
H	-3.34734500	2.59315800	-2.29843500
H	2.62745900	3.83483500	0.66110800
H	-3.29947000	0.81237100	-2.49096900
H	2.57481100	2.59481800	1.94905100
H	-1.80191100	1.74813000	-2.65118000
H	-0.95106900	-2.44275100	-2.61775100
H	0.82790800	-2.46401300	-2.67158700
H	0.87438800	-3.80257800	-0.76334200
H	-0.90378800	-3.79723900	-0.72083000
H	0.05468400	0.43346800	0.78086700

edt 2D*

Fe	1.25726500	0.18241400	-0.57034900
Fe	-1.25736500	0.18274700	0.57016100
S	0.60321200	1.30589700	1.38754000
S	-0.60319800	1.30544400	-1.38802400
P	2.66425800	-1.06452800	0.66165200
P	-2.66432400	-1.06480000	-0.66125800
O	1.48869400	-1.56261100	-2.91105900
O	3.32042900	2.08305100	-1.53690500
O	-1.48871000	-1.56132300	2.91158100
O	-3.31998900	2.08417000	1.53634600
C	1.37404300	-0.87753800	-1.96364500
C	2.50093000	1.35708000	-1.11542400
C	-1.37420100	-0.87658800	1.96390900
C	-2.50082300	1.35778800	1.11494300
C	0.32799400	3.01836500	0.69711700
C	-0.32772300	3.01814000	-0.69824400
C	3.60979300	-2.40754500	-0.22553700
C	4.04146800	-0.11457900	1.48781200
C	1.93690000	-2.00047200	2.10013000
C	-1.93704800	-2.00129100	-2.09941600
C	-4.04170000	-0.11532100	-1.48769100
C	-3.60963000	-2.40753400	0.22659800
H	-4.19080200	-1.96781500	1.04494800
H	-0.00009600	-0.81833600	0.00029100
H	1.31287500	3.49941600	0.67026000
H	-0.29791400	3.54636400	1.42635600
H	-1.31252900	3.49935700	-0.67158400
H	0.29826900	3.54574100	-1.42769800
H	4.28858100	-2.92234000	0.46633600
H	2.90619900	-3.13195700	-0.65038000
H	4.19078000	-1.96814200	-1.04419000
H	4.65595600	0.37585200	0.72476800
H	3.60122000	0.65360400	2.13281000
H	4.67145500	-0.78333000	2.08876500
H	2.72192100	-2.55517100	2.62982800
H	1.46043400	-1.29653000	2.79081600
H	1.17556000	-2.69824300	1.73631300
H	-2.72211700	-2.55610900	-2.62892000
H	-1.46054100	-1.29761000	-2.79033900
H	-1.17575200	-2.69899800	-1.73538600
H	-4.65619300	0.37532600	-0.72479000
H	-3.60158800	0.65267400	-2.13300800
H	-4.67165300	-0.78437200	-2.08834600
H	-4.28821300	-2.92290000	-0.46504800
H	-2.90588400	-3.13152100	0.65191200

TS
edt 2A*→2B*

Fe	1.38713300	-0.60272600	0.02121600
Fe	-1.43445200	-0.39429000	0.01646700
S	0.13282800	0.73245800	1.45840100
S	0.10643700	0.57147600	-1.56392000
P	3.37137300	0.61852600	0.02157900
P	-3.01558500	-0.05601900	-1.53359400
O	2.27014100	-2.28751900	2.24441200
O	-2.08602300	-3.27547400	0.03485400
O	2.21657100	-2.49416800	-2.05340000
O	-3.31985600	0.23022600	2.16083500
C	1.92771000	-1.60883600	1.35457300
C	-1.78311200	-2.14007200	-0.00537100
C	1.90634900	-1.73202200	-1.22087800
C	-2.57328900	-0.01434500	1.28507000
C	0.29332900	2.38791100	0.61771500
C	0.04879800	2.31611900	-0.89661800
C	4.86393800	-0.44143500	-0.35971500
C	-4.72543200	-0.64893000	-1.07687000
C	3.66387500	2.04811100	-1.15546300
C	-3.38123100	1.66941800	-2.15917100
C	3.88775700	1.35217800	1.66299500
C	-2.70696500	-0.97038800	-3.13045200
H	-1.74499900	-0.65074600	-3.54544400
H	4.77933900	-0.84081400	-1.37674500
H	-5.09989400	-0.07115900	-0.22464900
H	4.89763700	-1.28384700	0.34058200
H	-4.67832700	-1.70478800	-0.78808400
H	4.71665100	2.35868700	-1.13574400
H	-4.21724900	1.64809300	-2.87075100
H	3.03725600	2.90129800	-0.87287900
H	-2.49509200	2.06649400	-2.66677900
H	3.39364000	1.73728800	-2.17108300
H	-3.63783200	2.32131500	-1.31667200
H	5.79181100	0.13871500	-0.27389900
H	-5.41277300	-0.53500200	-1.92469200
H	4.85241200	1.86950300	1.58086900
H	-3.50762800	-0.77021000	-3.85461200
H	3.97136900	0.54381400	2.39851900
H	-2.66150900	-2.04515100	-2.92292600
H	3.12699100	2.05469300	2.02077700
H	-0.42152100	3.06309200	1.10507500
H	1.30504000	2.75119200	0.83745300
H	-0.94585400	2.70249400	-1.14179300
H	0.78983700	2.90534300	-1.45207700
H	0.05858500	-1.45788400	0.09888000

TS
edt 2A*→2C*

Fe	1.40336700	-0.33623500	0.03789400
Fe	-1.64474800	0.67125100	0.32001000
S	0.39460000	1.57924200	1.00446900
S	-0.24687900	0.25013700	-1.54480300
P	2.72782200	-1.26253700	-1.52795100
P	-3.18431300	-0.71441600	-0.50868200
O	3.61802500	-0.05999600	1.93592000
O	-2.72529000	0.77370400	3.02613900
O	0.54893400	-2.98305500	1.08141200
O	-2.99184000	3.12360100	-0.64142100
C	2.74110100	-0.17472300	1.16238300
C	-2.31124100	0.75100700	1.93235400
C	0.84220800	-1.92499700	0.66238400
C	-2.40824000	2.16738200	-0.29429200
C	0.68315500	2.69673200	-0.46244400
C	0.31380100	2.01506300	-1.80040000
C	4.06643000	-2.39931200	-0.89291100
C	-4.60522600	-1.16000700	0.61296100
C	1.87186700	-2.35553600	-2.77754300
C	-4.06022100	-0.15273100	-2.05770100
C	3.71556700	-0.12352200	-2.64131900
C	-2.54979700	-2.39035800	-1.01574400
H	-1.75464800	-2.26143200	-1.75860100
H	3.60857700	-3.19521800	-0.29440000
H	-5.15360700	-0.25238800	0.88902700
H	4.75205500	-1.83477700	-0.25130100
H	-4.21337800	-1.62086600	1.52645400
H	1.10089700	-1.77479300	-3.29560400
H	-4.75626900	-0.92310500	-2.41368300
H	1.38984200	-3.18634500	-2.25007400
H	-3.31067700	0.04871400	-2.83149700
H	2.59066300	-2.75291800	-3.50558200
H	-4.61208700	0.77162000	-1.85421600
H	4.62908000	-2.84639000	-1.72247200
H	-5.28667100	-1.86061400	0.11409600
H	4.34100900	-0.69985500	-3.33623400
H	-3.35940400	-2.99330000	-1.44700200
H	4.35455900	0.51867200	-2.02465400
H	-2.13151500	-2.89935300	-0.14123600
H	3.03214700	0.51037600	-3.21768600
H	0.07701800	3.59611600	-0.29845700
H	1.74156700	2.98289700	-0.43933900
H	-0.50826700	2.53959100	-2.30159100
H	1.17260300	1.98803200	-2.48172700
H	-1.10538700	-0.63990100	0.88552900

TS
edt 2A*→2D*

Fe	1.34295200	-0.45266800	0.26703500
Fe	-1.68190300	0.51618000	0.46098500
S	0.32613800	1.43349000	1.25231500
S	-0.23976700	0.20873100	-1.37715200
P	3.26988400	-0.01212100	1.35004400
P	-3.15074100	-0.84637800	-0.51567900
O	0.68399200	-2.74102000	2.04364100
O	-2.84881700	0.41225200	3.13262600
O	2.65190100	-2.15169200	-1.72802000
O	-3.06002600	2.99169800	-0.39352300
C	0.90678000	-1.80973600	1.36340900
C	-2.40120400	0.47289800	2.05305200
C	2.14361500	-1.46704600	-0.91811400
C	-2.46238900	2.03133300	-0.08359400
C	0.61473200	2.62101700	-0.16149700
C	0.32955800	1.97851800	-1.53766500
C	4.58251500	-1.33920800	1.29293900
C	-3.86890400	-0.25294800	-2.13078400
C	4.24988300	1.50214300	0.84753900
C	-2.47063100	-2.51626500	-0.97817700
C	3.08853500	0.25883500	3.18828700
C	-4.67246000	-1.29127200	0.46450500
H	-4.37146100	-1.77546000	1.40009500
H	4.90021600	-1.49889400	0.25656400
H	-3.04496500	-0.04758000	-2.82353200
H	4.16155500	-2.27644800	1.67434700
H	-4.43166400	0.67264500	-1.96597400
H	3.64515800	2.39847500	1.02611300
H	-3.23203000	-3.11576900	-1.49375400
H	4.49257900	1.44499500	-0.21954700
H	-2.14033800	-3.03354500	-0.07110700
H	5.17818800	1.57744600	1.42942800
H	-1.60420900	-2.38036300	-1.63520600
H	5.45099600	-1.05675400	1.90177200
H	-4.53231100	-1.01169600	-2.56520600
H	4.06017100	0.47934100	3.64937000
H	-5.31648000	-1.97140300	-0.10724500
H	2.66563700	-0.64449800	3.64211900
H	-5.23042400	-0.38003200	0.70765400
H	2.39806900	1.09136200	3.36187400
H	-0.03956600	3.48256900	0.01722100
H	1.65553500	2.96001500	-0.09598400
H	-0.46102400	2.52083800	-2.07044200
H	1.22713400	1.96503500	-2.16705900
H	-1.13478100	-0.82528900	0.93707000

TS_{edt 2C*→2D*}

Fe	1.89379500	-0.69789600	0.03712600
Fe	-1.37156800	-0.22121500	-0.34080600
S	0.22309500	-1.58423100	-1.39042400
S	0.00428100	-0.86585300	1.45328400
P	2.31682900	1.56352700	-0.12682200
P	-2.56252600	1.27876000	0.82263200
O	3.66739200	-1.13573100	2.33986900
O	-2.23964800	0.85282400	-2.91410300
O	3.93102400	-1.34225600	-1.96888100
O	-3.44869200	-2.30553300	-0.05013300
C	2.97240700	-0.95422600	1.40899900
C	-1.92213200	0.40822100	-1.87856700
C	3.12090900	-1.07965200	-1.16010200
C	-2.59768600	-1.50691900	-0.15282700
C	0.03625400	-3.09084300	-0.29716400
C	-0.09806100	-2.71396800	1.19939800
C	4.13673800	1.98827400	-0.04131800
C	-4.41085900	1.01209200	0.84481900
C	1.82581500	2.48261800	-1.68177500
C	-2.19208500	1.47414500	2.63997200
C	1.64785900	2.67687900	1.21908900
C	-2.46484700	3.03521900	0.20131900
H	-1.42794700	3.38395800	0.24343300
H	4.66422500	1.49747700	-0.86724900
H	-4.63758500	0.05369800	1.32453800
H	4.55352300	1.62009800	0.90310200
H	-4.78518700	0.98137100	-0.18483700
H	2.12781400	3.53734800	-1.62978300
H	-2.85678100	2.22824300	3.08078400
H	0.74194200	2.41266000	-1.82047600
H	-1.14902000	1.77625000	2.77912700
H	2.31518900	2.00764000	-2.54018000
H	-2.33576200	0.51288900	3.14441600
H	4.29185800	3.07312500	-0.10816900
H	-4.91477200	1.81996200	1.39036500
H	1.94856400	3.72135000	1.06212000
H	-3.09833100	3.69741700	0.80495600
H	2.02713500	2.32891100	2.18688700
H	-2.79804300	3.06694000	-0.84208200
H	0.55548800	2.60732800	1.22831000
H	0.70833200	-3.15835900	1.79407600
H	-1.06001900	-3.04613700	1.60818900
H	-0.84821700	-3.63436800	-0.65093100
H	0.92176400	-3.71281400	-0.47264500
H	-0.35081700	0.91617900	-0.45247600

edt 3A1

Fe	-0.98660900	-0.27597100	-0.48510600
Fe	1.39215600	0.54800800	-0.71521900
S	-0.40199800	1.57040200	-1.73941100
S	0.11249900	0.93526700	1.14784200
P	-3.03389600	-0.04815700	0.44678000
P	2.96219400	-0.57820000	0.56857100
O	0.81744900	-2.53846900	-0.84521800
O	2.94610100	3.02067700	-0.65871900
C	0.33978500	-1.47170000	-0.70173600
C	2.34570200	2.02414200	-0.67113000
C	-0.68131600	3.02759100	-0.60875100
C	-0.48253100	2.68746200	0.87368300
C	-4.14245300	-1.50738100	0.14791200
C	4.10376300	-1.69072600	-0.38318200
C	-3.03779300	0.08754300	2.29925700
C	4.11372100	0.55841400	1.48471400
C	-4.08330700	1.38696000	-0.11312400
C	2.32220000	-1.66846100	1.93590100
H	1.65938500	-1.09255000	2.59036200
H	-3.65160900	-2.41750600	0.50833700
H	4.66362100	-1.10328200	-1.11889600
H	-4.35036700	-1.61693500	-0.92135900
H	3.52161500	-2.45815800	-0.90382500
H	-2.51603500	0.99267800	2.62399500
H	4.79805300	-0.03634600	2.10146700
H	-2.52682500	-0.78197200	2.72503100
H	3.53276200	1.22610200	2.13035700
H	-4.07344700	0.11824200	2.65878400
H	4.69766300	1.16098600	0.78130000
H	-5.08782400	-1.36364900	0.68436300
H	4.80853600	-2.17366700	0.30423400
H	-5.07690700	1.31734800	0.34680700
H	3.17527600	-2.03575700	2.51956400
H	-4.18514600	1.36227200	-1.20324500
H	1.77736900	-2.52028400	1.51994600
H	-3.62219100	2.33505800	0.18159400
H	0.01829000	3.80249200	-0.94096600
H	-1.69682400	3.38197200	-0.81679100
H	0.26764900	3.33513100	1.34163200
H	-1.41332000	2.78861500	1.44369300
C	2.08777400	0.00835800	-2.26900400
O	2.53846400	-0.32722000	-3.28351400
C	-1.77879300	-0.97914600	-1.90523700
O	-2.28946600	-1.42085500	-2.85102400
H	-1.23856100	-1.40074100	0.48245000

edt 3A2

Fe	-1.08603800	0.47969600	0.23169900
Fe	1.23134900	-0.55789800	0.30278100
S	-0.66204200	-1.66123800	0.98115600
S	0.00324400	-0.34320800	-1.63255400
P	-3.32701700	0.16756900	0.09815200
P	2.79310100	0.93677200	-0.49447600
O	0.61353600	1.99565500	2.05934600
O	-1.48928100	3.05636200	-1.10786700
O	2.68776500	-2.89703100	-0.65891400
C	0.15318800	1.22943700	1.29627500
C	-1.33073800	2.03954500	-0.56358500
C	2.12315300	-1.95343700	-0.27759700
C	-1.03789800	-2.73173300	-0.50420000
C	-0.64135100	-2.08318500	-1.83695600
C	-4.30317500	1.70614500	0.45613200
C	4.02667900	1.55154800	0.75054600
C	-4.01852000	-0.39575200	-1.53837700
C	3.84607300	0.25480200	-1.86487800
C	-4.02214500	-1.04176400	1.32437900
C	2.11389300	2.50188400	-1.23490600
H	1.42456200	2.26238900	-2.05146600
H	-4.10051700	2.47440700	-0.29685800
H	4.59585300	0.70967900	1.15925500
H	-4.02339000	2.09268700	1.44187800
H	3.50450900	2.05978300	1.56832800
H	-3.64877100	-1.39704300	-1.78171900
H	4.53363100	1.02948000	-2.22471900
H	-3.71078600	0.30049200	-2.32564100
H	3.20280500	-0.07213000	-2.68909300
H	-5.11392100	-0.42403900	-1.48485600
H	4.42701100	-0.60058500	-1.50392300
H	-5.37361900	1.46893500	0.44716200
H	4.71775800	2.25361300	0.26881000
H	-5.11408400	-1.06904500	1.22586700
H	2.94478300	3.09783100	-1.63218800
H	-3.75199700	-0.72377700	2.33653900
H	1.59017200	3.08709600	-0.47313800
H	-3.61859200	-2.04462400	1.15531000
H	-0.49700200	-3.66988900	-0.33474500
H	-2.11026300	-2.95621000	-0.46575600
H	0.15786500	-2.64326200	-2.33456300
H	-1.48552200	-2.01446500	-2.53147600
C	1.99153900	-0.66093400	1.91535500
O	2.50756800	-0.77851000	2.94760700
H	-1.73996000	0.80681900	1.54326900

edt 3A3

Fe	1.08020900	-0.43568800	0.00144800
Fe	-1.33695200	0.19382400	0.54199300
S	0.50389000	1.03081200	1.64495000
S	-0.15699800	1.02735800	-1.26492900
P	3.21509200	0.22442900	-0.31796900
P	-3.19501700	0.04486300	-0.75125200
O	1.99939500	-2.41010000	1.98076500
O	-1.23770600	-2.73836100	0.26112700
O	1.22921600	-2.27154800	-2.29662100
O	-2.68670400	-0.15852500	3.11898500
C	1.63779900	-1.63113600	1.19885100
C	-1.08843700	-1.57822100	0.32170800
C	1.17020800	-1.55513500	-1.38346000
C	-2.15172800	-0.05323100	2.09460400
C	0.66902100	2.71136100	0.84826800
C	0.17282300	2.73918000	-0.59940600
C	4.33557500	-1.13869100	-0.90470100
C	-4.69343300	-0.62081700	0.11838200
C	3.49620500	1.56059700	-1.57950900
C	-3.76414100	1.66941200	-1.44502900
C	4.08593400	0.83770100	1.20578600
C	-3.04434100	-1.03386300	-2.25790500
H	-2.21231600	-0.68154500	-2.87757600
H	4.00951100	-1.49862900	-1.88607500
H	-4.95551900	0.03010000	0.95925900
H	4.31608100	-1.97315100	-0.19530300
H	-4.48414900	-1.62676200	0.49820800
H	3.04461200	2.49891300	-1.24321000
H	-4.65689900	1.51869400	-2.06399400
H	3.04562500	1.26654300	-2.53324300
H	-2.96787600	2.10201600	-2.06063500
H	4.57390900	1.71281900	-1.71580300
H	-3.99879100	2.35605500	-0.62490700
H	5.36191600	-0.76041300	-0.98386400
H	-5.53744800	-0.66717400	-0.58010600
H	5.11952500	1.10609500	0.95536200
H	-3.97326700	-0.98495800	-2.83877900
H	4.09172700	0.04877900	1.96542100
H	-2.85945400	-2.07125600	-1.96052600
H	3.57220000	1.71208200	1.61637500
H	0.09863000	3.39671100	1.48544900
H	1.72835400	2.98422600	0.92131200
H	-0.78320200	3.26602900	-0.68289900
H	0.89062900	3.21869100	-1.27455000
H	-1.98638300	1.54981400	0.72903400

edt 3A4

Fe	-1.05508700	-0.40755500	-0.17200600
Fe	1.34846800	0.35691300	-0.56912000
S	-0.52778400	1.44783400	-1.38957100
S	0.19571000	0.67474500	1.41616100
P	-3.15807300	0.07834800	0.48456200
P	3.05936600	-0.63856700	0.55710900
O	-2.20455600	-1.70404400	-2.55266800
O	1.12141600	-2.27312200	-1.83230400
O	-0.97526700	-2.88607300	1.41188900
O	3.04652100	2.71517500	-1.00010700
C	-1.73625500	-1.19689300	-1.61831500
C	1.04571700	-1.24583300	-1.27271200
C	-1.01329700	-1.90424500	0.78946100
C	2.36620800	1.80061800	-0.76682900
C	-0.69272800	2.85132300	-0.16858200
C	-0.15993900	2.50081200	1.22429600
C	-4.21261600	-1.43001300	0.74513300
C	4.42549200	-1.24197200	-0.54306300
C	-3.36820800	1.00298800	2.08495600
C	3.90738000	0.46430600	1.78742600
C	-4.14993900	1.06310700	-0.74244700
C	2.59419000	-2.12662200	1.56551000
H	1.85902300	-1.84009400	2.32504600
H	-3.81571500	-2.02564200	1.57401800
H	4.84483300	-0.40053200	-1.10508000
H	-4.22140300	-2.04379300	-0.16171500
H	4.02767900	-1.97699100	-1.25092400
H	-2.99338400	2.02626200	1.98511700
H	4.68429600	-0.10143000	2.31537700
H	-2.81695400	0.49377300	2.88215100
H	3.17003900	0.83083100	2.50950400
H	-4.43388200	1.03986300	2.34300000
H	4.36780800	1.31624400	1.27639500
H	-5.23854100	-1.12343100	0.98166100
H	5.21595400	-1.70685200	0.05826900
H	-5.16448100	1.21758200	-0.35511100
H	3.48710300	-2.52472400	2.06266200
H	-4.20463500	0.51744200	-1.69035500
H	2.16616600	-2.90152700	0.92169300
H	-3.68132900	2.03472800	-0.92630900
H	-0.15384300	3.69968800	-0.60694000
H	-1.75689900	3.11171100	-0.14298200
H	0.79403600	2.99905600	1.42707300
H	-0.86268000	2.78211600	2.01617800
H	1.95174700	0.29352500	-1.94345900

edt 3B

Fe	1.20078000	0.41857700	0.15717400
Fe	-1.32717500	0.51933300	0.04832400
S	-0.01097400	-0.51499000	-1.56353900
S	-0.16697100	-0.97259500	1.39661900
P	3.11748600	-0.74541800	-0.20307000
P	-3.33669100	-0.52350200	0.20393800
O	2.17799900	2.56742100	-1.59832000
O	-0.33959000	3.01596000	1.19988500
O	2.36509700	1.47695000	2.64698500
O	-2.45795200	2.22979300	-2.05129400
C	1.80172900	1.71678900	-0.90276500
C	-0.50233500	1.95400600	0.73424100
C	1.89709600	1.07683900	1.66267900
C	-2.02282900	1.56033100	-1.20682300
C	-0.04282500	-2.32053600	-1.09270500
C	-0.29441500	-2.54357400	0.40011300
C	3.32179300	-2.35795700	0.70304500
C	-4.76729600	0.65963600	0.14788200
C	3.47555100	-1.15872400	-1.98118700
C	-3.78612100	-1.76708100	-1.11022900
C	4.64763800	0.18981200	0.29157000
C	-3.63035600	-1.41723200	1.80725700
H	-2.89768800	-2.21612200	1.95682400
H	2.62344400	-3.10753000	0.31812100
H	-4.80312700	1.17072900	-0.81969300
H	3.13266100	-2.20514700	1.77079000
H	-4.65208100	1.40804000	0.93900600
H	4.43661000	-1.68315800	-2.04835700
H	-4.81170800	-2.12128600	-0.94836900
H	3.52779400	-0.23226200	-2.56291400
H	-3.10471500	-2.62290100	-1.07557500
H	2.68757700	-1.78848400	-2.40420000
H	-3.71585600	-1.29533900	-2.09617300
H	4.34590000	-2.72513300	0.56292000
H	-5.70433500	0.11040400	0.29784400
H	5.53494400	-0.39470900	0.02028800
H	-4.63945800	-1.84651100	1.80598200
H	4.65198300	0.36747600	1.37183500
H	-3.53635200	-0.70339500	2.63229700
H	4.68186600	1.15373300	-0.22746600
H	-0.81481200	-2.78595000	-1.71608900
H	0.92148200	-2.73674300	-1.40465400
H	-1.29946000	-2.93951100	0.58331800
H	0.41761600	-3.25172500	0.83840700
H	-2.11104700	1.02019100	1.22411700

edt 3C1

Fe	-1.27218000	-0.45846200	0.19857200
Fe	1.29509600	-0.46979000	0.28186900
S	-0.01234300	-2.33716400	0.41824100
S	0.05600400	-0.17463300	-1.63832700
O	2.85294100	-1.49607400	2.54483900
C	0.53431600	0.82283000	1.27967900
C	-2.60890800	-1.31433700	-0.53670600
C	2.22959200	-1.06610400	1.66600700
C	0.08876000	-2.99128000	-1.32764800
C	0.13776400	-1.88363300	-2.38705600
H	-0.70289900	-1.95151200	-3.08666700
H	1.07072900	-1.91403700	-2.95969100
H	0.98867400	-3.61512000	-1.35172600
H	-0.78600000	-3.63914800	-1.45497200
O	-3.47249900	-1.92367500	-1.02573000
C	-1.91003100	-0.58809300	1.86401000
O	-2.32845800	-0.68569700	2.94142400
O	0.37341700	1.70895500	2.03323400
H	2.28082800	-1.35038300	-0.45510700
P	-2.37394500	1.54177000	-0.18774500
P	2.89327500	0.96566300	-0.44661300
C	-3.14370600	1.58614900	-1.88186100
H	-3.65916100	2.54277000	-2.02900600
H	-2.36301400	1.47124200	-2.64153800
H	-3.86712300	0.77113700	-1.98858100
C	-3.82023800	1.84053100	0.94226800
H	-3.46753900	1.99621600	1.96751500
H	-4.36784200	2.73086300	0.61110700
H	-4.49423900	0.97710000	0.92604400
C	-1.46970600	3.16746800	-0.12651500
H	-0.63376200	3.15478200	-0.83266500
H	-2.16661200	3.96572600	-0.40940300
H	-1.09213200	3.35490300	0.88235300
C	3.74110600	0.41722800	-2.00467500
H	4.50054500	1.15282900	-2.29603400
H	4.21767200	-0.55470800	-1.83925500
H	3.00270500	0.32125000	-2.80809200
C	4.29094000	1.22869700	0.74767000
H	5.01778400	1.92937300	0.31964900
H	3.90419000	1.63850000	1.68724200
H	4.78867500	0.27531900	0.95454200
C	2.35907200	2.69772700	-0.86119600
H	1.91844000	3.17710300	0.01891800
H	3.22706400	3.28062900	-1.19252400
H	1.62168200	2.66582500	-1.67080600

edt 3C2

Fe	-1.27562900	-0.47383500	0.21971300
Fe	1.30269600	-0.36922300	0.49232000
S	-0.00702700	-2.19724300	0.98291100
S	0.19560900	-0.56004900	-1.51892400
O	3.67306900	-2.09953400	0.37014100
C	0.47531400	0.79070500	1.55710400
C	-2.48883100	-1.46390900	-0.55172800
C	2.72870900	-1.42066700	0.35689200
C	0.22159500	-3.23817300	-0.55335300
C	0.38185400	-2.39882600	-1.82961200
H	-0.36813400	-2.66146900	-2.58371700
H	1.37583100	-2.52144300	-2.27348300
H	1.09943800	-3.86732500	-0.36752400
H	-0.65866300	-3.88856000	-0.60292700
O	-3.26535100	-2.15668900	-1.07490400
C	-2.15785200	-0.34513000	1.76981400
O	-2.76468700	-0.28269100	2.75734400
O	0.21470500	1.59094400	2.37472100
H	1.92719900	-0.42064100	1.85833200
P	-2.31580300	1.45768700	-0.49654000
P	2.63106200	1.32426500	-0.25402700
C	-2.04193700	1.92646100	-2.27512600
H	-2.63983600	2.81245000	-2.52059600
H	-0.98343500	2.13746900	-2.45572800
H	-2.34160300	1.09377200	-2.92050200
C	-4.16993400	1.32032700	-0.39908100
H	-4.47778800	1.13555500	0.63588700
H	-4.62731800	2.25409200	-0.74736800
H	-4.52071800	0.49439300	-1.02672500
C	-2.00352500	3.03477900	0.44082100
H	-0.95427400	3.32919700	0.35847300
H	-2.63730100	3.82919900	0.02831500
H	-2.24503700	2.89148200	1.49915200
C	3.54097200	0.92743000	-1.82515200
H	4.18204300	1.77065000	-2.10905500
H	4.16193700	0.03655400	-1.68386800
H	2.81659300	0.73399700	-2.62385400
C	3.97004900	1.77905700	0.94878000
H	4.58660300	2.58792800	0.53879200
H	3.51953100	2.10706200	1.89197900
H	4.60263800	0.90686100	1.14540300
C	1.84279600	2.96357500	-0.63776500
H	1.39396100	3.38198700	0.26889600
H	2.60691100	3.65713900	-1.00889200
H	1.07435000	2.83651200	-1.40711300

edt 3D1

Fe	-1.13995100	0.43929300	0.43779800
Fe	1.14287500	-0.05690800	-0.58251200
S	-0.63271100	0.79740800	-1.74768100
S	0.69596200	1.76882800	0.73889400
P	-2.67649900	-1.16300200	-0.19647300
P	3.13185000	-0.31231200	0.48830800
O	-1.35331300	-0.21369600	3.30209700
O	0.33548000	-2.38511700	1.02653800
O	-3.10896500	2.57875600	0.63290800
O	1.76060400	-1.85899500	-2.80766400
C	-1.25827100	0.02279600	2.16925100
C	0.46905800	-1.36467000	0.45652800
C	-2.34092100	1.70763300	0.55872900
C	1.50709900	-1.17101200	-1.90649200
C	-0.20798000	2.61346900	-1.81491300
C	0.47218200	3.11337000	-0.53484800
C	-4.24054900	-0.44661000	-0.89928400
C	4.09311400	-1.81910700	-0.01584900
C	-2.12899800	-2.34328200	-1.52900600
C	4.31759900	1.08854300	0.21701800
C	-3.27866900	-2.28744400	1.15428600
C	3.03898100	-0.45139000	2.33946800
H	2.56025400	0.44345300	2.75171400
H	-3.99975800	0.17665700	-1.76745900
H	4.32116400	-1.77581300	-1.08620000
H	-4.74542800	0.16808500	-0.14656500
H	3.50365900	-2.71989400	0.18728000
H	-1.82899000	-1.78830300	-2.42460900
H	5.24699000	0.90255500	0.76867700
H	-2.96649400	-3.00478400	-1.78231600
H	3.86654000	2.02162100	0.57100300
H	-1.28905300	-2.94952300	-1.17667000
H	4.53773400	1.17978500	-0.85176600
H	-4.91100900	-1.25732700	-1.20873100
H	5.03087600	-1.86736200	0.55064700
H	-4.00769400	-2.99669700	0.74451600
H	4.05165000	-0.54064400	2.75090200
H	-3.75684400	-1.69821800	1.94431900
H	2.45700700	-1.33502600	2.62118400
H	-2.43473100	-2.84019400	1.58032500
H	0.43944300	2.72674300	-2.69072100
H	-1.15040700	3.13844200	-2.00808800
H	1.47641300	3.50024800	-0.73880800
H	-0.11089700	3.90036300	-0.04372700
H	2.06493700	0.80237400	-1.41963800

edt 3D2

Fe	-1.10865100	0.15404100	0.53899400
Fe	1.15319500	0.17213900	-0.61943600
S	-0.61604200	1.53535200	-1.19602700
S	0.75844200	1.13558200	1.43113900
P	-2.78807100	-0.81247900	-0.73811400
P	2.90805800	-0.97200800	0.27270100
O	-1.22223600	-1.94728800	2.59843900
O	0.05794000	-2.52570500	-0.87458000
O	-2.94510500	1.91807300	1.95709200
O	3.05933200	1.80811400	-2.14030100
C	-1.17223900	-1.12481600	1.77907300
C	0.32359700	-1.39751800	-0.66117600
C	-2.23447900	1.19806100	1.38173300
C	2.32027400	1.19069500	-1.48836900
C	-0.15559500	3.14291100	-0.36103700
C	0.54568800	2.93772100	0.98819800
C	-4.34931600	0.19657100	-0.75891100
C	3.73845700	-2.10470500	-0.93841000
C	-2.44458200	-1.05927400	-2.55255400
C	4.27328100	0.10846800	0.91791500
C	-3.36048800	-2.48778400	-0.17529600
C	2.50578800	-2.06217600	1.72229200
H	2.07937400	-1.45996100	2.53202900
H	-4.13601300	1.19550100	-1.15483900
H	4.13096500	-1.52023000	-1.77770700
H	-4.75251200	0.29247100	0.25472300
H	3.00865200	-2.82639100	-1.32065600
H	-2.14333500	-0.11129800	-3.01054500
H	5.07910400	-0.51931500	1.31676100
H	-3.36140000	-1.41722100	-3.03671600
H	3.88155600	0.74704700	1.71681500
H	-1.65296800	-1.80075700	-2.69185400
H	4.67082400	0.73700500	0.11448700
H	-5.09487800	-0.29352700	-1.39639800
H	4.56247000	-2.64181900	-0.45355200
H	-4.15721200	-2.84685000	-0.83777500
H	3.42380500	-2.54331600	2.08079400
H	-3.74543800	-2.42482000	0.84823600
H	1.78770200	-2.83436100	1.42801800
H	-2.52258800	-3.19206100	-0.20204900
H	0.47929900	3.67920000	-1.07479400
H	-1.09236500	3.70039400	-0.25093900
H	1.55520900	3.36350500	0.98812900
H	-0.01855800	3.38887200	1.81155500
H	1.24018700	-0.37486200	-2.01876700

edt 3A1*

Fe	-1.18372800	-0.61335700	-0.08911900
Fe	1.32463800	0.25090700	-0.48988500
S	-0.53230400	0.81155700	-1.80495500
S	-0.10150600	1.04143300	1.20910100
P	-3.28268200	0.02909100	0.61565600
P	2.81252200	-0.42942000	1.08824400
O	0.82868000	-2.72167800	0.10234500
O	2.78235600	2.76573400	-1.06638700
C	0.31788800	-1.65336000	-0.03914300
C	2.18311400	1.79388200	-0.80273500
C	-0.86667000	2.51417100	-1.12270500
C	-0.68033100	2.62494900	0.40341000
C	-4.51014200	-1.37737900	0.64327000
C	4.02809800	-1.72624100	0.53468900
C	-3.36968400	0.60268600	2.38953500
C	3.91832800	0.91762700	1.75243100
C	-4.29482600	1.34553500	-0.26255700
C	2.14847300	-1.16651300	2.67010500
H	1.46464500	-0.45380900	3.14376100
H	-4.08473600	-2.20774500	1.21736300
H	4.62368500	-1.33840600	-0.29916400
H	-4.70127700	-1.72460900	-0.37806400
H	3.46892900	-2.60420800	0.19354600
H	-2.75038600	1.49514300	2.52892300
H	4.58542000	0.51905300	2.52713200
H	-2.97047900	-0.19035800	3.03093000
H	3.29525300	1.71064400	2.18097400
H	-4.40583700	0.82511900	2.67520900
H	4.51810100	1.34217100	0.94022500
H	-5.45507800	-1.05706100	1.10011600
H	4.69441600	-2.01072100	1.35885100
H	-5.30876900	1.40541000	0.15471200
H	2.98212000	-1.38389100	3.35015700
H	-4.35565000	1.09911200	-1.32877600
H	1.60768100	-2.09027200	2.44593800
H	-3.80938300	2.32230600	-0.15712400
H	-0.18553600	3.19389600	-1.64787500
H	-1.89086900	2.76883900	-1.42050100
H	0.06779500	3.38745100	0.65167100
H	-1.61977200	2.90425700	0.89833600
C	2.09890800	-0.61636200	-1.81811800
O	2.62867900	-1.15538400	-2.71060800
C	-1.90539300	-1.78997500	-1.15813300
O	-2.38858200	-2.57779500	-1.87922900
H	-1.45623200	-1.43265400	1.15365800

edt 3A2*

Fe	-1.13876300	0.55365100	0.28145500
Fe	1.30381700	-0.57806900	0.29809500
S	-0.64533200	-1.62741600	1.03077600
S	-0.03612400	-0.23167000	-1.61579100
P	-3.38217500	0.09183400	0.04196400
P	2.80458900	0.91487900	-0.51674800
O	0.78289500	1.96263100	1.97544000
O	-1.56654900	3.23686600	-0.78336000
O	2.71513100	-2.96448500	-0.74560300
C	0.28791600	1.17340400	1.23524800
C	-1.39621400	2.15813400	-0.35212800
C	2.13153800	-2.01947000	-0.37068000
C	-1.02071800	-2.65959100	-0.48024000
C	-0.66217700	-1.97779300	-1.81526400
C	-4.46327100	1.58423700	0.34046200
C	4.14432900	1.45191800	0.66082600
C	-4.13023500	-0.56154800	-1.55218400
C	3.76807700	0.31501800	-1.99554500
C	-4.07121800	-1.09551600	1.30580400
C	2.15481400	2.55150000	-1.13379800
H	1.38915400	2.37982600	-1.89815100
H	-4.28974600	2.33276500	-0.44041600
H	4.71814600	0.57747000	0.98761900
H	-4.19654900	2.02488000	1.30733000
H	3.67849200	1.91413000	1.53830500
H	-3.75831200	-1.57253300	-1.75159900
H	4.45365100	1.09380400	-2.35311000
H	-3.83232300	0.08956900	-2.38195500
H	3.06073100	0.05439900	-2.79098200
H	-5.22598600	-0.59146200	-1.48824300
H	4.34083700	-0.57937500	-1.72736700
H	-5.52355100	1.30165700	0.34323900
H	4.81788600	2.17213900	0.17957500
H	-5.15751500	-1.19832800	1.18753900
H	2.97669800	3.13562700	-1.56757600
H	-3.84049000	-0.70987800	2.30461900
H	1.71208100	3.10960300	-0.30333300
H	-3.59666300	-2.07729000	1.20499800
H	-0.45905600	-3.59352600	-0.35708600
H	-2.08991700	-2.90570300	-0.43789600
H	0.13095000	-2.52931500	-2.33319500
H	-1.52810900	-1.92443800	-2.48624800
C	2.07718600	-0.73507900	1.87208600
O	2.61276700	-0.88607100	2.90105400
H	-1.77883500	0.87269500	1.60987900

edt 3A3*

Fe	-1.19152800	0.49179500	0.00595800
Fe	1.49690500	-0.18779500	0.56179900
S	-0.43201100	-0.91884200	1.67590500
S	0.17856600	-0.89376900	-1.26947900
P	-3.34686800	-0.34240800	-0.31723600
P	3.25108900	-0.05828700	-0.81001400
O	-2.15088400	2.44624700	1.97984200
O	1.27996200	2.76305300	0.46144400
O	-1.34959200	2.40752600	-2.21451200
O	2.99679500	-0.10277600	3.06068800
C	-1.74963500	1.66989100	1.19771800
C	1.19635300	1.59206800	0.46455300
C	-1.28088000	1.64779800	-1.32269500
C	2.39420100	-0.10357200	2.05811000
C	-0.56704200	-2.59823800	0.87470900
C	-0.18052100	-2.60075000	-0.61489200
C	-4.57139900	0.94577500	-0.90362600
C	4.86568000	0.47929400	-0.04867400
C	-3.69706200	-1.72027200	-1.54071800
C	3.71660800	-1.65103000	-1.65420500
C	-4.22302300	-0.97570400	1.21075700
C	3.08241800	1.11250900	-2.25114800
H	2.19403100	0.83490900	-2.82947800
H	-4.26694400	1.31462900	-1.88978000
H	5.14723600	-0.22171600	0.74495500
H	-4.57002100	1.79006400	-0.20453400
H	4.74288700	1.47434800	0.39377700
H	-3.22724800	-2.64975600	-1.19915600
H	4.56748100	-1.49832900	-2.33038100
H	-3.27230100	-1.45326000	-2.51525800
H	2.85380200	-2.00926300	-2.22670900
H	-4.77714500	-1.88631900	-1.64723600
H	3.97527000	-2.39777000	-0.89591100
H	-5.58574500	0.53064800	-0.96843300
H	5.66037600	0.51282500	-0.80476500
H	-5.25083200	-1.28715900	0.98218200
H	3.96942300	1.06405300	-2.89560900
H	-4.24367400	-0.17957000	1.96378700
H	2.95551000	2.13521700	-1.87977600
H	-3.67176900	-1.82413200	1.63105000
H	0.09112700	-3.25993900	1.45035200
H	-1.60217100	-2.93356400	1.01963900
H	0.73468700	-3.18184000	-0.77681100
H	-0.97643700	-3.02382400	-1.23975500
H	1.97999000	-1.64104700	0.64309000

edt 3A4*

Fe	-1.14215700	-0.46812800	-0.17747700
Fe	1.50120200	0.34179400	-0.60459400
S	-0.44779900	1.31646300	-1.49331400
S	0.21697400	0.61177200	1.37856800
P	-3.27680400	0.18827600	0.49914300
P	3.14356400	-0.58053600	0.58907300
O	-2.27606700	-1.83243000	-2.51836300
O	1.19101200	-2.32327700	-1.80529400
O	-1.10542300	-2.92460900	1.43326600
O	3.05972500	2.80806500	-0.94311100
C	-1.79800000	-1.29288500	-1.59317000
C	1.14719600	-1.28389600	-1.25863600
C	-1.11611000	-1.94235200	0.78941300
C	2.39317800	1.86713300	-0.72673400
C	-0.64968900	2.73937200	-0.30057300
C	-0.15131200	2.42390100	1.12068300
C	-4.44386100	-1.24961900	0.76414700
C	4.57979300	-1.22350100	-0.40719800
C	-3.53273600	1.12788200	2.10077000
C	3.96396800	0.53192300	1.83767800
C	-4.28212500	1.21864500	-0.70000200
C	2.66596400	-2.05257900	1.62506200
H	1.89540200	-1.75077500	2.34305800
H	-4.06490900	-1.87927800	1.57718500
H	5.01506500	-0.39901000	-0.98282500
H	-4.48690600	-1.85397600	-0.14922100
H	4.21411000	-1.98178200	-1.10836400
H	-3.11507600	2.13668100	2.01031700
H	4.72965400	-0.01751100	2.39970800
H	-3.01088300	0.60758600	2.91196800
H	3.19933800	0.90572600	2.52755800
H	-4.60084900	1.20518300	2.34321900
H	4.42801800	1.38190100	1.32567100
H	-5.45325000	-0.89939900	1.01676300
H	5.34677000	-1.66359100	0.24273800
H	-5.29253400	1.40641000	-0.31327100
H	3.53870400	-2.43872800	2.16719500
H	-4.35227600	0.68362300	-1.65400200
H	2.25837300	-2.84004100	0.98256700
H	-3.78297000	2.17674100	-0.88430500
H	-0.10488900	3.59063000	-0.72826900
H	-1.71779900	2.98727700	-0.30096800
H	0.78578700	2.95118300	1.33325000
H	-0.88818500	2.72052400	1.87714300
H	2.20437500	0.28128700	-1.93118400

edt 3B*

Fe	1.27192500	0.47759100	0.17429200
Fe	-1.44350600	0.60781900	0.05533300
S	-0.04008600	-0.35442900	-1.57800300
S	-0.19306600	-0.87195200	1.41847500
P	3.15479600	-0.86596000	-0.20962400
P	-3.34867100	-0.64981900	0.19022000
O	2.40293500	2.58006500	-1.54118500
O	-0.27995300	3.10287400	1.04329300
O	2.44282300	1.50947800	2.66013700
O	-2.73185100	2.33490100	-1.91534100
C	1.93912100	1.75079900	-0.85615700
C	-0.48029500	2.01907000	0.62790700
C	1.96237200	1.11466200	1.66802400
C	-2.22340900	1.64593100	-1.11602200
C	-0.07396400	-2.16244700	-1.12276700
C	-0.28174300	-2.41766700	0.37961400
C	3.36142300	-2.57120300	0.54621700
C	-4.89244800	0.38992400	0.05435000
C	3.56836000	-1.19238700	-2.00539100
C	-3.77588600	-2.03255600	-1.00932800
C	4.74524600	-0.06076600	0.35787600
C	-3.62682900	-1.46563900	1.84540600
H	-2.82146000	-2.17336900	2.06765000
H	2.66084100	-3.27525900	0.08340000
H	-4.96854700	0.81511600	-0.95231900
H	3.14693300	-2.51763400	1.61967200
H	-4.83105400	1.21245200	0.77493000
H	4.48086100	-1.79576400	-2.09811800
H	-4.79759500	-2.39463100	-0.83429800
H	3.71601600	-0.23168200	-2.51146700
H	-3.07762200	-2.86847000	-0.89049200
H	2.73689300	-1.70750200	-2.49836400
H	-3.69607900	-1.65379500	-2.03471900
H	4.38453900	-2.94087200	0.39736300
H	-5.78373900	-0.21641500	0.25944200
H	5.61505000	-0.66846500	0.07654300
H	-4.59134800	-1.98888500	1.85864700
H	4.72661000	0.06338700	1.44647600
H	-3.61478900	-0.68860500	2.61724700
H	4.83279400	0.93048100	-0.10137000
H	-0.86981300	-2.62287700	-1.72134900
H	0.87834800	-2.58752800	-1.46329700
H	-1.26547100	-2.86579300	0.56760900
H	0.46999400	-3.11003400	0.77718000
H	-2.23500000	1.09938700	1.23929600

edt 3C1*

Fe	-1.47460400	-0.49456700	0.12684100
Fe	1.47665300	-0.49147400	0.29554400
S	-0.03323600	-2.26177600	0.36023400
S	0.08585200	0.03202000	-1.53711800
O	3.26777900	-1.87509600	2.13599500
C	0.74186100	0.60048200	1.52411000
C	-2.77749500	-1.34312900	-0.76523300
C	2.54363400	-1.29831900	1.42138700
C	0.10865600	-2.80287200	-1.41911700
C	0.18035100	-1.61953300	-2.40368500
H	-0.65338500	-1.64080300	-3.11583200
H	1.12504400	-1.62831500	-2.96006800
H	1.01025900	-3.42332300	-1.48113400
H	-0.76834500	-3.43166300	-1.61546000
O	-3.64090000	-1.94924500	-1.28369400
C	-2.09424400	-0.70537100	1.77112800
O	-2.55408800	-0.86857900	2.83843200
O	0.49082800	1.34354600	2.39865300
H	2.27045500	-1.35515500	-0.68846900
P	-2.48234000	1.50888900	-0.07769600
P	2.95533600	1.02016800	-0.41531200
C	-2.93726200	1.95444400	-1.83313500
H	-3.44707700	2.92598100	-1.86834700
H	-2.02794100	1.98916900	-2.44268300
H	-3.59891000	1.18063200	-2.23807300
C	-4.13482600	1.64590500	0.77975900
H	-3.99653300	1.55793700	1.86284700
H	-4.61082500	2.60767300	0.55004700
H	-4.78246200	0.82822300	0.44450200
C	-1.64354400	3.07888500	0.49622700
H	-0.70408900	3.20989900	-0.05116900
H	-2.29289000	3.94518500	0.31401500
H	-1.41642000	3.00594000	1.56451300
C	3.64660400	0.69955500	-2.11398700
H	4.32098900	1.50820100	-2.42378900
H	4.18888500	-0.25194500	-2.10464300
H	2.81250800	0.62386400	-2.82065900
C	4.49970200	1.23191900	0.60962800
H	5.15990600	1.98924700	0.16810400
H	4.22279100	1.53728800	1.62512900
H	5.03154400	0.27582400	0.66801400
C	2.35929900	2.78126500	-0.57383000
H	2.02744200	3.14536300	0.40480500
H	3.15919400	3.43055700	-0.95192900
H	1.51444600	2.80315100	-1.27108400

edt 3C2*

Fe	-1.45601300	-0.48309400	0.19627600
Fe	1.46849100	-0.36718900	0.53990400
S	-0.02874900	-2.09709100	1.00640300
S	0.20429100	-0.40511200	-1.45679400
O	3.66608200	-2.28870000	0.22004400
C	0.64784600	0.80833300	1.60430100
C	-2.66378500	-1.53822800	-0.60770400
C	2.75873200	-1.54664900	0.26078000
C	0.18099900	-3.10439500	-0.55397200
C	0.36427000	-2.23391300	-1.81450300
H	-0.39329800	-2.47026700	-2.57120300
H	1.35730000	-2.38170100	-2.25576500
H	1.04460200	-3.76237500	-0.39706000
H	-0.71870400	-3.72592300	-0.62729900
O	-3.46351900	-2.25482900	-1.08501600
C	-2.24813100	-0.32762400	1.76599500
O	-2.82378600	-0.24971900	2.78656300
O	0.34879900	1.59758700	2.42173200
H	2.17288100	-0.48618600	1.86521200
P	-2.43647100	1.42893300	-0.48216800
P	2.79839300	1.23886500	-0.25350600
C	-2.36311100	1.80515300	-2.30933000
H	-2.92797100	2.71790400	-2.53885300
H	-1.31923300	1.92345200	-2.61787200
H	-2.78749900	0.96069800	-2.86383400
C	-4.27797700	1.46496700	-0.17083000
H	-4.46732600	1.37155500	0.90429700
H	-4.71714600	2.40183100	-0.53718600
H	-4.74886800	0.61778500	-0.68131400
C	-1.92857900	3.06453200	0.26938300
H	-0.87574000	3.26281300	0.04668900
H	-2.54486700	3.87999700	-0.13148300
H	-2.04687000	3.01586700	1.35724200
C	3.68579100	0.82075900	-1.83769600
H	4.29102600	1.66875800	-2.18250500
H	4.33430800	-0.04749000	-1.67770700
H	2.93619500	0.56752800	-2.59603300
C	4.18397500	1.75479700	0.88036500
H	4.80111200	2.53929900	0.42376600
H	3.75757200	2.12334700	1.82013500
H	4.80744200	0.88171200	1.10265700
C	2.01173400	2.87376400	-0.68364600
H	1.56587200	3.31274600	0.21545800
H	2.75856300	3.56620400	-1.09229300
H	1.22750800	2.70439600	-1.42981800

edt 3D1*

Fe	-1.31008900	0.51803800	0.38539000
Fe	1.29829100	-0.20299700	-0.57084700
S	-0.58324800	0.41695300	-1.81117000
S	0.64240300	1.73845400	0.57710100
P	-2.78444800	-1.13375700	-0.09915200
P	3.21404700	-0.15252100	0.56911400
O	-1.51960600	0.10449600	3.28658500
O	0.35437900	-2.34004500	1.24825900
O	-3.22905100	2.78437900	0.31472100
O	2.14431500	-2.08827300	-2.63111800
C	-1.41642700	0.24682100	2.12536600
C	0.58185200	-1.41321300	0.55791800
C	-2.48470500	1.87588700	0.30512800
C	1.79874600	-1.35776900	-1.78410400
C	-0.14858400	2.20462400	-2.11481200
C	0.47238900	2.88748100	-0.88172500
C	-4.19813800	-0.56020700	-1.17406800
C	4.41033100	-1.54897400	0.25834700
C	-2.19897700	-2.63170300	-1.05355100
C	4.26709300	1.35453000	0.28037700
C	-3.67230800	-1.92899900	1.33519200
C	3.06009900	-0.17700000	2.42697100
H	2.43724200	0.66698900	2.74352500
H	-3.78596200	-0.15110000	-2.10326600
H	4.68964900	-1.56414700	-0.80094600
H	-4.75410200	0.23052200	-0.65883800
H	3.92583500	-2.50042400	0.50539500
H	-1.71041000	-2.30451600	-1.97829500
H	5.16869300	1.32539700	0.90556000
H	-3.05412800	-3.27378800	-1.30160500
H	3.67732700	2.24408800	0.52785700
H	-1.48119600	-3.19768600	-0.45180200
H	4.54957000	1.39824600	-0.77678600
H	-4.87480400	-1.39282400	-1.40639900
H	5.31250200	-1.43074500	0.87188700
H	-4.40690800	-2.66217700	0.97862000
H	4.04882100	-0.09981500	2.89680600
H	-4.18134200	-1.15647000	1.92223500
H	2.57771200	-1.10860000	2.74228500
H	-2.93899000	-2.42806700	1.97837200
H	0.54645900	2.21078600	-2.96205800
H	-1.08072700	2.69795400	-2.41585700
H	1.47962800	3.25862900	-1.10585000
H	-0.14543200	3.72532200	-0.53692400
H	2.08832000	0.73568900	-1.49018000

edt 3D2*

Fe	-1.25403100	0.12827300	0.57555900
Fe	1.29124800	0.14309100	-0.66277300
S	-0.58898700	1.43659800	-1.22994600
S	0.71144100	0.98291600	1.45360200
P	-2.86270200	-0.73556400	-0.76091600
P	3.02624900	-0.91365900	0.25618100
O	-1.35639400	-2.10317500	2.48673900
O	0.16404100	-2.55518000	-0.94591400
O	-3.05393200	1.88948700	2.14515500
O	3.09481600	2.07480300	-1.95453400
C	-1.29529500	-1.22573600	1.70765200
C	0.45906700	-1.43371200	-0.72827200
C	-2.36479100	1.21588900	1.47356200
C	2.37048100	1.36686500	-1.36395800
C	-0.17847600	3.02192200	-0.33093500
C	0.53126200	2.78893000	1.01743400
C	-4.22666200	0.48609600	-1.12389900
C	3.95891300	-2.06621900	-0.87191900
C	-2.42999500	-1.29869700	-2.49153800
C	4.36749400	0.18643700	0.93416500
C	-3.81254800	-2.20682000	-0.11787400
C	2.62906900	-1.99695100	1.71898500
H	2.15165100	-1.38731900	2.49431400
H	-3.78673200	1.36812300	-1.60277700
H	4.34553000	-1.49885200	-1.72581100
H	-4.70326600	0.79513100	-0.18729700
H	3.27007600	-2.83182600	-1.24563100
H	-1.88355900	-0.50009600	-3.00602900
H	5.16007200	-0.41310500	1.39927200
H	-3.34848200	-1.52908600	-3.04687000
H	3.92600700	0.85428300	1.68212600
H	-1.79682100	-2.18953300	-2.44516600
H	4.79399900	0.78984600	0.12565000
H	-4.97816400	0.04299600	-1.79008600
H	4.79117000	-2.54826800	-0.34312600
H	-4.61542600	-2.48176400	-0.81367600
H	3.54506600	-2.44857300	2.12057800
H	-4.24347100	-1.96595200	0.86032300
H	1.93444600	-2.78811200	1.41729900
H	-3.12790200	-3.05380300	0.00171500
H	0.44378800	3.61903400	-1.00845900
H	-1.13432700	3.53963100	-0.19069100
H	1.54535200	3.20634300	1.00641700
H	-0.02676200	3.25102800	1.84037000
H	1.51830100	-0.33499000	-2.07432900

$[\text{Fe}_2(\mu\text{-pdt})(\text{CO})_4(\text{PMe}_3)_2]^+$ systems

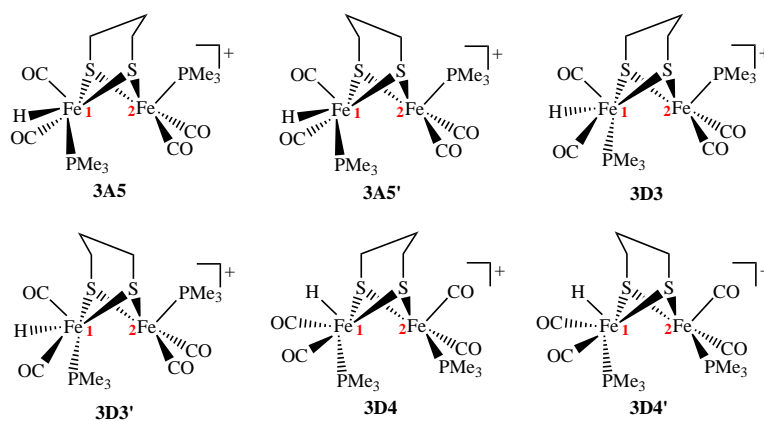


Figure A2: High energy isomers of $[\text{HFe}_2(\mu\text{-pdt})(\text{CO})_4(\text{PMe}_3)_2]^+$. Associated relative free energies and bond distances are reported in Table 3.7. Selected bond distances and bond angles are reported in Table A23 and Table A24, respectively.

Table A17: Selected bond distances of the unprotonated [$\text{Fe}_2(\mu\text{-pdt})(\text{CO})_4(\text{PMe}_3)_2$] from x-ray crystallography (in bold), compared to calculated values of all isomers and transition states inter-converting them.

Exp.	bond length/Å											
	Fe₁-Fe₂	Fe₁-S₁	Fe₁-S₂	Fe₂-S₁	Fe₂-S₂	Fe₁-CO₁	Fe₁-CO₂	Fe₂-CO₁	Fe₂-CO₂	Fe₁-P₁	Fe₂-P₂	
Exp.	2.557	2.320	2.320	2.317	2.317	1.762	1.771	1.642	1.696	2.273	2.279	
pdt 1A	2.5236	2.3086	2.3078	2.3033	2.2968	1.7563	1.7491	1.7547	1.7598	2.2386	2.2608	
pdt 1A'	2.5239	2.3183	2.3090	2.2919	2.2904	1.7547	1.7464	1.7528	1.7626	2.2392	2.2642	
pdt 1B	2.4892	2.3194	2.3144	2.3215	2.3281	1.7589	1.7561	1.7544	1.7556	2.2387	2.2409	
pdt 1C	2.5977	2.2834	2.2796	2.2944	2.2884	1.7507	1.7667	1.7515	1.7590	2.2592	2.2504	
pdt 1D	2.5662	2.2824	2.2852	2.2902	2.2899	1.7545	1.7537	1.7567	1.7513	2.2661	2.2668	
pdt 1D(B3LYP)	2.5632	2.3024	2.3031	2.3132	2.3149	1.7607	1.7643	1.7630	1.7594	2.2971	2.2932	
TS _{pdt 1A→1B}	2.5476	2.3130	2.3252	2.3337	2.3454	1.7628	1.7641	1.7450	1.7421	2.2393	2.2148	
TS _{pdt 1A→1C}	2.5717	2.3130	2.3320	2.3011	2.3144	1.7435	1.7380	1.7511	1.7672	2.2155	2.2684	
TS _{pdt 1A→1D}	2.5560	2.3352	2.3134	2.3109	2.3087	1.7426	1.7372	1.7510	1.7643	2.2145	2.2749	
TS _{pdt 1C→1D}	2.6739	2.3314	2.3354	2.2822	2.2833	1.7430	1.7417	1.7506	1.7551	2.2411	2.2681	
TS _{pdt 1C→1D-flip}	2.6828	2.3326	2.3339	2.2789	2.2710	1.7443	1.7430	1.7487	1.7611	2.2363	2.2803	
TS _{pdt 1A'→1C}	2.5529	2.3152	2.3337	2.3029	2.3045	1.7465	1.7398	1.7500	1.7681	2.2148	2.2805	
TS _{pdt 1A'→1D}	2.5554	2.3309	2.3171	2.3009	2.3105	1.7436	1.7411	1.7495	1.7660	2.2158	2.2738	
TS _{pdt 1A'→1B}	2.5445	2.3192	2.3285	2.3283	2.3445	1.7614	1.7607	1.7448	1.7421	2.2427	2.2136	
TS _{pdt 1A→1A'}	2.5437	2.2924	2.2870	2.2735	2.2748	1.7579	1.7493	1.7535	1.7625	2.2319	2.2620	
TS _{pdt 1B→1B}	2.5076	2.2981	2.3001	2.2981	2.3001	1.7585	1.7576	1.7585	1.7576	2.2338	2.2338	
TS _{pdt 1C→1C}	2.6281	2.2638	2.2613	2.2627	2.2639	1.7512	1.7658	1.7519	1.7664	2.2519	2.2628	
TS _{pdt 1D→1D}	2.5926	2.2625	2.2698	2.2686	2.2635	1.7556	1.7541	1.7556	1.7539	2.2659	2.2630	

Table A18: Selected bond angles of the unprotonated $[Fe_2(\mu\text{-pdt})(CO)_4(PMe_3)_2]$ from x-ray crystallography (in bold)[], compared to calculated values of all isomers and transition states inter-converting them.

Exp.	bond angle/°					
	$\angle S_1-Fe_1-S_2$	$\angle S_1-Fe_2-S_2$	$\angle Fe_1-S_1-Fe_2$	$\angle Fe_1-S_2-Fe_2$	$\angle L-Fe_1-Fe_2-L$	
	83.98	83.98	68.23	68.25	4.56	
pdt 1A	85.0185	85.3939	66.3494	66.4670	22.7418	
pdt 1A'	84.8972	85.9316	66.3838	66.5625	18.5125	
pdt 1B	85.2642	84.9073	64.8702	64.8463	14.5498	
pdt 1C	86.0129	85.5510	69.1438	69.3156	27.0657	
pdt 1D	85.2335	84.9451	68.2801	68.2377	6.8054	
pdt 1D (B3LYP)	85.2419	84.7292	67.4659	67.4253	14.0045	
TS _{pdt 1A→1B}	85.9943	85.0642	66.4945	66.1105	88.4103	
TS _{pdt 1A→1C}	84.9915	85.6665	67.7455	67.2104	84.1912	
TS _{pdt 1A→1D}	84.7557	85.4139	66.7519	67.1465	97.4949	
TS _{pdt 1C→1D}	84.8827	87.2295	70.8308	70.7409	101.6426	
TS _{pdt 1C→1D-flip}	84.9657	87.6848	71.1400	71.2528	90.2404	
TS _{pdt 1A'→1C}	85.5835	86.5419	67.1197	66.7870	96.8122	
TS _{pdt 1A'→1D}	85.5888	86.4352	66.9632	67.0367	101.5902	
TS _{pdt 1A'→1B}	85.3567	84.7886	66.3911	65.9825	91.0329	
TS _{pdt 1A→1A'}	84.1156	84.8251	67.7118	67.7830	15.4374	
TS _{pdt 1B→1B}	84.2225	84.2231	66.1288	66.0647	0.0284	
TS _{pdt 1C→1C}	85.0418	85.0062	70.9856	71.0066	11.2467	
TS _{pdt 1D→1D}	84.4015	84.4075	69.8057	69.7663	4.0411	

Table A19: Calculated gas phase and solvent corrected free energies and Fe Mulliken charges for isomers of $[(\mu\text{-H})\text{Fe}_2(\mu\text{-pdt})(\text{CO})_4(\text{PMe}_3)_2]^+$ and the transition states that connect them; either through rotation of the $\text{Fe}(\text{CO})_2(\text{PMe}_3)$ moiety or by the pdt bridge flip. Calculations using the B3LYP functional were carried out by Liu. [118]

Isomer	B3LYP		TPSS			
	Free Energies / kcal/mol				Mulliken charges	
	ΔG_g	ΔG_{solv}	ΔG_g	ΔG_{solv}	Fe ₁	Fe ₂
pdt 2A	4.8	5.2	4.9	5.3	-1.278	-0.148
pdt 2A'	3.7	6.4	5.0	6.0	-1.231	-0.073
pdt 2B	10.4	9.5	11.2	10.5	-0.811	-0.860
pdt 2C	3.0	3.2	4.9	6.4	-0.741	-0.481
pdt 2D	0.0	0.0	0.0	0.0	-0.654	-0.649
TS_{pdt 2A→2B}	"	"	29.2	28.7	-0.911	-0.667
TS_{pdt 2A→2C}	"	"	27.2	27.1	-0.497	-0.734
TS_{pdt 2A→2D}	"	"	25.1	26.2	-0.487	-0.607
TS_{pdt 2C→2D}	24.3	25.5	28.2	28.9	0.210	-1.139
TS_{pdt 2C→2D-flipped}	"	"	25.4	26.1	0.238	-1.045
TS_{pdt 2A'→2C}	20.4	21.9	25.2	25.2	-0.401	-0.668
TS_{pdt 2A'→2D}	20.1	21.0	23.0	24.1	-0.367	-0.539
TS_{pdt 2A'→2B}	28.2	29.0	31.3	31.9	-0.949	-0.215
TS_{pdt 2A→2A'}	3.9	4.2	12.0	12.3	-1.217	-0.054
TS_{pdt 2B→2B}	"	"	18.4	17.2	-0.743	-0.743
TS_{pdt 2C→2C}	"	"	11.7	12.4	-0.680	-0.566
TS_{pdt 2D→2D}	"	"	7.8	9.8	-0.539	-0.539

" data unavailable

Table A20: Selected bond distances of bridging hydride isomers of $[(\mu\text{-H})\text{Fe}_2(\mu\text{-pdt})(\text{CO})_4(\text{PMe}_3)_2]^+$ from x-ray crystallography (in bold), compared to calculated values of all isomers and transition states inter-converting them.

	bond length/Å												
	Fe₁-Fe₂	Fe₁-S₁	Fe₁-S₂	Fe₂-S₁	Fe₂-S₂	Fe₁-H	Fe₂-H	Fe₁-CO₁	Fe₁-CO₂	Fe₂-CO₁	Fe₂-CO₂	Fe₁-P₁	Fe₂-P₂
Exp.	2.578	2.265	2.265	2.265	2.292	1.710	1.711	1.782	1.776	1.775	1.781	2.251	2.254
pdt 2A	2.5864	2.3141	2.3299	2.3196	2.3107	1.6547	1.6610	1.7770	1.7759	1.7649	1.7778	2.2781	2.2972
pdt 2A'	2.5880	2.3256	2.3217	2.3094	2.3076	1.6719	1.6540	1.7785	1.7730	1.7632	1.7781	2.2743	2.2942
pdt 2B	2.5796	2.3330	2.3188	2.3272	2.3328	1.6442	1.6559	1.7808	1.7774	1.7772	1.7782	2.2809	2.2770
pdt 2C	2.6094	2.3000	2.3007	2.3007	2.3081	1.6815	1.6988	1.7608	1.7810	1.7627	1.7794	2.2960	2.3000
pdt 2D	2.6046	2.3022	2.3024	2.3069	2.3052	1.6778	1.6957	1.7610	1.7750	1.7624	1.7743	2.2959	2.2954
TS _{pdt 2A→2B}	2.6399	2.3056	2.3213	2.3954	2.3779	1.6369	1.6927	1.7798	1.7813	1.7574	1.7465	2.2785	2.2572
TS _{pdt 2A→2C}	2.6474	2.3734	2.3737	2.2966	2.3098	1.7022	1.6492	1.7554	1.7438	1.7673	1.7783	2.2577	2.2920
TS _{pdt 2A→2D}	2.6368	2.3660	2.3746	2.3056	2.3065	1.6969	1.6476	1.7543	1.7437	1.7677	1.7748	2.2607	2.2941
TS _{pdt 2C→2D}	2.6790	2.3712	2.3762	2.2956	2.3062	1.7188	1.6816	1.7521	1.7469	1.7678	1.7738	2.2503	2.2971
TS _{pdt 2C→2D-flipped}	2.6826	2.3742	2.3787	2.2928	2.2976	1.7310	1.6767	1.7524	1.7472	1.7661	1.7766	2.2480	2.3009
TS _{pdt 2A'→2C}	2.6513	2.3795	2.3714	2.2900	2.3033	1.7221	1.6466	1.7561	1.7429	1.7659	1.7794	2.2574	2.2936
TS _{pdt 2A'→2D}	2.6428	2.3652	2.3813	2.2972	2.2965	1.7166	1.6441	1.7548	1.7427	1.7661	1.7769	2.2599	2.2928
TS _{pdt 2A'→2B}	2.6366	2.3188	2.3205	2.3853	2.3739	1.6424	1.6786	1.7775	1.7760	1.7554	1.7471	2.2814	2.2596
TS _{pdt 2A→2A'}	2.6000	2.3000	2.3040	2.2943	2.2920	1.6749	1.6628	1.7789	1.7767	1.7631	1.7788	2.2678	2.2930
TS _{pdt 2B→2B}	2.5943	2.3114	2.3082	2.3114	2.3083	1.6566	1.6566	1.7806	1.7789	1.7806	1.7789	2.2746	2.2746
TS _{pdt 2C→2C}	2.6257	2.2811	2.2844	2.2832	2.2809	1.6993	1.6994	1.7609	1.7816	1.7611	1.7816	2.2946	2.2957
TS _{pdt 2D→2D}	2.6142	2.2839	2.2865	2.2864	2.2839	1.6871	1.6871	1.7621	1.7758	1.7621	1.7758	2.2935	2.2935

Table A21: Selected bond angles of the bridging hydride isomers of $[(\mu\text{-H})\text{Fe}_2(\mu\text{-pdt})(\text{CO})_4(\text{PMe}_3)_2]$ from x-ray crystallography (in bold)], compared to calculated values of all isomers and transition states inter-converting them.

Exp.	bond angle/°					
	$\angle \text{S}_1\text{-Fe}_1\text{-S}_2$	$\angle \text{S}_1\text{-Fe}_2\text{-S}_2$	$\angle \text{Fe}_1\text{-S}_1\text{-Fe}_2$	$\angle \text{Fe}_1\text{-S}_2\text{-Fe}_2$	$\angle \text{L-Fe}_1\text{-Fe}_2\text{-L}$	
Exp.	85.09	84.46	69.39	68.91	4.30	
pdt 2A	84.1861	84.4943	67.8579	67.7414	14.5862	
pdt 2A'	84.4150	85.0997	67.8819	67.9775	6.6244	
pdt 2B	84.0839	83.9049	67.2206	67.3613	8.9116	
pdt 2C	85.3908	85.2054	69.1085	68.9684	0.1922	
pdt 2D	85.6130	85.4393	68.8170	68.8412	0.6656	
TS _{pdt 2A→2B}	85.9210	82.6900	68.2981	68.3464	73.7757	
TS _{pdt 2A→2C}	82.6384	85.7506	69.0462	68.8249	75.3314	
TS _{pdt 2A→2D}	82.5639	85.3993	68.7105	68.5485	78.6349	
TS _{pdt 2C→2D}	83.4566	86.7333	70.0434	69.7797	81.3508	
TS _{pdt 2C→2D-flipped}	83.9045	87.6052	70.1475	69.9881	70.9578	
TS _{pdt 2A'→2C}	83.4216	86.9764	69.1631	69.0880	76.3313	
TS _{pdt 2A'→2D}	83.1198	86.5453	69.0411	68.7699	77.5099	
TS _{pdt 2A'→2B}	85.0050	82.3843	68.1642	68.3291	80.7233	
TS _{pdt 2A→2A'}	83.9046	84.3009	68.9324	68.9029	10.0152	
TS _{pdt 2B→2B}	83.3662	83.3662	68.2771	68.3830	0.0044	
TS _{pdt 2C→2C}	85.1266	85.1589	70.2794	70.1782	1.5078	
TS _{pdt 2D→2D}	84.6588	84.6613	69.7806	69.7801	4.5652	

Table A22: Calculated gas phase and solvent corrected free energies, Fe–Fe bond lengths, and Fe Mulliken charges of the terminal hydride isomers of $[HFe_2(\mu\text{-pdt})(CO)_4(PMe_3)_2]^+$. Energies are reported relative to the **2D** isomer.

Isomer	Free Energies / kcal/mol		Mulliken charges	
	ΔG_g	ΔG_{solv}	Fe ₁	Fe ₂
pdt 3A1	21.6	21.0	-1.262	-0.444
pdt 3A1'	20.2	20.3	-1.139	-0.470
pdt 3A2	21.1	20.3	-1.196	-0.570
pdt 3A2'	19.4	19.5	-1.129	-0.629
pdt 3A3	17.1	16.8	-0.632	-1.065
pdt 3A3'	17.6	18.4	-0.582	-1.257
pdt 3A4	21.2	20.9	-0.646	-0.916
pdt 3A4'	20.4	21.0	-0.585	-0.938
pdt 3B	26.2	25.0	-1.155	-0.634
pdt 3B'	25.7	25.4	-1.186	-0.524
pdt 3C1	17.3	16.6	-1.381	-0.494
pdt 3C1'	15.6	15.1	-1.165	-0.520
pdt 3C2	21.2	21.6	-0.667	-0.539
pdt 3C2'	20.8	21.3	-0.445	-0.666
pdt -3D1	13.6	14.4	-1.404	-0.487
pdt 3D1'	12.0	12.7	-1.191	-0.466
pdt 3D2	16.1	17.1	-1.181	-0.617
pdt 3D2'	15.9	17.2	-1.149	-0.630

Table A23: Selected bond distances of the terminal hydride isomers of $[Fe_2(\mu\text{-pdt})(CO)_4(PMe_3)_2]^+$.

	bond length/Å													
	Fe ₁ -Fe ₂	Fe ₁ -S ₁	Fe ₁ -S ₂	Fe ₂ -S ₁	Fe ₂ -S ₂	Fe-H	Fe ₁ -CO ₁	Fe ₁ -CO ₂	Fe ₂ -CO ₁	Fe ₂ -CO ₂	Fe-C _{semi}	Fe ₁ -P ₁	Fe ₂ -P ₂	
pdt 3A1	2.5428	2.3295	2.3213	2.3122	2.3031	1.5060	1.7732	1.7920	1.7565	1.7856	2.3121	2.2660	2.3275	
pdt 3A1'	2.5243	2.3209	2.3268	2.3216	2.3080	1.5011	1.7702	1.8162	1.7601	1.7878	2.2096	2.2626	2.3280	
pdt 3A2	2.5525	2.3204	2.3325	2.3059	2.3064	1.5024	1.7704	1.7907	1.7536	1.7867	2.3430	2.2701	2.3135	
pdt 3A2'	2.5380	2.3218	2.3308	2.3083	2.3185	1.4982	1.7676	1.8107	1.7561	1.7864	2.2454	2.2675	2.3108	
pdt 3A3	2.5622	2.3022	2.2970	2.3181	2.3237	1.5135	1.7884	1.7821	1.7686	1.8022	2.4450	2.2614	2.2727	
pdt 3A3'	2.5752	2.2906	2.2999	2.3172	2.3178	1.5156	1.7839	1.7817	1.7705	1.8015	2.5315	2.2555	2.2750	
pdt 3A4	2.5531	2.3083	2.3023	2.3141	2.3354	1.5006	1.7884	1.7788	1.7750	1.7811	2.4501	2.2612	2.2830	
pdt 3A4'	2.5696	2.2968	2.2974	2.3256	2.3236	1.5035	1.7838	1.7774	1.7760	1.7777	2.5802	2.2554	2.2824	
pdt 3B	2.5379	2.3365	2.3392	2.3305	2.3173	1.4972	1.7719	1.7986	1.7876	1.7832	2.3106	2.2727	2.2802	
pdt 3B'	2.5518	2.3307	2.3382	2.3244	2.3131	1.5014	1.7751	1.7858	1.7842	1.7819	2.4097	2.2761	2.2728	
pdt 3C1	2.5833	2.3142	2.2982	2.2936	2.2715	1.5135	1.7740	1.8009	1.7488	1.7873	2.5297	2.2749	2.3232	
pdt 3C1'	2.5665	2.3204	2.2937	2.2898	2.2799	1.5131	1.7723	1.8076	1.7492	1.7904	2.4233	2.2724	2.3259	
pdt 3C2	2.6129	2.3149	2.3119	2.2835	2.2797	1.5046	1.7766	1.7782	1.7446	1.7885	2.6095	2.2823	2.3183	
pdt 3C2'	2.5827	2.3231	2.3016	2.2961	2.2860	1.5028	1.7750	1.7858	1.7459	1.7911	2.4452	2.2767	2.3238	
pdt 3D1	2.5714	2.3064	2.3068	2.2750	2.2915	1.5145	1.7707	1.7980	1.7486	1.7857	2.4868	2.2746	2.3194	
pdt 3D1'	2.5559	2.3041	2.3099	2.2809	2.2945	1.5130	1.7692	1.8050	1.7501	1.7864	2.3937	2.2762	2.3167	
pdt 3D2	2.5556	2.3185	2.3132	2.2799	2.2935	1.5062	1.7771	1.7736	1.7497	1.7822	2.4962	2.2801	2.3316	
pdt 3D2'	2.5366	2.3088	2.3203	2.2859	2.3019	1.5040	1.7739	1.7862	1.7515	1.7846	2.3637	2.2805	2.3274	

Table A24: Selected bond angles of the terminal hydride isomers of $[Fe_2(\mu\text{-pdt})(CO)_4(PMe_3)_2]^+$.

	bond angle/ $^\circ$									
	$\angle S_1\text{-Fe}_1\text{-S}_2$	$\angle S_1\text{-Fe}_2\text{-S}_2$	$\angle Fe_1\text{-S}_1\text{-Fe}_2$	$\angle Fe_1\text{-S}_2\text{-Fe}_2$	$\angle L\text{-Fe}_1\text{-Fe}_2\text{-L}$	$\angle Fe\text{-Fe-C}_{semi}$	$\angle Fe\text{-C-O}_{semi}$			
pdt 3A1	85.0276	85.8385	66.4336	66.7134	35.9961	61.6243	157.5975			
pdt 3A1'	85.8928	86.3120	65.8771	65.9983	30.6584	58.5178	152.9164			
pdt 3A2	85.0448	85.9705	66.9712	66.7636	33.9449	62.4222	158.9690			
pdt 3A2'	85.8462	86.4437	66.4788	66.1706	33.8784	59.4044	154.7380			
pdt 3A3	85.6055	84.6350	67.3588	67.3522	2.2874	65.4651	162.7772			
pdt 3A3'	86.1361	85.1116	67.9537	67.7899	1.3530	68.0484	165.7164			
pdt 3A4	85.9639	85.0730	67.0540	66.7986	32.9405	66.0795	163.4776			
pdt 3A4'	86.7359	85.4630	67.5434	67.5683	17.6589	70.1258	167.0295			
pdt 3B	84.8464	85.4755	65.8855	66.0522	38.8046	61.6364	158.0145			
pdt 3B'	84.8348	85.5438	66.4849	66.5438	33.8045	64.7031	161.7880			
pdt 3C1	85.7549	86.8619	68.1989	68.8468	6.0133	67.7880	165.0586			
pdt 3C1'	85.8625	86.9037	67.6503	68.2710	1.5170	64.5865	161.6065			
pdt 3C2	85.7463	87.2381	69.2488	69.3666	15.0355	69.9890	166.1374			
pdt 3C2'	86.0721	87.0746	67.9877	68.5230	28.6258	65.1233	161.8506			
pdt 3D1	85.4296	86.5137	68.2825	68.0000	0.4506	66.6799	164.3655			
pdt 3D1'	85.6114	86.5098	67.7561	67.4340	0.4830	63.8877	161.0271			
pdt 3D2	85.5892	86.9523	67.5215	67.3877	23.5262	67.6573	164.7534			
pdt 3D2'	85.8737	86.8385	67.0157	66.5666	29.0133	63.5399	160.4680			

Table A25: Calculated gas phase and solvent corrected free energies and Fe Mulliken charges for the singly reduced isomers of $[\text{Fe}_2(\mu\text{-pdt})(\text{CO})_4(\text{PMe}_3)_2]$ and the transition states that connect them; either through rotation of the $\text{Fe}(\text{CO})_2(\text{PMe}_3)$ moiety or by the pdt bridge flip.

Isomer	Free Energies / kcal/mol		Mulliken charges	
	ΔG_g	ΔG_{solv}	Fe ₁	Fe ₂
pdt 2A*	3.7	4.1	-1.258	-0.118
pdt 2A'*	2.5	4.3	-1.144	-0.060
pdt 2B*	8.5	7.9	-0.797	-0.835
pdt 2C*	4.8	4.9	-0.661	-0.384
pdt 2D*	0.0	0.0	-0.597	-0.471
TS_{pdt 2A*→2B*}	22.7	21.7	-1.117	-0.391
TS_{pdt 2A*→2C*}	18.0	18.4	-0.527	-0.794
TS_{pdt 2A*→2D*}	18.0	19.2	-0.550	-0.755
TS_{pdt 2C*→2D*}	17.9	19.1	-0.021	-1.023
TS_{pdt 2C*→2D-flipped*}	14.9	16.0	-1.096	0.006
TS_{pdt 2A'→2C*}	14.8	15.1	-0.456	-0.781
TS_{pdt 2A'→2D*}	14.0	15.0	-0.499	-0.717
TS_{pdt 2A'→2B*}	24.6	24.2	-0.942	-0.261
TS_{pdt 2A*→2A'*}	11.6	12.1	-1.169	-0.063
TS_{pdt 2B*→2B*}	17.5	16.0	-0.731	-0.731
TS_{pdt 2C*→2C*}	12.5	12.8	-0.578	-0.483
TS_{pdt 2D*→2D*}	8.1	8.3	-0.564	-0.564

Table A26: Selected bond distances of the singly reduced isomers of $[(\mu-H)Fe_2(\mu-pdt)(CO)_4(PMe_3)_2]$ and transition states inter-converting them.

	bond length/Å												
	Fe ₁ -Fe ₂	Fe ₁ -S ₁	Fe ₁ -S ₂	Fe ₂ -S ₁	Fe ₂ -S ₂	Fe ₁ -H	Fe ₂ -H	Fe ₁ -CO ₁	Fe ₁ -CO ₂	Fe ₂ -CO ₁	Fe ₂ -CO ₂	Fe ₁ -P ₁	Fe ₂ -P ₂
pdt 2A*	2.7328	2.3631	2.3577	2.3641	2.3641	1.6850	1.6625	1.7601	1.7568	1.7910	1.7555	2.3555	2.2546
pdt 2A**	2.7311	2.3699	2.3558	2.3505	2.3620	1.7256	1.6390	1.7619	1.7580	1.7855	1.7552	2.3558	2.2519
pdt 2B*	2.7167	2.3700	2.3663	2.3640	2.3806	1.6454	1.6739	1.7603	1.7592	1.7607	1.7609	2.3372	2.3409
pdt 2C*	2.7709	2.3303	2.3620	2.3323	2.3749	1.6955	1.7274	1.7887	1.7593	1.7973	1.7579	2.2499	2.2547
pdt 2D*	2.7577	2.3631	2.3350	2.3407	2.3694	1.6817	1.7310	1.7893	1.7536	1.7959	1.7539	2.2513	2.2541
TS _{pdt 2A*→2B*}	3.1370	2.3566	2.3680	2.4172	2.3724	1.5079	2.4198	1.7517	1.7559	1.7542	1.7993	2.3319	2.2636
TS _{pdt 2A*→2C*}	3.2500	2.3767	2.3606	2.3466	2.3706	2.6511	1.5300	1.7548	1.7931	1.7865	1.7470	2.2650	2.2392
TS _{pdt 2A*→2D*}	3.2540	2.3474	2.3851	2.3518	2.3733	2.6604	1.5277	1.7557	1.7956	1.7870	1.7473	2.2640	2.2345
TS _{pdt 2C*→2D*}	3.3261	2.3713	2.3674	2.3499	2.3640	2.7946	1.5380	1.7552	1.7664	1.7838	1.7479	2.3042	2.2430
TS _{pdt 2C*→2D-flipped*}	3.2801	2.3481	2.3512	2.3564	2.3911	1.5380	2.7686	1.7815	1.7532	1.7686	1.7559	2.2471	2.2981
TS _{pdt 2A**→2C*}	3.1776	2.3932	2.3586	2.3356	2.3693	2.6137	1.5325	1.7545	1.7912	1.7831	1.7477	2.2745	2.2403
TS _{pdt 2A**→2D*}	3.1743	2.3457	2.4083	2.3463	2.3613	2.6002	1.5299	1.7556	1.7931	1.7840	1.7493	2.2717	2.2358
TS _{pdt 2A**→2B*}	2.8395	2.3557	2.3659	2.4092	2.4154	1.5973	1.8150	1.7577	1.7576	1.7465	1.7750	2.3389	2.2411
TS _{pdt 2A*→2A**}	2.7554	2.3453	2.3310	2.3305	2.3432	1.7283	1.6541	1.7624	1.7589	1.7865	1.7561	2.3399	2.2509
TS _{pdt 2B*→2B*}	2.7371	2.3472	2.3516	2.3472	2.3516	1.6682	1.6682	1.7612	1.7608	1.7612	1.7608	2.3271	2.3271
TS _{pdt 2C*→2C*}	2.8053	2.3051	2.3433	2.3074	2.3414	1.7387	1.7170	1.7909	1.7615	1.7926	1.7596	2.2468	2.2505
TS _{pdt 2D*→2D*}	2.7854	2.3118	2.3408	2.3408	2.3118	1.7188	1.7189	1.7917	1.7558	1.7917	1.7558	2.2515	2.2515

Table A27: Selected bond angles of the unprotonated singly reduced isomers of $[(\mu-H)Fe_2(\mu-pdt)(CO)_4(PMe_3)_2]$ and transition states inter-converting them.

	bond angle/°					
	$\angle S_1-Fe_1-S_2$	$\angle S_1-Fe_2-S_2$	$\angle Fe_1-S_1-Fe_2$	$\angle Fe_1-S_2-Fe_2$	$\angle L-Fe_1-Fe_2-L$	
pdt 2A*	84.7551	84.5940	70.6345	70.7270	15.4650	
pdt 2A**	84.8311	85.1227	70.6989	70.7433	6.6838	
pdt 2B*	84.7371	84.5551	70.0428	69.8242	9.1107	
pdt 2C*	85.3204	84.9817	72.9227	71.6000	1.6507	
pdt 2D*	85.7356	85.4654	71.7838	71.7723	2.0621	
TS _{pdt 2A*→2B*}	82.7157	81.3474	82.1525	82.8667	85.0785	
TS _{pdt 2A*→2C*}	80.2504	80.6606	86.9552	86.7770	64.4256	
TS _{pdt 2A*→2D*}	80.2354	80.3899	87.6487	86.2892	66.2326	
TS _{pdt 2C*→2D*}	80.1356	80.6433	89.5764	89.3321	68.3658	
TS _{pdt 2C*→2D-flipped*}	81.4587	80.4590	88.4082	87.5207	61.3244	
TS _{pdt 2A*→2C*}	81.3434	82.3283	84.4283	84.4566	67.6057	
TS _{pdt 2A*→2D*}	81.2673	82.2524	85.1470	83.4391	68.2903	
TS _{pdt 2A*→2B*}	84.8864	82.6699	73.1459	72.8562	78.0307	
TS _{pdt 2A*→2A**}	84.2121	84.2689	72.2119	72.2416	10.5907	
TS _{pdt 2B*→2B*}	83.7305	83.7305	71.3293	71.1760	0.0000	
TS _{pdt 2C*→2C*}	84.9073	84.8999	74.9172	73.5710	3.7416	
TS _{pdt 2D*→2D*}	85.1863	85.1865	73.5484	73.5485	3.0200	

Table A28: Calculated gas phase and solvent corrected free energies, Fe–Fe bond lengths, and Fe Mulliken charges of the singly reduced isomers of $[(H)Fe_2(\mu\text{-pdt})(CO)_4(PMe_3)_2]$. Energies are reported relative to the reduced **2D** isomer.

Isomer	Free Energies / kcal/mol		bond length / Å		Mulliken charges	
	ΔG_g	ΔG_{solv}	Fe ₁	Fe ₂	Fe ₁	Fe ₂
pdt 3A1*	17.1	15.5	-0.436	-1.481		
pdt 3A1**	14.7	14.1	-0.440	-1.315		
pdt 3A2*	16.2	14.4	-0.524	-1.388		
pdt 3A2**	13.9	13.5	-0.601	-1.212		
pdt 3A3*	11.0	10.3	-1.067	-0.585		
pdt 3A3**	8.6	9.5	-1.224	-0.461		
pdt 3A4*	14.4	14.0	-0.942	-0.603		
pdt 3A4**	12.3	13.1	-1.033	-0.460		
pdt 3B*	19.8	17.6	-1.273	-0.682		
pdt 3B**	19.7	17.8	-1.318	-0.483		
pdt 3C1*	9.9	9.3	-1.378	-0.371		
pdt 3C1**	10.5	9.9	-1.123	-0.440		
pdt 3C2*	13.6	13.4	-0.892	-0.383		
pdt 3C2**	14.0	14.1	-0.615	-0.523		
pdt 3D1*	7.2	7.6	-1.358	-0.395		
pdt 3D1**	7.3	7.6	-1.142	-0.397		
pdt 3D2*	10.8	11.4	-1.082	-0.448		
pdt 3D2**	11.0	11.8	-1.137	-0.608		

Table A29: Selected bond distances of the singly reduced terminal hydride isomers of $[(H)Fe_2(\mu-pdt)(CO)_4(PMe_3)_2]^{+}$.

	bond length/Å													
	Fe ₁ -Fe ₂	Fe ₁ -S ₁	Fe ₁ -S ₂	Fe ₂ -S ₁	Fe ₂ -S ₂	Fe-H	Fe ₁ -CO ₁	Fe ₁ -CO ₂	Fe ₂ -CO ₁	Fe ₂ -CO ₂	Fe-CO _{semi}	Fe ₁ -P ₁	Fe ₂ -P ₂	
pdt 3A1*	2.7014	2.3670	2.3483	2.3844	2.3435	1.5141	1.7911	1.7648	1.7468	1.8171	2.2505	2.2801	2.3019	
pdt 3A1**	2.6728	2.3699	2.3612	2.3850	2.3387	1.5103	1.7889	1.7649	1.7456	1.8467	2.1417	2.2780	2.3085	
pdt 3A2*	2.7069	2.3664	2.3479	2.3546	2.3724	1.5082	1.7893	1.7611	1.7457	1.8131	2.2802	2.2789	2.3060	
pdt 3A2**	2.6807	2.3799	2.3475	2.3541	2.3724	1.5053	1.7871	1.7607	1.7443	1.8409	2.1690	2.2735	2.3102	
pdt 3A3*	2.8345	2.3761	2.3453	2.3391	2.3340	1.5261	1.7464	1.8098	1.7641	1.7669	2.6502	2.2365	2.3445	
pdt 3A3**	2.8479	2.3696	2.3492	2.3440	2.3361	1.5308	1.7468	1.8042	1.7641	1.7661	2.7270	2.2365	2.3366	
pdt 3A4*	2.7893	2.3979	2.3453	2.3492	2.3460	1.5001	1.7700	1.7938	1.7643	1.7658	2.5810	2.2367	2.3409	
pdt 3A4**	2.8167	2.3853	2.3568	2.3467	2.3434	1.5035	1.7677	1.7855	1.7634	1.7646	2.7230	2.2365	2.3351	
pdt 3B*	2.6969	2.3766	2.3696	2.3699	2.3664	1.5040	1.7481	1.8216	1.7667	1.7695	2.2538	2.2945	2.3661	
pdt 3B**	2.7659	2.3816	2.3736	2.3604	2.3539	1.5085	1.7510	1.7918	1.7652	1.7693	2.4734	2.2857	2.3462	
pdt 3C1*	2.9679	2.3654	2.3352	2.3659	2.2988	1.5288	1.7494	1.7975	1.7907	1.7685	2.8984	2.2385	2.2566	
pdt 3C1**	2.9450	2.3724	2.3298	2.3555	2.2946	1.5245	1.7482	1.8039	1.7870	1.7694	2.8079	2.2394	2.2615	
pdt 3C2*	2.9570	2.3662	2.3441	2.3778	2.3032	1.5070	1.7667	1.7840	1.7902	1.7665	2.8906	2.2378	2.2531	
pdt 3C2**	2.9278	2.3764	2.3394	2.3650	2.3086	1.5040	1.7712	1.7907	1.7864	1.7672	2.7569	2.2375	2.2579	
pdt 3D1*	2.8922	2.3434	2.3571	2.3349	2.3256	1.5303	1.7482	1.7989	1.7952	1.7629	2.7817	2.2371	2.2686	
pdt 3D1**	2.8712	2.3461	2.3571	2.3309	2.3235	1.5277	1.7482	1.8068	1.7919	1.7636	2.6808	2.2358	2.2692	
pdt 3D2*	2.8722	2.3545	2.3645	2.3500	2.3213	1.5073	1.7706	1.7807	1.7919	1.7653	2.7805	2.2365	2.2606	
pdt 3D2**	2.7164	2.3544	2.3559	2.3468	2.3500	1.5050	1.7810	1.8156	1.7907	1.7634	2.3397	2.2296	2.2736	

Table A30: Selected bond angles of the singly reduced terminal hydride isomers of $[(H)Fe_2(\mu-pdt)(CO)_4(PMe_3)_2]^+$.

	bond angle/°							
	$\angle S_1-Fe_1-S_2$	$\angle S_1-Fe_2-S_2$	$\angle Fe_1-S_1-Fe_2$	$\angle Fe_1-S_2-Fe_2$	$\angle L-Fe_1-Fe_2-L$	$\angle Fe-Fe-C_{semi}$	$\angle Fe-C-O_{semi}$	
pdt 3A1*	85.8581	85.5715	69.2963	70.3070	29.7196	55.6843	151.7568	
pdt 3A1**	86.4673	86.6303	68.4019	69.3150	25.9624	52.8104	147.4581	
pdt 3A2*	85.9512	85.6648	69.9710	69.9804	29.5870	56.5158	152.8013	
pdt 3A2**	86.5049	86.5269	68.9782	69.2157	29.3514	53.5025	148.3900	
pdt 3A3*	83.7555	84.7768	73.8963	74.5269	4.5921	65.3089	164.9658	
pdt 3A3**	84.3560	85.2197	74.3392	74.8665	2.3159	67.5208	167.2883	
pdt 3A4*	84.3279	85.4020	71.9637	72.9631	29.1449	64.3203	163.0499	
pdt 3A4**	84.6272	85.7909	73.0563	73.6372	16.1183	68.3738	166.4890	
pdt 3B*	85.5388	85.7607	69.2460	69.4219	34.7978	55.8765	152.7757	
pdt 3B**	84.4223	85.3276	71.3600	71.6139	29.9154	61.4112	160.0344	
pdt 3C1*	83.6798	84.4623	77.7018	79.6502	11.1111	70.0586	169.2725	
pdt 3C1**	83.4346	84.5796	77.0545	79.1072	4.6157	67.6362	167.3945	
pdt 3C2*	83.8945	84.5260	77.1162	84.5260	9.5633	70.2192	167.6290	
pdt 3C2**	83.9065	84.8354	76.2666	78.0842	18.3619	66.5180	165.0406	
pdt 3D1*	83.9776	84.8653	76.3723	76.2857	2.3735	68.2064	167.3952	
pdt 3D1**	83.8696	84.9533	75.7434	75.6712	1.2738	65.3857	164.7762	
pdt 3D2*	84.3538	85.4165	75.2528	75.5989	25.2939	68.8600	166.4235	
pdt 3D2**	86.2766	86.5854	70.5951	70.5140	26.5516	58.1760	155.7279	

[Fe₂(μ-pdt)(CO)₄(PMe₃)₂] Cartesian Coordinates

pdt 1A

Fe	0.95609200	-0.51921600	0.07284500
Fe	-1.32162300	0.53012500	0.35475900
S	0.57295100	1.34413200	1.38088700
S	-0.10760500	0.67724500	-1.58942400
P	3.17984100	-0.35716100	-0.12661800
P	-2.69108500	-1.01013400	-0.57450400
O	0.93458300	-2.20082100	2.47183100
O	-2.23450400	-0.41405500	2.97632700
O	0.71599400	-2.87125900	-1.65182500
O	-3.19023100	2.77909000	0.16402200
C	0.94788300	-1.50821700	1.52423700
C	-1.84933800	-0.04776800	1.93097700
C	0.80626600	-1.92403700	-0.95836100
C	-2.43170700	1.88293900	0.22590100
C	1.19985100	2.90832400	0.56953300
C	0.54209500	2.40854600	-1.85861900
C	0.44243900	3.36816100	-0.67413200
C	4.05143400	-1.99291000	-0.36316500
C	-4.50426800	-0.62548000	-0.33799000
C	3.94790800	0.64482000	-1.51118500
C	-2.61614300	-1.31176900	-2.41386200
C	4.09145100	0.31236400	1.36209500
C	-2.60056000	-2.74238600	0.11499600
H	-1.60808400	-3.16130200	-0.07404300
H	3.71978600	-2.45312700	-1.30068800
H	-4.74444000	0.32065500	-0.83546000
H	3.78786800	-2.66274200	0.46321600
H	-4.71610900	-0.51759100	0.73190300
H	3.70057700	1.70446200	-1.38320000
H	-3.38065000	-2.04735800	-2.69552900
H	3.54453100	0.30525000	-2.47184600
H	-1.62637200	-1.68480200	-2.69457600
H	5.04028000	0.53144500	-1.51241900
H	-2.79443000	-0.36939500	-2.94242500
H	5.14056900	-1.85804400	-0.38926000
H	-5.13019900	-1.42589200	-0.75306300
H	5.17601100	0.30915900	1.19133200
H	-3.36314800	-3.37976300	-0.35139300
H	3.85610200	-0.31083400	2.23202400
H	-2.76654800	-2.71003300	1.19725300
H	3.75743800	1.33331800	1.57598700
H	0.84921800	4.34481300	-0.98780100
H	-0.61152000	3.53046300	-0.41817800
H	1.12770600	3.66831900	1.35755700
H	2.26461400	2.75007500	0.35055400
H	-0.04677100	2.79022400	-2.70236200
H	1.57987900	2.29728400	-2.19726500

pdt 1A'

Fe	0.97597400	-0.39916800	0.06810800
Fe	-1.34879100	0.54189600	0.35109400
S	0.49284000	1.47104000	1.35005800
S	-0.16861800	0.70648000	-1.60487500
P	3.19356200	-0.26324600	-0.21078000
P	-2.71024100	-1.02594800	-0.55162500
O	0.99244700	-1.97735100	2.53395300
O	-2.27994700	-0.35007900	2.98773800
O	0.73864300	-2.82437300	-1.54778300
O	-3.09862900	2.87114300	0.05825200
C	0.99229900	-1.32600000	1.55792800
C	-1.88542500	-0.00633500	1.93800800
C	0.83097000	-1.84569700	-0.89956100
C	-2.41659600	1.92013900	0.17102100
C	0.91523700	3.09731900	0.53502400
C	0.35948000	2.47648700	-1.89036500
C	1.39156200	3.03577000	-0.91434400
C	4.07785100	-1.86712600	0.16628200
C	-4.52416500	-0.65563300	-0.30041200
C	3.88247700	0.10164200	-1.91350000
C	-2.64876800	-1.34633600	-2.38871900
C	4.16094500	0.92027900	0.86848700
C	-2.59426000	-2.75178100	0.15107000
H	-1.59827500	-3.15968400	-0.04471600
H	3.69798800	-2.65520700	-0.49370000
H	-4.77533100	0.28629800	-0.80074200
H	3.87751600	-2.15695300	1.20383400
H	-4.72523800	-0.54300000	0.77106100
H	3.56106900	1.09408500	-2.24714500
H	-3.40716000	-2.09292600	-2.65759100
H	3.49082000	-0.64089400	-2.61791000
H	-1.65692900	-1.71151800	-2.67327800
H	4.97962300	0.05735300	-1.90910000
H	-2.84028600	-0.41156900	-2.92615800
H	5.16096300	-1.76258200	0.02026900
H	-5.14939000	-1.46225500	-0.70455200
H	5.24050300	0.80014900	0.70706900
H	-3.35263600	-3.40363500	-0.30206300
H	3.92168600	0.71619600	1.91808100
H	-2.74986400	-2.71222500	1.23468800
H	3.87498800	1.95363100	0.64518900
H	2.30898700	2.43488000	-0.97315600
H	1.65737200	4.05729000	-1.23595800
H	0.01604700	3.71964000	0.62945200
H	1.69541900	3.53316700	1.17300900
H	-0.56065500	3.07467500	-1.87849700
H	0.75964400	2.48634300	-2.91231800

pdt 1B

Fe	-1.26218300	-0.47598100	-0.06093200
Fe	1.22557600	-0.47056700	0.02199100
S	0.03016400	0.67329500	-1.60650200
S	-0.08529400	0.72493100	1.52937600
P	-3.28783700	0.47171100	0.04193000
P	3.29477100	0.38956400	0.02494900
O	-1.90112400	-2.37410800	-2.20096300
O	1.77914400	-2.36914100	2.18130300
O	-1.85455000	-2.49611300	1.97530600
O	1.77837900	-2.51359300	-1.99926900
C	-1.64068600	-1.61104000	-1.35018000
C	1.55055900	-1.60394100	1.32280700
C	-1.61181900	-1.68109100	1.16762000
C	1.55689100	-1.68906200	-1.19590300
C	0.03857800	2.52626500	-1.37129800
C	-0.16289900	2.56260700	1.18923800
C	0.58626300	3.05432200	-0.04708100
C	-3.82860100	1.05495200	1.73506800
C	4.64084200	-0.90733800	0.02513900
C	-3.72593300	1.95782600	-1.01222200
C	3.83630500	1.43141600	-1.43290900
C	-4.69172400	-0.68199400	-0.39439800
C	3.82867000	1.42478900	1.49042000
H	3.19259000	2.31158600	1.58061400
H	-3.14240100	1.82699400	2.10012600
H	4.54515100	-1.53047500	-0.87111500
H	-3.78848400	0.20895600	2.43012500
H	4.52846300	-1.54826400	0.90674600
H	-4.79051600	2.20528200	-0.90601200
H	4.89371000	1.71366100	-1.34361800
H	-3.50639000	1.73801000	-2.06304300
H	3.22486600	2.33729800	-1.50024900
H	-3.12946000	2.82310200	-0.70217700
H	3.68949400	0.84985400	-2.35006400
H	-4.85005600	1.45673100	1.70639900
H	5.63439900	-0.44084300	0.03900200
H	-5.66389800	-0.19314200	-0.24914700
H	4.87707000	1.73643200	1.39314200
H	-4.63511000	-1.57372500	0.24009800
H	3.70940300	0.82588400	2.40047800
H	-4.59475600	-0.99562400	-1.43987400
H	0.54278600	4.15697800	-0.06832500
H	1.64563200	2.78115400	0.04365200
H	0.64213300	2.90602000	-2.20609000
H	-0.99339800	2.86180000	-1.53257300
H	0.25208500	3.02943500	2.09181200
H	-1.22693800	2.82975300	1.13457000

pdt 1C

Fe	1.27792600	0.38245900	0.33500100
Fe	-1.32113300	0.30373400	0.31201200
S	-0.07601300	2.02964000	1.14940600
S	-0.00119700	0.50307300	-1.54509200
P	2.39114000	-1.42635800	-0.42699200
P	-2.19513000	-1.64354300	-0.45451900
O	3.54082900	2.16934200	-0.16548500
O	-1.76053500	-0.64773500	3.05288500
O	1.81896500	-0.56761400	3.06383000
O	-3.82216200	1.79488600	0.00962600
C	2.64767800	1.42554400	0.01906700
C	-1.55897500	-0.26640900	1.96191400
C	1.57643100	-0.17997300	1.98284600
C	-2.81739200	1.18913400	0.08778900
C	-0.07988600	3.50564700	0.00087400
C	0.02997100	2.24548500	-2.23295200
C	-0.68466000	3.29635800	-1.38715400
C	4.11457700	-1.55678800	0.28394900
C	-4.05399800	-1.60696800	-0.65546500
C	1.78189300	-3.16686100	-0.10818200
C	-1.69717300	-2.29129600	-2.13671500
C	2.74484300	-1.47419600	-2.25919500
C	-2.02264500	-3.16771200	0.61727400
H	-0.96627600	-3.38352300	0.80165100
H	4.05234300	-1.65395600	1.37365000
H	-4.32843000	-0.84730400	-1.39552800
H	4.67708300	-0.64699300	0.04794200
H	-4.51657300	-1.33965500	0.30118600
H	2.52148100	-3.90261600	-0.45023800
H	-2.25248000	-3.21139000	-2.35962000
H	0.83958500	-3.33547700	-0.63778600
H	-0.62233300	-2.49483200	-2.16799200
H	1.61166500	-3.29597900	0.96665100
H	-1.91846400	-1.53157800	-2.89354900
H	4.64021400	-2.42760400	-0.12849400
H	-4.42807200	-2.58655200	-0.97977600
H	3.33300400	-2.36390200	-2.51800000
H	-2.49783000	-4.03216500	0.13573400
H	3.30475000	-0.57281900	-2.53310800
H	-2.50669700	-2.98136000	1.58220600
H	1.80137800	-1.47243300	-2.81540500
H	1.08835200	2.49658900	-2.37829300
H	-0.44503100	2.16720000	-3.21915100
H	-0.64315700	4.25935000	-1.92418700
H	-1.74482700	3.03141700	-1.29320900
H	-0.64661300	4.26962600	0.54813600
H	0.96478200	3.83720300	-0.06265900

pdt 1D

Fe	1.15242300	0.22571900	0.55565200
Fe	-1.16696900	0.19327200	-0.54192400
S	0.62665900	1.36040100	-1.35693200
S	-0.69133900	1.24097000	1.43822000
P	2.53221800	-1.14738500	-0.60448100
P	-2.39834200	-1.34802800	0.57462500
O	1.00360900	-1.84101200	2.62922400
O	-0.77756300	-1.76036500	-2.68882600
O	3.20128700	1.96483600	1.72062500
O	-3.43480400	1.61323500	-1.73870200
C	1.04798300	-1.01264300	1.79295100
C	-0.92260200	-0.97868100	-1.82018300
C	2.40278800	1.25166600	1.23555400
C	-2.53329700	1.05885100	-1.22750900
C	0.49654400	3.19994500	-1.04857200
C	-0.57528100	3.09904900	1.27328000
C	-0.65120100	3.65097300	-0.14792900
C	4.21330700	-1.32284400	0.19222500
C	-4.13652700	-1.52859600	-0.08763400
C	2.99291100	-0.70910700	-2.35845500
C	-2.72638200	-1.12664800	2.39839600
C	2.04972700	-2.94386600	-0.78576900
C	-1.81353600	-3.12073400	0.51164900
H	-0.82217200	-3.19170400	0.96857600
H	4.70499600	-0.34449900	0.22799300
H	-4.67319800	-0.58143200	0.03608000
H	4.08782400	-1.68504100	1.21898800
H	-4.09487800	-1.76380900	-1.15719600
H	2.09932400	-0.71585600	-2.99061700
H	-3.38857300	-1.92957900	2.74726300
H	3.42514900	0.29673900	-2.38306100
H	-1.78554400	-1.15873700	2.95637300
H	3.72077400	-1.43657900	-2.74021000
H	-3.19792700	-0.15378200	2.57148700
H	4.84169300	-2.02741800	-0.36781500
H	-4.67607100	-2.32565200	0.44009100
H	2.84745300	-3.50427800	-1.29059300
H	-2.51194700	-3.77428600	1.05007900
H	1.87840200	-3.37715800	0.20584700
H	-1.74724600	-3.44494500	-0.53270400
H	1.12844800	-3.01677400	-1.37137400
H	-0.63315500	4.75270300	-0.09297400
H	-1.60894400	3.36966800	-0.60262300
H	0.38753800	3.63616900	-2.04936500
H	1.46909000	3.50846500	-0.64288900
H	-1.41287900	3.47673600	1.87345600
H	0.35994500	3.38881100	1.76888100

TS_{pdt 1A→1B}

Fe	1.16243900	-0.52020000	-0.04575500
Fe	-1.30033900	-0.12641100	0.46555700
S	0.44382700	0.81493400	1.69981300
S	-0.20566200	0.78102800	-1.40224100
P	3.25065300	0.25187300	-0.26503500
P	-3.20098900	0.03181600	-0.65444600
O	1.98256900	-2.54418200	1.91344400
O	-1.27368200	-3.02402000	0.17190000
O	1.37550200	-2.37802600	-2.30852900
O	-2.73161200	-0.18616400	3.01144600
C	1.64759300	-1.73784200	1.13528900
C	-1.17912900	-1.85026400	0.23814100
C	1.27879000	-1.64574500	-1.40106000
C	-2.16661100	-0.15441300	1.98078500
C	0.61430900	2.63499600	1.30597900
C	0.00649800	2.62366500	-1.17594000
C	-0.32524100	3.15026700	0.21813600
C	4.44930300	-1.02071100	-0.92785200
C	-4.66593000	-0.82502300	0.12434400
C	3.64400900	1.70635600	-1.37603300
C	-3.89406500	1.73831500	-0.98380500
C	4.10625500	0.74444100	1.32234400
C	-3.19975800	-0.72865100	-2.36026100
H	-2.41218000	-0.26398700	-2.96440800
H	4.15640700	-1.30732200	-1.94503300
H	-4.89880800	-0.36195100	1.09027500
H	4.41556900	-1.91490800	-0.29343300
H	-4.41142600	-1.87799300	0.29668900
H	3.20737900	2.62268700	-0.96145400
H	-4.84827000	1.67974200	-1.52645700
H	3.21610300	1.53165000	-2.37055400
H	-3.17279900	2.31163500	-1.57873200
H	4.73148300	1.83916600	-1.46312100
H	-4.04783800	2.25315000	-0.02760600
H	5.47419000	-0.62490100	-0.94260300
H	-5.54579700	-0.76525500	-0.53066200
H	5.13735600	1.07137700	1.12824500
H	-4.17450400	-0.59568000	-2.85001400
H	4.11872300	-0.11735100	2.00035400
H	-2.98034800	-1.79903400	-2.26597300
H	3.55100100	1.55238100	1.81223900
H	-0.27579400	4.25275500	0.19881500
H	-1.35646600	2.86442900	0.47885100
H	0.39761600	3.13260300	2.26045800
H	1.66518700	2.83594900	1.05153500
H	-0.66841900	3.06756600	-1.92082100
H	1.03310200	2.88124600	-1.46686200

TS_{pdt 1A→1C}

Fe	1.20905900	0.16126200	0.47228100
Fe	-1.34938200	0.34562100	0.30525700
S	-0.00152100	2.03915900	1.08352500
S	0.04594400	0.31340200	-1.53955600
P	2.87120000	-0.84152100	-0.58996800
P	-2.28537900	-1.55982900	-0.47344900
O	3.11195900	1.09524200	2.48367600
O	-2.23234800	-0.17398600	3.05828100
O	0.45183400	-2.24786400	1.92560700
O	-3.71627300	1.92117800	-0.38259200
C	2.36007300	0.72173800	1.65924500
C	-1.86233700	0.01964200	1.96742100
C	0.64874700	-1.26407800	1.29666100
C	-2.75448100	1.29185300	-0.14289600
C	0.17523000	3.40758600	-0.18336100
C	0.18227900	2.00433600	-2.33449500
C	-0.44212400	3.16099300	-1.55834200
C	4.08179600	-1.73759400	0.51529500
C	-3.62531700	-2.29442800	0.59773900
C	2.49042900	-2.18388000	-1.83483300
C	-3.17816500	-1.31601200	-2.09465000
C	4.00785700	0.26443700	-1.58287700
C	-1.23403100	-3.05195400	-0.85771000
H	-0.45069000	-2.75666100	-1.56459800
H	3.53982100	-2.49568500	1.09421900
H	-4.38796000	-1.53215800	0.79886500
H	4.53950500	-1.03007400	1.21612900
H	-3.19656300	-2.61870200	1.55330300
H	1.81572600	-1.79505700	-2.60619300
H	-3.97707100	-0.57608700	-1.96663900
H	2.00039000	-3.01864800	-1.31976600
H	-3.60960900	-2.26176000	-2.45015100
H	3.41816700	-2.54257100	-2.30212400
H	-2.46216200	-0.93688500	-2.83354100
H	4.86804200	-2.22413200	-0.07801300
H	-4.09237100	-3.15400300	0.09845700
H	4.82687100	-0.31189700	-2.03688300
H	-1.85312900	-3.84210000	-1.30496300
H	4.42354700	1.03589400	-0.92345700
H	-0.76714900	-3.41885800	0.06188500
H	3.43028400	0.75667700	-2.37510700
H	-0.31959900	4.07999800	-2.15749700
H	-1.52079700	2.99284300	-1.45288100
H	-0.30029900	4.27686200	0.28981500
H	1.25261900	3.60577200	-0.25833600
H	-0.30312100	1.90071100	-3.31412600
H	1.25475800	2.17442200	-2.49960800

TS_{pdt 1A→1D}

Fe	1.07845400	-0.27082500	-0.39927300
Fe	-1.22378000	0.36262900	0.50146700
S	0.70647100	1.47802500	1.10369700
S	-0.55857900	0.75494500	-1.67420400
P	3.14599400	-0.38456700	0.37644700
P	-2.62681900	-1.20674000	-0.35072000
O	0.31063100	-2.74940400	0.92283300
O	-1.43770300	-0.69326700	3.23166100
O	1.88531900	-1.55501200	-2.89663600
O	-3.31744500	2.36199000	0.92363300
C	0.53385800	-1.68154300	0.45830500
C	-1.33392300	-0.29453400	2.13755700
C	1.57739800	-1.03132300	-1.88768300
C	-2.47080500	1.57278400	0.73020500
C	0.82273900	3.16051200	0.29071800
C	-0.20773500	2.56672500	-1.98350200
C	-0.23187700	3.48577500	-0.76510900
C	4.14788900	-1.85149200	-0.20061900
C	-3.37239100	-2.40035600	0.87250600
C	4.29829600	1.03740100	-0.00835800
C	-4.13356800	-0.48113300	-1.17855500
C	3.32083400	-0.53723300	2.22948400
C	-1.98551500	-2.36061900	-1.66982500
H	-1.54872600	-1.77765900	-2.48872500
H	4.28047400	-1.80862800	-1.28791800
H	-3.90969600	-1.84535700	1.65095900
H	3.60608500	-2.77241600	0.04744700
H	-2.56580500	-2.97599100	1.34154700
H	3.89849300	1.95365100	0.44236300
H	-4.78131300	-1.27190600	-1.58108100
H	4.35126000	1.17418900	-1.09522800
H	-3.80358800	0.17166900	-1.99594900
H	5.30615500	0.84927800	0.38834700
H	-4.69773700	0.11936800	-0.45522300
H	5.13229100	-1.86608200	0.28675500
H	-4.06628200	-3.08654800	0.36829000
H	4.38013000	-0.55350300	2.52138700
H	-2.81131900	-2.97471400	-2.05533500
H	2.83800400	-1.46718200	2.55340500
H	-1.21350600	-3.00743700	-1.24158300
H	2.81560100	0.30570300	2.71414700
H	-0.05542600	4.51811800	-1.11429200
H	-1.22952500	3.47362500	-0.31001300
H	0.75482200	3.87611100	1.12061700
H	1.83307300	3.22473400	-0.13609800
H	-0.97457600	2.87686200	-2.70566300
H	0.76805600	2.59505700	-2.48569100

TS_{pdt 1C→1D}

Fe	-1.42182600	0.48609700	0.20306600
Fe	1.11722100	0.09863000	-0.51836400
S	-0.27033300	1.64813900	-1.46062900
S	0.46492100	0.90562100	1.51720800
P	-2.10053200	-1.62749300	-0.08462500
P	2.43985800	-1.30935100	0.66440100
O	-2.79543000	0.93872800	2.73884100
O	0.68775100	-1.87576500	-2.64160400
O	-3.73452000	1.39246300	-1.33047700
O	3.46372100	1.33938500	-1.74722100
C	-2.24806700	0.74581200	1.71591900
C	0.81109600	-1.07746700	-1.78696100
C	-2.80463100	1.00544600	-0.72428900
C	2.54681400	0.85064500	-1.19888700
C	0.10916100	3.36415900	-0.81601400
C	0.63319700	2.76981300	1.62938400
C	1.09371900	3.46024100	0.34846200
C	-3.73294000	-1.91957700	0.78854400
C	3.33718600	-2.61376300	-0.32602900
C	-2.58826300	-2.09746000	-1.83029400
C	3.86575500	-0.39577700	1.45540000
C	-1.18715900	-3.16882800	0.45601300
C	1.82347500	-2.28957300	2.13491000
H	1.17780300	-1.65176200	2.74999100
H	-4.45725900	-1.16074300	0.46820100
H	3.87604100	-2.12981900	-1.14978000
H	-3.59387700	-1.82795800	1.87249200
H	2.61517400	-3.31960300	-0.75354600
H	-3.04174300	-3.09875900	-1.84495600
H	4.51972100	-1.09183500	1.99853300
H	-1.71203100	-2.08591000	-2.48533000
H	3.46058100	0.34616600	2.15362100
H	-3.31514600	-1.36506000	-2.20113800
H	4.44587900	0.12521600	0.68508600
H	-4.12985700	-2.91761000	0.55565000
H	4.05047400	-3.16117500	0.30459000
H	-1.79418000	-4.06121000	0.24718300
H	2.67872200	-2.62898300	2.73468100
H	-0.98985400	-3.11075200	1.53232300
H	1.25549600	-3.16201000	1.79818800
H	-0.23713100	-3.23915600	-0.08376000
H	1.24915900	4.53006000	0.57113800
H	2.06774400	3.05372900	0.04455700
H	0.50165900	3.90725800	-1.68609600
H	-0.86419800	3.79722800	-0.55008100
H	1.36463400	2.93400700	2.43207200
H	-0.33960700	3.14778200	1.96895000

TS _{pdt 1C→1D-flip}			
Fe	-1.45581300	0.35483700	0.17025800
Fe	1.12887900	0.19554300	-0.53083600
S	-0.39199100	1.58992400	-1.49822700
S	0.38456400	0.93180600	1.48445400
P	-1.85295800	-1.83643100	-0.03344500
P	2.58096000	-1.09552800	0.66269700
O	-2.94988800	0.78599000	2.64166000
O	1.06880800	-1.70162500	-2.77065200
O	-3.81119600	0.88016900	-1.47315900
O	3.28321900	1.91644700	-1.49912200
C	-2.35302600	0.60911500	1.64279800
C	1.05352400	-0.94437100	-1.87113400
C	-2.85924500	0.64495100	-0.82409800
C	2.44759700	1.21188500	-1.06565900
C	-0.13340700	3.33152000	-0.86602200
C	0.44752700	2.80263200	1.57616700
C	-0.47729700	3.53876600	0.60816700
C	-3.48586400	-2.28248700	0.77201600
C	3.53308600	-2.38644300	-0.29319100
C	-2.17997700	-2.44239200	-1.77341000
C	3.96707200	-0.07092800	1.38616800
C	-0.81072200	-3.24633700	0.61703300
C	2.07291400	-2.04557700	2.19455600
H	1.39334100	-1.42911200	2.79321600
H	-4.27739400	-1.63386300	0.38001900
H	4.03250100	-1.90861000	-1.14351400
H	-3.41596200	-2.12642500	1.85452200
H	2.84281300	-3.14394800	-0.68069100
H	-2.53863000	-3.48030800	-1.75004100
H	4.66294700	-0.70886600	1.94632600
H	-1.26800300	-2.38617300	-2.37433000
H	3.53399800	0.67535600	2.06185300
H	-2.94410900	-1.80794500	-2.23532000
H	4.50852200	0.44732600	0.58819600
H	-3.74548400	-3.33015600	0.57012600
H	4.28297000	-2.86985800	0.34535000
H	-1.32848200	-4.19774800	0.43628600
H	2.96492200	-2.28609600	2.78628200
H	-0.65288700	-3.12307800	1.69336000
H	1.57036100	-2.97405900	1.91441900
H	0.15490000	-3.25605700	0.10241200
H	0.90740300	3.60161400	-1.08671600
H	-0.78902500	3.94324700	-1.49836800
H	1.49896200	3.07501100	1.41451300
H	0.17984500	3.03823700	2.61363900
H	-1.51423800	3.21640500	0.78181600
H	-0.42081500	4.61705700	0.83308700

TS_{pdt 1A'→1C}

Fe	1.15884100	0.02311600	0.50216700
Fe	-1.35615700	0.41508900	0.30600400
S	0.10671400	1.98161400	1.14816300
S	0.03794500	0.30221800	-1.52555000
P	2.89803500	-0.85955800	-0.54732300
P	-2.47445900	-1.37474100	-0.55796300
O	2.78538900	0.42427700	2.89671800
O	-2.39979600	-0.06359700	3.00954000
O	0.10463400	-2.49374600	1.51870600
O	-3.34125700	2.39699900	-0.51874600
C	2.13619400	0.26521500	1.92921800
C	-1.97048600	0.11609000	1.93676300
C	0.41359800	-1.45548900	1.03638500
C	-2.55870500	1.57803500	-0.20769200
C	0.31972800	3.36400400	-0.08914700
C	0.28903200	2.00658400	-2.25483400
C	1.06116100	2.98242700	-1.36796500
C	4.10723900	-1.79354700	0.52708300
C	-3.66103800	-2.25436700	0.58019300
C	2.53449100	-2.14860000	-1.85213800
C	-3.57518900	-0.89662200	-1.98761700
C	4.04666700	0.28616200	-1.48195300
C	-1.54458300	-2.81188400	-1.30808100
H	-0.81528500	-2.42953300	-2.02980500
H	3.57298300	-2.58642200	1.06296700
H	-4.38246000	-1.53701400	0.98677000
H	4.55278000	-1.11654400	1.26368400
H	-3.10039000	-2.69749100	1.41071300
H	1.91992200	-1.70764600	-2.64400700
H	-4.32676200	-0.17309300	-1.65388500
H	1.97767000	-2.97199000	-1.39126700
H	-4.07715800	-1.77963700	-2.40334400
H	3.46910900	-2.53479500	-2.27985500
H	-2.95663400	-0.42897900	-2.76219700
H	4.90124000	-2.24002400	-0.08524300
H	-4.19788300	-3.04382300	0.03901300
H	4.87089100	-0.27408400	-1.94374900
H	-2.25311700	-3.47652500	-1.81913200
H	4.45420600	1.03187000	-0.79008500
H	-1.02208000	-3.36338500	-0.52134300
H	3.47784700	0.80522400	-2.26165400
H	-0.67856800	3.76645300	-0.30571800
H	0.88375100	4.12528300	0.46458900
H	-0.70741100	2.39631100	-2.50035500
H	0.82915800	1.83054700	-3.19418500
H	2.03427800	2.54604300	-1.09860200
H	1.25551900	3.89957700	-1.94932600

TS_{pdt 1A'→1D}

Fe	1.04296600	-0.32827600	-0.35297400
Fe	-1.25071600	0.40830800	0.49926100
S	0.71237300	1.39856300	1.17735900
S	-0.51982800	0.77313500	-1.66196900
P	3.13785600	-0.49091800	0.35025100
P	-2.73814100	-1.07543900	-0.37034300
O	0.14541100	-2.67393200	1.11702200
O	-1.74234600	-0.49409000	3.24888500
O	1.65450700	-1.88943500	-2.74563100
O	-3.03182200	2.72165700	0.64997900
C	0.40960300	-1.63661800	0.60547500
C	-1.52425200	-0.16596500	2.14676500
C	1.41936300	-1.25469500	-1.78128700
C	-2.33242600	1.78076900	0.58290200
C	0.89118000	3.08540500	0.39472000
C	-0.14599900	2.58987800	-1.88998600
C	1.07714500	3.08683500	-1.12231300
C	4.09989500	-1.97910100	-0.23729200
C	-3.58202500	-2.22087200	0.83421400
C	4.31457300	0.90146300	-0.07182800
C	-4.17502500	-0.26448400	-1.23874100
C	3.35954300	-0.62785900	2.19907100
C	-2.12811800	-2.27059800	-1.66552100
H	1.29760100	4.11832300	-1.44531300
H	-1.67384200	-1.71777400	-2.49492200
H	4.20056100	-1.95151100	-1.32759200
H	-4.11389000	-1.63631400	1.59312700
H	3.55733300	-2.89024700	0.03906700
H	-2.82324500	-2.83469800	1.33213600
H	3.93193600	1.83426700	0.35688300
H	-4.84568100	-1.01523000	-1.67572700
H	4.36943500	1.01069900	-1.16085400
H	-3.78208000	0.38238300	-2.03128200
H	5.31842500	0.70247400	0.32707600
H	-4.73338500	0.35268200	-0.52609500
H	5.09673600	-1.99700500	0.22143700
H	-4.29397600	-2.87279400	0.31206000
H	4.42514500	-0.67777100	2.45811600
H	-2.96988800	-2.86687900	-2.04109000
H	2.85473500	-1.53505600	2.54955500
H	-1.37724400	-2.93245200	-1.22391100
H	2.89757100	0.23769900	2.68496600
H	0.00906800	3.66833800	0.69078800
H	1.76800100	3.52534700	0.88791400
H	-1.05045500	3.14815500	-1.61530300
H	0.01288700	2.69477000	-2.97038800
H	1.94253100	2.46137500	-1.38810400

TS_{pdt 1A'→1B}

Fe	1.04296600	-0.32827600	-0.35297400
Fe	-1.25071600	0.40830800	0.49926100
S	0.71237300	1.39856300	1.17735900
S	-0.51982800	0.77313500	-1.66196900
P	3.13785600	-0.49091800	0.35025100
P	-2.73814100	-1.07543900	-0.37034300
O	0.14541100	-2.67393200	1.11702200
O	-1.74234600	-0.49409000	3.24888500
O	1.65450700	-1.88943500	-2.74563100
O	-3.03182200	2.72165700	0.64997900
C	0.40960300	-1.63661800	0.60547500
C	-1.52425200	-0.16596500	2.14676500
C	1.41936300	-1.25469500	-1.78128700
C	-2.33242600	1.78076900	0.58290200
C	0.89118000	3.08540500	0.39472000
C	-0.14599900	2.58987800	-1.88998600
C	1.07714500	3.08683500	-1.12231300
C	4.09989500	-1.97910100	-0.23729200
C	-3.58202500	-2.22087200	0.83421400
C	4.31457300	0.90146300	-0.07182800
C	-4.17502500	-0.26448400	-1.23874100
C	3.35954300	-0.62785900	2.19907100
C	-2.12811800	-2.27059800	-1.66552100
H	1.29760100	4.11832300	-1.44531300
H	-1.67384200	-1.71777400	-2.49492200
H	4.20056100	-1.95151100	-1.32759200
H	-4.11389000	-1.63631400	1.59312700
H	3.55733300	-2.89024700	0.03906700
H	-2.82324500	-2.83469800	1.33213600
H	3.93193600	1.83426700	0.35688300
H	-4.84568100	-1.01523000	-1.67572700
H	4.36943500	1.01069900	-1.16085400
H	-3.78208000	0.38238300	-2.03128200
H	5.31842500	0.70247400	0.32707600
H	-4.73338500	0.35268200	-0.52609500
H	5.09673600	-1.99700500	0.22143700
H	-4.29397600	-2.87279400	0.31206000
H	4.42514500	-0.67777100	2.45811600
H	-2.96988800	-2.86687900	-2.04109000
H	2.85473500	-1.53505600	2.54955500
H	-1.37724400	-2.93245200	-1.22391100
H	2.89757100	0.23769900	2.68496600
H	0.00906800	3.66833800	0.69078800
H	1.76800100	3.52534700	0.88791400
H	-1.05045500	3.14815500	-1.61530300
H	0.01288700	2.69477000	-2.97038800
H	1.94253100	2.46137500	-1.38810400

TS_{pdt 1A→1A'}

Fe	0.95013200	-0.56787700	0.10122700
Fe	-1.33017000	0.52705600	0.36937800
S	0.55038200	1.27435100	1.40563200
S	-0.08582200	0.65450200	-1.53057900
P	3.16204900	-0.42206600	-0.15883800
P	-2.76868800	-0.91729400	-0.61105200
O	0.95217100	-2.22761200	2.51697100
O	-2.33456800	-0.43200100	2.95519300
O	0.58862900	-2.93084300	-1.58694800
O	-2.91371800	2.98111500	0.15263800
C	0.95655500	-1.54724900	1.56102400
C	-1.91514900	-0.05936600	1.92507800
C	0.73356000	-1.97863600	-0.91022300
C	-2.29808100	1.98267600	0.23103500
C	1.13369000	2.91591000	0.74886600
C	0.55300800	2.37011100	-1.85834300
C	1.08844400	3.32055100	-0.75104600
C	4.02922400	-2.05586300	-0.42138800
C	-4.56011000	-0.43503500	-0.38914600
C	3.86078200	0.58491700	-1.57338100
C	-2.68379800	-1.18647200	-2.45564200
C	4.12855200	0.25814900	1.28942900
C	-2.78220000	-2.66910700	0.03493800
H	-1.81157300	-3.13619500	-0.15695300
H	3.65966700	-2.52427600	-1.34047000
H	-4.73470900	0.53588700	-0.86606300
H	3.80266500	-2.72016100	0.42039400
H	-4.77892600	-0.33983000	0.68049300
H	3.56533300	1.63275200	-1.45216700
H	-3.47826800	-1.87845400	-2.76356900
H	3.45067200	0.21320800	-2.51915400
H	-1.70873400	-1.60203600	-2.72873300
H	4.95666400	0.51972000	-1.59926800
H	-2.80780900	-0.22720700	-2.96932600
H	5.11605200	-1.91863800	-0.49393100
H	-5.22767600	-1.18584300	-0.83157100
H	5.20858700	0.21612100	1.09589000
H	-3.57317200	-3.25238800	-0.45430500
H	3.89379700	-0.32938600	2.18386900
H	-2.95731200	-2.65520400	1.11620000
H	3.83255600	1.29603000	1.47525900
H	2.10978200	3.60465800	-1.03775900
H	0.49583500	4.24155500	-0.81193500
H	0.53269300	3.62171300	1.33378600
H	2.16231400	2.99367100	1.12294200
H	-0.29567700	2.84492700	-2.36428500
H	1.32789100	2.21068500	-2.61762300

TS_{pdt 1B→1B}

Fe	-1.25382700	-0.51165200	-0.02965000
Fe	1.25381000	-0.51169500	-0.02950400
S	0.00010900	0.60468900	-1.59900200
S	-0.00005600	0.68382100	1.48344700
P	-3.26303200	0.46105000	0.05365100
P	3.26300400	0.46101300	0.05355100
O	-1.87787600	-2.48263900	-2.10653800
O	1.83840000	-2.47156900	2.06884300
O	-1.83823900	-2.47181000	2.06848000
O	1.87760800	-2.48298900	-2.10617900
C	-1.62865400	-1.68898400	-1.28098300
C	1.59844700	-1.68033800	1.23724700
C	-1.59837200	-1.68044800	1.23698300
C	1.62850100	-1.68920000	-1.28071800
C	-0.00002500	2.45903200	-1.47776900
C	0.00013500	2.53271400	1.24809100
C	0.00013000	3.24291400	-0.13524700
C	-3.81872700	1.06870600	1.73313200
C	4.68502500	-0.66383400	-0.39871800
C	-3.64536000	1.94919600	-1.01772000
C	3.64512200	1.94898400	-1.01814400
C	-4.68509400	-0.66374400	-0.39862300
C	3.81896300	1.06896600	1.73283800
H	3.13087200	1.84098500	2.09383400
H	-3.13043400	1.84050200	2.09421800
H	4.57315500	-0.99154300	-1.43839000
H	-3.79452900	0.23203400	2.44018400
H	4.66252200	-1.54967500	0.24611900
H	-4.69417200	2.25295000	-0.90080200
H	4.69392000	2.25285000	-0.90138400
H	-3.45432800	1.69803100	-2.06712900
H	2.99728600	2.78537800	-0.73357100
H	-2.99757400	2.78558300	-0.73302100
H	3.45400500	1.69757100	-2.06747900
H	-4.83627900	1.47887400	1.68756300
H	5.64842600	-0.15109000	-0.27950500
H	-5.64848200	-0.15102000	-0.27922600
H	4.83658500	1.47893600	1.68704600
H	-4.66252100	-1.54968300	0.24607700
H	3.79469900	0.23247000	2.44009600
H	-4.57333400	-0.99129100	-1.43835700
H	-0.87266800	3.90906500	-0.15181200
H	0.87304300	3.90890600	-0.15188800
H	0.87746800	2.74456500	-2.06923900
H	-0.87775500	2.74439200	-2.06896100
H	0.87726400	2.85458100	1.82264900
H	-0.87682700	2.85482100	1.82277400

TS_{pdt 1C→1C}

Fe	1.29017600	0.28800200	0.38627100
Fe	-1.33599700	0.33509800	0.29883000
S	-0.02318000	1.94212300	1.20087300
S	0.04353800	0.48946900	-1.48960400
P	2.39792900	-1.47963800	-0.46178700
P	-2.29944900	-1.56583800	-0.46160900
O	3.64905300	2.00974400	0.18639500
O	-2.16517100	-0.48069300	2.99787200
O	1.55594700	-0.89730800	3.06302500
O	-3.53827200	2.11664800	-0.43683100
C	2.71603600	1.29406300	0.23928300
C	-1.80948600	-0.15463700	1.92859800
C	1.42471500	-0.41223700	2.00168100
C	-2.67122500	1.37472800	-0.15438100
C	0.02615100	3.48853400	0.17374000
C	0.09044000	2.19624800	-2.23187400
C	0.07911800	3.49722800	-1.38024800
C	4.02203200	-1.80426700	0.40079900
C	-4.16726500	-1.47870500	-0.43280300
C	1.67341200	-3.20446700	-0.46131400
C	-2.00604100	-2.09871300	-2.22839600
C	2.94160300	-1.30641500	-2.23901700
C	-2.04859900	-3.16072400	0.48446100
H	-0.99645600	-3.45598000	0.46425400
H	3.83338200	-2.03597800	1.45499300
H	-4.50653400	-0.66805300	-1.08661600
H	4.64676100	-0.90600200	0.34952900
H	-4.50169200	-1.26271500	0.58822900
H	2.39532200	-3.92577300	-0.86606900
H	-2.57804400	-3.00899200	-2.44913000
H	0.76543900	-3.22682600	-1.07208300
H	-0.94044900	-2.27905500	-2.39989300
H	1.41887600	-3.48608900	0.56667000
H	-2.32181500	-1.29293400	-2.89996500
H	4.55217900	-2.64384000	-0.06695300
H	-4.60771700	-2.42709300	-0.76662100
H	3.53252000	-2.17620100	-2.55366600
H	-2.66121100	-3.96255100	0.05193800
H	3.54626100	-0.39796800	-2.33854200
H	-2.34270700	-3.00396100	1.52809800
H	2.05693900	-1.20558800	-2.87724100
H	0.99684500	2.16867800	-2.84798600
H	-0.76716700	2.19738200	-2.91505400
H	0.97352000	4.06677800	-1.66175200
H	-0.77874400	4.09014800	-1.72084700
H	-0.86403600	4.03047000	0.51487400
H	0.89913600	4.01724900	0.57496500

TS_{pdt 1D→1D}

Fe	-1.16751600	0.19008100	-0.55459700
Fe	1.17483600	0.19634400	0.55677300
S	-0.64359300	1.26806300	1.37150900
S	0.65175400	1.25142700	-1.38365500
P	-2.48682100	-1.25147600	0.58674700
P	2.46763200	-1.27726200	-0.57954700
O	-0.94260400	-1.84223100	-2.65552700
O	0.96627300	-1.76099200	2.72905200
O	-3.26755800	1.88854700	-1.69064900
O	3.28044400	1.92033900	1.64235500
C	-1.02100500	-1.02584600	-1.81011700
C	1.04117200	-0.97971500	1.85131900
C	-2.44622900	1.19448400	-1.21654500
C	2.45772100	1.21435200	1.18910600
C	-0.50476700	3.11699900	1.24495400
C	0.51474500	3.10157500	-1.27874600
C	0.00542100	3.85788500	-0.02116200
C	-4.15113200	-1.50716100	-0.22212000
C	4.21019800	-1.38943600	0.08653000
C	-2.97639500	-0.84870800	2.34168000
C	2.78857500	-1.01948600	-2.40008300
C	-1.90215100	-3.01710600	0.76279600
C	1.95985300	-3.07522000	-0.54623200
H	0.98676100	-3.18583600	-1.03464500
H	-4.68954800	-0.55355300	-0.25449800
H	4.70193300	-0.41642400	-0.02339000
H	-4.00029000	-1.85451800	-1.25057600
H	4.17481100	-1.63978300	1.15289200
H	-2.08613900	-0.82598000	2.97824300
H	3.48521900	-1.78771200	-2.75973100
H	-3.44898300	0.13875500	2.37408200
H	1.84962400	-1.08610500	-2.95861700
H	-3.67622800	-1.60839600	2.71295000
H	3.21686900	-0.02479800	-2.56140100
H	-4.74862900	-2.24584400	0.32766100
H	4.78839500	-2.15375800	-0.44876100
H	-2.66613600	-3.62863900	1.26027000
H	2.70184900	-3.69437200	-1.06705300
H	-1.69666300	-3.43304700	-0.22971900
H	1.87539200	-3.41037500	0.49338900
H	-0.98108800	-3.03391400	1.35311800
H	0.81773000	4.51836400	0.30661400
H	-0.80592900	4.51569900	-0.35660500
H	0.12884200	3.36762700	2.10358300
H	-1.52067400	3.45497300	1.48291500
H	1.53062600	3.43635200	-1.52120100
H	-0.11925000	3.34245100	-2.13989400

pdt 2A

Fe	1.01858100	-0.58115300	0.12223100
Fe	-1.35682000	0.40739600	0.38605600
S	0.53687800	1.29355100	1.39057700
S	-0.12187900	0.55617000	-1.56132500
P	3.24233400	-0.21668800	-0.21230700
P	-2.90526500	-0.99356100	-0.57150600
O	1.62667000	-2.08746100	2.57085900
O	-2.40728400	-0.27235700	3.04577800
O	0.98761900	-2.95537800	-1.60998200
O	-3.12091100	2.72396400	0.06764800
C	1.41005900	-1.48452500	1.60160100
C	-1.99717800	0.00083800	1.99394300
C	1.02292700	-2.01491500	-0.92562000
C	-2.39800500	1.81864800	0.18855300
C	1.11198100	2.86465600	0.55717400
C	0.44905100	2.30517300	-1.87123700
C	0.36726400	3.28982300	-0.70576100
C	4.19245600	-1.79259100	-0.49300500
C	-4.67292100	-0.47610100	-0.31596900
C	3.80552000	0.83536200	-1.64189000
C	-2.80089900	-1.25953200	-2.40761800
C	4.13171600	0.52056000	1.24746100
C	-2.86997100	-2.72063500	0.11735500
H	-1.89780300	-3.18070200	-0.08775400
H	3.87459600	-2.26117500	-1.43057800
H	-4.85401500	0.48820600	-0.80242300
H	4.00997800	-2.49073900	0.33123000
H	-4.88221500	-0.37698600	0.75484100
H	3.52561800	1.88164600	-1.48339600
H	-3.59523600	-1.95065600	-2.71530700
H	3.35308200	0.47523400	-2.57202300
H	-1.82658000	-1.68107400	-2.67475900
H	4.89757800	0.77375400	-1.72382300
H	-2.92344800	-0.30458000	-2.92897700
H	5.26590900	-1.57506800	-0.54664600
H	-5.34550900	-1.22812000	-0.74555000
H	5.19659400	0.63685800	1.01209100
H	-3.66036700	-3.32364900	-0.34556100
H	4.02470800	-0.14362600	2.11183000
H	-3.02784000	-2.69226600	1.20083300
H	3.70902500	1.49570000	1.50796500
H	0.80022800	4.24396800	-1.04626100
H	-0.67995200	3.49865800	-0.46283000
H	0.99661500	3.62627900	1.33716500
H	2.18539100	2.73982600	0.36916000
H	-0.19040600	2.64244800	-2.69574300
H	1.46958700	2.21838300	-2.25937300
H	-0.52811100	-1.02718800	0.50525400

pdt 2A'

Fe	1.05981400	-0.54671100	0.21047600
Fe	-1.34694400	0.39008800	0.37609700
S	0.47374400	1.34737900	1.42594500
S	-0.05606600	0.50440500	-1.53321500
P	3.27370700	-0.23932500	-0.21000400
P	-2.87419000	-1.01598500	-0.60063500
O	1.66846900	-1.87148000	2.76263300
O	-2.55753400	-0.18859900	2.99200000
O	1.06604900	-3.01868600	-1.37453000
O	-2.88381400	2.82366300	-0.16181000
C	1.45195000	-1.34523300	1.75051500
C	-2.08114000	0.04270000	1.95784300
C	1.08498000	-2.03801500	-0.74819300
C	-2.28820000	1.84708700	0.05968900
C	0.86310700	2.97776500	0.60416400
C	0.43116000	2.28191600	-1.84430800
C	1.37405900	2.92874900	-0.83321300
C	4.26860300	-1.78386900	0.09559000
C	-4.64205000	-0.49233900	-0.35787800
C	3.75173500	0.17153100	-1.96241400
C	-2.75689400	-1.27671400	-2.43726800
C	4.16951700	0.99683300	0.85504500
C	-2.84967000	-2.74572700	0.08271600
H	-1.87773700	-3.20842000	-0.11776300
H	3.91975500	-2.59354700	-0.55419900
H	-4.80967800	0.48001800	-0.83356800
H	4.16633300	-2.09720000	1.13989200
H	-4.86098600	-0.40497900	0.71203700
H	3.30403700	1.11618300	-2.28366100
H	-3.54191100	-1.97449000	-2.75353600
H	3.39503800	-0.62677700	-2.62254300
H	-1.77609900	-1.68638900	-2.69940600
H	4.84352300	0.24329700	-2.03994400
H	-2.88572300	-0.32127000	-2.95656300
H	5.32646500	-1.58709000	-0.11578900
H	-5.31739200	-1.23243300	-0.80362700
H	5.23393800	1.00697000	0.59030400
H	-3.63905000	-3.34603100	-0.38550700
H	4.06054700	0.70371700	1.90501100
H	-3.01294400	-2.71914000	1.16550900
H	3.75628300	2.00127900	0.72838600
H	2.34330600	2.41747400	-0.85813600
H	1.55810900	3.96414200	-1.16103700
H	-0.05595000	3.57034900	0.68714900
H	1.61440400	3.43613200	1.25858900
H	-0.51254300	2.83479900	-1.92393800
H	0.89409500	2.26359700	-2.83805700
H	-0.49861300	-1.01243000	0.59723400

pdt 2B

Fe	-1.30699900	-0.56713400	-0.06755700
Fe	1.27172600	-0.56057300	0.00100600
S	0.02697600	0.55272700	-1.61981500
S	-0.07380900	0.62491800	1.49298400
P	-3.29466800	0.54346000	0.06754900
P	3.29687900	0.47830200	0.06654800
O	-2.22678800	-2.26521100	-2.28634600
O	2.05802100	-2.29692500	2.23839900
O	-2.21056300	-2.41896500	2.02797500
O	2.24715000	-2.36683000	-2.10112500
C	-1.88314000	-1.58854600	-1.40774700
C	1.76822400	-1.60338200	1.35308300
C	-1.87391700	-1.67321400	1.20305300
C	1.88024900	-1.64566400	-1.26815300
C	0.01823400	2.40577900	-1.42259100
C	-0.16542300	2.46144500	1.15129400
C	0.53549200	2.97407500	-0.10371400
C	-3.75364000	1.07175000	1.79323700
C	4.70820000	-0.73493200	0.13985000
C	-3.59806600	2.08004600	-0.94328400
C	3.77058000	1.50164100	-1.41526300
C	-4.74361300	-0.52123600	-0.41276400
C	3.65323300	1.54842700	1.54869400
H	2.95707800	2.39004400	1.60584000
H	-2.99078700	1.73649400	2.21045600
H	4.69946000	-1.37808600	-0.74650500
H	-3.82856600	0.18754800	2.43519300
H	4.62144400	-1.36133000	1.03394600
H	-4.65019200	2.37328000	-0.84025200
H	4.79001700	1.88654200	-1.28992800
H	-3.38127300	1.88615900	-1.99932800
H	3.08310100	2.34067500	-1.55369900
H	-2.97032600	2.90379200	-0.58867500
H	3.73141400	0.86764000	-2.30794300
H	-4.72040400	1.58940000	1.78028000
H	5.65930400	-0.19025000	0.17605300
H	-5.68002800	0.01457700	-0.21676300
H	4.67988900	1.93010100	1.49101500
H	-4.73321700	-1.44996500	0.16799600
H	3.54279200	0.94290100	2.45495800
H	-4.68882000	-0.77036000	-1.47792500
H	0.41613000	4.06888500	-0.13608100
H	1.61128300	2.78358400	-0.02015900
H	0.63312600	2.76348100	-2.25740600
H	-1.01217600	2.71855600	-1.62046500
H	0.27642400	2.91902500	2.04456700
H	-1.23181900	2.71770400	1.14351200
H	-0.02163200	-1.59244600	-0.06592500

pdt 2C

Fe	1.28363600	0.30856200	0.37329100
Fe	-1.32514300	0.27765700	0.32484900
S	-0.05556500	2.00237400	1.16539300
S	0.01899100	0.45587100	-1.54300500
P	2.46825200	-1.50444900	-0.38917400
P	-2.30537200	-1.67181500	-0.40224600
O	3.44848400	2.09972100	-0.44196300
O	-2.33357800	-0.25210000	3.03565900
O	2.20565300	-0.23789300	3.11321800
O	-3.67700400	1.83384800	-0.45741100
C	2.60016800	1.37319900	-0.11002500
C	-1.94358000	-0.03922300	1.96290700
C	1.85612200	-0.01341800	2.02876400
C	-2.72956200	1.22427600	-0.16348800
C	0.01868000	3.47141800	0.00948400
C	0.10182700	2.19181000	-2.23545600
C	-0.54912900	3.29117200	-1.39783000
C	4.19402400	-1.58482600	0.30413900
C	-4.15956900	-1.58517600	-0.53834300
C	1.81847000	-3.20719600	-0.01230600
C	-1.81570700	-2.31761100	-2.07671000
C	2.76461100	-1.55273400	-2.22474600
C	-2.07413300	-3.13082800	0.73092300
H	-1.00992300	-3.32272100	0.89423900
H	4.15668000	-1.68974300	1.39377300
H	-4.44801800	-0.85687200	-1.30352400
H	4.73916800	-0.66763900	0.05670700
H	-4.58887200	-1.27744700	0.42152400
H	2.53842800	-3.96345100	-0.34779300
H	-2.36610400	-3.24281200	-2.28609600
H	0.86873500	-3.36651500	-0.53164500
H	-0.74013000	-2.51528100	-2.11437700
H	1.66170600	-3.31309400	1.06679000
H	-2.05358300	-1.56832700	-2.83889500
H	4.72689600	-2.44403400	-0.12042500
H	-4.55780100	-2.56990800	-0.81055300
H	3.36273200	-2.43457100	-2.48407600
H	-2.54464100	-4.02159200	0.29749000
H	3.30415600	-0.64903900	-2.52949000
H	-2.54129800	-2.91601000	1.69823400
H	1.80895600	-1.58359000	-2.75787800
H	1.16645000	2.38915400	-2.40971600
H	-0.39358600	2.11676500	-3.21035300
H	-0.40583100	4.24281200	-1.93381500
H	-1.63081200	3.12753100	-1.34617300
H	-0.54136100	4.24721800	0.54477400
H	1.07297000	3.77341000	-0.01148400
H	-0.00552500	-0.69770200	0.76431700

pdt 2D

Fe	-1.16799400	0.07509200	0.55910600
Fe	1.17494700	0.06879400	-0.56588700
S	-0.67966800	1.11825900	-1.43917500
S	0.67751000	1.18798800	1.38415500
P	-2.65653100	-1.23299000	-0.58981400
P	2.72438800	-1.13975800	0.61182300
O	-1.30092600	-1.64836600	2.93409900
O	-3.33563000	1.77665600	1.54399100
O	1.40598300	-1.70817700	-2.89429800
O	3.14713100	1.99471200	-1.54522200
C	-1.24151300	-0.96774100	1.99454300
C	-2.46461500	1.11893400	1.14015800
C	1.30559600	-1.00815500	-1.97218200
C	2.37773700	1.21345400	-1.15473400
C	-0.50104600	2.97166200	-1.26616400
C	-0.49306300	3.53839900	0.15223200
C	0.62437300	3.02918900	1.06150600
C	-3.55208500	-2.50704900	0.42476000
C	-4.03996500	-0.28226600	-1.38636600
C	-1.94960000	-2.21683300	-1.99580800
C	2.07271500	-2.10547200	2.05746300
C	4.07138000	-0.10328500	1.36246300
C	3.66761200	-2.40850400	-0.36574600
H	4.16921800	-1.92376600	-1.21031300
H	0.02247500	-1.00787500	0.01574500
H	-1.35037700	3.37501400	-1.82962100
H	0.41582600	3.22456900	-1.81197600
H	-1.46593600	3.37207900	0.62761400
H	-0.37355600	4.62991800	0.06757900
H	1.61560100	3.28878300	0.67079200
H	0.52735000	3.46962900	2.06033800
H	-4.28230100	-3.03214800	-0.20205700
H	-2.83881200	-3.23173000	0.83124300
H	-4.07387200	-2.01902600	1.25510900
H	-4.63019500	0.22962900	-0.61889700
H	-3.62007200	0.46076600	-2.07207300
H	-4.68994200	-0.96768100	-1.94359400
H	-2.74975300	-2.79100200	-2.47821600
H	-1.49983400	-1.54025100	-2.72946000
H	-1.18434800	-2.90356000	-1.62066100
H	2.89777600	-2.63661500	2.54733800
H	1.60733200	-1.42407700	2.77683000
H	1.32805000	-2.83024700	1.71320700
H	4.63090800	0.40739400	0.57133500
H	3.62470500	0.64410400	2.02640300
H	4.75761100	-0.73706800	1.93696200
H	4.41797200	-2.88864300	0.27330200
H	2.98242500	-3.17057200	-0.75176500

TS_{pdt 2A→2B}

Fe	1.25091200	-0.57965700	-0.02354400
Fe	-1.32941700	-0.29066200	0.45357400
S	0.44748400	0.70390000	1.71506900
S	-0.15860700	0.67091100	-1.37917800
P	3.32225000	0.33011000	-0.29414700
P	-3.19046100	0.10250200	-0.76172300
O	2.34812000	-2.48393700	1.92929000
O	-2.16503000	-3.08147100	0.51403900
O	1.56541700	-2.40803400	-2.30607700
O	-2.75342800	0.31006900	2.93475500
C	1.93230400	-1.72238300	1.15864500
C	-1.84156600	-1.96036300	0.46833700
C	1.46567100	-1.68289300	-1.40542400
C	-2.19259700	0.07924300	1.93906700
C	0.52442700	2.53701200	1.37780700
C	-0.00686400	2.51517200	-1.12484200
C	-0.38616000	3.03254900	0.25951000
C	4.54702000	-0.90227800	-0.96465000
C	-4.74192400	-0.53714400	0.04356600
C	3.56679300	1.78291600	-1.43608400
C	-3.64637400	1.86550700	-1.14762300
C	4.13680700	0.87601100	1.28904300
C	-3.19092500	-0.73741800	-2.41999900
H	-2.33296500	-0.39727400	-3.01003200
H	4.27264800	-1.18520100	-1.98761300
H	-4.92378000	-0.00615000	0.98492200
H	4.55083500	-1.80206100	-0.33824300
H	-4.64601900	-1.60851300	0.25314300
H	3.15022100	2.69381300	-0.99224100
H	-4.60477900	1.87590000	-1.68368500
H	3.07840700	1.59114600	-2.39856900
H	-2.88037500	2.32746900	-1.77877600
H	4.64189300	1.93508900	-1.59941600
H	-3.74828700	2.43795700	-0.21856000
H	5.55373600	-0.46506300	-0.97166100
H	-5.59512000	-0.37889300	-0.62852500
H	5.13854500	1.27343800	1.07925900
H	-4.12186500	-0.50560400	-2.95391900
H	4.22510300	0.01856100	1.96644300
H	-3.11745100	-1.82151200	-2.27503600
H	3.53855400	1.64747800	1.78567600
H	-0.34253600	4.13324400	0.23991200
H	-1.42235800	2.74765900	0.49152300
H	0.24009000	2.99027400	2.33538200
H	1.57586200	2.78717900	1.18356400
H	-0.66491400	2.94429000	-1.89074900
H	1.02072400	2.78605000	-1.39109000
H	-0.10420100	-1.44576400	0.28115500

TS_{pdt 2A→2C}

Fe	1.17787100	-0.02848600	0.55931600
Fe	-1.42742600	0.34956800	0.31637500
S	-0.00328700	1.93848400	1.17017700
S	0.01280900	0.27189000	-1.49028600
P	2.88876900	-0.78217100	-0.70042500
P	-2.46117900	-1.52916000	-0.47757800
O	3.09320000	1.27486800	2.34248600
O	-2.60347900	0.03863400	2.99205900
O	1.30445100	-2.52997000	2.04919300
O	-3.62980300	2.01618500	-0.66705000
C	2.33415100	0.76262100	1.62028500
C	-2.15366400	0.16630500	1.93124100
C	1.27206100	-1.53673100	1.43267700
C	-2.73669300	1.36975900	-0.29457300
C	0.35170700	3.31600100	-0.04104700
C	0.27877800	1.97112500	-2.23204600
C	-0.23861600	3.16923600	-1.44070200
C	4.32261700	-1.40378700	0.31123000
C	-3.86618500	-2.16816400	0.55989900
C	2.50506000	-2.22339700	-1.81062700
C	-3.22851700	-1.32076100	-2.15857700
C	3.69920400	0.44631300	-1.84058300
C	-1.36689000	-3.01791900	-0.68444600
H	-0.55275800	-2.77614600	-1.37715100
H	3.99258600	-2.20792300	0.97856700
H	-4.62455600	-1.38556100	0.68049400
H	4.73957800	-0.59027800	0.91556500
H	-3.49921000	-2.46065100	1.55061100
H	1.71419500	-1.94708500	-2.51675500
H	-4.01792500	-0.56126000	-2.11525500
H	2.17108100	-3.07193500	-1.20235800
H	-3.66258000	-2.27105700	-2.49551900
H	3.40619100	-2.51276500	-2.36733700
H	-2.46026600	-0.99676800	-2.87002600
H	5.10214300	-1.78922300	-0.35805600
H	-4.32217500	-3.03999800	0.07360500
H	4.61822300	0.00856500	-2.25227500
H	-1.95051700	-3.85445200	-1.09030200
H	3.95075600	1.35923600	-1.28877200
H	-0.94321800	-3.30722800	0.28377500
H	3.02520600	0.69401800	-2.66782600
H	0.02534400	4.07529200	-2.01012700
H	-1.33325500	3.14861200	-1.38840900
H	-0.06100300	4.20351000	0.45458900
H	1.44377700	3.41860400	-0.06551500
H	-0.21640800	1.91706000	-3.20944900
H	1.35870100	2.05274200	-2.40118900
H	-0.33470900	-0.73078700	0.91306700

TS_{pdt 2A→2D}

Fe	1.09411800	-0.41544100	-0.33826700
Fe	-1.29398500	0.28581400	0.52345900
S	0.64381400	1.36066000	1.16018900
S	-0.57703600	0.66004800	-1.63828700
P	3.19890500	-0.24197700	0.45963600
P	-2.86285200	-1.12642600	-0.36234300
O	1.20211100	-3.22330500	0.43523600
O	-1.59583200	-0.77978600	3.24319200
O	2.10978400	-0.96248300	-3.02348100
O	-3.31153400	2.37419800	0.92965400
C	1.18362700	-2.09164900	0.14050400
C	-1.49091300	-0.35187300	2.16976900
C	1.71811800	-0.73863500	-1.94745800
C	-2.49490000	1.56483000	0.75012700
C	0.79520700	3.03829500	0.33989900
C	-0.16721400	2.45276900	-1.96577300
C	-0.21038100	3.38052200	-0.75613000
C	4.36331500	-1.49172800	-0.28058700
C	-4.09907200	-0.28158800	-1.46448800
C	4.10339800	1.36135200	0.19160700
C	-2.17307600	-2.48055500	-1.43296800
C	3.34819900	-0.54913200	2.28616200
C	-3.92411800	-2.02707800	0.87029300
H	-3.29979300	-2.66691900	1.50473100
H	4.48233100	-1.30760200	-1.35440700
H	-3.57047300	0.21923100	-2.28363200
H	3.97312100	-2.50533600	-0.13452200
H	-4.66221100	0.46414300	-0.89146300
H	3.66048500	2.14994800	0.80951800
H	-2.99364200	-3.04156200	-1.89898300
H	4.05293100	1.64991700	-0.86470900
H	-1.56745400	-3.16203600	-0.82490900
H	5.15497100	1.23266900	0.48045900
H	-1.54279000	-2.04344800	-2.21659200
H	5.34298700	-1.41139900	0.20775300
H	-4.79691600	-1.02063000	-1.87831000
H	4.39612100	-0.44217900	2.59618100
H	-4.66126000	-2.64869700	0.34590300
H	3.00714600	-1.56673200	2.51019200
H	-4.45043300	-1.30454100	1.50551600
H	2.72806600	0.16634200	2.83686000
H	0.01929700	4.39967300	-1.10717200
H	-1.22544300	3.41610500	-0.34414600
H	0.69987600	3.74257600	1.17553100
H	1.82129500	3.09843300	-0.04239700
H	-0.90854300	2.75898000	-2.71431500
H	0.81940900	2.44915700	-2.44559600
H	-0.34114500	-1.04323100	0.32116400

TS_{pdt 2C→2D}

Fe	-1.36043900	0.39218400	0.14245900
Fe	1.21633800	0.07151100	-0.49928500
S	-0.13119500	1.68787300	-1.42047900
S	0.49820900	0.82549300	1.56051200
P	-2.49868300	-1.52488800	-0.13537700
P	2.42197800	-1.53323000	0.60884400
O	-2.77132300	0.81038300	2.66029900
O	1.29026900	-1.40306700	-3.03728900
O	-3.44857100	1.72509600	-1.40507200
O	3.71975600	1.50220700	-1.03138100
C	-2.21038100	0.62461900	1.65281100
C	1.28090200	-0.80749500	-2.04027600
C	-2.60978100	1.16770600	-0.81414000
C	2.72495700	0.94918000	-0.78962600
C	0.13483000	3.37731800	-0.65907500
C	0.64875900	2.67890200	1.76962300
C	1.07896300	3.47054300	0.53731700
C	-4.34795800	-1.31359400	-0.10705900
C	3.46645700	-2.62511200	-0.47770700
C	-2.18972200	-2.37591900	-1.75813400
C	3.66801200	-0.81530400	1.79128900
C	-2.25164000	-2.84979600	1.14431000
C	1.50290400	-2.74820300	1.67274200
H	0.82901900	-2.21369700	2.35195400
H	-4.67386100	-0.68052900	-0.93921300
H	4.13497700	-2.00599600	-1.08771200
H	-4.65780300	-0.84949400	0.83659500
H	2.82907000	-3.21741200	-1.14465300
H	-2.84605800	-3.25100700	-1.85405800
H	4.22152100	-1.62489400	2.28441600
H	-1.14391000	-2.69515700	-1.81994700
H	3.14953500	-0.21636400	2.54844400
H	-2.39281400	-1.67775600	-2.57850300
H	4.37505700	-0.17579500	1.25042800
H	-4.82610700	-2.29753900	-0.19587000
H	4.06877800	-3.30281000	0.14071600
H	-2.88616400	-3.71428700	0.90830400
H	2.21683900	-3.33905700	2.26114600
H	-2.52674900	-2.45686300	2.13017800
H	0.92431900	-3.42525100	1.03455700
H	-1.20547500	-3.16465100	1.16901000
H	1.12897400	4.53183600	0.83019400
H	2.09566900	3.18507000	0.24178900
H	0.51904400	3.97774800	-1.49288200
H	-0.86991500	3.74156900	-0.41057100
H	1.38587500	2.79706700	2.57359700
H	-0.32492800	3.01285200	2.14928200
H	-0.19876500	-0.80976100	-0.27718100

TS_{pdt 2C→2D-flip}			
Fe	-1.36538500	0.30906000	0.13193400
Fe	1.23409500	0.12914100	-0.50574800
S	-0.20919300	1.62862400	-1.46765000
S	0.47430300	0.85524500	1.53735900
P	-2.36442700	-1.68900900	-0.11913600
P	2.57451100	-1.37182100	0.60982300
O	-2.80632900	0.66193300	2.64173000
O	1.51929400	-1.30551500	-3.05452500
O	-3.53960400	1.43791000	-1.45673000
O	3.50360500	1.94450300	-0.87762000
C	-2.23032200	0.50708300	1.63700200
C	1.42259700	-0.72912400	-2.04986200
C	-2.66286800	0.96657900	-0.84527200
C	2.61828200	1.20493900	-0.71956700
C	0.02824800	3.33800700	-0.75278300
C	0.57435200	2.71567500	1.68085300
C	-0.32654500	3.49491000	0.72429400
C	-4.21893300	-1.63340600	0.00862400
C	3.67622800	-2.41157300	-0.46964800
C	-2.06778200	-2.47354200	-1.77547700
C	3.78400800	-0.54382100	1.75644700
C	-1.93550500	-3.01780400	1.10484200
C	1.78353500	-2.63196600	1.72468400
H	1.08513500	-2.14082100	2.41006400
H	-4.63814900	-0.98827800	-0.76958800
H	4.29638200	-1.76367300	-1.09869800
H	-4.51627800	-1.24961400	0.99047700
H	3.07077400	-3.05573000	-1.11634900
H	-2.64922100	-3.40019500	-1.85682300
H	4.39022200	-1.30478900	2.26267300
H	-1.00348400	-2.69739200	-1.89573900
H	3.23676200	0.03986900	2.50409600
H	-2.37398500	-1.78091000	-2.56655700
H	4.44472700	0.12281200	1.19245200
H	-4.61561300	-2.64843800	-0.11371000
H	4.32552700	-3.03566800	0.15556700
H	-2.51618100	-3.92063900	0.87898500
H	2.56261600	-3.14176200	2.30458800
H	-2.17487100	-2.67664300	2.11764200
H	1.25141200	-3.37472200	1.12162300
H	-0.86970900	-3.24848600	1.04860300
H	1.06916100	3.61754900	-0.95881200
H	-0.62329900	3.96488400	-1.37250200
H	1.63196400	2.97685200	1.54912200
H	0.29443700	2.91627500	2.72132600
H	-0.12864400	-0.82450300	-0.29440000
H	-1.37401700	3.20225400	0.88230500
H	-0.24262600	4.56267500	0.97950800

TS_{pdt 2A'→2C}

Fe	1.14642900	-0.03982900	0.58016900
Fe	-1.45155600	0.40665000	0.29604300
S	0.00015700	1.97427400	1.12014100
S	-0.00470400	0.17874300	-1.48156100
P	2.83708300	-0.91511900	-0.63286200
P	-2.56689100	-1.45336500	-0.45019200
O	3.09649000	1.27991300	2.31149800
O	-2.80182300	0.29968200	2.90519800
O	1.18251100	-2.48356700	2.16376100
O	-3.32921700	2.28385800	-0.94336100
C	2.31966400	0.76178900	1.61199300
C	-2.27602900	0.34524900	1.87173800
C	1.18324200	-1.51166700	1.51290900
C	-2.59492700	1.52585700	-0.45129200
C	0.31431700	3.30421200	-0.14861700
C	0.27495300	1.85520000	-2.26752200
C	1.04377300	2.86108000	-1.41288300
C	4.24127400	-1.54927500	0.40832000
C	-3.97268300	-2.05377600	0.60704300
C	2.39909700	-2.38551500	-1.68179200
C	-3.34520800	-1.24824400	-2.12559900
C	3.69614100	0.22861400	-1.82013700
C	-1.51421400	-2.97171200	-0.65834500
H	-0.69662300	-2.75171000	-1.35288100
H	3.88187000	-2.32241000	1.09539400
H	-4.72129400	-1.26184100	0.71785400
H	4.67936600	-0.73163600	0.98990700
H	-3.60260200	-2.33270900	1.59941900
H	1.63290900	-2.10607100	-2.41196200
H	-4.10401600	-0.45902800	-2.09097900
H	2.02001700	-3.19166600	-1.04475300
H	-3.81772000	-2.18747900	-2.43756900
H	3.29512200	-2.73628500	-2.20856100
H	-2.57307600	-0.97024100	-2.85096100
H	5.01118800	-1.97777000	-0.24419500
H	-4.44046400	-2.92777000	0.13830600
H	4.52110700	-0.30853000	-2.30460200
H	-2.12086000	-3.79088900	-1.06298000
H	4.09876800	1.09106300	-1.27857400
H	-1.09744100	-3.27262900	0.30838100
H	2.99349300	0.57349900	-2.58462700
H	-0.66574300	3.74353400	-0.37424200
H	0.90635800	4.04970600	0.39479800
H	-0.71549600	2.23399900	-2.54773200
H	0.82362300	1.63382200	-3.19058900
H	-0.40688100	-0.66539100	0.98201600
H	2.02214500	2.44478600	-1.13747700
H	1.22934100	3.75531600	-2.02805300

TS_{pdt 2A'→2D}

Fe	1.05970900	-0.43942100	-0.33696000
Fe	-1.32233400	0.30158200	0.53534300
S	0.63803600	1.26080900	1.25218800
S	-0.58843900	0.72787100	-1.59860700
P	3.16620100	-0.35479400	0.47700200
P	-2.96082400	-1.00898600	-0.38909400
O	1.07940900	-3.27330800	0.33241400
O	-1.79022200	-0.76264200	3.23384000
O	2.07149500	-0.92230300	-3.03522600
O	-3.05201600	2.64963900	0.82168800
C	1.09480000	-2.13114100	0.07991400
C	-1.61507100	-0.34125600	2.16585700
C	1.67675300	-0.72426200	-1.95482700
C	-2.37567000	1.70810600	0.71236900
C	0.80776500	2.97133100	0.51484700
C	-0.18283700	2.53659300	-1.81134900
C	1.00826700	3.03500200	-0.99796400
C	4.29960000	-1.62628600	-0.27003200
C	-4.16528800	-0.08084800	-1.45722700
C	4.11529400	1.22432800	0.23343200
C	-2.33130600	-2.35023500	-1.51156800
C	3.29748800	-0.69013300	2.29874300
C	-4.05390400	-1.91775200	0.80826200
H	1.18856000	4.08601400	-1.27269600
H	-3.45457100	-2.61082700	1.40829700
H	4.40512400	-1.45469900	-1.34629500
H	-3.62294300	0.41352600	-2.27013300
H	3.90022600	-2.63245000	-0.10581700
H	-4.68800000	0.67515400	-0.86152500
H	3.63066200	2.04137400	0.77605300
H	-3.17578800	-2.86332300	-1.98737000
H	4.16431200	1.47089100	-0.83244300
H	-1.74814900	-3.07389600	-0.93257500
H	5.13415900	1.09206700	0.61833600
H	-1.69242000	-1.91148900	-2.28611900
H	5.28571900	-1.55167200	0.20382600
H	-4.89930200	-0.77666900	-1.88103300
H	4.34997700	-0.64008200	2.60390800
H	-4.81652600	-2.48240900	0.25895500
H	2.90747500	-1.69095300	2.51305100
H	-4.54733300	-1.20516100	1.47821800
H	2.71608700	0.04909400	2.85802000
H	-0.08369600	3.52747100	0.82995000
H	1.67036400	3.40371200	1.03558100
H	-1.10138100	3.08623000	-1.57021700
H	0.01248700	2.63964500	-2.88468600
H	-0.40931000	-1.04714200	0.31055000
H	1.90361900	2.46544900	-1.28217400

TS_{pdt 2A'→2B}

Fe	1.20486400	-0.57952100	0.02122500
Fe	-1.37845300	-0.28056400	0.45584900
S	0.36091700	0.65887400	1.79062100
S	-0.15974000	0.75473300	-1.29872000
P	3.31087600	0.22022200	-0.33903700
P	-3.19674400	0.19136900	-0.79995500
O	2.25948400	-2.49292700	1.98570600
O	-2.27099500	-3.05541700	0.39447200
O	1.44252500	-2.39741900	-2.27360900
O	-2.87234900	0.29360700	2.90100300
C	1.85958600	-1.73122600	1.20631800
C	-1.92516900	-1.93888100	0.39712500
C	1.37311300	-1.67541400	-1.36618500
C	-2.28329600	0.06903700	1.91891800
C	0.41617200	2.51069600	1.56267500
C	0.02819200	2.59032900	-0.97414100
C	0.89696300	3.01282800	0.20586700
C	4.54278700	-1.14727100	-0.62542700
C	-4.78952000	-0.41097300	-0.05234600
C	3.57230000	1.27897300	-1.84797500
C	-3.56976000	1.97741400	-1.16399100
C	4.10721000	1.14719200	1.06673300
C	-3.18403500	-0.60549200	-2.47746400
H	-2.29740500	-0.28400600	-3.03283000
H	4.25546600	-1.73637600	-1.50279200
H	-4.98255400	0.10647900	0.89315900
H	4.58512200	-1.80734400	0.24748400
H	-4.73533400	-1.48827500	0.13611700
H	2.97446200	2.19305100	-1.79525600
H	-4.56707100	2.04764100	-1.61562900
H	3.26892500	0.71268500	-2.73535200
H	-2.83461000	2.37472600	-1.87072800
H	4.63333900	1.54385500	-1.93219600
H	-3.55086600	2.56634900	-0.24088500
H	5.53702900	-0.71638100	-0.79474300
H	-5.61368100	-0.20971800	-0.74713700
H	5.13970300	1.40479100	0.80073500
H	-4.08779600	-0.31778500	-3.02869200
H	4.11272900	0.50477900	1.95412000
H	-3.16194700	-1.69434800	-2.36280600
H	3.55662100	2.06241300	1.30253300
H	-0.59410400	2.86933000	1.79288600
H	1.08481500	2.85502300	2.36088300
H	-0.98936600	2.97921000	-0.85928400
H	0.43710200	2.98452300	-1.91218900
H	-0.16650400	-1.43361600	0.31680100
H	1.93220600	2.69359100	0.04038500
H	0.90964400	4.11400600	0.23474400

TS_{pdt 2A→2A'}

Fe	1.01642900	-0.63284500	0.14690600
Fe	-1.36401700	0.38087000	0.40364800
S	0.51421900	1.21063000	1.42722700
S	-0.10443100	0.51534600	-1.50649500
P	3.21642700	-0.23921700	-0.23790000
P	-2.96364100	-0.91918400	-0.60075000
O	1.67122500	-2.14578000	2.58139500
O	-2.54377100	-0.27359800	3.01648800
O	0.96118400	-3.01261600	-1.57793700
O	-2.78561800	2.91035100	0.01299800
C	1.43051900	-1.54104300	1.61939900
C	-2.07941000	-0.01099300	1.98436900
C	1.00575300	-2.07046600	-0.89701000
C	-2.23635700	1.89566000	0.17374700
C	0.98395200	2.87362300	0.74142700
C	0.40596500	2.26728400	-1.85401400
C	0.89322500	3.25713300	-0.76117900
C	4.20246100	-1.79412100	-0.50640500
C	-4.70563700	-0.34855600	-0.28770400
C	3.68491400	0.79319400	-1.71253400
C	-2.90106300	-1.09019400	-2.45071700
C	4.12348200	0.57010400	1.16995300
C	-2.98014200	-2.68104300	-0.00626200
H	-2.02723600	-3.16159400	-0.25156100
H	3.86317700	-2.30077000	-1.41623600
H	-4.84833100	0.65435100	-0.70458100
H	4.07240400	-2.47100000	0.34500500
H	-4.89919800	-0.31377900	0.79001100
H	3.33230100	1.82004000	-1.57802600
H	-3.72103000	-1.73983000	-2.78056100
H	3.23627600	0.37144300	-2.61821400
H	-1.94425800	-1.52405900	-2.75851500
H	4.77656100	0.80345000	-1.81972700
H	-3.00455700	-0.10563300	-2.91888600
H	5.26601500	-1.54736000	-0.60856300
H	-5.41662500	-1.03805600	-0.75848100
H	5.18607800	0.66998900	0.91713600
H	-3.79759800	-3.23310400	-0.48549700
H	4.02362300	-0.04201500	2.07264000
H	-3.11860000	-2.70408400	1.08006000
H	3.70615000	1.56087700	1.37378600
H	1.88993700	3.60205900	-1.06213300
H	0.24368700	4.13748100	-0.82252600
H	0.34676600	3.54143100	1.33233800
H	2.00741000	3.02025400	1.10501900
H	-0.48785700	2.67006900	-2.34386800
H	1.16789900	2.15658000	-2.63296400
H	-0.55419500	-1.06533800	0.53602000

TS_{pdt 2B→2B}

Fe	-1.29713800	-0.60239300	-0.03445200
Fe	1.29714800	-0.60240700	-0.03442700
S	0.00003000	0.48929600	-1.60547300
S	-0.00000800	0.57918600	1.46531800
P	-3.26056300	0.54066100	0.07592300
P	3.26054400	0.54068400	0.07590200
O	-2.26522000	-2.34836900	-2.19436600
O	2.18971100	-2.38584000	2.12600300
O	-2.18970300	-2.38598900	2.12583900
O	2.26528300	-2.34850700	-2.19421700
C	-1.90282700	-1.65276200	-1.33847200
C	1.85412500	-1.66987600	1.27501600
C	-1.85412600	-1.66995000	1.27491200
C	1.90286800	-1.65284800	-1.33837600
C	0.00000500	2.33897000	-1.50650700
C	-0.00003600	2.42398200	1.21516800
C	-0.00001200	3.12787100	-0.16946700
C	-3.67385100	1.23691100	1.75144700
C	4.74105400	-0.52971800	-0.27906500
C	-3.53407600	1.97965800	-1.07271500
C	3.53409700	1.97955400	-1.07288600
C	-4.74105900	-0.52971300	-0.27917900
C	3.67375900	1.23710300	1.75137600
H	2.94204300	1.99725400	2.04206400
H	-2.94209100	1.99695200	2.04230500
H	4.69814100	-0.90140700	-1.30834900
H	-3.65730100	0.43445500	2.49645800
H	4.75664500	-1.38485000	0.40532300
H	-4.56354700	2.34272200	-0.96487600
H	4.56361500	2.34252000	-0.96517600
H	-3.36914100	1.66463200	-2.10867100
H	2.84460800	2.79300500	-0.82770700
H	-2.84447500	2.79301100	-0.82752000
H	3.36903900	1.66444900	-2.10880000
H	-4.67277300	1.68933600	1.73047100
H	5.66035800	0.05307500	-0.14604900
H	-5.66036400	0.05310000	-0.14625200
H	4.67272400	1.68943400	1.73043700
H	-4.75673100	-1.38483200	0.40522400
H	3.65706200	0.43474300	2.49648700
H	-4.69806100	-0.90142100	-1.30845100
H	-0.87094700	3.79425500	-0.18767000
H	0.87093100	3.79424300	-0.18764300
H	0.87579700	2.61169800	-2.10455600
H	-0.87579200	2.61166300	-2.10456600
H	0.87359400	2.74399100	1.79365400
H	-0.87370300	2.74396300	1.79361400
H	-0.00000900	-1.63251500	-0.05736500

TS_{pdt 2C→2C}

Fe	1.29561800	0.26183700	0.39090300
Fe	-1.32957800	0.27930400	0.34195100
S	-0.02179700	1.93456700	1.20920500
S	0.01781000	0.44225700	-1.49410400
P	2.42770100	-1.57052000	-0.40038900
P	-2.38773800	-1.61339000	-0.41193500
O	3.46055000	2.04576700	-0.43879000
O	-2.48478700	-0.21341000	3.00353900
O	2.24919500	-0.33328700	3.11040600
O	-3.40636300	2.09740000	-0.62610100
C	2.61276000	1.32153700	-0.10181200
C	-2.03108400	-0.01677700	1.95260500
C	1.88581900	-0.08997600	2.03469900
C	-2.59853900	1.35610000	-0.23409400
C	0.00702700	3.46324300	0.15713700
C	0.04443300	2.14457900	-2.24017000
C	0.03646000	3.45071300	-1.39686900
C	4.16173600	-1.69787600	0.26422700
C	-4.23496700	-1.42872700	-0.54008100
C	1.73311400	-3.25441700	-0.02107600
C	-1.92967200	-2.25538400	-2.09726400
C	2.69695500	-1.61888900	-2.24042200
C	-2.22392700	-3.10419400	0.69139200
H	-1.16937600	-3.35710500	0.83522600
H	4.14058000	-1.80264700	1.35425100
H	-4.48518400	-0.66085600	-1.27994500
H	4.72642800	-0.79505500	0.00765600
H	-4.64395600	-1.12891200	0.43109600
H	2.42194100	-4.03141000	-0.37392600
H	-2.51485800	-3.15610500	-2.31836400
H	0.76915500	-3.37820500	-0.52388900
H	-0.86213600	-2.49304600	-2.13888600
H	1.59137800	-3.36158900	1.05992300
H	-2.13990400	-1.48840200	-2.85002500
H	4.66488600	-2.57018900	-0.16984700
H	-4.68740000	-2.38097900	-0.84206500
H	3.27582800	-2.51046400	-2.50991800
H	-2.74856400	-3.95964200	0.24883100
H	3.24859400	-0.72420700	-2.55014600
H	-2.66470300	-2.88277300	1.66952100
H	1.73417800	-1.63265800	-2.76111500
H	0.93822300	2.11545600	-2.87349100
H	-0.82297700	2.12848500	-2.90961400
H	0.92203400	4.02192100	-1.69744700
H	-0.82989500	4.03274300	-1.73065700
H	-0.87744000	4.00589600	0.51004400
H	0.88257800	3.99731600	0.54379700
H	-0.03155200	-0.71911500	0.79595000

TS_{pdt 2D→2D}

Fe	-1.19679700	0.10221900	-0.52557400
Fe	1.19679300	0.10231700	0.52557000
S	-0.61672100	1.17242100	1.40988900
S	0.61668300	1.17256100	-1.40977800
P	-2.68173500	-1.25642200	0.57405900
P	2.68175900	-1.25630100	-0.57405500
O	-1.38836600	-1.63482500	-2.88903100
O	1.38869800	-1.63546100	2.88846100
O	-3.21784200	2.05752000	-1.33401100
O	3.21767000	2.05775400	1.33411600
C	-1.32259400	-0.94199700	-1.95635500
C	1.32278500	-0.94226400	1.95606800
C	-2.42762700	1.26405900	-1.01546200
C	2.42753500	1.26423500	1.01551700
C	-0.52112700	3.02129700	1.26252000
C	0.52096600	3.02142100	-1.26231000
C	-0.00009500	3.76182200	0.00013500
C	-4.28729300	-1.49021400	-0.33561100
C	4.28717100	-1.49041500	0.33578900
C	-3.23168200	-0.73253700	2.26970900
C	3.23199800	-0.73223800	-2.26955500
C	-2.08701700	-2.99965800	0.83384900
C	2.08688400	-2.99944100	-0.83413200
H	1.18989600	-2.99164700	-1.46198800
H	-4.79895600	-0.52697100	-0.43743000
H	4.79884000	-0.52721600	0.43799000
H	-4.09606300	-1.89595000	-1.33502000
H	4.09579900	-1.89647500	1.33503700
H	-2.37496800	-0.69541800	2.94978900
H	3.97053300	-1.44933800	-2.64823900
H	-3.68298400	0.26420600	2.22101200
H	2.37540400	-0.69520100	-2.94979700
H	-3.97004900	-1.44975300	2.64850300
H	3.68315600	0.26456100	-2.22072300
H	-4.93386000	-2.18313800	0.21597600
H	4.93379900	-2.18317100	-0.21593900
H	-2.86709300	-3.59400600	1.32454100
H	2.86664500	-3.59359300	-1.32556100
H	-1.84325100	-3.45493600	-0.13228100
H	1.84379200	-3.45507800	0.13200400
H	-1.19045500	-2.99207700	1.46232500
H	0.80936600	4.41967600	0.33604900
H	-0.80958500	4.41966700	-0.33572700
H	0.08428200	3.29283900	2.13455100
H	-1.54984700	3.33156100	1.47863700
H	1.54966700	3.33175800	-1.47841400
H	-0.08446300	3.29298000	-2.13432000
H	0.00004400	-0.96438400	0.00003100

pdt 2A*

Fe	1.05216100	-0.62841600	0.13308400
Fe	-1.45445500	0.43126500	0.38238900
S	0.49219300	1.26241400	1.43523800
S	-0.13813100	0.46885700	-1.58097400
P	3.32460800	-0.12017500	-0.22225600
P	-2.94434800	-0.97196900	-0.56332700
O	1.70875000	-2.12785900	2.56552900
O	-2.52745300	-0.20749700	3.03006000
O	1.06978000	-3.02383800	-1.55568300
O	-3.23627700	2.76283700	-0.01215400
C	1.45783000	-1.52099500	1.59479400
C	-2.09601900	0.04429000	1.96992700
C	1.07162700	-2.06437200	-0.87889000
C	-2.46842400	1.88336500	0.11630700
C	1.10292200	2.79552900	0.56287900
C	0.50863300	2.19293800	-1.87559200
C	0.38051200	3.19319800	-0.72477100
C	4.33279800	-1.67560300	-0.48571900
C	-4.71325300	-0.69270700	-0.03781800
C	4.02901100	0.93907500	-1.60693800
C	-3.09731400	-0.97113600	-2.42132500
C	4.20994100	0.59888600	1.26325100
C	-2.71298900	-2.78223200	-0.18064200
H	-1.74010500	-3.11132200	-0.55982200
H	4.03338800	-2.14987100	-1.42743900
H	-5.02222700	0.31973400	-0.32079000
H	4.13785500	-2.37911300	0.33171500
H	-4.79213300	-0.78992900	1.05073900
H	3.75483800	1.98947800	-1.45743400
H	-3.87995300	-1.67366700	-2.73568500
H	3.62244000	0.60240100	-2.56776500
H	-2.13921400	-1.25357800	-2.86945900
H	5.12422800	0.85866000	-1.63116400
H	-3.34985100	0.03995500	-2.75951400
H	5.40639300	-1.44867700	-0.51981400
H	-5.37808700	-1.42307700	-0.51611900
H	5.28153300	0.72521400	1.06095200
H	-3.50839100	-3.38395600	-0.63914500
H	4.07813900	-0.07786300	2.11504600
H	-2.72890300	-2.92264600	0.90602700
H	3.77319300	1.56679500	1.53245000
H	0.80668800	4.15175900	-1.06849500
H	-0.67701000	3.37950200	-0.50869800
H	1.00535700	3.59749900	1.30528000
H	2.17403100	2.64283800	0.37133300
H	-0.04994800	2.55630500	-2.74758000
H	1.55703800	2.07370600	-2.17347400
H	-0.54860300	-0.95293600	0.54729500

pd1 2A'*

Fe	1.04210100	-0.59966300	0.22187000
Fe	-1.48207900	0.43262800	0.36877200
S	0.40039600	1.31068500	1.46885000
S	-0.10942300	0.43567700	-1.55348000
P	3.31474600	-0.19079500	-0.24459800
P	-2.95308200	-0.97087000	-0.59946900
O	1.68769100	-1.94814200	2.74562900
O	-2.72983400	-0.07376800	2.96786200
O	1.04066900	-3.09590900	-1.31711900
O	-2.97829100	2.91407100	-0.22995100
C	1.43603100	-1.40799500	1.73699300
C	-2.22574500	0.12411400	1.92837100
C	1.04847500	-2.09719300	-0.69903800
C	-2.35771800	1.94230700	-0.00835500
C	0.78120100	2.92475500	0.61890900
C	0.37796800	2.21429300	-1.84043800
C	1.31634000	2.84635100	-0.81172200
C	4.35582400	-1.72236700	0.03740000
C	-4.74349700	-0.48920200	-0.38206300
C	3.85546400	0.23701900	-1.98935300
C	-2.85714600	-1.25699800	-2.44013100
C	4.28164400	1.03850000	0.79004700
C	-2.94054000	-2.71455600	0.06202200
H	-1.95759200	-3.16071100	-0.12304300
H	3.99514300	-2.53355000	-0.60548500
H	-4.91538800	0.48520400	-0.85303400
H	4.26143500	-2.04064200	1.08184000
H	-4.97050200	-0.40336000	0.68660100
H	3.42361600	1.19389500	-2.30169000
H	-3.64742100	-1.95251300	-2.75128300
H	3.48817600	-0.54134600	-2.66852000
H	-1.87658400	-1.66969100	-2.69944500
H	4.94955700	0.29433100	-2.06048700
H	-2.97564500	-0.30259600	-2.96439900
H	5.41269800	-1.52708200	-0.18595100
H	-5.40780500	-1.23588600	-0.83570800
H	5.34754700	1.02086400	0.52742700
H	-3.71658600	-3.32258400	-0.42063000
H	4.16374100	0.77280300	1.84704300
H	-3.11469200	-2.69195100	1.14355400
H	3.89235400	2.05225600	0.64721100
H	2.26895400	2.30323400	-0.81236400
H	1.53762300	3.87457500	-1.14623900
H	-0.14384700	3.51451000	0.66009300
H	1.52272600	3.41651500	1.26228700
H	-0.56042300	2.77974000	-1.91097000
H	0.85385300	2.22333600	-2.82954100
H	-0.60371700	-0.92746400	0.62390500

pdt 2B*

Fe	-1.37307100	-0.62571900	-0.06208400
Fe	1.34240300	-0.60955700	0.01930500
S	0.03248400	0.43220500	-1.65018800
S	-0.08144100	0.54573500	1.53753000
P	-3.32966400	0.64885200	0.03698200
P	3.35098500	0.59257900	0.03536600
O	-2.31570600	-2.35958700	-2.22885900
O	2.21825000	-2.28277200	2.26183600
O	-2.35441800	-2.41918600	2.03735200
O	2.35209900	-2.46379400	-2.01457300
C	-1.94836200	-1.66263700	-1.36309300
C	1.87506100	-1.61346400	1.36431700
C	-1.97205500	-1.69304400	1.20151100
C	1.95459300	-1.72001600	-1.20224600
C	-0.02932600	2.28254500	-1.43422300
C	-0.20793900	2.36657200	1.14699900
C	0.50072100	2.85055000	-0.11757200
C	-3.83979800	1.17021800	1.76189000
C	4.82391800	-0.56225200	0.09482000
C	-3.69381200	2.21906900	-0.93144800
C	3.83803300	1.63885800	-1.44308300
C	-4.82443300	-0.36370800	-0.45613800
C	3.76964000	1.71046500	1.48178700
H	3.07718200	2.55801300	1.52617000
H	-3.06774600	1.80580600	2.20911000
H	4.80932400	-1.21862700	-0.78253800
H	-3.94232200	0.27524600	2.38576800
H	4.76495700	-1.18495200	0.99466800
H	-4.74959100	2.50011400	-0.81892300
H	4.86488800	2.01278300	-1.33794400
H	-3.47829600	2.05373100	-1.99351100
H	3.15628700	2.48845000	-1.55833800
H	-3.06934800	3.04309800	-0.56857600
H	3.76827400	1.01897200	-2.34455900
H	-4.79479400	1.71131200	1.74447500
H	5.76501400	0.00271800	0.10731700
H	-5.75319300	0.19164100	-0.27153800
H	4.79768900	2.08749400	1.40352900
H	-4.83946000	-1.29598500	0.11973800
H	3.66353900	1.13348000	2.40776900
H	-4.75981200	-0.61696600	-1.52050700
H	0.41063600	3.94999500	-0.16138900
H	1.56960200	2.62478700	-0.03234400
H	0.55565500	2.68498800	-2.27172000
H	-1.07432000	2.57384100	-1.59165200
H	0.21340400	2.87480900	2.02403000
H	-1.27858300	2.60883200	1.10604000
H	-0.02738200	-1.57115400	-0.01270200

pdt 2C*

Fe	1.35889900	0.30539300	0.38184500
Fe	-1.41081000	0.30915700	0.30162400
S	-0.04583900	1.99048300	1.16748500
S	0.04077700	0.38605000	-1.57643500
P	2.47734400	-1.49771700	-0.36654500
P	-2.34574500	-1.62967600	-0.36951600
O	3.60422900	2.09393700	-0.34675900
O	-2.46203200	-0.15889000	2.99680000
O	2.20957700	-0.24946400	3.13198000
O	-3.77878300	1.90137100	-0.50891900
C	2.69358900	1.39265800	-0.10394000
C	-2.02764900	0.02070700	1.92231800
C	1.86827800	-0.02937600	2.03215200
C	-2.79932900	1.30614700	-0.25361400
C	0.09143000	3.42380100	-0.02465300
C	0.19430300	2.11583300	-2.26091400
C	-0.46400000	3.22593100	-1.43792200
C	4.18942700	-1.67214700	0.36139200
C	-4.21242400	-1.60441400	-0.44311800
C	1.79683700	-3.21312500	-0.07062900
C	-1.93358500	-2.31316300	-2.05774800
C	2.85369700	-1.55186800	-2.19395300
C	-2.07350400	-3.10944800	0.73919900
H	-1.00163500	-3.29020400	0.86173400
H	4.11906400	-1.78192000	1.44917600
H	-4.54143400	-0.86952700	-1.18577400
H	4.76945300	-0.76900300	0.14116200
H	-4.60929000	-1.30870900	0.53470800
H	2.49982300	-3.97808500	-0.42524200
H	-2.47252200	-3.25460600	-2.22542500
H	0.84716600	-3.32493900	-0.60359200
H	-0.85541500	-2.48131600	-2.14327200
H	1.61893300	-3.35134100	1.00189400
H	-2.21936300	-1.57912600	-2.81862000
H	4.70445400	-2.54545500	-0.05895800
H	-4.60463900	-2.59402200	-0.71014200
H	3.45301500	-2.43830600	-2.43856900
H	-2.55392200	-4.00527000	0.32466200
H	3.40902600	-0.64800500	-2.46894200
H	-2.49927500	-2.89423600	1.72575900
H	1.91574600	-1.56334700	-2.75876400
H	1.26892300	2.30434700	-2.38794100
H	-0.26554400	2.07435300	-3.25648300
H	-0.31827300	4.17434600	-1.98327000
H	-1.54526800	3.05555200	-1.38925600
H	-0.44583700	4.24361600	0.46886200
H	1.15726300	3.68663100	-0.05365800
H	-0.02011700	-0.59821200	0.77762000

pdt 2D*

Fe	1.25058100	0.09383400	-0.57374400
Fe	-1.25469700	0.08101200	0.57882200
S	0.63926100	1.10836500	1.47815700
S	-0.65235700	1.14190300	-1.44504100
P	2.64822000	-1.19390400	0.63826000
P	-2.68979900	-1.14863900	-0.64462100
O	1.44862300	-1.66480300	-2.90632100
O	3.44856600	1.79738200	-1.60131300
O	-1.51434200	-1.67199200	2.90912100
O	-3.29109300	2.00177700	1.54548100
C	1.34396800	-0.97339900	-1.96251500
C	2.55184100	1.19212800	-1.14423800
C	-1.38941900	-0.98095900	1.96780300
C	-2.47307800	1.27195300	1.12522600
C	0.41470600	2.95003400	1.27443200
C	0.44472500	3.49433000	-0.15661700
C	-0.65075000	2.97603700	-1.09332600
C	3.58233900	-2.52499200	-0.27856300
C	4.03398400	-0.27214800	1.48087300
C	1.91001500	-2.15342600	2.05486100
C	-1.98075000	-2.08941400	-2.08832800
C	-4.06609900	-0.18612300	-1.45684300
C	-3.64047600	-2.48467600	0.24853600
H	-4.21154000	-2.04182400	1.07232200
H	-0.02954700	-0.91785800	0.00441600
H	1.22734200	3.40248800	1.85688200
H	-0.53497000	3.19207300	1.76958900
H	1.42827400	3.30694500	-0.60206800
H	0.33037400	4.59023800	-0.09335500
H	-1.64852000	3.21062100	-0.69944000
H	-0.54828900	3.45335100	-2.07583200
H	4.26250800	-3.05367500	0.40127800
H	2.87352500	-3.23959300	-0.71105500
H	4.16107700	-2.07449600	-1.09273300
H	4.65101200	0.22891500	0.72698900
H	3.59884100	0.48424600	2.14265900
H	4.65882200	-0.95921600	2.06614400
H	2.69122300	-2.71711300	2.58066400
H	1.43011500	-1.45794900	2.75169300
H	1.15138500	-2.84470300	1.67324600
H	-2.77607800	-2.62701000	-2.62028200
H	-1.49377400	-1.38748900	-2.77367200
H	-1.23215500	-2.80291400	-1.72835200
H	-4.67086200	0.30761800	-0.68810300
H	-3.62330400	0.57800000	-2.10466600
H	-4.70568400	-0.84911100	-2.05398900
H	-4.32899900	-2.99216600	-0.43907800
H	-2.94057500	-3.21651500	0.66671900

TS_{pdt 2A*→2B*}

Fe	1.48248600	-0.68643900	-0.13870400
Fe	-1.57416100	-0.29196600	0.44603400
S	0.39883700	0.24653500	1.73444200
S	-0.19765300	0.49215400	-1.31999500
P	3.40614200	0.63160700	-0.14986800
P	-3.45354300	0.36944600	-0.62829300
O	2.73916600	-2.68593800	1.57966300
O	-2.11394800	-3.11019700	-0.32142100
O	2.08682200	-2.07181600	-2.64258000
O	-2.97141800	-0.54172400	3.00818600
C	2.26906000	-1.86258300	0.89403600
C	-1.84708500	-2.00200500	-0.04242600
C	1.87536200	-1.50464800	-1.64181200
C	-2.42371700	-0.43821000	1.97377600
C	0.51645600	2.10402000	1.57700100
C	-0.02533300	2.31434000	-0.94744800
C	-0.36627400	2.72215400	0.48980400
C	4.81693900	-0.27272500	-0.98217800
C	-5.03093300	-0.43262800	-0.03094400
C	3.63105900	2.32534500	-0.93438000
C	-3.95980600	2.17530500	-0.64037400
C	4.15409700	0.92434100	1.54137100
C	-3.49515200	-0.04086200	-2.44941100
H	-2.64158200	0.43016600	-2.94859000
H	4.60529200	-0.37557200	-2.05257700
H	-5.22020000	-0.14333300	1.00873700
H	4.91105800	-1.27560400	-0.55092300
H	-4.91799500	-1.52178600	-0.07326400
H	3.05972300	3.08151100	-0.38493500
H	-4.89991900	2.30970100	-1.19165100
H	3.28135400	2.30209700	-1.97305800
H	-3.17755600	2.77676400	-1.11666700
H	4.69261500	2.60574100	-0.91998100
H	-4.09220800	2.52408100	0.39030100
H	5.76203800	0.26962500	-0.85036100
H	-5.88260400	-0.13113200	-0.65397600
H	5.10093800	1.47362000	1.46128000
H	-4.43318300	0.30097100	-2.90596500
H	4.33705700	-0.04489500	2.01833100
H	-3.40477400	-1.12641700	-2.56974600
H	3.45929900	1.48638800	2.17452100
H	-0.29164400	3.82113500	0.56420900
H	-1.41163100	2.44783100	0.70140100
H	0.21510000	2.49066300	2.55891600
H	1.57264400	2.36186700	1.42417700
H	-0.70783600	2.81772900	-1.64543500
H	0.99518500	2.60670000	-1.21667200
H	0.35143700	-1.67782200	-0.03023900

TS_{pdt 2A*→2C*}

Fe	-1.50181000	-0.00922900	0.57354100
Fe	1.71305200	-0.40443000	0.30698600
S	-0.01022700	-1.78023200	1.10949200
S	0.00697300	0.17861000	-1.23214900
P	-3.30910200	0.59104400	-0.65272200
P	2.85910400	1.39548700	-0.37203400
O	-3.20504700	-0.92855200	2.77273100
O	3.14004200	-0.70317400	2.83236300
O	-1.11852700	2.68770000	1.75071600
O	3.52807100	-2.18960700	-1.19129900
C	-2.53026800	-0.55899400	1.88480000
C	2.59001600	-0.60043700	1.80512700
C	-1.24178000	1.62260300	1.26981100
C	2.72952900	-1.52446000	-0.64381200
C	-0.50802600	-2.99543800	-0.23320200
C	-0.36909300	-1.34651100	-2.25749100
C	-0.00084500	-2.70625400	-1.64928700
C	-4.61522700	1.53840900	0.28929400
C	4.46223000	1.74434900	0.51306500
C	-3.01126900	1.72726200	-2.10534700
C	3.38190000	1.39198600	-2.16196800
C	-4.35901500	-0.75611400	-1.43119100
C	1.95876500	3.01800100	-0.23588500
H	1.03008500	2.95534200	-0.81397800
H	-4.17100300	2.45182600	0.70018500
H	5.13408500	0.88627000	0.39768900
H	-4.98172300	0.92637100	1.12098000
H	4.26346800	1.88933800	1.58072000
H	-2.34615100	1.24182200	-2.82777000
H	4.05241900	0.54588600	-2.34861400
H	-2.51568400	2.63628200	-1.74624400
H	3.89224100	2.32821200	-2.42184400
H	-3.95839800	1.99182000	-2.59281600
H	2.48608100	1.27888100	-2.78286600
H	-5.45570200	1.80321600	-0.36520500
H	4.94483900	2.64260900	0.10747600
H	-5.20630500	-0.32895100	-1.98455400
H	2.57867000	3.83653100	-0.62405900
H	-4.73824400	-1.41365400	-0.64044000
H	1.70359700	3.20730300	0.81177000
H	-3.74987000	-1.35594600	-2.11674000
H	-0.41132900	-3.48462400	-2.31578700
H	1.08592900	-2.82993900	-1.67063500
H	-0.12321600	-3.96954500	0.09459400
H	-1.60449700	-3.03544000	-0.20008700
H	0.16840200	-1.21510400	-3.20565000
H	-1.44455700	-1.29361300	-2.47364200
H	0.99879800	0.63085400	1.17809000

$$\text{TS}_{\text{pdt } 2A^* \rightarrow 2D^*}$$

Fe	1.43989100	-0.51583200	-0.20946600
Fe	-1.61856700	0.36774200	0.46395800
S	0.49189700	1.23258500	1.03745000
S	-0.46022500	-0.03402900	-1.56812400
P	3.56419100	0.06604200	0.31423500
P	-3.20776200	-1.00762600	-0.29494200
O	1.24254200	-2.63482000	1.86027200
O	-2.34921400	0.15676900	3.27977800
O	2.36459600	-2.35831800	-2.29370600
O	-3.31690800	2.73675900	-0.01716000
C	1.29653800	-1.78137000	1.05630500
C	-2.07783400	0.26284500	2.14656800
C	2.00818500	-1.61631400	-1.45382800
C	-2.57099400	1.83922600	0.11633500
C	0.81321100	2.72162200	-0.05682000
C	0.07992100	1.60733300	-2.30321100
C	0.02396800	2.81883300	-1.36828500
C	4.73439000	-1.37381600	0.53011000
C	-4.09834200	-0.44522600	-1.83297300
C	4.52801300	1.11264000	-0.90903000
C	-2.60438300	-2.70011800	-0.77816000
C	3.83185700	0.99772500	1.91082400
C	-4.61625200	-1.39674100	0.86350700
H	-4.22077300	-1.85701600	1.77574000
H	4.77883200	-1.95124100	-0.40010500
H	-3.35312700	-0.25927200	-2.61433100
H	4.35853900	-2.02615600	1.32617300
H	-4.63643400	0.48633700	-1.62542400
H	4.01890400	2.07040900	-1.06718400
H	-3.42482500	-3.30094400	-1.19120100
H	4.57637700	0.58399900	-1.86811400
H	-2.18631300	-3.19620300	0.10433000
H	5.54761200	1.30410000	-0.54843900
H	-1.81223100	-2.59247400	-1.52757000
H	5.74165600	-1.02380500	0.79027300
H	-4.80763100	-1.20976800	-2.17453900
H	4.90355700	1.15317000	2.09085400
H	-5.32792600	-2.08387600	0.38868900
H	3.39773500	0.42122100	2.73506400
H	-5.13183900	-0.46891500	1.13616700
H	3.32049700	1.96554500	1.87088900
H	0.41628200	3.68727200	-1.92547600
H	-1.02153100	3.04767600	-1.14249600
H	0.59354200	3.60051700	0.56285000
H	1.89383100	2.70999200	-0.25385800
H	-0.57762100	1.78243100	-3.16437700
H	1.09587100	1.43738000	-2.68210800
H	-0.96841300	-0.96611800	0.82724000

TS_{pdt 2C*→2D*}

Fe	-1.80742600	-0.48302900	-0.03144300
Fe	1.45863500	-0.17312400	0.51581100
S	-0.23868800	-1.53532300	1.40204900
S	0.11369300	-0.41532500	-1.41320300
P	-2.33637400	1.75718500	0.07424000
P	2.82013100	1.22491900	-0.59006700
O	-3.50917900	-1.06336000	-2.36175400
O	2.07674100	0.88251000	3.16391100
O	-3.87252500	-1.15711900	1.93416300
O	3.64957300	-2.14957300	0.50956000
C	-2.84262600	-0.82247800	-1.42192400
C	1.86426600	0.43230100	2.10449400
C	-3.04939200	-0.87701400	1.14463400
C	2.72513400	-1.42770400	0.45452700
C	-0.22675800	-3.17165200	0.46689300
C	0.16737200	-2.21270900	-1.94463900
C	0.54480600	-3.22754000	-0.85856500
C	-4.17774700	2.08106900	0.12223900
C	4.35577500	1.74964200	0.33045000
C	-1.76488400	2.79226400	1.52592000
C	3.52586800	0.53994200	-2.17392100
C	-1.84241600	2.81610400	-1.38310500
C	2.13362100	2.85662500	-1.16753800
H	1.34606200	2.66099500	-1.90293000
H	-4.60741600	1.62511600	1.02126400
H	4.92323700	0.85999900	0.62607900
H	-4.64815000	1.62474600	-0.75618800
H	4.07011900	2.29643900	1.23609500
H	-2.13306500	3.82372500	1.44443700
H	4.16900200	1.28026200	-2.66660600
H	-0.67046800	2.79050600	1.56548100
H	2.69628700	0.27405900	-2.83853400
H	-2.14205900	2.34400100	2.45238600
H	4.10940600	-0.36081200	-1.95412900
H	-4.38707300	3.15866600	0.12794700
H	4.98712100	2.39138300	-0.29702100
H	-2.20236700	3.84697500	-1.26783100
H	2.92109100	3.46216700	-1.63437300
H	-2.26344800	2.37898200	-2.29554500
H	1.70585600	3.39975800	-0.31809200
H	-0.75256100	2.81786100	-1.47372900
H	0.38554600	-4.23418100	-1.28192600
H	1.61743000	-3.15273400	-0.65491600
H	0.20633700	-3.90030200	1.16385600
H	-1.28481000	-3.42194100	0.32216400
H	0.89510400	-2.27218100	-2.76424800
H	-0.82770400	-2.41796900	-2.35704800
H	0.46363600	0.99050800	0.66187100

TS _{pdt 2C*→2D-flip*}			
Fe	-1.82009100	0.38983600	-0.00052800
Fe	1.42773900	0.28505800	-0.44720600
S	-0.29561100	1.53882800	-1.44030100
S	0.04397500	0.52739700	1.43434800
P	-2.04819700	-1.89636000	-0.05177900
P	2.82110900	-1.17180800	0.54559900
O	-3.64072300	0.83668700	2.27080700
O	2.36224100	-0.46585100	-3.11294100
O	-3.89202300	0.71711200	-2.04670800
O	3.27444500	2.53704900	0.04215400
C	-2.92955500	0.66014700	1.35002100
C	2.01667500	-0.14661900	-2.04113400
C	-3.06402600	0.58089300	-1.22499700
C	2.51218400	1.66476600	-0.14023700
C	-0.19845500	3.21435500	-0.61248400
C	0.07476700	2.35610300	1.84353700
C	-0.66407400	3.26135900	0.84777000
C	-3.81105300	-2.48107000	0.16242200
C	4.63839100	-0.77253400	0.37596300
C	-1.56873300	-2.81395700	-1.61104400
C	2.66927700	-1.43429800	2.38547600
C	-1.18583800	-2.89004200	1.27593300
C	2.78013000	-2.91307600	-0.12380300
H	1.78321900	-3.34142300	0.02101700
H	-4.43001400	-2.06757000	-0.64199000
H	4.84978100	0.18666500	0.86116600
H	-4.20092800	-2.11907900	1.12047200
H	4.89386700	-0.68643100	-0.68636700
H	-1.75680800	-3.89154200	-1.51213000
H	3.38978700	-2.19152300	2.72006300
H	-0.50895100	-2.63881800	-1.82450500
H	1.65087700	-1.74689400	2.63609600
H	-2.15822200	-2.41872400	-2.44653400
H	2.86531500	-0.48714400	2.89998700
H	-3.86903600	-3.57708000	0.13576100
H	5.25455400	-1.55591400	0.83522800
H	-1.37919200	-3.96473200	1.16127400
H	3.52623500	-3.54255600	0.37767300
H	-1.53997300	-2.55551100	2.25764900
H	2.99135900	-2.88612300	-1.19879000
H	-0.10908800	-2.70190600	1.21549200
H	0.83298200	3.56799700	-0.72818800
H	-0.84810100	3.85960000	-1.21739300
H	1.12787800	2.64179000	1.95211800
H	-0.40506700	2.43699300	2.82711000
H	0.51768200	-0.93519700	-0.66683900
H	-1.73475400	3.01347600	0.87745100
H	-0.55941700	4.30117500	1.20219200

TS
pdt 2A^{1g} → 2C^{1g}

Fe	1.44588800	0.05018000	0.57848900
Fe	-1.69811600	0.41129400	0.29213800
S	-0.03504900	1.87445000	1.03273400
S	-0.01525500	-0.21394300	-1.25409400
P	3.26094200	-0.66632600	-0.59007900
P	-2.85166900	-1.40236500	-0.33955000
O	3.10498500	1.06672600	2.76748700
O	-3.20673500	0.84388300	2.75084500
O	1.08660000	-2.59251500	1.87487800
O	-3.27399900	2.25361100	-1.39681000
C	2.44966300	0.65696600	1.88329600
C	-2.62091700	0.68481000	1.75095800
C	1.19450000	-1.55194500	1.33909900
C	-2.60360200	1.53580700	-0.75424500
C	0.22494100	3.06923000	-0.37801700
C	0.22512500	1.31588500	-2.30610100
C	0.93062400	2.48419100	-1.60629400
C	4.67040100	-1.30416500	0.45825000
C	-4.43497300	-1.75569500	0.57973700
C	2.94278200	-2.12896000	-1.70886200
C	-3.41192300	-1.42584800	-2.11854800
C	4.18869600	0.47425400	-1.75656800
C	-1.93940700	-3.01852900	-0.20208700
H	-1.01940100	-2.95458200	-0.79373300
H	4.29791200	-2.09465400	1.11934900
H	-5.11925400	-0.90760800	0.46405800
H	5.06263100	-0.49053200	1.07851800
H	-4.21615200	-1.88256200	1.64576900
H	2.15900000	-1.86838000	-2.42869400
H	-4.09437100	-0.58836300	-2.30147400
H	2.58710600	-2.96969000	-1.10241200
H	-3.91919100	-2.36946100	-2.35695100
H	3.85685000	-2.42287700	-2.24116200
H	-2.53125500	-1.31213700	-2.76072900
H	5.47683600	-1.70467100	-0.16921700
H	-4.91408200	-2.66531800	0.19579200
H	5.06371000	-0.03747300	-2.17900400
H	-2.55891800	-3.84453200	-0.57470300
H	4.51917500	1.36730400	-1.21385300
H	-1.66933600	-3.19720700	0.84373100
H	3.52778300	0.78348200	-2.57396200
H	-0.75743800	3.48573600	-0.63282700
H	0.83881800	3.87653100	0.04159200
H	-0.76456600	1.60812800	-2.67792200
H	0.82636300	0.99118200	-3.16604100
H	-1.00494100	-0.58459800	1.22814900
H	1.93852600	2.16358600	-1.30228100
H	1.05563100	3.29296800	-2.34699800

TS _{pdt 2A^{**}→2D[*]}			
Fe	1.37545500	-0.50927700	-0.24279700
Fe	-1.59096200	0.35065200	0.49001200
S	0.50659600	1.20923200	1.09667700
S	-0.52284700	0.08742800	-1.59938000
P	3.52001600	-0.01065900	0.31644100
P	-3.22379500	-0.95347400	-0.30496800
O	1.23448100	-2.72399200	1.72490400
O	-2.33465500	0.07027100	3.29856800
O	2.19532800	-2.28152000	-2.42830000
O	-3.05407000	2.87274100	0.00598600
C	1.26369100	-1.82561200	0.96957100
C	-2.05567000	0.20135200	2.16982200
C	1.88353600	-1.56912600	-1.54688700
C	-2.43365600	1.88967600	0.16743500
C	0.69857100	2.76192700	0.06569100
C	-0.19624400	1.82664300	-2.18894700
C	0.92782900	2.54228200	-1.43423600
C	4.74632600	-1.39649500	0.05565200
C	-4.15928600	-0.28693200	-1.77349200
C	4.42989900	1.41469500	-0.49698200
C	-2.65828300	-2.61999800	-0.91041000
C	3.78559800	0.37384000	2.12504300
C	-4.60093400	-1.40433200	0.86977100
H	1.08265000	3.52988200	-1.90192100
H	-4.18260200	-1.92155400	1.74029500
H	4.81751700	-1.62875300	-1.01281000
H	-3.44089700	-0.05914000	-2.56874900
H	4.39452900	-2.29132700	0.58153600
H	-4.67916900	0.63481800	-1.48911200
H	3.91576100	2.35699900	-0.27652100
H	-3.49935500	-3.18617000	-1.33065000
H	4.44366200	1.26823000	-1.58317500
H	-2.21918700	-3.17275500	-0.07288400
H	5.46212000	1.47556900	-0.12712000
H	-1.88963000	-2.47745800	-1.67808600
H	5.73834100	-1.11898500	0.43491200
H	-4.88944800	-1.02093200	-2.13740900
H	4.84333900	0.58841700	2.32549600
H	-5.33179700	-2.05679500	0.37551000
H	3.46872400	-0.48955800	2.72099500
H	-5.10161400	-0.49237700	1.21432100
H	3.16921500	1.23205300	2.41348000
H	-0.19089200	3.37625900	0.25190300
H	1.56251100	3.28843100	0.49348400
H	-1.14227100	2.37898100	-2.12961300
H	0.07956600	1.72792300	-3.24651100
H	-0.96197700	-1.01376000	0.77843700
H	1.85385600	1.96417600	-1.57369600

$$\text{TS}_{\text{pdt } 2A^{*+} \rightarrow 2B^{*}}$$

Fe	1.29385200	-0.63363000	-0.03566600
Fe	-1.48836800	-0.31010500	0.43038200
S	0.32664400	0.41349100	1.83979200
S	-0.16272700	0.74446300	-1.29140100
P	3.39165200	0.37257800	-0.27481500
P	-3.28905700	0.32153400	-0.74480900
O	2.35995100	-2.67587900	1.77089100
O	-2.28680000	-3.12655900	0.07297500
O	1.65017500	-2.26611100	-2.44008400
O	-2.96822800	-0.00602200	2.93291500
C	1.94582100	-1.85370000	1.04870200
C	-1.93461100	-2.00845100	0.17117000
C	1.52543900	-1.60879500	-1.47944300
C	-2.38598300	-0.11871600	1.91624100
C	0.34960600	2.27670500	1.73089600
C	0.00988700	2.54755400	-0.82048800
C	0.84985400	2.87154500	0.41514000
C	4.71181200	-0.90540200	-0.63347200
C	-4.91310300	-0.31929000	-0.08181300
C	3.71355800	1.56294400	-1.68633200
C	-3.69818100	2.13173200	-0.99669200
C	4.18137100	1.24024200	1.18692200
C	-3.32291100	-0.31126300	-2.49918400
H	-2.42649000	0.03811600	-3.02252700
H	4.47338700	-1.42452400	-1.56863800
H	-5.10773200	0.11648400	0.90432400
H	4.73665500	-1.64334800	0.17618500
H	-4.85643900	-1.40831000	0.02383900
H	3.12960500	2.48051400	-1.55845900
H	-4.67399200	2.23417600	-1.48991900
H	3.40028600	1.08498700	-2.62177400
H	-2.93381900	2.59668900	-1.62835000
H	4.77928300	1.81916400	-1.74678400
H	-3.72504400	2.64371400	-0.02848200
H	5.69941800	-0.43492700	-0.72383900
H	-5.73532800	-0.06294900	-0.76190700
H	5.20590900	1.55471900	0.94918200
H	-4.22202800	0.04126500	-3.02125200
H	4.20256300	0.54380800	2.03319800
H	-3.31548600	-1.40674400	-2.48189400
H	3.59349200	2.11648600	1.48073500
H	-0.67395300	2.60593200	1.95108300
H	0.99594800	2.60413000	2.55578700
H	-1.00825900	2.93539000	-0.69308400
H	0.44740900	3.03269000	-1.70285000
H	-0.08415600	-1.42236400	0.13842200
H	1.88394500	2.54935100	0.24680900
H	0.87449600	3.96966500	0.52420600

TS_{pdt 2A*→2A*}			
Fe	1.05778500	-0.67782200	0.17052100
Fe	-1.46409900	0.40982300	0.39240700
S	0.45543100	1.18351900	1.46391500
S	-0.11351500	0.41565100	-1.52235600
P	3.29911400	-0.14886300	-0.24393900
P	-2.98137400	-0.93247000	-0.58882500
O	1.76146700	-2.15532300	2.60608400
O	-2.68548300	-0.13903500	2.99658900
O	1.04481600	-3.09895400	-1.48488100
O	-2.84169400	2.97870900	-0.12249000
C	1.48145500	-1.55995800	1.63620400
C	-2.19183000	0.07516800	1.95514100
C	1.05662300	-2.13070000	-0.82078300
C	-2.28324900	1.96389400	0.06755000
C	0.90386400	2.83740500	0.74515400
C	0.42446400	2.15841500	-1.87699600
C	0.84558300	3.17649100	-0.77516500
C	4.37695100	-1.66609400	-0.44364800
C	-4.75786000	-0.43033600	-0.31175800
C	3.84931400	0.84609800	-1.73559500
C	-2.93462100	-1.15234500	-2.44068300
C	4.20522700	0.73330300	1.13593000
C	-2.98001200	-2.69898900	0.00807200
H	-2.00570200	-3.14921600	-0.21041800
H	4.05873500	-2.22319900	-1.33234400
H	-4.92149300	0.56619600	-0.73738500
H	4.25542200	-2.31511400	0.43122000
H	-4.96116400	-0.38575100	0.76412700
H	3.47801200	1.87310800	-1.65155400
H	-3.74441300	-1.82220900	-2.75789200
H	3.43335700	0.39583900	-2.64433300
H	-1.96801000	-1.57188600	-2.73844300
H	4.94457700	0.86816800	-1.81023300
H	-3.04936300	-0.17764900	-2.92732200
H	5.43522000	-1.39274800	-0.54677600
H	-5.44546400	-1.14516800	-0.78180100
H	5.27504400	0.83231000	0.90975100
H	-3.77216000	-3.28037200	-0.48119900
H	4.08045500	0.16520200	2.06472500
H	-3.13357300	-2.71284700	1.09289100
H	3.77378400	1.72900900	1.28601900
H	1.84195200	3.54567600	-1.05313100
H	0.17212200	4.03601800	-0.87427100
H	0.23757000	3.51935000	1.28625100
H	1.91727000	3.02490300	1.12075300
H	-0.43071400	2.56808200	-2.42738800
H	1.23961800	2.03864800	-2.59967400
H	-0.59199700	-0.98235100	0.58586500

TS
 pdt 2B*→2B*

Fe	-1.36852900	-0.65389500	-0.01980600
Fe	1.36852900	-0.65389500	-0.01980700
S	-0.00000100	0.38180900	-1.62103600
S	0.00000100	0.48962300	1.51303100
P	-3.30267200	0.63886800	0.03784800
P	3.30267200	0.63886800	0.03784900
O	-2.35360200	-2.43823600	-2.12722100
O	2.34409300	-2.36970600	2.14842100
O	-2.34409200	-2.36970300	2.14842500
O	2.35360200	-2.43823400	-2.12722400
C	-1.96799600	-1.72244300	-1.28493900
C	1.95801100	-1.68063500	1.28348600
C	-1.95801000	-1.68063300	1.28348800
C	1.96799600	-1.72244200	-1.28494100
C	0.00000000	2.23436600	-1.50383800
C	0.00000100	2.33098300	1.24205100
C	-0.00000100	3.01765700	-0.15716800
C	-3.76726300	1.40201100	1.68296200
C	4.83598600	-0.38042600	-0.29695200
C	-3.60831000	2.07232000	-1.13257900
C	3.60830800	2.07232600	-1.13257100
C	-4.83598600	-0.38042900	-0.29694500
C	3.76726500	1.40200300	1.68296600
H	3.03113200	2.16268100	1.96445300
H	-3.03113700	2.16269900	1.96443900
H	4.78901600	-0.78987300	-1.31237800
H	-3.76234700	0.62113100	2.45192800
H	4.87843100	-1.21654000	0.41039700
H	-4.64027900	2.43662100	-1.04314500
H	4.64027700	2.43662800	-1.04313500
H	-3.42919900	1.73975900	-2.16155000
H	2.92031500	2.89333700	-0.90376400
H	-2.92031800	2.89333300	-0.90377500
H	3.42919800	1.73977000	-2.16154400
H	-4.76283100	1.86276400	1.63766900
H	5.74372700	0.22815300	-0.19317700
H	-5.74372700	0.22815100	-0.19317600
H	4.76282800	1.86276700	1.63767000
H	-4.87843200	-1.21653700	0.41041100
H	3.76236100	0.62111700	2.45192600
H	-4.78901500	-0.78988400	-1.31236800
H	-0.87170200	3.68491000	-0.17828200
H	0.87169900	3.68491100	-0.17828300
H	0.87726500	2.52576600	-2.09233100
H	-0.87726500	2.52576600	-2.09233200
H	0.87491000	2.67149500	1.80817700
H	-0.87490800	2.67149400	1.80817900
H	0.00000000	-1.60772600	-0.00278100

TS
pdt 2C*→2C*

Fe	1.38845500	0.25032200	0.41254600
Fe	-1.41501500	0.30258400	0.32627100
S	-0.00685900	1.90349700	1.20853400
S	0.04373900	0.32864000	-1.50493700
P	2.46187000	-1.55313800	-0.38952500
P	-2.46612200	-1.56108100	-0.37128300
O	3.58807300	2.09251900	-0.33125400
O	-2.59407000	-0.10901400	2.97945800
O	2.26550200	-0.34981800	3.14742600
O	-3.42742700	2.21153400	-0.72310100
C	2.71248700	1.35201900	-0.07773200
C	-2.10852900	0.04994600	1.92352800
C	1.90881600	-0.11473900	2.05538300
C	-2.63207000	1.44320800	-0.33039900
C	0.03317300	3.39757800	0.10606500
C	0.13652700	2.01426600	-2.27916300
C	0.11062000	3.33606800	-1.45080100
C	4.08911200	-1.92102300	0.44982900
C	-4.32894200	-1.43437100	-0.30807000
C	1.64330500	-3.23215700	-0.33296100
C	-2.20245200	-2.16174500	-2.11998800
C	2.98614700	-1.45636700	-2.17885300
C	-2.19300500	-3.11429800	0.63107400
H	-1.12952300	-3.37077500	0.63296500
H	3.91469300	-2.15470900	1.50580200
H	-4.66231100	-0.63864600	-0.98338500
H	4.73227600	-1.03564000	0.39292100
H	-4.63761300	-1.17533100	0.71102300
H	2.31303700	-4.00796800	-0.72656100
H	-2.80239900	-3.06140900	-2.30856200
H	0.72880600	-3.20743400	-0.93474000
H	-1.14233700	-2.37827200	-2.28619400
H	1.37982400	-3.47024700	0.70369600
H	-2.49498500	-1.36880100	-2.81697400
H	4.59349400	-2.76851700	-0.03170300
H	-4.79851800	-2.38239300	-0.60067400
H	3.55331300	-2.35097700	-2.46667600
H	-2.77368800	-3.95257600	0.22429500
H	3.61165000	-0.56768300	-2.31994300
H	-2.50279000	-2.92684000	1.66543300
H	2.09564500	-1.35995500	-2.80900800
H	1.06296300	1.97543600	-2.86420700
H	-0.69769300	2.02173700	-2.99064300
H	1.00979300	3.89510000	-1.73728600
H	-0.74115400	3.91804400	-1.82324900
H	-0.87039900	3.94401500	0.40139900
H	0.89162700	3.96392300	0.48652600
H	-0.05720600	-0.62861000	0.81335600

TS _{pdt 2D* → 2D*}			
Fe	-1.26274100	-0.06769600	0.58740600
Fe	1.26276900	-0.06772400	-0.58741000
S	-0.64200000	-1.06435000	-1.43757800
S	0.64201600	-1.06434900	1.43757800
P	-2.69303600	1.19256900	-0.61057200
P	2.69302400	1.19257000	0.61056200
O	-1.51870500	1.65067700	2.94676000
O	1.51882500	1.65063600	-2.94676800
O	-3.22337300	-2.09881000	1.49244300
O	3.22335300	-2.09889900	-1.49241900
C	-1.39624400	0.97529500	1.99350700
C	1.39631700	0.97525800	-1.99351800
C	-2.45205100	-1.30387600	1.10471300
C	2.45206100	-1.30392900	-1.10470100
C	-0.55118000	-2.91144000	-1.26747200
C	0.55111200	-2.91143800	1.26750800
C	-0.00004500	-3.63666800	0.00002400
C	-3.63643500	2.51776300	0.30576000
C	3.63630100	2.51785100	-0.30576800
C	-4.07413900	0.25351500	-1.44250700
C	4.07420700	0.25358300	1.44244100
C	-1.97390300	2.15586000	-2.03505400
C	1.97385400	2.15576900	2.03508700
H	1.48618000	1.46298100	2.72941500
H	-4.20567700	2.06460600	1.12514400
H	4.20561400	2.06474400	-1.12513000
H	-2.93204000	3.24043200	0.73217500
H	2.93182700	3.24042500	-0.73221400
H	-3.63597500	-0.49763400	-2.10848200
H	4.71349800	0.93127300	2.02319000
H	-4.67792600	-0.25537200	-0.68296300
H	3.63611100	-0.49757900	2.10844800
H	-4.71343000	0.93117100	-2.02329500
H	4.67797500	-0.25528900	0.68287300
H	-4.32542900	3.03792700	-0.37178900
H	4.32521900	3.03811100	0.37178500
H	-2.76265900	2.70767800	-2.56225300
H	2.76259500	2.70754900	2.56234700
H	-1.22266700	2.85771800	-1.65780200
H	1.22263100	2.85765600	1.65786000
H	-1.48625100	1.46312200	-2.72944800
H	0.80351900	-4.29566200	-0.35060800
H	-0.80363200	-4.29562700	0.35066700
H	0.03797300	-3.21448800	-2.14071500
H	-1.58390800	-3.23498500	-1.44424100
H	1.58382400	-3.23502600	1.44429400
H	-0.03806200	-3.21444000	2.14075200
H	-0.00000500	0.93965300	-0.00001300

pdt 3A1

Fe	-1.11461600	-0.58349000	-0.20820900
Fe	1.27101900	0.26446600	-0.44375700
S	-0.05344200	0.73460600	1.38082900
S	-0.48170600	1.07759800	-1.71377600
P	-3.18265900	-0.34567200	0.68697800
P	2.77287800	-0.74667400	1.01881200
O	0.71294500	-2.84834500	-0.37786600
O	-2.39091900	-1.91828800	-2.48947700
O	2.52454200	-0.89064400	-2.84562300
O	2.99339600	2.61400800	-0.64941800
C	0.20990700	-1.78579300	-0.31556400
C	-1.89070200	-1.40150100	-1.57666700
C	2.02731400	-0.44569400	-1.89707800
C	2.29331200	1.68953200	-0.54125800
C	4.02478000	-1.85763200	0.21417900
H	3.51046800	-2.67455400	-0.30260400
H	4.69429500	-2.27356800	0.97648600
H	4.61526300	-1.28833400	-0.51185400
C	2.07156600	-1.79895600	2.38675300
H	2.88351000	-2.06098900	3.07598100
H	1.63684900	-2.71428900	1.97614000
H	1.30375900	-1.23730300	2.92964400
C	3.80902600	0.47593200	1.96242300
H	4.48211100	-0.06378700	2.63949100
H	3.15720700	1.13180400	2.54988800
H	4.40544600	1.08519000	1.27578700
C	-0.99616700	2.79159900	-1.18139200
H	-0.69174800	3.42885400	-2.01981900
H	-2.09223400	2.77220100	-1.15883500
C	-0.70396800	2.48968500	1.36434100
H	-1.78186900	2.41658800	1.55477800
H	-0.24096800	2.94754800	2.24637100
C	-4.27761700	1.02368200	0.05056600
H	-3.85118000	2.00243900	0.29296500
H	-5.26925600	0.94480300	0.51334400
H	-4.37749400	0.93642600	-1.03672300
C	-3.21604100	-0.12541600	2.53243700
H	-4.25735500	-0.10665100	2.87603900
H	-2.72231300	0.80495800	2.82796300
H	-2.69002100	-0.96362900	3.00078800
C	-4.24757500	-1.85063200	0.45684700
H	-4.45103700	-2.01874900	-0.60558100
H	-5.19751700	-1.71006400	0.98602100
H	-3.72974500	-2.72683600	0.86096700
H	-1.36158100	-1.62493000	0.85121700
C	-0.41495900	3.33073200	0.12404000
H	0.66472000	3.48152900	0.02078800
H	-0.84966200	4.32882500	0.29350800

pdt 3A1'

Fe	1.09537700	-0.57091400	0.13238700
Fe	-1.27426000	0.23829000	0.45183700
S	0.00089600	0.81384000	-1.38377100
S	0.50356300	0.99777300	1.73722600
P	3.20695800	-0.38901300	-0.65982300
P	-2.89762400	-0.64082400	-0.96639300
O	-0.78004700	-2.80437500	0.09776800
O	2.26860100	-2.18185800	2.28427500
O	-2.51828100	-0.91565600	2.86187000
O	-2.68694200	2.78732600	0.68572900
C	-0.30813800	-1.72361400	0.13611300
C	1.80479800	-1.55065200	1.42489300
C	-2.02858900	-0.47343500	1.90813700
C	-2.14759700	1.76047900	0.58638800
C	-4.03315400	-1.88273200	-0.17996100
H	-3.44591600	-2.72424500	0.20177200
H	-4.75078000	-2.24789400	-0.92438600
H	-4.57884600	-1.41886700	0.64870900
C	-2.31442100	-1.50825400	-2.50776000
H	-3.18852000	-1.75441300	-3.12264000
H	-1.78842600	-2.43068800	-2.24589200
H	-1.64481900	-0.85200000	-3.07356900
C	-4.06019400	0.64177400	-1.64772300
H	-4.79172200	0.15768100	-2.30575600
H	-3.49656800	1.38550200	-2.22173800
H	-4.59065200	1.14575800	-0.83309100
C	0.91074700	2.75766300	1.27133500
H	0.00853400	3.34998100	1.46536800
H	1.66411200	3.04898600	2.01324900
C	0.48554800	2.61462100	-1.26804200
H	0.94107100	2.82994900	-2.24215000
H	-0.45066300	3.18211300	-1.20646500
C	4.45266900	0.49966700	0.40562600
H	4.14853800	1.53526800	0.58485700
H	5.43201600	0.49007200	-0.08876500
H	4.53124100	-0.01471400	1.36967500
C	3.37223200	0.39668900	-2.33566100
H	4.41224000	0.31459800	-2.67436000
H	3.09035900	1.45300700	-2.29267400
H	2.71344700	-0.12027400	-3.04087600
C	4.01571300	-2.04321000	-0.90512700
H	4.04100700	-2.59644000	0.03937800
H	5.04094600	-1.90252100	-1.26749500
H	3.44358400	-2.62255400	-1.63729500
H	1.29154900	-1.51862800	-1.01504400
C	1.44528300	2.98568100	-0.14010800
H	1.68697600	4.05544800	-0.24227100
H	2.38487500	2.43327300	-0.26620100

pdt 3A2

Fe	1.05778100	-0.60946700	0.19448400
Fe	-1.24176900	0.48383100	0.37305300
S	-0.06526000	0.35742000	-1.60669600
S	0.67171500	1.41424200	1.26199900
P	3.31191600	-0.34754200	0.13440800
P	-2.82826600	-0.93440000	-0.53463300
O	-0.68245800	-2.28798600	1.82930500
O	1.40948000	-3.01729200	-1.44522200
O	-2.47025400	0.42446100	3.04989700
O	-2.86302400	2.82036600	-0.28081800
C	-0.18968100	-1.45567100	1.16119100
C	1.27387900	-2.06878000	-0.78429900
C	-1.97452300	0.41544400	2.00117600
C	-2.19775500	1.89671800	-0.03289200
C	-4.06747600	-1.60025500	0.67819200
H	-3.54885500	-2.16545100	1.46002300
H	-4.77428900	-2.25967600	0.16067500
H	-4.61843000	-0.77369400	1.13986300
C	-2.18465300	-2.46222900	-1.37796600
H	-3.03100000	-3.00850300	-1.81239900
H	-1.67560400	-3.10959400	-0.65775300
H	-1.49125800	-2.18224000	-2.17793900
C	-3.87512100	-0.15282100	-1.85592100
H	-4.57944000	-0.89380300	-2.25252600
H	-3.23034000	0.20499800	-2.66592000
H	-4.43724300	0.69204700	-1.44467800
C	1.28874700	2.85859700	0.24855100
H	1.16509500	3.71436900	0.92283900
H	2.36590000	2.70296000	0.10812100
C	0.64896400	2.00991800	-2.10689900
H	1.67710000	1.79239200	-2.41697500
H	0.08054600	2.28563600	-3.00269200
C	4.02415400	0.58201500	1.57765800
H	3.65172100	1.61005600	1.61012900
H	5.11775300	0.59455900	1.49626000
H	3.72987200	0.07775100	2.50396000
C	4.08787600	0.46302900	-1.35670500
H	5.18035800	0.43139400	-1.26039800
H	3.77113300	1.50744100	-1.43964800
H	3.78981700	-0.07663300	-2.26222700
C	4.23036500	-1.96069900	0.22476500
H	3.89519300	-2.52221100	1.10310200
H	5.30537300	-1.76153300	0.30662400
H	4.04553700	-2.56044700	-0.67224300
H	1.69725900	-1.11862600	1.45500100
C	0.59328100	3.14095900	-1.08164000
H	1.08680800	4.01698800	-1.53230100
H	-0.44564100	3.43714200	-0.90290300

pdt 3A2'

Fe	1.04440500	-0.55396000	0.20764600
Fe	-1.26984700	0.47309000	0.38312500
S	-0.08617300	0.37251700	-1.60786000
S	0.61317300	1.45643500	1.28620800
P	3.30659600	-0.41015400	0.15116500
P	-2.86116700	-0.91679400	-0.55266900
O	-0.71618600	-2.24576000	1.80771700
O	1.41267300	-3.01955500	-1.33624500
O	-2.58428200	0.47658800	3.01918100
O	-2.64431600	2.92949100	-0.39490600
C	-0.26072100	-1.37903500	1.15334900
C	1.26344100	-2.04611200	-0.71431800
C	-2.05493200	0.44387500	1.98750600
C	-2.11472700	1.93967700	-0.08517400
C	-4.10957100	-1.60707800	0.63664200
H	-3.59550300	-2.18656200	1.41109100
H	-4.81158600	-2.25764900	0.10173200
H	-4.66545600	-0.79091900	1.11061000
C	-2.21128300	-2.42924600	-1.41866000
H	-3.05077000	-2.96804100	-1.87508000
H	-1.71174900	-3.08929900	-0.70281500
H	-1.50616700	-2.13579700	-2.20370600
C	-3.89571200	-0.10251000	-1.86376100
H	-4.60325300	-0.82876900	-2.28148600
H	-3.24439000	0.26889700	-2.66237800
H	-4.45444000	0.73703100	-1.43658600
C	1.05690400	2.96533400	0.28097600
H	0.17833100	3.62078600	0.31369300
H	1.84994700	3.44942100	0.86397700
C	0.49241300	2.08503800	-2.07728500
H	0.91326700	1.94966100	-3.08053500
H	-0.40615000	2.70621000	-2.17059400
C	4.06496200	0.93744500	1.18077500
H	3.81285800	1.92143100	0.77395400
H	5.15530200	0.81835200	1.18345500
H	3.68486300	0.86543200	2.20500700
C	4.11022200	-0.24006700	-1.52317000
H	5.20137400	-0.22868100	-1.40965700
H	3.78919600	0.68142800	-2.01848000
H	3.82253000	-1.09341800	-2.14689000
C	4.12183400	-1.93704500	0.82590900
H	3.82998800	-2.07140200	1.87279800
H	5.21131500	-1.83303500	0.75951200
H	3.81010300	-2.81890600	0.25697700
H	1.62118100	-1.00037700	1.51633600
C	1.52586700	2.72119400	-1.15167900
H	2.43010700	2.09951400	-1.14113100
H	1.81185900	3.69336600	-1.58348000

pdt 3A3

Fe	1.07004200	-0.49985200	0.17129600
Fe	-1.35833700	0.25599100	0.48219800
S	0.44468300	1.20123000	1.59096100
S	-0.10498000	0.64694600	-1.43500700
O	1.20042000	-2.83727800	-1.61539800
O	-1.24807500	-2.64111200	0.98672200
C	1.14581400	-1.91714600	-0.90635700
C	-2.28940900	0.40021600	1.97898800
C	-1.08400000	-1.50624100	0.74166000
C	0.65797900	2.94899500	0.97169800
C	0.34122800	2.46326800	-1.52682100
C	-0.05001600	3.31961500	-0.32774500
H	1.42108500	2.50368100	-1.71549100
H	-0.16873300	2.81291000	-2.43209600
H	0.19605800	4.36780600	-0.56134200
H	-1.13670400	3.26649800	-0.18048100
H	0.27534200	3.55553800	1.80116000
H	1.73890300	3.11805500	0.90898000
C	1.62582600	-1.39774700	1.61458900
O	1.97916900	-1.97678500	2.55620200
O	-2.90105100	0.55439300	2.95339500
H	-2.05634700	1.58770900	0.30939100
P	-3.12306600	-0.30513500	-0.83531600
P	3.19663800	-0.00864900	-0.42061900
C	-4.59492900	-0.96047600	0.08839100
H	-4.96801900	-0.20116400	0.78395400
H	-5.39096500	-1.22398900	-0.61830600
H	-4.30716300	-1.85217000	0.65615800
C	-2.79476700	-1.61728100	-2.11093600
H	-3.69491900	-1.77199200	-2.71822400
H	-1.97090300	-1.30142200	-2.75999900
H	-2.52769600	-2.55855200	-1.61913800
C	-3.80910300	1.10254600	-1.83153400
H	-3.02680800	1.49848900	-2.48771200
H	-4.65166900	0.75336900	-2.44050600
H	-4.14789700	1.89742100	-1.15876000
C	3.99487600	1.49591500	0.32552800
H	3.86466000	1.48485800	1.41274000
H	5.06553300	1.49011000	0.08655700
H	3.54948600	2.40768800	-0.08447500
C	3.47382900	0.19704000	-2.24891700
H	4.53274600	0.41233500	-2.43788400
H	3.19652200	-0.72772200	-2.76617500
H	2.86197200	1.01352200	-2.64379400
C	4.40279000	-1.35719100	0.01157800
H	4.07908700	-2.30570300	-0.43021900
H	5.39494500	-1.09960100	-0.37822600
H	4.46389100	-1.47418500	1.09866800

pdt 3A3'

Fe	1.05991000	-0.50338500	0.10159900
Fe	-1.37799900	0.21737400	0.51263900
S	0.45033800	1.06256900	1.65825500
S	-0.17006100	0.73411200	-1.39687400
O	1.10971000	-2.66762800	-1.89397100
O	-1.32544200	-2.72063200	0.77558700
C	1.09194100	-1.81699100	-1.10160600
C	-2.28799000	0.28788100	2.02968600
C	-1.17505500	-1.56884600	0.62923400
C	0.62723200	2.84837800	1.14184500
C	0.12563700	2.57982200	-1.37623700
C	1.06393700	3.11153400	-0.29642400
H	0.52925300	2.80187500	-2.37157100
H	-0.87001500	3.03107800	-1.29834300
H	2.07218400	2.70932200	-0.45467400
H	1.14037100	4.20247000	-0.42910700
H	-0.34397400	3.30621400	1.36128000
H	1.36449100	3.25818000	1.84296000
C	1.59153500	-1.53887600	1.45336000
O	1.93517400	-2.21028100	2.33609900
O	-2.88322100	0.39447200	3.02045500
H	-1.95379700	1.61769300	0.44527500
P	-3.19273100	-0.14942900	-0.80942100
P	3.21160900	-0.03150800	-0.38313500
C	-4.68996600	-0.79476700	0.08057600
H	-5.01038200	-0.07766400	0.84384400
H	-5.50759700	-0.95108000	-0.63328900
H	-4.44854500	-1.74667900	0.56617200
C	-2.94286900	-1.37874100	-2.18044800
H	-3.85739100	-1.45659500	-2.78089300
H	-2.11667400	-1.05008100	-2.82006300
H	-2.70501400	-2.36121200	-1.75927000
C	-3.81134500	1.36341900	-1.68824200
H	-3.01614300	1.76107100	-2.32799800
H	-4.68026900	1.10980900	-2.30745000
H	-4.09462600	2.12411500	-0.95315300
C	4.11748900	1.05588800	0.82443000
H	4.08498100	0.58954200	1.81508600
H	5.16257000	1.16202300	0.50804400
H	3.65686700	2.04580300	0.88739000
C	3.51484000	0.71445800	-2.06018200
H	4.59098700	0.86595900	-2.20914900
H	3.13542800	0.02948000	-2.82628200
H	2.99546400	1.67165900	-2.15841100
C	4.29669200	-1.54255300	-0.42448000
H	3.93653600	-2.24749400	-1.18097700
H	5.32384400	-1.24747700	-0.67096700
H	4.29192000	-2.03566500	0.55320800

pdt 3A4

Fe	-1.05959700	-0.47872100	-0.25820400
Fe	1.36205900	0.26826300	-0.56772700
S	-0.44164200	1.32272600	-1.56252400
S	0.15932600	0.52425100	1.41775000
O	-1.07990100	-3.02115000	1.22289500
O	3.26731700	2.43236900	-1.11691200
C	-1.07000700	-2.01197900	0.64346700
C	1.01272500	-1.34485100	-1.23708600
C	2.48910800	1.61433100	-0.82962400
C	-0.65108500	3.01007400	-0.79303300
C	-0.31475100	2.31673700	1.66910000
C	0.04815800	3.27626000	0.53986800
H	-1.38976900	2.33204400	1.88716100
H	0.21207500	2.59913800	2.58826000
H	-0.22342400	4.29512500	0.85957500
H	1.13541400	3.27501300	0.39996300
H	-0.26669700	3.69023200	-1.56268100
H	-1.73264700	3.17173800	-0.72232100
C	-1.74264900	-1.20007400	-1.74526900
O	-2.19746800	-1.65707000	-2.71041900
O	1.10395100	-2.38299500	-1.77740400
H	1.99677800	0.12352500	-1.91971300
P	-3.13389100	-0.03426300	0.52453300
P	3.00993200	-0.76772400	0.62534700
C	-3.29368000	-0.08565600	2.37783700
H	-4.33107300	0.12952000	2.66163900
H	-3.02121100	-1.08275900	2.73941900
H	-2.62832700	0.64712700	2.84399100
C	-3.93645000	1.57860900	0.05843900
H	-4.97381500	1.57610900	0.41554300
H	-3.40842600	2.41757800	0.52170100
H	-3.92845100	1.70103800	-1.02977300
C	-4.40770600	-1.27848800	-0.01469100
H	-5.36497900	-1.05700000	0.47234200
H	-4.53979000	-1.23727600	-1.10088100
H	-4.08774500	-2.28780500	0.26569100
C	3.85285900	0.32369900	1.86901300
H	4.61482000	-0.25180800	2.40806800
H	4.32999100	1.17061700	1.36513400
H	3.10896600	0.69866500	2.57971800
C	2.48327200	-2.23802500	1.63042700
H	2.08165300	-3.01805500	0.97574500
H	3.34864800	-2.63597100	2.17433000
H	1.71507900	-1.93582200	2.35043300
C	4.38650700	-1.41338000	-0.43765700
H	5.14966400	-1.89723300	0.18349400
H	3.98455900	-2.14013900	-1.15174000
H	4.84213500	-0.58630700	-0.99271700

pdt 3A4'

Fe	-1.03681800	-0.49083600	-0.18071800
Fe	1.38374200	0.26537100	-0.59552400
S	-0.47983500	1.22309600	-1.60461500
S	0.23735400	0.58384600	1.40027900
O	-0.89530400	-2.93057000	1.45538000
O	2.97092800	2.70655800	-0.98277800
C	-0.95548800	-1.96045500	0.81561500
C	1.13303800	-1.35820100	-1.27465400
C	2.33273300	1.75642000	-0.76962500
C	-0.68986500	2.94150700	-0.90507100
C	-0.05226900	2.42683700	1.55428500
C	-1.04578900	3.05107900	0.57637100
H	-0.40732600	2.55965700	2.58337700
H	0.93790900	2.89086500	1.47687300
H	-2.04121900	2.62297100	0.74662300
H	-1.12349500	4.12248700	0.82092800
H	0.23743400	3.47750700	-1.13961500
H	-1.48751100	3.38053000	-1.51661800
C	-1.68892700	-1.35170400	-1.60038900
O	-2.13367900	-1.90662400	-2.51888900
O	1.21529100	-2.39634300	-1.81025800
H	2.07616600	0.19084900	-1.92800800
P	-3.15225900	-0.10423400	0.49901400
P	3.10571100	-0.66804400	0.57615600
C	-3.36847600	0.48647700	2.24997300
H	-4.43792500	0.58201300	2.47448300
H	-2.91850900	-0.24467600	2.93012500
H	-2.87852700	1.45271200	2.39867900
C	-4.14325000	1.07041500	-0.55010500
H	-5.16708900	1.13730800	-0.16196000
H	-3.69198500	2.06672000	-0.55521800
H	-4.16950300	0.69225400	-1.57785400
C	-4.21236700	-1.63413600	0.47476500
H	-5.22701700	-1.38156700	0.80586700
H	-4.25953700	-2.04606000	-0.53878000
H	-3.79481000	-2.39071200	1.14748800
C	3.91693400	0.47319100	1.79675800
H	4.70825800	-0.06252700	2.33466700
H	4.35411900	1.33191400	1.27659200
H	3.16769900	0.82684700	2.51298900
C	2.66810200	-2.15111400	1.60309300
H	2.27583700	-2.94921900	0.96478700
H	3.56272200	-2.51371400	2.12376500
H	1.91000700	-1.87260700	2.34274000
C	4.49807500	-1.25312500	-0.50155300
H	5.29632600	-1.68669200	0.11278300
H	4.12571100	-2.00964000	-1.20054900
H	4.89756400	-0.40935100	-1.07444900

pdt 3B

Fe	1.23018800	-0.48443800	-0.17117100
Fe	-1.30367700	-0.55328300	-0.04569700
S	0.04098000	0.44823000	1.58540600
S	-0.13839200	0.81053300	-1.54275800
O	2.40497700	-1.60262200	-2.63306400
C	1.93583200	-1.17793900	-1.66003900
C	-1.97740000	-1.57915200	1.23224500
C	0.01107200	2.31319000	1.48774800
C	-0.19128700	2.60931200	-1.06164300
C	-0.75231300	2.93028000	0.32021100
H	0.82903500	2.98855200	-1.18265600
H	-0.80522200	3.07642900	-1.84157800
H	-0.74634200	4.02472900	0.44712600
H	-1.80059200	2.61190100	0.37001100
H	-0.44488500	2.61204700	2.43927300
H	1.05467600	2.65133800	1.50325200
C	1.83237700	-1.76165600	0.91772800
O	2.21025000	-2.60208400	1.62483300
C	-0.43977900	-1.99957800	-0.67552600
O	-0.29979700	-3.08686200	-1.09225500
O	-2.40387100	-2.24086900	2.08791500
H	-2.03857500	-1.09586200	-1.23187600
P	-3.39226400	0.32806800	-0.20811300
P	3.16971800	0.65716400	0.19543200
C	3.55643600	0.99222200	1.98484200
H	3.58780700	0.04403700	2.53220000
H	4.53289200	1.48608500	2.06115000
H	2.79124600	1.62826200	2.43901700
C	3.43104000	2.30249400	-0.63646600
H	4.47604600	2.60818200	-0.50266200
H	3.21423300	2.21610300	-1.70653300
H	2.78417900	3.06706900	-0.19490900
C	4.67538300	-0.29308600	-0.34874500
H	4.67812800	-0.40848200	-1.43750400
H	5.57840400	0.24879900	-0.04313600
H	4.68046700	-1.28618900	0.11323200
C	-4.09002100	1.22048200	1.27481400
H	-5.11925200	1.53547200	1.06296000
H	-4.09172700	0.53878900	2.13246900
H	-3.48764200	2.09885500	1.52585200
C	-3.67705300	1.48075000	-1.63730200
H	-4.74296900	1.73226600	-1.69563000
H	-3.09813900	2.40017500	-1.51134300
H	-3.36365200	0.98732800	-2.56324800
C	-4.67474500	-0.98645600	-0.49731600
H	-5.66823200	-0.52656600	-0.56075900
H	-4.45392500	-1.51033600	-1.43329500
H	-4.66817900	-1.71259800	0.32226500

pdt 3B'

Fe	-1.20128100	-0.47246100	0.12853800
Fe	1.34595500	-0.59173900	0.03228700
S	0.02544600	0.35285400	-1.65032800
S	0.18292500	0.83977300	1.45708300
O	-2.33168300	-1.60669800	2.60078000
C	-1.87344800	-1.17539100	1.62439500
C	2.06478500	-1.60512800	-1.23556500
C	0.18936800	2.21074900	-1.66764000
C	0.33960000	2.60870300	0.87746600
C	-0.32859100	2.96549000	-0.44685300
H	-0.10042800	3.19503200	1.69322400
H	1.41221100	2.83591400	0.85162400
H	-1.40965500	2.81207500	-0.35564300
H	-0.17842500	4.04265200	-0.62311700
H	1.25183400	2.40944600	-1.84510600
H	-0.35847800	2.52057000	-2.56580200
C	-1.77904900	-1.77039000	-0.94692900
O	-2.13073900	-2.62387500	-1.65139500
C	0.53784500	-2.04647000	0.68023100
O	0.35952100	-3.11660200	1.11990400
O	2.51146600	-2.25884200	-2.08604500
H	2.11742200	-1.11102300	1.21098600
P	3.36508600	0.43180800	0.26869200
P	-3.18101300	0.61516400	-0.12319200
C	-3.50014900	1.45142900	-1.75557700
H	-3.33932500	0.72750000	-2.56160100
H	-4.53866000	1.80347100	-1.78413600
H	-2.83005800	2.30204400	-1.90645100
C	-3.60650100	1.87610000	1.17931800
H	-4.60044400	2.29306400	0.97598400
H	-3.61559100	1.38385800	2.15796300
H	-2.87188300	2.68606700	1.20169900
C	-4.63773300	-0.54072100	-0.01691600
H	-4.64351500	-1.06031800	0.94681800
H	-5.56601200	0.03438100	-0.11825500
H	-4.58891400	-1.28274200	-0.82078700
C	3.87118400	1.80820500	-0.88755300
H	4.91356600	2.08389100	-0.68435100
H	3.78377600	1.47209900	-1.92645700
H	3.23941600	2.68969500	-0.73904600
C	3.67352600	1.14750800	1.95784500
H	4.69185900	1.55224400	2.00122400
H	2.95909100	1.94330600	2.18935900
H	3.56188200	0.35488300	2.70503100
C	4.78117000	-0.75834800	0.08774000
H	5.72015100	-0.25139300	0.33926100
H	4.63420600	-1.60915200	0.76130900
H	4.83884400	-1.12724300	-0.94150600

pdt 3C1

Fe	1.29185300	0.32738300	0.31763000
Fe	-1.28959800	0.31408600	0.41524800
S	0.03948100	2.09624300	0.99753800
S	-0.05218700	0.25078800	-1.53932000
O	-0.39513700	-2.16646600	1.73824100
C	-2.24185000	0.67784200	1.86716200
C	2.68541600	1.26322000	-0.17273700
C	-0.57219400	-1.15537300	1.16977300
C	-0.13416300	3.41578800	-0.31572600
C	-0.25635000	1.89896000	-2.40020500
C	0.39974300	3.09256700	-1.70969500
H	0.18341700	1.74697900	-3.39277100
H	-1.33732300	2.03987000	-2.51414500
H	1.48595600	2.94980300	-1.67456900
H	0.22280400	3.97763500	-2.34130700
H	-1.20302300	3.65913400	-0.33439200
H	0.40735500	4.27047600	0.10694000
O	3.61901600	1.90142200	-0.45456200
C	1.90598400	0.09623400	1.98009000
O	2.31458200	-0.04762500	3.05628800
O	-2.87494800	0.95756100	2.79840800
H	-2.20293100	1.35965200	-0.18750300
P	2.35759500	-1.59592200	-0.43230100
P	-2.93898200	-0.91435500	-0.55709800
C	3.24319900	-1.30633800	-2.04269100
H	3.73055800	-2.23301000	-2.36868200
H	2.51876100	-0.99072100	-2.80127700
H	4.00158900	-0.52566000	-1.92470600
C	3.70015000	-2.22412400	0.68984800
H	3.26885400	-2.55832900	1.63950000
H	4.21929600	-3.06491700	0.21448000
H	4.42178000	-1.42457200	0.89032200
C	1.36483500	-3.12465300	-0.80518500
H	0.57463800	-2.87875400	-1.52145400
H	2.02886200	-3.87781600	-1.24640200
H	0.91976900	-3.52197400	0.11101700
C	-3.71270400	-0.10285200	-2.03730800
H	-2.94855700	0.06621100	-2.80345700
H	-4.49978100	-0.74577800	-2.44978700
H	-4.14407700	0.85962700	-1.74278600
C	-2.47674700	-2.59418200	-1.20529500
H	-2.09553100	-3.21981700	-0.39165400
H	-3.35786500	-3.07422000	-1.64758600
H	-1.70486200	-2.48225900	-1.97383300
C	-4.38848100	-1.27474500	0.54766500
H	-4.84651500	-0.33729600	0.88045900
H	-5.13288200	-1.86623400	0.00119700
H	-4.05396500	-1.83776500	1.42588900

pdt 3C1'

Fe	1.28473600	0.35588600	0.31503000
Fe	-1.27785000	0.27435100	0.42995400
S	-0.01196000	2.09476800	1.01686700
S	-0.05342900	0.26932400	-1.54108700
O	-0.22011300	-2.15996900	1.70924000
C	-2.19980700	0.53976400	1.92014600
C	2.54804300	1.40413500	-0.28890900
C	-0.42362700	-1.14965400	1.14400700
C	-0.14595200	3.42244200	-0.29266000
C	-0.17003100	1.93209900	-2.39087700
C	-0.84781700	3.04365300	-1.59371600
H	0.85628300	2.19690500	-2.67255800
H	-0.72921900	1.72610300	-3.31124800
H	-0.88028600	3.94127900	-2.23158800
H	-1.88701500	2.76137200	-1.37805400
H	-0.69630000	4.22210200	0.21691900
H	0.87818100	3.77603700	-0.46534300
O	3.35405500	2.14614800	-0.68578500
C	1.98897100	0.19588600	1.95330100
O	2.45635200	0.10558900	3.01109400
O	-2.81815200	0.75272900	2.87855300
H	-2.32325100	1.23326100	-0.09630800
P	2.44710700	-1.50710100	-0.45174800
P	-2.86206600	-1.04762900	-0.52220000
C	3.32882900	-1.16110200	-2.05320700
H	3.85280600	-2.06334300	-2.39073700
H	2.59598900	-0.86269100	-2.81091200
H	4.05657700	-0.35393700	-1.92103100
C	3.80815800	-2.08779500	0.67364500
H	3.38385300	-2.45024400	1.61615000
H	4.36744700	-2.90020300	0.19441100
H	4.49189700	-1.25930700	0.88874100
C	1.53188000	-3.07758500	-0.85046000
H	0.75950400	-2.86834700	-1.59725100
H	2.24141100	-3.80479800	-1.26338700
H	1.07109100	-3.48965000	0.05130900
C	-3.64899400	-0.29292900	-2.02597800
H	-2.87983400	-0.09520600	-2.78016300
H	-4.39753200	-0.97763700	-2.44278600
H	-4.13076100	0.65134000	-1.75134100
C	-2.33441900	-2.72237300	-1.13254100
H	-1.92707100	-3.31399600	-0.30639300
H	-3.19680200	-3.24640100	-1.56171400
H	-1.56923100	-2.59782800	-1.90585700
C	-4.30763800	-1.43529700	0.57811900
H	-4.79796100	-0.50716700	0.89047300
H	-5.02820600	-2.06004200	0.03689800
H	-3.96272500	-1.97169400	1.46887900

pdt 3C2

Fe	-1.288087	0.378837	-0.267894
Fe	1.303344	0.219525	-0.561793
S	-0.019340	1.964508	-1.303647
S	0.202946	0.472069	1.459103
O	3.623674	2.018910	-0.463359
C	0.502109	-1.031987	-1.538377
C	-2.550969	1.394025	0.378604
C	2.696686	1.315257	-0.442536
C	0.294632	3.455963	-0.221611
C	0.561628	2.217872	2.042585
C	-0.094742	3.350555	1.253375
H	0.209185	2.234931	3.080276
H	1.654100	2.306970	2.049614
H	-1.184101	3.286166	1.348110
H	0.200791	4.296128	1.735226
H	1.357046	3.697471	-0.346873
H	-0.286409	4.249896	-0.705669
O	-3.404362	2.069394	0.796393
C	-2.161144	0.081583	-1.800280
O	-2.762966	-0.097299	-2.776861
O	0.234423	-1.894511	-2.286051
H	1.976791	0.179163	-1.906683
P	-2.324509	-1.506984	0.594772
P	2.653080	-1.409830	0.293868
C	-2.055127	-1.878798	2.396897
H	-2.661029	-2.747164	2.682653
H	-0.999259	-2.088364	2.591840
H	-2.351996	-1.012725	2.997762
C	-4.180063	-1.387377	0.487611
H	-4.488362	-1.258580	-0.555537
H	-4.629579	-2.306189	0.882506
H	-4.539564	-0.533694	1.071399
C	-2.005139	-3.137303	-0.244952
H	-0.954716	-3.420946	-0.141540
H	-2.636137	-3.908138	0.213988
H	-2.243690	-3.061077	-1.310822
C	3.572398	-0.913968	1.830919
H	4.209461	-1.740879	2.166990
H	4.198417	-0.038552	1.628453
H	2.851956	-0.665708	2.617746
C	3.985610	-1.928684	-0.889663
H	4.614227	-2.706087	-0.438923
H	3.528121	-2.315799	-1.806680
H	4.607105	-1.063902	-1.145617
C	1.870797	-3.022589	0.785869
H	1.428497	-3.503153	-0.092953
H	2.633829	-3.686634	1.209572
H	1.096158	-2.842777	1.538494

pdt 3C2'

Fe	-1.25524200	0.41842000	-0.29749100
Fe	1.30324300	0.16969100	-0.54797800
S	0.09749100	2.00763600	-1.23033700
S	0.19594500	0.39609900	1.48170600
O	3.81681800	1.65416000	-0.85253600
C	0.34072700	-1.06386000	-1.40870100
C	-2.37530400	1.55067200	0.41771100
C	2.81692000	1.09039800	-0.65654800
C	0.37237500	3.42886200	-0.04671700
C	0.40237600	2.11890600	2.18008600
C	1.09577100	3.12545600	1.26594500
H	-0.59893000	2.45237400	2.47659200
H	0.99080100	1.96801300	3.09263100
H	1.18391300	4.07455100	1.81841100
H	2.11888400	2.78698000	1.06103700
H	0.95064000	4.14826800	-0.63868500
H	-0.62107500	3.86053500	0.12735000
O	-3.08591300	2.33682700	0.90339500
C	-2.14089800	0.26884500	-1.84712600
O	-2.74200100	0.19405300	-2.83705500
O	0.04387800	-1.96635300	-2.10162100
H	1.82325100	0.03874400	-1.95181600
P	-2.50351900	-1.35821800	0.53041000
P	2.55504200	-1.52897800	0.30701700
C	-2.45281400	-1.58074000	2.37584300
H	-3.12807600	-2.39421700	2.66725800
H	-1.43357800	-1.81116300	2.70064000
H	-2.76931200	-0.65244400	2.86377800
C	-4.32166800	-1.13100300	0.19824600
H	-4.50572400	-1.11365000	-0.88136100
H	-4.88462000	-1.96098500	0.64182100
H	-4.67264800	-0.18891800	0.63246800
C	-2.21063300	-3.07413300	-0.12731500
H	-1.21888500	-3.42918500	0.16535900
H	-2.97123200	-3.74865300	0.28410400
H	-2.27507500	-3.07199500	-1.21981000
C	3.64987100	-1.01649300	1.71802900
H	4.24307100	-1.87364300	2.05869600
H	4.32458500	-0.21477500	1.40056200
H	3.02673500	-0.65552000	2.54356400
C	3.71168600	-2.27446700	-0.93727900
H	4.30275200	-3.07709800	-0.48009000
H	3.13283800	-2.68000600	-1.77441800
H	4.38626200	-1.50025800	-1.31836800
C	1.64648700	-2.99275700	1.00247500
H	1.10884100	-3.50783600	0.19989200
H	2.36104600	-3.68826600	1.45867100
H	0.93808000	-2.65118600	1.76522200

pdt 3D1

Fe	1.15259000	0.28934100	0.51959700
Fe	-1.15333500	-0.09945600	-0.54973800
S	-0.72864800	1.46715500	1.08938000
S	0.66146800	0.81783300	-1.63801400
O	-0.34373800	-2.63403400	0.71660800
C	2.38975100	1.47967400	0.85156700
C	-0.50214600	-1.55228000	0.28585600
C	-0.81583500	3.16956000	0.32241200
C	0.33028300	2.63440500	-1.92401300
C	0.27656100	3.52388900	-0.68458800
H	1.14710300	2.95039700	-2.58352400
H	-0.60628200	2.66622000	-2.49241400
H	1.25384400	3.54087700	-0.18868200
H	0.08556800	4.55327400	-1.02729700
H	-1.81386700	3.23504200	-0.12691300
H	-0.77265400	3.85007100	1.18069700
O	3.21419900	2.26650100	1.09277400
C	1.26359400	-0.39058600	2.16706900
O	1.35833900	-0.80408800	3.24787400
C	-1.52768600	-0.99843900	-2.02859000
O	-1.78248300	-1.54100800	-3.02373400
H	-2.03234600	0.91306500	-1.25398100
P	-3.16863900	-0.47254300	0.43663200
P	2.69817000	-1.22218500	-0.32068000
C	-4.27578700	1.01605900	0.46975100
H	-5.23087000	0.76074500	0.94428000
H	-3.79237300	1.81581600	1.04083200
H	-4.45580500	1.36193600	-0.55352300
C	-3.11513600	-1.01313600	2.21368800
H	-4.13642800	-1.09478500	2.60513800
H	-2.62023700	-1.98670500	2.29286000
H	-2.55919500	-0.27643100	2.80351600
C	-4.20482000	-1.77689500	-0.38555600
H	-5.14465800	-1.90577500	0.16450000
H	-4.42808800	-1.48055600	-1.41602300
H	-3.66183300	-2.72837500	-0.39893000
C	3.42123100	-2.40699100	0.91434300
H	2.62353000	-3.01925300	1.34854300
H	4.14910400	-3.06065800	0.41881400
H	3.92242400	-1.85311400	1.71561900
C	2.11185500	-2.33560800	-1.69239600
H	1.70348300	-1.73624200	-2.51283800
H	2.96536000	-2.91686600	-2.06228400
H	1.34534900	-3.02102900	-1.31977800
C	4.18301600	-0.39323900	-1.06945000
H	4.85875000	-1.14782100	-1.48943000
H	3.85363800	0.28201400	-1.86669800
H	4.71796200	0.18482300	-0.30866600

pdt 3D1'

Fe	1.14913300	0.27563900	0.54505000
Fe	-1.12946800	-0.08741300	-0.55439000
S	-0.75163400	1.39520800	1.17615900
S	0.66160600	0.93272100	-1.58408600
O	-0.23230600	-2.63457600	0.61515800
C	2.28899700	1.56287700	0.87161700
C	-0.39237100	-1.53018900	0.24120700
C	-0.76106600	3.15648000	0.55654900
C	0.39940100	2.77947600	-1.70522600
C	-0.80578700	3.34259700	-0.95758400
H	1.33859900	3.23861900	-1.37333400
H	0.29614000	2.95274600	-2.78250800
H	-0.85128900	4.42391700	-1.16286700
H	-1.72572900	2.89676100	-1.35847600
H	-1.65184400	3.59480600	1.02191800
H	0.11936400	3.63387700	1.00379300
O	3.01368600	2.44997400	1.08218100
C	1.32481100	-0.44205400	2.17151600
O	1.46390300	-0.87569800	3.23960400
C	-1.44618600	-0.96990300	-2.05465800
O	-1.66748300	-1.50544900	-3.06162800
H	-2.09996700	0.85402700	-1.23342400
P	-3.11654500	-0.60610600	0.42712900
P	2.75670100	-1.12550000	-0.36036000
C	-4.29416300	0.82408800	0.53598100
H	-5.22978700	0.50113500	1.00829500
H	-3.84307700	1.62179700	1.13528200
H	-4.50337700	1.20475300	-0.46919300
C	-3.02621200	-1.22763100	2.17612200
H	-4.04014100	-1.39725400	2.55822000
H	-2.46682300	-2.16819000	2.20965400
H	-2.52250300	-0.48477400	2.80397000
C	-4.09044400	-1.92008400	-0.45180200
H	-5.02699200	-2.11039000	0.08587300
H	-4.32007700	-1.59545100	-1.47220400
H	-3.50577300	-2.84546300	-0.49529000
C	3.55291100	-2.32374700	0.81512100
H	2.79255700	-2.99393200	1.23052600
H	4.30653300	-2.91790400	0.28442800
H	4.03533100	-1.78021800	1.63476200
C	2.20438000	-2.21008300	-1.76876000
H	1.74609700	-1.59944600	-2.55389600
H	3.07955300	-2.72668700	-2.18155800
H	1.48453800	-2.95278600	-1.41248000
C	4.19085500	-0.19965900	-1.09445400
H	4.89423200	-0.90579600	-1.55168300
H	3.81874600	0.48972000	-1.86022600
H	4.70935400	0.37248800	-0.31775200

pdt 3D2

Fe	1.11025000	0.09249400	0.53287500
Fe	-1.15730000	0.03200400	-0.64434700
S	-0.79725200	1.00101100	1.42505900
S	0.65529300	1.29325500	-1.35097700
O	-3.02545900	1.75092600	-2.12366600
C	2.26455600	1.10749600	1.36874100
C	-2.30089700	1.09837900	-1.48890100
C	-0.90029900	2.86055900	1.23919600
C	0.31478800	3.10213600	-1.02744000
C	0.20875800	3.53520400	0.43383100
H	1.15352100	3.61448600	-1.51323100
H	-0.59529600	3.34086700	-1.59079700
H	1.17236400	3.40067700	0.93833900
H	0.00523600	4.61783900	0.43970400
H	-1.88913400	3.05782000	0.80788800
H	-0.89439300	3.23214600	2.27024100
O	3.01937600	1.76994900	1.95899600
C	1.14772700	-1.16058300	1.79962000
O	1.18442700	-1.96971100	2.63297000
C	-0.35008400	-1.54719200	-0.65439100
O	-0.06939900	-2.67812200	-0.82112400
H	-1.31021000	-0.54051000	-2.02908400
P	-2.92933100	-1.08256400	0.25933700
P	2.80170300	-0.95326600	-0.68436000
C	-4.29038800	0.01849200	0.87909400
H	-4.68654200	0.62841500	0.06063600
H	-5.09850300	-0.59489000	1.29536500
H	-3.89413600	0.67437900	1.66131600
C	-3.76633200	-2.22596000	-0.93806600
H	-3.04401200	-2.96427500	-1.30236300
H	-4.60146800	-2.74329000	-0.45071000
H	-4.14376200	-1.65044100	-1.79031800
C	-2.54419400	-2.15224200	1.72809400
H	-3.47022600	-2.60651200	2.10054800
H	-1.84411700	-2.94481600	1.44486600
H	-2.09993100	-1.54137000	2.52135400
C	2.46836300	-1.36820300	-2.47007200
H	2.11706400	-0.47891700	-3.00325100
H	3.40419100	-1.71692200	-2.92361500
H	1.71727000	-2.15938800	-2.54263900
C	3.41040400	-2.56266200	0.01662100
H	2.58922100	-3.28705400	0.03684900
H	4.22211800	-2.95391300	-0.60833200
H	3.78136900	-2.41289500	1.03619200
C	4.33926900	0.08662800	-0.79873700
H	5.09288000	-0.43650400	-1.39946100
H	4.09877300	1.04380700	-1.27435700
H	4.74520000	0.27684600	0.20019900

pdt 3D2'

Fe	1.12111200	0.07737800	0.53630600
Fe	-1.13437800	0.04171700	-0.62383400
S	-0.79097300	0.93228700	1.49110300
S	0.63559500	1.36752600	-1.28723700
O	-3.08723200	1.45875500	-2.29379200
C	2.19914700	1.20623600	1.33092200
C	-2.32808400	0.94311200	-1.57737300
C	-0.76197100	2.79971400	1.47161900
C	0.34758100	3.15673000	-0.82547400
C	-0.83454700	3.45497400	0.09514900
H	1.29398600	3.50846300	-0.39637000
H	0.21019100	3.65328600	-1.79312200
H	-0.86810400	4.54611400	0.24292100
H	-1.77438600	3.17582600	-0.39729100
H	-1.63509500	3.07994100	2.07270900
H	0.13569400	3.10009800	2.02514300
O	2.87469600	1.98723300	1.86936400
C	1.25509200	-1.15954900	1.81572900
O	1.35401600	-1.94913900	2.66217700
C	-0.23550600	-1.50128100	-0.58378800
O	0.03460700	-2.63592200	-0.76269000
H	-1.17358500	-0.56566100	-1.99916100
P	-2.86738700	-1.15206500	0.25497200
P	2.84138100	-0.87012300	-0.71259500
C	-4.26272500	-0.09807000	0.87861400
H	-4.66427800	0.51635200	0.06627200
H	-5.05964000	-0.73794100	1.27604600
H	-3.88929000	0.55462700	1.67469800
C	-3.65409500	-2.30270200	-0.96829500
H	-2.90038300	-3.00381600	-1.34238700
H	-4.46979700	-2.86273200	-0.49542700
H	-4.05119100	-1.72606500	-1.81083100
C	-2.46115600	-2.23218200	1.71071100
H	-3.37756600	-2.71669900	2.06876400
H	-1.73840700	-3.00144100	1.42043100
H	-2.03980600	-1.62157900	2.51665200
C	2.49349800	-1.26249300	-2.50008500
H	2.09560300	-0.37787000	-3.00788600
H	3.43214900	-1.56432500	-2.98056900
H	1.77283800	-2.08181600	-2.57372800
C	3.52316600	-2.46708700	-0.05323100
H	2.72915400	-3.22103600	-0.03063000
H	4.33613600	-2.81840100	-0.69989100
H	3.90783500	-2.32080800	0.96175200
C	4.32995200	0.23822300	-0.82378400
H	5.10184400	-0.23697900	-1.44074900
H	4.04048800	1.19179600	-1.27915300
H	4.73583600	0.42884000	0.17527600

pdt 3A1*

Fe	-1.16930200	-0.67721500	-0.17417100
Fe	1.35547200	0.23906500	-0.46281000
S	-0.06178100	0.77964000	1.35429700
S	-0.46161900	0.82029700	-1.83202500
P	-3.25744600	-0.17126700	0.65195400
P	2.78394100	-0.60984500	1.09845500
O	0.82654900	-2.80814500	-0.24690700
O	-2.40178900	-2.40043100	-2.18141700
O	2.70463000	-1.03074200	-2.73752500
O	3.05613000	2.62675700	-0.86049100
C	0.30332000	-1.73894000	-0.25036300
C	-1.91132100	-1.70929500	-1.37229200
C	2.15046200	-0.54659100	-1.82855100
C	2.32321400	1.73469300	-0.64897800
C	4.14237800	-1.70123300	0.43952100
H	3.68651700	-2.56003600	-0.06556500
H	4.78598900	-2.05554000	1.25476100
H	4.74614500	-1.14461300	-0.28580500
C	2.09729000	-1.65297600	2.48750000
H	2.89437900	-1.86031000	3.21294300
H	1.71093700	-2.59391200	2.08548300
H	1.28350200	-1.10967100	2.98021800
C	3.71422300	0.69505800	2.05030900
H	4.35384100	0.23399700	2.81346500
H	2.98589000	1.35638300	2.53306800
H	4.33121800	1.28770900	1.36668200
C	-1.03851300	2.55068000	-1.43679000
H	-0.77520600	3.14460300	-2.32107500
H	-2.13320100	2.49393700	-1.38565300
C	-0.73741600	2.51036800	1.13990700
H	-1.81893200	2.44675500	1.32196900
H	-0.29739300	3.08761400	1.96305100
C	-4.36643100	1.21229100	0.02142700
H	-3.91185400	2.18756700	0.22788800
H	-5.35284000	1.16993200	0.50255800
H	-4.49014000	1.10759400	-1.06286500
C	-3.30952700	0.11463600	2.49703700
H	-4.34322300	0.26075700	2.83546900
H	-2.70762900	0.98798900	2.76727000
H	-2.87633400	-0.76109100	2.99209600
C	-4.43480300	-1.61323100	0.50044900
H	-4.66177000	-1.80050200	-0.55470600
H	-5.36834100	-1.40869500	1.03971300
H	-3.95641100	-2.50677200	0.91571500
H	-1.43966700	-1.62412000	0.97599000
C	-0.46477400	3.22250600	-0.18688300
H	0.61246400	3.37421900	-0.31060000
H	-0.91414600	4.22850100	-0.11610200

pdt 3A1*

Fe	-1.147097	-0.655555	-0.125100
Fe	1.358965	0.206693	-0.471273
S	-0.006499	0.813140	1.368335
S	-0.476439	0.788615	-1.838019
P	-3.281046	-0.213766	0.636773
P	2.865938	-0.557878	1.056413
O	0.871663	-2.772182	-0.149081
O	-2.346002	-2.533038	-2.010318
O	2.717018	-1.002279	-2.773412
O	2.769831	2.779028	-0.859031
C	0.387379	-1.680972	-0.188850
C	-1.859626	-1.779871	-1.254346
C	2.164659	-0.538268	-1.853588
C	2.181409	1.783329	-0.665900
C	4.197076	-1.672990	0.382341
H	3.719363	-2.548857	-0.070689
H	4.874085	-1.998058	1.182551
H	4.769823	-1.144567	-0.387869
C	2.243183	-1.546275	2.512633
H	3.074611	-1.740834	3.202196
H	1.826390	-2.494512	2.161004
H	1.461879	-0.977505	3.028453
C	3.832783	0.787481	1.910965
H	4.510240	0.358910	2.660099
H	3.126384	1.465703	2.402907
H	4.414317	1.354990	1.176579
C	-0.849475	2.579751	-1.478064
H	0.065473	3.145015	-1.697499
H	-1.600817	2.859884	-2.227995
C	-0.426017	2.610424	1.082458
H	-0.879316	2.947821	2.023890
H	0.524540	3.145013	0.957468
C	-4.561240	0.636986	-0.441940
H	-4.233427	1.649567	-0.701264
H	-5.533630	0.689900	0.065267
H	-4.669765	0.063992	-1.370356
C	-3.449802	0.697519	2.260376
H	-4.486386	0.654115	2.618771
H	-3.153307	1.745137	2.142161
H	-2.782649	0.229908	2.992862
C	-4.199723	-1.789571	1.039213
H	-4.272776	-2.414150	0.142227
H	-5.208476	-1.568760	1.411355
H	-3.636770	-2.342108	1.799138
H	-1.336889	-1.563710	1.066693
C	-1.376528	2.907536	-0.079937
H	-1.611570	3.985610	-0.053478
H	-2.320841	2.371782	0.080964

pdt 3A2*

Fe	1.10397600	-0.67561100	0.23965700
Fe	-1.32011100	0.52354200	0.35403700
S	-0.04064600	0.21920400	-1.61324700
S	0.64435800	1.39782800	1.29701000
P	3.36684100	-0.25574600	0.09583600
P	-2.85011700	-0.91394800	-0.53260400
O	-0.84298100	-2.20716300	1.78818000
O	1.48064200	-3.24059600	-1.10224800
O	-2.59152000	0.60249400	2.99288500
O	-2.90327000	2.89652900	-0.42984300
C	-0.31492900	-1.37076200	1.12888100
C	1.33490300	-2.20810300	-0.56380400
C	-2.07037200	0.54060600	1.94724300
C	-2.21315300	1.98513400	-0.16352200
C	-4.11534700	-1.57886100	0.66174300
H	-3.59436900	-2.11376300	1.46343300
H	-4.80665000	-2.26120200	0.15147700
H	-4.67973000	-0.74823100	1.09997000
C	-2.22581900	-2.47336200	-1.34527500
H	-3.06744500	-3.01635800	-1.79447700
H	-1.73888200	-3.11100800	-0.60147500
H	-1.50200100	-2.21242600	-2.12524300
C	-3.90578600	-0.19004300	-1.88817600
H	-4.61015500	-0.94067400	-2.26854900
H	-3.25238900	0.14556000	-2.70127000
H	-4.46320800	0.67168200	-1.50550300
C	1.30628800	2.77665900	0.22369300
H	1.20026500	3.68111200	0.83602900
H	2.38116200	2.58533900	0.09819600
C	0.73448300	1.83808300	-2.12505000
H	1.77878900	1.60157700	-2.36214900
H	0.23138800	2.11179900	-3.06104500
C	4.07553900	0.65360700	1.56484700
H	3.64673500	1.65759400	1.64507000
H	5.16737400	0.72661100	1.47945600
H	3.80963800	0.09938300	2.47127200
C	4.23649300	0.59778700	-1.33954800
H	5.32611100	0.55102400	-1.21050000
H	3.93230300	1.64820200	-1.40355600
H	3.96320800	0.09633100	-2.27545900
C	4.36911700	-1.83134200	0.16798900
H	4.04736600	-2.41843200	1.03489300
H	5.43905300	-1.60257400	0.25326200
H	4.19849600	-2.42616200	-0.73607600
H	1.74131600	-1.14708100	1.52270700
C	0.64858200	3.00559500	-1.13905600
H	1.15434900	3.86804300	-1.60750200
H	-0.39643900	3.30026100	-0.99928600

pdt 3A2''*

Fe	1.09501900	-0.62216800	0.24190000
Fe	-1.33877700	0.49432400	0.36998500
S	-0.06460800	0.22741800	-1.62232300
S	0.59509600	1.43653400	1.30960500
P	3.37983200	-0.30683800	0.11059100
P	-2.88500500	-0.90137400	-0.54094500
O	-0.86126600	-2.18628500	1.75166800
O	1.49754500	-3.22134700	-1.02397100
O	-2.65737200	0.63640200	2.98195800
O	-2.68147200	2.97734200	-0.51545000
C	-0.37898700	-1.30555900	1.10752600
C	1.33176300	-2.17674300	-0.51307400
C	-2.12107800	0.55240700	1.94630900
C	-2.11859700	1.99928100	-0.19626900
C	-4.15229600	-1.57880300	0.64371000
H	-3.63079400	-2.12496500	1.43758200
H	-4.84475200	-2.25371900	0.12526500
H	-4.71558700	-0.75362400	1.09345500
C	-2.26564300	-2.45080900	-1.37376100
H	-3.10861800	-2.99009400	-1.82484300
H	-1.77463500	-3.09438900	-0.63752900
H	-1.54546900	-2.18091800	-2.15398000
C	-3.93471100	-0.14646900	-1.88381700
H	-4.64497300	-0.88431400	-2.27808500
H	-3.27938800	0.19862700	-2.69136100
H	-4.48625000	0.71217300	-1.48536900
C	1.00854800	2.90794100	0.23750500
H	0.11627500	3.54711300	0.21756100
H	1.78914000	3.44695000	0.79095200
C	0.48663000	1.94122800	-2.11215100
H	0.92771000	1.81741300	-3.10941100
H	-0.41739000	2.55427200	-2.21728400
C	4.11204300	1.07187900	1.13730600
H	3.84620400	2.04639400	0.71430300
H	5.20514000	0.98202000	1.17759300
H	3.69632300	1.00862100	2.14894100
C	4.28166100	-0.12346700	-1.52737100
H	5.36826000	-0.08012400	-1.37587600
H	3.95462100	0.78281800	-2.04812100
H	4.03955500	-0.98791600	-2.15679400
C	4.29800600	-1.77406600	0.81461300
H	3.99008500	-1.91563500	1.85611200
H	5.38282100	-1.61451600	0.76672500
H	4.03908800	-2.67792400	0.25229700
H	1.65867800	-1.05486300	1.56889800
C	1.49972800	2.60827500	-1.18114400
H	2.39597400	1.97710300	-1.12904200
H	1.80358800	3.56391200	-1.64211900

pdt 3A3*

Fe	1.18256900	-0.56568500	0.17356300
Fe	-1.52579700	0.19437600	0.52166700
S	0.33266000	0.94573700	1.73895200
S	-0.13548300	0.61037700	-1.35979000
O	1.38983900	-2.80469100	-1.71770500
O	-1.30663100	-2.73720900	0.86700000
C	1.29646500	-1.91175400	-0.96089300
C	-2.51909700	0.31438300	1.95300100
C	-1.20989200	-1.57905300	0.69603200
C	0.65309600	2.71525200	1.23204500
C	0.35738500	2.41632300	-1.32195100
C	0.00721700	3.21062500	-0.06340700
H	1.43994900	2.43059900	-1.50522900
H	-0.13450600	2.86829900	-2.19286200
H	0.33153800	4.25389300	-0.22335000
H	-1.08302800	3.22420800	0.06048200
H	0.29162400	3.31754000	2.07510400
H	1.74464100	2.81521300	1.19210100
C	1.74135800	-1.55122900	1.52937500
O	2.12794000	-2.20215300	2.42394400
O	-3.18605700	0.45371800	2.90399700
H	-2.04404800	1.62359700	0.38877900
P	-3.20432100	-0.17876300	-0.90845800
P	3.32606700	0.17519600	-0.42084100
C	-4.82289700	-0.72440300	-0.16074800
H	-5.17955000	0.03769100	0.54105600
H	-5.57838100	-0.88443900	-0.94035000
H	-4.66659400	-1.65861000	0.39062600
C	-2.91092500	-1.48946300	-2.20128000
H	-3.77828500	-1.57414300	-2.86851200
H	-2.02305000	-1.22021200	-2.78412700
H	-2.73252200	-2.45263300	-1.71077300
C	-3.70713400	1.28887100	-1.93780700
H	-2.82759000	1.64998900	-2.48189800
H	-4.49551400	1.01699900	-2.65146600
H	-4.06564500	2.08507800	-1.27633700
C	4.16339900	1.70027100	0.28788300
H	4.10492500	1.67337800	1.38224700
H	5.21807900	1.74045900	-0.01615600
H	3.65854100	2.60567300	-0.06784900
C	3.62204900	0.42861600	-2.25427700
H	4.67530500	0.66414600	-2.45670900
H	3.34677100	-0.48923900	-2.78625300
H	2.99059100	1.24118000	-2.63091500
C	4.63991100	-1.10648400	-0.05338500
H	4.35266000	-2.05991900	-0.51123200
H	5.61716800	-0.79491700	-0.44508600
H	4.71347100	-1.25315300	1.03022500

pdt 3A3''*

Fe	1.17932100	-0.54761600	0.10144700
Fe	-1.53675500	0.19504000	0.52802100
S	0.35467300	0.93130400	1.71083800
S	-0.20919600	0.61016900	-1.39041700
O	1.30214900	-2.74233800	-1.84760200
O	-1.35576600	-2.74138200	0.85717300
C	1.24397800	-1.86777500	-1.06686400
C	-2.48724900	0.36040500	1.98417500
C	-1.27340500	-1.58219900	0.69337000
C	0.52074100	2.71789700	1.19897400
C	0.06125100	2.45772700	-1.34280400
C	0.97979400	2.97836400	-0.23653200
H	0.48643900	2.71186800	-2.32293600
H	-0.93636200	2.90786500	-1.26639700
H	1.98283000	2.55599000	-0.37642300
H	1.07553900	4.07034000	-0.36716400
H	-0.45788000	3.17441000	1.39230300
H	1.24877600	3.14793900	1.89985800
C	1.71185200	-1.58877300	1.42489900
O	2.09077600	-2.27640900	2.29556800
O	-3.12196100	0.53429300	2.95154400
H	-1.95715200	1.66113600	0.39656000
P	-3.26913000	-0.12927500	-0.84876200
P	3.36467600	0.12741200	-0.37613800
C	-4.87451900	-0.64076700	-0.04940200
H	-5.19319800	0.13008300	0.66106200
H	-5.65727600	-0.78646600	-0.80453400
H	-4.72080300	-1.57682500	0.49955200
C	-3.04810600	-1.44050700	-2.15496500
H	-3.93837900	-1.50444900	-2.79375400
H	-2.17434500	-1.18878900	-2.76622500
H	-2.87499000	-2.40903800	-1.67318200
C	-3.77435900	1.35298300	-1.85533000
H	-2.91143800	1.68626900	-2.44223600
H	-4.60294400	1.10528100	-2.53126900
H	-4.07643200	2.15981600	-1.17880800
C	4.27452300	1.23627600	0.83109400
H	4.25824700	0.76069500	1.81868100
H	5.31584400	1.39152400	0.51920600
H	3.77388500	2.20730200	0.91205000
C	3.73696200	0.93850000	-2.02574100
H	4.81174300	1.13104800	-2.14158000
H	3.40027200	0.26900000	-2.82591600
H	3.18902800	1.88257800	-2.11791700
C	4.56075400	-1.31110600	-0.44826200
H	4.23734900	-2.01608100	-1.22251600
H	5.57891500	-0.96765100	-0.67297400
H	4.55990500	-1.83195400	0.51600500

pdt 3A4*

Fe	-1.13955100	-0.52801900	-0.28447800
Fe	1.51800200	0.26075000	-0.59344000
S	-0.34829300	1.20220700	-1.65703900
S	0.18509400	0.45049200	1.39077100
O	-1.20175700	-3.05551800	1.21367700
O	3.27240300	2.56784300	-1.05128000
C	-1.16848600	-2.04364900	0.61810600
C	1.11610600	-1.37529100	-1.20949500
C	2.51895800	1.70852700	-0.77997700
C	-0.65269900	2.88200300	-0.90040200
C	-0.37656000	2.22243300	1.59150900
C	-0.01926000	3.18713200	0.46148800
H	-1.46308000	2.18528400	1.74387900
H	0.08181900	2.56445900	2.52816900
H	-0.35577400	4.19514300	0.76142700
H	1.07071200	3.24051300	0.36388500
H	-0.27910600	3.59635700	-1.64503400
H	-1.74345300	2.98927400	-0.85411500
C	-1.80154200	-1.27342900	-1.74194900
O	-2.26817600	-1.76266100	-2.69907700
O	1.17860800	-2.42892000	-1.73009200
H	2.24789200	0.11769800	-1.89611800
P	-3.24710500	0.07564300	0.53634400
P	3.10682500	-0.69801900	0.65521700
C	-3.43796800	0.01701700	2.39952500
H	-4.46914800	0.24957500	2.69618300
H	-3.17823300	-0.98848000	2.74945000
H	-2.75257200	0.72782400	2.87418700
C	-4.11955900	1.69166700	0.13594100
H	-5.14784000	1.68325600	0.52216200
H	-3.58014800	2.53372400	0.58421600
H	-4.14456300	1.83129200	-0.95109500
C	-4.58365300	-1.13480700	0.03451300
H	-5.53483400	-0.89994900	0.52993200
H	-4.72182800	-1.09793500	-1.05199200
H	-4.27302800	-2.14961000	0.30808100
C	3.91666100	0.39912100	1.92438200
H	4.66808300	-0.16137000	2.49473600
H	4.39613300	1.24785300	1.42473600
H	3.14439700	0.77506800	2.60436800
C	2.57835200	-2.16251500	1.67789000
H	2.19866900	-2.95270000	1.02159000
H	3.42633100	-2.54661200	2.25923200
H	1.77761900	-1.85299200	2.35882300
C	4.55472400	-1.36980800	-0.30491600
H	5.29187100	-1.83195300	0.36396900
H	4.18943300	-2.11601800	-1.01915600
H	5.02722700	-0.55459000	-0.86429600

pdt 3A4'*

Fe	-1.13644800	-0.52085300	-0.19504100
Fe	1.53756900	0.25226700	-0.62614800
S	-0.38126500	1.13337200	-1.67307000
S	0.27542800	0.48936300	1.38390500
O	-1.05797500	-2.97195400	1.42295800
O	3.06765900	2.73501400	-0.95358500
C	-1.08428100	-1.98972600	0.77932000
C	1.21708900	-1.38769700	-1.25541600
C	2.40938000	1.78534000	-0.74567100
C	-0.60101800	2.84733600	-0.96851300
C	0.01969900	2.33785600	1.50230400
C	-0.97739500	2.94143900	0.51150200
H	-0.33241400	2.51357600	2.52724400
H	1.01042100	2.79849400	1.39810200
H	-1.95543800	2.46797200	0.66276800
H	-1.09743200	4.01008200	0.76063300
H	0.32757200	3.39396100	-1.17630700
H	-1.39594000	3.29762500	-1.57748800
C	-1.76919600	-1.38399800	-1.59807700
O	-2.22491000	-1.95383700	-2.51610500
O	1.25953400	-2.43929800	-1.77643900
H	2.27517700	0.18142200	-1.93431600
P	-3.29534600	0.02472000	0.50799300
P	3.18034400	-0.63082000	0.60801100
C	-3.57388100	0.63711700	2.25813800
H	-4.64557700	0.72467900	2.48029200
H	-3.11381600	-0.07289100	2.95501300
H	-3.09670100	1.61314100	2.39893700
C	-4.32680500	1.22520900	-0.49782100
H	-5.34874100	1.29949000	-0.10305300
H	-3.86552000	2.21891600	-0.49308000
H	-4.36325400	0.87005500	-1.53429900
C	-4.43361200	-1.46216100	0.49678800
H	-5.44753100	-1.18751700	0.81576600
H	-4.47461000	-1.88055900	-0.51528700
H	-4.03711200	-2.22873600	1.17234300
C	3.95363400	0.50506300	1.86623500
H	4.72146800	-0.02455600	2.44424500
H	4.40803600	1.36270400	1.35828200
H	3.16983500	0.86394200	2.54250100
C	2.71934100	-2.10986100	1.64092100
H	2.34957600	-2.91151300	0.99298300
H	3.58934500	-2.46830900	2.20593600
H	1.92342800	-1.82335200	2.33715500
C	4.65093200	-1.24283500	-0.35819500
H	5.41695400	-1.65963300	0.30800900
H	4.31804800	-2.01462800	-1.06109000
H	5.07572600	-0.41129500	-0.93152600

pdt 3B*

Fe	-1.27707600	-0.54801700	0.19844000
Fe	1.41421300	-0.62216700	0.04163400
S	-0.01154100	0.28601000	-1.61892400
S	0.18298900	0.71959400	1.56878500
O	-2.45558000	-1.61678500	2.66618200
C	-1.97619200	-1.20254000	1.68303400
C	2.17213400	-1.66714300	-1.13713400
C	-0.05408600	2.14957700	-1.53896100
C	0.12402600	2.49968500	1.01716800
C	0.68128100	2.80770200	-0.37238100
H	-0.92133300	2.81856300	1.09846400
H	0.69400000	3.05147100	1.77646500
H	0.64587800	3.90142200	-0.51934200
H	1.73719400	2.51543000	-0.41156300
H	0.38794000	2.47985400	-2.48789800
H	-1.11032200	2.45147300	-1.54505400
C	-1.96988100	-1.78424500	-0.86116200
O	-2.43995400	-2.60014300	-1.55653900
C	0.38132800	-2.03178900	0.55581700
O	0.22926300	-3.14753000	0.91618500
O	2.67702900	-2.35906900	-1.93731400
H	2.13774500	-1.17755500	1.23750200
P	3.42519000	0.47119500	0.20021200
P	-3.19730300	0.77939300	-0.18786800
C	-3.65736400	0.97582200	-1.99250600
H	-3.74850100	-0.01816800	-2.44453300
H	-4.61105900	1.51010600	-2.09385000
H	-2.87464300	1.52085400	-2.53045900
C	-3.52828100	2.51456600	0.45754200
H	-4.57041600	2.79842200	0.25845600
H	-3.34908800	2.54455100	1.53868100
H	-2.86595500	3.23792100	-0.03083200
C	-4.73731600	-0.07462700	0.44756900
H	-4.70735000	-0.12267300	1.54187400
H	-5.63992400	0.46499100	0.13274200
H	-4.77391300	-1.09832300	0.05842000
C	4.17479300	1.42412000	-1.23485200
H	5.18254600	1.77906800	-0.98244600
H	4.23461900	0.75541700	-2.10144600
H	3.54792500	2.28070900	-1.50414300
C	3.65836000	1.63899300	1.64024200
H	4.71497600	1.91951600	1.73731800
H	3.05705900	2.54368900	1.50324400
H	3.32189900	1.13360000	2.55214500
C	4.80912800	-0.74227800	0.52236000
H	5.77183800	-0.22158800	0.60334600
H	4.59895000	-1.27989400	1.45307900
H	4.85923300	-1.47139600	-0.29357400

pdt 3B'*

Fe	-1.28574800	-0.51308400	0.14662600
Fe	1.47365700	-0.66874700	0.03968200
S	0.05119900	0.16167800	-1.66938400
S	0.20490100	0.75520300	1.46607200
O	-2.40477300	-1.61702700	2.62706100
C	-1.94045800	-1.19119900	1.63913000
C	2.27982800	-1.66411300	-1.15419000
C	0.23479100	2.01709500	-1.73445600
C	0.36774900	2.49633600	0.80843000
C	-0.29137200	2.80695800	-0.53574100
H	-0.07058700	3.13202000	1.58882400
H	1.44104700	2.72336300	0.76462600
H	-1.37287200	2.65318800	-0.44756400
H	-0.14167500	3.88101400	-0.74369600
H	1.30009700	2.21785400	-1.89967900
H	-0.30296100	2.32383100	-2.64127000
C	-1.92533400	-1.80749900	-0.87608500
O	-2.36649400	-2.65324100	-1.55596800
C	0.55447100	-2.10536600	0.58916400
O	0.33208300	-3.18770800	0.99047100
O	2.79997700	-2.32387500	-1.96967700
H	2.25766200	-1.16361800	1.22966700
P	3.38457800	0.56470400	0.26592800
P	-3.25273500	0.73542500	-0.13093100
C	-3.62352500	1.50121200	-1.80090600
H	-3.55224900	0.71825300	-2.56462100
H	-4.63109200	1.93688400	-1.81791300
H	-2.89023200	2.27863000	-2.03925400
C	-3.68761400	2.12003100	1.05892100
H	-4.68218400	2.52940300	0.83806500
H	-3.68049300	1.71659600	2.07829100
H	-2.94703300	2.92513400	1.00525700
C	-4.77958800	-0.32966500	0.07198700
H	-4.79146200	-0.76341900	1.07828300
H	-5.69175100	0.26264600	-0.07693800
H	-4.75569500	-1.14665100	-0.65784200
C	3.90192800	2.01578300	-0.81735500
H	4.92560700	2.32808500	-0.57108600
H	3.86305400	1.71353100	-1.87045200
H	3.22735400	2.86646700	-0.67163300
C	3.65442800	1.25656900	1.97917000
H	4.63385500	1.74771800	2.04207700
H	2.86817100	1.97168600	2.24038100
H	3.60793700	0.42808000	2.69391300
C	4.90799300	-0.50149400	0.09205900
H	5.80553100	0.06537500	0.36981700
H	4.80689600	-1.37593600	0.74353800
H	5.00606700	-0.84765900	-0.94260700

pdt 3C1*

Fe	-1.49677700	-0.38756300	0.25741900
Fe	1.46627900	-0.34579300	0.42216300
S	-0.05010200	-2.06061200	0.88377900
S	0.07972600	0.01927800	-1.45914700
O	0.53543200	1.85105700	2.17342100
C	2.52061700	-0.99655300	1.65724600
C	-2.86260200	-1.35999300	-0.37160100
C	0.77665400	0.95709100	1.45075400
C	0.17007100	-3.25695100	-0.53579300
C	0.31514900	-1.53332700	-2.47693500
C	-0.33200400	-2.79770500	-1.90800900
H	-0.12360400	-1.30871500	-3.45796600
H	1.39818400	-1.65992700	-2.59490700
H	-1.41887300	-2.66108000	-1.87001600
H	-0.14021900	-3.61799500	-2.62132000
H	1.24131600	-3.49279000	-0.55769000
H	-0.38001200	-4.15635500	-0.22985300
O	-3.80294600	-2.00370900	-0.66414500
C	-2.06365700	-0.24824000	1.92681200
O	-2.49572200	-0.17588600	3.01558400
O	3.23263400	-1.47423000	2.45267500
H	2.20484500	-1.36809900	-0.44188500
P	-2.50116100	1.55396900	-0.30277900
P	3.01444700	0.97785600	-0.50616000
C	-3.10851400	1.60348400	-2.06725000
H	-3.57794300	2.57021300	-2.29127300
H	-2.25644200	1.44272900	-2.73667400
H	-3.83628400	0.79939000	-2.22205200
C	-4.05180700	1.97228200	0.64674700
H	-3.80787600	2.11200700	1.70539400
H	-4.51136500	2.88858800	0.25478100
H	-4.76323800	1.14333100	0.56050600
C	-1.54767400	3.15781700	-0.19906300
H	-0.67055000	3.08953400	-0.85198400
H	-2.17614500	3.99795000	-0.52226800
H	-1.20966500	3.32237200	0.82904000
C	3.59533400	0.45681400	-2.19791600
H	2.73424900	0.43408700	-2.87487600
H	4.34604400	1.15735600	-2.58555900
H	4.02555000	-0.54854000	-2.13537900
C	2.55852200	2.76228100	-0.80365700
H	2.32259500	3.24694700	0.15005800
H	3.38282400	3.29761000	-1.29204200
H	1.67321100	2.79193700	-1.44825400
C	4.62575300	1.14514900	0.42029100
H	5.08309000	0.15658400	0.53853400
H	5.31740000	1.80412800	-0.11985300
H	4.43231600	1.55918600	1.41636900

pdt 3C1'*

Fe	1.48696800	0.39802200	0.27624600
Fe	-1.45146200	0.31018000	0.45180200
S	0.02800800	2.04799600	0.91999300
S	-0.06665700	0.00743300	-1.45058700
O	-0.39820600	-1.90472200	2.11294200
C	-2.49343100	0.85217100	1.74673200
C	2.72921600	1.44313000	-0.47074000
C	-0.66683600	-0.99613700	1.41721100
C	-0.07911500	3.27323300	-0.49188400
C	-0.09413500	1.58131100	-2.46625300
C	-0.72661800	2.80373700	-1.79862200
H	0.95275900	1.77152800	-2.73479700
H	-0.64520200	1.33895400	-3.38430500
H	-0.67013900	3.64119100	-2.51568000
H	-1.79079400	2.60321700	-1.61736800
H	-0.64867500	4.11953200	-0.08730800
H	0.95402100	3.60526200	-0.65701100
O	3.55968300	2.17066100	-0.87699200
C	2.14738700	0.31584400	1.91569200
O	2.63538600	0.28400200	2.98251400
O	-3.20248600	1.25206300	2.58647600
H	-2.28549200	1.32574300	-0.32101200
P	2.54573800	-1.50679200	-0.32781700
P	-2.96933500	-1.03396200	-0.49916400
C	3.13952800	-1.50322000	-2.09828700
H	3.64531000	-2.44658800	-2.34191500
H	2.27665000	-1.36702600	-2.75935400
H	3.83372500	-0.66867000	-2.24624700
C	4.11896500	-1.89663000	0.59684800
H	3.88975500	-2.07380800	1.65324700
H	4.60849700	-2.78425900	0.17608800
H	4.79818600	-1.03947900	0.52817500
C	1.64787600	-3.14479200	-0.25205600
H	0.75271200	-3.08708200	-0.88109000
H	2.29580700	-3.95280300	-0.61611100
H	1.34115900	-3.35160800	0.77812800
C	-3.59675100	-0.44145100	-2.14970600
H	-2.74025200	-0.31064600	-2.82030600
H	-4.30041100	-1.16178400	-2.58621400
H	-4.09238200	0.52640400	-2.01774800
C	-2.45045700	-2.78081300	-0.89929900
H	-2.16470300	-3.30087700	0.02162400
H	-3.26798400	-3.32593800	-1.38830100
H	-1.58578800	-2.74283000	-1.57123900
C	-4.55299200	-1.31228500	0.44751400
H	-5.03839700	-0.34853400	0.63722400
H	-5.23565200	-1.95934800	-0.11782200
H	-4.32435400	-1.77999200	1.41188200

pdt 3C2*

Fe	1.47183600	0.37167100	0.27168800
Fe	-1.46222400	0.22760700	0.60971400
S	0.05535800	1.88590700	1.27446400
S	-0.21409500	0.24692800	-1.40042900
O	-3.61179100	2.21602700	0.42436500
C	-0.68083300	-1.06399800	1.56036000
C	2.76564800	1.44898400	-0.33685000
C	-2.71932800	1.45346200	0.41406100
C	-0.20970900	3.31903000	0.10048700
C	-0.56188300	1.95118700	-2.09244000
C	0.14353100	3.10569400	-1.37622600
H	-0.22913000	1.91711900	-3.13787700
H	-1.65240500	2.07460600	-2.08217400
H	1.22719400	2.97930300	-1.47862100
H	-0.11631300	4.03656000	-1.90970800
H	-1.25738100	3.62279600	0.21901600
H	0.41854500	4.12097800	0.50890200
O	3.67539100	2.13367200	-0.63302600
C	2.19115600	0.03041200	1.84857000
O	2.72637100	-0.16440100	2.87518100
O	-0.39810100	-1.94595100	2.28312900
H	-2.15706100	0.27332400	1.94619000
P	2.48344700	-1.44993200	-0.58551600
P	-2.86228800	-1.27123100	-0.28540600
C	2.68452800	-1.46296000	-2.44084200
H	3.21743300	-2.36569000	-2.76648500
H	1.69641600	-1.41942000	-2.91017200
H	3.25227000	-0.57509600	-2.74143200
C	4.25042300	-1.67026200	-0.02232000
H	4.27488300	-1.82466700	1.06188600
H	4.71007600	-2.53223500	-0.52251800
H	4.82185800	-0.76580700	-0.25833000
C	1.79126800	-3.15512200	-0.25625900
H	0.79572400	-3.23851900	-0.70310200
H	2.44618600	-3.92424500	-0.68613000
H	1.70247200	-3.30851900	0.82458500
C	-3.74471000	-0.71066200	-1.82854800
H	-4.38620900	-1.51001700	-2.22056900
H	-4.35601800	0.17046300	-1.60570000
H	-2.99156600	-0.44214600	-2.57820400
C	-4.26112600	-1.80448500	0.82427000
H	-4.91401800	-2.53040600	0.32283800
H	-3.84435000	-2.25201100	1.73353700
H	-4.84566800	-0.92283600	1.10994300
C	-2.14563900	-2.89850400	-0.84304200
H	-1.68119700	-3.40889300	0.00758000
H	-2.92920200	-3.53781100	-1.26941100
H	-1.38496200	-2.69739900	-1.60572700

pdt 3C2''*

Fe	-1.45290800	0.38946200	-0.29022200
Fe	1.45433900	0.20763200	-0.58495800
S	-0.00470400	1.91306200	-1.24468800
S	0.17544100	0.23429000	1.41783800
O	3.76742300	2.01541400	-0.61624900
C	0.56473700	-1.05200600	-1.49509800
C	-2.61855400	1.54434300	0.41600400
C	2.81191600	1.34223500	-0.50342200
C	0.15091000	3.32212800	-0.02295700
C	0.23240300	1.93868600	2.18535200
C	0.83994000	3.04317600	1.31847100
H	-0.80158800	2.17602600	2.46511100
H	0.82088400	1.83360500	3.10581700
H	0.80348000	3.97977800	1.90167000
H	1.90096300	2.82541600	1.15056900
H	0.70742000	4.10155300	-0.55919300
H	-0.87439800	3.68246400	0.12929600
O	-3.40356900	2.32793900	0.80775500
C	-2.23543300	0.16186800	-1.85830300
O	-2.80371800	0.04267100	-2.87841700
O	0.25767900	-1.93376800	-2.21111000
H	2.09604000	0.18339500	-1.94498900
P	-2.54849100	-1.40228200	0.53879700
P	2.79402100	-1.35971600	0.28393200
C	-2.75187500	-1.43122700	2.39421700
H	-3.32554800	-2.31318600	2.70714200
H	-1.76307100	-1.43934800	2.86417700
H	-3.27891400	-0.52327000	2.70887100
C	-4.32460000	-1.53072600	-0.02416300
H	-4.35836700	-1.66847000	-1.11036000
H	-4.82647800	-2.37523500	0.46515200
H	-4.84994100	-0.60197800	0.22499900
C	-1.94093400	-3.13699100	0.19451800
H	-0.95354700	-3.27408200	0.64664000
H	-2.63621300	-3.87668300	0.61256500
H	-1.85181700	-3.28387100	-0.88708200
C	3.71502000	-0.85198600	1.82193000
H	4.34519200	-1.67300900	2.18689300
H	4.34090500	0.02045900	1.60548500
H	2.98029800	-0.58115500	2.58861700
C	4.15356400	-1.93635200	-0.85213600
H	4.78341300	-2.69418000	-0.36877900
H	3.70413300	-2.35659600	-1.75889900
H	4.76967000	-1.07667300	-1.13832200
C	2.01850300	-2.96413900	0.82851400
H	1.53565600	-3.44925000	-0.02660600
H	2.77846000	-3.63570600	1.24778700
H	1.26529900	-2.74420400	1.59337800

pdt 3D1*

Fe	1.32169000	0.32852900	0.52132800
Fe	-1.31283300	-0.16418300	-0.56567200
S	-0.66653700	1.40075600	1.07418300
S	0.60354900	0.58786000	-1.68523800
O	-0.41906800	-2.68958800	0.68998200
C	2.55297300	1.60484000	0.80026400
C	-0.63612000	-1.62652200	0.23404200
C	-0.77156400	3.05907600	0.21530800
C	0.25339400	2.38144600	-2.06530600
C	0.27475300	3.33252600	-0.86757700
H	1.02912500	2.67572800	-2.78414800
H	-0.71863800	2.39453400	-2.57381700
H	1.27508600	3.33337300	-0.41878500
H	0.09643900	4.35300800	-1.24863200
H	-1.78767400	3.12191000	-0.19524400
H	-0.66863300	3.79984900	1.01860700
O	3.38090100	2.39042700	1.08289200
C	1.41379800	-0.36654800	2.13884200
O	1.51468300	-0.79365900	3.22818000
C	-1.84424800	-0.97209000	-2.02200800
O	-2.21004300	-1.46059100	-3.02108800
H	-2.05939700	0.99951000	-1.22154600
P	-3.24542400	-0.36672900	0.54283200
P	2.80982500	-1.16523600	-0.31559000
C	-4.27307500	1.18203300	0.63809700
H	-5.19428400	1.00455000	1.20767000
H	-3.68479800	1.96423500	1.13024900
H	-4.52176900	1.51008200	-0.37686200
C	-3.12135100	-0.87564900	2.33124100
H	-4.11461500	-0.89678800	2.79777800
H	-2.66644400	-1.87012000	2.39639900
H	-2.48145600	-0.15964600	2.85852600
C	-4.45885700	-1.61109800	-0.13470500
H	-5.37044200	-1.63819500	0.47572600
H	-4.71928200	-1.34803700	-1.16598100
H	-3.99352100	-2.60330200	-0.13571500
C	3.84400000	-2.10817100	0.91798900
H	3.19151700	-2.74014300	1.53038300
H	4.58310300	-2.73634500	0.40453400
H	4.36212200	-1.40164400	1.57618100
C	2.20555800	-2.53707200	-1.43292600
H	1.62261500	-2.10298400	-2.25369700
H	3.06035500	-3.08830100	-1.84608400
H	1.56864000	-3.22224600	-0.86523500
C	4.10979200	-0.36737800	-1.39008800
H	4.79884700	-1.12153900	-1.79139500
H	3.60745500	0.14966300	-2.21497800
H	4.67106000	0.36637100	-0.80150500

pdt 3D1'*

Fe	1.31509100	0.31024900	0.54028200
Fe	-1.29010300	-0.16697900	-0.56832000
S	-0.67824200	1.34779700	1.13081800
S	0.61389100	0.67075800	-1.65323100
O	-0.30889500	-2.67805400	0.65380200
C	2.44095300	1.68459100	0.77402600
C	-0.53454000	-1.60432800	0.22387900
C	-0.62550700	3.07372100	0.41583000
C	0.42038100	2.51559400	-1.88687100
C	-0.70790600	3.19459200	-1.10712100
H	1.39581300	2.94697200	-1.62562600
H	0.25862000	2.65324400	-2.96319900
H	-0.68604400	4.26903500	-1.35910100
H	-1.67176100	2.79759100	-1.45140900
H	-1.46982400	3.60539500	0.87377300
H	0.30243900	3.51649600	0.79993600
O	3.16978400	2.58048700	0.99349400
C	1.47469700	-0.37697900	2.15660700
O	1.61620400	-0.79762900	3.24382800
C	-1.77154700	-1.00606400	-2.02447300
O	-2.10642500	-1.52304100	-3.02002500
H	-2.13232600	0.92785000	-1.22101000
P	-3.21809900	-0.45566300	0.52625500
P	2.85129600	-1.11098500	-0.33684300
C	-4.25501600	1.07944600	0.70996000
H	-5.16626600	0.86919900	1.28444800
H	-3.66246400	1.84139000	1.22774900
H	-4.52160000	1.45304000	-0.28453900
C	-3.09185200	-1.06334900	2.28354600
H	-4.08617600	-1.12278700	2.74444000
H	-2.62510700	-2.05431300	2.29385400
H	-2.46276100	-0.37072200	2.85371500
C	-4.42505400	-1.66654800	-0.22005500
H	-5.33815200	-1.72683800	0.38570400
H	-4.68303400	-1.35041500	-1.23693800
H	-3.95837900	-2.65677900	-0.27133100
C	3.89444500	-2.08806200	0.86257200
H	3.24814700	-2.75552900	1.44318800
H	4.64707000	-2.68176500	0.32816000
H	4.39651000	-1.40190300	1.55385200
C	2.28234900	-2.44488600	-1.51659500
H	1.70085000	-1.98624300	-2.32496300
H	3.14841300	-2.96758300	-1.94286300
H	1.64987300	-3.16092100	-0.98280600
C	4.14259500	-0.23893300	-1.36295200
H	4.86048200	-0.95591000	-1.78156000
H	3.63533200	0.29260700	-2.17556200
H	4.67300000	0.48986200	-0.74039500

pdt 3D2*

Fe	1.26886400	0.04972300	0.55755000
Fe	-1.31807000	0.01241200	-0.68969600
S	-0.73122200	0.81030100	1.45738100
S	0.60266400	1.17857000	-1.39293200
O	-3.11572500	1.98358000	-1.91909400
C	2.40815600	1.07014200	1.49123600
C	-2.38315100	1.25994200	-1.35625000
C	-0.84233600	2.67314100	1.30779900
C	0.29649800	2.98068700	-1.00409100
C	0.25025500	3.35445500	0.47937100
H	1.12430400	3.51303100	-1.48996000
H	-0.63128900	3.26198000	-1.51814800
H	1.22777800	3.15680100	0.93438500
H	0.08300400	4.44367500	0.54195000
H	-1.84005400	2.89214200	0.90489700
H	-0.79958000	3.04339400	2.33993200
O	3.14784500	1.64188000	2.20513000
C	1.26906300	-1.32830700	1.66091800
O	1.30808800	-2.22160600	2.42359900
C	-0.53532500	-1.58404600	-0.78660600
O	-0.23787900	-2.70114100	-1.00953500
H	-1.60886300	-0.45601600	-2.09258400
P	-3.08000400	-0.98337600	0.26207600
P	2.93033200	-0.81887500	-0.70552900
C	-4.27057600	0.16176800	1.12260700
H	-4.68270200	0.87688700	0.40243600
H	-5.08892100	-0.40738400	1.58126700
H	-3.72433500	0.70936000	1.89865000
C	-4.18406900	-1.93832400	-0.89613700
H	-3.59586700	-2.72252000	-1.38553700
H	-5.02432600	-2.39360400	-0.35643000
H	-4.56789700	-1.25979400	-1.66626700
C	-2.69479800	-2.22406100	1.59630200
H	-3.62100300	-2.60842200	2.04209300
H	-2.11962500	-3.05518600	1.17447600
H	-2.09166800	-1.73394500	2.36864200
C	2.54912900	-1.66688500	-2.32631000
H	1.93629200	-1.00002400	-2.94326800
H	3.48462700	-1.89677400	-2.85290400
H	1.99252500	-2.59054900	-2.14184600
C	4.03753700	-2.06929000	0.12729400
H	3.45961500	-2.96904700	0.36473500
H	4.87590500	-2.33721200	-0.52804800
H	4.42465900	-1.64682200	1.06135900
C	4.16009800	0.47086400	-1.26174600
H	4.95565200	0.01216000	-1.86326800
H	3.63276000	1.22075000	-1.86133600
H	4.59888800	0.96122700	-0.38592900

pdt 3D2''*

Fe	1.20237900	0.04244200	0.54730400
Fe	-1.24443700	0.06258400	-0.63238700
S	-0.76567200	0.87199400	1.52763800
S	0.62463400	1.30419600	-1.34516900
O	-3.15347900	1.66344500	-2.20248400
C	2.29624700	1.21541700	1.34358000
C	-2.39285400	1.11517300	-1.49561700
C	-0.63823800	2.73357000	1.52363600
C	0.47110000	3.08231900	-0.79108400
C	-0.68690400	3.41423000	0.15453400
H	1.43506700	3.34617700	-0.33576300
H	0.36266900	3.65610600	-1.72004800
H	-0.66850600	4.50477700	0.32379400
H	-1.64146700	3.18457600	-0.33410400
H	-1.48356200	3.07460800	2.13497800
H	0.28730500	2.98272700	2.05895400
O	3.00782500	1.93569600	1.93736100
C	1.33055300	-1.19295900	1.79908000
O	1.44297700	-1.98915800	2.65260700
C	-0.25302700	-1.45347200	-0.51007100
O	-0.00724600	-2.60576000	-0.67892200
H	-1.36913700	-0.55855400	-1.99757000
P	-2.94264600	-1.09890300	0.22677600
P	2.82928600	-0.86845700	-0.75377200
C	-4.35720500	-0.07839700	0.88305400
H	-4.77115400	0.53832100	0.07809000
H	-5.14471100	-0.72512300	1.29015700
H	-3.97522100	0.57766600	1.67295500
C	-3.77476200	-2.26104500	-0.96687500
H	-3.02697200	-2.96602200	-1.34684900
H	-4.58979200	-2.81393800	-0.48213200
H	-4.17228700	-1.68565300	-1.81044100
C	-2.55948000	-2.20501800	1.67734300
H	-3.47647600	-2.68386900	2.04358400
H	-1.84258600	-2.97516500	1.37405900
H	-2.11597000	-1.60260800	2.47827900
C	2.41363000	-1.43764400	-2.48477900
H	1.90558300	-0.62821600	-3.02052500
H	3.33823500	-1.70424800	-3.01287000
H	1.75292600	-2.30807700	-2.43840100
C	3.69626400	-2.36941300	-0.06596200
H	2.96365000	-3.17300900	0.06759000
H	4.48697300	-2.70606500	-0.74842900
H	4.13436300	-2.12793300	0.90883800
C	4.24924300	0.29267100	-1.09477100
H	4.99889200	-0.19346200	-1.73203600
H	3.85973800	1.18163500	-1.60335000
H	4.71492000	0.59962600	-0.15205000

[Fe₂(μ-odt)(CO)₄(PMe₃)₂] systems

Table A31: Calculated gas phase and solvent corrected free energies and Fe Mulliken charges of the isomers of [Fe₂(μ-odt)(CO)₄(PMe₃)₂]. Energies are reported relative to the **1A** isomer.

Isomer	Free Energies / kcal/mol		Mulliken charges	
	ΔG_g	ΔG_{solv}	Fe _a	Fe _b
odt 1A	0.0	0.0	-0.773	-0.312
odt 1A'	-2.9	-1.1	-0.663	-0.211
odt 1B	-0.8	-1.8	-0.571	-0.482
odt 1C	3.6	2.8	-0.391	-0.470
odt 1D	-0.7	-0.8	-0.403	-0.422
TS_{odt 1A→1B}	10.1	8.8	-0.602	-0.704
TS_{odt 1A→1C}	8.8	7.0	-0.998	-0.550
TS_{odt 1A→1D}	6.4	6.1	-0.882	-0.534
TS_{odt 1C→1D}	23.9	23.4	-0.297	-0.982
TS_{odt 1C→1D_{flipped}}	20.8	16.0	-0.091	-1.002
TS_{odt 1A'→1C}	7.2	5.9	-0.851	-0.545
TS_{odt 1A'→1D}	3.8	3.8	-0.710	-0.515
TS_{odt 1A'→1B}	8.7	7.0	-0.522	-0.851
TS_{odt 1A→1A'}	8.4	8.9	-0.642	-0.238
TS_{odt 1B→1B}	10.5	9.2	-0.499	-0.499
TS_{odt 1C→1C}	12.6	12.1	-0.337	-0.397
TS_{odt 1D→1D}	8.5	9.7	-0.542	-0.542

Table A32: Selected bond distances of the unprotonated [$Fe_2(\mu\text{-odt})(CO)_4(PMe_3)_2$] from x-ray crystallography (apical/basal)(in bold), compared to calculated values of all isomers and transition states inter-converting them.

	bond length/Å										
	Fe ₁ -Fe ₂	Fe ₁ -S ₁	Fe ₁ -S ₂	Fe ₂ -S ₁	Fe ₂ -S ₂	Fe ₁ -CO ₁	Fe ₁ -CO ₂	Fe ₂ -CO ₁	Fe ₂ -CO ₂	Fe ₁ -P ₁	Fe ₂ -P ₂
Exp.	2.523	2.270	2.267	2.255	2.256	1.752	1.751	1.767	1.763	2.211	2.228
odt 1A	2.5288	2.3117	2.3079	2.2976	2.2966	1.7562	1.7489	1.7625	1.7573	2.2395	2.2563
odt 1A'	2.5286	2.3133	2.3046	2.2934	2.2907	1.7541	1.7447	1.7547	1.7619	2.2419	2.2638
odt 1B	2.4945	2.3173	2.3147	2.3209	2.3230	1.7579	1.7563	1.7533	1.7536	2.2392	2.2438
odt 1C	2.6035	2.2842	2.2804	2.2879	2.2889	1.7524	1.7657	1.7579	1.7591	2.2577	2.2470
odt 1D	2.5796	2.2869	2.2856	2.2896	2.2928	1.7521	1.7566	1.7584	1.7512	2.2636	2.2524
TS _{odt 1A} →1B	2.5525	2.3197	2.3236	2.3294	2.3539	1.7636	1.7626	1.7426	1.7417	2.2423	2.2131
TS _{odt 1A} →1C	2.5714	2.3071	2.3324	2.3039	2.3148	1.7434	1.7397	1.7606	1.7640	2.2150	2.2675
TS _{odt 1A} →1D	2.5611	2.3334	2.3090	2.3081	2.3137	1.7418	1.7395	1.7603	1.7609	2.2154	2.2704
TS _{odt 1C} →1D	2.7061	2.3300	2.3301	2.2727	2.2791	1.7451	1.7417	1.7597	1.7603	2.2468	2.2608
TS _{odt 1C} →1D-flip	2.6900	2.3313	2.3335	2.2827	2.2752	1.7430	1.7432	1.7500	1.7601	2.2351	2.2779
TS _{odt 1A'} →1C	2.5784	2.3043	2.3440	2.3046	2.3205	1.7403	1.7407	1.7515	1.7686	2.2153	2.2753
TS _{odt 1A'} →1D	2.5616	2.3428	2.3107	2.3093	2.3151	1.7401	1.7397	1.7516	1.7655	2.2127	2.2767
TS _{odt 1A'} →1B	2.5491	2.3202	2.3244	2.3216	2.3438	1.7598	1.7592	1.7447	1.7443	2.2476	2.2153
TS _{odt 1A} →1A'	2.5492	2.2904	2.2869	2.2729	2.2741	1.7573	1.7495	1.7576	1.7619	2.2373	2.2597
TS _{odt 1B} →1B	2.5155	2.3016	2.2944	2.2944	2.3017	1.7596	1.7556	1.7556	1.7596	2.2390	2.2390
TS _{odt 1C} →1C	2.6260	2.2638	2.2644	2.2619	2.2649	1.7547	1.7647	1.7555	1.7653	2.2531	2.2638
TS _{odt 1D} →1D	2.5919	2.2652	2.2693	2.2693	2.2652	1.7591	1.7533	1.7591	1.7533	2.2646	2.2646

Table A33: Selected bond angles of the unprotonated $[\text{Fe}_2(\mu\text{-odt})(\text{CO})_4(\text{PMe}_3)_2]$ from x-ray crystallography (in bold), compared to calculated values of all isomers and transition states inter-converting them.

	bond angle/ $^\circ$					
	$\angle \text{S}_1\text{-Fe}_1\text{-S}_2$	$\angle \text{S}_1\text{-Fe}_2\text{-S}_2$	$\angle \text{Fe}_1\text{-S}_1\text{-Fe}_2$	$\angle \text{Fe}_1\text{-S}_2\text{-Fe}_2$	$\angle \text{L-Fe-Fe-L}$	
Exp.	84.22	84.79	67.79	67.82	15.68	
odt 1A	84.7274	85.3076	66.5445	66.6226	19.9092	
odt 1A'	85.0962	85.8730	66.5801	66.7671	7.3570	
odt 1B	85.3757	85.1055	65.0692	65.0764	5.8930	
odt 1C	85.7387	85.4557	69.4192	69.4702	20.5152	
odt 1D	85.9760	85.7446	68.6198	68.5875	37.7870	
TS _{odt 1A→1B}	85.6760	84.7703	66.5990	66.1393	93.6118	
TS _{odt 1A→1C}	84.9693	85.4428	67.7902	67.1902	90.7730	
TS _{odt 1A→1D}	84.9590	85.4281	66.9776	67.2871	96.1597	
TS _{odt 1C→1D}	84.9103	87.4319	72.0080	71.8944	66.7111	
TS _{odt 1C→1D-flip}	84.7497	87.2286	71.3150	71.4057	91.1735	
TS _{odt 1A'→1C}	85.6711	86.2097	68.0355	67.1138	93.1335	
TS _{odt 1A'→1D}	85.3256	85.9945	66.8175	67.2521	99.5245	
TS _{odt 1A'→1B}	85.4554	84.9811	66.6198	66.1923	96.8052	
TS _{odt 1A→1A'}	83.4561	84.1382	67.9220	67.9613	17.5327	
TS _{odt 1B→1B}	83.6753	83.6743	66.3648	66.3646	19.6241	
TS _{odt 1C→1C}	84.1574	84.1899	70.9349	70.8693	7.4841	
TS _{odt 1D→1D}	83.5764	83.5764	69.7229	69.7232	4.9643	

Table A34: Calculated gas phase and solvent corrected free energies and Fe Mulliken charges for isomers of $[(\mu\text{-H})\text{Fe}_2(\mu\text{-odt})(\text{CO})_4(\text{PMe}_3)_2]^+$ and the transition states that connect them; either through rotation of the $\text{Fe}(\text{CO})_2(\text{PMe}_3)$ moiety or by the odt bridge flip.

ΔG_g	Free Energies / kcal/mol		Mulliken charges	
	ΔG_{solv}	Fe ₁	Fe ₂	
odt 2A	3.5	4.5	-1.328	-0.138
odt 2A'	1.3	2.2	-1.105	-0.153
odt 2B	6.8	6.9	-0.955	-0.657
odt 2C	4.1	4.8	-0.774	-0.548
odt 2D	0.0	0.0	-0.685	-0.603
TS_{odt 2A→2B}	29.5	30.1	-1.082	-0.108
TS_{odt 2A→2C}	26.3	26.5	-0.517	-0.747
TS_{odt 2A→2D}	24.1	25.2	-0.477	-0.615
TS_{odt 2C→2D}	27.6	28.3	0.112	-1.090
TS_{odt 2C→2D-flipped}	27.4	28.3	0.202	-1.074
TS_{odt 2A'→2C}	25.4	25.7	-0.307	-0.750
TS_{odt 2A'→2D}	23.4	24.8	-0.351	-0.559
TS_{odt 2A'→2B}	28.3	28.4	-0.941	-0.257
TS_{odt 2A→2A'}	13.6	14.5	-1.180	-0.131
TS_{odt 2B→2B}	17.4	17.2	-0.735	-0.735
TS_{odt 2C→2C}	13.7	14.5	-0.693	-0.639
TS_{odt 2D→2D}	10.4	12.3	-0.574	-0.574

^u data unavailable

Table A35: Selected bond distances of the bridged protonated $[(\mu\text{-H})\text{Fe}_2(\mu\text{-odt})(\text{CO})_4(\text{PMe}_3)_2]\text{I}^+$ from x-ray crystallography (in bold) [], compared to calculated values of all isomers and transition states inter-converting them.

Exp.	bond length/Å												
	Fe ₁ -Fe ₂	Fe ₁ -S ₁	Fe ₁ -S ₂	Fe ₂ -S ₁	Fe ₂ -S ₂	Fe ₁ -H	Fe ₂ -H	Fe ₁ -CO ₁	Fe ₁ -CO ₂	Fe ₂ -CO ₁	Fe ₂ -CO ₂	Fe ₁ -P ₁	Fe ₂ -P ₂
2.579	2.271	2.262	2.262	2.262	2.271	1.737	1.737	1.780	1.776	1.780	1.776	2.243	2.243
2.5884	2.3155	2.3252	2.3157	2.3127	2.3127	1.6712	1.6575	1.7777	1.7762	1.7764	1.7738	2.2748	2.2902
2.5894	2.3226	2.3185	2.3126	2.3088	2.3088	1.6702	1.6642	1.7761	1.7709	1.7637	1.7783	2.2800	2.2948
2.5831	2.3295	2.3208	2.3285	2.3305	2.3305	1.6570	1.6542	1.7805	1.7779	1.7749	1.7752	2.2793	2.2833
2.6101	2.3004	2.3028	2.3014	2.3082	2.3082	1.6959	1.6909	1.7610	1.7810	1.7746	1.7759	2.2972	2.2919
2.6040	2.3035	2.3026	2.3062	2.3069	2.3069	1.6904	1.6891	1.7612	1.7754	1.7740	1.7711	2.2980	2.2905
TS _{odt 2A→2B}	2.6445	2.3189	2.3114	2.3847	2.3907	1.6423	1.6931	1.7812	1.7757	1.7532	1.7443	2.2808	2.2562
TS _{odt 2A→2C}	2.6503	2.3695	2.3684	2.2953	2.3106	1.7266	1.6421	1.7560	1.7449	1.7791	1.7745	2.2569	2.2866
TS _{odt 2A→2D}	2.6412	2.3653	2.3707	2.3045	2.3050	1.7179	1.6427	1.7546	1.7441	1.7787	1.7718	2.2608	2.2887
TS _{odt 2C→2D}	2.6834	2.3682	2.3738	2.2984	2.3055	1.7411	1.6713	1.7529	1.7479	1.7802	1.7708	2.2520	2.2927
TS _{odt 2C→2D-flipped}	2.6862	2.3750	2.3810	2.2978	2.3025	1.7357	1.6775	1.7512	1.7471	1.7675	1.7761	2.2455	2.3007
TS _{odt 2A'→2C}	2.6516	2.3736	2.3848	2.2944	2.3067	1.7210	1.6496	1.7533	1.7419	1.7672	1.7797	2.2548	2.2939
TS _{odt 2A'→2D}	2.6463	2.3774	2.3725	2.3021	2.3003	1.7183	1.6488	1.7527	1.7412	1.7671	1.7764	2.2568	2.2947
TS _{odt 2A'→2B}	2.6418	2.3150	2.3222	2.3804	2.3758	1.6387	1.6952	1.7752	1.7740	1.7565	1.7473	2.2858	2.2579
TS _{odt 2A→2A'}	2.6050	2.2958	2.3076	2.2940	2.2921	1.6760	1.6668	1.7775	1.7768	1.7681	1.7786	2.2763	2.2919
TS _{odt 2B→2B}	2.5994	2.3094	2.3035	2.3094	2.3035	1.6617	1.6618	1.7800	1.7783	1.7800	1.7783	2.2783	2.2783
TS _{odt 2C→2C}	2.6278	2.2812	2.2876	2.2811	2.2867	1.7000	1.6992	1.7656	1.7804	1.7660	1.7805	2.2937	2.2960
TS _{odt 2D→2D}	2.6166	2.2858	2.2877	2.2877	2.2858	1.6876	1.6876	1.7665	1.7749	1.7665	1.7749	2.2930	2.2930

Table A36: Selected bond angles of the bridged protonated $[(\mu\text{-H})\text{Fe}_2(\mu\text{-odt})(\text{CO})_4(\text{PMe}_3)_2]^+$ from x-ray crystallography (in bold)[1], compared to calculated values of all isomers and transition states inter-converting them.

	bond angle/°					
	$\angle \text{S}_1\text{-Fe}_1\text{-S}_2$	$\angle \text{S}_1\text{-Fe}_2\text{-S}_2$	$\angle \text{Fe}_1\text{-S}_1\text{-Fe}_2$	$\angle \text{Fe}_1\text{-S}_2\text{-Fe}_2$	$\angle \text{L-Fe}_1\text{-Fe}_2\text{-L}$	
Exp.	85.06	85.06	69.30	69.30	5.22	
odt 2A	84.5408	84.8188	67.9593	67.8467	11.3272	
odt 2A'	84.9600	85.4095	67.9226	68.0547	5.4868	
odt 2B	84.5651	84.3714	67.3594	67.4674	4.2752	
odt 2C	85.7811	85.6316	69.1089	68.9514	1.5015	
odt 2D	86.0369	85.8749	68.7902	68.7957	0.2219	
TS _{odt 2A→2B}	85.7281	82.5397	68.4052	68.4217	73.2460	
TS _{odt 2A→2C}	83.1270	86.0703	69.2205	68.9898	79.2898	
TS _{odt 2A→2D}	83.0620	85.8810	68.8735	68.7721	79.6289	
TS _{odt 2C→2D}	84.1550	87.2974	70.1846	69.9665	80.0840	
TS _{odt 2C→2D-flipped}	84.0049	87.5463	70.1561	69.9738	78.6787	
TS _{odt 2A'→2C}	83.3745	86.9112	69.2014	68.8069	77.3897	
TS _{odt 2A'→2D}	83.2814	86.5909	68.8537	68.9684	79.1986	
TS _{odt 2A'→2B}	85.5384	82.9133	68.4599	68.4220	80.3845	
TS _{odt 2A→2A'}	83.5719	83.9599	69.1607	68.9881	11.4730	
TS _{odt 2B→2B}	83.1452	83.1452	68.4947	68.4947	0.0000	
TS _{odt 2C→2C}	84.6341	84.6575	70.3354	70.1248	1.2509	
TS _{odt 2D→2D}	84.1333	84.1333	69.7941	69.7941	4.5168	

Table A37: Calculated gas phase and solvent corrected free energies, Fe–Fe bond lengths, and Fe Mulliken charges of the isomers of $[(H)Fe_2(\mu\text{-odt})(CO)_4(PMe_3)_2]^+$. Energies are reported relative to the **2D** isomer.

Isomer	Free Energies / kcal/mol		Mulliken charges	
	ΔG_g	ΔG_{solv}	Fe ₁	Fe ₂
odt 3A1	21.1	21.2	-0.437	-1.301
odt 3A1'	18.6	18.7	-1.151	-0.538
odt 3A2	17.2	17.3	-1.209	-0.596
odt 3A2'	20.2	20.6	-1.146	-0.674
odt 3A3	17.2	17.6	-1.478	-0.463
odt 3A3'	15.0	15.6	-0.645	-1.379
odt 3A4	19.9	20.4	-0.711	-0.966
odt 3A4'	18.0	18.4	-0.479	-0.953
odt 3B	22.9	22.4	-1.204	-0.687
odt 3B'	22.3	21.8	-1.267	-0.509
odt 3C1	22.9	22.1	-1.563	-0.391
odt 3C1'	17.2	16.8	-1.526	-0.455
odt 3C2	20.6	20.7	-1.138	-0.559
odt 3C2'	17.1	17.2	-1.083	-0.664
odt 3D1	13.9	14.7	-1.475	-0.493
odt 3D1'	13.4	14.5	-1.459	-0.497
odt 3D2	16.5	17.4	-1.129	-0.623
odt 3D2'	16.1	17.3	-1.144	-0.681

Table A38: Calculated selected bond distances of the terminally protonated $[(H)Fe_2(\mu\text{-odt})(CO)_4(PMe_3)_2]^+$ isomers.

	bond length/Å													
	Fe ₁ -Fe ₂	Fe ₁ -S ₁	Fe ₁ -S ₂	Fe ₂ -S ₁	Fe ₂ -S ₂	Fe-H	Fe ₁ -CO ₁	Fe ₁ -CO ₂	Fe ₂ -CO ₃	Fe ₂ -CO ₄	Fe-CO _{semi}	Fe ₁ -P ₁	Fe ₂ -P ₂	
odt 3A1	2.5357	2.3265	2.3186	2.3205	2.3078	1.5044	1.7727	1.8059	1.7710	1.7829	2.2621	2.2632	2.3220	
odt 3A1'	2.5327	2.3228	2.3294	2.3179	2.3052	1.4984	1.7692	1.8042	1.7571	1.7881	2.2769	2.2726	2.3302	
odt 3A2	2.5475	2.3186	2.3271	2.3080	2.3133	1.5014	1.7699	1.8030	1.7674	1.7830	2.2977	2.2671	2.3074	
odt 3A2'	2.5493	2.3279	2.3265	2.3059	2.3108	1.4967	1.7657	1.8008	1.7531	1.7868	2.3194	2.2774	2.3126	
odt 3A3	2.5737	2.2907	2.3026	2.3184	2.3218	1.5139	1.7842	1.7838	1.7675	1.8015	2.5123	2.2580	2.2695	
odt 3A3'	2.5757	2.2906	2.3022	2.3140	2.3172	1.5165	1.7818	1.7805	1.7712	1.8053	2.4999	2.2598	2.2785	
odt 3A4	2.5696	2.3026	2.2950	2.3208	2.3319	1.4990	1.7872	1.7779	1.7899	1.7775	2.5374	2.2565	2.2802	
odt 3A4'	2.5691	2.2994	2.3005	2.3243	2.3228	1.5030	1.7821	1.7762	1.7769	1.7819	2.5381	2.2595	2.2833	
odt 3B	2.5499	2.3422	2.3340	2.3249	2.3101	1.4952	1.7706	1.7922	1.7863	1.7826	2.3966	2.2822	2.2728	
odt 3B'	2.5500	2.3305	2.3372	2.3209	2.3195	1.5007	1.7740	1.7952	1.7820	1.7811	2.3624	2.2726	2.2766	
odt 3C1	2.5779	2.2958	2.3182	2.2754	2.2898	1.5179	1.7747	1.8052	1.7598	1.7853	2.4771	2.2754	2.3256	
odt 3C1'	2.5724	2.2931	2.3240	2.2768	2.2865	1.5155	1.7711	1.8030	1.7487	1.7895	2.4741	2.2686	2.3307	
odt 3C2	2.6128	2.3109	2.3229	2.2750	2.2923	1.5041	1.7785	1.7881	1.7555	1.7875	2.5452	2.2946	2.3068	
odt 3C2'	2.6029	2.3101	2.3276	2.2738	2.2917	1.5014	1.7925	1.7837	1.7445	1.7922	2.5146	2.2905	2.3171	
odt 3D1	2.5709	2.3071	2.3046	2.2920	2.2788	1.5153	1.7707	1.8035	1.7584	1.7831	2.4621	2.2756	2.3135	
odt 3D1'	2.5683	2.3107	2.3023	2.2917	2.2767	1.5139	1.7675	1.8012	1.7486	1.7865	2.4628	2.2717	2.3173	
odt 3D2	2.5523	2.3129	2.3159	2.2983	2.2853	1.5054	1.7771	1.7802	1.7603	1.7797	2.4516	2.2815	2.3252	
odt 3D2'	2.5542	2.3170	2.3149	2.2952	2.2790	1.5024	1.7876	1.7772	1.7492	1.7851	2.4549	2.2794	2.3309	

Table A39: Calculated selected bond angles of the terminally protonated $[(H)Fe_2(\mu-odt)(CO)_4(PMe_3)_2]^+$ isomers.

	bond angle/ $^\circ$										
	$\angle S_1-Fe_1-S_2$	$\angle S_1-Fe_2-S_2$	$\angle Fe_1-S_1-Fe_2$	$\angle Fe_1-S_2-Fe_2$	$\angle L-Fe_1-Fe_2-L$	$\angle Fe-Fe-C_{semi}$	$\angle Fe-C-O_{semi}$				
odt 3A1	86.6190	85.3448	67.5291	67.4680	23.8847	68.6621	165.9419				
odt 3A1'	86.9026	85.8044	67.5072	67.5145	17.6513	68.6493	165.9947				
odt 3A2	85.6450	86.2083	66.8183	66.5935	31.7324	60.9465	157.0259				
odt 3A2'	85.9295	86.8048	66.7530	66.6955	24.7379	61.6359	157.8285				
odt 3A3	85.5262	84.4596	67.8866	67.6319	4.6652	67.4383	164.9314				
odt 3A3'	86.3352	85.4462	68.0229	67.7760	2.4213	66.9326	164.8118				
odt 3A4	86.6190	85.3448	67.5291	67.4680	23.8847	68.6621	165.9419				
odt 3A4'	86.9026	85.8044	67.5072	67.5145	17.6513	68.6493	165.9947				
odt 3B	84.9717	85.9083	66.2333	66.6012	28.0169	64.2550	161.0360				
odt 3B'	85.2950	85.9189	66.4900	66.4042	30.2619	63.0876	160.0185				
odt 3C1	85.8552	87.0024	68.6575	68.0327	1.8219	66.1149	164.1135				
odt 3C1'	85.5377	86.7958	68.5109	67.8205	0.2374	66.1753	163.6000				
odt 3C2	86.4960	88.0735	69.4608	68.9575	13.1816	67.6978	165.7594				
odt 3C2'	86.4644	88.1815	69.1935	68.5893	18.3995	66.9662	165.1441				
odt 3D1	85.8609	86.8194	67.9717	68.2345	0.0395	65.8083	163.5792				
odt 3D1'	85.5219	86.5595	67.8368	68.2308	0.5703	65.9210	163.3750				
odt 3D2	86.0500	87.1096	67.2126	67.3740	23.9845	66.1613	163.4718				
odt 3D2'	86.0864	87.4428	67.2557	67.5541	22.1912	66.2517	163.4949				

Table A40: Calculated gas phase and solvent corrected free energies and Fe Mulliken charges for isomers of the singly reduced bridged protonated $[(\mu - H)Fe_2(\mu\text{-odt})(CO)_4(PMe_3)_2]$ and the transition states that connect them; either through rotation of the $Fe(CO)_2(PMe_3)$ moiety or by the odt bridge flip.

ΔG_g	Free Energies / kcal/mol		Mulliken charges	
	ΔG_{solv}	Fe ₁	Fe ₂	
odt 2A*	4.3	5.3	-1.273	-0.155
odt 2A'*	-0.3	1.0	-1.119	-0.105
odt 2B*	4.9	5.0	-0.912	-0.700
odt 2C*	4.4	4.5	-0.645	-0.506
odt 2D*	0.0	0.0	-0.571	-0.480
TS_{odt 2A*→2B*}	22.6	22.9	-1.222	-0.402
TS_{odt 2A*→2C*}	16.9	18.3	-0.573	-0.788
TS_{odt 2A*→2D*}	16.1	17.6	-0.583	-0.767
TS_{odt 2C*→2D*}	16.2	17.8	-0.143	-1.124
TS_{odt 2C*→2D-flipped*}	16.0	17.3	-0.071	-1.170
TS_{odt 2A'→2C*}	14.3	15.6	-0.400	-0.828
TS_{odt 2A'→2D*}	15.2	16.6	-0.749	-0.829
TS_{odt 2A'→2B*}	21.3	21.6	-1.068	-0.472
TS_{odt 2A*→2A'*}	11.9	13.3	-1.159	-0.136
TS_{odt 2B*→2B*}	15.5	15.4	-0.741	-0.741
TS_{odt 2C*→2C*}	13.8	14.4	-0.568	-0.582
TS_{odt 2D*→2D*}	9.1	9.8	-0.594	-0.462

Table A41: Calculated selected bond distances of the singly reduced bridged protonated $[(\mu-H)Fe_2(\mu-odt)(CO)_4(PMe_3)_2]$ isomers.

	bond length/Å												
	Fe ₁ -Fe ₂	Fe ₁ -S ₁	Fe ₁ -S ₂	Fe ₂ -S ₁	Fe ₂ -S ₂	Fe ₁ -H	Fe ₂ -H	Fe ₁ -CO ₁	Fe ₁ -CO ₂	Fe ₂ -CO ₁	Fe ₂ -CO ₂	Fe ₁ -P ₁	Fe ₂ -P ₂
odt 2A*	2.7285	2.3552	2.3651	2.3564	2.3646	1.7133	1.6487	1.7603	1.7584	1.8015	1.7518	2.3606	2.2476
odt 2A**	2.7254	2.3714	2.3541	2.3528	2.3641	1.7043	1.6579	1.7583	1.7548	1.7890	1.7554	2.3449	2.2533
odt 2B*	2.7112	2.3678	2.3685	2.3645	2.3751	1.6703	1.6577	1.7608	1.7595	1.7571	1.7572	2.3426	2.3318
odt 2C*	2.7645	2.3293	2.3683	2.3315	2.3689	1.7277	1.6984	1.7922	1.7592	1.8076	1.7542	2.2509	2.2475
odt 2D*	2.7515	2.3662	2.3361	2.3355	2.3715	1.7081	1.7060	1.7922	1.7540	1.8051	1.7508	2.2538	2.2483
TS _{odt 2A*→2B*}	3.2321	2.3597	2.3645	2.4149	2.3762	1.5044	2.5778	1.7550	1.7530	1.7517	1.8007	2.3306	2.2628
TS _{odt 2A*→2C*}	3.2548	2.3752	2.3534	2.3435	2.3716	2.7246	1.5296	1.7552	1.7936	1.7979	1.7438	2.2673	2.2346
TS _{odt 2A*→2D*}	3.2633	2.3475	2.3783	2.3480	2.3699	2.7364	1.5281	1.7553	1.7961	1.7986	1.7448	2.2648	2.2315
TS _{odt 2C*→2D*}	3.3362	2.3703	2.3524	2.3543	2.3589	2.8606	1.5353	1.7566	1.7666	1.7993	1.7477	2.2982	2.2420
TS _{odt 2C*→2D-flipped*}	3.2963	2.3954	2.3608	2.3540	2.3516	2.7920	1.5368	1.7536	1.7711	1.7841	1.7528	2.2950	2.2475
TS _{odt 2A**→2C*}	3.2626	2.3974	2.3686	2.3401	2.3672	2.7434	1.5307	1.7525	1.7923	1.7859	1.7486	2.2678	2.2388
TS _{odt 2A**→2D*}	3.3817	2.3829	2.3612	2.3435	2.3562	2.9519	1.5253	1.7575	1.8053	1.7838	1.7501	2.2774	2.2387
TS _{odt 2A**→2B*}	3.1959	2.3640	2.3738	2.3958	2.3600	1.5071	2.5294	1.7498	1.7512	1.7547	1.8013	2.3277	2.2622
TS _{odt 2A*→2A**}	2.7579	2.3381	2.3392	2.3300	2.3410	1.7231	1.6595	1.7613	1.7578	1.7933	1.7559	2.3451	2.2504
TS _{odt 2B*→2B*}	2.7441	2.3413	2.3486	2.3413	2.3486	1.6750	1.6750	1.7597	1.7605	1.7597	1.7605	2.3344	2.3344
TS _{odt 2C*→2C*}	2.8041	2.3042	2.3471	2.3085	2.3406	1.7426	1.7118	1.7972	1.7599	1.7987	1.7585	2.2478	2.2493
TS _{odt 2D*→2D*}	2.7910	2.3066	2.3438	2.3420	2.3117	1.7146	1.7243	1.7967	1.7547	1.7964	1.7552	2.2508	2.2515

Table A42: Calculated selected bond angles of the singly reduced bridged protonated $[(\mu - H)Fe_2(\mu - odt)(CO)_4(PMe_3)_2]$ isomers.

	bond angle/°					
	$\angle S_1-Fe_1-S_2$	$\angle S_1-Fe_2-S_2$	$\angle Fe_1-S_1-Fe_2$	$\angle Fe_1-S_2-Fe_2$	$\angle L-Fe_1-Fe_2-L$	
odt 2A*	84.8698	84.8529	70.7738	70.4624	5.7800	
odt 2A**	85.2882	85.4831	70.4638	70.5663	5.4889	
odt 2B*	85.0110	84.9368	69.9072	69.7174	5.0877	
odt 2C*	85.5092	85.4459	72.7585	71.4034	2.8922	
odt 2D*	85.9266	85.8202	71.6344	71.5287	2.0035	
TS _{odt 2A*→2B*}	81.9516	80.5639	85.2033	85.9675	60.9882	
TS _{odt 2A*→2C*}	80.3642	80.6397	87.2211	87.0765	66.1135	
TS _{odt 2A*→2D*}	80.3122	80.4770	88.0517	86.8301	66.5286	
TS _{odt 2C*→2D*}	80.1369	80.3302	89.8434	90.1670	63.0908	
TS _{odt 2C*→2D-flipped*}	80.2305	81.2771	87.8990	88.7745	58.3701	
TS _{odt 2A**→2C*}	80.5396	81.7572	87.0433	87.0910	61.0247	
TS _{odt 2A**→2D*}	79.2902	80.1902	91.3652	91.5908	85.3430	
TS _{odt 2A**→2B*}	81.3455	80.9720	84.3538	84.9293	73.2085	
TS _{odt 2A*→2A**}	83.5842	83.7199	72.4257	72.2088	11.3749	
TS _{odt 2B*→2B*}	83.3833	83.3840	71.7502	71.4943	0.0026	
TS _{odt 2C*→2C*}	84.1010	84.1529	74.8754	73.4788	3.4639	
TS _{odt 2D*→2D*}	84.3602	84.2888	73.7951	73.6676	1.8856	

Table A43: Calculated gas phase and solvent corrected free energies, Fe–Fe bond lengths, and Fe Mulliken charges of the isomers of the singly reduced $[(\mu\text{-H})\text{Fe}_2(\mu\text{-odt})(\text{CO})_4(\text{PMe}_3)_2]$. Energies are reported relative to the **2D** isomer.

Isomer	Free Energies / kcal/mol		Mulliken charges	
	ΔG_g	ΔG_{solv}	Fe ₁	Fe ₂
odt 3A1*	15.6	14.8	-1.483	-0.384
odt 3A1'*	11.3	10.7	-1.334	-0.503
odt 3A2*	10.9	10.4	-1.378	-0.542
odt 3A2'*	14.8	13.9	-1.263	-0.643
odt 3A3*	11.5	12.2	-1.278	-0.606
odt 3A3'*	6.5	6.7	-0.516	-1.317
odt 3A4*	12.8	13.6	-0.635	-1.018
odt 3A4'*	9.7	10.5	-0.431	-1.036
odt 3B*	15.5	14.5	-1.307	-0.665
odt 3B'*	16.0	14.8	-1.396	-0.515
odt 3C1*	8.4	8.2	-1.438	-0.394
odt 3C1'*	9.6	9.8	-1.356	-0.446
odt 3C2*	13.4	13.7	-0.812	-0.398
odt 3C2'*	12.7	13.4	-0.786	-0.504
odt 3D1*	7.3	7.7	-1.440	-0.388
odt 3D1'*	8.0	8.9	-1.399	-0.395
odt 3D2*	10.1	10.8	-1.069	-0.451
odt 3D2'*	11.2	12.0	-1.036	-0.550

Table A44: Calculated selected bond distances of the singly reduced terminally protonated $[(H)Fe_2(\mu\text{-}odt)(CO)_4(PMe_3)_2]^{+}$ isomers and transition states interconverting them.

	bond length/Å													
	Fe ₁ -Fe ₂	Fe ₁ -S ₁	Fe ₁ -S ₂	Fe-H	Fe ₁ -CO ₁	Fe ₁ -CO ₂	Fe ₂ -CO ₃	Fe ₂ -CO ₄	Fe-CO _{semi}	Fe ₁ -P ₁	Fe ₂ -P ₂			
odt 3A1*	2.6797	2.3408	2.3787	1.5127	1.7464	1.8368	1.8064	1.7618	2.1806	2.3024	2.2763			
odt 3A1*	2.6789	2.3397	2.3862	1.5068	1.7431	1.8307	1.7894	1.7659	2.2084	2.3097	2.2784			
odt 3A2*	2.6877	2.3768	2.3490	1.5024	1.7417	1.8277	1.7866	1.7606	2.2364	2.3099	2.2760			
odt 3A2*	2.6895	2.3720	2.3505	1.5083	1.7447	1.8292	1.8031	1.7577	2.2211	2.3070	2.2714			
odt 3A3*	2.8657	2.3321	2.3386	1.5236	1.7666	1.7643	1.7445	1.8076	2.7357	2.3411	2.2321			
odt 3A3*	2.8497	2.3348	2.3428	1.5338	1.7627	1.7613	1.7470	1.8079	2.7102	2.3319	2.2388			
odt 3A4*	2.8240	2.3451	2.3418	1.4997	1.7649	1.7632	1.7811	1.7878	2.6888	2.3382	2.2338			
odt 3A4*	2.7966	2.3445	2.3504	1.5031	1.7616	1.7609	1.7699	1.7915	2.6572	2.3304	2.2374			
odt 3B*	2.7392	2.3815	2.3718	1.5008	1.7463	1.8019	1.7652	1.7689	2.4162	2.2961	2.3552			
odt 3B*	2.7184	2.3797	2.3648	1.5080	1.7492	1.8102	1.7623	1.7668	2.3425	2.2913	2.3427			
odt 3C1*	2.9780	2.3340	2.3639	1.5320	1.7497	1.7997	1.7995	1.7653	2.8902	2.2388	2.2520			
odt 3C1*	2.9882	2.3680	2.3295	1.5220	1.7467	1.8013	1.7884	1.7692	2.9123	2.2343	2.2581			
odt 3C2*	2.9611	2.3644	2.3403	1.5064	1.7678	1.7875	1.8008	1.7627	2.8695	2.2383	2.2485			
odt 3C2*	2.9808	2.3761	2.3425	1.5031	1.7806	1.7839	1.7886	1.7666	2.8857	2.2345	2.2556			
odt 3D1*	2.8928	2.3556	2.3431	1.5327	1.7485	1.8018	1.8049	1.7597	2.7698	2.2384	2.2644			
odt 3D1*	2.9181	2.3571	2.3421	1.5232	1.7463	1.8027	1.7934	1.7638	2.8077	2.2330	2.2690			
odt 3D2*	2.8402	2.3618	2.3537	1.5066	1.7734	1.7868	1.8016	1.7623	2.6938	2.2359	2.2599			
odt 3D2*	2.8474	2.3641	2.3528	1.5045	1.7855	1.7849	1.7896	1.7649	2.6899	2.2318	2.2668			

Table A45: Calculated selected bond angles of the singly reduced terminally protonated $[(H)Fe_2(\mu-odt)(CO)_4(PMe_3)_2]^+$ isomers and transition states inter-converting them.

	bond angle/°									
	$\angle S_1-Fe_1-S_2$	$\angle S_1-Fe_2-S_2$	$\angle Fe_1-S_1-Fe_2$	$\angle Fe_1-S_2-Fe_2$	$\angle L-Fe_1-Fe_2-L$	$\angle Fe-Fe-C_{semi}$	$\angle Fe-C-O_{semi}$			
odt 3A1*	86.2547	86.1826	69.6373	68.7016	26.3720	53.9035	149.1798			
odt 3A1**	86.6808	86.6391	69.4968	68.5926	17.7728	54.8238	150.4272			
odt 3A2*	86.6654	86.7046	69.3389	69.3311	20.4769	55.5157	151.3986			
odt 3A2**	86.2514	86.3200	69.5527	69.3570	27.7705	54.9809	150.6211			
odt 3A3*	84.2564	83.2174	75.5327	74.9529	2.3196	67.3146	167.0375			
odt 3A3**	85.4267	84.5762	74.9640	74.4564	1.3890	66.8917	166.9411			
odt 3A4*	85.5151	84.3260	73.9660	73.2577	21.9560	67.0227	165.6446			
odt 3A4**	86.0769	85.0968	72.9957	72.4561	15.3322	66.6621	165.2526			
odt 3B*	85.1982	85.9332	70.4724	70.8391	23.8016	60.1593	158.4909			
odt 3B**	85.5721	85.9986	69.9841	70.1607	26.1225	58.2476	155.9676			
odt 3C1*	83.6281	84.3106	79.9783	78.0292	7.8208	69.4986	169.1906			
odt 3C1**	82.9978	83.9633	78.5016	80.4324	5.8642	69.9402	169.5447			
odt 3C2*	84.0430	84.5148	77.3416	79.1309	11.8561	69.3741	167.3326			
odt 3C2**	83.5076	84.5641	77.9916	79.6917	12.8483	69.4069	167.5881			
odt 3D1*	84.1495	85.0623	76.3405	76.4406	0.6433	67.7763	167.3552			
odt 3D1**	83.4189	84.4773	77.1082	77.3716	1.5412	68.3472	167.8184			
odt 3D2*	84.9273	85.8179	74.5540	74.3126	23.3051	66.7738	164.8599			
odt 3D2**	84.8449	85.8771	74.6983	74.6749	22.2150	66.4711	164.8245			

[Fe₂(μ-mpdt)(CO)₄(PMe₃)₂] systems

Table A46: Calculated gas phase and solvent corrected free energies, Fe–Fe bond lengths, and Fe Mulliken charges of the isomers of [Fe₂(μ-mpdt)(CO)₄(PMe₃)₂]. Energies are reported relative to the 1A isomer.

Isomer	Free Energies / kcal/mol		Mulliken charges	
	ΔG_g	ΔG_{solv}	Fe _a	Fe _b
mpdt 1A1	0.0	0.9	-0.652	-0.321
mpdt 1A2	7.6	7.6	-0.710	-0.352
mpdt 1A1'	0.04	1.6	-0.715	-0.169
mpdt 1A2'	7.9	7.4	-0.673	-0.265
mpdt 1B1	2.7	8.8	-0.401	-0.501
mpdt 1B2	12.1	3.2	-0.439	-0.680
mpdt 1C1	4.0	3.2	-0.439	-0.331
mpdt 1C2	9.3	9.3	-0.350	-1.029
mpdt 1D1	-0.9	-0.9	-0.443	-0.507
mpdt 1D2	4.0	4.0	-0.629	-0.765
TS _{mpdt 1A1→1B1}	9.9	8.0	-0.474	-0.682
TS _{mpdt 1A1'→1B1}	12.2	11.1	-0.453	-0.679
TS _{mpdt 1A1→1C1}	10.6	9.5	-0.934	-0.520
TS _{mpdt 1A1'→1C1}	^u	^u	^u	^u
TS _{mpdt 1A1→1D1}	7.2	7.4	-0.742	-0.525
TS _{mpdt 1A1'→1D1}	^u	^u	^u	^u
TS _{mpdt 1C1→1D1}	19.6	19.5	-0.990	-0.084
TS _{mpdt 1C1→1D1^{flipped}}	22.4	22.3	-1.111	-0.115
TS _{mpdt 1A1→1A2'}	11.8	12.5	-0.579	-0.198
TS _{mpdt 1A2→1A1'}	11.3	11.2	-0.671	-0.151

^u transition state not found

Table A47: Selected bond distances of the unprotonated [$\text{Fe}_2(\mu\text{-mpdt})(\text{CO})_4(\text{PMe}_3)_2$] from x-ray crystallography (in bold)(unpublished), compared to calculated values of all isomers and transition states inter-converting them.

Exp.	bond length/Å										
	$\text{Fe}_1\text{-Fe}_2$	$\text{Fe}_1\text{-S}_1$	$\text{Fe}_1\text{-S}_2$	$\text{Fe}_2\text{-S}_1$	$\text{Fe}_2\text{-S}_2$	$\text{Fe}_1\text{-CO}_1$	$\text{Fe}_1\text{-CO}_2$	$\text{Fe}_2\text{-CO}_1$	$\text{Fe}_2\text{-CO}_2$	$\text{Fe}_1\text{-P}_1$	$\text{Fe}_2\text{-P}_2$
mpdt 1A1	2.585(3)	2.248(3)	2.253(3)	2.253(3)	2.248(3)	1.771(12)	1.757(11)	1.771(12)	1.757(11)	2.229(3)	2.229(3)
mpdt 1A1'	2.5258	2.3057	2.3033	2.3038	2.2945	1.7563	1.7492	1.7550	1.7597	2.2363	2.2594
mpdt 1A2	2.5264	2.3171	2.3063	2.2913	2.2882	1.7552	1.7464	1.7526	1.7624	2.2377	2.2626
mpdt 1A2'	2.5170	2.3137	2.3118	2.3205	2.2886	1.7552	1.7481	1.7551	1.7607	2.2408	2.2589
mpdt 1B1	2.5229	2.3226	2.3217	2.3021	2.3036	1.7511	1.7476	1.7511	1.7632	2.2501	2.2594
mpdt 1B2	2.4892	2.3168	2.3117	2.3214	2.3266	1.7589	1.7562	1.7545	1.7556	2.2381	2.2405
mpdt 1C1	2.4862	2.3298	2.3210	2.3236	2.3456	1.7604	1.7557	1.7512	1.7563	2.2411	2.2568
mpdt 1C2	2.6001	2.2889	2.2848	2.2777	2.2803	1.7508	1.7658	1.7533	1.7616	2.2650	2.2599
mpdt 1D1	2.5782	2.2890	2.3123	2.2890	2.3170	1.7498	1.7662	1.7460	1.7486	2.2580	2.2395
mpdt 1D2	2.5660	2.2837	2.2843	2.2925	2.2925	1.7501	1.7581	1.7514	1.7503	2.2692	2.2492
	2.5392	2.2974	2.3037	2.2978	2.3198	1.7501	1.7604	1.7475	1.7424	2.2815	2.2384
TS _{mpdt 1A1} →1B1	2.5486	2.3117	2.3222	2.3328	2.3428	1.7628	1.7640	1.7447	1.7421	2.2403	2.2151
TS _{mpdt 1A1'} →1B1	2.5450	2.3180	2.3257	2.3258	2.3401	1.7615	1.7608	1.7451	1.7422	2.2426	2.2143
TS _{mpdt 1A1} →1C1	2.5736	2.3077	2.3333	2.2940	2.3145	1.7428	1.7382	1.7506	1.7675	2.2149	2.2704
TS _{mpdt 1A1'} →1C1	"	"	"	"	"	"	"	"	"	"	"
TS _{mpdt 1A1} →1D1	2.5580	2.3317	2.3104	2.3075	2.3082	1.7426	1.7376	1.7509	1.7648	2.2138	2.2718
TS _{mpdt 1A1'} →1D1	"	"	"	"	"	"	"	"	"	"	"
TS _{mpdt 1A1'} →1D1	2.6849	2.2667	2.2774	2.3356	2.3305	1.7484	1.7617	1.7435	1.7436	2.2830	2.2320
TS _{mpdt 1C1} →1D1	2.6763	2.2781	2.2783	2.3316	2.3284	1.7503	1.7549	1.7417	1.7429	2.2707	2.2407
TS _{mpdt 1C1} →1D1 ^{flipped}	2.5401	2.2985	2.2828	2.2775	2.2772	1.7582	1.7479	1.7528	1.7617	2.2318	2.2623
TS _{mpdt 1A1} →1A2'	2.5421	2.2906	2.2866	2.2762	2.2753	1.7574	1.7500	1.7529	1.7622	2.2318	2.2608

" transition state not found

Table A48: Selected bond angles of the unprotonated $[Fe_2(\mu\text{-mpdt})(CO)_4(PMe_3)_2]$ from x-ray crystallography (in bold)(unpublished), compared to calculated values of all isomers and transition states inter-converting them.

Exp.	bond angle/°					
	$\angle S_1-Fe_1-S_2$	$\angle S_1-Fe_2-S_2$	$\angle Fe_1-S_1-Fe_2$	$\angle Fe_1-S_2-Fe_2$	$\angle L_{ap}-Fe_1-Fe_2-L_{ap}$	
mpdt 1A1	84.64(11)	84.64(11)	70.10(9)	70.10(9)	5.89	
mpdt 1A1'	84.7353	84.9785	66.4522	66.6431	22.1634	
mpdt 1A2	84.6481	85.6540	66.4865	66.7152	36.0954	
mpdt 1A2'	83.5814	83.9423	65.7956	66.3381	22.9723	
mpdt 1B1	83.5730	84.4329	66.1213	66.1127	55.5778	
mpdt 1B2	85.0572	84.6170	64.9144	64.9113	14.5538	
mpdt 1C1	83.9281	83.5212	64.5890	64.3808	60.5381	
mpdt 1C2	84.9460	85.3092	69.4118	69.4385	3.6193	
mpdt 1D1	84.9703	84.8615	68.5505	67.6866	64.4646	
mpdt 1D2	86.0140	85.4892	68.2116	68.1067	48.1809	
	84.9177	84.5424	67.0882	66.6235	71.8414	
TS _{mpdt 1A1→1B1}	85.7806	84.8369	66.5579	66.2277	104.0438	
TS _{mpdt 1A1'→1B1}	85.0618	84.5626	66.4641	66.1109	98.5825	
TS _{mpdt 1A1→1C1}	84.7311	85.4701	68.0082	67.2434	104.0112	
TS _{mpdt 1A1'→1C1}	"	"	"	"	"	
TS _{mpdt 1A1→1D1}	84.5215	85.1205	66.9226	67.2641	92.9568	
TS _{mpdt 1A1'→1D1}	"	"	"	"	"	
TS _{mpdt 1C1→1D1}	87.4305	84.5991	71.3593	71.2667	71.4847	
TS _{mpdt 1C1→1D1^{flipped}}	86.8228	84.4339	70.9738	71.0284	59.9815	
TS _{mpdt 1A1→1A2'}	83.5913	84.1924	67.4316	67.7021	15.4546	
TS _{mpdt 1A2→1A1'}	83.7439	84.3265	67.6463	67.7284	18.7610	

" transition state not found

Table A49: Calculated gas phase and solvent corrected free energies and Fe Mulliken charges for isomers of $[(\mu\text{-H})\text{Fe}_2(\mu\text{-mpdt})(\text{CO})_4(\text{PMe}_3)_2]^+$ and the transition states that connect them; either through rotation of the $\text{Fe}(\text{CO})_2(\text{PMe}_3)$ moiety or by the mpdt bridge flip. Energies are reported relative to the **2A1** isomer

ΔG_g	Free Energies / kcal/mol		Mulliken charges	
	ΔG_{solv}	Fe ₁	Fe ₂	
mpdt 2A1	0.0	0.0	-1.258	-0.123
mpdt 2A1'	7.1	6.0	-1.090	-0.099
mpdt 2A2	-0.5	-0.4	-1.281	-0.155
mpdt 2A2'	8.7	8.6	-1.172	-0.094
mpdt 2B1	5.5	4.6	-0.771	-0.603
mpdt 2B2	15.1	13.4	-0.682	-0.936
mpdt 2C1	-0.8	-1.0	-0.780	-0.503
mpdt 2C2	7.4	6.6	-0.756	-0.413
mpdt 2D1	-5.2	-5.6	-0.706	-0.609
mpdt 2D2	2.5	1.5	-0.680	-0.643

Table A50: Calculated selected bond distances of the bridged protonated $[(\mu-H)Fe_2(\mu-mpdt)(CO)_4(PMe_3)_2]^+$ isomers and transition states inter-converting them.

	bond length/Å													
	Fe ₁ -Fe ₂	Fe ₁ -S ₁	Fe ₁ -S ₂	Fe ₂ -S ₁	Fe ₂ -S ₂	Fe ₁ -H	Fe ₂ -H	Fe ₁ -CO ₁	Fe ₁ -CO ₂	Fe ₂ -CO ₁	Fe ₂ -CO ₂	Fe ₁ -P ₁	Fe ₂ -P ₂	
mpdt 2A1	2.5888	2.3097	2.3232	2.3228	2.3094	1.6561	1.6610	1.7776	1.7763	1.7649	1.7776	2.2763	2.2956	
mpdt 2A1'	2.5883	2.3169	2.3335	2.3433	2.2915	1.6449	1.6607	1.7760	1.7743	1.7635	1.7803	2.2835	2.2971	
mpdt 2A2	2.5882	2.3239	2.3203	2.3076	2.3060	1.6712	1.6539	1.7786	1.7731	1.7628	1.7780	2.2733	2.2938	
mpdt 2A2'	2.5882	2.3274	2.3346	2.3153	2.3141	1.6772	1.6357	1.7784	1.7736	1.7642	1.7771	2.2863	2.2923	
mpdt 2B1	2.5795	2.3305	2.3169	2.3274	2.3313	1.6442	1.6553	1.7807	1.7774	1.7774	1.7782	2.2799	2.2771	
mpdt 2B2	2.5831	2.3357	2.3241	2.3280	2.3405	1.6276	1.6594	1.7799	1.7764	1.7773	1.7788	2.2900	2.2921	
mpdt 2C1	2.6107	2.2986	2.3034	2.2996	2.3041	1.6784	1.7017	1.7600	1.7804	1.7617	1.7799	2.2949	2.2999	
mpdt 2C2	2.6025	2.3038	2.3077	2.2855	2.3269	1.6674	1.7015	1.7610	1.7803	1.7630	1.7769	2.2924	2.3060	
mpdt 2D1	2.6058	2.3005	2.2986	2.3059	2.3042	1.6772	1.6956	1.7606	1.7748	1.7629	1.7741	2.2971	2.2949	
mpdt 2D2	2.6054	2.3060	2.3039	2.3026	2.3065	1.6640	1.6994	1.7610	1.7735	1.7615	1.7736	2.2965	2.3005	

Table A51: Calculated selected bond angles of the bridged protonated $[(\mu-H)Fe_2(\mp\text{-mpdt})(CO)_4(PMe_3)_2]^+$ isomers and transition states inter-converting them.

	bond angle/ °				
	$\angle S_1-Fe_1-S_2$	$\angle S_1-Fe_2-S_2$	$\angle Fe_1-S_1-Fe_2$	$\angle Fe_1-S_2-Fe_2$	$\angle L-Fe_1-Fe_2-L$
mpdt 2A1	83.9534	83.9691	67.9523	67.9502	14.5161
mpdt 2A1'	82.8580	83.1920	67.4748	68.0526	22.6500
mpdt 2A2	84.1200	84.8071	67.9479	68.0351	6.6462
mpdt 2A2'	82.6335	83.3446	67.7627	67.6620	10.4198
mpdt 2B1	83.8590	83.6090	67.2547	67.4120	8.6149
mpdt 2B2	82.4881	82.2992	67.2655	67.2506	8.6879
mpdt 2C1	84.9650	84.9265	69.1903	69.0292	1.7306
mpdt 2C2	83.8041	83.7801	69.0935	68.3235	6.7305
mpdt 2D1	85.3997	85.1474	68.9008	68.9610	0.0709
mpdt 2D2	84.1165	84.1379	68.8517	68.8213	2.0895

Table A52: Calculated gas phase and solvent corrected free energies, Fe–Fe bond lengths, and Fe Mulliken charges of the isomers of $[HFe_2(\mu\text{-mpdt})(CO)_4(PMe_3)_2]^+$. Energies are reported relative to the 2A1 isomer.

Isomer	Free Energies / kcal/mol		Mulliken charges	
	ΔG_g	ΔG_{solv}	Fe ₁	Fe ₂
mpdt 3A1	15.9	14.8	-1.236	-0.416
mpdt 3A12	24.7	22.8	-1.130	-0.632
mpdt 3A1'	14.6	14.2	-1.103	-0.516
mpdt 3A12'	23.3	21.4	-1.091	-0.535
mpdt 3A2	16.0	14.9	-1.216	-0.559
mpdt 3A22	23.8	21.3	-1.169	-0.614
mpdt 3A2'	14.8	14.6	-1.126	-0.688
mpdt 3A22'	22.2	20.6	-1.056	-0.723
mpdt 3A3	12.0	11.1	-0.622	-1.120
mpdt 3A32	18.4	16.9	-0.697	-0.907
mpdt 3A3'	12.2	11.8	-0.524	-1.231
mpdt 3A32'	20.8	19.7	-0.534	-1.177
mpdt 3A4	15.7	15.0	-0.647	-0.872
mpdt 3A42	22.6	21.1	-0.660	-1.211
mpdt 3A4'	15.0	15.3	-0.497	-0.982
mpdt 3A42'	24.0	22.8	-0.533	-1.007
mpdt 3B	21.0	19.7	-0.638	-1.161
mpdt 3B'	20.1	18.5	-0.464	-1.178
mpdt 3B2	30.1	27.3	-0.702	-1.193
mpdt 3B2'	31.7	29.3	-0.566	-1.119
mpdt 3C1	11.6	10.2	-1.395	-0.517
mpdt 3C12	19.1	17.3	-1.370	-0.547
mpdt 3C1'	10.8	9.3	-1.306	-0.480
mpdt 3C12'	16.3	14.0	-0.988	-0.519
mpdt 3C2	15.9	15.5	-0.723	-0.540
mpdt 3C22	23.5	22.3	-0.741	-0.455
mpdt 3C2'	15.7	15.4	-0.442	-0.693
mpdt 3C22'	21.6	20.9	-0.742	-0.794
mpdt 3D1	8.1	8.3	-1.390	-0.500
mpdt 3D12	14.8	13.7	-1.415	-0.501
mpdt 3D1'	7.1	7.3	-1.253	-0.463
mpdt 3D12'	13.0	12.5	-0.906	-0.579
mpdt 3D2	11.3	11.6	-1.125	-0.625
mpdt 3D22	18.5	18.3	-1.175	-0.678
mpdt 3D2'	10.6	10.9	-1.130	-0.678
mpdt 3D22'	17.1	16.7	-1.344	-0.680

Table A53: Selected bond distances of the terminally protonated $[(H)Fe_2(\mu\text{-mpdt})(CO)_4(PMe_3)_2]^+$ isomers **3** calculated using DFT.

	bond length/Å													
	Fe ₁ -Fe ₂	Fe ₁ -S ₁	Fe ₁ -S ₂	Fe ₂ -S ₁	Fe ₂ -S ₂	Fe-H	Fe ₁ -CO ₁	Fe ₁ -CO ₂	Fe ₂ -CO ₃	Fe ₂ -CO ₄	Fe-CO _{semi}	Fe ₁ -P ₁	Fe ₂ -P ₂	
mpdt 3A1	2.5368	2.3258	2.3207	2.3058	2.3084	1.5051	1.7736	1.7924	1.7577	1.7850	2.3062	2.2644	2.3314	
mpdt 3A12	2.5287	2.3325	2.3293	2.2888	2.3361	1.5017	1.7749	1.7887	1.7592	1.7814	2.3235	2.2690	2.3312	
mpdt 3A1'	2.5265	2.3201	2.3238	2.3228	2.3057	1.5022	1.7697	1.8146	1.7595	1.7876	2.2127	2.2609	2.3256	
mpdt 3A12'	2.5297	2.3313	2.3153	2.3361	2.3247	1.4993	1.7696	1.8323	1.7659	1.7855	2.1301	2.2698	2.3165	
mpdt 3A2	2.5543	2.3170	2.3292	2.3066	2.3016	1.5022	1.7703	1.7905	1.7542	1.7868	2.3454	2.2704	2.3150	
mpdt 3A22	2.5535	2.3239	2.3406	2.3229	2.2859	1.5015	1.7697	1.7845	1.7534	1.7892	2.3604	2.2722	2.3208	
mpdt 3A2'	2.5392	2.3208	2.3297	2.3033	2.3145	1.4978	1.7673	1.8101	1.7555	1.7865	2.2475	2.2668	2.3120	
mpdt 3A22'	2.5344	2.3130	2.3356	2.3229	2.3315	1.4960	1.7670	1.8283	1.7633	1.7846	2.1492	2.2719	2.3117	
mpdt 3A3	2.5634	2.2992	2.2929	2.3153	2.3217	1.5135	1.7882	1.7822	1.7680	1.8023	2.4473	2.2601	2.2726	
mpdt 3A32	2.5503	2.3095	2.3011	2.3023	2.3202	1.5022	1.7886	1.7815	1.7667	1.8056	2.4049	2.2652	2.2745	
mpdt 3A3'	2.5748	2.2887	2.3012	2.3152	2.3163	1.5154	1.7837	1.7818	1.7708	1.8006	2.5306	2.2568	2.2741	
mpdt 3A32'	2.5822	2.2924	2.3040	2.3286	2.3264	1.5141	1.7820	1.7803	1.7692	1.7966	2.5866	2.2668	2.2732	
mpdt 3A4	2.5582	2.3074	2.2966	2.3142	2.3350	1.5008	1.7885	1.7785	1.7746	1.7808	2.4609	2.2605	2.2798	
mpdt 3A42	2.5454	2.3161	2.3107	2.2936	2.3518	1.4985	1.7890	1.7789	1.7708	1.7849	2.3801	2.2695	2.2805	
mpdt 3A4'	2.5687	2.2941	2.2981	2.3218	2.3235	1.5039	1.7836	1.7776	1.7754	1.7777	2.5743	2.2557	2.2817	
mpdt 3A42'	2.5776	2.2986	2.2998	2.3336	2.3366	1.5032	1.7828	1.7748	1.7749	1.7731	2.6226	2.2665	2.2802	

Table A54: Selected bond distances of the terminally protonated $[(H)Fe_2(\mu\text{-mpdt})(CO)_4(PMe_3)_2]^{+}$ isomers **3B**, **3C** and **3D** calculated using DFT.

	bond length/Å													
	Fe ₁ -Fe ₂	Fe ₁ -S ₁	Fe ₁ -S ₂	Fe ₂ -S ₁	Fe ₂ -S ₂	Fe-H	Fe ₁ -CO ₁	Fe ₁ -CO ₂	Fe ₂ -CO ₃	Fe ₂ -CO ₄	Fe-CO _{semi}	Fe ₁ -P ₁	Fe ₂ -P ₂	
mpdt 3B	2.5365	2.3143	2.3275	2.3376	2.3362	1.4974	1.7834	1.7876	1.7720	1.7978	2.3120	2.2761	2.2718	
mpdt 3B'	2.5484	2.3118	2.3223	2.3384	2.3281	1.5017	1.7822	1.7842	1.7753	1.7860	2.4044	2.2718	2.2756	
mpdt 3B2	2.5378	2.3320	2.3438	2.3502	2.3166	1.4945	1.7841	1.7889	1.7730	1.8121	2.1914	2.2994	2.2778	
mpdt 3B2'	2.5541	2.3016	2.3311	2.3494	2.3381	1.5005	1.7786	1.7842	1.7763	1.7767	2.4817	2.2773	2.2851	
mpdt 3C1	2.5840	2.3120	2.2958	2.2921	2.2705	1.5135	1.7739	1.8005	1.7486	1.7875	2.5281	2.2738	2.3231	
mpdt 3C12	2.5735	2.3215	2.3015	2.3167	2.2586	1.5157	1.7745	1.7986	1.7517	1.7824	2.5222	2.2715	2.3225	
mpdt 3C1'	2.5608	2.3232	2.2956	2.2901	2.2805	1.5153	1.7726	1.8081	1.7505	1.7894	2.3899	2.2733	2.3240	
mpdt 3C12'	2.5394	2.3253	2.2840	2.3057	2.2963	1.5041	1.7714	1.8172	1.7538	1.7887	2.3064	2.2752	2.3223	
mpdt 3C2	2.6137	2.3140	2.3111	2.2818	2.2776	1.5050	1.7757	1.7775	1.7453	1.7885	2.6123	2.2786	2.3192	
mpdt 3C22	2.6196	2.3192	2.3190	2.2831	2.2613	1.5051	1.7763	1.7744	1.7433	1.7875	2.6514	2.2767	2.3258	
mpdt 3C2'	2.5833	2.3206	2.3010	2.2969	2.2854	1.5026	1.7740	1.7863	1.7459	1.7901	2.4378	2.2775	2.3227	
mpdt 3C22'	2.5611	2.3372	2.2834	2.3145	2.2967	1.5005	1.7683	1.7956	1.7505	1.7902	2.3319	2.2778	2.3246	
mpdt 3D1	2.5709	2.3044	2.3062	2.2724	2.2927	1.5139	1.7703	1.7983	1.7486	1.7861	2.4893	2.2763	2.3164	
mpdt 3D12	2.5698	2.3156	2.3107	2.2669	2.2962	1.5143	1.7694	1.7931	1.7472	1.7863	2.5072	2.2732	2.3263	
mpdt 3D1'	2.5553	2.3025	2.3071	2.2819	2.2919	1.5116	1.7683	1.8060	1.7493	1.7864	2.3882	2.2741	2.3165	
mpdt 3D12'	2.5354	2.2975	2.3063	2.2969	2.3064	1.5003	1.7664	1.8132	1.7526	1.7852	2.3101	2.2762	2.3154	
mpdt 3D2	2.5590	2.3168	2.3109	2.2788	2.2912	1.5066	1.7770	1.7737	1.7491	1.7820	2.5019	2.2795	2.3278	
mpdt 3D22	2.5635	2.3245	2.3183	2.2816	2.2854	1.5060	1.7762	1.7686	1.7477	1.7800	2.5460	2.2799	2.3298	
mpdt 3D2'	2.5366	2.3074	2.3171	2.2844	2.3029	1.5037	1.7732	1.7867	1.7512	1.7847	2.3582	2.2823	2.3264	
mpdt 3D22'	2.5234	2.2921	2.3323	2.2996	2.3197	1.5018	1.7665	1.7969	1.7553	1.7834	2.2689	2.2831	2.3211	

Table A55: Selected bond angles of the terminally protonated $[HFe_2(\mu\text{-mpdt})(CO)_4(PMe_3)_2]^+$ isomers, **3A** calculated using DFT.

	bond angle/°									
	$\angle S_1\text{-Fe}_1\text{-S}_2$	$\angle S_1\text{-Fe}_2\text{-S}_2$	$\angle Fe_1\text{-S}_1\text{-Fe}_2$	$\angle Fe_1\text{-S}_2\text{-Fe}_2$	$\angle L\text{-Fe}_1\text{-Fe}_2\text{-L}$	$\angle Fe\text{-Fe-C}_{semi}$	$\angle Fe\text{-C-O}_{semi}$			
mpdt 3A1	84.8130	85.5479	66.4201	66.4618	35.0123	61.5705	157.4300			
mpdt 3A12	83.6609	84.4734	66.3416	65.6429	40.8019	62.3699	158.3199			
mpdt 3A1'	85.5217	85.8726	65.9344	66.1486	32.0280	58.5794	153.0990			
mpdt 3A12'	84.8277	84.5109	65.6374	66.0754	59.1707	55.7367	148.6190			
mpdt 3A2	84.8158	85.6813	67.0696	66.9508	33.8644	62.4576	159.1114			
mpdt 3A22	83.5201	84.7589	66.6687	66.9880	41.1556	63.0274	159.6856			
mpdt 3A2'	85.5591	86.3123	66.6119	66.2851	35.0100	59.4498	154.8444			
mpdt 3A22'	84.8755	84.7453	66.2818	65.7803	62.3053	56.2629	149.6687			
mpdt 3A3	85.4174	84.3955	67.4909	67.4864	3.1086	65.5114	162.8266			
mpdt 3A32	84.2337	83.9654	67.1439	66.9866	3.1117	64.3914	161.3886			
mpdt 3A3'	85.9053	84.9508	68.0095	67.7816	2.3128	68.0377	165.6460			
mpdt 3A32'	84.7208	83.4112	67.9409	67.7887	3.5842	69.7907	166.7801			
mpdt 3A4	85.6653	84.6355	67.2209	67.0506	32.5282	66.3186	163.6976			
mpdt 3A42	84.4267	84.0014	67.0315	66.1685	43.2091	63.8847	161.0847			
mpdt 3A4'	86.4388	85.2139	67.6234	67.5310	17.6470	69.9462	166.9091			
mpdt 3A42'	85.1941	83.5857	67.6177	67.5464	23.1310	71.4384	167.8420			

Table A56: Selected bond angles of the terminally protonated $[HFe_2(\mu\text{-mpdt})(CO)_4(PMe_3)_2]^+$ isomers, **3B**, **3C** and **3D** calculated using DFT.

	bond angle/°									
	$\angle S_1\text{-Fe}_1\text{-S}_2$	$\angle S_1\text{-Fe}_2\text{-S}_2$	$\angle Fe_1\text{-S}_1\text{-Fe}_2$	$\angle Fe_1\text{-S}_2\text{-Fe}_2$	$\angle L\text{-Fe}_1\text{-Fe}_2\text{-L}$	$\angle Fe\text{-Fe-C}_{semi}$	$\angle Fe\text{-C-O}_{semi}$			
mpdt 3B1	85.1597	84.4426	66.0824	65.8961	39.1960	61.7249	158.0846			
mpdt 3B1'	85.1704	84.4398	66.4607	66.4596	34.8447	64.6095	161.7118			
mpdt 3B12	83.6398	83.8346	65.6388	65.9848	69.5950	57.6471	152.5887			
mpdt 3B12'	83.9302	82.7324	66.6104	66.3255	42.3475	67.1699	164.1865			
mpdt 3C1	85.4821	86.5361	68.2838	68.9262	4.8824	67.7211	165.0205			
mpdt 3C12	84.3665	85.4431	67.4005	68.7086	13.9627	67.8106	165.2196			
mpdt 3C1'	85.2286	86.3490	67.4302	68.0559	0.2434	63.6145	160.8109			
mpdt 3C12'	84.8037	84.9741	66.5050	67.3403	0.8797	61.3067	157.5058			
mpdt 3C2	85.5342	87.0685	69.3167	69.4395	16.1930	70.0748	166.3298			
mpdt 3C22	84.1388	86.2914	69.3840	69.7570	10.4900	71.2998	166.8628			
mpdt 3C2'	85.7954	86.7133	68.0334	68.5599	28.4562	64.8549	161.4677			
mpdt 3C22'	85.1339	85.3544	66.8112	67.9992	42.4555	61.8033	157.7142			
mpdt 3D1	85.2014	86.2557	68.3457	67.9770	0.3669	66.7726	164.5092			
mpdt 3D12	83.8219	85.2516	68.2080	67.8070	1.4773	67.4586	164.8776			
mpdt 3D1'	85.4080	86.2376	67.7491	67.5042	0.2016	63.7137	160.7779			
mpdt 3D12'	84.9285	84.9399	66.9879	66.6886	1.5367	61.5551	157.5944			
mpdt 3D2	85.3257	86.6660	67.6700	67.5659	24.8279	67.7653	164.8271			
mpdt 3D22	83.9688	85.6917	67.6289	67.6721	28.9512	69.2180	165.7726			
mpdt 3D2'	85.6993	86.5625	67.0649	66.6035	29.2342	63.3513	160.2077			
mpdt 3D22'	84.9686	85.0893	66.6723	65.6978	42.1263	60.6243	156.6207			

[Fe₂(μ-dmdt)(CO)₄(PMe₃)₂] systems

Table A57: Calculated gas phase and solvent corrected free energies, Fe–Fe bond lengths, and Fe Mulliken charges of the isomers of [Fe₂(μ-dmpdt)(CO)₄(PMe₃)₂]. Energies are reported relative to the **1A** isomer.

Isomer	Free Energies / kcal/mol		bond length / Å	Mulliken charges	
	ΔG_g	ΔG_{solv}		Fe–Fe	Fe _a
dmpdt 1A	0.0	0.0	2.515	-0.741	-0.325
dmpdt 1A'	-0.6	-0.4	2.525	-0.583	-0.324
dmpdt 1B	3.8	3.2	2.486	-0.423	-0.538
dmpdt 1C	1.2	1.2	2.579	-0.469	-0.959
dmpdt 1D	-3.8	-3.1	2.551	-0.658	-0.726

Table A58: Selected bond distances of the unprotonated $[\text{Fe}_2(\mu\text{-dmpdt})(\text{CO})_4(\text{PMe}_3)_2]$ from x-ray crystallography (in bold)(unpublished), compared to DFT calculated values for all isomers.

	bond length/Å											
	Fe₁-Fe₂	Fe₁-S₁	Fe₁-S₂	Fe₂-S₁	Fe₂-S₂	Fe₁-CO₁	Fe₁-CO₂	Fe₂-CO₁	Fe₂-CO₂	Fe₁-P₁	Fe₂-P₂	
Exp.	2.569	2.250	2.253	2.248	2.259	1.757	1.758	1.763	1.741	2.234	2.210	
dmpdt 1A	2.5147	2.3177	2.3113	2.3228	2.2898	1.7555	1.7476	1.7561	1.7601	2.2415	2.2594	
dmpdt 1A'	2.5245	2.3219	2.3214	2.3015	2.2999	1.7501	1.7480	1.7506	1.7637	2.2509	2.2603	
dmpdt 1B	2.4863	2.3286	2.3191	2.3221	2.3448	1.7605	1.7557	1.7513	1.7565	2.2407	2.2584	
dmpdt 1C	2.5792	2.2865	2.3085	2.2879	2.3174	1.7495	1.7668	1.7460	1.7477	2.2589	2.2382	
dmpdt 1D	2.5410	2.2975	2.3082	2.2957	2.3240	1.7507	1.7619	1.7460	1.7391	2.2903	2.2351	

Table A59: Selected bond angles of the unprotonated $[\text{Fe}_2(\mu\text{-dmpdt})(\text{CO})_4(\text{PMe}_3)_2]$ from x-ray crystallography (in bold)(unpublished), compared to DFT calculated values for all isomers.

	bond angle/ °			
	$\angle \text{S}_1\text{-Fe}_1\text{-S}_2$	$\angle \text{S}_1\text{-Fe}_2\text{-S}_2$	$\angle \text{Fe}_1\text{-S}_1\text{-Fe}_2$	$\angle \text{Fe}_1\text{-S}_2\text{-Fe}_2$
Exp.(1D)	83.45	83.37	69.67	69.41
dmpdt 1A	83.3754	83.7360	65.6271	66.2590
dmpdt 1A'	83.4377	84.3717	66.1896	66.2233
dmpdt 1B	83.7104	83.2842	64.6353	64.4275
dmpdt 1C	84.6795	84.4452	68.6422	67.7735
dmpdt 1D	84.5611	84.2434	67.1737	66.5343

Table A60: Calculated gas phase and solvent corrected free energies, Fe–Fe bond lengths, and Fe Mulliken charges of the isomers of $[(\mu\text{-H})\text{Fe}_2(\mu\text{-dmpdt})(\text{CO})_4(\text{PMe}_3)_2]^+$. Energies are reported relative to the **1A** isomer.

Isomer	Free Energies / kcal/mol		Mulliken charges	
	ΔG_g	ΔG_{solv}	Fe ₁	Fe ₂
dmpdt 2A	0.0	0.0	-1.295	-0.132
dmpdt 2A'	0.7	1.7	-0.924	-0.147
dmpdt 2B	7.4	7.0	-0.703	-0.619
dmpdt 2C	-1.2	-1.1	-0.825	-0.414
dmpdt 2D	-5.7	-5.9	-0.773	-0.615

Table A61: Calculated selected bond distances of the bridged protonated $[(\mu-H)Fe_2(\mu-dmpdt)(CO)_4(PMe_3)_2]^+$ isomers.

	bond length/Å												
	Fe ₁ -Fe ₂	Fe ₁ -S ₁	Fe ₁ -S ₂	Fe ₂ -S ₁	Fe ₂ -S ₂	Fe ₁ -H	Fe ₂ -H	Fe ₁ -CO ₁	Fe ₁ -CO ₂	Fe ₂ -CO ₁	Fe ₂ -CO ₂	Fe ₁ -P ₁	Fe ₂ -P ₂
dmpdt 2A	2.5880	2.3166	2.3323	2.3523	2.2886	1.6414	1.6593	1.7763	1.7740	1.7647	1.7804	2.2815	2.2973
dmpdt 2A'	2.5899	2.3301	2.3297	2.3150	2.3116	1.6764	1.6354	1.7789	1.7731	1.7636	1.7770	2.2904	2.2928
dmpdt 2B	2.5815	2.3399	2.3273	2.3369	2.3470	1.6231	1.6568	1.7794	1.7760	1.7772	1.7781	2.2923	2.3033
dmpdt 2C	2.6035	2.3011	2.3093	2.2852	2.3289	1.6677	1.6999	1.7605	1.7799	1.7638	1.7760	2.2902	2.3067
dmpdt 2D	2.6053	2.3066	2.3061	2.3061	2.3022	1.6622	1.7001	1.7609	1.7734	1.7619	1.7740	2.2954	2.3002

Table A62: Calculated selected bond angles of the bridged protonated $[(\mu\text{-H})\text{Fe}_2(\mu\text{-dmpdt})(\text{CO})_4(\text{PMe}_3)_2]^+$ isomers.

	bond angle/ °				
	$\angle \text{S}_1\text{-Fe}_1\text{-S}_2$	$\angle \text{S}_1\text{-Fe}_2\text{-S}_2$	$\angle \text{Fe}_1\text{-S}_1\text{-Fe}_2$	$\angle \text{Fe}_1\text{-S}_2\text{-Fe}_2$	$\angle \text{L-Fe}_1\text{-Fe}_2\text{-L}$
dmpdt 2A	82.5672	82.7291	67.3218	68.1131	24.6349
dmpdt 2A'	82.4543	83.1770	67.7726	67.8333	9.4616
dmpdt 2B	82.2737	81.9160	67.0068	67.0453	8.0037
dmpdt 2C	83.5150	83.4288	69.1731	68.2909	9.5411
dmpdt 2D	83.7705	83.8681	68.7774	68.8502	0.2689

Table A63: Calculated gas phase and solvent corrected free energies, Fe–Fe bond lengths, and Fe Mulliken charges of the isomers of $[\text{HFe}_2(\mu\text{-dmpdt})(\text{CO})_4(\text{PMe}_3)_2]^+$. Energies are reported relative to the 2A isomer.

Isomer	Free Energies / kcal/mol		Mulliken charges	
	ΔG_g	ΔG_{solv}	Fe ₁	Fe ₂
dmpdt 3A1	17.2	25.2	-1.137	-0.638
dmpdt 3A1'	14.2	22.2	-1.031	-0.623
dmpdt 3A2	16.7	24.7	-1.207	-0.630
dmpdt 3A2'	12.9	20.8	-1.011	-0.842
dmpdt 3A3	10.5	18.4	-0.664	-0.940
dmpdt 3A3'	12.8	20.8	-0.347	-1.196
dmpdt 3A4	14.1	22.0	-0.677	-1.087
dmpdt 3A4'	15.7	23.6	-0.307	-1.101
dmpdt 3B1	21.1	29.1	-0.728	-1.141
dmpdt 3B1'	22.2	30.2	-0.340	-1.144
dmpdt 3C1	10.7	18.6	-1.431	-0.562
dmpdt 3C1'	7.7	15.7	-1.024	-0.604
dmpdt 3C2	16.0	24.0	-0.861	-0.444
dmpdt 3C2'	13.2	21.2	-0.709	-0.876
dmpdt 3D1	7.3	7.6	-1.402	-0.491
dmpdt 3D1'	4.1	4.7	-0.942	-0.655
dmpdt 3D2	10.5	10.8	-1.268	-0.630
dmpdt 3D2'	8.8	9.2	-1.185	-0.753

Table A64: Selected bond distances of the terminally protonated $[HFe_2(\mu-dmpdt)(CO)_4(PMe_3)_2]^+$ calculated using DFT.

	bond length/Å													
	Fe ₁ -Fe ₂	Fe ₁ -S ₁	Fe ₁ -S ₂	Fe ₂ -S ₁	Fe ₂ -S ₂	Fe-H	Fe ₁ -CO ₁	Fe ₁ -CO ₂	Fe ₂ -CO ₃	Fe ₂ -CO ₄	Fe-CO _{semi}	Fe ₁ -P ₁	Fe ₂ -P ₂	
dmpdt 3A1	2.5314	2.3315	2.3244	2.2887	2.3364	1.5020	1.7751	1.7878	1.7598	1.7807	2.3264	2.2655	2.3254	
dmpdt 3A1'	2.5305	2.3279	2.3156	2.3321	2.3235	1.5000	1.7694	1.8314	1.7648	1.7852	2.1326	2.2683	2.3181	
dmpdt 3A2	2.5524	2.3200	2.3392	2.3277	2.2831	1.5004	1.7698	1.7854	1.7538	1.7890	2.3468	2.2737	2.3228	
dmpdt 3A2'	2.5349	2.3109	2.3350	2.3215	2.3342	1.4972	1.7671	1.8289	1.7640	1.7844	2.1401	2.2723	2.3119	
dmpdt 3A3	2.5480	2.3132	2.3056	2.2990	2.3244	1.5015	1.7881	1.7813	1.7661	1.8059	2.3801	2.2688	2.2750	
dmpdt 3A3'	2.5843	2.2931	2.3073	2.3279	2.3266	1.5140	1.7815	1.7801	1.7692	1.7959	2.5941	2.2742	2.2730	
dmpdt 3A4	2.5448	2.3136	2.3106	2.2929	2.3595	1.4986	1.7893	1.7792	1.7702	1.7837	2.3716	2.2685	2.2806	
dmpdt 3A4'	2.5796	2.2976	2.2987	2.3346	2.3349	1.5034	1.7828	1.7745	1.7744	1.7722	2.6377	2.2727	2.2807	
dmpdt 3B1	2.5378	2.3308	2.3424	2.3526	2.3156	1.4946	1.7843	1.7887	1.7728	1.8107	2.1904	2.2977	2.2814	
dmpdt 3B1'	2.5499	2.3024	2.3467	2.3543	2.3375	1.4998	1.7766	1.7839	1.7771	1.7761	2.4886	2.2893	2.2845	
dmpdt 3C1	2.5749	2.3233	2.3042	2.3133	2.2585	1.5161	1.7744	1.7967	1.7512	1.7828	2.5238	2.2707	2.3228	
dmpdt 3C1'	2.5383	2.3221	2.2829	2.3051	2.2968	1.5025	1.7711	1.8177	1.7538	1.7885	2.3079	2.2760	2.3241	
dmpdt 3C2	2.6167	2.3208	2.3186	2.2911	2.2614	1.5054	1.7752	1.7721	1.7447	1.7868	2.6388	2.2788	2.3243	
dmpdt 3C2'	2.5604	2.3365	2.2822	2.3143	2.2977	1.5006	1.7677	1.7959	1.7507	1.7901	2.3283	2.2771	2.3215	
dmpdt 3D1	2.5725	2.3139	2.3138	2.2751	2.2909	1.5137	1.7685	1.7925	1.7488	1.7849	2.5210	2.2747	2.3195	
dmpdt 3D1'	2.5346	2.2948	2.3059	2.2984	2.3070	1.4992	1.7664	1.8134	1.7530	1.7850	2.2991	2.2751	2.3143	
dmpdt 3D2	2.5630	2.3258	2.3180	2.2808	2.2838	1.5062	1.7757	1.7674	1.7490	1.7802	2.5460	2.2794	2.3307	
dmpdt 3D2'	2.5211	2.2887	2.3349	2.3022	2.3208	1.5015	1.7654	1.7976	1.7556	1.7830	2.2589	2.2829	2.3205	

Table A65: Selected bond angles of the terminally protonated $[HFe_2(\mu-dmpdt)(CO)_4(PMe_3)_2]^+$ calculated using DFT.

	bond angle/°									
	$\angle S_1-Fe_1-S_2$	$\angle S_1-Fe_2-S_2$	$\angle Fe_1-S_1-Fe_2$	$\angle Fe_1-S_2-Fe_2$	$\angle L-Fe_1-Fe_2-L$	$\angle Fe-Fe-C_{semi}$	$\angle Fe-C-O_{semi}$			
dmpdt 3A1	83.3709	84.0446	66.4388	65.7931	44.6918	62.4106	158.3989			
dmpdt 3A1'	84.6189	84.3485	65.7796	66.1134	60.1678	55.8035	148.6753			
dmpdt 3A2	83.2662	84.3366	66.6204	67.0222	42.9314	62.5971	159.1624			
dmpdt 3A2'	84.5392	84.3207	66.3509	65.7618	64.1085	55.9587	149.2122			
dmpdt 3A3	83.8301	83.7253	67.0690	66.7766	3.5060	63.6248	160.4034			
dmpdt 3A3'	84.4753	83.2720	68.0014	67.7909	4.5198	70.0041	166.8851			
dmpdt 3A4	84.0848	83.4485	67.0652	66.0274	45.9678	63.6240	160.7644			
dmpdt 3A4'	84.9536	83.3217	67.6740	67.6505	22.6171	71.9219	71.9219			
dmpdt 3B1	83.3892	83.4944	65.6187	66.0212	72.6329	57.6245	152.4974			
dmpdt 3B1'	83.4387	82.5161	66.3892	65.9604	47.9354	67.5205	164.4860			
dmpdt 3C1	83.7880	85.0396	67.4676	68.7041	13.7046	67.8508	165.2643			
dmpdt 3C1'	84.6817	84.7544	66.5359	67.3172	1.4402	61.3764	157.6422			
dmpdt 3C2	83.7917	85.7667	69.1309	69.6722	10.4478	70.9688	166.5562			
dmpdt 3C2'	84.7891	84.9500	66.8025	67.9786	44.0922	61.7019	157.5621			
dmpdt 3D1	83.5328	84.9240	68.1869	67.9274	1.4282	67.8627	165.0875			
dmpdt 3D1'	84.6571	84.5503	66.9836	66.6589	1.7981	61.2139	157.0385			
dmpdt 3D2	83.5336	85.3214	67.6029	67.6867	29.8486	69.2438	165.8404			
dmpdt 3D2'	84.5723	84.5925	66.6169	65.5713	43.5458	60.3443	156.1758			

[Fe₂(μ-mpdt-S)(CO)₄(PMe₃)₂] systems

Table A66: Calculated gas phase and solvent corrected free energies, Fe–Fe bond lengths, and Fe Mulliken charges of the isomers of [Fe₂(μ-mpdt-S)(CO)₄(PMe₃)]. Energies are reported relative to the **1A1** isomer.

Isomer	Free Energies / kcal/mol		Mulliken charges	
	ΔG_g	ΔG_{solv}	Fe ₁	Fe ₂
mpdt-S 1A1	0.0	0.0	-0.175	-0.760
mpdt-S 1A2	0.5	0.3	-0.110	-0.838
mpdt-S 1B	2.9	1.8	-0.480	-0.469
TS_{mpdt-S1A1→1B}	10.9	9.7	-0.863	-0.563
TS_{mpdt-S1A1→1A2}	13.9	14.7	-0.171	-0.692
TS_{mpdt-S1B→1B}	15.8	15.4	-0.463	-0.404

Table A67: Selected bond distances of the unprotonated $[\text{Fe}_2(\mu\text{-mpdt-S})(\text{CO})_4(\text{PMe}_3)_2]$ from x-ray crystallography (unpublished), compared to calculated values of all isomers and transition states inter-converting them.

Exp.	bond length/Å											
	Fe ₁ -Fe ₂	Fe ₁ -S ₁	Fe ₁ -S ₂	Fe ₂ -S ₁	Fe ₂ -S ₂	Fe ₁ -CO ₁	Fe ₁ -CO ₂	Fe ₂ -CO ₁	Fe ₂ -CO ₂	Fe ₁ -P ₁	Fe ₂ -S _{apical}	
2.539	2.242	2.262	2.256	2.267	1.763	1.774	1.768	1.766	2.221	2.254		
2.5317	2.2884	2.2816	2.3000	2.2906	1.7528	1.7646	1.7588	1.7560	2.2561	2.2618		
2.5257	2.2848	2.2893	2.3009	2.2931	1.7525	1.7621	1.7637	1.7515	2.2563	2.2635		
2.4772	2.3192	2.3094	2.3114	2.3083	1.7590	1.7557	1.7566	1.7614	2.2350	2.2598		
2.5309	2.2834	2.2819	2.3095	2.3008	1.7513	1.7650	1.7614	1.7550	2.2589	2.3019		
2.5391	2.3171	2.3320	2.3180	2.3204	1.7458	1.7448	1.7638	1.7679	2.2136	2.2670		
2.4778	2.3055	2.3157	2.3188	2.3154	1.7575	1.7601	1.7603	1.7592	2.2350	2.2973		

Table A68: Selected bond angles of the unprotonated $[\text{Fe}_2(\mu\text{-mpdt-S})(\text{CO})_4(\text{PMe}_3)_2]$ from x-ray crystallography (in bold)(unpublished), compared to calculated values of all isomers and transition states inter-converting them.

Exp.	bond angle/°					
	$\angle \text{S}_1\text{-Fe}_1\text{-S}_2$	$\angle \text{S}_1\text{-Fe}_2\text{-S}_2$	$\angle \text{Fe}_1\text{-S}_1\text{-Fe}_2$	$\angle \text{Fe}_1\text{-S}_2\text{-Fe}_2$	$\angle \text{L-Fe-Fe-L}$	
mpdt-S 1A1	86.30	85.83	68.73	68.19	4.99	
mpdt-S 1A2	86.8749	86.3882	66.9759	67.2440	6.7941	
mpdt-S 1B	86.9046	86.4349	66.8385	66.8945	19.2889	
TS _{mpdt-S1A1→1A2}	86.0361	86.2396	64.6833	64.8875	12.6703	
TS _{mpdt-S1A1→1B}	86.8527	85.7986	66.8750	67.0450	13.3062	
TS _{mpdt-S1B1→1B}	85.9279	86.1754	66.4337	66.1538	98.0795	
	85.9282	85.6308	64.7963	64.6914	5.9745	

Table A69: Calculated gas phase and solvent corrected free energies, Fe–Fe bond lengths, and Fe Mulliken charges of the isomers of $[(\mu\text{-H})\text{Fe}_2(\mu\text{-mpdt-S})(\text{CO})_4(\text{PMe}_3)_2]^+$. Energies are reported relative to the **2A1** isomer.

Isomer	Free Energies / kcal/mol		bond length / Å	Mulliken charges	
	ΔG_g	ΔG_{solv}	Fe–Fe	Fe _a	Fe _b
mpdt-S 2A1	0.0	0.0	-0.316	-1.185	
mpdt-S 2A2	0.3	0.1	-0.248	-1.204	
mpdt-S 2B	5.9	5.4	-0.869	-0.524	
TS_{mpdt-S2A1→2A2}	3.5	3.1	-0.222	-1.241	
TS_{mpdt-S2A1→2B1}	26.6	26.3	-0.298	-0.862	
TS_{mpdt-S2B1→2B}	19.9	20.5	-0.819	-0.532	

Table A70: Selected bond distances of the bridged protonated $[(\mu\text{-H})\text{Fe}_2(\mu\text{-mpdt-S})(\text{CO})_4(\text{PMe}_3)_2]^+$ from x-ray crystallography [1], compared to calculated values of all isomers.

Exp.	bond length/Å												
	$\text{Fe}_1\text{-Fe}_2$	$\text{Fe}_1\text{-S}_1$	$\text{Fe}_1\text{-S}_2$	$\text{Fe}_2\text{-S}_1$	$\text{Fe}_2\text{-S}_2$	Fe-H	$\text{Fe}_1\text{-CO}_1$	$\text{Fe}_1\text{-CO}_2$	$\text{Fe}_2\text{-CO}_3$	$\text{Fe}_2\text{-CO}_4$	$\text{Fe-CO}_{\text{semi}}$	$\text{Fe}_1\text{-P}_1$	$\text{Fe}_2\text{-S}_{\text{apical}}$
2.566	2.276	2.273	2.265	2.261	1.575	1.651	1.766	1.796	1.806	1.796	1.796	2.247	2.247
2.5727	2.2988	2.2973	2.2990	2.3103	1.6915	1.6534	1.7597	1.7823	1.7829	1.7882	2.2961	2.2818	
2.5744	2.2967	2.3041	2.3113	2.2990	1.6913	1.6542	1.7595	1.7814	1.7924	1.7788	2.2977	2.2812	
2.5658	2.3172	2.3200	2.3090	2.3162	1.6777	1.6325	1.7808	1.7819	1.7820	1.7903	2.2731	2.2839	
$\text{TS}_{\text{mpdt-S2A1} \rightarrow \text{2A2}}$	2.5766	2.2945	2.3053	2.3167	2.2953	1.6922	1.6532	1.7593	1.7811	1.7932	1.7782	2.2985	2.2870
$\text{TS}_{\text{mpdt-S2A1} \rightarrow \text{2B1}}$	2.6247	2.3796	2.3677	2.2966	2.3120	1.7197	1.6125	1.7565	1.7472	1.7818	1.7885	2.2585	2.2851
$\text{TS}_{\text{mpdt-S2B1} \rightarrow \text{2B}}$	2.5593	2.3026	2.3195	2.3235	2.3175	1.6973	1.6115	1.7810	1.7853	1.7903	1.7883	2.2656	2.2875

Table A71: Selected bond angles of the bridged protonated $[(\mu-H)Fe_2(\mu-mpdt-S)(CO)_4(PMe_3)_2]^+$ from x-ray crystallography (in bold), compared to calculated values of all isomers.

Exp.	bond angle/°					
	$\angle S_1-Fe_1-S_2$	$\angle S_1-Fe_2-S_2$	$\angle Fe_1-S_1-Fe_2$	$\angle Fe_1-S_2-Fe_2$	$\angle L-Fe_1-Fe_2-L$	
mpdt-S 2A1	85.69	85.15	68.93	68.91	6.37	
mpdt-S 2A2	86.4060	86.0980	68.0509	67.8857	1.4559	
mpdt-S 2B	86.4516	86.2293	67.9275	68.0108	1.2732	
TS _{mpdt-S2A1→2A2}	84.9769	85.2486	67.3685	67.2041	3.3447	
TS _{mpdt-S2A1→2B1}	86.3793	86.0952	67.9374	68.1177	2.3664	
TS _{mpdt-S2B1→2B}	83.3103	86.4135	68.2639	68.2204	82.7337	
	85.1671	84.7416	67.1748	66.9963	6.6013	

Table A72: Calculated gas phase and solvent corrected free energies, Fe–Fe bond lengths, and Fe Mulliken charges of the isomers of $[HFe_2(\mu\text{-mpdt-S})(CO)_4(PMe_3)_2]^+$. Energies are reported relative to the **2A** isomer.

Isomer	Free Energies / kcal/mol		Mulliken charges	
	ΔG_g	ΔG_{solv}	Fe ₁	Fe ₂
mpdt-S 3A1	15.1	14.9	-1.394	-0.709
mpdt-S 3A1'	15.8	15.7	-1.361	-0.740
mpdt-S 3A2	17.8	18.1	-0.904	-0.849
mpdt-S 3A2'	17.6	17.9	-0.920	-0.852
mpdt-S 3B	21.4	20.4	-1.257	-0.685
mpdt-S 3B'	21.9	20.9	-1.236	-0.648

Table A73: Selected bond distances of the terminally protonated $[HFe_2(\mu\text{-mpdt-S})(CO)_4(PMe_3)_2]^+$ calculated using DFT.

	bond length/Å													
	Fe₁-Fe₂	Fe₁-S₁	Fe₁-S₂	Fe₂-S₁	Fe₂-S₂	Fe-H	Fe₁-CO₁	Fe₁-CO₂	Fe₂-CO₃	Fe₂-CO₄	Fe-CO_{semi}	Fe₁-P₁	Fe₂-S_{typical}	
mpdt-S 3A1	2.5372	2.3013	2.3026	2.2810	2.2982	1.5139	1.7736	1.8144	1.7909	1.7988	2.3960	2.2793	2.2682	
mpdt-S 3A1'	2.5407	2.3000	2.3048	2.2909	2.2861	1.5146	1.7723	1.8128	1.8006	1.7894	2.4068	2.2807	2.2671	
mpdt-S 3A2	2.5348	2.3081	2.3083	2.2924	2.2881	1.5038	1.7742	1.7899	1.8009	1.7862	2.4513	2.2832	2.2645	
mpdt-S 3A2'	2.5372	2.3155	2.3059	2.2823	2.2959	1.5049	1.7748	1.7878	1.7907	1.7907	2.4684	2.2829	2.2670	
mpdt-S 3B	2.5160	2.5160	2.3254	2.3104	2.3126	1.5008	1.7753	1.8105	1.7901	1.8022	2.2630	2.2596	2.2798	
mpdt-S 3B'	2.5156	2.3259	2.3151	2.3182	2.3205	1.5010	1.7758	1.8128	1.7974	1.7895	2.2507	2.2583	2.2749	

Table A74: Selected bond angles of the terminally protonated $[HFe_2(\mu\text{-mpdt-S})(CO)_4(PMe_3)_2]^+$ calculated using DFT.

	bond angle/°									
	$\angle S_1-Fe_1-S_2$	$\angle S_1-Fe_2-S_2$	$\angle Fe_1-S_1-Fe_2$	$\angle Fe_1-S_2-Fe_2$	$\angle L-Fe_1-Fe_2-L$	$\angle Fe-Fe-C_{semi}$	$\angle Fe-C-O_{semi}$			
mpdt-S 3A1	86.6178	87.2034	67.2390	66.9356	1.1028	64.3304	162.0602			
mpdt-S 3A1'	86.6262	87.2810	67.2041	67.2031	3.2144	64.6153	162.2633			
mpdt-S 3A2	86.9546	87.8081	66.8671	66.9345	16.6426	66.4880	164.1254			
mpdt-S 3A2'	86.9466	87.9768	66.9801	66.9199	17.6587	67.0281	164.4692			
mpdt-S 3B	86.0755	86.5321	65.7366	65.8340	30.5701	60.4952	156.7212			
mpdt-S 3B'	86.1786	86.2312	65.5963	65.7322	40.3728	60.0814	156.3496			

Appendix B

Protonation mechanisms of the [Fe₂(μ-(Xdt)(CO)₄(PMe₃)₂ model systems

Table B1: Free energy comparison between the TPSS and B3LYP functionals for the solvent mediated terminal path leading to bridging hydrides. Energies are reported in kcal/mol relative to 1A. Calculations using the B3LYP functional carried out by Lui.[118]

Reaction coordinate	pdt		edt	odt
	TPSS	B3LYP		
1A → 6Aba	+17.5	+13.7	+14.8	+12.8
6Aba → TS_{6Aba-6HAba}	+13.1	+15.6	+15.1	+13.8
TS_{6Aba-6HAba} → 6HAba	-34.8	-41.1	-34.4	-33.7
6HAba → 2A	-4.4	-4.1	-4.1	-2.3
1A' → 6A'ba	+15.8	+13.6	+14.8	+18.6
6A'ba → TS_{6A'ba-6HA'ba}	+13.6	+14.8	+15.1	+12.2
TS_{6A'ba-6HA'ba} → 6HA'ba	-32.9	-42.1	-34.4	-32.7
6HA'ba → 2A'	-4.7	-1.4	-4.1	-8.6
1B → 6Bba	+15.0	+15.2	+16.2	+17.1
6Bba → TS_{6Bba-6BHba}	+7.8	+9.9	+8.4	+8.0
TS_{6Bba-6BHba} → 6BHba	-24.7	-33.5	-23.7	-24.4
6BHba → 2B	-3.8	-3.3	-6.5	-5.9
1B → 6Bba'	+14.6	<i>a</i>	*****	*****
6Bba' → TS_{6Bba'-6BHba'}	+5.8	<i>a</i>	*****	*****
TS_{6Bba'-6BHba'} → 6BHba'	-22.6	<i>a</i>	*****	*****
6BHba' → 2B	-3.5	<i>a</i>	*****	*****
1C → 6Cba	+16.9	+13.8	+16.5	+16.8
6Cba → TS_{6Cba-6HCba}	+16.7	+16.5	+16.2	+15.3
TS_{6Cba-6HCba} → 6HCba	-40.3	-48.3	-38.0	-7.1
6HCba → 2C	-3.1	-3.3	-7.1	-3.9
1D → 6Dba	+17.0	+16.2	+18.0	+19.3
6Dba → TS_{6Dba-6HDba}	+18.2	+17.2	+16.1	+15.1
TS_{6Dba-6HDba} → 6HDba	-41.4	-50.7	-40.6	-41.3
6HDba → 2D	-7.4	-4.7	-6.4	-6.2

^a data not available from B3LYP calculations

Table B2: Free energy comparison between the TPSS and B3LYP functionals for the solvent mediated terminal paths leading to terminal hydrides **3A**. Energies are reported in kcal/mol relative to **1A**. Calculations using the B3LYP functional were carried out by Lui.[118]

Reaction coordinate	<i>pdt</i>			<i>odt</i>
	TPSS	B3LYP	<i>edt</i>	
1A → 8Aba	+19.5	+17.9	+20.6	<i>b</i>
8Aba → TS _{8Aba-8HAba}	+11.5	+10.4	+7.8	<i>b</i>
TS _{8Aba-8HAba} → 8HAba	-19.5	-22.3	-17.1	<i>b</i>
8HAba → 3A1	-3.7	-2.0	-4.4	<i>b</i>
1A' → 8A'ba	+20.3	+17.4	+20.6	<i>b</i>
8A'ba → TS _{8A'ba-8HA'ba}	+8.9	+9.2	+7.8	<i>b</i>
TS _{8A'ba-8HA'ba} → 8HA'ba	-17.0	-21.4	-17.1	<i>b</i>
8HA'ba → 3A1'	-5.1	-1.9	-4.4	<i>b</i>
1A → 10Aba	+15.1	<i>a</i>	+20.0	+16.9
10Aba → TS _{10Aba-10HAba}	+12.8	<i>a</i>	+10.4	+10.7
TS _{10Aba-10HAba} → 10HAba	-18.0	<i>a</i>	-16.1	-18.3
10HAba → 3A2	-2.9	<i>a</i>	-7.6	-6.0
1A' → 10A'ba	+14.9	<i>a</i>	+20.0	+13.6
10A'ba → TS _{10A'ba-10HA'ba}	+9.2	<i>a</i>	+10.4	+12.5
TS _{10A'ba-10HA'ba} → 10HA'ba	-15.2	<i>a</i>	-16.1	-18.8
10HA'ba → 3A2'	-3.5	<i>a</i>	-7.6	-0.5
1A → 6Aap	+15.7	+13.5	+15.6	+16.3
6Aap → TS _{6Aap-6HAap}	+14.0	+15.1	+10.5	+9.7
TS _{6Aap-6HAap} → 6HAap	-20.4	-24.1	-17.8	-18.1
6HAap → 3A3	-5.8	-3.7	-3.6	-3.8
1A' → 6A'ap	+16.2	+13.3	+15.6	<i>b</i>
6A'ap → TS _{6A'ap-6HA'ap}	+11.6	+13.2	+10.5	<i>b</i>
TS _{6A'ap-6HA'ap} → 6HA'ap	-20.2	-22.8	-17.8	<i>b</i>
6HA'ap → 3A3'	-3.5	-4.6	-3.6	<i>b</i>
1A → 9Aba	+15.1	+12.0	+19.3	+16.9
9Aba → TS _{9Aba-9HAba}	+4.7	+6.6	+3.0	+1.9
TS _{9Aba-9HAba} → 9HAba	-7.4	-14.4	-5.6	-7.2
9HAba → 3A4	-4.8	-1.3	-8.9	-5.1
1A' → 9A'ba	+15.0	+14.3	+19.3	+14.0
9A'ba → TS _{9A'ba-9HA'ba}	+3.8	+4.5	+3.0	+4.1
TS _{9A'ba-9HA'ba} → 9HA'ba	-6.7	-15.6	-5.6	-9.4
9HA'ba → 3A4'	-5.2	-0.9	-8.9	-3.1

^a data not available from B3LYP calculations, ^b TS could not be found

Table B3: Free energy comparison for the solvent mediated terminal paths leading to terminal hydrides **3B** and **3B'**. Energies are reported in kcal/mol relative to **1A**.

Reaction coordinate	pdt		edt	odt
	TPSS	B3LYP		
1B → 7Bba	+15.5	^a	+16.2	+17.8
7Bba → TS _{7Bba-7HBba}	+12.2	^a	+13.6	+10.0
TS _{7Bba-7HBba} → 7HBba	-16.2	^a	-15.0	-16.1
7HBba → 3B	-2.6	^a	-4.5	-1.4
1B → 7B'ba	+14.8	^a	+16.2	16.2
7B'ba → TS _{7B'ba-7HB'ba}	+12.4	^a	+13.6	12.3
TS _{7B'ba-7HB'ba} → 7HB'ba	-14.7	^a	-15.0	15.3
7HB'ba → 3B'	-3.3	^a	-4.5	3.6

^a data not available from B3LYP calculations

Table B4: Free energy comparison between the TPSS and B3LYP functionals for the solvent mediated terminal paths leading to terminal hydrides **3C**. Energies are reported in kcal/mol relative to **1A**. Calculations using the B3LYP functional were carried out by Lui.[118]

Reaction coordinate	pdt		edt	odt
	TPSS	B3LYP		
1C → 6Cap	+16.5	^a	^b	+16.3
6Cap → TS _{6Cap-6HCap}	+8.5	^a	^b	+7.1
TS _{6Cap-6HCap} → 6HCap	-19.6	^a	^b	-17.0
6HCap → 3C1	-5.4	^a	^b	-8.3
1C → 6C'ap	+16.5	+12.9	^b	+16.5
6C'ap → TS _{6C'ap-6HC'ap}	+6.7	+9.6	^b	+6.2
TS _{6C'ap-6HC'ap} → 6HC'ap	-18.7	-24.4	^b	-17.1
6HC'ap → 3C1'	-5.7	-3.7	^b	-4.9
1C → 7Cba	+16.5	^a	+14.5	+16.5
7Cba → TS _{7Cba-7HCba}	+2.4	^a	+4.1	+1.9
TS _{7Cba-7HCba} → 7HCba	-12.3	^a	-7.6	-8.2
7HCba → 3C2	-1.3	^a	-4.8	-5.8
1C → 8Cba	+15.6	+11.9	+14.5	+16.3
8Cba → TS _{8Cba-8HCba}	+2.3	+4.0	+4.1	+7.1
TS _{8Cba-8HCba} → 7HCba	-8.9	-15.5	-7.6	-17.0
7HCba → 3C2'	-4.0	-2.4	-4.8	-8.3

^a data not available from B3LYP calculations, ^b TS could not be found

Table B5: Free energy comparison between the TPSS and B3LYP functionals for the solvent mediated terminal paths leading to terminal hydrides **3D**. Energies are reported in kcal/mol relative to **1A**. Calculations using the B3LYP functional were carried out by Lui.[118]

Reaction coordinate	<i>pd</i> t		<i>edt</i>	<i>odt</i>
	TPSS	B3LYP		
1D → 6Dap	<i>b</i>	+12.7	<i>b</i>	+16.1
6Dap → TS _{6Dap-6HDap}	<i>b</i>	+11.0	<i>b</i>	+5.8
TS _{6Dap-6HDap} → 6HDap	<i>b</i>	-25.6	<i>b</i>	-15.7
6HDap → 3D1'	<i>b</i>	-4.9	<i>b</i>	-4.7
1D → 8Dba	+18.0	<i>a</i>	+14.9	+17.0
8Dba → TS _{8Dba-8HDba}	+1.4	<i>a</i>	+3.8	+2.9
TS _{8Dba-8HDba} → 8HDba	-9.7	<i>a</i>	-8.9	-8.5
8HDba → 3D2	-6.3	<i>a</i>	-5.9	-7.0
1D → 8D'ba	+15.0	+16.1	+14.9	+18.6
8D'ba → TS _{8D'ba-8HD'ba}	+3.0	+0.3	+3.8	+0.7
TS _{8D'ba-8HD'ba} → 8HD'ba	-8.9	-14.5	-8.9	-9.7
8HD'ba → 3D2'	-6.3	-4.6	-5.9	-5.4

^a data not available from B3LYP calculations, ^b TS could not be found

[Fe₂(μ-pdt)(CO)₄(PMe₃)₂] Cartesian Coordinates

6Aba

Fe	0.55888500	0.98403700	0.38793100
Fe	0.77735700	-1.36541500	-0.49563000
H	-3.58010200	0.24476500	0.28018700
S	2.58356500	-0.12492000	0.13923200
S	0.24069400	0.41825800	-1.84130400
P	0.99085400	3.20215900	0.39741500
P	1.06243300	-2.76051100	1.29030300
O	0.92018500	0.67504300	3.27781900
O	-2.34428100	1.09021200	0.58298200
O	-2.00484600	-2.26189400	-0.65329600
O	1.97776000	-3.12269700	-2.50722100
C	0.78589400	0.80521400	2.12080900
C	-1.14503200	1.04151100	0.50604300
C	-0.88301900	-1.90323600	-0.58428600
C	1.50490400	-2.44214600	-1.68026900
C	-0.25800900	-2.72111000	2.60984000
H	-0.27887800	-1.73607800	3.08587700
H	-0.05319400	-3.48550300	3.36982300
H	-1.23447400	-2.92005300	2.15450600
C	2.62794600	-2.63476300	2.29125300
H	2.61546400	-3.39802200	3.07925800
H	2.71009200	-1.64145700	2.74341900
H	3.49300600	-2.79224700	1.63884200
C	1.05083200	-4.56124500	0.80737500
H	1.13324500	-5.19897600	1.69614100
H	1.89156600	-4.76604000	0.13575000
H	0.11922600	-4.79314800	0.27933000
C	1.65924900	0.84306000	-2.97978100
H	1.85586200	-0.07013600	-3.55544000
H	1.24652500	1.59359200	-3.66539900
C	2.92996400	1.36866900	-2.31815400
H	3.65620300	1.60776400	-3.11208000
H	2.71171300	2.30965000	-1.79767900
C	3.59182500	0.39548400	-1.34688100
H	4.49694200	0.84270700	-0.91835400
H	3.87889400	-0.53707000	-1.84820800
C	0.54597600	4.18964100	-1.12500300
H	1.14683300	3.86563800	-1.98052700
H	0.71351700	5.26014500	-0.95122300
H	-0.51040600	4.01961700	-1.36104400
C	2.72263600	3.77739800	0.79357100
H	2.76262600	4.87304200	0.83771700
H	3.42977900	3.42043500	0.03800100

Continued on next page

*Continued from previous page***6Aba**

H	3.01698800	3.36381000	1.76450400
C	0.01358000	4.11090100	1.70293100
H	-1.05791100	3.97216000	1.52033300
H	0.24665100	5.18282100	1.68428000
H	0.25547400	3.70813000	2.69254000
O	-4.48544000	-0.22308600	0.12802100
C	-4.70152000	-0.52163300	-1.34039700
H	-3.73596700	-0.93757200	-1.63280900
H	-4.87999800	0.43522800	-1.84039200
C	-5.56965900	0.48488100	0.89979200
H	-6.40011400	-0.22391700	0.90523900
H	-5.13892300	0.54652900	1.90236100
C	-5.83037100	-1.51866700	-1.50321000
H	-6.80784700	-1.10295700	-1.23381000
H	-5.87371600	-1.79621500	-2.56391400
H	-5.63984800	-2.42711200	-0.92219100
C	-5.93013400	1.84287200	0.32365600
H	-6.39578600	1.76792200	-0.66517100
H	-6.66291200	2.30505100	0.99749800
H	-5.05765700	2.50359000	0.27001400

TS_{6Aba→6HAba}

Fe	1.11683900	0.43425300	0.07253300
Fe	-0.95213000	-1.02259400	-0.54503800
H	-0.81231600	1.30856500	-0.14791100
S	0.47627700	-1.47846200	1.18075500
S	0.94255400	-0.86777900	-1.82736000
P	3.34820500	0.54693300	0.54577300
P	-2.63343400	-1.17495700	1.01430200
O	0.52761600	1.91138500	2.53627400
O	1.58271100	2.57311700	-1.87494800
O	-2.48068400	0.28428200	-2.68481100
O	-1.58263000	-3.70762400	-1.51186500
C	0.75514900	1.33637300	1.54303400
C	1.35535100	1.75097700	-1.07371700
C	-1.88132500	-0.20046300	-1.80595400
C	-1.35118400	-2.63825100	-1.09887300
C	-2.62272000	-0.03295300	2.48841600
H	-1.70880900	-0.22272700	3.06249000
H	-3.49473300	-0.23055100	3.12416500
H	-2.62224300	1.01446000	2.17670300
C	-2.66344900	-2.83371900	1.86848600
H	-3.48312900	-2.85808300	2.59708400
H	-1.71365100	-2.99446800	2.38908200

Continued on next page

*Continued from previous page***TS**_{6Aba→6HAba}

H	-2.81255100	-3.63260800	1.13446400
C	-4.38627300	-1.11531200	0.37060800
H	-5.09315400	-1.28081900	1.19268000
H	-4.50887000	-1.91153200	-0.37258000
H	-4.61828500	-0.16126000	-0.11262400
C	1.85846500	-2.49554800	-1.75157100
H	1.15204900	-3.24429400	-2.12922200
H	2.65722900	-2.38817400	-2.49572700
C	2.44764500	-2.90439700	-0.40377200
H	2.92931900	-3.88744100	-0.52949200
H	3.24415600	-2.20323500	-0.13003500
C	1.45400200	-3.01570400	0.75008500
H	1.97921000	-3.27835500	1.67641600
H	0.70110700	-3.78987100	0.55886200
C	4.55141000	0.20403800	-0.83760700
H	4.45293500	-0.82223300	-1.20295700
H	5.57855000	0.36676900	-0.48868500
H	4.33853800	0.89010700	-1.66504100
C	3.98627700	-0.43962700	1.99428500
H	5.04384300	-0.20530900	2.16754900
H	3.87993400	-1.51351000	1.81693400
H	3.40510100	-0.17329300	2.88412500
C	3.86851700	2.26924400	1.03856800
H	3.65637700	2.97068900	0.22450800
H	4.94415400	2.28686800	1.25228200
H	3.32195900	2.58469400	1.93380900
O	-1.51613800	2.38211100	0.01819500
C	-2.95421400	2.36104000	-0.31777900
H	-3.21971400	1.31176700	-0.18650700
H	-3.06532500	2.62006700	-1.37567800
C	-0.87246100	3.71969500	-0.03908600
H	-1.28678300	4.28451800	0.80265300
H	0.17662000	3.51189700	0.17397700
C	-3.77405000	3.26585000	0.59436900
H	-3.57588700	4.32886700	0.41791800
H	-4.83674300	3.09306800	0.38102000
H	-3.59704200	3.04457000	1.65318500
C	-1.05566900	4.43354900	-1.37131100
H	-2.09652300	4.72786400	-1.54784900
H	-0.45506900	5.35191500	-1.34795300
H	-0.70540200	3.82322100	-2.20981400

6HAba

Fe	0.85163300	0.83758100	-0.04265800
----	------------	------------	-------------

Continued on next page

*Continued from previous page***6HAb**

Fe	0.09183400	-1.60716300	-0.42118300
H	-0.53567600	-0.08877000	-0.21542100
S	1.34186700	-0.92567600	1.39412500
S	1.70605500	-0.55631700	-1.69206400
P	2.52356500	2.36543300	0.18717100
P	-1.56211400	-2.27586500	1.01969900
O	-0.58102400	2.18136400	2.14069300
O	-0.41242100	2.41381900	-2.17537700
O	-1.70777000	-1.70252600	-2.74193000
O	1.13173800	-4.33004300	-0.70166600
C	-0.02315500	1.64365200	1.27323600
C	0.10513900	1.81203900	-1.32802100
C	-0.99549600	-1.67936300	-1.82418400
C	0.70450000	-3.25147200	-0.58642800
C	-2.30474800	-0.94799400	2.07852900
H	-1.52393000	-0.50441100	2.70552600
H	-3.07274500	-1.38964500	2.72595700
H	-2.75525900	-0.17553700	1.44208500
C	-1.00737500	-3.56010700	2.24456600
H	-1.83637400	-3.81967300	2.91410500
H	-0.17591300	-3.16150300	2.83530600
H	-0.67429600	-4.46162900	1.71895000
C	-3.03937500	-3.07332600	0.21979900
H	-3.74501800	-3.40519500	0.99108900
H	-2.72254300	-3.93823700	-0.37342000
H	-3.53899900	-2.35519600	-0.43846700
C	3.36337800	-1.32623800	-1.29973000
H	3.24851900	-2.39208800	-1.53049800
H	4.04267700	-0.89704000	-2.04607700
C	3.92243700	-1.11473600	0.10535200
H	4.89849700	-1.62267000	0.15809800
H	4.11747500	-0.04805000	0.26403600
C	3.06013800	-1.64157600	1.25020300
H	3.53369900	-1.41717700	2.21333400
H	2.92397900	-2.72772000	1.18611800
C	3.79211400	2.44175800	-1.17290400
H	4.38675000	1.52455900	-1.20474000
H	4.45712000	3.29806000	-1.00714700
H	3.27728100	2.56013800	-2.13249300
C	3.49937800	2.31522100	1.77225600
H	4.24780200	3.11710000	1.77306100
H	4.00095200	1.35123100	1.89516100
H	2.81297000	2.46114700	2.61359900
C	1.88403700	4.11520000	0.20047000
H	1.38228100	4.33902600	-0.74695200
H	2.72033100	4.81178500	0.33487700

Continued on next page

*Continued from previous page***6HAba**

H	1.17102800	4.24994100	1.02075900
O	-3.67440200	1.50299700	0.05420500
C	-4.39302700	1.29300300	-1.18391100
H	-3.70264100	0.72327900	-1.81766900
H	-4.57793400	2.25802200	-1.68002500
C	-4.18388500	2.59572500	0.85494700
H	-5.28345300	2.55672600	0.89021800
H	-3.81083700	2.40121400	1.86767200
C	-5.70411300	0.52372900	-0.99186500
H	-6.41708100	1.07800500	-0.36928200
H	-6.17917200	0.34972400	-1.96656200
H	-5.52006300	-0.44922200	-0.51911500
C	-3.70588700	3.96634100	0.36534300
H	-4.06020400	4.18504500	-0.64940600
H	-4.09093300	4.75213800	1.02900300
H	-2.61023200	4.01809500	0.36881500

6A'ba

Fe	0.52493400	1.00883400	0.39321100
Fe	0.88152600	-1.32835000	-0.48246300
S	2.57736800	-0.06984300	0.40667100
S	0.52256800	0.49115700	-1.86007600
P	0.89171000	3.23538700	0.31588900
P	0.93161000	-2.71447900	1.32555200
O	0.61511500	0.80384200	3.31671900
O	-2.38614700	1.09709700	0.34301900
O	-1.89321600	-2.13782500	-0.92759200
O	2.15299100	-3.25086300	-2.29153200
C	0.58584600	0.89228500	2.14861700
C	-1.18329600	1.04845900	0.35423700
C	-0.77362400	-1.81155400	-0.74877500
C	1.67200700	-2.47823600	-1.55518100
C	-0.52342100	-2.61452000	2.48991100
C	2.37957100	-2.62310900	2.49210500
C	0.91244200	-4.52044600	0.86247600
C	2.08041900	1.05669100	-2.72720500
C	3.36016200	0.31378600	-2.35426400
C	3.78696800	0.49904800	-0.90032200
C	0.11403400	4.12410800	-1.13013600
C	2.62762000	3.92456300	0.31270300
C	0.14240100	4.15139100	1.75860500
O	-4.49531300	-0.28872900	0.01126600
C	-4.77065500	-0.61428600	-1.44129500
C	-5.55995100	0.40961700	0.81845300

Continued on next page

*Continued from previous page***6A'ba**

C	-5.89583100	-1.62398300	-1.54063400
C	-5.96092500	1.75849100	0.24737400
H	3.24389600	-0.75341800	-2.57616800
H	-3.59628500	0.20932100	0.11173000
H	-0.56618400	-1.61903000	2.94176000
H	-0.42825900	-3.36784800	3.28203700
H	-1.44869200	-2.79521300	1.93169300
H	2.27762400	-3.40198700	3.25816800
H	2.41519200	-1.64032400	2.97211800
H	3.31066900	-2.77244800	1.93583500
H	0.86880600	-5.14596600	1.76252300
H	1.81687200	-4.76539700	0.29541400
H	0.03998900	-4.72925700	0.23321800
H	1.85473700	0.91782800	-3.79134200
H	2.17550400	2.13394700	-2.53896400
H	4.01606100	1.54748500	-0.67606700
H	4.68782700	-0.09061200	-0.69090000
H	0.54608900	3.76687000	-2.07079300
H	0.27050700	5.20697900	-1.04733400
H	-0.96066000	3.91171800	-1.14457700
H	2.60146100	5.01921900	0.38629000
H	3.13990400	3.64630300	-0.61416300
H	3.18716700	3.51756600	1.16206400
H	-0.92512900	3.91396000	1.82822400
H	0.26531000	5.23457800	1.63609500
H	0.62993300	3.83614400	2.68773300
H	-3.81334000	-1.02453700	-1.76733400
H	-4.98053700	0.33219800	-1.94891800
H	-6.37970900	-0.31021800	0.86065500
H	-5.09257700	0.48502100	1.80355000
H	-6.86530600	-1.21241900	-1.23785700
H	-5.98036700	-1.91981300	-2.59386000
H	-5.67389300	-2.52114100	-0.95307300
H	-6.46162900	1.67073700	-0.72309200
H	-6.67482100	2.21483500	0.94508500
H	-5.10037500	2.43073100	0.15767600
H	4.17343200	0.68494200	-2.99902000

TS_{6A'ba→6HA'ba}

Fe	1.10653800	0.42955500	0.02878800
Fe	-0.96181100	-1.05341400	-0.52394500
S	0.52217100	-1.47707200	1.17078100
S	0.89496100	-0.91404800	-1.84851000
P	3.33109900	0.46534000	0.57529200

Continued on next page

Continued from previous page

TS_{6A'ba→6HA'ba}

P	-2.58538700	-1.12282100	1.09498400
O	0.59510300	1.99187500	2.45699200
O	1.61708100	2.47686800	-2.00811200
O	-2.48313900	0.37299800	-2.58613200
O	-1.93324100	-3.61235000	-1.54872300
C	0.78641000	1.38077600	1.47684700
C	1.38033400	1.69668900	-1.16918500
C	-1.88631800	-0.16005000	-1.73406300
C	-1.52716600	-2.60984500	-1.10413500
C	-2.47291700	0.03934000	2.54849100
C	-2.64846400	-2.77071400	1.96522000
C	-4.35118000	-0.98281300	0.50681600
C	1.85483800	-2.51725900	-1.78963600
C	1.55844700	-3.48151100	-0.64081800
C	1.69146800	-2.88298100	0.75639900
C	4.58674500	-0.42036200	-0.48245200
C	3.75796600	-0.09775100	2.30236200
C	4.02296000	2.19620500	0.58681500
O	-1.37719500	2.49424800	-0.02988700
C	-2.83198300	2.49002200	-0.27781500
C	-0.71114200	3.81530200	-0.14199500
C	-3.58107600	3.42537900	0.66388100
C	-0.92955400	4.49713300	-1.48545700
H	0.55960700	-3.91473900	-0.76146200
H	-0.67681200	1.40651000	-0.16928000
H	-1.54994500	-0.18148400	3.09592900
H	-3.33199700	-0.10993800	3.21414400
H	-2.43739100	1.08035000	2.21753600
H	-3.44208500	-2.76115100	2.72246800
H	-1.68582300	-2.96071600	2.45127600
H	-2.84994700	-3.56870500	1.24275700
H	-5.03957400	-1.12024900	1.34939600
H	-4.53457900	-1.76659500	-0.23698900
H	-4.55041500	-0.01434200	0.03764300
H	1.61324500	-2.98948400	-2.74965600
H	2.91282800	-2.23330400	-1.82020800
H	2.70542100	-2.50818000	0.93847800
H	1.47357400	-3.64233500	1.51677600
H	4.46157700	-1.50463500	-0.40166600
H	5.59772200	-0.15597200	-0.14832800
H	4.46287500	-0.12114900	-1.52902600
H	4.83296100	0.03077000	2.47944100
H	3.49159100	-1.14830700	2.45225700
H	3.19919100	0.50685400	3.02500200
H	3.98916500	2.62125400	-0.42186300
H	5.06254700	2.18117800	0.93537100

Continued on next page

Continued from previous page

TS_{6A'ba}→6HA'ba

H	3.42980000	2.82621400	1.25886400
H	-3.10460200	1.44764400	-0.10888600
H	-3.00260000	2.73001100	-1.33245400
H	-1.08125900	4.41085200	0.69921800
H	0.34136800	3.59101800	0.03747600
H	-3.37551500	4.48121600	0.45531400
H	-4.65751900	3.26855400	0.51751300
H	-3.34392200	3.21959700	1.71413200
H	-1.97149700	4.80374400	-1.63248400
H	-0.31401700	5.40549500	-1.50944200
H	-0.62002900	3.85705200	-2.31783800
H	2.26827700	-4.32101500	-0.71857600

6HA'ba

Fe	0.77208500	0.90646700	0.00397600
Fe	0.24164800	-1.59200400	-0.41041800
S	1.40595400	-0.81745300	1.43352200
S	1.78902000	-0.37460300	-1.62907000
P	2.34923200	2.54369000	0.12610400
P	-1.39278000	-2.38563800	0.98978800
O	-0.72051700	2.09276400	2.24070700
O	-0.66541700	2.41527100	-2.06717200
O	-1.51529000	-1.70601300	-2.76102900
O	1.22893700	-4.32449300	-0.78450700
C	-0.13791600	1.62341600	1.35046100
C	-0.08157900	1.83601800	-1.24663500
C	-0.81842400	-1.67888200	-1.83190500
C	0.86719200	-3.22815200	-0.62248600
C	-2.28826100	-1.11357300	1.99586200
C	-0.77266800	-3.60269000	2.25046300
C	-2.75638300	-3.31842500	0.13856000
C	3.54134600	-0.82781000	-1.15344200
C	3.71804400	-1.81097200	0.00176300
C	3.19766600	-1.32975000	1.35556200
C	3.13301700	2.98947600	-1.50287800
C	3.80528900	2.33427000	1.26966000
C	1.65731000	4.17958300	0.68468900
O	-3.75859100	1.30193500	0.03935400
C	-4.37577100	1.19620600	-1.26527900
C	-4.41956200	2.23533800	0.92653400
C	-5.59173900	0.26481100	-1.27249400
C	-4.00442800	3.68768600	0.67360100
H	3.25130300	-2.76726500	-0.25679300
H	-0.51404000	-0.12909900	-0.16846900

Continued on next page

*Continued from previous page***6HA'ba**

H	-1.57861100	-0.61071000	2.66134000
H	-3.05722000	-1.60762100	2.60337100
H	-2.75765400	-0.37745500	1.33054800
H	-1.60094600	-3.93013600	2.89057200
H	-0.00403600	-3.12516100	2.86689600
H	-0.34041900	-4.47482600	1.74838300
H	-3.45578700	-3.71453700	0.88433400
H	-2.33635900	-4.14955700	-0.43873700
H	-3.29580500	-2.65059300	-0.54099000
H	3.95409900	-1.25485700	-2.07497200
H	4.06525400	0.11644500	-0.96041800
H	3.77326400	-0.47887400	1.73678000
H	3.27231000	-2.13528800	2.09592900
H	3.62227400	2.11796700	-1.94814500
H	3.87034200	3.78737100	-1.35331600
H	2.35848000	3.33989400	-2.19343600
H	4.38277000	3.26667900	1.29157400
H	4.45594300	1.52713300	0.91937400
H	3.45488400	2.10263300	2.28129400
H	0.82220700	4.47169100	0.03860700
H	2.43671600	4.94927500	0.63400700
H	1.29621200	4.10200900	1.71566700
H	-3.58973400	0.80634100	-1.92304300
H	-4.64920700	2.19713900	-1.63270300
H	-5.51156900	2.12125100	0.84630800
H	-4.12580500	1.92554300	1.93697400
H	-6.39272300	0.63413500	-0.62041500
H	-5.99772200	0.18931200	-2.29004100
H	-5.31240400	-0.74211600	-0.93752900
H	-4.28193300	4.02278200	-0.33351600
H	-4.50467900	4.34822600	1.39448500
H	-2.92061500	3.80491500	0.79329100
H	4.79601500	-2.01157400	0.10960200

8Aba

Fe	-0.10659600	1.03660700	0.15232600
Fe	-1.41467100	-1.13003900	0.37172800
S	-1.28998500	0.06754300	-1.58076000
S	-2.08922700	0.83835400	1.34080500
P	-0.10428200	3.27235700	-0.23516400
P	-0.55025000	-2.87733300	-0.77222200
O	2.50572400	0.41365200	-0.96893200
O	1.27530600	1.30483100	2.72446800
O	-0.09496200	-2.01551700	2.83536800

Continued on next page

*Continued from previous page***8Aba**

O	-3.93591600	-2.56776100	0.75326700
C	1.39294000	0.64198900	-0.56025600
C	0.69252800	1.19697900	1.71266000
C	-0.62960800	-1.64391600	1.86030200
C	-2.93277100	-1.99484300	0.55697400
C	-1.63322800	-3.45695600	-2.17275700
C	-0.31090600	-4.44023000	0.21416500
C	1.09882700	-2.68725800	-1.62483300
C	-3.53240300	1.58962900	0.41575500
C	-3.96341600	0.87588800	-0.86381400
C	-2.92174200	0.88959400	-1.97910400
C	-0.73557300	4.33207600	1.16488900
C	-0.98068700	4.01395500	-1.70976600
C	1.61504700	3.96449300	-0.46574400
O	4.59716900	-0.70266900	-0.04684200
C	5.75977700	-0.03006500	-0.73822600
C	5.64333400	-0.27314300	-2.23028000
C	4.61746700	-0.64832100	1.46779000
C	3.58646700	-1.62118400	2.00113100
H	3.81363700	-2.64622100	1.68982900
H	-4.87458900	1.36929000	-1.23977800
H	-1.18551700	-4.32525400	-2.67216600
H	-1.75146700	-2.64100400	-2.89383700
H	-2.61899100	-3.73265800	-1.78305700
H	0.03275400	-5.25562500	-0.43387900
H	-1.26198300	-4.72468500	0.67796900
H	0.42373600	-4.27218700	1.00909700
H	1.32843500	-3.58494100	-2.21270700
H	1.88139200	-2.53715000	-0.87380300
H	1.06269400	-1.81570000	-2.28697100
H	-4.34649800	1.57432500	1.15040600
H	-3.27556900	2.63934200	0.22170700
H	-2.69467100	1.90754700	-2.31429900
H	-3.29037400	0.32864100	-2.84673400
H	-0.16092400	4.11150500	2.07122300
H	-0.63448000	5.39686200	0.91998000
H	-1.78775400	4.10402200	1.36431200
H	-0.73342500	5.07976000	-1.79380400
H	-0.67404700	3.49678000	-2.62553600
H	-2.06461700	3.91421700	-1.59071000
H	1.58287200	5.05611900	-0.56979500
H	2.23132500	3.70567200	0.40304900
H	2.06701200	3.52953000	-1.36436600
H	3.70780300	-0.30206500	-0.40504000
H	-4.23760300	-0.16005100	-0.63151800
H	6.63653100	-0.51010700	-0.29668600

Continued on next page

*Continued from previous page***8Aba**

H	5.72394400	1.02961100	-0.46209100
H	6.51341200	0.18786300	-2.71425200
H	5.65158200	-1.34406500	-2.45862300
H	4.74120800	0.18628500	-2.64804500
H	5.64193300	-0.93117800	1.72163800
H	4.42786300	0.39320900	1.74901100
H	3.61762300	-1.57686900	3.09695100
H	2.57014700	-1.35370400	1.69523500

TS_{8Aba→8HAba}

Fe	-0.68638900	-0.47582400	0.44267100
Fe	1.82114600	-0.10587000	0.39932600
S	0.56395100	-0.42192800	-1.53050100
S	0.86816500	-2.05745500	1.12200400
P	-2.47576100	-1.64224000	-0.36848500
P	2.63258300	1.85353400	-0.50692300
O	-0.31663200	2.37009900	1.06743000
O	-1.80500500	-0.69746700	3.13889500
O	2.24983000	0.78756400	3.16383500
O	4.46522000	-1.33019700	0.19673900
C	-0.38324700	1.23350600	0.71874100
C	-1.36191300	-0.60924900	2.05981900
C	2.08652500	0.43264600	2.06750900
C	3.40946100	-0.83003300	0.22655300
C	3.48291700	2.99929900	0.68664700
C	1.51309600	3.01219000	-1.45012600
C	3.94750800	1.52906000	-1.78734700
C	1.28800900	-3.42629400	-0.08227500
C	1.74931900	-3.03771900	-1.48733300
C	0.78973900	-2.13300200	-2.25557900
C	-2.33637600	-3.50379400	-0.24750300
C	-2.99744500	-1.41898800	-2.14869600
C	-4.11313700	-1.40700000	0.50200300
O	-2.95666500	1.74117700	-0.31494300
C	-3.49006900	2.25091200	0.99965900
C	-2.57246100	2.83996500	-1.26256600
C	-2.32966600	2.26425300	-2.64441100
C	-4.95873500	2.61474300	0.87201200
H	1.87824300	-3.96795200	-2.06408100
H	2.76156500	3.35285300	1.43130300
H	3.90527100	3.85786600	0.15091600
H	4.28847500	2.46451200	1.20176100
H	2.12726300	3.75355400	-1.97578300
H	0.83994500	3.52267100	-0.75647300

Continued on next page

Continued from previous page

TS_{8Aba→8HAba}

H	0.93261600	2.43835100	-2.18100300
H	4.29965400	2.47678000	-2.21267000
H	3.52532600	0.90760100	-2.58481400
H	4.79469200	1.00091900	-1.33820100
H	2.08108100	-3.98326100	0.43112300
H	0.40262100	-4.07099100	-0.11540500
H	-0.20470300	-2.58490300	-2.34978400
H	1.17187700	-1.94795000	-3.26649100
H	-1.59453400	-3.87962600	-0.95856400
H	-3.30575200	-3.96398700	-0.47624800
H	-2.03031700	-3.77942500	0.76743500
H	-3.75589700	-2.16720500	-2.41022200
H	-2.13930300	-1.52001000	-2.82039200
H	-3.42378900	-0.41958200	-2.27508600
H	-4.00884600	-1.63256900	1.56865600
H	-4.86254000	-2.07882400	0.06628700
H	-4.45734700	-0.37537900	0.38408100
H	-2.08079800	1.03118200	-0.11040200
H	-3.32502800	1.41515500	1.68394700
H	-2.85303600	3.09086000	1.29469700
H	-3.42132100	3.52791600	-1.24686100
H	-1.69004300	3.32385700	-0.83251600
H	-1.53629100	1.50807900	-2.63338000
H	-3.24452800	1.83161800	-3.06309900
H	-2.01202000	3.08404700	-3.30139900
H	-5.55906600	1.75972800	0.54282900
H	-5.31709700	2.92276300	1.86260800
H	-5.12628000	3.45396300	0.18762400
H	2.73488900	-2.56022100	-1.44350100

8HAba

Fe	-0.18272200	-0.87810400	0.53899000
Fe	1.98708100	0.38421200	0.25893300
S	0.70175200	-0.29818000	-1.53072600
S	1.89585700	-1.82454900	0.97200900
P	-1.82240300	-2.26979900	-0.17185600
P	1.78821800	2.57186100	-0.50069100
O	-0.35271800	1.75767200	1.76916100
O	-1.00243000	-1.68007900	3.23630900
O	3.16266300	1.19653200	2.83605900
O	4.58314300	0.01987600	-1.03468300
C	0.01397200	0.80391700	1.17736200
C	-0.68344300	-1.35534700	2.16559200
C	2.68951900	0.88092200	1.82488100

Continued on next page

*Continued from previous page***8HAb**

C	3.55215100	0.18916200	-0.52024000
C	2.18646900	3.88202000	0.75452400
H	1.50479100	3.79119200	1.60674000
H	2.07235500	4.87471400	0.30258300
H	3.21719500	3.76219500	1.10515700
C	0.13440900	3.10952200	-1.16780300
H	0.24075100	4.11637000	-1.58998400
H	-0.60965300	3.12903300	-0.36683200
H	-0.19321700	2.41919900	-1.95201300
C	2.92584200	2.96225000	-1.91960900
H	2.75922100	3.99464200	-2.24944500
H	2.72006800	2.27996300	-2.75175700
H	3.97105200	2.84825700	-1.61402300
C	2.52832100	-2.94320900	-0.37845800
H	3.55921000	-2.63268200	-0.58728000
H	2.56958400	-3.92765000	0.10331400
C	1.68859800	-3.01362200	-1.65093100
H	2.15199500	-3.75262200	-2.32368200
H	0.68775700	-3.39026000	-1.40454400
C	1.56504500	-1.69889500	-2.41753100
H	0.97192600	-1.84171400	-3.32879000
H	2.54739900	-1.31409500	-2.71689300
C	-1.64371800	-4.06933800	0.28341400
H	-0.73604300	-4.49388500	-0.15608200
H	-2.51654400	-4.62827000	-0.07673400
H	-1.58306300	-4.16146300	1.37324400
C	-2.13360600	-2.28280300	-2.00318900
H	-3.02150800	-2.89225500	-2.21176000
H	-1.27624900	-2.70346500	-2.53756800
H	-2.30445000	-1.25645100	-2.34217200
C	-3.48282500	-1.82846000	0.52197200
H	-3.44922200	-1.84850800	1.61668600
H	-4.22746700	-2.55561600	0.17489100
H	-3.75819800	-0.82004200	0.18660700
H	-1.38510000	-0.08020900	0.13327600
O	-4.14198500	1.44677500	-0.29592800
C	-4.27576300	2.15304300	0.95827700
H	-3.46536700	1.76240600	1.58483500
H	-4.08631200	3.22683300	0.78722300
C	-4.91432400	2.02644100	-1.36628800
H	-5.99082100	1.93822500	-1.15248800
H	-4.67008600	3.10000100	-1.44638500
C	-4.56940000	1.29644500	-2.65920300
H	-3.49753800	1.38213800	-2.87931500
H	-4.83383100	0.23384200	-2.58891100
H	-5.12987600	1.73110200	-3.49620300

Continued on next page

*Continued from previous page***8HAba**

C	-5.62893200	1.94774500	1.64641600
H	-5.83006500	0.87999300	1.79879900
H	-5.61839700	2.43870600	2.62853300
H	-6.45588400	2.37934500	1.07021900

8A'ba

Fe	-0.61170400	-1.02130900	-0.08173700
Fe	-0.63474100	1.46268500	-0.53617100
S	-1.75429100	0.51850100	1.22822800
S	-1.74815000	-0.04735500	-1.85584900
P	-1.43176300	-2.89536000	0.88069500
P	0.38589500	2.79656700	1.00210200
O	2.07900100	-0.77120400	0.98152400
O	0.64826000	-2.63712200	-2.17030900
O	1.68446900	1.49182700	-2.32747900
O	-2.20658300	3.68591400	-1.60543500
C	0.91474000	-0.80456300	0.65140500
C	0.13069600	-1.98928900	-1.34028500
C	0.74078100	1.48969600	-1.62549200
C	-1.57014400	2.82079200	-1.13976300
C	-0.79445200	4.01624500	1.77075700
H	-0.27191900	4.64349600	2.50362700
H	-1.59905700	3.46587000	2.27025500
H	-1.22854800	4.65295700	0.99294600
C	1.72739200	3.91242800	0.34656200
H	2.08222700	4.59123800	1.13156400
H	1.33148400	4.50064100	-0.48865800
H	2.56671800	3.31126600	-0.02022100
C	1.18163700	2.06467900	2.52519700
H	1.48577300	2.87021900	3.20542400
H	2.05762400	1.47259900	2.24535000
H	0.46001700	1.41471900	3.03238300
C	-3.59137800	0.09337600	-1.59400400
H	-3.85819100	1.13205100	-1.82615200
H	-4.01821000	-0.54912200	-2.37363800
C	-4.10573600	-0.32659400	-0.21971200
H	-5.20645600	-0.27388600	-0.23080000
H	-3.83733100	-1.37652700	-0.03881700
C	-3.60080600	0.53725700	0.93343200
H	-4.03903800	0.20538200	1.88279800
H	-3.86613900	1.59136500	0.78634900
C	-2.45289000	-4.04863400	-0.17522900
H	-1.86863900	-4.34399200	-1.05384200
H	-2.73322700	-4.94507200	0.39218400

Continued on next page

*Continued from previous page***8A'ba**

H	-3.36085100	-3.54213000	-0.51946100
C	-2.46480300	-2.73727100	2.42605000
H	-2.68015000	-3.73144200	2.83780600
H	-1.92083300	-2.14215900	3.16707900
H	-3.40939100	-2.23323500	2.19655000
C	-0.07689500	-4.04063200	1.45822900
H	-0.50181400	-4.94951200	1.90202100
H	0.55447800	-4.31906500	0.60699800
H	0.53948400	-3.52662200	2.20386200
H	3.35957400	-0.49723000	0.23645000
O	4.29144200	-0.30386300	-0.18346500
C	4.32438800	-0.58433200	-1.67405300
H	3.45457200	-0.03363500	-2.03945500
H	5.24094200	-0.08408100	-1.99850400
C	5.39453200	-0.89484600	0.65020300
H	5.20711800	-1.97033400	0.72577800
H	6.29706800	-0.70691900	0.06247400
C	5.41257800	-0.19380000	1.99546100
H	5.57674500	0.88261000	1.87901600
H	4.48620100	-0.36746800	2.55366600
H	6.24209500	-0.60829200	2.58185400
C	4.29270400	-2.06377100	-2.00831700
H	3.38966400	-2.55181200	-1.62720000
H	4.27294700	-2.14851700	-3.10263400
H	5.18291700	-2.59445100	-1.65277700

TS_{8A'ba→8HA'ba}

Fe	-0.67894587	-0.47472586	0.44254234
Fe	1.81370287	-0.10696814	0.39945466
S	0.58050869	-0.43886688	-1.52322918
S	0.88472269	-2.07439388	1.12927582
P	-2.46831787	-1.64114186	-0.36861366
P	2.62504745	1.85221270	-0.50669112
O	-0.30959391	2.36891321	1.06693247
O	-1.79758063	-0.69637257	3.13881125
O	2.24192360	0.78552579	3.16105156
O	4.45687141	-1.33088231	0.19696615
C	-0.37620891	1.23232021	0.71824347
C	-1.35448863	-0.60815457	2.05973525
C	2.07861860	0.43060779	2.06472556
C	3.40111241	-0.83071831	0.22678015
C	3.38886976	3.04123986	0.70295534
C	1.52826592	2.96519894	-1.52830684
C	4.00914107	1.53316134	-1.71345863

Continued on next page

Continued from previous page

 $TS_{8A'ba \rightarrow 8HA'ba}$

C	1.30456669	-3.44323288	-0.07500318
C	0.61729328	-3.24097078	-1.32212206
C	0.80629669	-2.14994088	-2.24830718
C	-2.59810518	-3.41299609	0.21716444
C	-2.68668216	-1.83802211	-2.21379714
C	-4.17013117	-1.03941442	0.11702296
O	-2.95955611	1.74404844	-0.29942628
C	-3.45969588	2.30011745	1.00945702
C	-2.58543651	2.80864416	-1.28917756
C	-2.37789748	2.18747574	-2.65701040
C	-4.92725487	2.67465459	0.90157238
H	2.62352637	3.39257960	1.40343488
H	3.81803728	3.89860398	0.17072428
H	4.17953751	2.53590450	1.26841440
H	2.15108768	3.71011821	-2.03852768
H	0.81007259	3.47350297	-0.87969066
H	0.99798269	2.36340498	-2.27468017
H	4.36069866	2.48019497	-2.14079249
H	3.64130857	0.88615395	-2.51750044
H	4.84451311	1.03412732	-1.21195650
H	2.39980945	-3.41352395	-0.12310323
H	1.02315636	-4.37483982	0.42854471
H	0.30462011	-2.16368219	-3.22305626
H	1.88574094	-2.22644816	-2.42483907
H	-1.81621609	-4.02631716	-0.24073698
H	-3.57569495	-3.82536917	-0.06222485
H	-2.48495201	-3.44421354	1.30618489
H	-3.49117730	-2.55527119	-2.41828499
H	-1.75995464	-2.18760314	-2.67936975
H	-2.95239700	-0.87027093	-2.64900890
H	-4.25566400	-0.99055849	1.20780426
H	-4.92982000	-1.72900179	-0.27045985
H	-4.35230800	-0.04605800	-0.30331339
H	-2.08028383	1.03062966	-0.11019919
H	-3.28789609	1.48458377	1.71611678
H	-2.80853131	3.14239113	1.26427233
H	-3.42720497	3.50532813	-1.27718444
H	-1.68942364	3.29679602	-0.89341917
H	-1.59166987	1.42400672	-2.63895777
H	-3.30561519	1.75123837	-3.04234397
H	-2.06670754	2.98301236	-3.34612339
H	-5.54260507	1.81587957	0.61233369
H	-5.26128417	3.01718788	1.88933523
H	-5.10152731	3.49367166	0.19475655
H	0.83280019	-4.13132745	-1.87504319
H	-0.44214138	-3.19072395	-1.18079454

8HA'ba

Fe	-0.18272200	-0.87810400	0.53899000
Fe	1.98708100	0.38421200	0.25893300
S	0.70175200	-0.29818000	-1.53072600
S	1.89585700	-1.82454900	0.97200900
P	-1.82240300	-2.26979900	-0.17185600
P	1.78821800	2.57186100	-0.50069100
O	-0.35271800	1.75767200	1.76916100
O	-1.00243000	-1.68007900	3.23630900
O	3.16266300	1.19653200	2.83605900
O	4.58314300	0.01987600	-1.03468300
C	0.01397200	0.80391700	1.17736200
C	-0.68344300	-1.35534700	2.16559200
C	2.68951900	0.88092200	1.82488100
C	3.55215100	0.18916200	-0.52024000
C	2.18646900	3.88202000	0.75452400
H	1.50479100	3.79119200	1.60674000
H	2.07235500	4.87471400	0.30258300
H	3.21719500	3.76219500	1.10515700
C	0.13440900	3.10952200	-1.16780300
H	0.24075100	4.11637000	-1.58998400
H	-0.60965300	3.12903300	-0.36683200
H	-0.19321700	2.41919900	-1.95201300
C	2.92584200	2.96225000	-1.91960900
H	2.75922100	3.99464200	-2.24944500
H	2.72006800	2.27996300	-2.75175700
H	3.97105200	2.84825700	-1.61402300
C	2.52832100	-2.94320900	-0.37845800
H	3.55921000	-2.63268200	-0.58728000
H	2.56958400	-3.92765000	0.10331400
C	1.68859800	-3.01362200	-1.65093100
H	2.15199500	-3.75262200	-2.32368200
H	0.68775700	-3.39026000	-1.40454400
C	1.56504500	-1.69889500	-2.41753100
H	0.97192600	-1.84171400	-3.32879000
H	2.54739900	-1.31409500	-2.71689300
C	-1.64371800	-4.06933800	0.28341400
H	-0.73604300	-4.49388500	-0.15608200
H	-2.51654400	-4.62827000	-0.07673400
H	-1.58306300	-4.16146300	1.37324400
C	-2.13360600	-2.28280300	-2.00318900
H	-3.02150800	-2.89225500	-2.21176000
H	-1.27624900	-2.70346500	-2.53756800
H	-2.30445000	-1.25645100	-2.34217200
C	-3.48282500	-1.82846000	0.52197200
H	-3.44922200	-1.84850800	1.61668600

Continued on next page

*Continued from previous page***8HA'ba**

H	-4.22746700	-2.55561600	0.17489100
H	-3.75819800	-0.82004200	0.18660700
H	-1.38510000	-0.08020900	0.13327600
O	-4.14198500	1.44677500	-0.29592800
C	-4.27576300	2.15304300	0.95827700
H	-3.46536700	1.76240600	1.58483500
H	-4.08631200	3.22683300	0.78722300
C	-4.91432400	2.02644100	-1.36628800
H	-5.99082100	1.93822500	-1.15248800
H	-4.67008600	3.10000100	-1.44638500
C	-4.56940000	1.29644500	-2.65920300
H	-3.49753800	1.38213800	-2.87931500
H	-4.83383100	0.23384200	-2.58891100
H	-5.12987600	1.73110200	-3.49620300
C	-5.62893200	1.94774500	1.64641600
H	-5.83006500	0.87999300	1.79879900
H	-5.61839700	2.43870600	2.62853300
H	-6.45588400	2.37934500	1.07021900

9Aba

Fe	0.92559400	-0.87271000	-0.35662500
Fe	-0.13769400	1.31180000	0.32639500
S	0.20348500	-0.43699800	1.79870200
S	2.12463900	1.08652200	-0.14740800
O	1.02046300	-0.71052400	-3.27950300
O	-1.14421800	3.11635700	2.40188000
C	1.00065000	-0.75486700	-2.11000600
C	-0.67772600	2.43548100	1.56707100
C	1.52821000	0.01134900	3.03676200
C	3.16018700	1.13143700	1.41161000
C	2.36889700	1.24431000	2.71179000
C	-0.34015600	-2.08402200	-0.43430000
O	-1.20053100	-2.88394500	-0.48085600
P	2.62693300	-2.34684200	-0.24920900
P	-0.14466900	2.98189400	-1.19260200
C	4.20956900	-1.80602000	-1.07234600
C	3.22025500	-2.95778200	1.41303300
C	2.27574100	-3.95372000	-1.12780900
C	0.90328900	4.44174800	-0.70770200
C	0.44377300	2.61782100	-2.91892500
C	-1.81115400	3.76045400	-1.48368900
O	-4.64710300	-0.99140100	0.11314000
C	-4.71147900	-2.40418000	-0.41163500
C	-4.85290000	-2.33990800	-1.92013300

Continued on next page

*Continued from previous page***9Aba**

C	-4.85689000	-0.78386100	1.59188200
C	-3.83393400	-1.49774300	2.45743700
C	-1.56999500	0.63611800	-0.30623600
O	-2.61724300	0.23326400	-0.75471500
H	-3.79164300	-0.50126400	-0.21917600
H	-2.81028700	-1.16998300	2.24383300
H	3.80058200	0.24002300	1.40473500
H	3.80459700	2.00864700	1.27861800
H	3.07841300	1.40043100	3.54063300
H	1.72374600	2.13193100	2.66723300
H	0.97654400	0.16201500	3.97253500
H	2.15283100	-0.88274000	3.15279400
H	4.97203300	-2.59065000	-0.99039300
H	4.01215300	-1.60209400	-2.13045900
H	4.57836900	-0.88593300	-0.60835200
H	3.96997700	-3.74661700	1.27340500
H	3.67261600	-2.13752400	1.98051200
H	2.37334400	-3.35789400	1.98135800
H	3.16164600	-4.60051600	-1.11519200
H	1.44501200	-4.47036600	-0.63468100
H	1.99419800	-3.74852900	-2.16659900
H	0.82127900	5.23497100	-1.46127000
H	0.57382900	4.82583700	0.26364600
H	1.94732800	4.12070900	-0.62867100
H	-0.19490300	1.85749300	-3.37927300
H	0.41318100	3.53505400	-3.52017900
H	1.47229500	2.24363300	-2.88195400
H	-1.72148600	4.60379600	-2.17918100
H	-2.49704200	3.01819000	-1.90636000
H	-2.22017700	4.11994300	-0.53290300
H	-5.59224400	-2.82442000	0.08153200
H	-3.80029300	-2.91292000	-0.08593000
H	-4.92751800	-3.36836400	-2.29501900
H	-5.75731800	-1.79689900	-2.21363500
H	-3.97662700	-1.87630900	-2.38602200
H	-5.88233000	-1.12717400	1.75391900
H	-4.81633400	0.30432200	1.68809900
H	-4.05572300	-1.24371300	3.50229900
H	-3.89834800	-2.58727900	2.36214200

TS_{9Aba→9HAba}

Fe	1.44572800	-0.25294000	-0.50868300
Fe	-0.86307600	0.51219300	0.26182500
S	0.21111700	-1.35965600	1.09130000

Continued on next page

*Continued from previous page***TS**_{9Aba→9HAba}

S	1.12961300	1.60500700	0.80057200
O	2.18437400	1.40192800	-2.81950000
O	-2.98725700	0.66048200	2.28331800
C	1.88763700	0.75935700	-1.89231300
C	-1.04348600	-0.02286900	-1.40347900
C	-2.11222200	0.62041600	1.50206500
C	0.69045400	-1.06978900	2.87277800
C	1.57393400	1.32998000	2.59887000
C	0.66901800	0.37382600	3.37006400
C	1.31536900	-1.71240000	-1.50876100
O	1.23430700	-2.67789500	-2.15707000
O	-1.35868100	-0.28912600	-2.51016700
P	3.62216300	-0.63911600	-0.06177400
P	-1.57051900	2.54492400	-0.47374400
C	4.66093500	0.88916800	0.16960200
C	4.06871600	-1.68361200	1.41569800
C	4.52122400	-1.51178600	-1.43942700
C	-1.63912900	3.85422600	0.84432300
C	-0.55772600	3.34193100	-1.81160500
C	-3.28992500	2.57184000	-1.18278300
O	-3.06348900	-1.67934800	-0.05452800
C	-2.52608800	-2.94933600	-0.59670500
C	-2.61788600	-4.05405400	0.44507600
C	-4.33271800	-1.22136600	-0.64755900
C	-5.50732200	-2.08018400	-0.19897500
H	-5.58348000	-2.09880700	0.89371600
H	2.62301800	1.00956100	2.62892100
H	1.52271100	2.33411000	3.03645100
H	-0.02916800	-1.67472000	3.43740100
H	1.67863500	-1.52825900	2.99437800
H	-2.16082200	-0.70320200	-0.00426700
H	5.70558300	0.60686500	0.34927100
H	4.60354200	1.50662000	-0.73322500
H	4.29086800	1.47729700	1.01488500
H	5.14963300	-1.87154900	1.41758300
H	3.80092300	-1.16482600	2.34171300
H	3.53509400	-2.63900800	1.37107400
H	5.58885600	-1.58742200	-1.20021600
H	4.11100900	-2.51791600	-1.57647600
H	4.40138600	-0.95184800	-2.37340900
H	-2.00337100	4.79644500	0.41711800
H	-2.30983500	3.53728700	1.64989200
H	-0.63334400	4.00260200	1.25087500
H	-0.55564600	2.70976100	-2.70525300
H	-0.98618600	4.32071100	-2.05960100
H	0.47058600	3.47650500	-1.46115800

Continued on next page

*Continued from previous page***TS_{9Aba→9HAba}**

H	-3.53557900	3.57983900	-1.53778200
H	-3.35418800	1.86894700	-2.02028800
H	-4.00874500	2.28151300	-0.40868400
H	-3.08240000	-3.17809300	-1.51337400
H	-1.48603500	-2.73608800	-0.86218800
H	-2.17669400	-4.97045500	0.03148600
H	-2.05686500	-3.77834200	1.34462100
H	-3.65567800	-4.26545000	0.72326000
H	-4.21423300	-1.21073100	-1.73930800
H	-4.43332300	-0.19414600	-0.28581000
H	-6.43216000	-1.64963800	-0.60411200
H	-5.43011100	-3.10785300	-0.57227500
H	0.99062100	0.37089500	4.42414200
H	-0.35865300	0.75568300	3.35413900

9HAba

Fe	1.62456800	-0.41962200	-0.44132700
Fe	-0.64570800	0.55645800	0.20251500
S	0.36061300	-1.19433700	1.33018100
S	1.38785800	1.66010500	0.51406100
O	2.49530800	0.80361600	-2.97084500
O	-2.63876300	1.06220200	2.29652500
C	2.15138700	0.32532800	-1.96687600
C	-0.63919500	-0.22207900	-1.39598900
C	-1.79813500	0.90962600	1.50442900
C	0.85084300	-0.60234400	3.03205800
C	1.87550400	1.65010400	2.32097200
C	0.93780600	0.90549900	3.26509700
C	1.48191700	-2.05688500	-1.14342800
O	1.40265800	-3.12543800	-1.59105800
O	-0.95066200	-0.65636000	-2.44109600
P	3.78909700	-0.79147800	0.09412900
P	-1.43112900	2.39812400	-0.88943400
C	4.87367400	0.72159600	0.09147200
C	4.16676600	-1.60887300	1.72194100
C	4.66562400	-1.89936700	-1.11702200
C	-1.57173500	3.91670800	0.17119700
C	-0.42035200	2.98238000	-2.33383700
C	-3.13133400	2.16087500	-1.59016700
O	-4.66677000	-1.85559300	-0.01959500
C	-4.44498200	-3.27152600	-0.13946100
C	-3.00962500	-3.50961400	-0.59203000
C	-6.00935200	-1.56648500	0.40617800
C	-6.19293600	-0.05490700	0.46650000

Continued on next page

*Continued from previous page***9HAba**

H	-6.04258400	0.39126500	-0.52468800
H	2.89613400	1.25153400	2.36860900
H	1.91920200	2.71251500	2.58789300
H	1.29679700	1.06145000	4.29518400
H	-0.06088500	1.35484200	3.21375100
H	0.08630500	-1.04235500	3.68375100
H	1.80039300	-1.10126500	3.25729100
H	-1.87479300	-0.28655100	0.02909500
H	5.90343500	0.43365100	0.33625000
H	4.85435300	1.17935000	-0.90340000
H	4.51972800	1.45745600	0.81984700
H	5.23579900	-1.85156400	1.76517200
H	3.92520700	-0.93745600	2.55157500
H	3.58041400	-2.52886700	1.81833200
H	5.72885000	-1.96080100	-0.85545900
H	4.23141300	-2.90421900	-1.09083800
H	4.56872800	-1.49737300	-2.13130100
H	-1.94480400	4.75393400	-0.43090000
H	-2.26210900	3.73444400	1.00128700
H	-0.58420800	4.16938200	0.57194700
H	-0.34972000	2.19176500	-3.08762600
H	-0.89972400	3.86272700	-2.77886100
H	0.58538500	3.25381500	-1.99527600
H	-3.46318600	3.07514200	-2.09687900
H	-3.11849500	1.33101500	-2.30479100
H	-3.82875900	1.91469800	-0.78292600
H	-5.15774500	-3.69373200	-0.86921900
H	-4.63347900	-3.75701200	0.83446300
H	-2.82539200	-4.58648500	-0.69669200
H	-2.82474000	-3.03230900	-1.56200800
H	-2.30007700	-3.10874900	0.14274900
H	-6.18734800	-2.02074000	1.39681800
H	-6.72499900	-2.01612900	-0.30405700
H	-7.21004800	0.18603600	0.80030200
H	-5.48387500	0.39324300	1.17376100

9A'ba

Fe	1.01425200	-0.74345400	-0.45478600
Fe	-0.18841800	1.32102300	0.38924800
S	0.09968200	-0.58075700	1.66302000
S	2.09237700	1.22790600	0.07700500
O	1.51838600	-0.26232000	-3.29715100
O	-0.91097200	2.98970900	2.68868100
C	1.32476600	-0.43030800	-2.15497100

Continued on next page

*Continued from previous page***9A'ba**

C	-0.58047500	2.36437800	1.75328700
C	1.31255600	-0.24219600	3.04241400
C	2.95966300	1.24330700	1.73487900
C	2.75671000	0.01549900	2.61888200
C	-0.30365100	-1.82695900	-0.83420900
O	-1.20601200	-2.54075200	-1.08231000
P	2.58033400	-2.36285100	-0.35458500
P	-0.18867000	3.08299700	-1.04073100
C	4.37252700	-1.84605400	-0.41846400
C	2.51699600	-3.55862900	1.07938200
C	2.49538200	-3.54068200	-1.79888100
C	0.83435700	4.52483600	-0.45842400
C	0.42742300	2.83507100	-2.77746500
C	-1.85894400	3.86355800	-1.30778100
O	-4.67083800	-1.10747400	0.14840500
C	-4.66702900	-2.41530400	-0.60441900
C	-4.90992200	-2.11574000	-2.07068800
C	-4.82075300	-1.16137200	1.64858600
C	-3.72978100	-1.95823200	2.34104100
C	-1.70967400	0.78495600	-0.18160600
O	-2.79724000	0.44091700	-0.57068600
H	3.36130400	0.14802700	3.53099500
H	-3.87652000	-0.50328400	-0.12991300
H	-2.73129100	-1.54821100	2.14928400
H	4.02282100	1.36258300	1.49248700
H	2.61759600	2.15720100	2.23577700
H	0.90139700	0.60516900	3.60500800
H	1.25856900	-1.13258400	3.68134200
H	5.02441900	-2.72859200	-0.42294400
H	4.53986600	-1.26650100	-1.33308900
H	4.62194400	-1.21593400	0.44092600
H	3.30016600	-4.32012900	0.97521200
H	2.64977100	-3.03256300	2.02998300
H	1.53654600	-4.04794400	1.08782600
H	3.27106400	-4.31184200	-1.71369600
H	1.51135300	-4.02192200	-1.82312100
H	2.63849700	-2.98941800	-2.73455600
H	0.76956200	5.34956900	-1.17901400
H	0.47157200	4.86513000	0.51736100
H	1.87776300	4.20706000	-0.36072600
H	-0.16710800	2.06583200	-3.27998900
H	0.35500200	3.77760400	-3.33475100
H	1.47308600	2.51258800	-2.75008000
H	-1.76600600	4.75607900	-1.93835800
H	-2.52962500	3.14766600	-1.79541000
H	-2.28923900	4.14820100	-0.34106800

Continued on next page

Continued from previous page

9A'ba

H	-5.48159600	-2.98053000	-0.14353100
H	-3.70223700	-2.89400500	-0.41714000
H	-4.93530600	-3.07171800	-2.60856700
H	-5.86752400	-1.60660000	-2.22098200
H	-4.09985800	-1.51402200	-2.49662700
H	-5.82211900	-1.57787200	1.78798500
H	-4.82313900	-0.10395100	1.92575100
H	-3.91641600	-1.89606600	3.42130900
H	-3.75183800	-3.01802900	2.06374600
H	3.15045400	-0.87175300	2.10701800

TS_{9A'ba→9HA'ba}

Fe	1.48283100	-0.13512400	-0.50152700
Fe	-0.88779500	0.48164800	0.23782100
S	0.21729000	-1.43549700	0.91148700
S	1.02539800	1.58081700	0.95092600
O	2.17536400	1.81769900	-2.57911100
O	-2.80680200	0.45118500	2.46014900
C	1.90249100	1.05275600	-1.74191400
C	-1.12989700	0.05599400	-1.45298600
C	-2.03145800	0.48625900	1.58015900
C	0.60116500	-1.28429100	2.73278900
C	1.27678700	1.20200500	2.76540000
C	1.64494300	-0.23745400	3.11372600
C	1.38254400	-1.45291400	-1.67970700
O	1.32225000	-2.32755700	-2.44883000
O	-1.43795500	-0.15249000	-2.57209400
P	3.64694400	-0.62805400	-0.11022700
P	-1.66252500	2.54598700	-0.33258200
C	4.65392400	0.62868500	0.82710300
C	3.99501000	-2.24455000	0.75006200
C	4.64247100	-0.81241300	-1.67424200
C	-1.78153700	3.74327000	1.08617300
C	-0.67711100	3.49231100	-1.59168100
C	-3.38216700	2.57604200	-1.04354600
O	-3.08808700	-1.70198000	-0.10132800
C	-2.57739100	-2.92795000	-0.75972900
C	-2.59695400	-4.09995700	0.20993700
C	-4.39901700	-1.22229400	-0.57474800
C	-5.53260000	-2.12862300	-0.11432400
H	-5.53598700	-2.22815400	0.97667200
H	2.07515000	1.88430600	3.08162500
H	0.34875900	1.50840400	3.26307000
H	2.60298600	-0.49233300	2.64427100

Continued on next page

*Continued from previous page***TS_{9A'ba}→9HA'ba**

H	1.80149400	-0.29401500	4.20293000
H	-0.35862400	-1.09804500	3.22978600
H	0.94496600	-2.28474600	3.02247900
H	-2.19685800	-0.72458800	-0.04302100
H	5.69825200	0.29790000	0.88713000
H	4.60652800	1.58726200	0.29909800
H	4.26008200	0.76661000	1.83841100
H	5.07711800	-2.41974200	0.79309100
H	3.59061000	-2.24026000	1.76683800
H	3.51859700	-3.05524500	0.18807600
H	5.68421700	-1.05181400	-1.42868800
H	4.22560000	-1.61618200	-2.29045600
H	4.61462900	0.12122600	-2.24610800
H	-2.16277400	4.70730900	0.72828200
H	-2.45559000	3.34982900	1.85446300
H	-0.78577100	3.88496700	1.51947200
H	-0.63428200	2.93198700	-2.53106900
H	-1.15031500	4.46579400	-1.76945100
H	0.33999100	3.64977400	-1.21866800
H	-3.65596300	3.59895200	-1.32858900
H	-3.42774400	1.93064200	-1.92707300
H	-4.09373300	2.21343200	-0.29342700
H	-3.18936800	-3.10146500	-1.65272600
H	-1.55726800	-2.68623800	-1.07405100
H	-2.18809500	-4.98534200	-0.29452500
H	-1.97282000	-3.88343700	1.08373000
H	-3.61278400	-4.33239700	0.54620000
H	-4.35416400	-1.13091100	-1.66837600
H	-4.48536200	-0.22547000	-0.13281000
H	-6.48637000	-1.68287200	-0.42486900
H	-5.47070700	-3.12497800	-0.56696900

9HA'ba

Fe	1.53162800	-0.37248600	-0.51449800
Fe	-0.69848000	0.59063500	0.30742000
S	0.36200600	-1.24268700	1.26137500
S	1.34924800	1.65961800	0.54200600
O	2.15173000	1.04309900	-3.01500300
O	-2.22165800	1.13772800	2.75780700
C	1.91730100	0.48744500	-2.01922100
C	-0.94107500	-0.13639400	-1.29040700
C	-1.57990000	0.96590500	1.80138700
C	0.98938000	-0.74150500	2.94753400
C	1.75889300	1.65944700	2.36769500

Continued on next page

*Continued from previous page***9HA'ba**

C	2.09780900	0.30813900	2.99275500
C	1.27962800	-1.93343500	-1.33609800
O	1.13670900	-2.95835700	-1.86514500
O	-1.33883700	-0.56246800	-2.30695700
P	3.70049800	-0.91654400	-0.22331600
P	-1.53707400	2.49870400	-0.61868900
C	4.83747900	0.46329900	0.29499100
C	4.06526400	-2.31537400	0.94991700
C	4.51380000	-1.51297700	-1.78775800
C	-1.54797500	3.96587000	0.52167300
C	-0.63669200	3.13293100	-2.11336100
C	-3.29822100	2.34746700	-1.18094600
O	-4.39520100	-1.42593000	0.15425000
C	-5.28624300	-1.40958400	-0.98060800
C	-4.91143400	-2.41415500	-2.07567500
C	-4.60925500	-2.55515400	1.02358600
C	-3.74040600	-2.38576200	2.26410100
H	-3.99698700	-1.46149700	2.79583500
H	2.61512400	2.33924600	2.45467300
H	0.90263800	2.12883400	2.86660000
H	3.00270400	-0.09532500	2.52234000
H	2.34853500	0.48303900	4.05122600
H	0.10739000	-0.42155500	3.51498200
H	1.34316400	-1.68166900	3.38802600
H	-1.99493000	-0.17888300	0.29264800
H	5.87038900	0.09492500	0.32542500
H	4.76321000	1.27755700	-0.43376700
H	4.56193500	0.84868200	1.28080800
H	5.14556300	-2.50580000	0.96640100
H	3.72437000	-2.07891200	1.96200300
H	3.54496600	-3.21567700	0.60523500
H	5.56087700	-1.76698700	-1.58287000
H	3.99787100	-2.40185100	-2.16560800
H	4.47882200	-0.72954000	-2.55209100
H	-1.93713800	4.84339700	-0.00870700
H	-2.17954000	3.76199000	1.39271300
H	-0.52535700	4.16863000	0.85684100
H	-0.66864500	2.38968500	-2.91652900
H	-1.11103500	4.05942000	-2.45887200
H	0.40653800	3.33828400	-1.85119400
H	-3.65173800	3.30712200	-1.57681500
H	-3.36437700	1.58462000	-1.96391200
H	-3.92772900	2.04125300	-0.33870700
H	-6.31917600	-1.57915300	-0.63164400
H	-5.22787100	-0.38535900	-1.36943900
H	-5.59662300	-2.30408400	-2.92706900

Continued on next page

*Continued from previous page***9HA'ba**

H	-3.88877300	-2.23601700	-2.42925700
H	-4.98461100	-3.45042400	-1.72427100
H	-4.35379800	-3.49164700	0.50216200
H	-5.67703000	-2.59937200	1.29962000
H	-3.89607900	-3.23231300	2.94508900
H	-2.67802000	-2.35535600	1.99112800

10Aba

Fe	-0.21138000	1.06803200	-0.41881300
Fe	-0.79812100	-1.24218800	0.42856000
S	-2.37670000	0.28333700	-0.26045100
S	-0.04398300	0.43874600	1.80869600
P	-0.58810700	3.29639300	-0.47554300
P	-1.63568000	-2.66829100	-1.12209000
O	-0.27816400	0.82771900	-3.33840700
O	1.92966400	-2.19485600	-0.01284400
O	-1.57167500	-3.05775400	2.59148700
C	-0.27943800	0.90924700	-2.17058400
C	0.82570600	-1.80378700	0.15730700
C	-1.31572900	-2.32946600	1.70888700
C	-0.83384900	-4.35002100	-1.12215900
C	-1.60782400	-2.20867300	-2.92562100
C	-3.42978600	-3.07947500	-0.84529500
C	-1.41364000	1.03638200	2.93088300
C	-3.28665800	1.06537000	1.17796400
C	-0.66960300	4.27339700	1.11437000
C	-2.13452400	3.84787000	-1.36070400
C	0.72681200	4.22798400	-1.41456900
C	-2.83445300	0.61029300	2.56245800
O	4.71324400	-0.33126600	0.35914600
C	4.53674800	-0.98133000	1.71647000
C	5.10981800	-1.26736600	-0.76140400
C	5.42825500	-0.43898600	-1.99065100
C	4.19520200	0.09237700	2.73007700
C	1.50452700	1.09996700	-0.41080400
O	2.70249700	1.11981100	-0.38231300
H	3.87719100	0.19983800	0.09407300
H	0.22399800	-4.25737500	-1.39122800
H	-1.33289400	-5.01039000	-1.84182700
H	-0.90389900	-4.78890000	-0.12071900
H	-2.07150400	-3.00876100	-3.51643400
H	-0.57541600	-2.06176400	-3.25827400
H	-2.16454600	-1.27845400	-3.07746900
H	-3.77935700	-3.79276700	-1.60188000

Continued on next page

*Continued from previous page***10Aba**

H	-4.01961000	-2.15893500	-0.90932500
H	-3.55723500	-3.51476100	0.15169300
H	-1.14054400	0.63430900	3.91413100
H	-1.32076600	2.12814700	2.97714900
H	-3.19984900	2.15330300	1.06322500
H	-4.33536200	0.79201800	1.01085500
H	-1.55288600	3.97860200	1.69063600
H	-0.73298800	5.34651800	0.89398600
H	0.22548800	4.07835200	1.71529000
H	-2.19135000	4.94324600	-1.38606400
H	-3.02144000	3.44995100	-0.85711700
H	-2.11955800	3.46172000	-2.38575100
H	1.69253500	4.10721500	-0.91119600
H	0.47975100	5.29537000	-1.47101400
H	0.80635000	3.82256600	-2.42944800
H	3.75873300	-1.74111000	1.59850400
H	5.51102300	-1.44205900	1.89805300
H	4.27526900	-1.96160800	-0.89602100
H	5.98541300	-1.78433000	-0.36089200
H	5.75384400	-1.12593400	-2.78187900
H	4.54846200	0.10166600	-2.35579500
H	6.23974700	0.26961300	-1.79474500
H	4.15800000	-0.38593700	3.71707400
H	4.96182500	0.87416600	2.75711300
H	3.21166300	0.53611100	2.54001100
H	-3.51973300	1.04174200	3.31029400
H	-2.92948100	-0.48008900	2.63783500

TS_{10Aba→10HAba}

Fe	-0.62484300	-0.37701100	-0.49994400
Fe	1.63706500	0.15697400	0.55779400
S	1.27863700	-1.68043000	-0.76591000
S	-0.17186900	-0.59103900	1.76956700
P	-2.51729700	-1.64978000	-0.46032000
P	2.99796400	0.98152600	-1.09965700
O	-0.22405700	2.49911100	-0.88942400
O	-0.90932100	-0.38800300	-3.41051100
O	1.58084600	2.71697800	2.00043500
O	3.92552200	-0.73362600	2.13878100
C	-0.34059300	1.35973700	-0.58169100
C	-0.79361300	-0.37785000	-2.24529600
C	1.58470300	1.71471500	1.40521100
C	3.00526500	-0.39893500	1.50175600
C	3.59868500	2.72332100	-0.84712200

Continued on next page

*Continued from previous page***TS**_{10Aba→10HAba}

H	2.74273900	3.40661600	-0.83172600
H	4.27611000	3.00784900	-1.66128900
H	4.13050500	2.79876100	0.10778000
C	2.31422600	1.02249500	-2.82927600
H	3.08772500	1.40100500	-3.50905400
H	1.44206200	1.68094300	-2.87191600
H	2.02786000	0.01199400	-3.13867500
C	4.57032000	0.01238700	-1.31712300
H	5.15724500	0.43146100	-2.14335100
H	4.31894600	-1.03013600	-1.54094500
H	5.16448200	0.04786200	-0.39796000
C	0.00110100	-2.38382100	2.28226100
H	0.02707000	-2.34208300	3.37755800
H	-0.92588800	-2.89211300	1.98861100
C	1.33557400	-3.25389900	0.24326400
H	0.54162000	-3.89282900	-0.16015200
H	2.29544700	-3.71040700	-0.02634600
C	-3.59280500	-1.63587000	1.06940300
H	-2.99334600	-1.84086900	1.96199700
H	-4.38309000	-2.39127200	0.97973800
H	-4.05753700	-0.65133100	1.18451900
C	-2.26453900	-3.48530100	-0.71754600
H	-1.71059700	-3.91764200	0.12092200
H	-1.69478800	-3.64442300	-1.63954800
H	-3.23543600	-3.99039300	-0.79853000
C	-3.78210900	-1.32895200	-1.79788300
H	-4.10274000	-0.28284600	-1.78618900
H	-4.65505000	-1.97595300	-1.64887700
H	-3.34263100	-1.54166000	-2.77811700
H	-2.03015000	1.03306800	0.13853700
C	1.23594500	-3.11806000	1.76297100
O	-2.75723100	1.82770500	0.59804700
C	-3.95915800	2.24209300	-0.17057900
H	-4.64555300	1.38617900	-0.19442500
H	-4.40785900	3.04632500	0.41981100
C	-2.87198300	1.84598500	2.08685000
H	-2.13091200	1.11166700	2.41496200
H	-3.87934700	1.48958400	2.33373400
C	-2.58798700	3.24070700	2.62038000
H	-2.65852100	3.21349000	3.71548400
H	-1.57945300	3.56690500	2.34662500
H	-3.31447100	3.97836400	2.25949800
C	-3.55155800	2.72446500	-1.55241200
H	-4.45485100	3.05646900	-2.07962700
H	-2.85552000	3.56581000	-1.48330000
H	-3.08499100	1.92913900	-2.14311700

Continued on next page

*Continued from previous page***TS_{10Aba}→_{10HAba}**

H	1.22341800	-4.13479500	2.18830300
H	2.13651700	-2.63309900	2.15447100

10HAba

Fe	0.25546900	-0.46592100	0.56201700
Fe	-1.85273700	0.43390300	-0.56773500
S	-1.76124900	-1.63333600	0.44010100
S	0.02188800	-0.22911800	-1.73231400
P	2.09822000	-1.79309000	0.40895500
P	-3.36955100	1.06496900	1.06201700
O	-0.09323800	2.33151000	1.31426600
O	0.26755600	-0.97450800	3.45039700
O	-1.62471900	3.15684000	-1.66624500
O	-4.00773500	-0.09500900	-2.46182900
C	-0.15937800	1.24376700	0.87363200
C	0.27372400	-0.76617900	2.30489700
C	-1.69229100	2.09258900	-1.20821200
C	-3.14116800	0.09083100	-1.70496300
C	-3.80984200	2.86971400	1.08149500
H	-2.91074200	3.46666600	1.26889700
H	-4.54508400	3.06368500	1.87164000
H	-4.23525200	3.16018400	0.11468700
C	-2.88328500	0.72201800	2.82457500
H	-3.71149900	1.01336500	3.48227900
H	-1.99402400	1.29983500	3.09323000
H	-2.68344000	-0.34666500	2.95388500
C	-5.01166200	0.20765400	0.92010700
H	-5.66633500	0.52211900	1.74165000
H	-4.85768700	-0.87561600	0.97299500
H	-5.48783000	0.45633100	-0.03398600
C	-0.22505300	-1.87744800	-2.57811900
H	-0.18577900	-1.62481200	-3.64442600
H	0.66280800	-2.48010300	-2.34956800
C	-1.72287900	-3.02406200	-0.80932300
H	-0.94795400	-3.70994800	-0.44945500
H	-2.69274600	-3.51985100	-0.68629000
C	3.23288900	-1.41397800	-1.01005100
H	2.70169100	-1.46351200	-1.96511900
H	4.04976700	-2.14647500	-1.01046100
H	3.64668100	-0.40613200	-0.87851700
C	1.84267800	-3.63986900	0.31556600
H	2.81654500	-4.14276700	0.36711700
H	1.35492900	-3.91432700	-0.62517000
H	1.22028300	-3.96982200	1.15438400

Continued on next page

*Continued from previous page***10HAba**

C	3.23388500	-1.62305500	1.86764100
H	3.51580300	-0.57128600	1.98117200
H	4.13485800	-2.22308800	1.69377400
H	2.74438300	-1.96872300	2.78357600
H	1.51168500	0.35006100	0.48549500
C	-1.51002700	-2.64641000	-2.27457900
O	4.97224300	1.64724700	-0.33600700
C	6.39740700	1.55620900	-0.14337400
H	6.89977800	1.53177300	-1.12582200
H	6.74884400	2.45379000	0.39345200
C	4.61249800	2.85789900	-1.03041100
H	5.07823000	2.85789200	-2.03111900
H	5.00673100	3.72535600	-0.47416100
C	3.09494300	2.93668800	-1.13775500
H	2.80787800	3.85483700	-1.66595700
H	2.69499400	2.08171200	-1.69735400
H	2.63682300	2.95597700	-0.14141600
C	6.71102900	0.29911700	0.65805700
H	7.79305600	0.21923100	0.82063800
H	6.21980300	0.33266500	1.63840000
H	6.38007400	-0.60033300	0.12377400
H	-1.47817800	-3.58297400	-2.85422400
H	-2.37405100	-2.08706500	-2.64825600

10A'ba

Fe	0.49857900	-0.97362700	-0.47193700
Fe	0.53647500	1.35899300	0.52550400
S	2.39700600	0.34479300	-0.33205700
S	0.29684600	-0.54468900	1.79976200
P	1.12899900	-3.14424500	-0.58309600
P	0.85984400	3.01540200	-0.99479900
O	0.61386700	-0.69884100	-3.38626300
O	-2.35261500	1.82750000	0.52273000
O	1.36321600	3.04794100	2.76917900
C	0.58260500	-0.79003100	-2.21972800
C	-1.18507300	1.63390000	0.52288900
C	1.05589700	2.39839500	1.84348700
C	-0.30657100	4.45912500	-0.82519000
C	0.76131300	2.62560900	-2.81272100
C	2.52229100	3.84389500	-0.86115600
C	1.85305700	-0.83936900	2.79196100
C	3.58725200	-0.11737600	1.03367500
C	0.95430000	-4.21376200	0.93857900
C	2.85992100	-3.51654000	-1.17371300

Continued on next page

*Continued from previous page***10A'ba**

C	0.11313600	-4.11246800	-1.81349600
C	3.11172200	-1.19559000	2.00346600
O	-4.67435000	-0.51578900	0.31624200
C	-4.67205700	-0.16901100	1.79090200
C	-5.23918700	0.54939500	-0.59653900
C	-5.29875500	-0.00534000	-2.00633600
C	-4.16224700	-1.36399100	2.57137800
C	-1.19773400	-1.21317300	-0.49006600
O	-2.38426300	-1.38426600	-0.50725500
H	-3.73852500	-0.79395400	0.00223500
H	-1.33301000	4.13668900	-1.03095600
H	-0.03121100	5.25590600	-1.52675700
H	-0.26017500	4.84723100	0.19847000
H	0.89347900	3.54403700	-3.39838300
H	-0.20960200	2.17746900	-3.04673400
H	1.55003700	1.91393300	-3.07618900
H	2.60421500	4.65011900	-1.60066500
H	3.30879500	3.10336900	-1.04004400
H	2.64585200	4.26003000	0.14455200
H	1.99919100	0.07054100	3.38714800
H	1.59164800	-1.65429200	3.47849100
H	4.49507500	-0.44717200	0.51409400
H	3.81286300	0.82009400	1.55687400
H	1.61750200	-3.86231500	1.73512000
H	1.20145700	-5.25562500	0.69853800
H	-0.07920000	-4.16035000	1.29814200
H	3.01650300	-4.59966600	-1.25237800
H	3.59628400	-3.09310700	-0.48318800
H	3.00438700	-3.05604400	-2.15739900
H	-0.94150200	-4.08956400	-1.51694700
H	0.45220400	-5.15481000	-1.85846500
H	0.20815800	-3.66115900	-2.80721000
H	2.94852500	-2.13123600	1.45335300
H	3.92172600	-1.39036600	2.72524200
H	-4.05300000	0.72623300	1.89856300
H	-5.72266400	0.05309800	1.99435600
H	-4.59163900	1.42448300	-0.49062200
H	-6.22917700	0.74333600	-0.17613400
H	-5.75282500	0.76024200	-2.64795700
H	-4.30049900	-0.22529100	-2.40011500
H	-5.91906800	-0.90643600	-2.05509900
H	-4.23970700	-1.11949500	3.63832600
H	-4.76853600	-2.25544900	2.37842400
H	-3.10929700	-1.57338000	2.35429700

TS_{10A'ba→10HA'ba}

Fe	0.56953500	-0.44144000	0.47518800
Fe	-1.65508700	0.24652700	-0.54971400
S	-1.36397900	-1.72188500	0.60949100
S	0.13922500	-0.42541000	-1.81938000
P	2.45563200	-1.72924200	0.48631800
P	-3.03985800	0.95234600	1.14328400
O	0.25663800	2.43014000	0.96730000
O	0.84451000	-0.57535700	3.38182500
O	-1.69379400	2.88454800	-1.84326600
O	-3.78951600	-0.78632300	-2.25098400
C	0.30030200	1.29455100	0.61531100
C	0.72180200	-0.51715300	2.21842300
C	-1.65375700	1.84994800	-1.30672300
C	-2.95300100	-0.35625300	-1.55879200
C	-3.54599400	2.74215800	1.09994700
H	-2.65566500	3.37643700	1.17080900
H	-4.21540700	2.96170000	1.94049100
H	-4.06415900	2.96278900	0.16039300
C	-2.41534000	0.74696500	2.88336000
H	-3.20046600	1.05156300	3.58647600
H	-1.53042800	1.37148200	3.03883800
H	-2.15880200	-0.30209200	3.06291400
C	-4.66368900	0.04763900	1.18705600
H	-5.26399900	0.38729200	2.03971200
H	-4.47015900	-1.02650100	1.28191500
H	-5.21872100	0.22839200	0.26021500
C	-0.21649600	-2.09784300	-2.57465200
H	-1.13137900	-1.96273600	-3.16435700
H	0.60989600	-2.26670000	-3.27598300
C	-1.47070300	-3.15643400	-0.58531300
H	-1.48409800	-4.04109300	0.06262600
H	-2.44903000	-3.08388800	-1.07488200
C	3.30327700	-2.12113700	-1.13089000
H	2.61849400	-2.64199700	-1.80628800
H	4.17956200	-2.75531000	-0.94729700
H	3.62604300	-1.18966700	-1.60726200
C	2.23459500	-3.41412200	1.26811100
H	3.18108900	-3.96810600	1.24236200
H	1.46354800	-3.98985400	0.74827000
H	1.92340500	-3.28042300	2.31012300
C	3.89799200	-1.10965700	1.50000200
H	4.31089300	-0.20786200	1.03958700
H	4.67826600	-1.87950700	1.53913600
H	3.57051900	-0.88087000	2.51963700
H	1.99820700	0.89392600	-0.06312300
C	-0.34044000	-3.27084900	-1.60578900

Continued on next page

*Continued from previous page***TS_{10A'}ba→10HA'**

H	0.61119500	-3.40907400	-1.07835100
H	-0.50967900	-4.18386300	-2.19906400
O	2.95007000	1.49786700	-0.40164100
C	3.38373300	2.49772000	0.61900000
H	2.70881400	3.35548300	0.55317400
H	3.20439100	1.97656300	1.56317900
C	2.92425200	1.93394000	-1.83632300
H	2.39966800	1.10699000	-2.32305500
H	3.97354000	1.94205300	-2.14717000
C	2.23139800	3.26643700	-2.07473200
H	2.19148800	3.42570400	-3.16011500
H	1.20458600	3.26853100	-1.69695100
H	2.77942600	4.11019400	-1.64043100
C	4.84625600	2.86506400	0.42992700
H	5.13954800	3.53301000	1.24963900
H	5.49304100	1.98091400	0.46276700
H	5.02179800	3.40156700	-0.50950100

10HA'

Fe	0.19659200	-0.43818100	0.55636400
Fe	-1.88737700	0.42658700	-0.60879100
S	-1.78933400	-1.64499000	0.42561100
S	0.01703000	-0.20935100	-1.74383300
P	2.11574400	-1.65176500	0.59169100
P	-3.50348000	1.03607500	0.92687100
O	-0.30218400	2.34570400	1.27713400
O	0.18408700	-0.81727300	3.46290000
O	-1.78077500	3.11369100	-1.80840000
O	-3.80891100	-0.48746100	-2.60862700
C	-0.35121600	1.26602000	0.80833900
C	0.19203900	-0.65867000	2.30887400
C	-1.80340200	2.06522200	-1.31128800
C	-3.05829700	-0.10995700	-1.80161200
C	-3.97394500	2.83355100	0.91966700
H	-3.09304300	3.44453200	1.14495600
H	-4.74667800	3.01954300	1.67519300
H	-4.35943700	3.11503400	-0.06631800
C	-3.10128600	0.70738900	2.71325900
H	-3.96589700	0.98315300	3.32927900
H	-2.23757200	1.30413000	3.02206000
H	-2.88485100	-0.35651800	2.85697700
C	-5.12169400	0.15088700	0.70220800
H	-5.82944300	0.46810300	1.47743600
H	-4.95656800	-0.92910700	0.78258400

Continued on next page

*Continued from previous page***10HA'ba**

H	-5.54321600	0.37742500	-0.28288200
C	-0.32971400	-1.80931900	-2.64205200
H	-1.18280200	-1.60645100	-3.30067300
H	0.55136400	-1.95230000	-3.27942800
C	-1.79298200	-2.98679800	-0.87315500
H	-1.88164100	-3.91192000	-0.29158600
H	-2.71669600	-2.86287500	-1.45060000
C	3.02984300	-1.78998700	-1.01798600
H	2.44743800	-2.35391600	-1.75237200
H	3.98084500	-2.30636300	-0.83910400
H	3.23059000	-0.78361300	-1.39881800
C	1.98357100	-3.40283600	1.22217200
H	2.97482300	-3.87310200	1.20669800
H	1.29426700	-3.99157000	0.60933100
H	1.61154300	-3.38575900	2.25254800
C	3.39784100	-0.91304800	1.71105400
H	3.74019500	0.03762100	1.28577700
H	4.24906300	-1.60024700	1.78816200
H	2.98281000	-0.74221800	2.70960000
H	1.38518600	0.46341300	0.44987900
C	-0.56554000	-3.04698800	-1.77893900
H	0.32557500	-3.24531500	-1.16987800
H	-0.68744100	-3.90922000	-2.45373800
O	5.12354500	1.60546700	-0.33001900
C	6.55758400	1.47450000	-0.39086700
H	6.89789600	1.67145100	-1.42199600
H	7.02014300	2.22925000	0.26783600
C	4.70259600	2.92809700	-0.71616200
H	5.03883100	3.13160600	-1.74747200
H	5.17812400	3.67094500	-0.05303500
C	3.18496000	3.01364600	-0.61662900
H	2.84792200	4.01510000	-0.91273400
H	2.70889700	2.28166800	-1.28144100
H	2.85080900	2.83159400	0.41231300
C	6.95030100	0.06877100	0.04629600
H	8.04029400	-0.04505700	-0.00342900
H	6.63366500	-0.12181100	1.07905500
H	6.49827900	-0.68486800	-0.61094500

6Aap

Fe	1.77937100	-0.25801900	-0.46651800
Fe	-0.54069100	0.60898000	0.09599200
S	1.35533800	1.05848800	1.37618700
S	0.07582000	-1.60772700	0.32062300

Continued on next page

*Continued from previous page***6Aap**

P	3.74424600	-1.15540400	0.16333300
P	-0.82919900	2.84580600	-0.01754300
O	3.09729200	1.96903200	-1.83855600
O	1.68676400	-1.83149700	-2.94440500
O	-0.94736000	0.42773000	-2.79779500
O	-3.26661900	0.05277500	0.93079900
C	2.56454900	1.09293500	-1.27568300
C	1.71566300	-1.19953700	-1.96299600
C	-0.69880800	0.47451300	-1.64968800
C	-2.11716900	0.35838800	0.67377600
C	-1.22356800	3.62240100	1.62722900
C	-2.25478400	3.39223900	-1.08444000
C	0.56799800	3.90354100	-0.63981800
C	0.12235000	-2.03987100	2.13836800
C	0.11311800	-0.86371200	3.11333400
C	1.31039500	0.07135400	2.96590900
C	3.73738900	-2.76965900	1.09797900
C	4.82630900	-0.06906300	1.22426500
C	4.88281600	-1.54253300	-1.26090900
O	-4.93600000	-1.03707900	-0.58953300
C	-6.29726000	-0.81484000	0.00967000
C	-4.59390200	-2.43919300	-1.01929000
C	-3.36117500	-2.38706600	-1.90038900
C	-6.50916700	-1.55908700	1.31733800
H	0.10788800	-1.26925800	4.13840200
H	-1.39557700	4.69975200	1.51100500
H	-0.38083000	3.45893300	2.30718600
H	-2.11712300	3.15117000	2.05074300
H	-2.36117000	4.48330600	-1.05189900
H	-3.18044800	2.92962500	-0.72393100
H	-2.08282100	3.07653400	-2.11901100
H	0.28284300	4.96171300	-0.58547300
H	0.80206300	3.64204300	-1.67649200
H	1.45503600	3.73543600	-0.02034400
H	-0.76660200	-2.66520200	2.28834100
H	1.00421100	-2.67612100	2.28252000
H	2.25884900	-0.47598500	3.03661500
H	1.30092400	0.83237800	3.75530200
H	3.16984700	-3.51733500	0.53328100
H	4.76491000	-3.12536000	1.24450400
H	3.26734100	-2.63210100	2.07750200
H	5.78792200	-0.56171400	1.41491500
H	5.00054300	0.88019700	0.70627700
H	4.33199000	0.14432000	2.17726400
H	5.84263200	-1.92233500	-0.88971000
H	4.42298700	-2.29568000	-1.90983700

Continued on next page

*Continued from previous page***6Aap**

H	5.05787800	-0.63413900	-1.84808800
H	-4.18929400	-0.60862400	0.02565600
H	-6.33390200	0.27118400	0.12803000
H	-6.98681300	-1.11899400	-0.78262100
H	-4.45293100	-3.03334600	-0.11071300
H	-5.48700300	-2.77184400	-1.55568500
H	-3.52205800	-1.74328900	-2.77109400
H	-2.47758700	-2.04727700	-1.34878200
H	-3.16054300	-3.40591000	-2.25564600
H	-5.76488500	-1.27213000	2.06862500
H	-7.49976200	-1.28397000	1.70153400
H	-6.49770300	-2.64653400	1.18483300
H	-0.81188300	-0.28522100	2.98266800

TS_{6Aap→6HAap}

Fe	-1.78374300	0.19386900	0.32628600
Fe	0.75626200	0.53745800	0.33064200
S	-0.44747100	-0.19064200	-1.55003300
S	-0.28073200	-1.22154600	1.41465800
P	-3.57063600	-1.07193700	-0.31769500
P	1.52871700	2.24250500	-0.96130300
O	-3.09786000	2.49323100	-0.94328900
O	-3.03037200	0.64865900	2.95285200
O	-0.51028500	2.72702800	1.76034600
O	2.83476900	0.93079200	2.32822900
C	-2.56241100	1.58356200	-0.44722400
C	-2.53234200	0.48262800	1.91532000
C	-0.25648300	1.75163000	1.14177700
C	2.03815500	0.71998100	1.48041400
C	2.65013200	1.84111200	-2.39856000
C	2.49476200	3.54286700	-0.04526300
C	0.21043600	3.25586700	-1.80056600
C	-0.03496200	-2.85744300	0.54951100
C	0.49856900	-2.82467300	-0.88260400
C	-0.34609500	-2.02959300	-1.87270000
C	-3.65878200	-2.89459700	0.07432900
C	-3.96642900	-1.01140000	-2.13917300
C	-5.17272500	-0.46749500	0.41928300
O	3.34869100	-1.40143800	0.10841000
C	4.12552300	-1.30510800	-1.15590300
C	4.06052700	-1.83609600	1.35965900
C	5.33620400	-1.06090900	1.64024600
C	4.69260000	-2.65812900	-1.55396900
H	1.51527500	-2.41811700	-0.87486900

Continued on next page

*Continued from previous page***TS_{6Aap}→6HAap**

H	2.84533800	2.74992800	-2.98123600
H	2.16589200	1.09794900	-3.04201100
H	3.60453800	1.44827400	-2.03325000
H	2.75012700	4.36764700	-0.72123200
H	3.41463700	3.11194100	0.36385100
H	1.88969000	3.92702100	0.78318700
H	0.67757300	4.05322100	-2.39162400
H	-0.44443000	3.70439700	-1.04715000
H	-0.38395300	2.61784100	-2.46329300
H	0.66595000	-3.39750800	1.19845400
H	-0.99737500	-3.37753800	0.60847300
H	-1.37315700	-2.41051100	-1.91968200
H	0.08046200	-2.10371000	-2.88070000
H	-3.45882600	-3.05628100	1.13916300
H	-4.66324900	-3.26642100	-0.16389600
H	-2.92884000	-3.45346100	-0.51951100
H	-4.84743200	-1.63070400	-2.34749300
H	-4.17929000	0.02486000	-2.42295800
H	-3.12112600	-1.36528000	-2.73709500
H	-6.01327200	-1.02200400	-0.01513000
H	-5.16774000	-0.61477600	1.50441600
H	-5.29989400	0.60002600	0.20932600
H	2.55477200	-0.57965100	0.24853200
H	4.90151700	-0.54405300	-1.01958700
H	3.37806200	-0.94672900	-1.86860300
H	4.23221800	-2.90755000	1.22120200
H	3.30078600	-1.68393000	2.12947900
H	5.72465100	-1.40531000	2.60739900
H	6.11413200	-1.24655000	0.89068100
H	5.14276600	0.01290500	1.72372800
H	5.45864200	-3.01132400	-0.85464800
H	3.90293500	-3.41322600	-1.63454400
H	5.16851300	-2.55335200	-2.53715400
H	0.56505300	-3.86541900	-1.24123200

6HAap

Fe	2.11407200	-0.16154200	0.07437000
Fe	-0.34266400	-0.80890600	0.40171100
S	0.46212000	0.26932000	-1.48207500
S	0.73253200	0.87787700	1.57013600
P	3.65788500	1.47662200	-0.16165600
P	-1.70118800	-2.02507600	-0.95668000
O	3.42287100	-1.82761400	-1.97424400
O	3.69820700	-1.26299700	2.29894000

Continued on next page

*Continued from previous page***6HAap**

O	1.25236900	-3.28064800	0.54440200
O	-1.65926100	-1.56548600	2.90663100
C	2.91014000	-1.17568800	-1.16003200
C	3.07148500	-0.82561200	1.42379200
C	0.79617600	-2.20528900	0.44612700
C	-1.11730200	-1.29605200	1.91521600
C	-2.84569500	-1.00029800	-1.99234100
C	-2.83078100	-3.19435900	-0.05949800
C	-0.84269100	-3.11095900	-2.19897000
C	0.09071100	2.53550900	0.98287100
C	-0.84632100	2.52562100	-0.22108000
C	-0.21846700	2.00833000	-1.51158600
C	4.00215100	2.42461000	1.40119300
C	3.35928000	2.80684400	-1.42716300
C	5.34214200	0.84425300	-0.63305300
O	-4.67833800	1.16842200	-0.08430600
C	-5.54995600	1.95241700	-0.93304400
C	-5.15953200	1.01586100	1.27206200
C	-6.20369200	-0.09605500	1.41124600
C	-5.33202400	3.45942600	-0.76989400
H	-1.74347400	1.93823000	0.01418700
H	-3.47531100	-1.66183100	-2.60039600
H	-2.25088900	-0.36366700	-2.65713000
H	-3.47199900	-0.37274200	-1.34519800
H	-3.44515300	-3.74721600	-0.78040600
H	-3.48530000	-2.62844800	0.61157100
H	-2.24142500	-3.90462700	0.53069300
H	-1.58939700	-3.59007300	-2.84385600
H	-0.25849100	-3.88247700	-1.68699700
H	-0.17322000	-2.50089700	-2.81565300
H	-0.42803900	2.93090200	1.86405700
H	0.97309600	3.16441800	0.80585400
H	0.60603000	2.64358800	-1.85357400
H	-0.96739500	1.97971700	-2.31213200
H	4.37751800	1.73862200	2.16813700
H	4.75458800	3.19899600	1.20855200
H	3.08358000	2.88893500	1.77277800
H	4.25438300	3.43636200	-1.50557900
H	3.14857200	2.35300400	-2.40125800
H	2.51365600	3.43439600	-1.12801400
H	6.06125800	1.67225900	-0.63459900
H	5.67017400	0.08540200	0.08556700
H	5.30801400	0.39529600	-1.63131700
H	-1.61995000	-0.00386700	0.35280300
H	-6.60056800	1.68584200	-0.74182700
H	-5.30949600	1.63954800	-1.95681900

Continued on next page

*Continued from previous page***6HAap**

H	-5.55953100	1.97419800	1.63769500
H	-4.26760700	0.77986500	1.86561700
H	-6.50179900	-0.19771100	2.46326500
H	-7.10785800	0.11710200	0.82808100
H	-5.79567900	-1.05718700	1.07427400
H	-5.56013800	3.79583800	0.24916600
H	-4.29285200	3.72681400	-0.99906800
H	-5.98942600	4.00855000	-1.45714200
H	-1.17792400	3.56140900	-0.39985100

6A'ap

Fe	-1.807406	-0.163452	0.417424
Fe	0.555597	0.648975	-0.050666
S	-1.187486	0.863661	-1.552183
S	-0.026428	-1.581649	0.026932
P	-3.709909	-1.254517	-0.100710
P	0.806468	2.896874	-0.205477
O	-3.247467	2.251914	1.227217
O	-1.870566	-1.194391	3.162516
O	0.943135	0.808730	2.853728
O	3.270931	0.020032	-0.874978
C	-2.662523	1.297767	0.886518
C	-1.835518	-0.779945	2.070859
C	0.727212	0.733075	1.702469
C	2.129150	0.348904	-0.615980
C	1.246411	3.471042	-1.920637
H	1.388789	4.558801	-1.937559
H	0.435432	3.198421	-2.604369
H	2.167681	2.976781	-2.247965
C	2.196688	3.584865	0.826830
H	2.299968	4.664349	0.662603
H	3.134101	3.086759	0.554673
H	1.995418	3.398696	1.887390
C	-0.611497	4.014306	0.241635
H	-0.315471	5.060501	0.094396
H	-0.892660	3.858755	1.287818
H	-1.473049	3.789631	-0.395010
C	0.069657	-2.286304	-1.701520
H	1.087803	-2.084172	-2.058152
H	-0.034974	-3.369884	-1.562062
C	-0.970506	-1.783721	-2.699871
H	-0.825887	-2.327786	-3.647804
H	-1.974508	-2.041894	-2.340725
C	-0.901865	-0.288380	-2.997534

Continued on next page

Continued from previous page

6A'ap

H	-1.670584	-0.013321	-3.730429
H	0.076785	-0.009210	-3.406695
C	-3.649552	-3.118831	-0.176077
H	-3.287521	-3.497172	0.786313
H	-4.650108	-3.524149	-0.372633
H	-2.963813	-3.453888	-0.960472
C	-4.572403	-0.765824	-1.680803
H	-5.521949	-1.306539	-1.779753
H	-4.766669	0.311958	-1.654966
H	-3.939398	-0.982430	-2.546893
C	-5.065560	-0.992728	1.152365
H	-5.965289	-1.548302	0.860713
H	-4.731681	-1.339329	2.136455
H	-5.307847	0.073335	1.219318
H	4.251356	-0.592175	0.013267
O	5.041109	-1.005688	0.578661
C	6.319300	-0.973074	-0.215137
H	6.429489	0.088532	-0.450712
H	7.084706	-1.268703	0.507597
C	4.663215	-2.316686	1.217241
H	4.349214	-2.991613	0.414576
H	5.597960	-2.666573	1.664045
C	3.577805	-2.059177	2.243863
H	3.908639	-1.339402	2.999543
H	2.650763	-1.707993	1.778678
H	3.358491	-3.010639	2.744917
C	6.280437	-1.853658	-1.452722
H	5.460981	-1.569013	-2.121978
H	7.224132	-1.710171	-1.994416
H	6.201151	-2.917879	-1.204756

TS_{6A'ap→6HA'ap}

Fe	1.74742500	0.21236500	-0.18654200
Fe	-0.76439000	0.64209800	-0.43575100
S	0.18811300	-0.32827700	1.45116400
S	0.36939800	-1.00911300	-1.60074500
P	3.54226600	-1.07453200	0.33656700
P	-1.59155700	2.30373900	0.89173400
O	2.81293700	2.38268400	1.47241500
O	3.22671500	1.09974400	-2.56508000
O	0.46131500	2.86821100	-1.88112300
O	-3.02281000	0.83223600	-2.26452000
C	2.37083400	1.52066400	0.82106400
C	2.62388700	0.76342400	-1.62714900

Continued on next page

Continued from previous page

TS_{6A'ap→6HA'ap}

C	0.11501300	1.92201000	-1.27599700
C	-2.15380800	0.69490500	-1.47415400
C	-2.80425800	1.84502000	2.23298000
H	-3.04266700	2.73223800	2.83242800
H	-2.35703600	1.08362500	2.88190300
H	-3.72995700	1.46254600	1.79079900
C	-2.51356200	3.63153100	-0.03204600
H	-2.85645700	4.40483800	0.66570300
H	-3.37766500	3.19900600	-0.54750000
H	-1.85428700	4.08617700	-0.77914900
C	-0.34822500	3.28817800	1.86445300
H	-0.86652400	4.07023300	2.43305600
H	0.37305000	3.75389100	1.18635700
H	0.18446100	2.63129400	2.55969100
C	-0.03366600	-2.71332600	-0.95378000
H	-1.11978400	-2.83264500	-1.03247800
H	0.43007000	-3.39181400	-1.68077500
C	0.45588200	-3.04398500	0.45383700
H	0.19384500	-4.09245100	0.67281500
H	1.54973100	-2.98796800	0.47287400
C	-0.11482700	-2.17321800	1.57026000
H	0.31986800	-2.46302500	2.53481000
H	-1.20035500	-2.29893200	1.64159600
C	3.97762100	-2.45780600	-0.83623900
H	4.13552900	-2.03163000	-1.83316700
H	4.89866400	-2.95259700	-0.50403600
H	3.17282300	-3.19587300	-0.89811400
C	3.61139400	-1.84818100	2.03371100
H	4.58860500	-2.32412200	2.18260600
H	3.47255100	-1.06210600	2.78403400
H	2.82478900	-2.59791700	2.16135600
C	5.13496800	-0.10368000	0.33155500
H	5.97440700	-0.76980000	0.56485000
H	5.29794100	0.34470500	-0.65422400
H	5.09196000	0.69445000	1.08015100
H	-2.43066400	-0.64190500	-0.21238400
O	-3.12454200	-1.53781100	-0.00561400
C	-3.87971900	-1.46382600	1.27469100
H	-4.73648400	-0.79893200	1.12290900
H	-3.16497700	-0.99079800	1.95226500
C	-3.84491100	-2.06414000	-1.21877200
H	-3.88757500	-3.14649300	-1.06563000
H	-3.14777300	-1.83499100	-2.02800400
C	-5.21234600	-1.44335200	-1.44719900
H	-5.59213100	-1.83380500	-2.40026400
H	-5.93571100	-1.71800300	-0.67105100

Continued on next page

*Continued from previous page***TS_{6A'ap}→6HA'ap**

H	-5.15007200	-0.35457300	-1.53747200
C	-4.28876400	-2.85046900	1.74476600
H	-5.02224000	-3.31656800	1.07743500
H	-3.42072900	-3.51200200	1.84208200
H	-4.75696600	-2.75298900	2.73237900

6HA'ap

Fe	2.01783500	-0.10201400	0.09518500
Fe	-0.37494600	-0.99924700	0.42290100
S	0.31174300	0.22259900	-1.41905800
S	0.56840400	0.70815400	1.66920000
P	3.46895500	1.59452300	-0.21465700
P	-1.70413100	-2.19851400	-0.97754000
O	3.41183700	-1.64712600	-1.98683500
O	3.66426800	-1.14282600	2.30237200
O	1.39097300	-3.36482700	0.44836900
O	-1.63174500	-1.93668200	2.89846900
C	2.86168900	-1.04254500	-1.15963500
C	3.01848400	-0.72826900	1.43032200
C	0.83152700	-2.33772100	0.40423300
C	-1.11240900	-1.59427500	1.91745200
C	-2.85136400	-1.16720600	-2.00727000
H	-3.50733900	-1.82523300	-2.59048500
H	-2.25795900	-0.55474500	-2.69567700
H	-3.44754700	-0.50979100	-1.36293500
C	-2.83144600	-3.40518800	-0.12664800
H	-3.43414200	-3.94124400	-0.86988500
H	-3.49664600	-2.86838400	0.55805000
H	-2.24039200	-4.12775400	0.44664400
C	-0.82007200	-3.23947000	-2.23940300
H	-1.55147200	-3.70372900	-2.91200500
H	-0.23698900	-4.02168400	-1.74247600
H	-0.14491300	-2.60399200	-2.82336400
C	-0.33520900	2.27707900	1.20949700
H	-1.39229800	2.06903100	1.40866300
H	0.01708400	3.01176500	1.94425600
C	-0.13357900	2.80567800	-0.20743400
H	-0.71988600	3.73365700	-0.30142400
H	0.91723000	3.08485000	-0.35396600
C	-0.57867800	1.86432000	-1.32273300
H	-0.40387600	2.32701300	-2.30170300
H	-1.64276700	1.61885000	-1.22920100
C	3.46485400	2.91404000	1.09578400
H	3.63483000	2.44514300	2.07090900

Continued on next page

*Continued from previous page***6HA'ap**

H	4.26296100	3.63894800	0.89413800
H	2.50133100	3.43066900	1.11843400
C	3.35408300	2.49962100	-1.83615700
H	4.12684700	3.27718500	-1.87766800
H	3.51327200	1.78751600	-2.65313600
H	2.36909900	2.95856600	-1.95804500
C	5.24615700	1.04189000	-0.20943900
H	5.90027300	1.90836100	-0.36532800
H	5.49297100	0.57527500	0.75000400
H	5.41638700	0.31641300	-1.01193600
H	-1.66291400	-0.20594300	0.41132800
O	-4.26351100	1.46646400	-0.11766200
C	-5.12016800	2.28197300	-0.95364200
H	-6.17430200	2.01516800	-0.78378000
H	-4.86795400	1.99871600	-1.98305500
C	-4.76298900	1.28255800	1.22839800
H	-5.15183500	2.23595300	1.61808800
H	-3.88212900	1.01315600	1.82430400
C	-5.82504800	0.18329800	1.32525100
H	-6.13563400	0.05671300	2.37087400
H	-6.71994700	0.42555500	0.73921000
H	-5.42631800	-0.77367700	0.96616300
C	-4.89883600	3.78245700	-0.74235800
H	-5.13744800	4.08986100	0.28344400
H	-3.85695500	4.05508400	-0.95300600
H	-5.54702500	4.35387300	-1.41999600

6Bba

Fe	-1.20746000	-0.36816800	0.01578300
Fe	1.27985900	-0.33556000	-0.13639500
S	-0.08071400	0.84138100	-1.60869100
S	0.09606500	0.81172700	1.51587100
P	-3.24518100	0.57118700	0.24019000
P	3.34920400	0.58354200	-0.16747800
O	-1.92435900	-2.27874200	-2.09087800
O	1.78486600	-2.49282600	1.75082900
O	-1.63968600	-2.41928600	2.05033100
O	1.83512600	-2.13626000	-2.38047800
C	-1.65038000	-1.49746400	-1.26425000
C	1.58481900	-1.58079700	0.99698300
C	-1.47717900	-1.57296400	1.24167800
C	1.61744200	-1.40392900	-1.49486000
C	-0.03810600	2.68777900	-1.33482700
C	-0.02178300	2.65721500	1.23367100

Continued on next page

*Continued from previous page***6Bba**

C	0.61255600	3.18883400	-0.04820800
C	-3.68616400	1.10937000	1.97241600
C	4.69939200	-0.70286300	-0.23582000
C	-3.71386200	2.07259100	-0.76670500
C	3.82249900	1.66693200	-1.61215100
C	-4.64973900	-0.58880800	-0.16004100
C	3.87880900	1.57537900	1.32302400
H	3.23903200	2.45477500	1.44665700
H	-2.97919500	1.86901500	2.32289600
H	4.58209800	-1.31341100	-1.13791400
H	-3.62192000	0.24568100	2.64346700
H	4.62910000	-1.35474700	0.64214700
H	-4.77421100	2.31085100	-0.61463800
H	4.87159300	1.97861000	-1.53302900
H	-3.53583600	1.87584700	-1.82955000
H	3.18484900	2.55552800	-1.65193400
H	-3.11297300	2.93484100	-0.45827100
H	3.68118800	1.09899900	-2.53840500
H	-4.70389500	1.51838800	2.00388100
H	5.68643800	-0.22437900	-0.25122900
H	-5.61621400	-0.11319200	0.04803300
H	4.92239500	1.89839800	1.22003300
H	-4.55698200	-1.49744900	0.44534900
H	3.77803600	0.94881800	2.21623700
H	-4.60537200	-0.86841100	-1.21842700
H	0.54893100	4.28923000	-0.03661500
H	1.67998600	2.93573500	-0.05409300
H	0.50294100	3.07209600	-2.20833100
H	-1.07647000	3.03012400	-1.41503400
H	0.46635600	3.09862100	2.11122800
H	-1.08865500	2.91054300	1.28108100
O	0.78313200	-4.77981400	2.40048800
H	1.11586200	-3.85439300	2.09950300
C	-0.15613500	-5.38970900	1.38244000
H	-0.32804400	-6.39507900	1.77506000
H	-1.07468200	-4.79618600	1.41218200
C	0.23988600	-4.70369400	3.81029700
H	-0.07083800	-5.73084800	4.01745800
H	-0.62509200	-4.03478300	3.77402000
C	1.34644100	-4.22673300	4.73026500
H	0.94922900	-4.21726600	5.75301100
H	2.20775400	-4.90234900	4.70174300
H	1.66798800	-3.20916100	4.48430500
C	0.52154600	-5.39646800	0.02674700
H	-0.14364200	-5.91710500	-0.67359200
H	0.67884900	-4.38444600	-0.35993300

Continued on next page

*Continued from previous page***6Bba**

H	1.47458600	-5.93518700	0.05791900
---	------------	-------------	------------

TS_{6Bba→6HBba}

Fe	1.27916300	-0.10589200	-0.02886500
Fe	-1.27281100	-0.02601100	-0.01287200
S	-0.05262500	-1.13360500	-1.62544600
S	-0.01441500	-1.27083000	1.48420700
P	3.19939200	-1.31522200	0.20765700
P	-3.33052000	-0.99463600	-0.08629700
O	2.43038700	1.24032500	-2.36697100
O	-2.14794100	1.40711300	2.38969300
O	2.18562700	1.62767500	2.15767000
O	-2.08425600	1.83009900	-2.13412700
C	1.96697000	0.75129700	-1.41140900
C	-1.79120400	0.87708400	1.41002000
C	1.82387600	0.94713600	1.27843500
C	-1.76042700	1.10592400	-1.27645400
C	-0.10542500	-2.99271100	-1.46158800
C	0.02567700	-3.10409900	1.10926800
C	-0.67317800	-3.56558600	-0.16594800
C	3.55759900	-1.90180600	1.94168600
C	-4.70557600	0.26484800	-0.07339600
C	3.51585700	-2.84109000	-0.82098900
C	-3.77604700	-1.98452000	-1.60318700
C	4.72740100	-0.31204800	-0.15877800
C	-3.83104000	-2.07324400	1.35094200
H	-3.16261600	-2.93341200	1.45011800
H	2.77159600	-2.57579300	2.29599000
H	-4.62278500	0.91741500	-0.94905400
H	3.59634600	-1.03713200	2.61269600
H	-4.64512500	0.87536400	0.83405100
H	4.54750000	-3.17880200	-0.66181400
H	-4.82950600	-2.28685400	-1.55521200
H	3.37210300	-2.61077000	-1.88228100
H	-3.15110300	-2.87814600	-1.69028600
H	2.83578000	-3.64901600	-0.53270000
H	-3.61774200	-1.36002400	-2.48936800
H	4.52216400	-2.42336700	1.96785400
H	-5.67678900	-0.24401600	-0.09711000
H	5.62489200	-0.90465000	0.05551100
H	-4.85991300	-2.42797600	1.21351100
H	4.73632200	0.58874900	0.46476600
H	-3.77310400	-1.48138600	2.27130500
H	4.73709200	-0.01383600	-1.21251900

Continued on next page

*Continued from previous page***TS_{6Bba}→6HBba**

H	-0.60236300	-4.66420300	-0.21783700
H	-1.74049200	-3.32729900	-0.09676800
H	-0.70909400	-3.31689100	-2.31821400
H	0.92018600	-3.33476200	-1.63715000
H	-0.44350500	-3.56532300	1.98680100
H	1.08338100	-3.39463100	1.10837000
H	0.13475300	1.66135600	-0.02040300
O	0.16228500	2.98160900	-0.03697100
C	-0.96145300	3.81773200	0.43554500
H	-1.82350300	3.14947100	0.42112000
H	-1.11710300	4.58984600	-0.32592300
C	-0.71973300	4.40127900	1.82212600
H	-1.62440100	4.94001500	2.13263000
H	-0.52113600	3.61406700	2.55616500
H	0.10904400	5.11823900	1.83315900
C	1.36511800	3.73311400	-0.45293700
H	2.16910600	2.99593500	-0.43703300
H	1.56479700	4.47156900	0.33095100
C	1.20190300	4.36662500	-1.82865800
H	2.14584400	4.85649700	-2.10061800
H	0.97537200	3.61164900	-2.58818200
H	0.41767400	5.13223500	-1.84037300

6HBba

Fe	-1.33574500	-0.40362800	-0.10144800
Fe	1.24243200	-0.42533600	-0.04603800
S	0.00143500	0.73158200	-1.63767900
S	-0.08333700	0.74207100	1.47715600
P	-3.30886800	0.72926900	0.06160900
P	3.27760700	0.59436100	0.02357500
O	-2.29211500	-2.03818500	-2.35114000
O	2.04806200	-2.19694500	2.15612700
O	-2.27934700	-2.27129400	1.96180800
O	2.19715200	-2.19239000	-2.18955400
C	-1.93079500	-1.38994000	-1.45832600
C	1.74479100	-1.49511600	1.28226000
C	-1.91941600	-1.52471200	1.14795900
C	1.83456100	-1.49082700	-1.33830700
C	0.01232000	2.58028700	-1.40331800
C	-0.16033700	2.58585300	1.17235600
C	0.53993600	3.11725600	-0.07524400
C	-3.76117000	1.22945000	1.79797400
C	4.67959600	-0.63162700	0.05991600
C	-3.59885300	2.28913100	-0.91797500

Continued on next page

*Continued from previous page***6HBba**

C	3.75108200	1.64754400	-1.43776100
C	-4.77208700	-0.30742500	-0.43822200
C	3.65860900	1.62859900	1.52564800
H	2.97740700	2.48075800	1.60435100
H	-2.99333600	1.88255400	2.22440900
H	4.65716700	-1.25766400	-0.83833500
H	-3.83881200	0.33417300	2.42402000
H	4.59509000	-1.27446900	0.94242700
H	-4.64852900	2.58930000	-0.81001000
H	4.77596600	2.01761500	-1.31224600
H	-3.38270200	2.11411800	-1.97745900
H	3.07206100	2.49749100	-1.54874900
H	-2.96442800	3.10048800	-0.54706500
H	3.69640000	1.03619500	-2.34529900
H	-4.72505700	1.75258300	1.79660100
H	5.63551500	-0.09557700	0.09808300
H	-5.70171800	0.23456300	-0.22736600
H	4.69125400	1.99430200	1.47093700
H	-4.77100900	-1.24976100	0.12025800
H	3.54214300	1.00606800	2.41959000
H	-4.72245800	-0.53210400	-1.50906200
H	0.43128900	4.21367000	-0.08500700
H	1.61404400	2.91437600	0.00036300
H	0.62756200	2.94925600	-2.23299000
H	-1.01563900	2.90716800	-1.59093000
H	0.28924600	3.02244400	2.07229600
H	-1.22432300	2.85246100	1.17411200
H	-0.06170900	-1.44280800	-0.12111700
O	-0.09319000	-5.54704900	0.03986500
C	-0.09147000	-6.37119400	1.21854800
H	-0.99410000	-7.00754100	1.22206900
H	0.78874100	-7.03792600	1.19856500
C	-0.12304500	-6.34370100	-1.15665900
H	-1.02255800	-6.98443200	-1.14869600
H	0.76024100	-7.00636100	-1.17878600
C	-0.06019000	-5.47447000	2.44988700
H	-0.06179700	-6.08916900	3.35911400
H	0.84352500	-4.85335800	2.45569500
H	-0.93894800	-4.81905900	2.47510300
C	-0.13223300	-5.41816700	-2.36675900
H	0.76624300	-4.78952400	-2.38174600
H	-0.15320900	-6.01069900	-3.29031100
H	-1.01720500	-4.77053400	-2.35386600

6B'ba

Fe	1.00705000	-0.95412700	0.30277100
Fe	-0.21962800	1.21268400	0.25169500
S	1.98813900	1.04996900	0.95669500
S	0.53758000	0.15992000	-1.67776800
P	2.65785000	-2.43160400	-0.12895000
P	-0.37426300	3.44094100	-0.11060400
O	0.90218100	-1.67723400	3.14106400
O	-2.91854500	0.45369100	-0.53537500
O	-1.23663500	-2.71344100	-0.32131100
O	-1.03436800	1.37595400	3.06440500
C	0.95212500	-1.38258500	2.01060800
C	-1.80350700	0.76733100	-0.22014900
C	-0.30898600	-2.02296800	-0.08061100
C	-0.68893200	1.32504100	1.94803200
C	3.15919400	1.77644500	-0.30738200
C	2.02475600	0.96878100	-2.46227000
C	3.29542300	1.00935200	-1.61889100
C	3.03486000	-2.85748400	-1.90832300
C	-2.10000800	4.09440200	0.16466000
C	4.34229400	-2.08129700	0.59612300
C	0.61852400	4.52319300	1.03949800
C	2.31259700	-4.12688800	0.57200800
C	0.02229700	4.17236100	-1.78372300
H	1.09807500	4.10579400	-1.97963800
H	3.41221500	-1.98006600	-2.44315900
H	-2.43870300	3.82002400	1.17018900
H	2.11318400	-3.19237900	-2.39703400
H	-2.78137700	3.64905500	-0.56895600
H	5.02519800	-2.91820200	0.40288300
H	0.42355600	5.58354000	0.83546500
H	4.23908200	-1.93815700	1.67742900
H	1.68798400	4.32162500	0.91947500
H	4.76255400	-1.16686000	0.16457000
H	0.34204900	4.29448700	2.07441800
H	3.78443100	-3.65732900	-1.95854500
H	-2.12103300	5.18634100	0.06101200
H	3.14711800	-4.80709900	0.36115600
H	-0.27453000	5.22869600	-1.80911300
H	1.39812000	-4.53080400	0.12345700
H	-0.51564900	3.62569300	-2.56607500
H	2.17127900	-4.05756200	1.65623200
H	2.83307300	2.80908600	-0.48444100
H	4.12413400	1.81484200	0.21278200
H	1.70746600	1.97606600	-2.75800000
H	2.19332700	0.39042200	-3.37921100
O	-4.51920000	-1.55321600	-0.37184900

Continued on next page

*Continued from previous page***6B'ba**

H	-3.83999400	-0.78088500	-0.41436100
C	-4.39737400	-2.30014400	0.93840400
H	-5.19573600	-3.04404200	0.87837200
H	-3.41455800	-2.78098400	0.93322000
C	-4.40937100	-2.40768300	-1.61612800
H	-5.16286300	-3.18336300	-1.45797800
H	-3.40276400	-2.83607200	-1.61112700
C	-4.70301200	-1.53926300	-2.82354400
H	-4.65640100	-2.17849400	-3.71412400
H	-5.70501100	-1.10144000	-2.76581000
H	-3.95963100	-0.74347500	-2.94202800
C	-4.59507800	-1.31879700	2.07703000
H	-4.57295700	-1.88803000	3.01475300
H	-3.79246500	-0.57522000	2.12156600
H	-5.56394200	-0.81357600	2.00461100
H	3.61980100	-0.01506800	-1.39890700
H	4.09441500	1.47785400	-2.21624400

TS_{6B'ba→6HB'ba}

Fe	1.27575600	0.00501500	0.02531900
Fe	-1.26341200	-0.17926800	0.02578300
S	0.08432500	-1.30569800	-1.47255400
S	0.09391300	-1.14665800	1.63890300
P	3.37734400	-0.86909900	0.03171700
P	-3.14321700	-1.45201800	-0.19062100
O	1.98371200	1.58215000	-2.34279300
O	-2.43757900	1.19304800	2.33911400
O	2.05142900	1.80590500	2.20643200
O	-2.18926400	1.46270500	-2.22202700
C	1.70157200	0.98284500	-1.37907400
C	-1.97246200	0.68567100	1.39448600
C	1.73970000	1.11180500	1.31983000
C	-1.82654900	0.82221400	-1.31335700
C	0.11969400	-3.13418600	-1.07568100
C	0.24219600	-3.00109400	1.49239100
C	0.84369800	-3.54822500	0.20143200
C	3.93358700	-1.82469900	1.53429500
C	-4.70166900	-0.48516400	0.14326100
C	3.87342700	-1.93460700	-1.41726900
C	-3.47712500	-2.10241800	-1.90651300
C	4.68706900	0.45699900	-0.04440500
C	-3.41136900	-2.95670100	0.88132000
H	-2.70605200	-3.74950200	0.61198200
H	3.34565600	-2.73829900	1.66235100

Continued on next page

*Continued from previous page***TS_{6B'ba}→6HB'ba**

H	-4.73557700	0.39626900	-0.50655500
H	3.80009000	-1.19570000	2.42141000
H	-4.72190700	-0.15618900	1.18774100
H	4.93596700	-2.19690500	-1.34226300
H	-4.42326300	-2.65720100	-1.91767000
H	3.70385400	-1.37144200	-2.34163900
H	-2.66787600	-2.76034200	-2.23820200
H	3.27936400	-2.85252300	-1.45533600
H	-3.54383100	-1.26106200	-2.60449000
H	4.99320200	-2.09080000	1.43524200
H	-5.58130500	-1.10954800	-0.05432200
H	5.68309100	-0.00193400	-0.05257300
H	-4.43187200	-3.33171400	0.73439900
H	4.60397200	1.11466600	0.82751100
H	-3.27188600	-2.69370100	1.93554000
H	4.56163600	1.05363900	-0.95427900
H	-0.92480300	-3.46820400	-1.06441500
H	0.60289200	-3.58606400	-1.95041000
H	-0.76336400	-3.39799100	1.66944500
H	0.86167800	-3.28450500	2.35218600
H	-0.22243500	1.63062500	0.04463300
O	-0.30864100	2.95276000	0.11616900
C	-1.61962700	3.62961500	0.20022700
H	-2.33473700	2.81312100	0.30274600
H	-1.79748300	4.12629400	-0.75962100
C	-1.69917400	4.58516500	1.38391200
H	-2.72510500	4.96999600	1.44742500
H	-1.46651900	4.07168300	2.32317000
H	-1.03203600	5.44702100	1.26844600
C	0.84632600	3.83819100	-0.14789200
H	1.69535000	3.15568800	-0.18925400
H	0.96163400	4.47575500	0.73551900
C	0.71702700	4.64067800	-1.43664900
H	1.66757800	5.16255600	-1.60687700
H	0.52840000	3.98995900	-2.29726000
H	-0.06761700	5.40367800	-1.37986600
H	1.89360800	-3.24263300	0.13249900
H	0.83984700	-4.64873700	0.25909200

6HB'ba

Fe	-0.30094200	-1.27144100	0.01004100
Fe	-0.29670500	1.30632600	0.07631500
S	-1.45640000	0.07215800	-1.50659200
S	-1.44388300	-0.02607600	1.60791900

Continued on next page

*Continued from previous page***6HB'ba**

P	-1.34252900	-3.29497500	-0.06820800
P	-1.40977200	3.29149100	-0.08024700
O	1.46182000	-2.08409900	-2.19660200
O	1.34604000	2.23882600	2.33015300
O	1.45553400	-2.25665200	2.14839600
O	1.58297100	2.23609900	-1.98225600
C	0.76319800	-1.77825600	-1.32105000
C	0.69502700	1.88674900	1.43567500
C	0.75833300	-1.88154900	1.29900900
C	0.83115900	1.88230300	-1.17049300
C	-3.29913600	0.16539900	-1.19967700
C	-3.29277900	-0.01745100	1.37531600
C	-3.83646400	-0.53426000	0.04571200
C	-2.39796000	-3.76350900	1.39317300
C	-0.35758800	4.74240600	0.42287000
C	-2.38289600	-3.65872600	-1.57038100
C	-1.90521100	3.75296400	-1.81558600
C	-0.13127400	-4.70962900	-0.11202600
C	-2.96667900	3.59467400	0.90000300
H	-3.78375700	2.96803600	0.52842100
H	-3.23930100	-3.07484100	1.50989400
H	0.58503100	4.73146300	-0.13501700
H	-1.78360400	-3.72063300	2.29933500
H	-0.13409300	4.68852900	1.49375300
H	-2.76226400	-4.68651900	-1.51763000
H	-2.41713600	4.72285200	-1.81226100
H	-1.75955200	-3.54858400	-2.46456100
H	-2.56731300	2.99360000	-2.24339800
H	-3.22574100	-2.96579800	-1.64674300
H	-1.00918200	3.82141900	-2.44164900
H	-2.78052700	-4.78326300	1.26349800
H	-0.88891100	5.67842300	0.21315800
H	-0.67720300	-5.65977800	-0.15447800
H	-3.25735700	4.64716600	0.79340000
H	0.49531000	-4.69806500	0.78605100
H	-2.79352500	3.37565400	1.95919900
H	0.51206400	-4.62756000	-0.99441600
H	-3.55548600	1.23183800	-1.19710100
H	-3.74070900	-0.27650000	-2.10099000
H	-3.60890600	1.01303900	1.56734100
H	-3.66726100	-0.63218900	2.20289100
H	0.72965600	0.02177400	0.09155000
O	4.83539200	-0.00212800	-0.00929100
C	5.62218800	0.01576700	1.19403200
H	6.27737900	-0.87303800	1.21754500
H	6.27030100	0.91001200	1.19556300

Continued on next page

*Continued from previous page***6HB'ba**

C	5.66931600	-0.00787000	-1.18099900
H	6.32769600	-0.89428300	-1.15819400
H	6.31398200	0.88882200	-1.17654000
C	4.68652100	0.02690100	2.39628200
H	5.27127300	0.03887000	3.32493800
H	4.04609700	0.91707100	2.38187200
H	4.05053800	-0.86648200	2.40154400
C	4.78253300	-0.02732400	-2.41976900
H	4.13664000	0.85838100	-2.44884100
H	5.40462600	-0.03057900	-3.32394300
H	4.15208400	-0.92447700	-2.43231500
H	-3.64513000	-1.61017200	-0.03425600
H	-4.93166400	-0.41412900	0.05699100

7Bba

Fe	0.65154200	-1.18071800	0.13992400
Fe	0.11569000	1.24779700	0.28830200
S	2.08537800	0.32924200	1.13800300
S	0.76355500	0.22860000	-1.70411700
O	-1.75207000	-2.35186300	-1.04142500
C	-0.76596700	-1.89096200	-0.58404300
C	-0.35590600	1.48668800	1.96941900
C	3.59192800	0.67636000	0.08674000
C	2.49814100	0.66736200	-2.23423700
C	3.34728600	1.42633800	-1.21924700
C	0.15947900	-1.70809100	1.74427200
O	-0.21364500	-2.05869400	2.79777900
C	-1.51151000	1.10506200	-0.21600300
O	-2.66533500	0.98160500	-0.52211400
O	-0.69310500	1.63775100	3.07905700
P	0.39245900	3.46836900	-0.06560300
P	2.01997700	-2.93994400	-0.19215800
C	3.38014500	-3.16888700	1.06527600
C	2.93900800	-3.10660800	-1.80980800
C	1.14886900	-4.58616700	-0.09189800
C	1.77121900	4.34931500	0.83444700
C	0.56645500	4.06199400	-1.82727600
C	-1.08512100	4.46033900	0.49776500
O	-4.62904000	-0.65918500	-0.21003700
C	-4.47918100	-1.63059200	0.94032200
C	-4.14702500	-0.85538000	2.19983500
C	-4.97210400	-1.28819900	-1.54299300
C	-5.23224000	-0.18235000	-2.54670200
H	-4.33494500	0.41799600	-2.73024000

Continued on next page

*Continued from previous page***7Bba**

H	2.97485400	-0.27556800	-2.52719600
H	2.36137700	1.26614300	-3.14331400
H	4.32239000	1.65201000	-1.68087900
H	2.86982300	2.38807700	-0.99459500
H	4.24765000	1.26026400	0.74401000
H	4.07835400	-0.29049900	-0.09658300
H	2.93788800	-3.24008400	2.06505500
H	3.94864800	-4.08323200	0.85348000
H	4.06007200	-2.31055800	1.05249400
H	3.45539500	-4.07379300	-1.85536600
H	2.23235300	-3.03218100	-2.64348600
H	3.68177300	-2.30708500	-1.90303300
H	0.39957900	-4.65617100	-0.88822900
H	1.86579500	-5.40978400	-0.19735500
H	0.64270400	-4.67210400	0.87608000
H	1.73100700	5.42809400	0.63783000
H	1.65855100	4.17135600	1.90971800
H	2.74622300	3.96208400	0.52175400
H	0.62375500	5.15725800	-1.85745700
H	1.46504200	3.64018800	-2.28804400
H	-0.30554700	3.72712900	-2.40005700
H	-0.92570900	5.52957400	0.31056600
H	-1.97725900	4.12863800	-0.04530200
H	-1.24748700	4.30397600	1.57008100
H	-5.45812600	-2.11435800	0.98656300
H	-3.70566600	-2.34591600	0.64544000
H	-4.11880200	-1.57013100	3.03182600
H	-3.16269300	-0.37966100	2.14236000
H	-4.91205200	-0.10320400	2.41950600
H	-5.86467400	-1.87871800	-1.32142200
H	-4.13061700	-1.93587100	-1.80616500
H	-5.52255700	-0.65359500	-3.49408700
H	-6.05079800	0.46801800	-2.22084000
H	-3.79909300	-0.05842800	-0.30404500

TS_{7Bba→7HBba}

Fe	1.55187500	-0.49631500	0.25310300
Fe	-0.81982400	0.34041400	0.46485900
S	1.06290400	1.65293800	0.91179400
S	0.23116400	-0.01374600	-1.60194500
O	1.73523300	-3.25803500	-0.73401400
C	1.64970000	-2.16717700	-0.32966100
C	-1.27521400	0.59372700	2.14547200
C	1.50460100	2.87105800	-0.43803600

Continued on next page

Continued from previous page

TS_{7Bba→7HBba}

C	0.70637800	1.54825000	-2.50124700
C	0.65038600	2.84765300	-1.70251100
C	1.91329800	-0.92300400	1.93495100
O	2.12072200	-1.21337300	3.04370800
C	-0.82382500	-1.38696100	0.80039500
O	-0.93349300	-2.49901800	1.19041800
O	-1.56682500	0.75955900	3.26415300
P	-2.52670700	1.79733800	-0.02574500
P	3.74381200	-0.17053500	-0.19690300
C	4.60412100	1.07043200	0.89498000
C	4.25837400	0.34039400	-1.91620000
C	4.79068200	-1.68769300	0.07187600
C	-2.25602100	3.52195500	0.64917100
C	-3.05642200	2.12064300	-1.79014600
C	-4.18294600	1.41665200	0.74363100
O	-3.17180100	-1.48980900	-0.73794500
C	-2.90610000	-1.74196900	-2.18385800
C	-2.04027200	-2.96219600	-2.46265700
C	-3.75386900	-2.66093600	-0.01276600
C	-4.36630300	-2.21536200	1.30289900
H	-5.21251700	-1.53763400	1.15050000
H	1.71053500	1.36208000	-2.89865500
H	0.02077100	1.59810600	-3.35643300
H	0.98437400	3.66754000	-2.35904900
H	-0.39033400	3.06510200	-1.43674600
H	1.42352900	3.84930000	0.05148900
H	2.56367000	2.70750700	-0.67341100
H	-2.22365800	-0.90995400	-0.18738100
H	4.49770700	0.76115100	1.94033000
H	5.66927000	1.11867000	0.63699300
H	4.15716800	2.06293800	0.78360000
H	5.35345100	0.35826100	-1.98239300
H	3.86517700	-0.37561200	-2.64622800
H	3.87669900	1.33888600	-2.15294900
H	4.49243200	-2.47993200	-0.62278100
H	5.84796100	-1.44543700	-0.08966100
H	4.65842900	-2.05044900	1.09704600
H	-3.13338300	4.14851200	0.44574800
H	-2.10312600	3.45677600	1.73208100
H	-1.37095200	3.98530500	0.20356800
H	-3.81254000	2.91548600	-1.80448700
H	-2.20923200	2.42195900	-2.41267800
H	-3.49631700	1.20930600	-2.20783100
H	-4.87242700	2.25017500	0.56245800
H	-4.58951300	0.50670900	0.29482600
H	-4.07406100	1.26877000	1.82305100

Continued on next page

*Continued from previous page***TS_{7Bba→7HBba}**

H	-3.89919400	-1.81875700	-2.64181300
H	-2.41539100	-0.82212600	-2.51163700
H	-1.86600600	-3.00692800	-3.54544900
H	-1.06608500	-2.88619600	-1.96928700
H	-2.52572900	-3.89887700	-2.16824800
H	-2.95176700	-3.38914800	0.13433300
H	-4.50997000	-3.06337000	-0.69648400
H	-4.73687700	-3.11044300	1.81832700
H	-3.62714500	-1.74075300	1.95604200

7HBba

Fe	-1.91425700	0.54678800	0.26688600
Fe	0.32544700	-0.54716000	0.73475700
S	-1.63367200	-1.75274800	0.31718200
S	-0.16536500	0.53200100	-1.27353300
O	-1.88124800	3.48679300	0.07463000
C	-1.88628000	2.32908500	0.16680400
C	0.44078500	-1.38881700	2.28898400
C	-1.68546300	-2.48095900	-1.40343200
C	-0.41715200	-0.64889500	-2.69224300
C	-0.53446600	-2.12903300	-2.34025100
C	-2.82166400	0.47301900	1.79959800
O	-3.39463800	0.42503800	2.80931100
C	-0.07689700	0.95022000	1.63911700
O	0.04187000	1.82755100	2.40856600
O	0.49492100	-1.95045200	3.30593800
P	2.21261000	-1.69099400	0.17325700
P	-3.90225300	0.53289000	-0.84192800
C	-5.01149500	-0.90419400	-0.43220300
C	-3.91438600	0.59713700	-2.70297100
C	-4.98205100	1.98448600	-0.40142100
C	2.08861800	-3.55366300	0.12322400
C	3.04051100	-1.21221600	-1.41747100
C	3.57569500	-1.43161300	1.40777400
O	5.19119600	1.59673400	-0.47300800
C	4.83709600	2.97172200	-0.22763300
C	3.37551000	3.03785000	0.19675500
C	6.57643400	1.47118900	-0.85055100
C	6.89386000	0.00251600	-1.10307800
H	6.28450600	-0.39336800	-1.92503600
H	-1.29878300	-0.29020200	-3.23431400
H	0.45197100	-0.47715900	-3.33907000
H	-0.67148500	-2.69329900	-3.27675400
H	0.40696300	-2.47689800	-1.89891900

Continued on next page

*Continued from previous page***7HBba**

H	-1.71026200	-3.56229900	-1.22313600
H	-2.65140300	-2.19817400	-1.83967500
H	1.54154900	0.31649300	0.82425700
H	-5.21227500	-0.90756000	0.64444700
H	-5.95878300	-0.80402400	-0.97597100
H	-4.53694900	-1.85320500	-0.69747800
H	-4.94668000	0.72819000	-3.05031100
H	-3.30825400	1.44127100	-3.04863800
H	-3.51774200	-0.33102800	-3.12546400
H	-4.52311900	2.91717900	-0.74538700
H	-5.96253700	1.86956300	-0.87879100
H	-5.11648700	2.03547600	0.68448200
H	3.07490900	-3.97864400	-0.10138600
H	1.75589900	-3.91497100	1.10246800
H	1.37240500	-3.88527600	-0.63469600
H	3.93645200	-1.83191500	-1.54532600
H	2.37448800	-1.36328400	-2.27120300
H	3.33974200	-0.15992800	-1.35795900
H	4.42791500	-2.07055600	1.14701500
H	3.89075400	-0.38329000	1.37747700
H	3.23384400	-1.68213200	2.41703000
H	5.49076700	3.38173900	0.56114000
H	5.00481400	3.56093900	-1.14562000
H	3.08696900	4.08057700	0.37967300
H	2.72201100	2.63368000	-0.58676500
H	3.21246000	2.47296700	1.12316200
H	7.21143400	1.87306200	-0.04257700
H	6.76358700	2.07131800	-1.75758300
H	7.95021400	-0.10821800	-1.37761900
H	6.71065200	-0.59615400	-0.20200100

7B'ba

Fe	0.75725000	-1.09214900	0.15505000
Fe	-0.00316300	1.27596400	0.31639400
S	1.98608000	0.52640500	1.26251400
S	0.83620500	0.37876800	-1.64981600
O	-1.52030200	-2.40401700	-1.11896200
C	-0.58293500	-1.88049000	-0.62811100
C	-0.54230500	1.52397400	1.97905300
C	3.51500400	1.07538900	0.34437300
C	2.54040100	1.04454500	-2.03166400
C	3.66386700	0.60170700	-1.09931100
C	0.23276500	-1.65830400	1.73275100
O	-0.16771900	-2.02789500	2.76934900

Continued on next page

*Continued from previous page***7B'ba**

C	-1.60416000	1.00446200	-0.22332600
O	-2.74365700	0.79762500	-0.54244700
O	-0.91826000	1.67845500	3.07540600
P	0.13776100	3.48155400	-0.16665600
P	2.19635600	-2.78970300	-0.21131900
C	3.81551700	-2.80482800	0.71912600
C	2.70246500	-3.11862400	-1.97852400
C	1.50103900	-4.45203000	0.27524300
C	1.70229200	4.43576700	0.19712700
C	-0.19667800	3.92791000	-1.94749400
C	-1.13325700	4.51807600	0.72189300
O	-4.56629200	-0.98294700	-0.19896300
C	-4.31092200	-1.92878800	0.95374500
C	-4.08369000	-1.11869300	2.21453900
C	-4.85874100	-1.64841400	-1.52610400
C	-5.27490400	-0.58199600	-2.51984400
H	-4.46369900	0.12655800	-2.71864400
H	2.73919100	0.70384900	-3.05521900
H	2.45550000	2.13839200	-2.05465900
H	3.53046900	2.16974500	0.40880200
H	4.34365600	0.69751000	0.95610400
H	3.60770400	-2.75632900	1.79387600
H	4.37364600	-3.72327500	0.49771600
H	4.42660900	-1.93931500	0.44489700
H	3.35822000	-3.99650200	-2.03583900
H	1.80123900	-3.29902400	-2.57521900
H	3.22268500	-2.25060900	-2.39593500
H	0.58234000	-4.64729600	-0.28913300
H	2.22706900	-5.24747300	0.06654400
H	1.26528600	-4.45312100	1.34515500
H	1.54619600	5.50517100	0.00635800
H	1.98387600	4.29198400	1.24602900
H	2.51804100	4.08024200	-0.44144900
H	-0.17201600	5.01630000	-2.08406600
H	0.54793800	3.46288100	-2.60191600
H	-1.18452700	3.54771400	-2.22945600
H	-1.07190500	5.56458700	0.39886300
H	-2.13580400	4.13213300	0.50569800
H	-0.96370800	4.46363400	1.80292900
H	-5.22550100	-2.52579100	0.99386800
H	-3.45640800	-2.54872600	0.66608500
H	-3.97674600	-1.82413000	3.04807800
H	-3.16330700	-0.52826500	2.16467800
H	-4.93513700	-0.46334300	2.42621500
H	-5.66708400	-2.34427000	-1.28777800
H	-3.95072000	-2.18865500	-1.81000500

Continued on next page

*Continued from previous page***7B'ba**

H	-5.52298200	-1.08367200	-3.46364400
H	-6.16140300	-0.03962800	-2.17483400
H	-3.79358900	-0.30905900	-0.30539100
H	4.61604800	0.99287800	-1.49350500
H	3.73951400	-0.49257400	-1.12218600

TS_{7B'ba→7HB'ba}

Fe	1.56094100	-0.44643200	0.29612200
Fe	-0.84252500	0.30400400	0.45863400
S	0.97212800	1.72157100	0.79990700
S	0.22336700	-0.15567000	-1.58416500
O	1.79157700	-3.28057400	-0.43052500
C	1.68209600	-2.15877200	-0.12852000
C	-1.28073000	0.56499800	2.14552500
C	1.19557300	2.90560100	-0.63236300
C	0.66696900	1.34252800	-2.60351800
C	1.65531100	2.31016700	-1.95977600
C	1.85286400	-0.72786600	2.01795100
O	2.00395700	-0.92906000	3.15548600
C	-0.94092600	-1.41958600	0.78857300
O	-1.04080600	-2.54062000	1.14762500
O	-1.56469000	0.72851900	3.26625500
P	-2.46512800	1.86791100	-0.03036100
P	3.76362300	-0.22071300	-0.15655800
C	4.58123300	1.38553000	0.32055200
C	4.31771100	-0.51179800	-1.91513500
C	4.81129600	-1.45696000	0.76411200
C	-2.23614200	3.47438000	0.89923200
C	-2.76144500	2.48955000	-1.76946300
C	-4.20836100	1.45693700	0.49338400
O	-3.26420600	-1.42509400	-0.75861400
C	-3.01206700	-1.66154900	-2.20724400
C	-2.18635300	-2.90448900	-2.50720600
C	-3.90001500	-2.57505100	-0.04920900
C	-4.49357300	-2.11014100	1.26900300
H	-5.29459600	-1.37922600	1.11877200
H	1.09323700	0.92087600	-3.52200700
H	-0.27148200	1.84043700	-2.87179400
H	0.24489800	3.44057600	-0.74946300
H	1.93450300	3.62752500	-0.26330400
H	-2.28700100	-0.89278300	-0.18891000
H	4.38522100	1.58478100	1.37966100
H	5.66370500	1.31595100	0.15627700
H	4.18096100	2.21477200	-0.27076500

Continued on next page

Continued from previous page

TS_{7B'ba}→7HB'ba

H	5.40891400	-0.42192500	-1.98410700
H	4.02021900	-1.52158300	-2.21899100
H	3.85349600	0.20817800	-2.59670100
H	4.50419800	-2.47546700	0.50318300
H	5.86773000	-1.32140500	0.50267000
H	4.68830300	-1.31710800	1.84337400
H	-3.04106600	4.17350900	0.64111900
H	-2.26646000	3.27306800	1.97535700
H	-1.27048200	3.93095800	0.66332700
H	-3.63804600	3.14922800	-1.77257000
H	-1.89628600	3.05992400	-2.12143800
H	-2.94197000	1.65499600	-2.45494300
H	-4.84746700	2.33894700	0.36366900
H	-4.59277100	0.63239700	-0.11271500
H	-4.21634400	1.16067300	1.54799700
H	-4.00766500	-1.69787000	-2.66494000
H	-2.49309700	-0.75235200	-2.52156600
H	-2.01968800	-2.94253100	-3.59146500
H	-1.20749800	-2.86213800	-2.01837100
H	-2.69976100	-3.82856400	-2.22009200
H	-3.13392400	-3.34259100	0.09258600
H	-4.67286000	-2.93669900	-0.73713300
H	-4.92075100	-2.98640700	1.77258400
H	-3.73088700	-1.68787400	1.93124800
H	1.83981600	3.13706200	-2.66445700
H	2.61342300	1.79713000	-1.81504300

7HB'ba

Fe	1.61910000	-0.49206800	0.44305700
Fe	-0.56235300	0.82159800	0.58380800
S	1.54818200	1.81981800	0.43575900
S	0.10136500	-0.36279500	-1.30918100
O	1.23681900	-3.41128300	0.44257200
C	1.37178800	-2.25687000	0.45666100
C	-0.81695600	1.79864900	2.04274100
C	1.81850100	2.58448400	-1.24514700
C	0.60235000	0.80934600	-2.67231000
C	1.86225900	1.63893100	-2.44179200
C	2.30273100	-0.40789200	2.08569500
O	2.72188200	-0.34132400	3.16700200
C	-0.51358700	-0.63463200	1.60927400
O	-0.80228200	-1.47284100	2.37417900
O	-0.95130700	2.44131900	3.00181500
P	-2.17630000	2.04369200	-0.46421000

Continued on next page

*Continued from previous page***7HB'ba**

P	3.68290300	-0.88742000	-0.41630400
C	4.87122200	0.54375500	-0.49157400
C	3.74506100	-1.67250800	-2.10418700
C	4.64937800	-2.11105500	0.60243800
C	-1.74152500	3.65662400	-1.30294900
C	-3.12614900	1.10620500	-1.75461300
C	-3.51794600	2.59055900	0.69927300
O	-4.29200100	-2.03578700	-0.43534800
C	-4.12670900	-3.16351300	-1.31618600
C	-3.35046200	-2.72302800	-2.55125200
C	-5.05612200	-2.39183200	0.73253300
C	-5.19043700	-1.16877500	1.63095800
H	-4.20431700	-0.82287800	1.96611100
H	0.73255700	0.16141100	-3.54757400
H	-0.26608000	1.45060900	-2.86434800
H	2.72088300	0.96523000	-2.34187400
H	2.04195900	2.24263800	-3.34589200
H	1.03371700	3.34072000	-1.35500800
H	2.77334600	3.11515400	-1.14698200
H	-1.88510800	0.11771400	0.55131600
H	4.95604100	0.98836100	0.50592300
H	5.85552100	0.18151300	-0.81270500
H	4.52492700	1.30999800	-1.19050300
H	4.78828900	-1.86700600	-2.38215900
H	3.19782000	-2.62119200	-2.07431200
H	3.28431300	-1.02645300	-2.85718900
H	4.10922500	-3.06094400	0.67128500
H	5.62457900	-2.28734500	0.13271200
H	4.80600100	-1.71728800	1.61223500
H	-2.66744200	4.14655200	-1.62962500
H	-1.21734400	4.31234200	-0.59911100
H	-1.10849700	3.48647700	-2.17939600
H	-3.91722300	1.74965200	-2.15938900
H	-2.46884400	0.78734400	-2.56999600
H	-3.56767300	0.21367400	-1.29463100
H	-4.32838200	3.05625300	0.12576600
H	-3.90853300	1.72467100	1.24263700
H	-3.12517300	3.31702200	1.41810300
H	-3.58930700	-3.96611600	-0.78176500
H	-5.11936900	-3.55319000	-1.60011400
H	-3.20533500	-3.57919600	-3.22221300
H	-3.89984100	-1.94809300	-3.10038000
H	-2.36441200	-2.33081900	-2.27254000
H	-4.54686500	-3.21302500	1.26545800
H	-6.05010900	-2.75553100	0.42055100
H	-5.69909300	-0.35337100	1.10105100

Continued on next page

*Continued from previous page***7HB'ba**

H	-5.78274700	-1.42051700	2.51939300
---	-------------	-------------	------------

6Cba

Fe	-0.11000200	1.25188200	0.42003800
Fe	-0.85334000	-1.21857200	0.17425900
H	3.49961600	-0.10937500	-0.85353200
S	-2.22280200	0.46317100	0.85924700
S	0.57821700	-0.46319500	1.79223400
P	-0.91958100	2.68956400	-1.15305900
P	-2.23244800	-1.74303600	-1.56216100
O	0.70157000	3.39816300	2.24592400
O	2.38743100	0.91030300	-1.04525300
O	1.40082000	-2.39008400	-1.29505600
O	-1.76022200	-3.51453600	1.74245800
C	0.31249800	2.56195700	1.52422200
C	1.33465300	1.03751500	-0.47314300
C	0.49512900	-1.91369700	-0.71370700
C	-1.42376900	-2.60338100	1.08702400
C	-2.05583500	-0.91300400	-3.22727900
H	-2.31689600	0.14723900	-3.15464200
H	-2.72115600	-1.39159000	-3.95689900
H	-1.01976800	-1.00372000	-3.57217100
C	-4.05565400	-1.57528500	-1.22056700
H	-4.63771800	-1.91047500	-2.08774700
H	-4.29603400	-0.53218300	-0.98960900
H	-4.31271900	-2.18895800	-0.35010600
C	-2.09022600	-3.53602800	-2.05439300
H	-2.80240500	-3.76865200	-2.85557700
H	-2.29891900	-4.17474900	-1.18961400
H	-1.07326300	-3.74308100	-2.40537500
C	-0.24425700	-0.41886800	3.47053100
H	-0.56810100	-1.44858100	3.66795600
H	0.56834900	-0.17410200	4.16519200
C	-1.39431300	0.57406800	3.62741500
H	-1.75866700	0.50383000	4.66527100
H	-1.02397000	1.59756400	3.49315400
C	-2.57734800	0.32772100	2.69402000
H	-3.36093100	1.07328700	2.87447800
H	-3.01142300	-0.66860000	2.84251600
C	-2.75928800	2.77982500	-1.44743400
H	-3.15294600	1.80417900	-1.74819500
H	-2.96733000	3.51817100	-2.23183100
H	-3.25993100	3.07684300	-0.52025700
C	-0.22833700	2.50133900	-2.87691600

Continued on next page

*Continued from previous page***6Cba**

H	-0.71441900	3.20259500	-3.56624000
H	-0.37158000	1.47675700	-3.23138400
H	0.84666200	2.71279400	-2.85245800
C	-0.52473700	4.48175200	-0.81817500
H	-1.00324600	4.79912300	0.11449000
H	-0.88505800	5.10908400	-1.64275500
H	0.55853900	4.60775800	-0.71413400
O	4.27322700	-0.78091800	-0.73280100
C	4.30179700	-1.34859100	0.66992200
H	3.27260600	-1.21958800	1.01843500
H	4.97482600	-0.71289100	1.25370700
C	5.55553600	-0.25546000	-1.31881300
H	6.27591000	-1.05699800	-1.14024100
H	5.32987300	-0.20150300	-2.38688300
C	4.72614100	-2.80194800	0.60964400
H	5.75236400	-2.92317300	0.24406200
H	4.68929700	-3.20502800	1.62985700
H	4.04221500	-3.38163800	-0.01797000
C	5.97254500	1.08129900	-0.72900400
H	6.18691400	1.01633300	0.34348400
H	6.89622300	1.39469500	-1.23227000
H	5.21394400	1.85233600	-0.90209900

TS_{6Cba→6HCba}

Fe	1.51766000	-0.18245300	-0.26351500
Fe	-1.10797800	-0.79949800	-0.44627600
H	-0.55205800	1.30944500	-0.42899600
S	0.34035300	-1.47977700	1.19322400
S	0.54992600	-1.43892300	-1.89359000
P	2.25000700	1.14600400	1.46950600
P	-2.64415400	-0.41790000	1.22484700
O	4.17745800	-1.38782500	-0.28175000
O	2.44769400	1.58728100	-2.40950000
O	-2.44941300	0.70807500	-2.57197100
O	-2.59494600	-3.23980200	-1.08759400
C	3.09935200	-0.93617300	-0.25193700
C	2.02363800	0.93842700	-1.53411900
C	-1.89912300	0.14320000	-1.70538500
C	-2.00461100	-2.27557700	-0.78916400
C	-2.34579400	0.78898900	2.62129400
H	-1.48872600	0.42690000	3.19970700
H	-3.22560600	0.82391600	3.27552300
H	-2.12640600	1.79474100	2.25306100
C	-2.97163400	-1.95908400	2.22609800

Continued on next page

*Continued from previous page***TS**_{6Cba→6HCba}

H	-3.70763600	-1.74323700	3.01012300
H	-2.03726100	-2.29463200	2.68825200
H	-3.35859800	-2.75404800	1.58050000
C	-4.37639900	-0.02540000	0.64412600
H	-5.05471900	0.06093800	1.50158000
H	-4.71762400	-0.84349600	-0.00058600
H	-4.41341400	0.90020900	0.06073400
C	0.90097800	-3.26123400	-1.64649900
H	-0.04116500	-3.77433600	-1.87295200
H	1.61168200	-3.49907600	-2.44718300
C	1.47620000	-3.69549600	-0.29673100
H	1.55464400	-4.79452700	-0.31212500
H	2.49902700	-3.31941600	-0.19185300
C	0.66226600	-3.31209500	0.93902100
H	1.19100300	-3.62924000	1.84577700
H	-0.32799600	-3.78297500	0.93805000
C	1.15234500	2.32060900	2.41671600
H	0.71369600	3.06108900	1.74323800
H	1.74619400	2.82933500	3.18611900
H	0.34607000	1.75952800	2.89686700
C	3.67101300	2.25273400	0.98402700
H	4.07143000	2.76586700	1.86662300
H	3.34160900	3.00212500	0.25542600
H	4.46595600	1.65279400	0.52755900
C	2.99343000	0.15261700	2.85985700
H	2.22398500	-0.49373100	3.29608600
H	3.39029800	0.82351900	3.63123200
H	3.80501600	-0.47339500	2.47463300
O	-0.77267700	2.54681400	-0.34160800
C	-2.19644700	2.96164900	-0.37550700
H	-2.71132100	2.11062100	0.07104700
H	-2.50570300	3.04820100	-1.42115300
C	0.15746600	3.46466000	-1.05433800
H	0.09436200	4.41672600	-0.51732500
H	1.13441800	3.02170300	-0.86279700
C	-2.43020600	4.24211900	0.41490700
H	-1.98128000	5.11890200	-0.06487000
H	-3.51222700	4.41940500	0.46563300
H	-2.04855200	4.16214500	1.43939000
C	-0.12812200	3.61454300	-2.54156200
H	-1.07060300	4.13822900	-2.73673200
H	0.67896700	4.21476000	-2.98009000
H	-0.14251700	2.64611100	-3.05082900

6HCba

Fe	-0.68016900	-1.33680700	-0.37621100
Fe	-1.25580800	1.20848500	-0.30125600
H	0.07383900	0.17919100	-0.25282900
S	-1.92178300	-0.31933000	1.28645900
S	-2.11844500	-0.28043700	-1.82876400
P	0.82521900	-2.16436400	1.15370700
P	-0.13544900	2.53568900	1.20008900
O	-1.81756300	-4.02604900	-0.56214900
O	1.22013000	-1.74540900	-2.57924500
O	0.09760800	2.64105500	-2.48487300
O	-3.66608200	2.86269000	-0.21134200
C	-1.38809600	-2.94603600	-0.47623300
C	0.46667900	-1.60066400	-1.70705300
C	-0.44167000	2.08000900	-1.62188500
C	-2.69180000	2.22468000	-0.24600200
C	-0.28610900	2.12211200	3.00856000
H	-1.33507000	2.20761100	3.31211200
H	0.32158900	2.82185500	3.59516800
H	0.04119800	1.09697600	3.20374100
C	-0.69422100	4.31158000	1.16741300
H	-0.07966800	4.90882500	1.85180500
H	-1.74348000	4.38193300	1.47335400
H	-0.59438800	4.71318800	0.15301800
C	1.69302200	2.71052500	0.90468200
H	2.14390900	3.30834800	1.70640900
H	1.84803200	3.22547400	-0.05019800
H	2.18390400	1.73530500	0.84692200
C	-3.91376200	-0.62757000	-1.43951200
H	-4.41823500	0.34489800	-1.49140900
H	-4.25117300	-1.22712300	-2.29318300
C	-4.22313500	-1.35619700	-0.13247300
H	-5.31772600	-1.46214100	-0.06674400
H	-3.81784600	-2.37343200	-0.16547600
C	-3.75560300	-0.65241100	1.14076600
H	-3.98768100	-1.26738900	2.01808400
H	-4.24451600	0.32051300	1.27080200
C	2.10560600	-1.02351700	1.85886800
H	2.74416700	-0.63065000	1.05650600
H	2.72377000	-1.57825800	2.57625400
H	1.61489200	-0.19651700	2.38058300
C	1.85712200	-3.56450100	0.49195700
H	2.49497400	-3.96116200	1.29086200
H	2.49124700	-3.20578600	-0.32558200
H	1.21110000	-4.36597100	0.11772600
C	0.02670300	-2.91743700	2.65544300
H	-0.55085400	-2.15436000	3.18684200

Continued on next page

*Continued from previous page***6HCba**

H	0.79673600	-3.32636700	3.32104900
H	-0.64847700	-3.72445700	2.35022300
O	4.36312000	0.27813100	-0.27690200
C	4.60089800	0.13278000	-1.69920200
H	3.81402700	-0.54211600	-2.05571800
H	5.56875600	-0.36452100	-1.86508000
C	5.53939800	0.66264100	0.47486600
H	6.10896200	1.42007700	-0.08494100
H	5.15585300	1.14183500	1.38461000
C	4.53926400	1.46739600	-2.44669800
H	5.30591900	2.16757100	-2.09204200
H	4.70937600	1.30142400	-3.51880400
H	3.55538000	1.93697100	-2.32453800
C	6.42681700	-0.53279300	0.83335200
H	6.81647400	-1.03222900	-0.06224300
H	7.28634500	-0.19528700	1.42774400
H	5.86677700	-1.26838400	1.42401800

7Cba

Fe	0.17442600	1.09324100	0.41048900
Fe	-1.21775700	-1.08581500	0.15702000
S	-2.10525900	0.96412500	0.63400600
S	0.21879500	-0.66549300	1.88984100
P	-0.09884900	2.86306000	-0.97339200
P	-2.38223700	-1.25653400	-1.79438200
O	2.42207600	0.04812900	-1.13380200
O	1.46417900	2.82957700	2.38504600
O	0.75267800	-2.94152300	-0.96720700
O	-2.88796300	-3.07867500	1.49917000
C	1.47216700	0.45447900	-0.50854700
C	0.90278700	2.17605700	1.58777500
C	-0.03531300	-2.19075400	-0.52039000
C	-2.24746000	-2.26210000	0.95832000
C	-3.88348200	-0.17968300	-2.03243700
H	-4.34986600	-0.40449300	-2.99945000
H	-3.61276400	0.87898300	-1.98770800
H	-4.59626700	-0.38186600	-1.22572200
C	-3.10484100	-2.95688900	-2.04972900
H	-3.60116800	-3.01410500	-3.02620900
H	-3.83296700	-3.17565900	-1.26164600
H	-2.30682800	-3.70654100	-2.00674300
C	-1.42922300	-1.04816600	-3.38492200
H	-2.09441000	-1.17262300	-4.24846900
H	-0.64087700	-1.80785700	-3.42646100

Continued on next page

*Continued from previous page***7Cba**

H	-0.96332300	-0.06061800	-3.42062900
C	-0.66061700	-0.19719100	3.47273300
H	-0.44833600	-1.03098200	4.15297200
H	-0.14413200	0.69422900	3.84998900
C	-2.16841100	0.02714100	3.36806000
C	-2.58313500	1.16268400	2.43588200
H	-2.15214000	2.12116400	2.74962800
H	-3.67519700	1.26072800	2.42392100
C	-1.11252400	4.24143400	-0.23905600
H	-0.65135500	4.57481200	0.69701700
H	-1.17259300	5.08684700	-0.93552600
H	-2.11946900	3.86830300	-0.02423500
C	-0.87232500	2.66428500	-2.65691600
H	-0.97300600	3.64339000	-3.14129600
H	-0.23780200	2.02150300	-3.27634800
H	-1.86281100	2.21013800	-2.55708800
C	1.49951400	3.72274600	-1.39963400
H	1.30861600	4.61532900	-2.00808900
H	2.01368900	4.01735100	-0.47823900
H	2.14495000	3.03652200	-1.95966000
H	3.58317600	-0.85779000	-0.84058600
O	4.41810900	-1.45919800	-0.70799600
C	4.08475000	-2.74594800	0.01692800
H	3.22002800	-3.11407100	-0.53964600
H	4.95604400	-3.37574500	-0.18247000
C	5.59009500	-0.66265300	-0.20719700
H	5.28613600	-0.18625700	0.73011300
H	6.35939200	-1.41619000	-0.01809200
C	5.98983800	0.32781500	-1.28453900
H	6.26788400	-0.18540900	-2.21079800
H	5.18713200	1.04427500	-1.49072300
H	6.86020800	0.88957400	-0.92315500
C	3.80159700	-2.54885900	1.49453100
H	2.94817200	-1.88234000	1.66594700
H	3.54111900	-3.53200500	1.90822200
H	4.67716100	-2.18358900	2.04322000
H	-2.66351500	-0.90221600	3.06351600
H	-2.54169200	0.26527500	4.37745300

TS_{7Cba→7HCba}

Fe	0.74733600	0.22046100	0.45327800
Fe	-1.55535300	-0.74447800	-0.31885400
S	-1.18836200	0.21914700	1.70822900
S	0.28809000	-2.01228600	0.10793500

Continued on next page

*Continued from previous page***TS**_{7Cba→7HCba}

P	1.06177000	2.39161300	1.05218600
P	-3.13298600	0.82588400	-0.90692900
O	0.64540900	1.27737300	-2.28413600
O	2.98793300	-0.34071100	2.26563500
O	-1.39917300	-1.48970400	-3.16133700
O	-3.62242700	-2.70475100	0.30336900
C	0.61857800	0.77480400	-1.21442900
C	2.08576100	-0.11268900	1.54704700
C	-1.44924600	-1.18746700	-2.03717000
C	-2.79848700	-1.91269600	0.06386400
C	-4.59486400	0.05818400	-1.77126900
H	-4.26180600	-0.47395900	-2.66921400
H	-5.30856300	0.83863900	-2.06185500
H	-5.09404500	-0.65318100	-1.10500600
C	-2.63527800	2.14341000	-2.12389000
H	-3.49826900	2.78003500	-2.35417400
H	-2.27513500	1.67138600	-3.04403200
H	-1.82970000	2.75512400	-1.71191300
C	-3.95515000	1.76398500	0.47328900
H	-4.69624300	2.45705200	0.05757000
H	-3.21445200	2.31695300	1.05811500
H	-4.45362700	1.05141000	1.13951300
C	0.23774800	-2.86412800	1.77159600
H	0.18380000	-3.93078700	1.52315500
H	1.21180800	-2.66938800	2.23692400
C	-0.91243500	-2.48656500	2.70457700
C	-0.97361300	-1.01321200	3.10262500
H	-0.06430400	-0.70025000	3.62941800
H	-1.83209100	-0.83842300	3.76174700
C	1.03342200	2.69554200	2.88842300
H	0.04494200	2.43706400	3.28354100
H	1.24308700	3.75213800	3.09445300
H	1.78960700	2.07535200	3.38116500
C	-0.11659600	3.68429000	0.41729800
H	0.15991100	4.66458000	0.82390700
H	-1.13779200	3.44408400	0.72943000
H	-0.06390100	3.72301800	-0.67562300
C	2.70785300	3.08870000	0.53792200
H	3.51524100	2.47195000	0.94643200
H	2.81673200	4.11720300	0.90307600
H	2.77923800	3.08593800	-0.55487500
H	2.24602800	-0.20769300	-0.54882100
O	3.33700000	-0.62566600	-1.12679100
C	3.71591700	-1.98752500	-0.68065600
H	3.24436500	-2.09616900	0.29827700
H	3.26184800	-2.70743800	-1.37236800

Continued on next page

*Continued from previous page***TS_{7Cba→7HCba}**

C	3.39603600	-0.44204000	-2.60132800
H	4.04816100	-1.23542000	-2.97978600
H	2.38352700	-0.59479400	-2.98983400
C	3.95231200	0.93320500	-2.92838000
H	3.30050200	1.72766900	-2.55242000
H	4.95773900	1.05931100	-2.51168500
H	4.01167900	1.03822200	-4.01926500
C	5.22966500	-2.11583800	-0.58934500
H	5.64006700	-1.38131400	0.11201100
H	5.47799000	-3.12065700	-0.22408400
H	5.71468800	-1.98772700	-1.56446500
H	-0.79266200	-3.07429800	3.62894900
H	-1.86698800	-2.79552400	2.26429300

7HCba

Fe	-0.38584500	1.13479700	-0.19108200
Fe	1.99619700	-0.59098500	-0.58758100
S	1.58213500	1.01805900	1.11475200
S	1.10426800	0.99897100	-1.99432000
P	-1.60766300	1.39151100	1.67033700
P	2.38538900	-2.15530300	0.98783500
O	-1.42885200	-1.60980300	-0.38767700
O	-0.95845700	3.93943600	-0.83681900
O	1.28034900	-2.70529000	-2.49927000
O	4.84388300	-0.57950900	-1.40432700
C	-0.88171600	-0.57409400	-0.29746200
C	-0.64780900	2.84745200	-0.53788100
C	1.52588500	-1.85296500	-1.72937100
C	3.72900400	-0.52674700	-1.03143800
C	3.29395200	-3.66323500	0.36678600
C	0.95286100	-2.94814000	1.89162300
C	3.48476500	-1.61333800	2.39510600
C	2.17858800	2.53060800	-1.89167500
C	3.11477800	2.66048900	-0.68444600
C	2.46078900	2.61850500	0.69907600
C	-1.14407200	2.86890600	2.70935200
C	-1.54871400	0.02457400	2.93604100
C	-3.43426700	1.62696700	1.40726000
O	-5.10446600	-0.86759200	-0.45190000
C	-4.84562600	-0.51269200	-1.82523400
C	-5.19233000	-2.28497200	-0.23215500
C	-5.41436200	-2.52007600	1.25830400
C	-6.09104000	-0.60004400	-2.71502300
H	3.88516100	1.88292800	-0.73557800

Continued on next page

*Continued from previous page***7HCba**

H	2.68691800	-4.17485400	-0.38796800
H	3.50376300	-4.35308600	1.19398700
H	4.23652900	-3.35192800	-0.09663700
H	1.31675300	-3.70720300	2.59645100
H	0.27904600	-3.41317100	1.16397000
H	0.39593700	-2.18160300	2.43952700
H	3.65762500	-2.44112600	3.09500400
H	3.01381800	-0.77225400	2.91457900
H	4.44232700	-1.27518200	1.98330600
H	2.77666900	2.50131200	-2.81146500
H	1.49803100	3.38852200	-1.96155800
H	1.72323100	3.42188100	0.82114100
H	3.23370500	2.73882300	1.46904600
H	-0.08825200	2.78442000	2.99017300
H	-1.76260900	2.91330100	3.61491400
H	-1.28721500	3.78696700	2.12911700
H	-2.18522600	0.27261200	3.79490500
H	-0.51335100	-0.09457600	3.27461600
H	-1.89471600	-0.91205000	2.48634300
H	-3.58825000	2.50229700	0.76545800
H	-3.94795300	1.78584500	2.36464600
H	-3.85514000	0.74641900	0.90633300
H	-1.56731600	1.15760900	-1.12555900
H	-4.48030000	0.52035300	-1.78573900
H	-4.03326800	-1.14492700	-2.22062300
H	-6.02753500	-2.71211600	-0.81212600
H	-4.25812300	-2.76421800	-0.57150700
H	-4.57741500	-2.11772300	1.84221600
H	-6.33839900	-2.03261100	1.59250100
H	-5.49406700	-3.59586800	1.46237700
H	-6.89520000	0.02750900	-2.31123300
H	-5.84933200	-0.24656800	-3.72686000
H	-6.46239900	-1.62893100	-2.80200600
H	3.63529000	3.62934100	-0.77924100

8Cba

Fe	0.47149700	0.53196000	0.34037600
Fe	-1.70571900	-0.85133400	0.05958500
S	-1.59546100	1.10189600	1.26387900
S	0.10079100	-1.53957400	1.27557000
P	0.69709500	2.69461400	-0.21538200
P	-3.19773100	0.00843400	-1.43778800
O	0.79814200	-0.30569600	-2.43458900
O	3.25885000	0.27149300	1.11032600

Continued on next page

*Continued from previous page***8Cba**

O	-1.28135100	-3.08915400	-1.79991000
O	-3.74875100	-2.12848500	1.70855800
C	0.52995000	-0.02364200	-1.31782800
C	2.08569100	0.46641500	0.85767800
C	-1.43659300	-2.18971500	-1.07131500
C	-2.94922100	-1.61809200	1.02491800
C	-4.21000600	1.47744500	-0.90590800
H	-4.89498300	1.76827500	-1.711178400
H	-3.55777800	2.31751000	-0.65136900
H	-4.78712800	1.21031700	-0.01388900
C	-4.52782000	-1.21625300	-1.89390800
H	-5.22322700	-0.76823300	-2.61416800
H	-5.08107100	-1.51220800	-0.99598400
H	-4.07624600	-2.10975200	-2.33865100
C	-2.55713400	0.49782100	-3.11861600
H	-3.38807900	0.81176300	-3.76230900
H	-2.04627100	-0.35726700	-3.57415800
H	-1.83820000	1.31668900	-3.02580200
C	-0.17151600	-1.36666800	3.11624700
H	-1.03352500	-2.00205700	3.35677800
H	0.72183200	-1.82147100	3.56140600
C	-0.35856700	0.05975400	3.62995200
H	-0.42038800	0.01933800	4.72952400
H	0.52390300	0.66196600	3.36897800
C	-1.61475800	0.74792200	3.10122100
H	-1.73470300	1.73496600	3.56374900
H	-2.51933400	0.16285600	3.30809200
C	-0.66501800	3.57395300	-1.13331600
H	-1.59011700	3.51829300	-0.55095000
H	-0.39520300	4.62680500	-1.28224000
H	-0.81786400	3.10184100	-2.10894000
C	2.17772000	3.08353200	-1.27933700
H	2.23969800	4.16023400	-1.47923400
H	3.08971100	2.76302000	-0.76361600
H	2.09778100	2.54330600	-2.22937800
C	0.95021700	3.80284900	1.25898300
H	1.10101800	4.84252700	0.94225200
H	0.06748700	3.74231900	1.90485600
H	1.82300700	3.45929300	1.82453400
O	4.79399400	-1.39447900	0.01804100
H	4.11110200	-0.71780900	0.45339300
C	4.18429700	-2.16184100	-1.13113000
H	5.04722700	-2.58946200	-1.64913800
H	3.67636900	-1.43522900	-1.77272200
C	6.11987800	-0.73017300	-0.22049300
H	6.36418100	-0.31552200	0.76099000

Continued on next page

*Continued from previous page***8Cba**

H	6.79376100	-1.56220900	-0.44280400
C	3.25706100	-3.21703800	-0.56229100
H	2.43018700	-2.77276900	0.00330000
H	2.82511400	-3.77387100	-1.40376200
H	3.80330600	-3.91937600	0.07608000
C	6.07846400	0.32134900	-1.31631200
H	5.37401700	1.12560900	-1.07670900
H	7.08015400	0.76261200	-1.39690400
H	5.82534400	-0.10658300	-2.29270900

TS_{8Cba→8HCba}

Fe	-0.57086800	0.42130200	0.30103200
Fe	1.71141300	-0.75721100	0.25661500
S	0.69131900	0.07959000	-1.65240700
S	-0.31706500	-1.82027300	0.65731100
P	-1.29809800	2.38842800	-0.53898600
P	3.60629100	0.49602900	-0.13495200
O	1.39001900	1.93047000	1.83024000
O	-2.11420300	0.77511400	2.74788900
O	2.56964000	-1.42814200	2.99018100
O	2.86442700	-3.15302100	-0.96628000
C	0.85978300	1.14337700	1.11462000
C	-1.51489700	0.61470600	1.74847700
C	2.23524900	-1.14650100	1.91308900
C	2.42335200	-2.18867700	-0.47921500
C	4.80977200	-0.31195200	-1.30374600
H	5.67559900	0.34349700	-1.45686800
H	4.32097100	-0.49626800	-2.26683200
H	5.15193300	-1.26747600	-0.89243900
C	4.64738500	0.84708900	1.36574400
H	5.51598100	1.45343300	1.08187200
H	4.99389100	-0.09300400	1.80823500
H	4.04854500	1.39080000	2.10415400
C	3.41232900	2.18438700	-0.89274300
H	4.40615500	2.59947500	-1.10004200
H	2.88623000	2.84070000	-0.19397300
H	2.84719400	2.10448700	-1.82710100
C	-0.77295300	-2.85550100	-0.83526500
H	0.04498500	-3.57259800	-0.97607700
H	-1.65302700	-3.41765100	-0.49938400
C	-1.08895200	-2.10198300	-2.12634400
H	-1.42716000	-2.83897900	-2.87295400
H	-1.92026800	-1.40655800	-1.94640900
C	0.09007900	-1.33219400	-2.71486600

Continued on next page

*Continued from previous page***TS_{8Cba→8HCba}**

H	-0.19548200	-0.86241500	-3.66379300
H	0.94985900	-1.98612000	-2.90399000
C	-1.85879000	2.40068100	-2.32231200
H	-2.65145200	1.66609900	-2.49609100
H	-2.22464000	3.39871500	-2.59405400
H	-1.00427200	2.14091400	-2.95628400
C	-0.07268200	3.79397600	-0.57657900
H	-0.55244600	4.69940200	-0.96812100
H	0.30416100	3.98635300	0.43315000
H	0.76564800	3.52150800	-1.22564900
C	-2.72392700	3.20002600	0.35214300
H	-2.99488500	4.13999800	-0.14371300
H	-3.59692900	2.53937700	0.37116100
H	-2.43092900	3.41266200	1.38615700
H	-2.48627200	-0.22960800	0.16048900
O	-3.49753300	-0.81531600	0.03538700
C	-3.86886800	-1.69612600	1.19229500
H	-4.24692800	-2.61545600	0.73505900
H	-2.89765200	-1.89463400	1.65526100
C	-4.58487900	-0.13361600	-0.70926200
H	-5.14611900	0.48768000	-0.00309300
H	-4.04113400	0.50878000	-1.40584100
C	-4.85994000	-1.07012000	2.15938300
H	-5.85023500	-0.92395000	1.71258800
H	-4.98137200	-1.76756100	2.99833500
H	-4.48981700	-0.12358900	2.56562900
C	-5.46410600	-1.14009400	-1.43537500
H	-6.19473600	-0.58807700	-2.04022900
H	-4.87194100	-1.77338600	-2.10511000
H	-6.02514100	-1.77656600	-0.74184900

8HCba

Fe	-0.29389200	0.34333700	0.49873900
Fe	2.03732400	-0.70106000	0.27705300
S	0.70224300	-0.22470400	-1.52026300
S	0.23755600	-1.78649100	1.15873100
P	-1.41027300	2.06368100	-0.48170900
P	3.71479200	0.64598400	-0.60691400
O	1.68306300	2.29189100	1.48450100
O	-1.67787800	0.63686500	3.06609900
O	3.38835200	-0.81225100	2.89609000
O	3.21955100	-3.16015400	-0.74457900
C	1.07407600	1.39295600	1.03150500
C	-1.11498800	0.53914800	2.05546400

Continued on next page

*Continued from previous page***8HCba**

C	2.85543700	-0.75678800	1.86665000
C	2.77936400	-2.16064600	-0.33849600
C	4.75896500	-0.23703800	-1.86897600
H	5.52233400	0.44633000	-2.25983800
H	4.12701100	-0.58249100	-2.69448000
H	5.25224100	-1.10184100	-1.41302800
C	4.96724200	1.27969900	0.61284600
H	5.71527100	1.88728000	0.08973800
H	5.46822400	0.43990300	1.10609000
H	4.46733800	1.89283100	1.37018300
C	3.22107100	2.18956600	-1.52524500
H	4.11624900	2.63313400	-1.97799900
H	2.77655000	2.90923400	-0.83205700
H	2.50299900	1.93755500	-2.31270500
C	-0.48649500	-3.02858100	-0.03619300
H	0.31421100	-3.75183500	-0.23517100
H	-1.25520300	-3.53258700	0.56146900
C	-1.09070100	-2.47565300	-1.32406500
H	-1.51196600	-3.32265000	-1.88893700
H	-1.92215700	-1.80057300	-1.07961400
C	-0.09684800	-1.75789100	-2.23283500
H	-0.59691300	-1.40131800	-3.14108200
H	0.72846200	-2.41316300	-2.53666400
C	-2.17471400	1.61696100	-2.11331800
H	-2.84977400	0.76844900	-1.96009000
H	-2.74144300	2.47380600	-2.49808300
H	-1.39398000	1.34748100	-2.83242400
C	-0.46203200	3.61911200	-0.86426100
H	-1.13945700	4.35820300	-1.30896100
H	-0.03000000	4.03131000	0.05361200
H	0.34170300	3.39864900	-1.57426800
C	-2.86527100	2.67313200	0.49329000
H	-3.34412700	3.49738100	-0.04929800
H	-3.57756600	1.84759500	0.60853100
H	-2.54472800	3.03096000	1.47746500
H	-1.65863900	-0.17260800	0.09832500
O	-4.78713900	-0.23758800	-0.15069300
C	-5.00216800	-1.18873500	0.91973800
H	-5.58591100	-2.04501000	0.54764500
H	-4.00129500	-1.55500500	1.18050300
C	-5.95197200	-0.02690900	-0.98476200
H	-6.85777200	0.01300000	-0.36088200
H	-5.81206200	0.96669000	-1.42872400
C	-5.67559900	-0.56097700	2.14340500
H	-6.67459100	-0.17575800	1.90455900
H	-5.78984700	-1.31497000	2.93372200

Continued on next page

*Continued from previous page***8HCba**

H	-5.07069000	0.26325800	2.54007700
C	-6.08959000	-1.08852200	-2.07970400
H	-6.96431100	-0.86869700	-2.70615500
H	-5.20014300	-1.10088200	-2.72232900
H	-6.22606900	-2.09184300	-1.65745300

6Cap

Fe	0.47520800	0.44909400	0.26460700
Fe	-1.76000500	-0.84524500	-0.00752400
S	-1.43892600	0.84044200	1.51367600
S	0.15478200	-1.75471900	0.84302200
P	0.68548300	2.68940600	0.07450800
P	-3.27304900	0.35919800	-1.21138600
O	0.78180500	0.02159500	-2.61258200
O	3.26417700	0.08895700	0.98736100
O	-1.51068500	-2.62968700	-2.32756900
O	-3.85387000	-2.40299100	1.30633600
C	0.55593200	0.16350000	-1.46286800
C	2.09172700	0.32797600	0.77421200
C	-1.59600800	-1.90922000	-1.41220200
C	-3.01323700	-1.77476500	0.78992300
C	-4.21344700	1.70155800	-0.32947200
H	-4.90711800	2.19104900	-1.02413400
H	-3.52567400	2.44001700	0.09159800
H	-4.77867500	1.25184500	0.49433700
C	-4.65950300	-0.68594300	-1.88859100
H	-5.35138900	-0.06522400	-2.47097300
H	-5.20586500	-1.15700300	-1.06445000
H	-4.25218400	-1.47147200	-2.53429600
C	-2.62836400	1.17537000	-2.75460800
H	-3.42473700	1.73346500	-3.26216500
H	-2.23615100	0.40471900	-3.42707800
H	-1.80814100	1.84932600	-2.49441400
C	0.16750600	-1.88427700	2.70896300
H	0.23495000	-2.96220200	2.90042600
H	1.10182700	-1.41392200	3.03973500
C	-1.04314500	-1.29822900	3.43283600
C	-1.21997900	0.20956800	3.26457900
H	-0.35609700	0.75676900	3.66192400
H	-2.11779100	0.54638600	3.79627500
C	-0.73197500	3.77321900	-0.46684900
H	-1.59367900	3.58863700	0.18220500
H	-0.43971600	4.82746400	-0.38535600
H	-1.00300400	3.55966000	-1.50533600

Continued on next page

*Continued from previous page***6Cap**

C	2.05167300	3.25697700	-1.06140500
H	2.13469400	4.35068000	-1.05296800
H	3.00243500	2.82398400	-0.73022200
H	1.84586400	2.91737300	-2.08256800
C	1.14713500	3.48419600	1.69437000
H	1.29171100	4.56479200	1.57044100
H	0.34386300	3.30554700	2.41750700
H	2.06850000	3.03022400	2.07434700
O	4.84016800	-1.22505600	-0.49209600
H	4.15808300	-0.71472400	0.12619700
C	4.11260200	-1.96707200	-1.59421100
H	4.91298000	-2.26253000	-2.27746700
H	3.44467200	-1.24608900	-2.07749900
C	3.39264500	-3.15241800	-0.98489800
H	2.60717100	-2.84084700	-0.28760200
H	2.90991800	-3.70483300	-1.80132500
H	4.09576000	-3.82435700	-0.48133600
H	-0.92062300	-1.50051900	4.50945200
H	-1.95342600	-1.82305300	3.12070100
C	5.91123900	-0.27291500	-0.94882200
H	6.54935800	-0.88269400	-1.59342000
H	5.41864600	0.51027500	-1.53661600
C	6.64481800	0.25375600	0.27019900
H	5.98336000	0.83077800	0.92521800
H	7.09956200	-0.56353800	0.83953300
H	7.44496100	0.91910100	-0.07736000

TS_{6Cap→6HCap}

Fe	-0.58913900	0.46293800	0.32685900
Fe	1.66863900	-0.76255700	0.22000000
S	0.66399400	0.22095900	-1.63628600
S	-0.37274400	-1.80919400	0.49771300
P	-1.31084600	2.43662000	-0.49715400
P	3.57792100	0.50523300	-0.07536600
O	1.36332400	1.94676400	1.90076400
O	-2.23938800	0.68929300	2.72400000
O	2.36868300	-1.42710500	2.99706700
O	3.04413200	-3.14232600	-0.78091400
C	0.79258600	1.20596500	1.17136400
C	-1.58221500	0.58011500	1.75444900
C	2.09932200	-1.15248900	1.90007000
C	2.48571900	-2.18163700	-0.42361500
C	4.81594200	-0.27060300	-1.23069400
C	4.57588900	0.79753200	1.46696400

Continued on next page

Continued from previous page

TS_{6Cap→6HCap}

C	3.42522400	2.21605800	-0.79130900
C	-0.87290700	-2.71874200	-1.06789900
C	-0.07559700	-2.46575600	-2.34570000
C	-0.07810800	-1.01647500	-2.82154700
C	-2.10878500	2.42723100	-2.18890300
C	0.00479900	3.72810300	-0.77595400
C	-2.50672900	3.40649300	0.55711500
O	-3.56901700	-0.76378000	0.05790500
C	-3.78783400	-1.75832500	1.16472300
C	-4.62085800	0.28304200	-0.05474200
C	-4.35039800	-3.06678400	0.63278700
C	-5.92358700	-0.26941100	-0.61000400
H	-0.52654000	-3.08429000	-3.13884400
H	5.68420800	0.39056600	-1.33862200
H	4.35659300	-0.42719600	-2.21292500
H	5.14879700	-1.23693600	-0.83819100
H	5.45948800	1.40200100	1.22846700
H	4.89974000	-0.16063800	1.88756700
H	3.96250200	1.32360400	2.20594100
H	4.43043700	2.63239600	-0.92990200
H	2.86115800	2.85551400	-0.10733500
H	2.91552100	2.16503300	-1.75893200
H	-0.79978300	-3.77550800	-0.78372200
H	-1.93021500	-2.47334800	-1.22225000
H	-1.09651400	-0.66187300	-3.02294000
H	0.50999200	-0.91798600	-3.74151900
H	-2.92845900	1.70442200	-2.24535500
H	-2.48829300	3.42692000	-2.43482800
H	-1.34847000	2.14075000	-2.92417900
H	-0.44743400	4.64180800	-1.18077300
H	0.50011900	3.95910600	0.17275600
H	0.74218300	3.34380700	-1.48757900
H	-2.77917200	4.34284300	0.05541400
H	-3.41283100	2.83009800	0.76489900
H	-2.02397100	3.63922300	1.51302100
H	-2.47622200	-0.24745600	0.13951400
H	-2.79230200	-1.89277200	1.59833900
H	-4.44039600	-1.27246400	1.89801700
H	-4.74308800	0.73094300	0.93911500
H	-4.17563200	1.01372700	-0.73298800
H	-3.68084200	-3.51860300	-0.10598400
H	-4.43717300	-3.76232200	1.47801600
H	-5.34261700	-2.94971000	0.18712300
H	-6.60110600	0.57555100	-0.78924300
H	-5.76243800	-0.78764700	-1.56165400
H	-6.42112700	-0.94519700	0.09328800

Continued on next page

Continued from previous page

TS_{6Cap}→6HCap

H	0.95412200	-2.81898000	-2.23029100
---	------------	-------------	-------------

6HCap

Fe	-0.30662400	0.34727100	0.50607100
Fe	2.03929800	-0.69680400	0.26541900
S	0.69007900	-0.19478900	-1.51608800
S	0.25116000	-1.78865100	1.14310600
P	-1.47019500	2.04286500	-0.46689200
P	3.67237100	0.71451100	-0.60374400
O	1.61284800	2.33311200	1.53911200
O	-1.75880900	0.53190300	3.04781900
O	3.32447200	-0.70027900	2.91753600
O	3.49285200	-3.06806700	-0.60430800
C	0.99907600	1.44487600	1.07619500
C	-1.17036500	0.48060700	2.04851000
C	2.81817600	-0.69148100	1.87337200
C	2.91306000	-2.11095600	-0.27907300
C	4.71735400	-0.10242300	-1.90922600
C	4.92892100	1.33353400	0.61939400
C	3.13785700	2.27543800	-1.46868500
C	-0.54380000	-2.99249700	-0.04425200
C	-0.04258900	-2.98715700	-1.48656700
C	-0.21824400	-1.66513600	-2.22912000
C	-2.24026200	1.59735100	-2.09544300
C	-0.54975100	3.61518100	-0.84952800
C	-2.92675600	2.62296700	0.52312500
O	-4.86559500	-0.21505600	-0.13795400
C	-5.01391600	-1.26044500	0.85214600
C	-6.03210100	-0.03721200	-0.97717300
C	-5.76958700	-0.79447800	2.09966400
C	-6.05276600	-1.00664300	-2.16260100
H	-0.61448000	-3.75227900	-2.03546400
H	5.45235600	0.61608500	-2.29119900
H	4.07977400	-0.44090500	-2.73323400
H	5.24479400	-0.96525000	-1.48966300
H	5.66202900	1.96571900	0.10436400
H	5.44759000	0.48799300	1.08380900
H	4.42953600	1.91854100	1.39896600
H	4.02066500	2.74715000	-1.91743500
H	2.68734900	2.96692400	-0.75139200
H	2.41703600	2.03211900	-2.25629000
H	-0.35752100	-3.96961800	0.41720300
H	-1.61806200	-2.78093600	0.01280500
H	-1.27121500	-1.36419600	-2.27310400

Continued on next page

*Continued from previous page***6HCap**

H	0.16458700	-1.75236000	-3.25265600
H	-2.91486300	0.74865800	-1.94044700
H	-2.81107800	2.45431000	-2.47393400
H	-1.46396500	1.33263200	-2.82110700
H	-1.24088700	4.34383600	-1.29033200
H	-0.12150600	4.03358700	0.06731900
H	0.25486800	3.40938900	-1.56292700
H	-3.41723600	3.44880600	-0.00669200
H	-3.63090600	1.78907200	0.63059200
H	-2.60470800	2.97207000	1.50992400
H	-1.62614700	-0.23848500	0.04886400
H	-5.50537600	-2.13649600	0.40029200
H	-3.98860500	-1.55038200	1.11446300
H	-6.94727700	-0.13615300	-0.37429100
H	-5.97865100	1.00046300	-1.32943300
H	-6.79643000	-0.48981500	1.86293400
H	-5.82514100	-1.61393800	2.82872100
H	-5.25589000	0.05185300	2.57138900
H	-6.93851700	-0.81994100	-2.78427900
H	-5.16038900	-0.87499900	-2.78765900
H	-6.09238900	-2.05168600	-1.83064000
H	1.00668800	-3.30156800	-1.52299600

6C'ap

Fe	0.47149700	0.53196000	0.34037600
Fe	-1.70571900	-0.85133400	0.05958500
S	-1.59546100	1.10189600	1.26387900
S	0.10079100	-1.53957400	1.27557000
P	0.69709500	2.69461400	-0.21538200
P	-3.19773100	0.00843400	-1.43778800
O	0.79814200	-0.30569600	-2.43458900
O	3.25885000	0.27149300	1.11032600
O	-1.28135100	-3.08915400	-1.79991000
O	-3.74875100	-2.12848500	1.70855800
C	0.52995000	-0.02364200	-1.31782800
C	2.08569100	0.46641500	0.85767800
C	-1.43659300	-2.18971500	-1.07131500
C	-2.94922100	-1.61809200	1.02491800
C	-4.21000600	1.47744500	-0.90590800
H	-4.89498300	1.76827500	-1.71178400
H	-3.55777800	2.31751000	-0.65136900
H	-4.78712800	1.21031700	-0.01388900
C	-4.52782000	-1.21625300	-1.89390800
H	-5.22322700	-0.76823300	-2.61416800

Continued on next page

*Continued from previous page***6C'ap**

H	-5.08107100	-1.51220800	-0.99598400
H	-4.07624600	-2.10975200	-2.33865100
C	-2.55713400	0.49782100	-3.11861600
H	-3.38807900	0.81176300	-3.76230900
H	-2.04627100	-0.35726700	-3.57415800
H	-1.83820000	1.31668900	-3.02580200
C	-0.17151600	-1.36666800	3.11624700
H	-1.03352500	-2.00205700	3.35677800
H	0.72183200	-1.82147100	3.56140600
C	-0.35856700	0.05975400	3.62995200
H	-0.42038800	0.01933800	4.72952400
H	0.52390300	0.66196600	3.36897800
C	-1.61475800	0.74792200	3.10122100
H	-1.73470300	1.73496600	3.56374900
H	-2.51933400	0.16285600	3.30809200
C	-0.66501800	3.57395300	-1.13331600
H	-1.59011700	3.51829300	-0.55095000
H	-0.39520300	4.62680500	-1.28224000
H	-0.81786400	3.10184100	-2.10894000
C	2.17772000	3.08353200	-1.27933700
H	2.23969800	4.16023400	-1.47923400
H	3.08971100	2.76302000	-0.76361600
H	2.09778100	2.54330600	-2.22937800
C	0.95021700	3.80284900	1.25898300
H	1.10101800	4.84252700	0.94225200
H	0.06748700	3.74231900	1.90485600
H	1.82300700	3.45929300	1.82453400
O	4.79399400	-1.39447900	0.01804100
H	4.11110200	-0.71780900	0.45339300
C	4.18429700	-2.16184100	-1.13113000
H	5.04722700	-2.58946200	-1.64913800
H	3.67636900	-1.43522900	-1.77272200
C	6.11987800	-0.73017300	-0.22049300
H	6.36418100	-0.31552200	0.76099000
H	6.79376100	-1.56220900	-0.44280400
C	3.25706100	-3.21703800	-0.56229100
H	2.43018700	-2.77276900	0.00330000
H	2.82511400	-3.77387100	-1.40376200
H	3.80330600	-3.91937600	0.07608000
C	6.07846400	0.32134900	-1.31631200
H	5.37401700	1.12560900	-1.07670900
H	7.08015400	0.76261200	-1.39690400
H	5.82534400	-0.10658300	-2.29270900

$TS_{6C'ap \rightarrow 6HC'ap}$

Fe	-0.57086800	0.42130200	0.30103200
Fe	1.71141300	-0.75721100	0.25661500
S	0.69131900	0.07959000	-1.65240700
S	-0.31706500	-1.82027300	0.65731100
P	-1.29809800	2.38842800	-0.53898600
P	3.60629100	0.49602900	-0.13495200
O	1.39001900	1.93047000	1.83024000
O	-2.11420300	0.77511400	2.74788900
O	2.56964000	-1.42814200	2.99018100
O	2.86442700	-3.15302100	-0.96628000
C	0.85978300	1.14337700	1.11462000
C	-1.51489700	0.61470600	1.74847700
C	2.23524900	-1.14650100	1.91308900
C	2.42335200	-2.18867700	-0.47921500
C	4.80977200	-0.31195200	-1.30374600
H	5.67559900	0.34349700	-1.45686800
H	4.32097100	-0.49626800	-2.26683200
H	5.15193300	-1.26747600	-0.89243900
C	4.64738500	0.84708900	1.36574400
H	5.51598100	1.45343300	1.08187200
H	4.99389100	-0.09300400	1.80823500
H	4.04854500	1.39080000	2.10415400
C	3.41232900	2.18438700	-0.89274300
H	4.40615500	2.59947500	-1.10004200
H	2.88623000	2.84070000	-0.19397300
H	2.84719400	2.10448700	-1.82710100
C	-0.77295300	-2.85550100	-0.83526500
H	0.04498500	-3.57259800	-0.97607700
H	-1.65302700	-3.41765100	-0.49938400
C	-1.08895200	-2.10198300	-2.12634400
H	-1.42716000	-2.83897900	-2.87295400
H	-1.92026800	-1.40655800	-1.94640900
C	0.09007900	-1.33219400	-2.71486600
H	-0.19548200	-0.86241500	-3.66379300
H	0.94985900	-1.98612000	-2.90399000
C	-1.85879000	2.40068100	-2.32231200
H	-2.65145200	1.66609900	-2.49609100
H	-2.22464000	3.39871500	-2.59405400
H	-1.00427200	2.14091400	-2.95628400
C	-0.07268200	3.79397600	-0.57657900
H	-0.55244600	4.69940200	-0.96812100
H	0.30416100	3.98635300	0.43315000
H	0.76564800	3.52150800	-1.22564900
C	-2.72392700	3.20002600	0.35214300
H	-2.99488500	4.13999800	-0.14371300
H	-3.59692900	2.53937700	0.37116100

Continued on next page

*Continued from previous page***TS_{6C'ap}→6HC'ap**

H	-2.43092900	3.41266200	1.38615700
H	-2.48627200	-0.22960800	0.16048900
O	-3.49753300	-0.81531600	0.03538700
C	-3.86886800	-1.69612600	1.19229500
H	-4.24692800	-2.61545600	0.73505900
H	-2.89765200	-1.89463400	1.65526100
C	-4.58487900	-0.13361600	-0.70926200
H	-5.14611900	0.48768000	-0.00309300
H	-4.04113400	0.50878000	-1.40584100
C	-4.85994000	-1.07012000	2.15938300
H	-5.85023500	-0.92395000	1.71258800
H	-4.98137200	-1.76756100	2.99833500
H	-4.48981700	-0.12358900	2.56562900
C	-5.46410600	-1.14009400	-1.43537500
H	-6.19473600	-0.58807700	-2.04022900
H	-4.87194100	-1.77338600	-2.10511000
H	-6.02514100	-1.77656600	-0.74184900

6HC'ap

Fe	-0.29389200	0.34333700	0.49873900
Fe	2.03732400	-0.70106000	0.27705300
S	0.70224300	-0.22470400	-1.52026300
S	0.23755600	-1.78649100	1.15873100
P	-1.41027300	2.06368100	-0.48170900
P	3.71479200	0.64598400	-0.60691400
O	1.68306300	2.29189100	1.48450100
O	-1.67787800	0.63686500	3.06609900
O	3.38835200	-0.81225100	2.89609000
O	3.21955100	-3.16015400	-0.74457900
C	1.07407600	1.39295600	1.03150500
C	-1.11498800	0.53914800	2.05546400
C	2.85543700	-0.75678800	1.86665000
C	2.77936400	-2.16064600	-0.33849600
C	4.75896500	-0.23703800	-1.86897600
H	5.52233400	0.44633000	-2.25983800
H	4.12701100	-0.58249100	-2.69448000
H	5.25224100	-1.10184100	-1.41302800
C	4.96724200	1.27969900	0.61284600
H	5.71527100	1.88728000	0.08973800
H	5.46822400	0.43990300	1.10609000
H	4.46733800	1.89283100	1.37018300
C	3.22107100	2.18956600	-1.52524500
H	4.11624900	2.63313400	-1.97799900
H	2.77655000	2.90923400	-0.83205700

Continued on next page

*Continued from previous page***6HC'ap**

H	2.50299900	1.93755500	-2.31270500
C	-0.48649500	-3.02858100	-0.03619300
H	0.31421100	-3.75183500	-0.23517100
H	-1.25520300	-3.53258700	0.56146900
C	-1.09070100	-2.47565300	-1.32406500
H	-1.51196600	-3.32265000	-1.88893700
H	-1.92215700	-1.80057300	-1.07961400
C	-0.09684800	-1.75789100	-2.23283500
H	-0.59691300	-1.40131800	-3.14108200
H	0.72846200	-2.41316300	-2.53666400
C	-2.17471400	1.61696100	-2.11331800
H	-2.84977400	0.76844900	-1.96009000
H	-2.74144300	2.47380600	-2.49808300
H	-1.39398000	1.34748100	-2.83242400
C	-0.46203200	3.61911200	-0.86426100
H	-1.13945700	4.35820300	-1.30896100
H	-0.03000000	4.03131000	0.05361200
H	0.34170300	3.39864900	-1.57426800
C	-2.86527100	2.67313200	0.49329000
H	-3.34412700	3.49738100	-0.04929800
H	-3.57756600	1.84759500	0.60853100
H	-2.54472800	3.03096000	1.47746500
H	-1.65863900	-0.17260800	0.09832500
O	-4.78713900	-0.23758800	-0.15069300
C	-5.00216800	-1.18873500	0.91973800
H	-5.58591100	-2.04501000	0.54764500
H	-4.00129500	-1.55500500	1.18050300
C	-5.95197200	-0.02690900	-0.98476200
H	-6.85777200	0.01300000	-0.36088200
H	-5.81206200	0.96669000	-1.42872400
C	-5.67559900	-0.56097700	2.14340500
H	-6.67459100	-0.17575800	1.90455900
H	-5.78984700	-1.31497000	2.93372200
H	-5.07069000	0.26325800	2.54007700
C	-6.08959000	-1.08852200	-2.07970400
H	-6.96431100	-0.86869700	-2.70615500
H	-5.20014300	-1.10088200	-2.72232900
H	-6.22606900	-2.09184300	-1.65745300

6DbA

Fe	0.72507800	-1.08365800	0.39972900
Fe	-1.37201900	0.15395200	-0.41388000
S	0.08482300	-0.99322800	-1.79644800
S	-1.40938300	-1.79487600	0.82603900

Continued on next page

*Continued from previous page***6Db**

P	2.69493200	0.00769600	-0.02634200
P	-2.70877900	1.00437300	1.19020200
O	1.87219500	-3.76839200	0.45341500
O	0.20838500	2.59178100	-0.60291700
O	1.10902100	-0.44305500	3.23947300
O	-3.35274300	0.69672600	-2.49339000
C	1.44860400	-2.67887000	0.43360300
C	-0.39332300	1.53961300	-0.46188200
C	0.93906100	-0.68373700	2.10811100
C	-2.60969600	0.40945600	-1.62551900
C	-0.66712500	-2.60183900	-2.38512100
C	-1.85936900	-3.27792900	-0.21947700
C	-1.97865000	-3.01008300	-1.71709200
C	3.07259600	0.54871600	-1.77175000
C	-3.22748200	2.77298900	0.90921900
C	3.04809000	1.55204000	0.95944300
C	-4.34272700	0.13543800	1.37885900
C	4.19363400	-1.02765100	0.37195700
C	-2.05135100	1.04431000	2.92866000
H	-1.82746400	0.02418800	3.25681800
H	3.04257400	-0.31731400	-2.44072700
H	-3.72931100	2.85535500	-0.06173800
H	4.06843400	1.00784200	-1.80530300
H	-2.34279600	3.41964700	0.91374900
H	3.04993400	1.30815000	2.02729600
H	-4.95747200	0.63858000	2.13546500
H	2.27371300	2.30051900	0.76739700
H	-4.16174400	-0.89989800	1.68619200
H	4.02951000	1.95833300	0.68454600
H	-4.87010300	0.13531300	0.41876100
H	2.32544100	1.27431100	-2.10842600
H	-3.91501500	3.10215300	1.69775300
H	5.11180100	-0.44894000	0.21284900
H	-2.79763000	1.48526200	3.60123000
H	4.21026600	-1.91763500	-0.26640500
H	-1.13125600	1.63689200	2.96210800
H	4.14720100	-1.35040900	1.41795600
H	-2.33417700	-3.93180800	-2.20555900
H	-2.73912500	-2.23727700	-1.89184200
H	-0.81684900	-2.45259600	-3.46112800
H	0.11064000	-3.36402600	-2.24917200
H	-2.82297000	-3.60592800	0.18862300
H	-1.11586200	-4.05355500	0.00119800
H	0.10132700	3.30334100	-1.87547200
C	-0.67222500	5.08755900	-2.71750200
H	-1.68156100	4.87282000	-2.34806100

Continued on next page

*Continued from previous page***6Dba**

H	-0.71677700	5.45533900	-3.74476800
C	-0.50492200	2.79047200	-3.84028300
H	-0.17260200	1.81954100	-3.46245100
H	-1.59663200	2.85349500	-3.78289000
C	0.05931100	3.11326400	-5.20952500
H	1.15363700	3.07376400	-5.20592600
H	-0.31097200	2.35620200	-5.91233700
H	-0.26809900	4.09168800	-5.57851900
C	0.12617700	5.99907900	-1.80464800
H	1.13195600	6.17316400	-2.20090600
H	-0.39362900	6.96344900	-1.74730400
H	0.19899100	5.59407700	-0.78908200
O	0.04179500	3.76922600	-2.82099100

TS_{6Dba→6HDb}

Fe	0.83506700	-0.86885300	0.55902200
Fe	-1.42488300	-0.01129800	-0.59184300
S	0.19195500	-1.29874100	-1.58568900
S	-1.32306300	-1.49917400	1.11453900
P	3.05718200	-0.64963500	-0.05801100
P	-2.75666200	1.21622500	0.85412300
O	1.54248400	-3.41232200	1.83196400
O	-1.35960500	2.24296000	-2.45333600
O	1.19672300	0.84635600	2.91176800
O	-3.75995000	-0.91754800	-2.09512800
C	1.29547500	-2.40836000	1.28632600
C	-1.29667500	1.34746300	-1.69930000
C	1.03064500	0.16976400	1.96781900
C	-2.83236800	-0.59070700	-1.46423800
C	-0.33032100	-3.09617900	-1.71365700
C	-1.62558600	-3.25444300	0.52803500
C	-1.60998300	-3.49750000	-0.98095600
C	3.51777200	-0.52909900	-1.86433000
C	-3.27091100	2.92153800	0.30122700
C	4.06701300	0.68898000	0.76070400
C	-4.40632900	0.39317900	1.12136200
C	4.10130400	-2.13171500	0.40111400
C	-2.21395700	1.49149800	2.61817200
H	-1.98081400	0.52672600	3.08049900
H	3.15868900	-1.42535300	-2.38051100
H	-3.76150800	2.85885300	-0.67626700
H	4.60978300	-0.47256700	-1.95235400
H	-2.39870300	3.57682000	0.20930600
H	4.06043400	0.52011900	1.84354100

Continued on next page

Continued from previous page

TS_{6Dba}→6HDb

H	-5.00662100	0.97853700	1.82821300
H	3.64280800	1.67437400	0.55742600
H	-4.24343700	-0.61055900	1.52860900
H	5.10225500	0.64812500	0.40056100
H	-4.94568900	0.31155000	0.17223500
H	3.07107400	0.34183800	-2.34758200
H	-3.96969100	3.35406800	1.02712600
H	5.13582400	-1.95436500	0.08319300
H	-3.03267000	1.96872400	3.17091600
H	3.72329000	-3.03205000	-0.09440300
H	-1.32760500	2.12974000	2.67126400
H	4.08253600	-2.29099300	1.48410600
H	-1.75691000	-4.57824400	-1.13871200
H	-2.46884200	-3.00294600	-1.44539200
H	-0.44871700	-3.27458300	-2.78901700
H	0.53428800	-3.67288100	-1.36306600
H	-2.61477400	-3.49584800	0.93544900
H	-0.88880700	-3.87369200	1.05176500
H	0.77928300	1.14255700	-0.15690900
C	0.70883000	3.30484700	0.50716200
H	-0.03334800	2.77065500	1.10609900
H	0.19696300	4.00015200	-0.16771900
C	1.57242900	2.61275200	-1.76825200
H	1.50330900	1.66025400	-2.30066800
H	0.74915400	3.25371100	-2.09465800
C	2.92337200	3.28851200	-1.94403700
H	3.74904700	2.66426100	-1.58800500
H	3.07088500	3.46838100	-3.01734100
H	2.96554300	4.25918800	-1.43934700
C	1.74935200	3.99071700	1.37940700
H	2.50361000	4.51748400	0.78626500
H	1.23621800	4.73334500	2.00482300
H	2.24263400	3.27461200	2.04371000
O	1.30600400	2.23983700	-0.34557300

6HDb

Fe	0.79158700	-1.63384700	0.64790100
Fe	-1.17634400	-0.57486000	-0.67252000
S	0.15649600	-2.28129900	-1.47082400
S	-1.42920900	-1.90527800	1.19417900
P	2.81417800	-0.86276200	-0.12466600
P	-2.16821000	1.12561400	0.50861900
O	1.74925100	-4.29792600	1.38499200
O	-0.18160400	1.22771800	-2.76453900

Continued on next page

*Continued from previous page***6HDba**

O	1.38909400	-0.44937700	3.26924300
O	-3.66537400	-1.10230100	-2.11753400
C	1.38452100	-3.22950400	1.09861900
C	-0.58215800	0.52091900	-1.93204200
C	1.14128700	-0.90402000	2.22685200
C	-2.67685000	-0.91661600	-1.52987200
C	-0.68662800	-3.94851800	-1.41080300
C	-2.00753200	-3.63522200	0.78510700
C	-2.03270400	-4.02125100	-0.69295400
C	3.09765900	-0.85163000	-1.96259500
C	-2.24728000	2.76850900	-0.35029900
C	3.19316900	0.89121400	0.36653000
C	-3.93439000	0.77571800	0.97219300
C	4.28544500	-1.80219900	0.51700500
C	-1.37933300	1.52879200	2.14043500
H	-1.38415200	0.64290900	2.78368200
H	3.03138400	-1.86894800	-2.36050500
H	-2.72474100	2.65529400	-1.32999000
H	4.09545100	-0.44208000	-2.16329800
H	-1.23069000	3.16413000	-0.47847200
H	3.22853800	0.97039300	1.45849600
H	-4.33413500	1.60931300	1.56223700
H	2.42173000	1.57035200	-0.01266800
H	-3.97900000	-0.14363300	1.56614300
H	4.16801000	1.18445200	-0.04208700
H	-4.54286900	0.65041800	0.07028100
H	2.34568800	-0.23113100	-2.46024600
H	-2.83687800	3.46783200	0.25551700
H	5.21194800	-1.33981500	0.15588500
H	-1.94677100	2.33001500	2.62974600
H	4.24321600	-2.84068200	0.17107700
H	-0.34872300	1.85949200	1.97926800
H	4.28296100	-1.79493300	1.61258600
H	-2.38356300	-5.06362800	-0.75537700
H	-2.77243800	-3.41420100	-1.22629100
H	-0.80899700	-4.21497600	-2.46702000
H	0.04493000	-4.63711400	-0.97084800
H	-3.01777600	-3.68533400	1.20791100
H	-1.36304000	-4.30219400	1.37054400
H	0.23455400	-0.13707800	0.14595400
C	0.96136500	5.12526200	0.68550500
H	-0.02086800	5.09538800	1.18088800
H	1.07586900	6.12352900	0.23878400
C	1.24562700	4.63390100	-1.68062300
H	0.96094000	3.82653300	-2.36503500
H	0.60125200	5.50299800	-1.89357100

Continued on next page

*Continued from previous page***6HDb**

C	2.72054300	4.99977500	-1.86667900
H	3.36473500	4.13482300	-1.66487900
H	2.89332000	5.32626700	-2.90087500
H	3.02259800	5.82082600	-1.20443600
C	2.07389800	4.85260700	1.69816000
H	3.06252900	4.90997300	1.22771400
H	2.03265000	5.59185900	2.50941500
H	1.95846000	3.85548300	2.14195100
O	0.93763800	4.12298700	-0.36218600

8Db

Fe	-0.45635300	0.65933300	0.16895200
Fe	1.99762500	-0.12489100	0.14783600
S	0.26918800	-1.35228200	1.01677000
S	1.21195700	1.57971800	1.46055800
P	-0.78231400	2.76486100	-0.60482100
P	2.38919800	-1.72484000	-1.45612600
O	-3.14920800	0.31747700	1.21172900
O	-0.83166500	-0.43010600	-2.52301200
O	3.42105200	1.78422400	-1.56140100
O	4.34541300	-0.82876200	1.74078900
C	-2.01876500	0.54409500	0.82895200
C	-0.60594100	-0.00071500	-1.44713800
C	2.83017700	1.03746200	-0.88243900
C	3.39745600	-0.57699300	1.10376800
C	1.26698600	-3.21158100	-1.54098100
H	1.62170200	-3.88484500	-2.33129400
H	0.24256900	-2.89757900	-1.76352900
H	1.27828800	-3.73457600	-0.57944100
C	4.06336800	-2.53023200	-1.29686300
H	4.22082600	-3.23932300	-2.11878700
H	4.13346200	-3.06110300	-0.34140000
H	4.84480700	-1.76296600	-1.32851700
C	2.42944600	-1.15186300	-3.23035000
H	2.65409400	-2.00071800	-3.88799200
H	3.20680000	-0.39021400	-3.35188100
H	1.46156600	-0.72400100	-3.50679900
C	0.99762400	1.09567200	3.25485500
H	1.74612900	1.69365100	3.78813500
H	0.00035500	1.45524900	3.53765500
C	1.17203600	-0.38386100	3.58666400
C	0.17901600	-1.30771400	2.88537000
H	-0.85620800	-1.04256200	3.13501000
H	0.35252700	-2.34781200	3.18840200

Continued on next page

Continued from previous page

8DbA

C	0.65101200	3.69773300	-1.33484900
H	1.01478800	3.18457200	-2.23032700
H	0.33165200	4.71337400	-1.59975800
H	1.46205300	3.75309200	-0.60164900
C	-1.39802000	3.93854700	0.70301600
H	-1.58771400	4.92815100	0.26900700
H	-2.32232000	3.54814100	1.14271200
H	-0.64118900	4.02627800	1.48975500
C	-2.08290800	2.92908200	-1.93041800
H	-2.21174900	3.98100000	-2.21313000
H	-1.78979900	2.35082000	-2.81327400
H	-3.03578400	2.54046100	-1.55362800
H	-4.11069500	-0.64895600	0.71211200
O	-4.83502100	-1.35160600	0.40122900
C	-5.10765600	-1.25361400	-1.07352100
H	-5.70967000	-2.13909500	-1.29522600
H	-4.14386100	-1.31073200	-1.58956200
C	-4.54392600	-2.71864400	0.96210300
H	-4.41782700	-2.51660600	2.02893700
H	-5.47630300	-3.26752800	0.80281300
C	-3.33274000	-3.38413800	0.33243000
H	-3.48541600	-3.59751500	-0.73155700
H	-2.42222800	-2.78726300	0.46068800
H	-3.18125700	-4.34488100	0.84177600
C	-5.85670300	0.04038600	-1.33161400
H	-6.80566800	0.06331300	-0.78630200
H	-5.25856200	0.91535400	-1.05422400
H	-6.06973500	0.10299500	-2.40605900
H	1.03486300	-0.50299600	4.67387300
H	2.19753500	-0.70152000	3.36536400

TS_{8DbA→8HDbA}

Fe	0.70205400	-0.59484700	0.11611100
Fe	-1.81077200	-0.11852800	-0.10566300
S	-0.51235300	0.73662100	1.56818800
S	-0.95721100	-2.15293000	0.46787900
P	1.61067300	-2.14952500	-1.26585100
P	-2.35568500	2.06033500	-0.65704900
O	0.62317200	1.09921200	-2.28398400
O	2.81037600	-1.14123000	2.08314600
O	-2.55576100	-1.05335800	-2.78948800
O	-4.46116500	-0.61245300	1.00980300
C	0.56353500	0.46148900	-1.28704300
C	1.97308000	-0.93921000	1.28360000

Continued on next page

*Continued from previous page***TS**_{8Db \rightarrow 8HDb}

C	-2.24761000	-0.69285600	-1.72498700
C	-3.39891000	-0.38348900	0.58246300
C	-3.15976600	2.31073600	-2.31611000
C	-1.03093700	3.37410700	-0.65497700
C	-3.59612300	2.78357800	0.52845600
C	-1.10827800	-2.52645600	2.29480000
C	-1.59004100	-1.38893400	3.19353100
C	-0.69422800	-0.15132900	3.20494900
C	3.20307300	-1.65917900	-2.09768500
C	0.56016400	-2.70770300	-2.69366000
C	2.06248700	-3.74781300	-0.42871800
O	3.00219300	1.54179400	0.22173900
C	3.40175700	2.20180800	-1.04338600
C	2.84647400	2.42884000	1.40730000
C	3.99412100	2.23290100	2.38670100
C	4.84687100	2.67531000	-0.99944900
H	-2.61352200	-1.10501600	2.92225700
H	-2.45972600	2.02615000	-3.10904800
H	-3.44100100	3.36334000	-2.44094400
H	-4.05685300	1.68711400	-2.39521400
H	-1.50714800	4.35717600	-0.75402100
H	-0.34884200	3.21276000	-1.49398700
H	-0.47582100	3.33396500	0.28858300
H	-3.81232400	3.82421600	0.25808500
H	-3.18454900	2.74933100	1.54326000
H	-4.52526800	2.20513900	0.50296700
H	-1.81169300	-3.36598400	2.34151800
H	-0.11857700	-2.88762800	2.60077300
H	0.32257500	-0.39034400	3.53925700
H	-1.10770900	0.60842200	3.87884100
H	3.02268300	-0.80631000	-2.76138400
H	3.59052100	-2.49515300	-2.69273100
H	3.94566200	-1.38142900	-1.34147900
H	1.09725300	-3.47029300	-3.27079600
H	0.33182600	-1.85577400	-3.34212900
H	-0.37503100	-3.13434000	-2.31652000
H	2.80158000	-3.56315600	0.35791600
H	2.48045700	-4.44770000	-1.16231000
H	1.16307800	-4.18484600	0.01751400
H	2.06253300	0.72132900	0.10811000
H	3.25405800	1.42575100	-1.79693900
H	2.69626600	3.02070600	-1.23107400
H	2.77777300	3.45614900	1.03026100
H	1.88149600	2.14148100	1.83846800
H	4.05387700	1.18934700	2.71221800
H	4.95598100	2.52590900	1.95350400

Continued on next page

*Continued from previous page***TS_{8DBa→8HDBa}**

H	3.81119800	2.86014800	3.26927200
H	5.52726300	1.84893500	-0.76596400
H	5.11002400	3.07020100	-1.98928100
H	4.99755600	3.48128400	-0.27248900
H	-1.63525000	-1.77686500	4.22384600

8HDBa

Fe	-0.33959100	-0.87219700	-0.15611400
Fe	1.89654400	0.30139700	0.22320700
S	0.83765500	0.26151500	-1.79558500
S	1.64776200	-1.98074900	0.25462300
P	-1.29534700	-2.17470600	1.45132100
P	1.70082500	2.61977000	0.15004500
O	-0.86252700	1.23129800	1.80524300
O	-1.92275400	-2.28582500	-2.18394700
O	2.52047800	0.32291500	3.10014800
O	4.71576500	0.38876900	-0.51236600
C	-0.48302700	0.44226000	1.01765600
C	-1.25723400	-1.77763700	-1.37414100
C	2.26522100	0.31428800	1.96605200
C	3.58380100	0.36363300	-0.23633800
C	1.87503800	3.49041900	1.78274400
C	0.13749600	3.34276900	-0.56054100
C	3.01081000	3.40815000	-0.90827700
C	2.22353600	-2.81581900	-1.31694200
C	2.65175000	-1.89916300	-2.46129600
C	1.56226100	-0.97355300	-2.99903900
C	-3.08170100	-1.77793400	1.75067100
C	-0.51250600	-2.08229600	3.13282200
C	-1.27977700	-3.99285000	1.07219600
O	-3.76739000	1.46076300	-0.51289300
C	-4.28925000	2.42541100	0.42379600
C	-4.31698200	1.56136100	-1.84891500
C	-5.18899800	0.35319900	-2.19478100
C	-5.73694400	2.15971900	0.84901100
H	2.97803800	-2.54153600	-3.29466300
H	1.08409400	3.15812600	2.46324600
H	1.79440300	4.57390700	1.63466700
H	2.84964000	3.25921300	2.22606400
H	0.24599400	4.43408700	-0.59181400
H	-0.72484000	3.08104600	0.05798700
H	-0.01744000	2.96386000	-1.57576000
H	2.85156400	4.49224300	-0.94859200
H	2.95275300	2.99600600	-1.92172300

Continued on next page

*Continued from previous page***8HDba**

H	4.00556800	3.20591000	-0.49788400
H	3.06823900	-3.43701400	-0.99782300
H	1.40210300	-3.47847300	-1.61641600
H	0.71141500	-1.53706000	-3.40095400
H	1.96184800	-0.34654700	-3.80478800
H	-3.17620500	-0.72543700	2.03660100
H	-3.48382400	-2.41583400	2.54696000
H	-3.65108400	-1.93796400	0.82901600
H	-1.03361400	-2.76378700	3.81596700
H	-0.58000000	-1.06118100	3.52146700
H	0.54033800	-2.37649500	3.06447400
H	-1.81548900	-4.18775200	0.13732900
H	-1.76430200	-4.54341800	1.88757400
H	-0.24280900	-4.33101000	0.97317500
H	-1.56817800	-0.05069100	-0.45818700
H	-3.62001900	2.36141400	1.29052200
H	-4.19478700	3.43883300	-0.00336300
H	-4.88875900	2.49713200	-1.94353500
H	-3.46174500	1.62232100	-2.53798000
H	-4.61285800	-0.57577600	-2.10236000
H	-6.06114800	0.28775600	-1.53379000
H	-5.54479500	0.43067900	-3.23126700
H	-5.83950300	1.15336700	1.27370200
H	-6.03957800	2.89030700	1.61143500
H	-6.43153500	2.25355400	0.00499900
H	3.52733600	-1.31229900	-2.16131700

8D'ba

Fe	-0.44516200	0.68687900	0.15622000
Fe	2.00130100	-0.10817200	0.12406600
S	0.32023200	-1.22900500	1.18864000
S	1.28831900	1.74455300	1.26087200
P	-0.80888000	2.69463700	-0.81204200
P	2.40850100	-1.90114800	-1.26417700
O	-3.17754600	0.38683600	1.10570100
O	-0.64551900	-0.60672500	-2.45847900
O	3.49090100	1.57171600	-1.76806500
O	4.20325600	-0.64508700	1.96560200
C	-2.03068400	0.58815300	0.75540500
C	-0.46686600	-0.10352500	-1.40421800
C	2.87576700	0.91405400	-1.02272900
C	3.33726900	-0.45925900	1.20203700
C	1.24180200	-3.35638600	-1.22240800
H	1.62013100	-4.14097900	-1.88942600

Continued on next page

*Continued from previous page***8D'ba**

H	0.24809200	-3.04328600	-1.55794300
H	1.16887400	-3.74287200	-0.20074600
C	4.04764400	-2.71754900	-0.91502000
H	4.21837800	-3.54632000	-1.61317700
H	4.06067300	-3.09887800	0.11176900
H	4.85296300	-1.98270200	-1.02424400
C	2.54248500	-1.55850600	-3.09212000
H	2.77924900	-2.48694400	-3.62606800
H	3.33845600	-0.82855900	-3.27343400
H	1.59525400	-1.15618500	-3.46377800
C	1.20872100	1.42622600	3.10128300
H	2.21449100	1.11420700	3.40862500
H	1.01274700	2.41481300	3.53373500
C	0.14298200	0.42820400	3.54480000
H	0.12872300	0.40323400	4.64664700
H	-0.84424400	0.77801500	3.21149700
C	0.38278100	-0.99502500	3.04408800
H	-0.38698900	-1.67296600	3.43328100
H	1.36176600	-1.37400800	3.36364200
C	0.58926000	3.48378300	-1.75034100
H	0.89704100	2.83281900	-2.57479500
H	0.26596300	4.45283200	-2.15074200
H	1.44123800	3.63639400	-1.07988200
C	-1.30740000	4.02643000	0.38663900
H	-1.49457200	4.96864400	-0.14314600
H	-2.21297500	3.71918800	0.92093900
H	-0.49898900	4.16894100	1.11139800
C	-2.19528900	2.72622400	-2.05703600
H	-2.32022100	3.73613100	-2.46614800
H	-1.97503700	2.03014100	-2.87367300
H	-3.12771100	2.41974100	-1.56955300
H	-4.10070000	-0.63850600	0.68952200
O	-4.81097000	-1.38299100	0.43730900
C	-5.11396800	-1.38876900	-1.03382200
H	-5.69078500	-2.30506500	-1.18684700
H	-4.15889300	-1.44884100	-1.56575100
C	-4.47245400	-2.70154900	1.07913500
H	-4.35083900	-2.43105600	2.13124900
H	-5.38541700	-3.29133200	0.95785900
C	-3.24046100	-3.36248900	0.48585600
H	-3.38431300	-3.63327700	-0.56631300
H	-2.34867900	-2.73283600	0.58547400
H	-3.06193200	-4.29149600	1.04303300
C	-5.90927400	-0.13789300	-1.35838200
H	-6.84665300	-0.10833000	-0.79367500
H	-5.33363200	0.77104300	-1.15190100

Continued on next page

*Continued from previous page***8D'ba**

H	-6.14709900	-0.15191900	-2.42933400
---	-------------	-------------	-------------

TS_{8D'ba→8HD'ba}

Fe	0.69539000	-0.62900100	0.11549700
Fe	-1.80194000	-0.10460000	-0.07268800
S	-0.49492800	0.63641300	1.64774600
S	-0.98546600	-2.18712700	0.40692600
P	1.54141700	-2.10890600	-1.38286100
P	-2.33482900	2.08794300	-0.60477100
O	0.50041700	1.17056300	-2.19548700
O	3.03985900	-1.16603900	1.79491000
O	-2.77481800	-1.01449100	-2.69450300
O	-4.28719000	-0.59204000	1.37433000
C	0.45266300	0.48288900	-1.22866700
C	2.09233400	-0.96511100	1.12893800
C	-2.37601100	-0.65580500	-1.66009200
C	-3.30814300	-0.36355500	0.78144900
C	-2.81671400	2.41335000	-2.37250800
H	-1.98014400	2.15916800	-3.03167900
H	-3.07179800	3.47237000	-2.49887500
H	-3.68288800	1.80012900	-2.64286700
C	-1.08278600	3.43428200	-0.28531900
H	-1.55086600	4.40703600	-0.48075500
H	-0.22431100	3.30851000	-0.95121600
H	-0.75380000	3.39221100	0.75810800
C	-3.80450500	2.72287200	0.34608800
H	-4.00972100	3.76357800	0.06750700
H	-3.59610100	2.66937900	1.42041000
H	-4.68650400	2.11181600	0.12706600
C	-1.25108900	-2.61750800	2.20689100
H	-2.32998600	-2.54026000	2.38764000
H	-0.97455300	-3.67693300	2.26587500
C	-0.44232400	-1.80017000	3.20988200
H	-0.63876800	-2.20391700	4.21620100
H	0.62901000	-1.93331300	3.01622900
C	-0.78344900	-0.31168700	3.23543500
H	-0.16455800	0.20875300	3.97591800
H	-1.83651800	-0.14261600	3.49302600
C	3.10047600	-1.57137100	-2.24731900
H	2.89392300	-0.68442300	-2.85642100
H	3.46422800	-2.37345600	-2.90092900
H	3.87177300	-1.33343800	-1.50641300
C	0.43369100	-2.58703100	-2.79698600
H	0.94779400	-3.31713700	-3.43388200

Continued on next page

*Continued from previous page***TS_{8D'ba}→8HD'ba**

H	0.18218200	-1.70170300	-3.38995100
H	-0.48687800	-3.03395100	-2.40776700
C	2.01973500	-3.74945600	-0.64972200
H	2.77282000	-3.60403400	0.13180100
H	2.42669300	-4.40244500	-1.43129300
H	1.13195300	-4.21668000	-0.21091600
H	1.99080400	0.74610100	0.11019200
O	2.89555500	1.61177100	0.22317500
C	3.30412600	2.26798300	-1.03911900
H	3.16741900	1.48868700	-1.79153900
H	2.59677100	3.08285400	-1.23784400
C	2.72008500	2.49850900	1.40512500
H	2.65569400	3.52526300	1.02595600
H	1.75009500	2.20942100	1.82348200
C	3.85361200	2.30635700	2.40193700
H	3.91345800	1.26289300	2.72760800
H	4.82102500	2.60188500	1.98300700
H	3.65565900	2.93305200	3.28169200
C	4.74672700	2.74843000	-0.98129800
H	5.42799000	1.92536200	-0.73880100
H	5.01925600	3.14377400	-1.96838500
H	4.88549700	3.55558900	-0.25316700

8HD'ba

Fe	-0.31167100	-0.90635300	-0.16284800
Fe	1.86276600	0.34485600	0.21742900
S	0.81204000	0.25357000	-1.81231900
S	1.71715500	-1.95320200	0.24182100
P	-1.19532900	-2.19942200	1.49348500
P	1.63888800	2.65731300	0.14242500
O	-0.80348800	1.19065200	1.81224200
O	-2.13294900	-2.23832400	-2.03507200
O	2.65395000	0.38379400	3.05474800
O	4.59878400	0.36320600	-0.78871700
C	-0.39332400	0.42320500	1.01470500
C	-1.36264600	-1.76476500	-1.29981500
C	2.32922400	0.37137000	1.93867500
C	3.50912500	0.38572800	-0.37697500
C	1.75389000	3.52846000	1.77998900
H	0.96103200	3.16883100	2.44407900
H	1.64147700	4.60910000	1.63187700
H	2.72707100	3.32768000	2.24069100
C	0.07717300	3.34589700	-0.60347400
H	0.14944500	4.44056900	-0.61522000

Continued on next page

*Continued from previous page***8HD'ba**

H	-0.79439500	3.04515200	-0.01580700
H	-0.03555500	2.97819200	-1.62843400
C	2.95958800	3.47744700	-0.87811400
H	2.78797400	4.56012000	-0.90616800
H	2.92977600	3.08108300	-1.89897400
H	3.94804000	3.28152000	-0.44911000
C	2.45861800	-2.68144600	-1.31023000
H	3.49832900	-2.33479200	-1.34868300
H	2.47096100	-3.75975100	-1.11211100
C	1.70905700	-2.38779400	-2.60661200
H	2.21483600	-2.93111700	-3.42066500
H	0.68992900	-2.78996000	-2.54400900
C	1.66456800	-0.91216500	-2.99942500
H	1.10603200	-0.78315700	-3.93387300
H	2.67171200	-0.50266800	-3.14716700
C	-2.97401800	-1.81404500	1.84782400
H	-3.06878200	-0.75710300	2.11711900
H	-3.34203300	-2.43976700	2.66975400
H	-3.57294000	-1.99839500	0.94969400
C	-0.35628000	-2.07773400	3.14573600
H	-0.83450800	-2.76953700	3.84949800
H	-0.43788000	-1.05684100	3.53214600
H	0.70101600	-2.34339900	3.04094700
C	-1.17406900	-4.02025000	1.13072500
H	-1.74242300	-4.22919600	0.21849700
H	-1.62088200	-4.56862800	1.96881600
H	-0.13798400	-4.34688200	0.99342800
H	-1.53139800	-0.05660000	-0.40964500
O	-3.68142600	1.42710000	-0.47597900
C	-4.17800500	2.36886200	0.49747400
H	-3.51570300	2.24784600	1.36334300
H	-4.04827700	3.39518500	0.11197600
C	-4.22594000	1.59432600	-1.80810900
H	-4.74191200	2.56445500	-1.87566000
H	-3.36720000	1.62491600	-2.49459600
C	-5.16477500	0.44850800	-2.18983100
H	-4.64420000	-0.51421200	-2.11928900
H	-6.04441600	0.41580800	-1.53659500
H	-5.50801200	0.57503500	-3.22577300
C	-5.63595400	2.13584100	0.90610300
H	-5.77678300	1.11552100	1.28386200
H	-5.91444500	2.84136700	1.70067200
H	-6.32322300	2.29418400	0.06592800

Appendix C

Isomerisation pathways of the terminal hydrides of $[\text{HFe}_2(\mu\text{-(pdt)})(\text{CO})_4(\text{PMe}_3)_2]^+$ to bridging hydrides

Table C1: Free energy comparison between the pdt, edt and odt dithiolate bridge in the isomerisation pathways leading to the bridging hydrides **2A** and **2B** from the terminal hydride **3A3**. Energies are reported in kcal/mol. For the pdt bridge a comparison between the TPSS and B3LYP functionals is reported. Calculations using the B3LYP functional were carried out by Lui.[118]

Reaction coordinate	B3LYP		TPSS	
	pdt	pdt	odt	edt
$\text{TS}_{3\text{A3}\rightarrow 3\text{B}}$	^a	16.7	13.5	13.5
$\text{TS}_{3\text{A3}'\rightarrow 3\text{B}'}$	18.3	13.9	16.1	13.5
$\text{TS}_{3\text{B}\rightarrow 2\text{A}}$	^a	6.9	11.0	9.6
$\text{TS}_{3\text{B}'\rightarrow 2\text{A}'}$	12.5	8.1	9.7	9.6
$\text{TS}_{3\text{A3}\rightarrow 6\text{AInt}}$	^a	14.7	15.0	13.9
$\text{TS}_{3\text{A3}'\rightarrow 6\text{AInt}'}$	13.6	13.1	14.8	13.9
$\text{TS}_{6\text{AInt}\rightarrow 2\text{A}}$	^a	8.5	11.9	10.2
$\text{TS}_{6\text{AInt}'\rightarrow 2\text{A}'}$	6.4	11.7	11.7	10.2
$\text{TS}_{3\text{A3}\rightarrow 3\text{A4}}$	^a	15.3	16.3	21.4
$\text{TS}_{3\text{A3}'\rightarrow 3\text{A4}'}$	20.1	13.1	16.5	21.4
$\text{TS}_{3\text{A4}\rightarrow 2\text{B}}$	^a	12.0	13.2	11.8
$\text{TS}_{3\text{A4}'\rightarrow 2\text{B}}$	16.8	13.2	14.1	11.8

^a data not available from B3LYP calculations

Table C2: Free energy comparison between the pdt, edt and odt dithiolate bridge in the isomerisation pathway leading to the bridging hydride **2D**, **2A** and **2A'** from the terminal hydride **3C1**. Energies are reported in kcal/mol. For the pdt bridge a comparison between the TPSS and B3LYP functionals is given. Calculations using the B3LYP functional were carried out by Lui.[118]

Reaction coordinate	B3LYP		TPSS	
	pdt	pdt	odt	edt
TS _{3C1→3A2}	^a	15.3	11.5	14.6
TS _{3C1'→3A2'}	22.3	17.9	14.5	14.6
TS _{3A2→2D}	^a	10.9	14.9	11.1
TS _{3A2'→2D}	13.2	10.8	10.5	11.1
TS _{3C1→3D2}	^a	24.8	19.8	24.3
TS _{3C1'→3D2'}	29.0	24.8	24.5	24.3
TS _{3D2→2A}	^a	14.3	14.7	12.8
TS _{3D2'→2A'}	18.3	13.1	14.3	12.8
TS _{3C1→6CInt}	^a	20.7	15.7	21.2
TS _{3C1'→6CInt'}	26.7	23.0	21.3	21.2
TS _{6CInt→2D}	^a	5.5	3.4	5.7
TS _{6CInt'→2D}	3.1	3.5	6.3	5.7

^a data not available from B3LYP calculations

Table C3: Free energy comparison between the pdt, edt and odt dithiolate bridge in the isomerisation pathway leading to the bridging hydride **2C**, **2A** and **2A'** from terminal hydride **3D1**. Energies are reported in kcal/mol. For the pdt bridge a comparison between the TPSS and B3LYP functionals is given. Calculations using the B3LYP functional were carried out by Lui.[118]

Reaction coordinate	B3LYP		TPSS	
	pdt	pdt	odt	edt
TS _{3D1→3A1}	^a	34.1	32.9	30.9
TS _{3D1'→3A1'}	37.6	34.6	32.0	30.9
TS _{3A1→2C}	^a	11.2	11.7	12.5
TS _{3A1'→2C}	14.5	8.9	12.1	12.5
TS _{3D1→3C2}	^a	25.7	25.4	24.8
TS _{3D1'→3C2'}	29.7	24.9	25.5	24.8
TS _{3C2→2A}	^a	12.0	12.9	8.5
TS _{3C2'→2A'}	16.5	11.1	15.8	8.5
TS _{3D1→6DInt}	^a	17.4	18.0	17.2
TS _{3D1'→6DInt'}	23.2	19.7	18.5	17.2
TS _{6DInt→2C}	^a	19.4	17.5	17.9
TS _{6DInt'→2C}	16.3	14.8	16.4	17.9

^a data not available from B3LYP calculations

Appendix D

Characterising the Normal Modes of Tris(acetylacetonate)iron(III) Using NIS and DFT

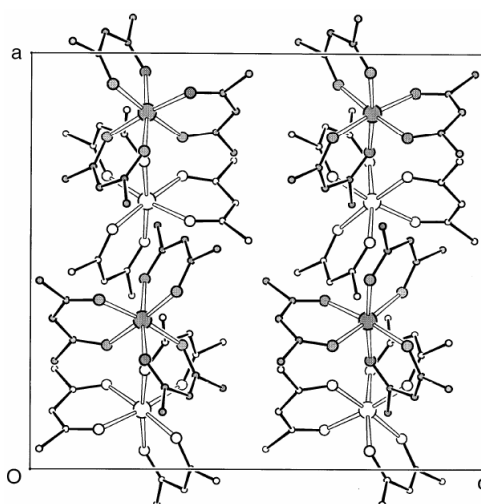


Figure D1: Contents of one unit cell of tris(acetylacetonate)iron(III) showing the latent symmetry elements that are present in this crystal structure. These are the pseudo threefold axes of the molecules being almost parallel to each other and to that of the crystallographic baxis, and the near tetragonal intermolecular symmetry about each molecule within one layer. Atoms in the upper layer are darkened for easy visualisation of the latter symmetry.

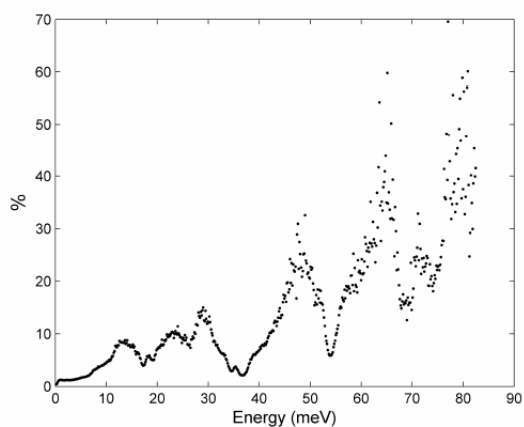


Figure D2: The relative errors in the PDOS spectrum for each energy value (in %). They depend on the numbers of accumulated counts at each energy transfer in the NIS spectrum.

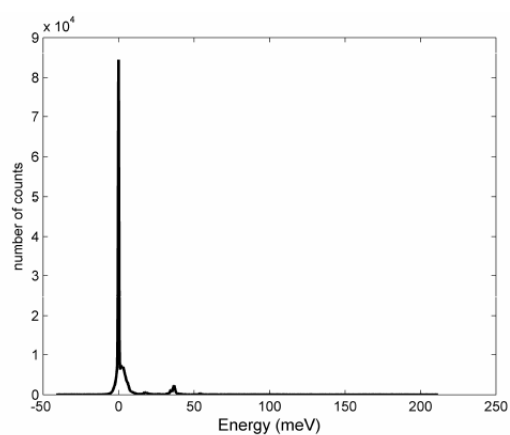


Figure D3: The relative errors in the PDOS spectrum for each energy value (in %). They depend on the numbers of accumulated counts at each energy transfer in the NIS spectrum.

$^{57}\text{Fe}(\text{acac})_3$ Cartesian Coordinates

Fe⁵⁷(acac)₃

Fe	0.00000000	0.00000000	0.00000000
O	2.02300267	0.00000000	0.00000000
O	-0.16171283	2.01652838	0.00000000
O	0.13888750	0.01694612	-2.01815829
O	-2.01175692	-0.15552180	-0.14555669
O	0.00578964	-2.01775059	0.14555674
O	0.00578994	0.13979789	2.01815825
C	2.84605569	0.00127407	-0.96682452
C	1.15991348	0.03012699	-2.77281037
C	-0.95627654	-2.84631932	0.13706792
C	-2.76076958	-1.18074191	-0.13706754
C	-0.06268968	1.15861003	2.77281093
C	-0.22623485	2.83705013	0.96682496
C	2.48637807	0.01948965	-2.32107283
C	-2.30705227	-2.49946931	-0.00000022
C	-0.17932581	2.47997967	2.32107305
C	-0.01240515	0.87413777	4.25395987
C	-0.36093976	4.28901690	0.57836203
C	-4.23730239	-0.90744939	-0.28679139
C	-0.56582917	-4.29628144	0.28679127
C	0.87233227	0.05751039	-4.25395995
C	4.30414418	-0.01693423	-0.57836180
H	3.27603329	0.02567941	-3.05822833
H	-3.03975501	-3.29328235	-0.00000035
H	-0.23627830	3.26760294	3.05822869
H	-0.09439358	1.77791778	4.85639678
H	-0.82192394	0.18876115	4.51538595
H	0.92675128	0.36695984	4.48759352
H	-1.27269597	4.41725808	-0.00992728
H	-0.39223219	4.95185071	1.44215692
H	0.47795930	4.56809039	-0.06333370
H	-4.41014809	-0.39426468	-1.23578811
H	-4.83635481	-1.81656779	-0.25346602
H	-4.55942047	-0.23094319	0.50818324
H	-1.42415157	-4.96608856	0.25346573
H	0.13426153	-4.56329145	-0.50818402
H	-0.04047021	-4.42755142	1.23578845
H	1.77977389	0.04802996	-4.85639642
H	0.25385932	-0.80420521	-4.51538657
H	0.29170391	0.95311956	-4.48759310
H	4.96735824	0.00485789	-1.44215697
H	4.51526571	0.84158832	0.06333376
H	4.50485759	-0.91552138	0.00992790

Appendix E

Measuring the Rate of Interfacial Transfer Using Muon Spectroscopy

Allyl Alcohol Cartesian Coordinates

Centrally muoniated allyl alcohol

C	1.93505200	0.15606900	0.00189200
C	0.59850400	-0.49849500	-0.02795200
C	-0.55810700	0.49071800	0.07684600
O	-1.77707600	-0.24401800	-0.04817900
H	0.50984100	-1.23929500	0.77380300
H	2.09110400	1.12383500	-0.46197000
H	2.80762600	-0.37570800	0.35886800
H	0.46388200	-1.06188600	-0.96716700
H	-0.47557200	1.24215500	-0.72085400
H	-0.51496000	1.01352100	1.04113800
H	-2.51801000	0.35976800	0.05689800

Terminally muoniated allyl alcohol

C	0.00000000	0.00000000	0.00000000
C	0.00000000	0.00000000	1.48885900
C	1.27005000	0.00000000	2.25580300
O	0.99735100	-0.31580700	3.62306500
H	0.71849500	-0.72256200	-0.40618700
H	-0.98696600	-0.24295900	-0.40048600
H	1.76135500	0.99076600	2.18967000
H	1.97602900	-0.72527000	1.81805100
H	1.78981700	-0.15045700	4.14213900
H	-0.90842600	0.21252000	2.04117700
H	0.27990100	0.98146400	-0.41879600